

Related Pergamon Titles of Interest

BOOKS

JAPANESE SOCIETY OF MECHANICAL ENGINEERS
Visualized Flow

NISHIMURA
Automatic Control in Aerospace

TANIDA
Atlas of Visualization

URBANSKI
Chemistry & Technology of Explosives, Volumes 1–4

JOURNALS

Acta Astronautica

Advances in Space Research

COSPAR Information Bulletin

Microgravity Quarterly

Progress in Aerospace Science

Space Technology

Full details of all Pergamon publications/free specimen copy of any Pergamon journal available on request from your nearest Pergamon office.

SOLID ROCKET PROPULSION TECHNOLOGY

Edited by

Alain Davenas

*ancien élève de l'Ecole Polytechnique
Technology and Research Director, SNPE, France*



PERGAMON PRESS

OXFORD • NEW YORK • SEOUL • TOKYO

U.K.	Pergamon Press Ltd, Headington Hill Hall, Oxford OX3 0BW, England
U.S.A.	Pergamon Press, Inc, 660 White Plains Road, Tarry- town, NY 10591-5153, U.S.A.
KOREA	Pergamon Press Korea, Room 613 Hanaro Building, 194-4 Insa-Dong, Chongno-ku, Seoul 110-290, Korea
JAPAN	Pergamon Press Japan, Tsunashima Building Annex, 3-20-12 Yushima, Bunkyo-ku, Tokyo 113, Japan

English translation Copyright © 1993 Pergamon Press Ltd.

Translation of: Technologie des propergols solides.
Copyright © Société Nationale des Poudres et Explosifs, and Masson, Paris, 1988

All Rights Reserved. No part of this publication may be reproduced, stored in a retrieval system or transmitted in any form or by any means: electronic, electrostatic, magnetic tape, mechanical, photocopying, recording or otherwise, without permission in writing from the copyright holders

First English edition 1993

Library of Congress Cataloging-in-Publication Data

Technologie des propergols solides. English.

Solid rocket propulsion technology/edited by Alain Davenas.

p. cm.

Translation of: Technologie des propergols solides.

Includes bibliographical references.

1. Solid propellant rockets. I. Davenas, Alain. II. Title.
TL783.3.T4313 1991 662'.26—dc20 90-25612

British Library Cataloguing in Publication Data

Solid rocket propulsion technology.

1. Aerospace vehicles. Engines

I. Davenas, Alain

629.1

ISBN 0-08-040999-7

Foreword

THIS book is a translation, with some slight adaptations, of *Technologie des propergols solides*, published in French in 1989.

There are few books on solid propellants and their use in rocket propulsion, and few of these present a comprehensive review of the field.

There are many reasons for this. For the most part, applications of this technology, with the exception of fireworks displays, have been limited to the fields of advanced armament and space activities. Therefore, most of it has been protected by industrial or military security classifications. It was thus necessary to wait for the moment when a significant quantity of data would be disclosed through open literature or patents.

These restrictions on the free flow of information led to different designs and methods in different countries. In France, for instance, there has been intensive use of trimmed axisymmetric grain designs with high loading fractions which have not been developed in any other countries, and for which the design and production methods were protected by a "secret" classification for a long time. In the USSR a very specific composite propellant formulation has been used in a family of missiles, with a binder that uses a derivative of a terpenic resin found only in the Ural forests of the USSR.

The technology of propellants is, like other technology, subject to the influence of fashionable trends. In France today, for example, Finocyl grain designs are currently popular. The main reason for this is probably that Finocyl geometries are very adaptable to various flow rate or thrust requirements. There are, however, cases where a simple star-shaped design would have satisfied the main requirements, and also offered some better secondary characteristics.

While the original objective was to present, to the extent possible, a universal body of knowledge, factors such as restricted information flow, specific industrial developments in various countries and fashionable trends have sometimes made this difficult. Readers may therefore find a French flavor to some of the chapters.

As already stated, we tried to cover all aspects of the field, and consequently this is a long book. We had to be as concise as possible on each subject; therefore we often refer the reader to what we feel is essential material for additional information. One original intention was that each chapter should be readable independent of the others, implying a great amount of redun-

dancy. Because of space limitations we discovered that this could not be done. Therefore, some chapters refer to other chapters. This practice was, however, kept to a minimum, and we used a traditional approach: each chapter uses concepts already developed in previous chapters.

After a first chapter reviewing the fundamentals of rocket propulsion, the second chapter develops all the descriptive aspects. The second chapter is recommended to anyone who is interested only in reading about one of the more specialized subjects found in later chapters. The subsequent chapters present the specific design methods and the theoretical physics underlying them. These are chapters where, after the fundamental mechanisms involved in the working of propulsion systems are presented, the rules of the art and specialized engineering methods are then deduced.

The last part of the book deals with the industrial production of the most important motor component: the propellant, and the inert materials, such as thermal insulations and bonding materials.

Some subjects of common interest to different chapters are covered in only one of them. Hence, processes used to manufacture composite propellants, used for composite double-base propellants (Chapter 11), are covered in Chapter 10. Non-destructive testing techniques used for every type of grain are also found in Chapter 10. Some mechanisms for the transition from deflagration to detonation are described in Chapter 11. The decomposition of nitrate esters and critical dimensions for cracking by internal pressure are discussed only in Chapter 9; vulnerability issues are discussed in Chapter 8, etc.

All authors who contributed to this work belong to the same company: Société Nationale des Poudres et Explosifs — SNPE. The reason for this is quite simple. SNPE originated from a famous official French governmental organization: the “Service des Poudres”. For several centuries this organization held the monopoly in France for the production of “explosive substances” (substances that can deflagrate or detonate). During the 19th century and the first part of the 20th century it was one of the great French chemical groups where fundamental research in the field of physical chemistry was most advanced. SNPE has kept the mandate, for reasons of national interest, to develop all types of products for propulsion applications and for all basic research programs in this area, differing from most other countries, where companies often specialized in only one family of products.

Daniel Quentin had the original idea for this project, and stimulated the first drafts. The requirements of his professional activities took him very far away from France, making it impossible for him to participate directly in later drafts. Even though there is now little left from the voluminous first drafts, these had the great merit of resulting in internal documents on each subject that are proving to be extremely valuable for our company.

I was assisted, for the French version of this book, by a very conscientious editorial committee that included Claude Grosmaire, Roland Lucas and

Bernard Zeller, later replaced — again because of the press of other professional duties — by Rene Couturier.

The French edition of this book was published by Masson, Paris, at the beginning of 1989 with the usual high standards of this publisher. It found quickly a significant audience (relatively speaking!) but its diffusion would nowadays stay essentially limited to French-speaking countries.

The publication of an English version was considered at an early stage. Pergamon Press, with its dynamic policy, agreed to publish it despite the limited audience of this specialized subject. We asked Mrs Anne Baron, Daniel Quentin's assistant, to make a first draft of translation. This draft was then reviewed by the authors with the help of their knowledge of the vocabulary of their technical field. Then we asked some English-speaking colleagues, knowledgeable in the field, to check our translation. We wish to express all our gratitude to Miss Carol Jones (Chapter 13), Professor Beddini (4) and to Tom Boggs (9), John Consaga (11), Ron Derr (3), Geoffrey Evans (9), Ray Feist (2), Joseph Hildreth (1), Frank Roberto (8, 10, 14), Bert Sobers (12), Frank Tsë (6) and Andy Victor (5).

Some of the problems we encountered during the translation were due to the fact that some concepts that are represented by one word in one language needed a long sentence for their translation — and this to my surprise is true both ways (for instance “autoserrage” for “burning area to port area ratio” or “indice structural” for “ratio of inert mass to propellant mass for a given motor”, etc.). Another difficulty was that terminology has sometimes still to be standardized even if some progress is being made in this area (for example in low visible signature propellants, hazards classification, etc.). This is particularly true for propellant formulations. We have developed in French a specific terminology to name propellants according to their main components, which is compact, efficient and (of course!) Cartesian. It was used for the French version but there is no English equivalent so we had to decide, for the English vocabulary, somewhat arbitrarily. Some traces of the French names may be found in some chapters. In case of possible ambiguities we have made a special presentation, in an addendum, of the decisions we have taken to name propellants in English, and the rules of French terminology.

Since the French edition was published, at the beginning of 1989, there has not been much important evolution in solid propulsion technology, so the changes made are quite limited.

Some developments on program management were suppressed in Chapter 8 because they were very specific to the French organization. A small addition was made in Chapter 12 on integral boosters that were briefly mentioned in the French edition, and in Chapter 7 on XDT (delayed detonation through shock). Some developments related to clean propellants for future space boosters and continuous-mixing processes of composite

propellant, which may become important in the near future were added to Chapter 14. Some “fresh” references were added to some chapters.

On behalf of myself and my co-authors I would like to record our gratitude to our colleagues at SNPE, whose names do not always appear, for their generous cooperation in the preparation of this book. We would also like to thank all those who have provided illustrations.

Finally I would like to thank my wife Cathy for her patience and understanding during the summers of 1987 and 1988 (French version) and 1989 (English version) while I was assuming my editorial duty, and to thank my supervisor, Pierre Dumas, who encouraged me with this work, even when business was brisk, also all our French, British and American colleagues and friends who helped us in this task.

ALAIN DAVENAS

Note on International Nomenclature for Solid Propellant Compositions

TERMINOLOGY for propellants has still to be standardized. Many equivalent names for the same propellant can be found in the literature (or in this book); besides that the French have developed a specific terminology for composite and high-energy propellants which is described in Chapter 2, Section 3.2.1. This is probably due to the fact that authors sometimes refer to the chemical composition, sometimes to the production process and sometimes to some functional characteristics such as smoke or mechanical properties (e.g. elastomeric modified double-base).

Homogeneous propellants are also called (surprisingly) double-base propellants (based on nitrocellulose and a nitric ester). The two main types are extruded double-base or EDB (in French SD for “sans dissolvant”, meaning without solvent) and cast double-base or CDB (in French Epictète!). When energetic solids are introduced into this propellant it becomes a CMDB, for composite modified double-base. This name is used only for cast propellants even if some EDBs can contain oxidizers or energetic solids. Elastomeric modified cast double-base or EMCDB propellants have been developed. They are cast double-base propellants in which an elastomeric binder has been added to the double-base. They can involve the addition of energetic solids. In French, since it is a composite propellant, the rules for nomenclature apply: these propellants are nitrargols (generic term). If they contain AP they will become nitalites. If they contain HMX they will be nitramites, etc. These propellants will be minimum smoke propellants if their formula contains only or mostly C, H, O, N.

In English composite propellants are generally named according to their binder, e.g. HTPB or polyurethane propellants, etc., which of course leaves ambiguity except for the fact that most industrial composite propellants use AP for oxidizer, and this is generally implied. The presence of a solid fuel is less clear, since more and more “reduced smoke” propellants, i.e. without metallic fuel, are used in practical applications. In French the names will vary according to the main ingredients of the composition. For instance a composite propellant based on polybutadiene, AP, Al will be a butalane. Without Al it will be a butalite, etc.

So-called high-energy propellants are generally composite propellants with an energetic binder. The most typical use a nitroglycerine plasticized binder and are called XLDB for crosslinked double-base even if there is almost no nitrocellulose in the binder. In French they are nitrargols (nitra for the binder). Minimum smoke XLDB based on HMX, for instance, are nitramites.

The terms “minimum smoke” and “reduced smoke” are themselves not sufficient to differentiate propellants clearly. A working group of AGARD is now trying to define more clearly the level of smoke, in order to be able to compare different propellants made in different countries or organizations. The idea is to characterize the level of primary and the level of secondary smoke of any propellant. In order to be independent of the method and hardware used to measure optical transmission, the classification will be made by reference to two given defined propellants, and the level of smoke will be considered as higher than or lower than ...

CHAPTER 1

Propulsion Elements for Solid Rocket Motors

ROLAND LUCAS

1. Principles of Propulsion

1.1. INTRODUCTION

Rocket launches have become a familiar spectacle. Newspapers, movies and television frequently show us the images of the first moments of lift-off. Impressed by the large quantity of gases released at the lift-off of the rocket, a knowledgeable spectator will deduce the relationship between cause and effect. As a perceptive observer he will have in fact discovered the principle of propulsion, which links reaction force to the ejection of a mass.

Expressed by an equation and applied to rockets, this principle is:

$$F = q \cdot V_e$$

where F is the reaction force which we call thrust, q is the gas mass flow rate and V_e the exhaust velocity of the gases.

Following his logical line of reasoning, the observer will then wonder about the origin of such a volume of gas ensuring for many seconds the propulsion of the rocket. If his creative mind leads him to think of the burning of a solid mass, on board the rocket, he will then have imagined the concept of solid fuel rockets.

1.2. MAIN COMPONENTS OF A ROCKET MOTOR

The rocket motor (Fig. 1) is designed to ensure the combustion under pressure of the propellant grain it contains. The resulting gases are expanded through the nozzle, whose function is to convert this pressure into supersonic exhaust.

As a rule, such a rocket motor has five major components.

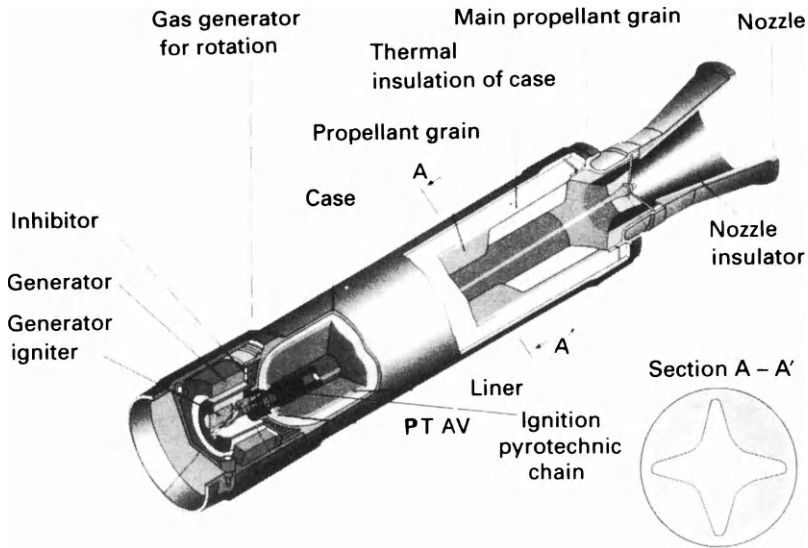


FIG. 1.1. Typical rocket motor.

1.2.1. The case

Made either from metal (high-resistance steels) or from composite materials by filament winding (glass, kevlar, carbon), the case must be capable of withstanding the internal pressure resulting from the motor operation, approximately 3–25 MPa, with a sufficient safety coefficient, usually of the order of 1.4.

1.2.1.1. Ballistic missiles and space launchers

For ballistic missiles and space launchers, special industrial resources have been developed to manufacture cases with an internal volume of up to about 10 cubic meters.

(a) Metal cases

Several types of steel are used for the metal cases (such as AMS 6487 or AMS 6520) whose main characteristics are their great mechanical strength, usually greater than 1000 MPa, and the ease with which they can be shaped.

For the cylindrical body, two manufacturing methods are used:

- wrapping-welding of long steel sheets, requiring longitudinal welding;
- flow turning of rough forgings, avoiding the drawback of welding and offering the possibility of progressive thicknesses.

The technique used for the production of the end closures of the cases involves the machining of solid thermal press forgings. Consequently grooves for handling, and for the interfacing between the various stages, can be obtained from a solid steel block. The end closures and cylindrical body are welded together. The additional manufacturing cycles involve various thermal treatments (hardening, tempering), finish machining, surface treatments (anti-corrosion) and a pressurization test above the maximum expected operating pressure (over-test coefficient of the order of 1.15).

Quality control testing is performed at every stage of the manufacture, including tests of metal properties, X-ray and ultrasonic testing [1].

(b) Composite material cases

The so-called filament-wound cases use composite materials spun into filaments (glass, kevlar, carbon) and a matrix consisting of thermosetting resin of a polyester, epoxide or polyamide type. An overview of these composite materials for propulsion application is shown in ref. [2].

Based on the internal pressure requirements during operation, the design analysis of a case of this type is done in two stages: a preliminary design phase, followed by a testing phase [3]. The first phase is based on the principle that the case has rigidity only in the direction of the filaments. Geometry, corresponding thicknesses, as well as the winding law ensuring the fiber stability requirement (elimination of the risk of slippage during the winding) can be rapidly determined. The second stage uses the computational methods with finite elements by considering the material as a homogeneous orthotropic solid, and enables verification of the structural integrity of the whole.

Once the design has been completed, and the manufacturing parameters determined, manufacture of the case may begin. The fibers, impregnated with resin, are wound on a mandrel shaped as required with the help of a special lathe. The mandrel, an agglomerate of sand, or a metallic piece fitting, is first coated with the thermal insulation intended for the case and is equipped with metal polar bosses at both ends. These metal bosses help strengthen the forward and aft openings and provide the connection with the other components, such as the ignition system and the nozzle. There are two winding methods: the wet process which involves continuous impregnation during manufacture or the dry process, which uses previously impregnated fibers. Two successive types of filament winding are necessary:

- the first filament winding is a succession of loops tangential to the two openings: this is “helix” or “polar” winding, designed to cover the domes and the case;
- the second filament winding covers only the cylindrical section, perpendicular to the generatrix: this is the “hoop” winding.

The entire part is then cured in an oven, with temperature (from 60° to 150°C) and duration (approximately 20 h) depending on the material used; then the mandrel is removed. If it is an agglomerate of sand, a hydraulic process is used to disintegrate the mandrel. The manufacturing process ends with final machining. A series of tests is performed before delivery, i.e., ultrasound tests for structural integrity of the winding and the bonding of the internal thermal insulation.

1.2.1.2. Tactical missiles and rockets

Similar manufacturing processes are used for both tactical missiles and rockets. A comparison between metal cases and cases made of fiber-reinforced plastics is provided in ref. [4].

(a) Metal cases

The selection of manufacturing technique is based on the performance requirements and includes:

- Helical wrapped-welded techniques, which are very well suited for large industrial production.
- Wrapped-welded techniques along the length of the generatrix, used for mid-size or small production runs;
- Flow forming, which does away with the drawbacks of welding along the generatrix and has the advantage of very good precision and very good inside surface conditions — this technique can be used for large-scale production but requires substantial investments.
- Metallic strips which are first coated with an adhesive and then wound in an helical configuration on a mandrel [5]. The number of layers wound is a function of the thickness desired. This technique allows the manufacture of metal cases with a very high level of mechanical strength under normal operational conditions and, according to the inventors of the process, shows specific advantages in the field of insensitive munitions. In the case of unplanned stimuli (fire, bullet impact) resulting in the ignition of the propellant inside the case, the strip laminate technique prevents the usual explosion caused by confinement of the gases until rupture. Composite material cases may offer similar advantages.

As a rule the manufacturing processes described above require that the end closures, which are press-forged and machined, be welded to the case. Sometimes the assembly of the forward end closure and the case, press-forged, is accomplished by a flow forming process to minimize the number of weld beads.

Because of the scale of industrial production, manufacturing costs require the use of metal that can be welded and machined, and that is not too

expensive. Steel type AMS 6520 is commonly used for tactical engines. The machining technology for this type of steel allows a minimum thickness of approximately 1 mm.

Aluminum-copper (AMS 2014) and aluminum-zinc-magnesium (AMS 7075) alloys are also used for small-caliber rockets.

(b) Wound composite material cases

Specific performance characteristics of metals (modulus E and maximum strength σ_R divided by density ρ) are at best equal or inferior to the characteristics of wound fiberglass. Composite materials such as glass-epoxy, kevlar-epoxy and carbon-epoxy are used when performance requirements are important. However, with these materials, strain/stress induced through pressurization or TVC loads induced by ignition or TVC, may lead to significant hoop strains (1–2%), causing greater problems for the structural integrity of the propellant grain. Nevertheless, the winding technique is increasingly used for the production of tactical missile cases [6,7], and rockets [8]. The French company “Société Européenne de Propulsion” [9] has developed an interesting process using a method called structural assembly. The casting-curing cycle of the propellant grain is done in a rubber tube. The whole, serving as a mandrel, is then wrapped with impregnated filaments, thereby integrating the forward- and aft-end closures and, if necessary, a blast tube.

1.2.2. *Propellant grain*

Two main configurations — free-standing grain and case-bonded grain — with various central port geometries are used to fulfill the required performance objectives.

- Free-standing grains. Free-standing grains are contained inside a cylindrical plastic cartridge (PVC, etc.). They are secured inside the case by various support elements such as wedges, springs or grids.
- Case-bonded grains. These are obtained by casting the propellant, before polymerization has occurred, directly into a case already provided with thermal insulation. Additional manufacturing steps (molding, curing, machining, control) required for the propellant grain are performed on the loaded case.

1.2.3. *Thermal insulation*

The combustion temperature of propellant grains, ranging from approximately 1500 to 3500 K, requires the protection of the inside surface of the case.

The design of the internal insulation involves the following four major steps [10]:

- analysis of the internal thermal insulation environment: the nature of the propellant gases, internal aerodynamics, etc.;
- selection of the material: reduced scale tests designed to assess specimens in conditions simulating firing are performed;
- determination of the thickness in the various areas of the case necessary to withstand the heat;
- determination of the dimensions and thickness needed to withstand mechanical strains on the case and propellant grain.

In areas where flow erosion is high (high gas velocity in the vicinity of the case wall), dense and possibly even rigid materials made of asbestos, silicate and carbon fibers impregnated with a heat-proof resin (phenolic, polyamide) may be used. Today, however, elastomers are being increasingly preferred to these types of material. The use of elastomers has allowed significant improvements in insulation by the addition of a reinforcing filler. Due to the ban on asbestos filler, which has been used for many years, alternate insulation materials have been developed as a replacement for the asbestos-containing materials [11]. These reinforcing fillers are either in the form of fibers (silicate, kevlar and carbon) or in the form of powder fillers (silicate and carbon). Various densities can be obtained, in order to decrease the weight of inert parts in the motor.

Thermal insulation for the cylindrical part of the case, which is exposed only at the end of burning, can be provided by the liner, a rubber compound with low fillers that is sprayed. The liner's main function is to allow a good bond between the propellant and the case or the thermal rubber compound. Industrial production and the characteristics of this type of material are specifically discussed in Chapter 13.

1.2.4. The nozzle

The general shape of a nozzle (Fig. 2), called the nozzle profile, includes three major parts:

- the convergent zone of the nozzle, which channels the flow of propellant combustion gases;
- the throat: selection of throat dimensions determines the operating point of the rocket motor;
- the exit cone of the nozzle, which increases the exhaust velocity of the gases in their expansion phase, consequently improving the propulsive effect.

Since 1970, thermal and physical property improvements of the materials with, on the one hand, developments of new computer codes and, on the

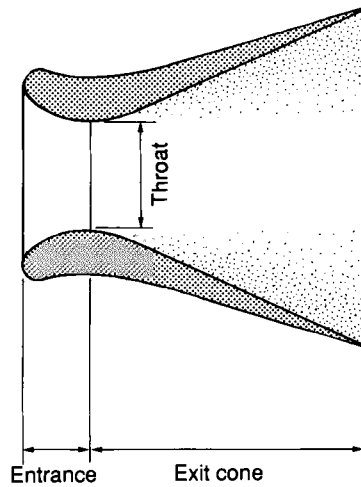


FIG. 1.2. Nozzle diagram.

other hand, performance of experimental studies, have made possible important nozzle design improvements [12]. Currently, the shape and complexity of a nozzle depend on the expected level of performance and on the field of application of the rocket motor (space, ballistic missiles, tactical missiles). Its design requires knowledge of the following parameters [13]:

- Internal operating pressure of the motor, which affects the structural integrity of the nozzle and the ablation of the thermal materials.
- Burning time, often negligible for small rocket motors (a few seconds) but in the case of large rocket motors (measured by the minute) an essential factor in the determination of the thickness required to withstand thermal transfer.
- Throat diameter, which will determine the operating pressure.
- Type of propellant used: the gases and the propellant's burning temperature determine the selection of the thermal materials.
- Space available; often a function of equipment necessary for the guidance of the missile; for example, the nozzles located at the end of a blast tube on some tactical engines.
- Expansion ratio (exit cone area A_s versus nozzle throat area A_t , i.e. $\varepsilon = A_s/A_t$) must allow a pressure in the exit section equal to the ambient pressure to allow maximum efficiency. Because space is usually limited on ballistic missiles, the concept of the extendible nozzle exit cone (during flight) permits an increase in this ratio during operation.
- Submergence of the nozzle into the burning chamber, defined as the ratio of the integrated length versus total length, to minimize the external part of the nozzle. This technology is used particularly on ballistic and space

missiles. The external nozzle, less complex technologically and less costly, is used for the propulsion of tactical missiles and in situations where overall vehicle length is not a constraint. The nozzle is sometimes placed at the end of an insulated metal tube. Use of this blast tube provides space for the devices that activate the steering controls of the missile.

- Thrust vector control which, in ballistics and space motors, uses the principle of a movable nozzle permitting thrust vector control angles ranging from 3° to 15° . The various mechanical systems used include flexible bearing, ball and socket, hydraulic bearing and rotatable exit cone. These techniques cannot be used with tactical missiles. They are replaced by aerodynamic systems — fins — acting on the nozzle jet or, when the atmosphere is sufficiently dense, aerodynamic fins mounted on the case. Non-guided rockets require a spinning action to ensure flight stability. This requirement is taken into account when designing the nozzle. Various systems such as gas deflectors and slanted slots are included, which use the gas flow in the exit cone, or special motors are included to start the spin.
- Interface with the case, which must take into account the geometry selected — nozzle integration or maximum displacement of the nozzle — and the concern to minimize inert part mass.
- Performance, cost, reliability, environment and service life; often conflicting parameters which are used to select the final technical design.

In the case of ballistic and space missiles, performance requirements often lead to the design of materials with good thermal and mechanical stress characteristics, which are well suited for use in the production of large parts. There are currently three major families:

- Traditional composite materials (carbon-epoxy, glass-epoxy) for the body of the nozzle, sometimes replaced by metals (steel, aluminum).
- Ablative materials, made of refractory fiber reinforcements such as carbon, graphite and silica and a matrix obtained from the polymerization of a resin, generally phenolic. These materials are generally used for the duct and as insulation between the duct and the nozzle body.
- Thermostable insulators with a refractory matrix and ceramic or reinforcement carbon. They provide both insulation and structural integrity. They have no degassing at high temperatures and are used mainly for the nozzle walls. Carbon-carbon is particularly well suited for the manufacture of parts from a single block. It is composed of a carbon reinforcement (fabrics, fibers, pultruded sticks) and a carbon matrix obtained by a multistep liquid or gas process (densification process). It is known for its low density (1.5–2) and related excellent structural integrity at high temperatures. The design and development of new solid rocket motor (SRM) nozzles may incorporate these materials in several ways [15].

Frequently the entrance and throat region will be fabricated as a single piece of carbon-carbon material called an ITE (integral throat-entrance). A variation of this application is a single-piece throat, exit cone component called an ITEC or integral throat-exit-cone [16]. Carbon-carbon materials are used to construct very thin-walled structures for fixed and extendable segments of exit cones.

Finally a new concept is under development: the nozzleless solid rocket motor. This approach may use a high-strength, low-burn-rate propellant to form a nozzle. In this case [14], SRM cost reductions of 10–20% are expected.

1.2.5. *The ignition system*

The ignition system brings the energy necessary to the surface of the propellant to start burning. There are three stages:

- *Initiator*: a pyrotechnic element designed to transform an ignition signal such as shock, electrical impulse or light into the steady burning of a pyrotechnic substance.
- *Booster charge*: a charge, powder, pellets or propellant micro-rocket that transmits the flame between the primer and the main grain.
- *Main charge*: a charge, powder, pellets or propellant rocket that ignites the propellant grain.

Ignition systems for large propellant grains (ballistic missiles, space) use this three-stage process. The main charge burns for a few tenths of a second, delivering a discharge approximately a tenth of the flow rate of the propellant grain.

Ignition systems for small propellant grains are usually limited to a primer linked to a primary powder charge (instantaneous and very high release of gases during a few milliseconds) or a primer and an increment (a few tens of milliseconds).

The ignition materials have a high specific energy. They are designed to release either gases or solid particles, based on applications. Pyrotechnic ignition compounds include one or several generally metallic reducers, e.g., Al, Mg, B, Zn, C, and others, and one or several oxidizers or metallic oxides, e.g., NH_4ClO_4 , CuO , Fe_2O_3 , BaO , BaO_2 , and others. Binary ignition compounds are the most used. Sometimes such compounds are designed to fit very specific applications, as was the case of the IFOC system (Initiateur à Fonctionnement par Onde de Choc; in English: shock wave primer), used on the Ariane rocket [17]. This compound is ignited by a shock wave and must not under any circumstances detonate.

2. Fundamental Equations of Internal Ballistics

2.1. INTRODUCTION

The objective of internal ballistics of propellant rocket motor is to provide the motor design engineer with the means to predict or understand the burning characteristics.

The following paragraphs provide a closer view of rocket motor operation. For more detailed information on the equations below, the reader is referred to classic books or technical papers [18–20].

To begin with, there are two fundamental definitions [21]:

- *Burning pressure*: this is the static pressure measured at the head end of the internal gas flow; in other words, it is the pressure at the forward end of the combustion chamber. It is, by definition, an absolute pressure.
- *Burning rate*: this is the linear regression rate of the flame edge, measured at a specific time and a specific distance on the propellant burning surface. The steady-state burning rate of a propellant (excluding the ignition phase and thrust tail-off) is defined by the ratio of minimum web to be burned (minimum distance traveled by the flame edge from the start of combustion to the time the flame reaches the outside contour of the grain) versus steady-state burning time. The burning rate is a function of the combustion chamber pressure.

2.2. PROPELLANT GRAIN FLOW RATE

For preliminary calculations it may be assumed that propellants burn in parallel layers, and that the burning rate is only a function of the pressure. Under these conditions the flow rate resulting from the combustion at a given time is:

$$q = \rho \cdot S \cdot v \quad (1)$$

where ρ is the density of the propellant, S the burning surface and v the burning rate of the propellant at a given time.

2.3. NOZZLE FLOW RATE AND DISCHARGE COEFFICIENT

A nozzle, like any other opening, allows a flow rate which is proportional to the opening area — here, the area of the throat, A_t — and to the pressure upstream of the nozzle — here, chamber pressure, p .

The proportionality coefficient is called the propellant discharge coefficient, indicated by C_D .

Where q' is the gas flow rate passing through the nozzle,

$$q' = C_D \cdot p \cdot A_t \quad (2)$$

where p is combustion pressure at a given time.

Presuming that gases are ideal, it can be shown [19,20] that coefficient C_D is affected only by the nature and temperature of the gases flowing through the nozzle, or

$$C_D = \frac{\Gamma(\gamma)}{\sqrt{\gamma r T}}; \quad \Gamma(\gamma) = \gamma \cdot \left(\frac{2}{\gamma + 1} \right)^{\gamma + 1/2(\gamma - 1)} \quad (3)$$

where:

- T is the combustion temperature (ranging from 2000 to 3000 K);
- γ is the ratio of specific heats of combustion gases at constant pressure and constant volume ($\gamma = c_p/c_v$ with an approximate value of 1.2);
- r is R/\mathcal{M} where R is the universal gas constant (8.134 J/kg · K) and \mathcal{M} is the molar weight in kg (approximately 29×10^{-3} kg for propellant gases).

REMARK: T and γ are not very susceptible to pressure variations, particularly in the case of propellant with a low level of aluminum. Therefore, in many cases, the independence of C_D from pressure is accepted.

The discharge coefficient is expressed in seconds/meter, i.e. the inverse of the flow rate: meters/second. A typical value of C_D is in the range of 6.5×10^{-4} s/m. The average experimental flow rate coefficient is calculated by using eqn (4), which is obtained from eqn (2) by calculating the integral of both sides of the equation as a function of the burning time of the propellant grain:

$$C_D = \frac{M_p}{\int p(t) A_t(t) dt} \quad (4)$$

where M_p is the mass of propellant ejected and $p(t)$, $A_t(t)$, the equations for evolution of chamber pressure and of the nozzle throat area during combustion.

2.4. ROCKET MOTOR OPERATING POINT; KLEMMUNG (BURNING AREA TO THROAT AREA RATIO)

2.4.1. Operating point

The rocket motor operation point corresponds to the equality of the gas flow rates:

- created from the combustion of the propellant grain;
- ejected by the nozzle.

Based on eqns (1) and (2), this relation is given by:

$$\rho \cdot S \cdot v = C_D \cdot p \cdot A_t \quad (5)$$

REMARK: For preliminary calculations this equation does not take into account the volume of gas filling the space resulting from the combustion of the propellant inside the combustion chamber.

Relation (5) can also be written:

$$v = \frac{C_D}{\rho} \cdot \frac{A_t}{S} \cdot p \quad (6)$$

According to the above equations, at any given time in the combustion chamber of a rocket motor (A_t and S having values specific to the rocket motor) containing a known propellant (which defines C_D and ρ), the burning rate is proportional to pressure p .

The burning rate of a propellant, in terms of an intrinsic property of the material, is easily obtained by using small motors which have a constant propellant burning area S , and so a constant operation pressure p . (Refer to Chapter 4, Section 4). Within a common range of pressure (from 3 to 30 MPa depending on the propellant), several successive values may be obtained by selecting different values of the A_t/S ratio.

A law defined by the following equation:

$$v = ap^n (n < 1) \quad (7)$$

is often found to be a good expression of the phenomena.

The rocket motor operating point (v_o, p_o) at a given time will be such that eqns (6) and (7) are simultaneously validated.

On a graph with coordinates v and p (Fig. 3), the rocket motor operating

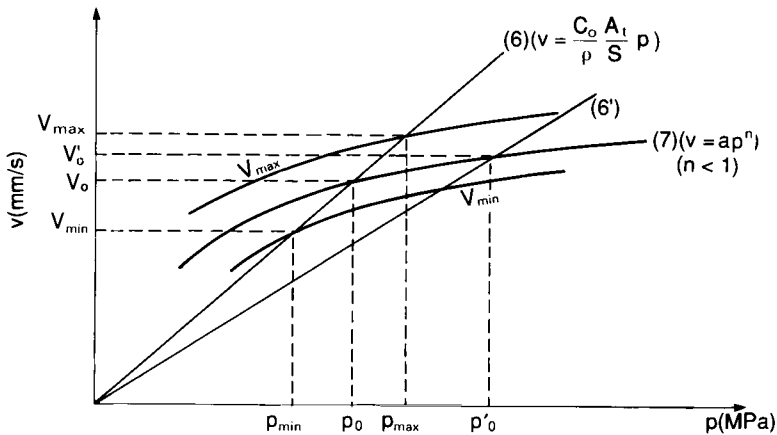


FIG. 1.3. Operating point of a rocket motor.

point is located at the intersection of the straight line of eqn (6) and the curve of eqn (7).

2.4.2. *Klemmung*

The *klemmung* of a rocket motor is the ratio between the propellant burning surface area and the throat nozzle area.

$$K = \frac{S}{A_t} \quad (8)$$

Equation (6) can be written in the form:

$$v = \frac{C_D}{\rho} \cdot \frac{1}{K} \cdot p \quad (9)$$

Figure 3 shows that for a given propellant grain (law $v = a p^n$ determined), the operating point of a rocket motor (v_o, p_o) is a function of the value of the *klemmung*.

Specifically, all other parameters being equal, a fluctuation in the value of K , either voluntarily induced to obey a thrust law or involuntary and deriving from an operational defect (e.g. a crack in the propellant grain causing a sudden increase of S , or a nozzle obstruction), results in a shift toward a new operating point corresponding to a new burning pressure (p'_o) and a new burning rate (v'_o).

2.5. USEFUL EQUATIONS

Equation (5) can be used in the form:

$$p = \frac{\rho \cdot S \cdot v}{C_D \cdot A_t} \quad (10)$$

effect of the burning law:

$$v = a \cdot p^n \quad (n < 1)$$

Equation (10) can be used in the form:

$$p^{n-1} = \frac{\rho \cdot S \cdot a}{C_D \cdot A_t} \quad (11)$$

This last equation is useful for preliminary propellant grain design, excluding combustion phenomena covered in greater detail in Chapter 4.

With any given grain using a known propellant, there is:

- ρ : constant;
 a and n : presumed constant in the pressure zone analyzed;
 C_D : presumed constant for the major part of the pressure rise of the combustion;
 A_i : generally fluctuates so little that it can be assumed constant.

Relation (11) shows that, once the equation of the evolution of grain burning surface is known, the equation for propellant internal pressure can be determined, thereby demonstrating the importance of determining the initial burning surface, then calculating its evolution to be able to find the internal pressure law of the rocket motor best suited for the mission of the missile.

2.6. TEMPERATURE COEFFICIENTS

Propellant temperature affects the rate of burning. Because of the wide temperature ranges required for some tactical all-weather missiles, from -45°C to 60°C or more, a detailed knowledge of these variations is mandatory.

The equations for burning rate and pressure at various temperatures can be calculated from measurements. Curves v_{\max} and v_{\min} in Fig. 3 are an example of data obtained.

When characterizing the temperature sensitivity of a propellant, a constant klemmung ratio is generally preferred because it corresponds to a motor operating at various temperatures.

Coefficient π_k expressing the temperature sensitivity is written in the form:

$$\pi_k = \frac{1}{v} \cdot \left(\frac{\partial v}{\partial \theta} \right)_k$$

Approximately 0.25% for 1°C is a typical value found in composite propellants.

When v_{\max} and v_{\min} correspond to extreme temperature requirements for a tactical missile, Fig. 3 shows that the value of operating pressure can vary between p_{\max} and p_{\min} simply due to temperature changes.

Temperature sensitivity at constant pressure, π_p , is sometimes required. It is given by:

$$\pi_p = \frac{1}{v} \cdot \left(\frac{\partial v}{\partial \theta} \right)_p$$

with a burning rate law $v = ap^n$, it is easily demonstrated that:

$$\pi_p = (1 - n) \cdot \pi_k$$

3. Rocket Motor Thrust

3.1. THEORY OF OPERATION OF A NOZZLE

The nozzle expansion process involves the study of very complex transformations, chemical reactions, heat transfer, gas flow, etc.

Modelling the nozzle operation necessitates the use of simplifying assumptions that will lead to a model with results close to the actual performance of the rocket motor it represents.

Some aspects of this question have been covered in the specialized literature [18–20].

Some of the most important simplifying assumptions are:

- combustion and subsequent expansion of the combustion products are two separate phenomena that happen respectively in the combustion chamber and in the nozzle;
- the expansion in the nozzle is an isentropic phenomenon, in other words, adiabatic and reversible;
- one-dimensional flow;
- gas flow velocity at the entrance of the nozzle is very low and the gas kinetic energy is negligible;
- gas flow through the nozzle occurs without separating from the wall.

Combustion gases are known to remain in the nozzle for a period of 10^{-4} to 10^{-3} s; that information permits us to set the solution between two extreme models:

- the time needed to reach chemical balance is long compared with the time the gases remain in the nozzle; the gas composition does not evolve: it is a frozen equilibrium flow;
- the time needed to reach chemical balance is short compared with the time the gases remain in the nozzle; the gas remains in chemical equilibrium as a function of the local temperature and pressure through the expansion and in each area of the nozzle: it is a shifting equilibrium flow.

Working with the assumptions given above, a simplified method can be used by presuming that the combustion products are ideal with a constant molecular weight and γ .

Using the following variables:

- p , T and ρ : pressure, temperature and density of the gases;
- V : gas flow velocity;
- A : a cross-section of the nozzle;
- R : universal gas constant $\left(r = \frac{R}{\mathcal{M}}\right)$;

- a : the speed of sound ($a = \sqrt{\gamma r T}$);
 M : the Mach number ($M = V/a$);

and the following equations:

- the Mariotte law: $\frac{p}{\rho} = r \cdot T = \frac{R \cdot T}{M}$
- continuity equation: $\rho \cdot A \cdot v = cst^e$
- Saint-Venant equation: $V^2 = 2 \cdot c_p \cdot \Delta T$
- Mayer formula: $c_p - c_v = r = \frac{R}{M}$

and using the following subscripts:

- index 0: for the values of the parameters at the beginning of the convergent zone of the nozzle, in other words the values obtained during the propellant combustion;
- index t: for the values of the parameters at the throat of the nozzle;
- index s: for the values of the parameters at the exit plane of the nozzle;

The following is demonstrated:

3.1.1. *The Hugoniot formula*

$$\frac{dA}{A} = \frac{dV}{V} (M^2 - 1)$$

showing that, on a convergent-divergent nozzle:

- gas velocity increases continuously;
- gas velocity is equal to the speed of sound at the throat section ($M = 1$).

3.1.2. *The existence of a maximum exhaust velocity*

This velocity is reached through isentropic expansion of the gases, until absolute vacuum.

$$V_L = \sqrt{2 \cdot c_p \cdot T_o} = \sqrt{2 \cdot \frac{\gamma}{\gamma - 1} \cdot r \cdot T_o}$$

3.1.3. *The existence of various relationships between the operational parameters*

- In any section of the nozzle:

$$\frac{p}{p_o} = \left(\frac{T}{T_o} \right)^{\gamma/\gamma - 1} = \left(\frac{\rho}{\rho_o} \right)^{\gamma}$$

- At the nozzle throat:

$$\frac{p_t}{p_o} = \left(\frac{2}{\gamma + 1} \right)^{\gamma/(\gamma-1)}$$

$$\frac{T_t}{T_o} = \frac{2}{\gamma + 1}$$

- At the exit cone section:

$$V_s = V_L \sqrt{1 - \left(\frac{p_s}{p_o} \right)^{(\gamma-1)/\gamma}}$$

where p_o/p_s is the expansion ratio.

Because exhaust velocity is of primary importance in the determination of thrust, we need to write in its complete form:

$$V_s = \sqrt{\frac{2}{\gamma-1} \cdot \frac{R}{\mathcal{M}} \cdot T_o \left[1 - \left(\frac{p_s}{p_o} \right)^{(\gamma-1)/\gamma} \right]} \quad (12)$$

where V_s increases when T_o does or when the molar mass \mathcal{M} of the exhaust gases decreases.

3.2. DETERMINATION OF THE THRUST

Where p_a is the ambient pressure and q the gas mass flow rate of the nozzle:

$$F = q \cdot V_s + (p_s - p_a)A_s$$

This equation demonstrates:

- that thrust increases when ambient pressure (p_a) decreases. Thrust is maximum in vacuum, i.e.:

$$F_{\text{vacuum}} = q \cdot V_s + p_s \cdot A_s$$

- and that for a given ambient pressure (constant p_a) after taking into account the differential equation:

$$dF = V_s \cdot dq + q \cdot dV_s + A_s \cdot d(p_s - p_a) + (p_s - p_a) \cdot dA_s$$

where q and p_a are constant, thrust is maximum when $p_s = p_a$, that is:

$$F = q \cdot V_s$$

in which case we have the optimum expansion ratio of the nozzle; p_s is a function of p_o and of the geometry of the nozzle and, because of that, it cannot be constantly equal to p_a , which varies during flight.

- When $p_s > p_a$ the jet bursts at the exit cone. It is under-expanded.
- When $p_s < p_a$ the jet separates from the wall of the nozzle. It is over-expanded. (The Summerfield criterion, which is valid for the half-

angles of the exit cone of a nozzle smaller than 15° , indicates that separation occurs in an area where pressure is close to $0.4 p_a$.)

3.3. THRUST COEFFICIENT

For practical reasons related to the design of the propellant grain, it is useful to use a proportionality coefficient, which is the ratio between the thrust on the one hand and the chamber pressure and throat area on the other hand. The relation is:

$$F = C_F \cdot p_o \cdot A_t \quad (13)$$

Combining with eqns (12) and (13), it is solved by:

$$C_F = \sqrt{\frac{2\gamma^2}{\gamma-1} \cdot \left(\frac{2}{\gamma+1}\right)^{(\gamma+1)/\gamma} \cdot \left[1 - \left(\frac{p_s}{p_o}\right)^{(\gamma-1)/\gamma}\right]} + \frac{p_s - p_a}{p_o} \cdot \frac{A_s}{A_t}$$

C_F is a parameter that does not depend on units of measure and depends solely on combustion gases (γ) of the ratio between sections $\varepsilon = A_s/A_t$ and on the ratio p_o/p_a . (p_o/p_s is expressed only as a function of γ and of A_s/A_t).

C_F indicates the efficiency of a nozzle for a given propellant grain and given nozzle geometry. Figure 4 shows the evolution of C_F as a function of the ratio $\varepsilon = A_s/A_t$ for various values for the p_o/p_a ratio.

These same results can be displayed in the form of tables, based on the values on γ .

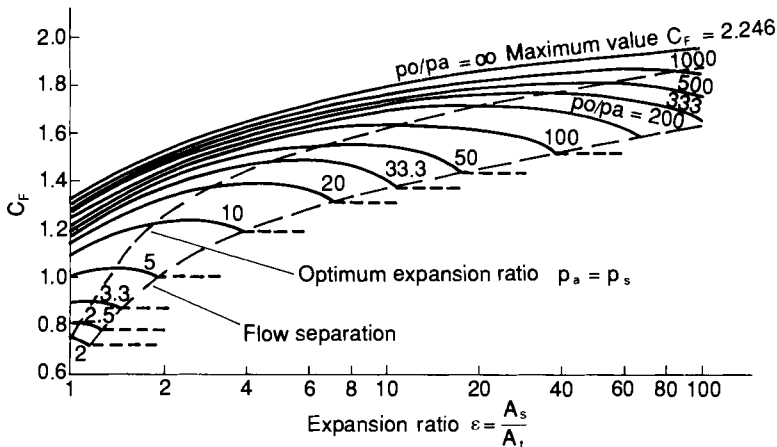


FIG. 1.4. C_F diagram.

4. Specific Impulse

4.1. INTRODUCTION

Suppose we have several rocket motors with identical structures (shape and equipment) and nozzles, and loaded with different propellant grains.

A comparison of their performance is easily done by measuring the intensity of the thrust F obtained by each of the motors during operation.

All things being equal, the various compositions of propellant grains can be compared by dividing thrust F obtained by the weight flow rate of propellant burned.

This ratio — the thrust obtained versus the weight flow rate — for a given rocket motor allows us to determine the intrinsic characteristics of the propellant grain used.

This is known as the specific impulse of the propellant grain. Because its dimensional equation is time, this value is expressed in seconds. At this point it is already clear that, because specific impulse can only be measured through the operation of a rocket motor, its experimental measurement is highly dependent on the rocket motor and its operating point.

4.2. DEFINITIONS AND RELATIONS

Instantaneous specific impulse is the ratio of thrust versus the weight flow rate of the propellant at a particular instant; it is given by:

$$I_s = \frac{F}{g_0 \cdot q} \quad (14)$$

where g_0 is the standard acceleration due to gravity ($g_0 = 9.80665 \text{ m/s}^2$) and q the mass flow rate of the propellant.

From the previous equation we can write:

$$I_s = \frac{F}{g_0 q} = \frac{p C_F A_t}{g_0 p C_D A_t} : I_s = \frac{C_F}{g_0 C_D} \quad (15)$$

To measure performance of the propellant it is preferable, for practical reasons, to take into account total duration of combustion. By combining the second side of eqn (14) with the total combustion time (t_c), we obtain the average specific impulse of the propellant or of the rocket motor:

$$I_{sm} = \frac{\int_0^{t_c} F \cdot dt}{g_0 \int_0^{t_c} q \cdot dt} = \frac{\int_0^{t_c} F \cdot dt}{g_0 \cdot M_p}$$

where M_p is the total mass of propellant burned.

The integral of thrust F as a function of total combustion time (t_c) is called the total impulse of the rocket motor; it is given by:

$$I_{\text{Ft}} = \int_0^{t_c} F \, dt$$

Based on the preceding equations, we can deduce that:

$$I_{\text{sm}} = \frac{I_{\text{Ft}}}{g_0 \cdot M_p} \quad (16)$$

and

$$I_{\text{Ft}} = g_0 \cdot M_p \cdot I_{\text{sm}} \quad (17)$$

4.3. PRACTICAL APPLICATIONS

The definitions introduced in the preceding paragraph and related equations are used by the designers to guide them in the selection of the best performances.

4.3.1. *Propellant formulation*

Equation (15) shows a direct connection between specific impulse and nozzle discharge coefficient C_D . Based on the expression for C_D (see Section 2.3 of this chapter), we obtain a proportionality relationship between I_s and $\sqrt{T/M}$. To design highly energetic propellants the researcher will seek the propellants with high combustion temperatures T that produce combustion gases with the lowest possible molar mass.

4.3.2. *Preliminary propellant grain design*

Preliminary design analyses of a rocket motor always require the determination of a thrust level F which must be available for a length of time t necessary to perform the assigned mission.

This requirement is translated into the level of total impulse to be obtained:

$$I_{\text{FT}} = F \times t.$$

Using eqn (17) and based on the value selected for the average specific impulse (I_{sm}), the expert is able to deduce the required weight of the corresponding propellant. This equation is of great use for all calculations for preliminary propellant grain design.

4.3.3. Preliminary missile design

A rocket with a total mass M moves vertically at a speed V . Where R is the resultant from aerodynamic forces expressing air drag and F the thrust delivered by the rocket motor, the equation of motion is:

$$M \cdot \frac{dV}{dt} = F + M \cdot g + R$$

$$M \cdot \frac{dV}{dt} = q \cdot g_0 \cdot I_s + M \cdot g + R$$

$$\frac{dV}{dt} = \frac{1}{M} \cdot \frac{dM}{dt} \cdot g_0 \cdot I_s + g + \frac{R}{M}$$

By integrating this equation between t_0 and t_1 which correspond to ignition and propellant burn-out ($t_c = t_1 - t_0$) and neglecting air drag the velocity increase is:

$$\Delta V = g_0 \cdot I_s \cdot \ln \frac{M_0}{M_1} + g \cdot t_c$$

Assuming that I_s and g remain constant during the t_c combustion time and where:

M_0 = total weight of the rocket ($M_0 = M_p + M_1$)

M_p = propellant weight

M_1 = rocket weight at burn-out

and

ρ = the density of the propellant

v = the volume of the propellant grain

we can write the following equation:

$$\Delta V = g_0 \cdot I_s \cdot \ln \left(1 + \frac{\rho v}{M_1} \right) + g \cdot t_c$$

All other things being equal (g , t_c), the velocity increase of the rocket is therefore a function of:

$$g_0 \cdot I_s \cdot \ln \left(1 + \frac{\rho v}{M_1} \right)$$

This equation is very useful for preliminary design analyses.

- When $M_p = \rho v$ is small compared to M_1 (the first stages of ballistic missiles), ΔV becomes a function of:

$$g_0 \cdot I_s \cdot \frac{\rho \cdot v}{M_1} \quad (22)$$

and the product $\rho \cdot v I_s$ is an important criterion for the comparison of propellant grains.

- When $M_p = \rho \cdot v$ is high compared to M_1 (the last stages of ballistic missiles), ΔV is a function of:

$$g_0 \cdot I_s \cdot \ln \frac{\rho \cdot v}{M_1}$$

in which case ρ intervenes only through its logarithm. Specific impulse alone is then an interesting criterion for the comparison of propellants.

These results suggest that propellants could be compared using a performance index such as:

$$I_s \cdot \rho^\alpha \quad \text{where } 0 < \alpha < 1$$

where α is dependent on the rocket motor in which the propellant is to be used. This theory has been developed in various references [18,22].

4.4. DETERMINATION OF THE AVERAGE STANDARD SPECIFIC IMPULSE

Experimental measurement of specific impulse is available only through operating a rocket motor. Consequently, its value is related to the rocket motor.

In addition, eqn (15):

$$I_s = \frac{C_F}{g_0 \cdot C_D}$$

shows that for a given propellant (γ constant), the value of I_s is dependent on C_F , therefore on the ratio of sections $\varepsilon = A_s/A_1$ and p_o/p_a which are inherent to the operating characteristics in the rocket motor.

These remarks illustrate why there is a certain amount of confusion concerning the comparison of the performance of propellants. To be fully convinced, it should be enough to note:

- that p_o is the internal operating pressure of the rocket motor and is therefore related to the combustion chamber characteristics;
- that p_a is the pressure outside of the missile and is therefore related to ambient test conditions;
- that ε is related to the geometry characteristics of the nozzle and their evolution during operation.

Luckily, it is commonly agreed that specific impulse is the parameter that should be used to discuss the performance of propellant grains or rocket motors. This means that, in practice, the exact operating conditions of a rocket motor must be established to allow measurement of the average standard specific impulse:

- The expansion ratio p_o to p_s has been established. Its value, in the United States, has been set at 68, where p_o is 1000 psi and $p_s = p_a$ is 14.7 psi (atmospheric pressure under normal conditions). In France, p_o was in the past assigned 70 atmospheres and a value of $p_s = p_a$ of 1 atmosphere; this ratio is therefore 70.
- The nozzle must be adjusted for the ambient pressure at sea level: $p_s = p_a = 0.10133$ MPa.
- The exit area is shaped like a cone with a 15° half-angle.

To obtain comparable data between propellants, the tests must be performed with identical rocket motors, known as standard rocket motors. The propellant grain geometries used are well suited to obtain the desired precise data (e.g. a combustion pressure that is as constant as possible, geometric parameters that are simple to measure, etc.).

Two types of geometry are commonly used; they are described in greater detail in Chapter 3, Section 5.5. They are:

- the 10-branch star-shaped propellant grains, named 'Mimosa';
- the cylindrical shape, a propellant grain from the United States, named 'Bates'.

These rocket motors are manufactured and tested very carefully to ensure good reproducibility and high-quality results. There may, however, still be some small differences from the standard operating conditions defined above. After analyzing the results, the necessary compensations are calculated; a detailed discussion of these corrective measures is found in Chapter 3, Section 5.9; they are based on the proportionality laws between specific impulse and thrust coefficient (C_F). The results of these measurements and calculations allow us to obtain the average standard specific impulse of the propellant, expressed by I_{sm}^s .

In conclusion, we see that great caution is necessary when discussing specific impulse. Indeed, a rigorous performance comparison between various propellants requires:

- identical rocket motors (shape, mass, insulation, shape and material of the nozzle, etc.);
- operating points corresponding to standard conditions;
- identical unit systems;
- test conditions and equipment sufficient to secure a good level of precision.

4.5. AVERAGE SPECIFIC IMPULSE OF A ROCKET MOTOR

For a given propellant it is possible to assess the performance of the future rocket motor by determining a predicted average specific impulse.

There are various methods to calculate and optimize the performance of a

rocket motor. An excellent synthesis of the research done by Working Group 17 under the AGARD (Advisory Group for Aerospace Research and Development) is available [23], in which the three main steps of this process are well described:

4.5.1. Calculation of the theoretical specific impulse of the propellant

This step uses the thermodynamics computer programs based on main algorithms developed by the Lewis Research Center of NASA [24]. In addition, there are two complementary data banks on thermodynamic properties of the various components of the propellants and other products likely to result from combustion and subroutines tailored to the needs of the user (presentation of results). The use of this software and various thermodynamic calculations performed are discussed in depth in Chapter 3.

Based on the chemical composition of the propellant, this software program calculates the various thermochemical characteristics of the combustion gases and the theoretical specific impulse of an ideal rocket motor having no losses, for the required operating point (p_o , p_a and ϵ). The major simplifying assumptions are:

- uniaxial, isentropic and non-viscous flow;
- chemical equilibrium of the gases during expansion;
- kinetic and thermal equilibrium between the solid and gaseous phases of the flow.

4.5.2. Determination of losses due to flow conditions in the nozzle

These losses result from the discrepancies between real properties of the flow of the gaseous mixture and the characteristics corresponding to the simplifying assumptions above. They belong, in general, to the following six categories:

- Losses through flow expansion because the flow is in fact bidimensional. They are a function of the half-angle of the exit cone and of its convex shape.
- Two-phase losses, resulting from velocity and temperature lag between the solid and the gaseous phases.
- Boundary layer losses, caused by the viscosity effect and by the heat exchange at the nozzle wall.
- Losses through chemical kinetics because of a delay in the establishment of chemical equilibrium of the gas flow.
- Losses due to the submergence of the nozzle into the propellant grain, resulting in a modification of the flow at the inlet of the nozzle.

- Losses due to erosion of the throat area through ablation, resulting in a decrease of nozzle expansion ratio.

4.5.3. *Determination of losses due to chamber combustion conditions*

With a radial burning propellant grain these losses are fairly limited compared to the losses due to the flow conditions in the nozzle. They are mainly caused by heat exchange at the walls and incomplete combustion.

The research done by Working Group 17 AGARD [23] permits comparison of the performance predictions done by various companies, using the steps described above. These forecasts were done for two different rocket motors. They were later compared to the experimental results.

Rocket motor	Average specific impulse forecast	Actual measurements
no. 1	289.6–294.5 s according to various companies	293.12 s
no. 2	292.8–299.1 s according to various companies	296.7 s

Complex programs are necessary to estimate the average specific impulse of a rocket motor. With such tools the designer is also able to improve the profile of the nozzle duct and, as a result, to optimize the performance of the rocket motor. The process involves successive iterations between profile modifications and calculation of corresponding losses, while at the same time taking into account the thermal characteristics of the materials.

4.6. EFFICIENCY

4.6.1. *Propulsive efficiency*

An estimation of the losses in the nozzle will be made experimentally by calculating the propulsive efficiency of the nozzle:

$$\eta_F = \frac{\overline{C_F}}{C_F}$$

with:

C_F obtained from the theoretical calculations described in the preceding section;

$\overline{C_F}$ obtained by using the firing data in the equation:

$$\overline{C_F} = \frac{\int F \cdot dt}{\overline{A_t} \cdot \int p \cdot dt}$$

where $\overline{A_t}$ is the average throat area during firing.

4.6.2. *Combustion efficiency*

Similarly, the combustion efficiency, which will indicate losses inside the combustion chamber, will be calculated by writing:

$$\eta^* = \frac{C_D}{\overline{C_D}}$$

with:

C_D obtained from the above theoretical calculation;

$\overline{C_D}$ obtained by using the firing data in the equation:

$$\overline{C_D} = \frac{M_p}{A_t \int p \cdot dt}$$

where M_p is the mass of propellant burned.

As a rule, losses inside the combustion chamber are limited and correspond to about 10% of the losses in the nozzle. This rule does not apply, however, to the end-burning propellant grains. In this particular case the importance of thermal losses in the combustion chamber increases with the regression of the flame front, leading to a drop of the specific impulse of the motor [25].

4.6.3. *Overall efficiency of the rocket motor*

The overall efficiency accounts for all losses in the rocket motor (nozzle and combustion chamber). It is written as a function of the average specific impulse:

$$\eta = \frac{I_{sm} \text{ (measured)}}{I_{sm} \text{ (theoretical, without calculating the losses)}}$$

Based on the equations described in this section, we see that:

$$\eta = \eta^* \cdot \eta_F$$

5. A Special Case: Ramjets and Ramrockets

5.1. GENERALITIES: AIR-BREATHING MOTORS

By definition, an air-breathing motor uses the oxygen in the air to function. Consequently, unlike rocket propulsion, a rocket engine using an air-breathing motor needs the outside environment to ensure its propulsion.

This type of motor is finding its application in the ramjet working technology which, in spite of a rather early design — proposed in 1911 by R. Lorin — is currently the object of renewed interest in the area of missile

propulsion [26,27]. However, their operation assumes the use of boosters to allow reaching supersonic speeds.

During the propulsive phase of the ramjet the specific impulse (which is the impulse supplied by the mass unit of burned propellant), because of its use of atmospheric gases, is four to six times greater than the specific impulse of conventional propellants. These values are significant, however, only under operating conditions equivalent to those found during flight. For example, under specific experimental conditions (Mach 2, altitude 0) and a chamber pressure of 0.57 MPa, the average specific impulse will be in the range 1000–1300 s, depending on the propellant families.

5.2. DESCRIPTION OF A RAMJET

A typical ramjet includes the following components (see simplified drawing in Fig. 5):

- An air inlet, followed by a divergent diffuser section, located between sections 1 and 2, allowing the intake and compression (with temperature rise) of the quantity of air required for combustion.
- A fuel injection and air/fuel mixing system, located between sections 2 and 2'. For solid propellant motors, called ducted rockets or ramrockets, the liquid fuel is replaced by gases produced by the combustion of a propellant grain located in a primary chamber. The injection of these gases and their mixing with air takes place in an area located before the combustion chamber (Fig. 6).
- A combustion chamber where the mixture is burned, also called the secondary chamber (sections 2' to 3), where the temperature rises (to approximately 2.200 K at 0.8 MPa in this particular case) at the same time as the gas flow increases.
- An ejection system for the combustion products through a convergent-divergent nozzle, assumed to be sonic at the throat (sections 3 to 5).

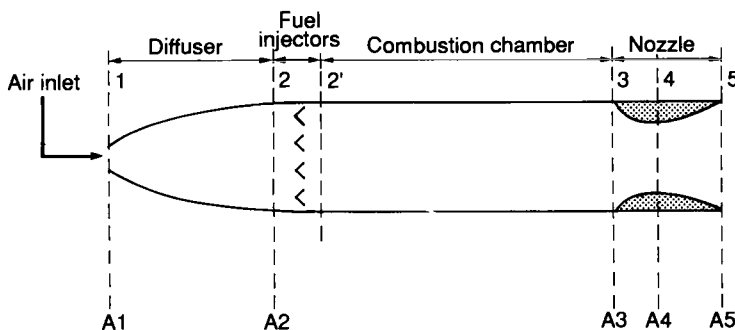


FIG. 1.5. Drawing of a ramjet.

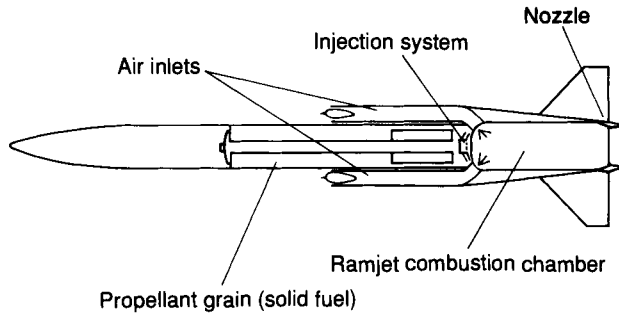


FIG. 1.6. Drawing of a solid-fuel ramjet.

To operate correctly, the ramjet must be ignited at supersonic speeds (around Mach 1.5). It has been clearly established that this method of propulsion is of no interest under Mach 1 because the compression ratio is too low under such conditions.

5.3. PRINCIPLES OF OPERATION

Let us assume that the ramjet is a hollow axisymmetric shape, placed in a uniform supersonic flow with a velocity V_0 and equipped with an adjustable cover to allow variations in the exit plane A_4 (Figs 5 and 7).

Three types of operational modes are possible:

5.3.1. *Subcritical mode*

The cover is pulled back a little. The frontal shock wave is located in front of the inlet. A thin-stream jet of cross-section A_0 in front of the shock penetrates into the diffuser. When traversing the shock wave the flow becomes subsonic and is subjected to a recompression inside the diffuser. In the vicinity of the exit the flow accelerates and becomes sonic at S.

The resultant of the pressure force (internal pressure greater than external pressure) is directed toward the front, creating a thrust. The subcritical rate is characterized by a mass flow rate:

$$q_m = \rho_0 \cdot V_0 \cdot A_0 \quad (23)$$

5.3.2. *Critical mode*

The opening section S is further opened. The flow increases and the frontal shock wave moves closer to the inlet. The mass flow rate reaches its maximum value when the shock attaches itself to the rim of the air inlet:

$$q_m = \rho_0 \cdot V_0 \cdot A_1 \quad (24)$$

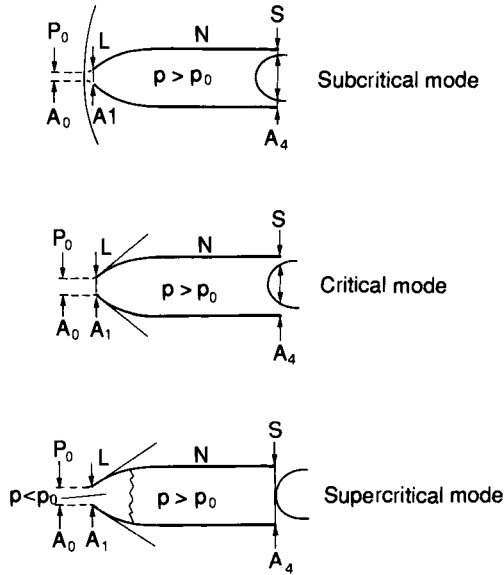


FIG. 1.7. Ramjet operating principles.

The flow in the diffuser is completely subsonic, the internal pressure remains greater than the external pressure. A thrust forward results. This operational rate corresponds to *optimal performance*.

5.3.3. Supercritical mode

When further increasing exit plane S , the external flow is not subject to any modification (constant rate q_m); the plane portion of the shock wave, however, moves into the diffuser. The thrust/drag balance is either positive or negative based on the position of the shock wave, because the internal pressure in front of and behind the shock is respectively smaller and greater than the atmospheric pressure.

5.4. EQUIVALENCE OF THERMAL AND MECHANICAL OBSTRUCTIONS

Removing the rear obstruction, and assuming that we supply a certain quantity Q of heat to the flow, between N and S : analyzing two neighboring sections of the flow between which dQ is supplied, a demonstration based on the classic laws of flow [28] leads to the equation:

$$(1 - M^2) \frac{dV}{V} = \frac{dQ}{T \cdot \rho} \cdot \frac{K^2}{a^2} - \frac{dA}{A} \quad (25)$$

where:

$$K^2 = \frac{\partial p}{\partial s} \text{ (where } s \text{ is the entropy of the flow gases);}$$

$$a^2 = \text{the square of the speed of sound;}$$

$$V, \rho, p, T = \text{velocity, density, pressure and temperature of the flow gases;}$$

$$A = \text{area of entrance section and } M \text{ is the Mach number.}$$

This equation shows that the addition of heat ($dQ > 0$) affects the velocity in the same way as a reduction of the cross-section ($dA < 0$), which explains the expression “thermal obstruction of the flow”.

5.5. PROPULSION EQUATIONS

Looking at the ramjet in Fig. 5: conventional thrust is determined by applying the law of momentum [28,29].

$$F = p_5 A_5 (1 + \gamma M_5^2) - p_0 A_1 \varepsilon (1 + \gamma M_0^2) - p_0 (A_5 - A_0) \quad (26)$$

N.B.: The evolution of the value of a parameter is indicated with the value of its index, which stands for the section analyzed. The index i is used for generative pressure.

Assuming an operation at critical mode ($\varepsilon = A_0/A_1 = 1$) we use:

- (1) Efficiency of the air intake

$$\eta_{o2} = \frac{p_{i2}}{p_{i0}}$$

- (2) The characteristics of the motor rating

$$\eta_{25} = \frac{p_{i5}}{p_{i2}}$$

- (3) The parameters of the geometry of the ejector

$$\sigma_{25} = \frac{A_5}{A_2} \text{ and } \frac{p_5}{p_{i5}} = \bar{\omega}(M_5)$$

$$\text{where } \bar{\omega}(M) = \left(1 + \frac{\gamma - 1}{2} M^2\right)^{-\gamma/(\gamma - 1)}$$

(for an isentropic expansion of a thermally ideal gas, γ is constant in permanent rating).

- (4) The evolution of cross-section A of a stream tube

$$\frac{A}{A_c} = \frac{1}{M} \left(\frac{2}{\gamma + 1} + \frac{\gamma - 1}{\gamma + 1} M^2 \right)^{\gamma + 1/2(\gamma - 1)} \equiv \Sigma(M)$$

where A_c (the critical area) indicates the surface that would be taken by this flow tube if the isentropic expansion reached $M = 1$.

(5) The equations

$$\frac{A_o}{A_{co}} = \sum_o \text{ and } \frac{A_2}{A_{c2}} = \sum_2$$

which, by writing the conservation of flow from infinitely upstream to section A_2 ($p_{i0} A_{co} = p_{i2} A_{c2}$), leads to:

$$\eta_{o2} = \frac{p_{i2}}{p_{i0}} = \frac{A_1}{A_2} \cdot \frac{\sum_2}{\sum_o}$$

with the assumption ($\varepsilon = A_o/A_1 = 1$) which has been selected.

(6) External drag

$$X_{\text{ext}} = p_o (A_5 - A_o)$$

Equation (26) can be written:

$$\frac{F}{p_o A_2} = \eta_{o2} \left[\sigma_{25} \cdot \eta_{25} \cdot \frac{\bar{\omega}_5}{\bar{\omega}_o} (1 + \gamma M_5^2) - \frac{\sum_o}{\sum_2} (1 + \gamma M_o^2) \right] - \frac{X_{\text{ext}}}{p_o A_2} \quad (27)$$

or:

$$\frac{F}{p_o A_2} = \eta_{o2} \cdot \mathcal{F} - \frac{X_{\text{ext}}}{p_o A_2} \quad (28)$$

\mathcal{F} depends solely on the geometry of the ejector (σ_{25}, M_5) on the flight Mach number and on the motor rating (η_{25}, M_2). Any increase $\Delta\eta_{o2}$ of efficiency in the air intake results, all other things being equal, in a proportional increase of the net thrust:

$$\Delta \left(\frac{F}{p_o A_2} \right) = \mathcal{F} \cdot \Delta\eta_{o2}$$

Finally, it is normal to use the value of thrust related to section A_5 . A thrust coefficient is determined:

$$C_F = \frac{F}{1/2 \cdot \gamma \cdot M_o^2 \cdot p_o \cdot A_5}$$

In the case of critical operation, eqn (26) is used to write:

$$C_F = 2 \left(\frac{p_5}{p_o} \cdot \frac{1 + \gamma M_5^2}{\gamma M_o^2} - \frac{A_o}{A_5} - \frac{1}{\gamma M_o^2} \right) \quad (29)$$

Bibliography

1. BRUNER, G., La qualité métallurgique dans les industries aérospatiales, *L'Aéronautique et l'Astronautique*, 83, April 1980, pp. 13-18.
2. PARR, C. H., Composite for propulsion applications — an overview, 24th Joint Propulsion Conference, Boston, Massachusetts, AIAA-88-3127, July 1988.
3. DENOST, J. P., Conception des structures de propulseurs bobinées, *Design Methods in Solid Rocket Motors*, AGARD-LS-150, 1987, pp. 23-44.
4. LANGROCK, W. J., Solid rocket motor case design, *Design Methods in Solid Rocket Motors*, AGARD-LS-150, revised version 1988, pp. 1-16.
5. BADHAM, H. and THROP, G. P., Considerations for designers of cases for small solid propellant rocket motors, *Design Methods in Solid Rocket Motors*, AGARD-LS-150, 1987, pp. 1-20.
6. EVANS, P. R., Composite motor case design, *Design Methods in Solid Rocket Motors*, AGARD-LS-150, 1987, pp. 4.1-4.11.
7. GERLACH, H., Composite motor cases for tactical rockets, 24th Joint Propulsion Conference, Boston, Massachusetts, AIAA-88-3327, July 1988.
8. MAGNESS, R. W., Development of a high performance rocket motor for the VT-1 tactical missile, 24th Joint Propulsion Conference, Boston, Massachusetts, AIAA-88-3325, July 1988.
9. SOCIÉTÉ EUROPÉENNE DE PROPULSION, Brevet Français 83-15263, publication 2 552 494, 1983.
10. TRUCHOT, A., Conception et dimensionnement des protections thermiques internes d'un propulseur à poudre, *Design Methods in Solid Rocket Motors*, AGARD-LS-150, 1987, pp. 1-13.
11. YEZZI, C. A. and MOORE, B. B., Characterization of Kevlar/EPDM rubbers for use as rocket motor case insulators, 22nd Joint Propulsion Conference, Huntsville, Alabama, AIAA-86-1489, June 1986.
12. HILDRETH, J. H., Advances in solid rocket nozzle design and analysis technology in the United States since 1970, *Design Methods in Solid Rocket Motors*, AGARD-LS-150, 1987, pp. 1-15.
13. TRUCHOT, A., Conception et dimensionnement des tuyères de propulseurs à poudre, *Design Methods in Solid Rocket Motors*, AGARD-LS-150, 1987, pp. 1-27.
14. ALBERT, L., Nozzleless booster hardware demonstration progress to date, 24th Joint Propulsion Conference, Boston, Massachusetts, AIAA-88-3366, July 1988.
15. GENTIL, P., Design and development of a new SRM nozzle based on carbon-carbon and carbon-ceramic material, 24th Joint Propulsion Conference, Boston, Massachusetts, AIAA-88-3366, July 1988.
16. ELLIS, P. A., Testing of NOVOLTEXTM 3-D carbon-carbon integral throat and exit cones (ITECs), 24th Joint Propulsion Conference, Boston, Massachusetts, AIAA-88-3361, July 1988.
17. CHOTARD, P., Ignition by shock, Proceedings Fourth international pyrotechnics seminar, Steamboat Village, Colorado, 22-26 July 1974.
18. SUTTON, G. P., *Rocket Propulsion Elements*, 5th edn, Wiley, New York, 1986.
19. WILLIAMS, F. A., BARRERE, M. and HUANG, N. C., Fundamental aspects of solid propellant rockets, AGARDOGRAPH no. 116, Technivision Services, Slough, England, October 1969.
20. TIMNAT, Y. M., *Advanced Chemical Rocket Propulsion*, 1st edn, Academic Press, New York, 1987.
21. NAPOLY, C. and BOISSON, J., Paramètres d'autopropulsion, Laboratoire de Balistique, Sevran, no. 693, 1963.
22. Pire, Trajectoires phase propulsée, Trajectoires phase balistique, Engins balistiques et spatiaux à propergols solides, ADERA, St Médard en Jalles, 1985.
23. Report of the propulsion and energetics panel, Working Group 17, performance of rocket motors with metallized propellants, AGARD-AR-230, 1986.
24. GORDON, S. and MCBRIDE, B. J., Computer program for calculation of complex chemical equilibrium compositions, rocket performance, etc., NASA LEWIS, SP-273, 1971.
25. BANON, S. and ASTIER, J., The contribution of inert material to end burning propellant grain performances, 22nd Joint Propulsion Conference, Huntsville, Alabama, AIAA-86-1421, June 1986.

26. THOMAS, A. N. Jr, The outlook for ramjets and ramjet derivatives in U. S. military applications, AGARD Conference proceedings, no. 307, 1981, pp. 4.1-4.33. NATO Confidential.
27. MARGUET, R. and CAZIN, Ph., Ramjet research in France: realities and perspectives, 7th International Symposium on Air Breathing Engines, Beijing, People's Republic of China, ISABE-85-7022, September 1985, pp. 215-224.
28. CARRIÈRE, P., Aérodynamique interne des réacteurs, Ecole Nationale Supérieure de l'Aéronautique, Troisième année, Première partie: prises d'air, 1966, Troisième partie: stato-réacteur, 1965.
29. CRISPIN, B., Ramjet and ramrocket. Propulsion systems for missiles. Introduction and overview, AGARD-LS-136, October 1984.

CHAPTER 2

Solid Propellant Grain Design

BERNARD ZELLER*

To design a solid propellant grain is to conceive and to define a grain which satisfies various requirements. This chapter describes the methods and procedures used today to design propellant grains. It describes and analyses:

- the various types of grain and the various families of propellant which are available and used today,
- the detailed requirements that a solid propellant grain must satisfy,
- the methods which are used to precisely define the propellant, the architecture and the configuration of the grain, and more specifically the methods used in order to ensure required ballistic performances though maintaining structural integrity of the grain (which is submitted to mechanical loads all through its life),
- an overview on a method of solid propellant grain reliability assessment.

The last section comprises a more specific treatment of some special cases.

1. Introduction

During the past 20 years, requirements on performance, reliability and cost of solid propellant rocket motors (and also on schedules and cost of development) have become more and more stringent. This, in turn, has a direct effect on solid propellant grain design methods and procedures, and on development program content.

The need for improved performance is the consequence of the need for longer ranges, higher velocities and more powerful payloads. The improvement of reliability originates from the need for higher availability of weapon systems, for lower malfunction probability and for longer service life. A decrease of duration and cost of a development program directly reduces the total cost of the program.

*With participation of B. Plantif, M. Vidal and M. Menez-Coutenceau.

During the same period of time, energetic, kinetic, mechanical and aging propellant properties have also been largely improved. Furthermore, the power of scientific computers has greatly increased, and the use of microcomputers has spread widely within the project manager's community.

Due to the pressure of competition (tactical missiles, space launchers) or for technical/political reasons (strategic missiles), the time assigned to designers for performing grain preliminary design* has decreased considerably.

It seems appropriate to present a synthesis of the various methods used today for designing solid propellant grains, within the larger frame of solid propellant rocket motor design.

Design of propellant grains involves vast knowledge and numerous techniques. This is due to the nature of propellants, the geometry and architecture of propellant grains and to their operation modes in rocket motors.

Grains are made of solid propellant put into a given configuration during manufacture; their surface is generally locally restricted or inhibited (to prevent ignition and combustion) by a flame-resistant adhesive material. Other parts of the grain may be bonded by a liner to the motor case (case-bonded grains).

Weights of propellant grains range from just a few grams to several metric tonnes, chamber pressures from a few tenths to more than 30 MegaPascal (MPa); operating times from a few milliseconds to a few minutes.

Manufacture, fielding, storage and operation of a propellant grain (within a rocket motor) involve numerous phenomena related to chemistry, thermodynamics, geometry, combustion, fluid dynamics, mechanics of continuous media, etc. In the present chapter, it is not possible to comprehensively analyse all the aspects of grain design which precisely define a propellant grain which can be industrially manufactured and which must satisfy requirements on storage and operation in various conditions. So it is assumed that the reader is familiar with the basic knowledge of solid propulsion (Chapter 1), internal ballistics and structural analysis (Chapters 4 and 6).

Main points discussed include:

- a description of various types of grain and associated propellants (including French terminology);
- an analysis of requirements for solid propellant grains;
- a review of mechanical and ballistic design methods used today, particularly in France;

*The result of a preliminary design is a first propellant grain definition which generally demonstrates how initial requirements may almost totally be satisfied. Additional modifications of the grain, often involving the use of large computer codes, are needed in order to establish the final design.

- a method of assessing propellant grain reliability;
- a description of some special designs used for very specific applications.

2. Description of Grain Geometries and Associated Propellants

In this section, various types of grain configurations and of propellants are presented, and also general principles on configuration and propellant selection.

2.1. GRAIN CONFIGURATIONS

There are two main types of grain architecture: free-standing grains and case-bonded grains. Grains of the first type are introduced into rocket motor cases (cartridge-loaded) after manufacture. Grains of the second type are bonded to the motor case during the casting (or injection) and curing steps of the propellant grain manufacturing process (Fig. 1).

There is not a single, well-defined, procedure for selecting a free-standing grain architecture or a case-bonded grain architecture for a given rocket motor, except when one of these two architectures is obviously most appropriate for a specific reason. Nevertheless, case-bonded grains generally give higher performances than free-standing grains for equal available volumes. However free-standing grains are largely widespread because this type of architecture may present significant advantages, for instance from the point of view of cost and of overall industrial management. Today, the trend is toward case-bonded architectures, due to the demand for higher performances.

2.1.1. Case-bonded grain configurations

When propellant grains have an outer diameter larger than 500 mm or a weight of more than 300 kg, they are almost always case-bonded. High-performance, middle-sized grains (outer diameter between 100 mm and

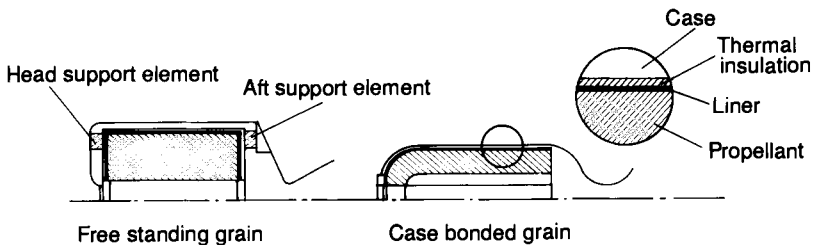


FIG. 2.1. Case bonded grain.

500 mm, weight between 10 and 300 kg) are case-bonded, but free-standing middle-sized grains are very common. For small rocket motors free-standing grains are generally used.

Case-bonded grains generally have a central port, the outer surface of the grain is bonded by a liner (and a thermal insulation) to the motor case. During firing, combustion of the propellant is initiated on the internal surface of the central port and proceeds radially toward the case (and to a certain extent longitudinally depending on the exact geometry). Exact grain geometry is obtained during manufacture of the grain either by direct casting in the case around the mandrel or by machining the port after casting and curing have been completed.

2.1.1.1. *Axisymmetric configurations*

AXIL: Axisymmetric grain with annular slots. The slots are circular; their axis is the same as the grain axis. They are located all along the central port (Fig. 2).

AXAR: Axisymmetric grain with annular slots. This configuration is similar to AXIL, except that the slots are located near the aft-end of the central port (Fig. 3).

CONOCYL (contraction of cone and cylinder): Axisymmetric grain with annular slots. The tips of the annular slots are inclined toward grain head-end so that a part of the grain is cone-shaped (Fig. 4).



FIG. 2.2. Axil configuration.

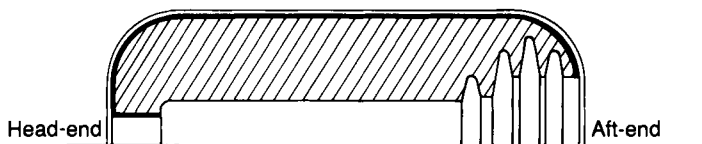


FIG. 2.3. Axar configuration.

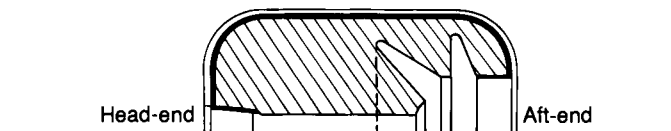


FIG. 2.4. Conocyl configuration.

2.1.1.2. Cylindrical configurations

STAR: The cross-section of the central port has the shape of an n -points star. The contour of the star is constant along the axis [in some cases it may be slightly tapered for manufacture practicality (Fig. 5)].

WAGON WHEEL: The cross-section of the central port looks like a wagon wheel (Fig. 6). Numerous parent configurations exist, such as dendrite, anchor and dogbone configurations.

Other configurations may be obtained, derived from some of the above-described configurations. For example, bipropellant star configuration (to eliminate sliver), or AXAR configuration having a stress-relieving annular slot in the head-end area. Full head-end web grains are also used. Simpler configurations such as internal-burning tube are commonly used; the ends are usually unrestricted to function as a burning surface control; they may also be partially restricted.

2.1.1.3. Three-dimensional geometries

The above-described configurations are considered as one- or two-dimensional, though of course being actually three-dimensional. They are either axisymmetric or cylindrical, with, often, an order " n " symmetry. It is therefore not too difficult to calculate burning area versus web burned or stress-strain field. Today, three-dimensional configurations are becoming more and more popular among the designer community; they are also much more difficult to design. Most of these configurations are referred to as

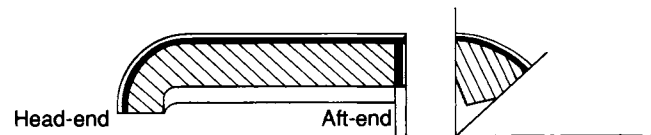


FIG. 2.5. Star configuration.

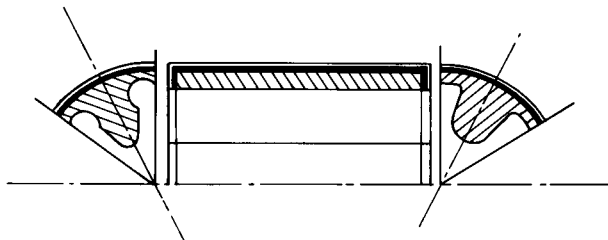


FIG. 2.6. Wagon wheel configuration.

“finocyl”, which is a contraction of fin and cylinder. The fins may be located either at the head-end or at the aft-end of the grain (and sometimes at both ends); they merge into a central cylindrical port. They may have the shape of slots, which simplifies the geometry (Fig. 7).

Often, for stress-relieving, there are annular slots. These configurations require three-dimensional analysis for calculating burning area versus web burned, as well as stress-strain field or gas flow inside the central port.

2.1.1.4. End-burning grains

An end-burning configuration is not well adapted to case-bonded architecture because of problems of structural integrity. However, it is possible to manufacture such case-bonded grains using stress-relieving grain support and retention systems which allow thermal shrinkage due to propellant cooling after curing, though permitting pressure to equilibrate during firing.

2.1.2. Free-standing grain configurations

Free-standing grains are generally smaller than case-bonded grains. Because they are not bonded to the case wall, except sometimes locally, they allow configurations which cannot be obtained with case-bonded grains (for instance an internal-external burning tube).

Final checking of the grains is easier than in the case of case-bonded grains. They are loaded into the motor case during final assembly of the rocket motor. Various support systems may be used to ensure proper operation during firing. During missile service life it is often possible, if necessary, to replace the grain independently of other motor components.

2.1.2.1. Cylindrical configurations

Star, wagon wheel and tube configurations similar to those described above may be found for free-standing grains. Grain ends are generally simpler: they are plane and may be restricted or not. Rod and shell and cruciform type grains may also be found.

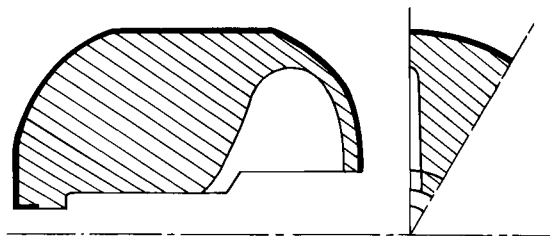


FIG. 2.7. Finocyl configuration.

2.1.2.2. *Configurations with evolving port cross-section*

To reach high-volume loading fractions for free-standing grains a configuration was developed: the cross-section of the central port is right circular in the forward section and becomes progressively star-shaped in the aft section of the grain (Fig. 8). In France this configuration is referred to as “trompette” (trumpet), though it does not much resemble the shape of a trumpet.

2.1.2.3. *End-burning grains*

The orientation of burning is totally in the longitudinal direction. This configuration is wide-spread because gas generation rate is almost constant, volumetric loading fraction is high and grain manufacture is easy. Side and head faces are restricted. Burning times are long and thrust levels are low or moderate. Thermal insulation and inhibitor play important roles, respectively, to protect the chamber walls from the continuous exposure to hot gas and to restrict the combustion to the desired area. They also generate pyrolysis gaseous products during firing, which must be taken into account in the total amount of gas generated by the grain. They are used mainly for the sustaining phase of the flight of some missiles. Anomaly of combustion may be observed on this type of grain, which is known as “coning”.

2.1.3. *General principles for selection of grain configuration*

A practical procedure for selecting the grain configuration/propellant combination is discussed at Section 4. Hereafter only basic principles are discussed.

For selection of the grain configuration, the main factors which are taken into account are:

- volume available for the propellant grain;
- grain length to diameter ratio (L/D);
- grain diameter to web thickness ratio (D/e);
- thrust versus time curve: this gives a good idea of what should be the burning area versus web burned curve (neutral, regressive, progressive, dual-level);

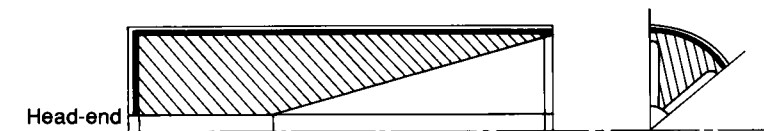


FIG. 2.8. Trumpet configuration.

- volumetric loading fraction: this can be estimated from required total impulse and actual specific impulse of available propellants;
- critical loads (thermal cycles, pressure rise at ignition, acceleration, internal flow);
- manufacture practicality, which depends on case geometry (some grain configurations are more or less easy to obtain);
- fabrication cost: this can be the critical factor for selecting a given configuration.

There is no definite procedure to select a grain configuration in order to satisfy a set of requirements, because there are often several technical solutions to the propulsion problem.

Practically, there are some general trends in selecting configurations, based on the shape of the burning area versus web burned curve (which is qualitatively close to the thrust versus time curve). Table 1 summarizes these trends. Table 2 presents the main characteristics of commonly encountered grain configurations.

2.2. PROPELLANT SELECTION

There are several solid propellant families which differ with respect to composition, manufacturing processes and ability to be processed into certain configurations. These families are comprehensively presented in Chapters 8, 9, 10 and 11.

2.2.1. *Propellant families*

Five families of propellants are commonly manufactured and used, and are described more specifically in other chapters of this book.

- Solventless extruded double-base propellants (EDB); the main ingredients of which are nitrocellulose and nitroglycerine. The configuration is obtained by extrusion through a die having the desired shape. The outer diameter is limited to about 300 mm because of equipment limitations. Additional grain machining may be performed.
- Cast double-base propellants (CDB); the ingredients are similar or parents to those of EDB propellants; they are obtained by casting a mixture of nitroglycerine and triacetin into a mold containing nitrocellulose-based casting powder.
- Composite modified cast double-base propellants (CMCDB), which are derived from CDB propellants by addition of RDX, HMX, or ammonium perchlorate and possibly nitroglycerin, in the casting powder.
- Composite propellants based on a non-energetic polymeric binder and on ammonium perchlorate, which may also contain aluminum powder.

TABLE 1 *Burning area neutrality versus grain configuration*

Burning area neutrality	Grain configuration	Remarks and comments
Good neutrality (less than 15% relative change in burning area)	Wagon wheel dendrite	Short burning times (≤ 3 s), low volumetric loading fraction
	Trumpet	A constant burning area versus web burned is obtained by progressive cylinder zone and degressive slots or trumpet zone
	Tube and slots	Case-bonded grain, $L/D \leq 1$ for third stage of strategic missiles
	Axial	Case-bonded grains, $2 \leq L/D \leq 4$ for first and second stages of strategic missiles
	Finocyl Axar Conocyl Tube (end faces may be restricted) Bipropellant star	Volumetric loading fraction less than 0.8
Dual level	End-burning	Two different propellants. Internal propellant has a higher burning rate than external propellant by a factor of about 2. It is a costly configuration requiring long manufacture cycles (two curing stages). But neutrality is kept, even for high volumetric fraction, and slivers are eliminated. Long burning times, low or moderate thrust
	Remark: the lower the volumetric loading fraction, the better the neutrality. A constant burning area can be accurately obtained by adding axisymmetric slots in the central port or by restricting specific propellant surfaces. It raises grain cost because it requires additional phases during manufacture	
Progressive	Trumpet	The ratio of the two levels can be adjusted by varying the geometry of the aft-end section
	Slotted tube Axar Bipropellant star End-burning (with annular slots in the aft-end face)	Volumetric fraction may reach 0.88. L/D may reach 10 Adjusted by number and geometry of the annular slots Adjusted by the geometry of the stars and propellant burning rates Adjusted by the geometry of the annular slot(s) (boost with radial burning, sustain with end-burning)
Regressive	Tube (right circular port section) Star	The most common is the grain with restricted faces With restricted end faces; slivers induce long tail-off
	Tube with internal External burning Star with internal- external burning End-burning with tapered aft-end	Unrestricted end faces and low to moderate L/D ratio Long burning time, low to moderate thrust

TABLE 2 *Main characteristics of common grain configurations*

Configuration	Volumetric loading fraction	Web thickness	Burning area	Burning area neutrality	Sliver fraction	Web fraction	Comments
Star	0.75-0.90	intermediate	intermediate	good	5-10%	3.5-5.5	Case-bonded and free-standing grains
Trumpet	0.88-0.95	large	intermediate	excellent	0%	> 2	Free-standing grains
Slotted tube	0.75-0.85	large	large	good	0%	≈ 3	Case-bonded grains
Wagon wheel	0.5-0.7	small	very large	excellent	5-10%	6-12	Free-standing and case-bonded grains
Finocyl	0.85-0.95	large	large	good to excellent	0%	2-3	Mainly case-bonded grains, high L/D
Axil	0.88-0.93	intermediate	large	excellent	5%	3	Case-bonded grains, $L/D \approx 1$
Axar	0.88-0.95	large	large	good to excellent	0%	2-3	Case-bonded grains, high L/D
Star (with full head-end web)	0.75-0.85	intermediate	intermediate	good	5-10%	3	Case-bonded grains
Bipropellant star	0.9	large	intermediate	excellent	< 5%	2.5-3	Case-bonded grains
End-burning grains	0.98-1	very large	small	excellent	0%	1	Low thrust

- High-energy propellants based on an energetic binder highly plasticized by a liquid nitric ester, and on RDX or HMX, which may also contain ammonium perchlorate and aluminum, which is called XLDB, for “crosslinked double-base”, even if there is very little or no nitrocellulose in the binder and a very high level of energetic solids in the formulation.

There is a terminology commonly used in France for the last three of these propellant families, that will sometimes be used in the present book. It is based on the following principles: the name of a propellant is made up of a prefix, one consonant, and a suffix.

The prefix gives some information on the binder:

nitra energetic binder (usually containing nitric esters);
buta binder based on carboxy- or hydroxy-terminated polybutadiene;
iso binder based on polyurethane.

The middle letter indicates the nature of the main energetic filler.

l ammonium perchlorate;
m octogen (HMX) or hexogen (RDX);
p potassium perchlorate.

The suffix indicates the nature of the metallic fuel.

ane aluminum;
abe beryllium;
aze zirconium;
ite no metal added.

The most common of these propellants are:

- Nitramite* E: Nitrocellulose/nitroglycerine binder filled with RDX or HMX. “E” indicates that this family of propellants is obtained through a process very similar to the one used for manufacturing CDB propellants (known in France as “Epictete”).
- Isolite*: Polyurethane binder and ammonium perchlorate.
- Isolane*: Polyurethane binder, ammonium perchlorate and aluminum.
- Butalite*: Polybutadiene binder and ammonium perchlorate.
- Butalane*: Polybutadiene binder, ammonium perchlorate and aluminum.
- Nitramite* G: Elastomeric binder, plasticized with a mixture of liquid nitric esters, and filled with RDX or HMX and possibly some ammonium perchlorate. The letter G indicates that

*Trade marks of SNPE.

the manufacturing process is the slurry cast (global) process.

- Nitralane*: Elastomeric binder plasticized with a liquid nitric ester, and filled with HMX, ammonium perchlorate and aluminum.

Besides the main ingredients, propellants may contain several other ingredients, generally in small amounts, used as stabilizers, afterburning suppressants, combustion instabilities suppressants and burning rate modifiers. One of the important tasks of propellant designers is to find a practical way (filler, particle size, burning rate modifier, etc.) to control burning rate, which is a key factor in designing solid propellant grains.

2.2.2. Propellant selection

Selection of a propellant for designing a given grain is based on numerous criteria and, here again, there is no strict procedure for selecting a given composition. The type of architecture (case-bonded or free-standing), energy and burning rate criteria, structural integrity considerations, smokelessness and safety considerations, may lead toward a given propellant family. Each of the propellant families covers a certain range of properties, and it is necessary that the properties of the selected propellant allow design and manufacture of a grain satisfying all the requirements. Table 3 summarizes some properties of the main propellant families. The information presented is very succinct and would need more thorough development. However, it allows, in combination with Tables 1 and 2, a first approach in the selection of the couple configuration/propellant which is detailed in Section 4.3.

3. Solid Propellant Grain Requirements

This section addresses technical requirements that propellant grains must meet. That requirements are settled as the consequence of an agreement between the rocket motor designer and the propellant grain designer. They must be clear, complete and consistent, so that the propellant grain designer may precisely define the grain and eventually build the corresponding engineering development program.

Requirements are divided into those related to functional specifications, those related to operational specifications and interface requirements. They are detailed below.

* Trade mark of SNPE.

TABLE 3 *Main characteristics of common propellants*

Propellant	Maximum delivered specific impulse in standard conditions (70/1)	Maximum density (kg/dm ³)	Range of burning rates at 7 MPa (or at the plateau) (mm/s)	Pressure exponent	Temperature coefficient	Architecture	Smoke	Hazard classification* Card Gap Test (number of cards)	Sensitivity to electrostatic discharge	Manufacturing cost	Ingredients cost
Extruded double-base EDB	225 s	1.65	5-40 (plateau)	≈ 0	very low	free standing	no	1.3 110	no	low	low
Cast double-base CDB	215 s	1.60	4-22 (plateau)	≈ 0	very low	free standing	no	1.3 100	no	high	low
Cast composite modified double-base Nitramite E	230 s	1.70	3-28 (plateau)	0-0.2	low	free standing and case-bonded	no	1.3 150	no	high	moderate (RDX)
Non aluminized composite polybutadiene propellant Butalite	240 s	1.73	4-60	0.3-0.5	low to moderate	free standing and case-bonded	secondary smoke	1.3 0	no	moderate	low
Aluminized composite polybutadiene propellant Butalane	245 s	1.86	5.5-80	0.2-0.5	low to moderate	free standing and case-bonded	primary and secondary smoke	1.3 0	often	moderate	low
Non aluminized cross-linked double base Nitramite G	245 s (with AP) 235 s (without AP)	1.79 1.75	10-25 5-10	0.45-0.6	moderate	case bonded	no (secondary smoke with AP)	1.3 180	no	moderate	moderate (RDX) fairly high (HMX)
Aluminized cross-linked double base NEPE Nitalane	254 s	1.86	9-25	0.5-0.7	moderate	case-bonded smoke	primary and secondary smoke	1.3 180	no	moderate	fairly high (HMX)

* According to French regulations.

Notes: AP: ammonium perchlorate; Card Gap Test is French Gap Test.

3.1. REQUIREMENTS RELATED TO FUNCTIONAL SPECIFICATIONS

3.1.1. *Main internal ballistics requirements*

Average, minimum and peak values of chamber pressure, thrust, total impulse and burning times must be specified within the full operating temperature range. Envelopes of thrust versus time or mass flow rate versus time curves may also be specified.

3.1.2. *Special requirements*

Other requirements are necessary to the designer in order to define a satisfactory propellant grain:

- Maximum weight of propellant grain.
- Maximum weight of total inert (thermal insulation, liner and restrictor).
- Maximum axial and transverse acceleration undergone by the propellant grain during operation of the rocket motor.
- Rocket spin rate (for instance for unguided rockets).
- Dispersions on pressure, thrust, total impulse and burning time have to be specified. Depending on the corresponding requirements, manufacturing process and control operations may be strongly affected and thus the cost of the grain also.
- Plume characteristics (emission and transmission in the visible, infrared and electromagnetic wavelengths range).

3.2. REQUIREMENTS RELATED TO OPERATIONAL SPECIFICATIONS

Depending on environmental conditions, definition of the propellant grain may be significantly affected. Such conditions must therefore be well defined in order to be correctly taken into account during the grain structural design phase.

3.2.1. *Long-term storage*

Desired maximum shelf-life, related temperature cycles and storage conditions must be defined. Particular conditions (relative humidity, salty atmospheres, etc.) which could directly affect propellant grain behavior must be specified.

3.2.2. Thermal environmental conditions

The nature and number of thermal cycles undergone by missiles (for instance during operational flights for airborne missiles) must be defined. Generally they are the limiting factors for structural grain design because very low temperatures may be encountered.

3.2.3. Acceleration, handling and transportation

- Acceleration before and during rocket motor operation: longitudinal acceleration undergone by the rocket motor must be specified, as well as radial acceleration due to rocket spin.
- Handling and transportation: dynamic loadings such as shocks and vibrations encountered during handling (drops) and transportation must also be specified.

3.2.4. Reliability

A level of reliability is more and more commonly required. It is essential to define in which conditions it has to be satisfied. The principle of a method of reliability assessment is discussed in Section 5.

3.2.5. Maintainability

The content and the planning of missiles surveillance, inspection, and maintenance must be defined, as far as they may have an effect on rocket motor environmental conditions.

3.2.6. Safety and vulnerability

These requirements are related to safety and survivability of persons and materials. At present they are not often taken directly into account during grain design analysis. They may induce an *a priori* selection of a type of propellant (e.g. a non-detonable propellant or a propellant having a large critical detonation diameter) or, during engineering development, the performance of safety and vulnerability tests.

3.3. INTERFACE SPECIFICATIONS

Close environment has an important effect on grain behavior during its life and operation. It is often prescribed by the rocket motor designer. The grain designer must take special care that its definition is complete.

3.3.1. Case geometry and properties

A blueprint of the case, or at least its geometry (length, configuration of head and aft-ends), is mandatory in order to perform grain preliminary design analysis. Physical and mechanical characteristics of the case have a direct effect on structural and ballistic design:

- type of case (metal, filament winding/resin, etc.);
- thermal expansion coefficient;
- hoop and longitudinal strains as function of internal pressure;
- maximum allowable peak pressure (depending on ultimate elastic elongation of case material);
- maximum temperature allowable at case wall at the end of motor firing.

3.3.2. Thermal insulations

Nature and geometry of thermal insulations (especially for case-bonded grains) must be known in order to settle grain definition, either from a ballistic point of view (case wall surfaces subjected to high-temperature combustion products), or on a structural point of view (configuration of stress-relieving flaps and boots). Thermal diffusivity, specific heat capacity and mechanical properties data must also be available.

3.3.3. Support system

In the case of free-standing grains the support elements ensure that combustion gas may flow between the grain and the case wall during pressurization due to ignition. The support system must be well determined so that prediction of grain operation may be possible at any temperature.

3.3.4. Nozzle

The characteristics of the nozzle have a dramatic effect on practical ballistic performance of a rocket motor. The following characteristics are of particular interest to the grain designer:

- number and orientation of the nozzles (the angle between nozzle center line and rocket motor center line must be known);
- degree of nozzle submergence;
- erosion of the nozzle (diameter evolution) versus operation time at throat and exit planes;
- angle of the exit cone (or a dimensioned sketch, in the case of a contoured nozzle);
- failure pressure of the frangible closure disk (this allows definition of ignition system and control of pressurization at ignition);

- dimensions of the blast pipe (between chamber and nozzle), when existing; this affects rocket motor efficiency.

3.3.5. Ignition system

The conditions of propellant grain ignition depend on its configuration (location, volume, design). Important characteristics are:

- pressure at the end of ignition,
- pressurization rate (which affects structural integrity during firing).

Minimum and maximum values of delivered pressure and pressurization rate must be accurately known because they are important factors governing grain structural integrity. An envelope of ignition pressure versus time is of interest for this task.

4. Ballistic and Structural Grain Design Methods

4.1. INPUT

In order to design a propellant grain, two types of data are needed:

- Technical specifications: the preceding section gives an almost complete list of these specifications. They are the reduction of functional, operational and interface requirements that must be satisfied in order that the rocket motor fulfill its assigned mission.
- A data bank on propellants, liners, inhibitors and thermal insulations: this allows the grain designer to have at his disposal, quickly and with a low probability of error, chemical, physical, kinetic, mechanical, thermodynamic, etc. characteristics of the various candidate materials which may be used in a rocket motor. The values of these characteristics will be used as input data in analytical and computational design tools.

4.2. PROCEDURE

When performing a solid propellant grain design analysis, two levels of design accuracy have to be distinguished:

4.2.1. First level

This is the level of preliminary design analysis. The tools used at this level must be simple and friendly enough to be operated by propellant grain project managers themselves. They are usually small computer codes based on analytical models, or even graphs which give, very simply, the first results.

In any case, the method involves four main stages:

- selection of a propellant/configuration couple;
- definition of grain geometry satisfying internal ballistic and structural integrity (versus temperature cycles related loads) requirements;
- approximate assessment of erosive burning and potential combustion instabilities;
- assessment of grain structural integrity during pressure rise at ignition.

The method is iterative: depending on the results obtained at the third or fourth stage it allows restarting at the second or even the first stage if it appears that the first definition needs strong modifications.

For a few years, grain designers have been requested to quickly provide fairly precise preliminary design analysis for a given project. In order to satisfy this request a computer-aided grain preliminary design analysis method (MIDAP*) has been developed in France. This method is discussed in detail in Section 4.5.

4.2.2. *Second level*

This is the level of final grain design. The tools required for this task are more sophisticated. They are operated by grain design experts, and are mainly finite differences or finite element computer codes based on two- or three-dimensional models of physical phenomena related to internal ballistics, fluid dynamics, continuous media structural analysis, etc. They allow accurate calculations and therefore optimization of the grain final definition.

The principle of the method is parent to the one developed for preliminary design analysis, but it starts from the final result of this analysis; that is to say the geometry and the propellant selected at the end of the preliminary design analysis.

Starting from this geometry, the evolution of grain burning surface area versus web burned is accurately calculated. Taking into account propellant properties, one obtains the evolution of chamber pressure versus time $p(t)$, and thrust versus time $F(t)$. If necessary, the effect of erosive burning has to be taken into consideration at this stage. The results must then be compared with corresponding requirements (maximum pressure, combustion time, total impulse, etc.). Afterwards the structural safety factor (related to thermal cycles and pressure rise loads) must be assessed with the aid of advanced structural analysis computer codes.

If the results are satisfactory and the design is correct, the propellant grain definition is accepted for starting engineering development. If this is not the

* MIDAP: Méthode Informatisée de Définition des Avants-Projets (computer-aided grain preliminary design).

case, grain definition must be modified so as to increase the safety factor in the critical grain area. Additional structural analysis must be performed in order to check the benefits of geometry modification. Evolution of burning area versus web burned, pressure, and thrust versus time must also be checked so that the ballistic requirements remain satisfied. It may happen that, after these modifications, some of the requirements are no longer satisfied. In this event, selection of the couple propellant/geometry has to be changed or, if there is no other possibility, modification of some requirements has to be considered, in cooperation with the rocket motor designer.

4.3. BALLISTIC DESIGN ANALYSIS

4.3.1. *Basic equations*

Basic equations of solid propellant rocket motor internal ballistics are:

- | | | |
|-------|------------------------------|--|
| (I) | $p = \rho S V_c / C_D A_t$ | p = chamber pressure
ρ = propellant mass density
S = propellant grain burning area
V_c = propellant burning rate |
| (II) | $V_c = f(p)$ (often ap^n) | C_D = propellant discharge coefficient
A_t = nozzle throat area
a = burning rate coefficient |
| (III) | $F = p C_F A_t$ | n = burning rate pressure exponent
F = motor thrust (specific impulse multiplied by propellant weight flow rate)
C_F = nozzle thrust coefficient |

A quick examination of the basic solid propulsion equations indicates the effects of various parameters on motor operation and therefore on motor and propellant grain design:

- evolution of burning area versus web burned is directly connected to pressure evolution versus time;
- sensitivity of burning rate to factors such as propellant initial temperature, rocket motor acceleration, chamber pressure, gas flow, will have an effect on motor operation;
- ρ and C_D , which are specific for a propellant, may be considered for propellant selection;
- initial values, and possible evolutions during firing, of A_t and C_F , which are directly related to nozzle definition (and also to propellant nature), must be accurately known.

In the following sections, the series of stages encountered in ballistic design analysis is described.

and an optimum expansion ratio nozzle) measured for the propellant likely to be selected. This first calculation is iterative, for the value of I_{sms} has to be corrected so as to be representative of the average conditions of motor operation:

- (a) average chamber pressure (P_c) estimated from the specified maximum pressure
- (b) nozzle expansion ratio depending on maximum allowable nozzle exit cone diameter

$$\varepsilon = \frac{A_s}{A_t}$$

A_s is limited by the specification on maximum diameter of nozzle exit cone, A_t equals $M_p/P_c \cdot C_D \cdot t_c$, where t_c (burn time) is specified.

- Assessment of volumetric loading fraction (C_R) required to obtain specified total impulse, given the mass density of the propellant likely to be selected and the volume available for the propellant grain.
- Selection of grain configurations. For each family of grain configuration an empirical maximum volumetric loading fraction has been determined. Thus, given the volumetric fraction required, one or several configurations can be selected. Other criteria, such as processing practicality, difficulty of structural analysis, propellant web thickness, have also to be taken into consideration.
- Definition of propellant burning rate $V_c: V_c = e_b/t_c$.
- Verification of consistency between specific impulse, density, and burning rate (at the average chamber pressure).

This approach must be completed by an accurate calculation of nozzle throat diameter generating a maximum pressure lower than that required by the specifications. This step requires a precise definition of grain geometry in order to calculate burning area evolution which is needed for the determination of A_t :

$$A_t = \frac{\rho \cdot S \cdot V_c}{C_D \cdot p_{\text{max}}}$$

On Fig. 9 the various steps of the method are represented by the path from A to B, then to C and D, or to C' and D'.

4.3.3. *Calculation of propellant grain burning area*

Accurate prediction of chamber pressure evolution versus time depends on accurate calculation of propellant burning area versus web burned. Computational tools which are commonly used belong to two families: one for “two-

dimensional" configurations, the other for "three-dimensional" configurations. Actual grain configurations are three-dimensional, but in numerous cases their geometry is defined by only two coordinates (r, θ) or (r, z); in that case, configurations are said to be two-dimensional.

4.3.3.1. Two-dimensional geometry computer codes (Fig. 10)

These programs calculate the evolution of burning area of the following propellant grain configurations:

- grains with a constant port area section;
- axisymmetric grains, presenting a symmetry of revolution with respect to motor center line;
- end-burning grains with axisymmetric slots on the aft-end face.

These various codes require the description (expressed in plane coordinates) of the initial burning area, and of every section of the propellant grain. The computing time can be adjusted according to the level of accuracy desired. Because of the rapidity at which the computations can be done, a visual display of the computed burning areas is possible. As a rule the level of accuracy is excellent. In a more complex case, where the local burning rate of the propellant is not assumed to be independent of the curvilinear abscissa, the evolution of the burning area as a function of time can be computed with the help of a specially designed computerized numerical model [1].

4.3.3.2. Three-dimensional geometry computer codes

These codes allow the calculation of burning area of complex configurations, for example finocyl grains having one or several axisymmetric slots. One initial method, limited to the existence of a constant burning rate

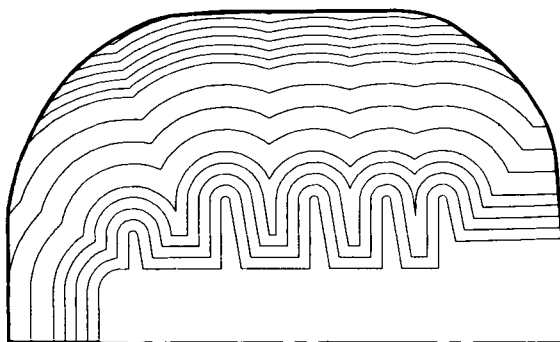


FIG. 2.10. Two dimensional burning area evolution.

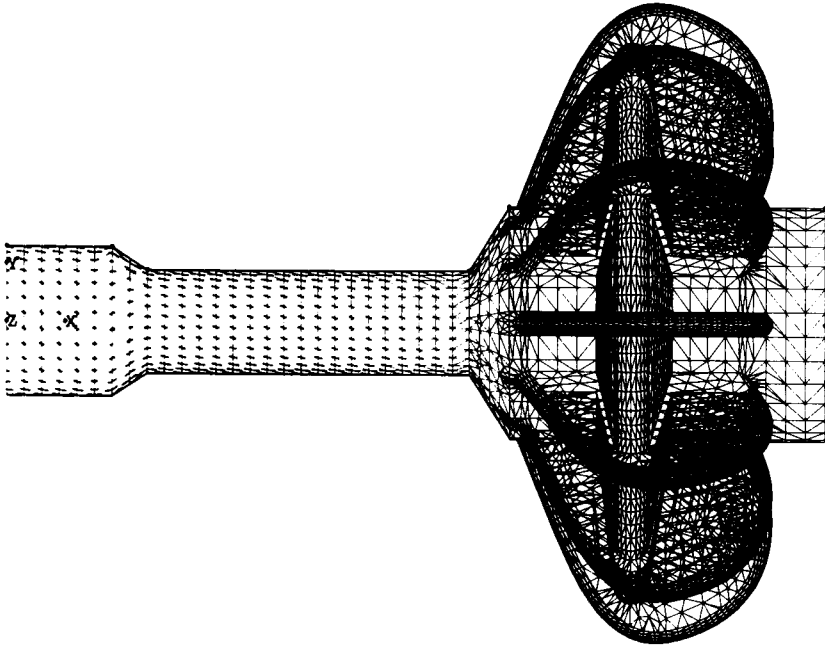


FIG. 2.11. Initial grid of burning area.

throughout the whole grain, uses for each computation step the principle of generation of a surface at a constant distance from the initial surface. This software requires the generation of an initial volumetric grid with a density suitable for the level of accuracy required in the highly three-dimensional zones.

A grid generation can be performed only by an internal ballistics expert, and the analysis of the evolution of the grain burning area, in spite of the existence of grid generation preprocessed data, represents the largest amount of work.

Another method, which allows the burn rate to be a variable function of time and space, uses automatic grid generation and management of the burning area evolution. The assessment of the perpendicular for each triangle of the grid is done utilizing a numerical model using hyperbolic nonlinear differential equations [2]. This method has allowed the development of a very friendly software which requires only the definition of the initial grain geometry (burning area and restricted area—Fig. 11) and parameters that will guide the computation, e.g. level of accuracy of the results, computer time, burning rate versus pressure law, selection of intermediary stages for visualization, etc. (Fig. 12).

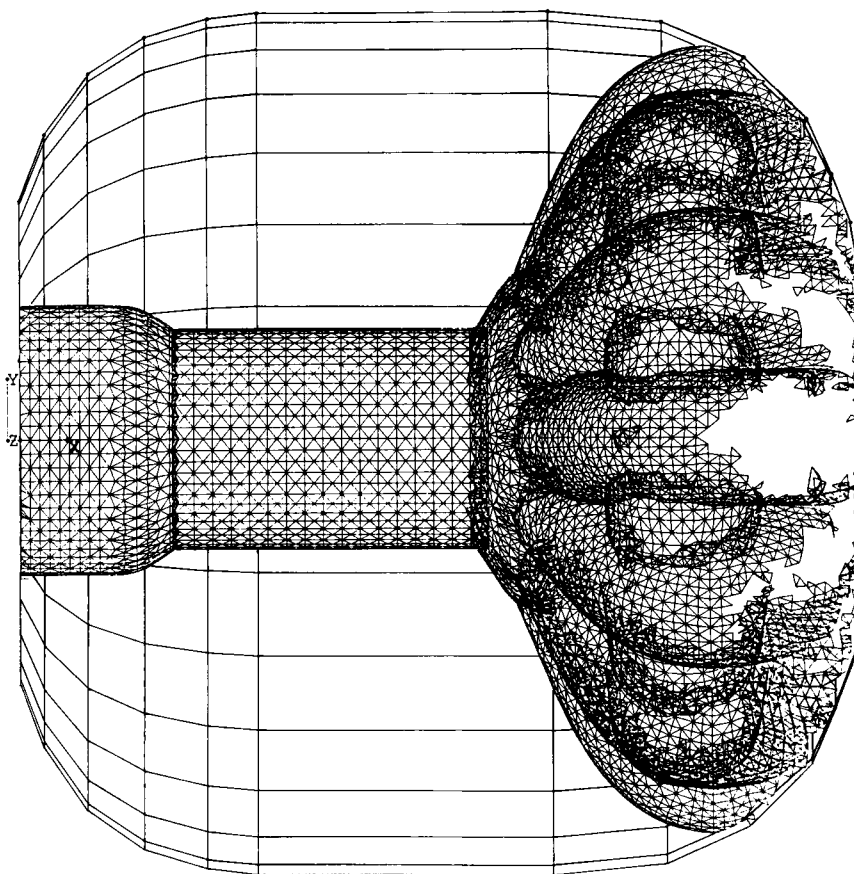


FIG. 2.12. Burning surface evolution, intermediary stage.

4.3.4. *Propellants burning rates*

Burning rate is one of the major propellant characteristics. It is measured on standard ballistic evaluation motors and it is stored in the data bank mentioned earlier (Section 4.1). It is sensitive to several factors:

- *Pressure.* In the pressure range in which rocket motors operate, a de Saint Robert's burning rate law ($V = ap^n$) is generally preferred. It is also possible to directly use plots of actually measured burning rates versus pressure. The lower the pressure exponent, the more stable the rocket motor internal ballistics.
- *Temperature.* Environmental and use conditions of rocket motors may correspond to a wide temperature range. It is therefore necessary to know burning rate sensitivity to initial propellant temperature. It is generally

expressed at a given burning surface to throat area ratio, K , as a coefficient defined by:

$$\pi_K = \frac{1}{V} \left(\frac{\partial V}{\partial \theta} \right)_K$$

where θ is the propellant temperature.

- *Acceleration.* Propellant burning rate is sensitive to acceleration, but it is taken into account only when it is more than $10g$.
- *Manufacturing process.* “Hump” effect is the result of change in burning rate as a function of web burned (enhancement of burning rate in radially burning grains in the zone between central port and motor case walls). It is related to manufacturing process. Empirical correlations, drawn from experience, are generally applied to take account of this phenomenon in ballistic design.
- *Internal flow.* Combustion products interact with propellant combustion phenomena and may locally change the burning rate law, which is no longer the one expected. Because of the significant effect of this phenomenon, it is discussed in more detail in the following section.

Burning rate laws, evolution of burning surface versus web burned, and basic internal ballistics equations provide pressure versus time and thrust versus time evolutions. In the simple case where internal flows do not significantly interact with burning rate, eqns (I) and (II) of Section 4.3.1, combined with $V_c = de/dt$, lead to a differential equation which is numerically solved and which provides web burned versus time $e(t)$, burning area versus time $S(t)$, pressure versus time $P(t)$ and thrust versus time $F(t)$.

4.3.5. Effect of internal flows

It is often assumed that flow velocity in the central port exit plane is low enough that it can be neglected in internal ballistics analysis. It is then assumed that flow is accelerated only in the convergence zone of the nozzle so that it reaches sonic velocity at the nozzle throat. In fact this assumption is not satisfactory, because flow calculations demonstrate that velocities of the order of 100–150 m/s are observed in the port exit plane after complete ignition and pressurization. Depending on grain configuration and on propellant properties, two types of phenomenon may be generated:

- a pressure drop between forward and aft-end of the central port,
- a local increase of propellant burning rate due to erosive burning.

4.3.5.1. Criteria for occurrence of non-desired phenomena

When performing a ballistic design analysis one has to quickly assess the magnitude of the phenomena connected with internal flow. Table 4 sum-

TABLE 4 *Intensity of phenomena due to internal flow*

J	K	Erosive burning	Pressure drop
< 0.2	< 50 50 to 100 100 to 150 > 150	no yes when $v < 10$ mm/s yes when $v < 20$ mm/s yes; very important when $v < 10$ mm/s	Low $< 5\%$ P forward end
0.2 to 0.35	< 50 50 to 100 100 to 150 > 150	no yes when $v < 10$ mm/s yes when $v < 20$ mm/s yes; very important when $v < 10$ mm/s	Approximately 10% P forward end when $J = 0.3$
0.35 to 0.5	< 50 50 to 150 > 150	yes when $v < 10$ mm/s yes when $v < 20$ mm/s yes; very important when $v < 10$ mm/s	Approximately 10% P forward end when $J = 0.4$
0.5 to 0.8	< 50 and 50 to 150 > 150	yes; very important when $v < 20$ mm/s yes; very important when $v < 10$ mm/s	40% of P forward may be observed
1	any value	yes; (a) very important when $v < 20$ mm/s (b) low when $v < 30$ mm/s	The pressure in the sonic section is $P \approx 0.56 P$ forward

marizes the knowledge empirically acquired in this field as the result of numerous solid propellant grain design analyses. This table involves a factor J , which is defined as:

$$J = \frac{K_p}{K}$$

$$K_p = S'/A_c$$

$$K = S/A_t$$

A_c = area of a given cross-section of central port

S' = propellant burning area upstream of the above cross-section

S = propellant grain burning area

A_t = nozzle throat area

4.3.5.2. Pressure drop

Pressure drop is related to a decrease of pressure from grain head-end to grain aft-end. It induces an increase of head-end pressure at the first phase of

motor firing, and therefore maximum pressure generally increases. Pressure drops are generally due to:

- energy losses inside the flow, and to phenomena occurring at the interface of flow and propellant surface or to sharp changes of port section or of flow direction,
- side injections from burning propellant walls.

One of the critical steps in rocket motor operation therefore occurs just after ignition when port sections (through which combustion gas must flow) are minimum. Average pressure drop values encountered are of the order of 0.1 MPa between head- and aft-end. In some cases, for special configurations, pressure drops of more than 1 MPa have been observed.

A gaseous flow is fully characterized by the knowledge of local velocities and pressures. Computer codes have been developed in order to determine such characteristics; they are named PROCNE 2 and PROCNE 3 (depending on whether geometry is respectively two- or three-dimensional). They allow:

- description of unsteady phases during pressure rise at ignition,
- calculation of steady flow just after ignition, in the whole cavity and in the nozzle convergence section.

In order to use these codes one has to generate a grid of the combustion chamber. Order “ n ” symmetry (when existing) is taken into account so as to reduce the analysis to a sector of $2\pi/n$ (n = symmetry number). Figure 13 presents an example of a grid created inside the cavity of a finocyl propellant grain having a symmetry number of 32. Results may be presented either as gas velocity or pressure field (Fig. 14) or as curves representing, for instance, gas velocity as a function of radial distance to the central axis in central port cross-section.

4.3.5.3. *Erosive burning*

Enhancement of propellant burning rate due to tangential gas flow (compared to propellant burning rate without tangential flow) is known as erosive burning. It occurs when the propellant burning surface is subjected to

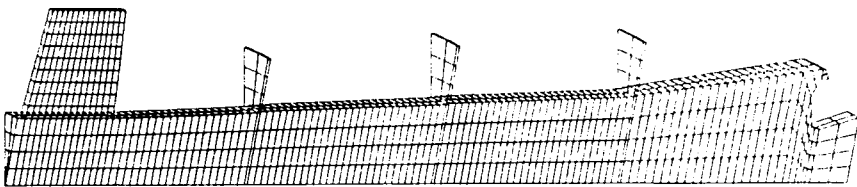


FIG. 2.13. Three dimensional flow inside rocket motor, grid of central cavity.

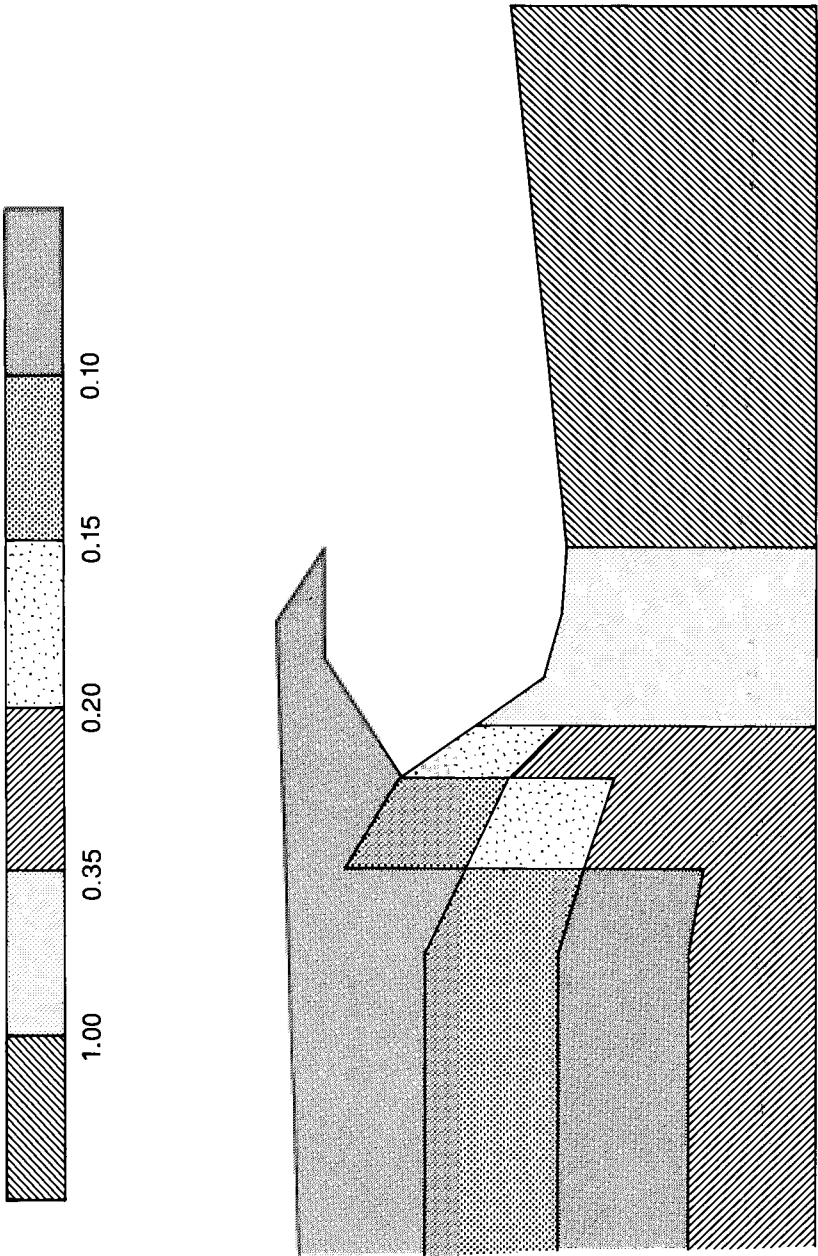


FIG. 2.14. Three dimensional flow inside a rocket motor: velocity field (Mach number of the flow).

a high-velocity combustion gas flow parallel to it. The phenomenon is due to an increase of heat transfer from the flame zone to the propellant surface. There are numerous physical models to explain and to quantify this phenomenon [3]. Practically, a simple computer code (COMBEROS), based on a monodimensional flow model, allows the calculation of the head-end and aft-end pressure evolution in a grain experiencing erosive burning. The erosive burning law selected for the model is:

$$V_e = V_0[1 + \alpha(G - G_0)]$$

V_e = burning rate with erosive burning;

V_0 = burning rate without erosive burning;

G = mass flow rate unit in the given port cross-section;

G_0 = mass flow rate unit threshold (beyond which erosive burning occurs).

Both α and G_0 are obtained empirically.

The COMBEROS code is used systematically in preliminary ballistic design analysis. It implies that grain geometry can be described by the cross-section contour perimeter evolution along the grain axis. Erosive burning is calculated in several cross-sections of the central port according to local flow characteristics (static pressure P and local mass flow rate G) and to the above erosive burning law. The ignition phase is simulated as an unsteady phenomenon; time steps range from 1 to 5 ms. A complete motor firing may be simulated, using a steady-state model and time steps generally ranging from 0.05 to 0.1 s (Fig. 15). A more comprehensive investigation of erosive burning

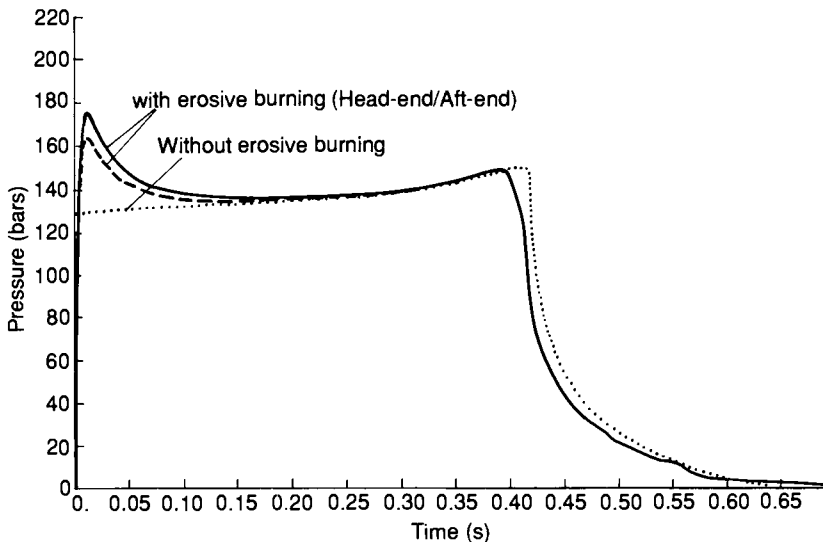


FIG. 2.15. Pressure versus time with, and without, erosive burning.

in propellant grains, though keeping a one-dimensional geometry assumption, may be performed with a more sophisticated code [4].

4.3.6. Combustion instabilities

Grain design must incorporate an assessment of combustion stability during motor firing. The phenomenon of combustion instability may occur when perturbations excite oscillation modes of the chamber cavity. Interaction with combustion, flow, particles, nozzle, etc., may induce either an increase or a decrease of the phenomenon. When it increases, pressure vibrations and pressure increase may consequently be driven to an unacceptable level. In order to assess combustion stability, a two-step procedure is followed [5].

Pressure inside the combustion chamber cavity is assumed to be:

$$\frac{p'}{p_0} = \sum_{i=1}^n e^{\alpha_i t} e^{j\omega_i t} \Psi_i(M)$$

p_0 = average chamber pressure;

p' = instantaneous pressure at point M ;

ω_i = pulsation of mode of rank i and of frequency f_i ;

Ψ_i = spatial form of mode of rank i ;

M = point in grain cavity;

α_i = damping coefficient (when $\alpha_i < 0$), or gain factor (when $\alpha_i > 0$) of the mode of rank i .

The first step of the analysis consists in calculating the various acoustic modes specific to the grain cavity. A finite-element two-dimensional computer code, VASAX, is used. An example of a two-dimensional grid and the corresponding results are presented respectively in Figs 16 and 17 (the rank of the mode is 3).

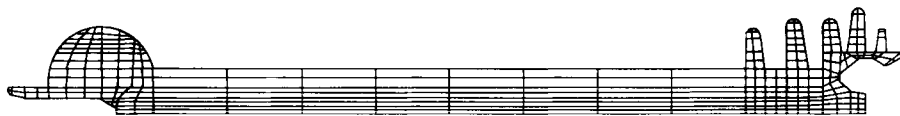


FIG. 2.16. Combustion instabilities: grid of a motor cavity for calculation of acoustical modes.

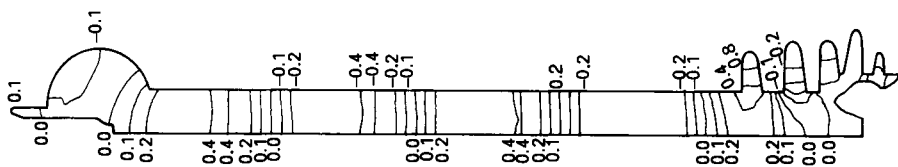


FIG. 2.17. Combustion instabilities: pressure contour lines.

The second step of the analysis consists of calculating the value of α . These calculations need not only the results of the first step, but also data describing propellant response to pressure, effect of condensed particles, etc. The computer code AVER is used.

Depending on the value of α (equal to the algebraic sum of the various gain and damping factors), it is possible to evaluate the grain propensity to experience combustion instabilities: for a mode of frequency f_i , a value of α_i , larger than $0.1 f_i$ indicates that there is a significant probability that combustion instability may occur. The grain configuration (or propellant) has to be modified.

4.4. STRUCTURAL DESIGN ANALYSIS

4.4.1. Principles of structural design analysis*

Various loads are imposed on propellant grains throughout their lifetime, from their manufacture until motor firing. These loads depend not only on the rocket motor's own characteristics but also on manufacturing temperature, environmental and operational conditions. Various factors affect loads imposed on a grain (especially a case-bonded grain):

- curing temperature;
- acceleration of gravity;
- type and number of thermal cycles undergone during storage and transportation (for instance captive flights for airborne missiles);
- acceleration during boost phase;
- pressurization during grain ignition.

The goal of structural analysis is to calculate a safety factor defined as:

$$K = \frac{C}{S}$$

where C is the propellant (or bond) structural capability (allowable), and S is a function related to stress/strain induced in the propellant grain region undergoing the more severe loads (margin of safety may be defined as $C - S$ or $C/S - 1$). In order to compare them, C and S must be of the same physical nature.

The safety factor must be higher than 1 during the rocket motor lifetime, including motor firing. According to this definition it is assumed that grain cracking or propellant/liner debonding induce significant modifications to rocket motor internal ballistics having consequences ranging from failure of

*This section may use notions developed in Chapter 6.

missile mission to rocket motor explosion. It is assumed that failure at the most stressed (strained) point does not depend on the stress (strain) gradient in the surrounding region.

If the safety factor calculated for a given propellant grain and given imposed loads is lower than the required value, the propellant grain system has to be redesigned until a satisfactory safety factor is obtained.

Assessment of capability variations (due to manufacturing process, to material reproducibility, to mechanical testing, to aging, etc.) and of induced stress/strain variations (due to uncertainties of boundary conditions, imposed loads and stress/strain determination methods) allows, as a result of a probabilistic analysis, estimation of reliability of a series of propellant grains of a given definition. This subject is discussed in Section 5.

The procedure followed in order to predict safety factors comprises two major aspects: it must define how to assess propellant and propellant–liner bond structural capabilities on one hand, and how to determine induced stress/strain in various loading conditions encountered by the grain, on the other hand. This procedure is schematically presented in Fig. 1 of Chapter 6 of this book.

Propellant and propellant–liner bond capabilities are determined by performing various mechanical tests and require a failure criterion which is defined as the critical value (at failure) of a function related to the state of stress (or strain) of propellant or bond.

Determination of induced stress/strain involves a structural analysis requiring input data such as geometry, boundary conditions (e.g. case displacement), and propellant and bond mechanical behavior.

Results are expressed using the same function selected for failure criterion so that they may be directly compared to propellant and bond capabilities. Experimental validation of the procedure has to be performed, either on the propellant grain itself or on subscale analogs, whenever new elements — such as uncommon grain configurations, new propellants or new bonding systems — have to be considered in safety factor assessment.

4.4.2. Assessment of structural capabilities and of mechanical behavior

Propellant or propellant–liner bond capability is the maximum mechanical loading which can be imposed on the propellant or the bond before failure occurs. Capability is determined by performing tensile (and other) testing on various specimens. The main parameters affecting propellant and propellant–liner bond capability are:

- loading rates (which are very different when thermal cooling or pressurization at ignition have to be simulated);
- temperature;
- surrounding pressure (when simulating ignition pressurization).

As a whole, the experimental work performed on this subject has led to the conclusion [6–8] that propellant behavior is:

- viscoelastic, as evidenced by relaxation tests;
- nonlinear, although considered linear for small deformations;
- Incompressible (Poisson's ratio is very close to 0.5), until dewetting is significant enough to cause volume variations during tensile testing.

The function which expresses propellant capabilities is described in Section 4.4.4.

4.4.3. *Determination of induced stress/strain fields*

The determination of induced stress/strain fields in the propellant grain requires a knowledge of:

- geometry on which loads are imposed;
- boundary conditions which describe imposed loads;
- propellant and propellant–liner bond behavior.

In most cases the geometry is three-dimensional, loads are static, dynamic or thermally induced and propellant behavior is viscoelastic and nonlinear. Loads which are the limiting factors in structural grain design are generally:

- thermally induced, in the case of grains for tactical missiles (low-temperature cycling);
- pressurization-induced, in the case of grains for large ballistic missiles (stored in almost isothermal conditions).

At the preliminary design phase the expected maximum value of stress/strain induced in the grain is quickly assessed using analytical expressions. For instance, in the case of fairly simple internally perforated grains, the following expressions are commonly used:

$$\varepsilon = 2\alpha \cdot \Delta T \cdot K_1 \cdot C \cdot (b/a)^2$$

for a thermally induced strain.

- ε is the equivalent strain at the grain inner bore surface;
- α is the propellant thermal expansion coefficient (assumed to be at least an order of magnitude higher than the case material thermal expansion coefficient);
- ΔT is the difference between stress free temperature and temperature at which induced strain has to be estimated (ΔT may be as large as 100°C);
- K_1 and C are corrective coefficients taking into account respectively central port exact geometry and end effects;
- b and a are respectively grain outer and inner radii.

In the case of a pressurization-induced strain,

$$\varepsilon = k \cdot \varepsilon_{\theta s} \cdot \beta \cdot K_t \cdot C \cdot (b/a)^2$$

$\varepsilon_{\theta s}$ is hoop strain of the empty case submitted to ignition maximum pressure;

β takes into account case stiffness increase due to propellant grain;

k is an empirical coefficient.

These values of ε are input data for a first assessment of the grain safety factor.

The final design phase involves extensive use of computational methods based on finite-element techniques applied to grain stress/strain field analysis. The procedure comprises three stages:

4.4.3.1. The determination of the induced stress/strain field

This assumes a linear behavior for the material. The stress/strain field is governed by the incompressible behavior of practically all of the propellant grain.

The mechanical load establishing the boundary conditions is expressed either as prescribed displacement, or as prescribed forces at the nodal points of surface elements. Several different computer analysis programs, either two- or three-dimensional, may be used for this phase.

A typical program will have the following characteristics:

- Finite-element method.
- Quadratic elements with 20 nodal points.
- Quadratic surface elements with eight nodal points to allow accurate assessment of stress/strain at the surface of the grain. The use of surface elements increases the accuracy by dramatically reducing the uncertainties caused by the fairly loose extrapolations necessary to calculate maximum stress/strain when there are no skin elements.
- HERRMAN reformulation on incompressibility.

The level of accuracy of the results is a function of the precision of the grid generated to represent the geometries. The number of nodal points must be limited because of computer capacity and CPU time. A typical grid will include 7000 nodal points and 1000 elements.

Figure 18 shows an example of a two-dimensional grid.

4.4.3.2. Post-processing analysis

The assumption is made that the propellant behavior is linear and incompressible. The regions of the grain where the stress/strain is the greatest are identified. Figure 19 gives a three-dimensional grid example with stress contour lines for equal stress. The maximum stress occurs, in this case, at the forward slot bore junction.

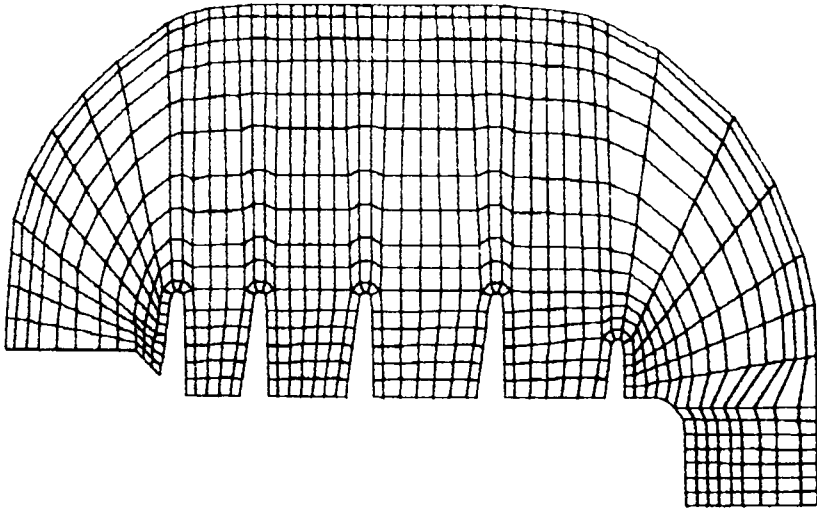


FIG. 2.18. Two dimensional grid network.

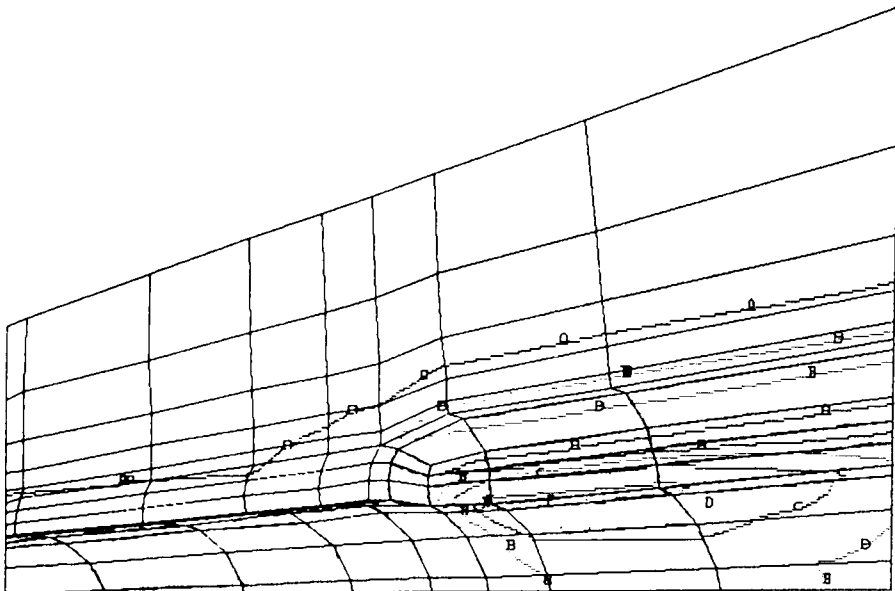


FIG. 2.19. Three dimensional grid network.

4.4.3.3 *Determination of stress/strain in the regions experiencing the greatest induced load*

Starting with the above results, the determination of strain/stress in the most highly loaded regions is refined by introducing a viscoelastic nonlinear model for thermally induced strain/stress, and an elastic nonlinear model for pressure-induced stress at ignition.

(a) Thermally induced load

The structural model used is a viscoelastic nonlinear model. It provides, at any moment of an imposed thermal cycle, the values of the principal stresses in the propellant (σ_{1th} , σ_{2th} , σ_{3th}). The numerical method used is incremental with respect to the time, the principles consists in calculating stresses at a given time t from the values known at time $t - \Delta t$. For that purpose, the effect of the thermal cycles are handled as successive stresses with simultaneous relaxation of the stresses observed at the preceding time [9].

The results of this program have been compared many times with the results of tests performed on propellant grains. The program itself is continuously being improved.

(b) Pressurization-induced stress at ignition

This structural model requires propellant master curves and data characteristics of the pressurization (pressure rise time, final pressure, temperature). It provides the values of the main stresses (σ_{1p} , σ_{2p} , σ_{3p}) corresponding to the maximum pressure.

When performing a structural analysis of a propellant grain at the time of firing, which occurs after the effect of a thermal cycle, the maximum stresses will be determined by adding the principal stresses resulting from the thermally induced stresses and pressure-induced stresses, provided that the principal directions for both stresses are identical. This is true for external surfaces, where the most stressed areas are frequently located.

4.4.4. *Determination of structural safety factor*

At the stage of preliminary design analysis, simple analytical formulas provide the magnitude of strain either due to thermal loading or due to pressure rise (see Section 4.4.3.). In both cases, propellant capability is obtained from the master maximum strain curves at t/a_T corresponding to the loading conditions. So a first assessment of the safety factor is:

$$K = \frac{\varepsilon \text{ (due to thermal loading or pressure rise loading)}}{e_m \text{ (at } t/a_T \text{ corresponding to the loading conditions)}}$$

Propellant capability (Section 4.4.2.) is related to uniaxial tensile tests; it is represented by maximum stress (σ_m) or maximum strain (e_m). Induced stress (strain) (Section 4.4.3.) is the result of a stress (strain) analysis; it is expressed as principal stresses ($\sigma_1, \sigma_2, \sigma_3$) (strains, $\varepsilon_1, \varepsilon_2, \varepsilon_3$) in the most severely stressed (strained) region of the grain.

In order to be able to directly compare capability and induced stress (strain), failure criteria are needed [10]. They are based on an equivalence between principal stresses and an equivalent uniaxial stress defined by:

Von Mises criterion

$$\sigma_0 = [(\sigma_1 - \sigma_2)^2 + (\sigma_2 - \sigma_3)^2 + (\sigma_3 - \sigma_1)^2]^{1/2}/a^{1/2}$$

or

Stassi criterion:

$$\sigma_0 = [(\sigma_1 + \sigma_2 + \sigma_3) + [(\sigma_1 + \sigma_2 + \sigma_3)^2 + b[(\sigma_1 - \sigma_2)^2 + (\sigma_2 - \sigma_3)^2 + (\sigma_3 - \sigma_1)^2]]^{1/2}]/c$$

a, b, c are coefficients which generally depend on the propellant, but do not depend on strain rate and temperature.

According to the magnitudes of ($\sigma_1, \sigma_2, \sigma_3$), it is either the Stassi criterion or the Von Mises criterion that is used. The Stassi criterion is used mainly in the case of thermally induced stresses, and the Von Mises criterion is used mainly for pressure-induced stress at propellant grain ignition (ignition at 7 Mpa). The parameters of the induced pressure on the propellant grain to determine these criteria are obtained experimentally by performing tensile tests under atmospheric and various other pressures, at various temperatures and stress rates.

The propellant grain safety factor is then defined as the ratio of the maximum stress (obtained in a uniaxial tensile test performed at the strain rate and temperature equivalent to those applied to the grain) to the principal maximum uniaxial stress (obtained from the failure criterion, either from Stassi or from Von Mises criteria, depending on the type of stresses encountered in the most stressed region of the grain), equivalent to the maximum three-dimensional state of stress calculated in the propellant grain:

$$K_\sigma = \frac{S_m(t/a_T)}{\sigma_0(S, VM)}$$

The safety factor may also be defined as:

$$K_\varepsilon = \frac{e_m(t/a_T)}{\varepsilon_0(S, VM)}$$

Where ε_0 is the ratio of equivalent uniaxial stress to the modulus.

There are other methods to predict safety factors; these are discussed in Chapter 6, Section 6. In addition, an analysis of most of these methods was recently published [11].

In the case of propellant liner bonds the problem is a different one because of the presence at all points of the interface of two different materials—the propellant and the liner. The tensors representing stress/strain on both sides, propellant grain and liner, are different. Only the force applied to the interface is continuous. Its components are: a perpendicular strength, σ_n , and a shear strength, τ . The safety factor is determined by comparing the modulus of interface strength (components σ_n and τ) to the modulus of the interface force at the time of failure, obtained under identical conditions on a propellant liner bond specimen.

In most cases the propellant liner bonds are designed for failure to occur in a propellant grain area close to the interface. Furthermore, should the propellant in this area have the same properties as the bulk of the propellant, the safety factor will be calculated the same way, and:

$$K_{\text{bond}} = \min.[K_{\text{strength at bond}}, K_{\text{propellant}}]$$

4.5. COMPUTER-AIDED PRELIMINARY DESIGN OF PROPELLANT GRAINS

4.5.1. *General description*

As mentioned in Section 4.2., there is an increasing pressure to have, as early as the preliminary design phase, quick and relatively accurate results defining the propellant grain. Moreover, further changes in technical requirements need to be easily taken into account. A computer code satisfying these needs is now on service. It is named MIDAP [12] and it involves, today, around 20,000 statements in its newest version. Figure 20 presents the general architecture of the code. Each type of grain configuration (star-shaped, slotted tube, axisymmetric, finocyl, etc.) is individually treated inside the code. The procedure for any of these configurations is the one which is generally followed to perform propellant grain preliminary design analysis (it is described in Section 4.2.). The architecture of the code is modular so that any addition of a new module, or any improvement of an existing module, may be very simply worked out.

Runs are controlled by the user from the graphic terminal. CPU time is negligible as compared to time spent by the user performing the design analysis.

The process is iterative and, besides the input of technical specifications, the user has only to answer yes or no to the option proposed on the screen. Results are presented either as tables or as curves. The block diagram

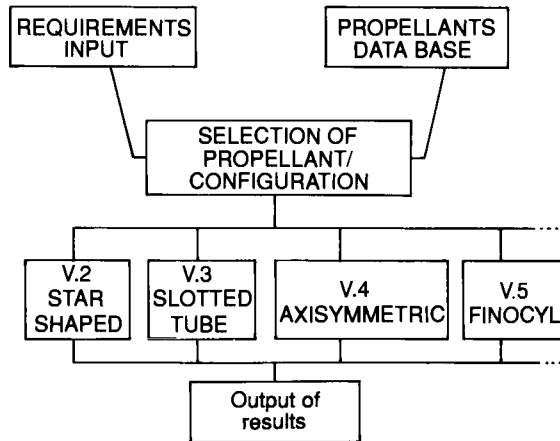


FIG. 2.20. General structure of preliminary design analysis computer code.

presented in Fig. 20 emphasizes the role of propellant/configuration selection, which provides several possibilities, ranked according to a given set of criteria. The selection of propellant/configuration depends:

- on the one hand, on technical requirements (total impulse, burning time, etc.);
- on the other hand, on semi-quantitative requirements related, for instance, to manufacturing process practicality, industrial and economical aspects, etc.

Due to the dual nature of the criteria, an expert system was selected and implemented for this critical stage of preliminary design analysis.

4.5.2. Description of the code

All the branches of the code have the same basic structure. The slotted tube branch is detailed below. On the flow chart of Fig. 21 the main stages of the analysis appear. Two possibilities are provided to the user:

- design of a case-bonded (or free-standing) grain meeting technical requirements;
- for a given rocket motor, calculation of motor operation (pressure versus time, thrust versus time, etc.).

In the case of slotted tube configurations, geometrical characteristics which are taken into account for design analysis are:

- cylindrical motor case, presenting possibly thermal insulation overthickness in the aft-end zone (slotted zone);

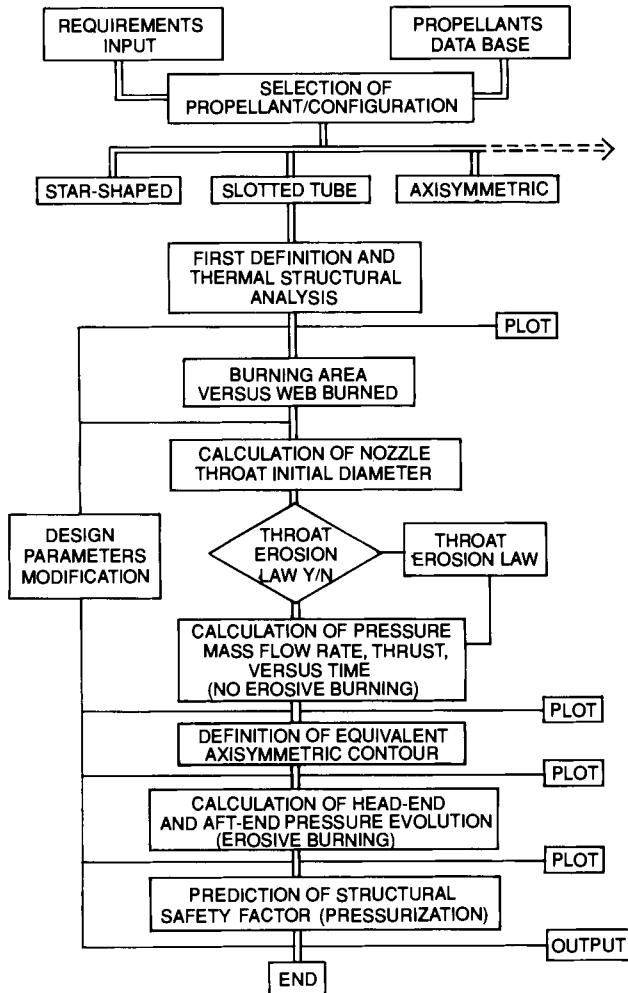


FIG. 2.21.

- plane grain aft-end zone (slotted zone);
- cylindrical central port;
- slot walls may be parallel or not (star-shaped);
- possibility of a tapered port in grain aft zone (in order to limit erosive burning effects).

The successive steps of the analysis are:

- First definition of the grain and thermal structural analysis. This definition meets various requirements, the priorities of which are ranked as follows:
 - (1) Structural integrity (for thermally induced strains) corresponding to a safety factor higher than 2.

- (2) Maximum operating pressure.
- (3) Total impulse.
- (4) Evolution of pressure versus time.
- (5) Burning time.

The structural analysis is based on data obtained from regression analysis of stress/strain field determination results, performed with the aid of three-dimensional computer codes on various selected slotted tube geometries.

- Burning area evolution. This task is performed by dividing the grain into three parts as described in Section 4.3.3.
- Determination of nozzle throat initial diameter. This is the minimum throat diameter value consistent with the specification on maximum acceptable pressure.
- Determination of pressure, mass flow rate and thrust evolutions versus time. In a first approach, erosive burning is not taken into account. The calculations provide expansion ratio, and thus nozzle optimum expansion ratio and exit diameter. Nozzle exit diameter is then compared to corresponding requirement. Afterwards, ratios K (burning area to nozzle throat area) and J (burning area to central port cross-section) are calculated. If needed, a tapered zone is designed in the grain slots region so as to meet a criterion on J (maximum permitted value). Burning area versus time is then calculated again.
- Definition of equivalent axisymmetric longitudinal port contour. This is based on equal flow rates in any port cross-section for actual (three-dimensional) and equivalent (two-dimensional axisymmetric) contours. It allows a simplified analysis of erosive burning which is taken into account at the following stage.
- Calculation of head-end and aft-end pressure evolution. At this stage, erosive burning is taken into account. The module provides pressure evolution inside grain central port, as well as peak pressure at ignition and pressure rise time.
- Prediction of safety factor related to ignition pressurization. Preliminary structural design analysis is performed, as described in Section 4.3.3.

5. Propellant Grain Reliability

Reliability is the probability that a system will fulfill a required mission in given conditions and during a given period of time. Reliability must be considered:

- at the design phase—the system must be designed so that its reliability will meet the requirement;
- at the realization phase—it must be demonstrated that the reliability requirement has been met.

Reliability of a solid propellant rocket motor results from the reliabilities of constitutive elements, such as case, thermal insulation, igniter, nozzle, propellant grain, etc. Grain reliability has several components; but main components are ballistic and structural reliability. In the case of case-bonded grains, past experience and analysis performed according to FMECA (failure modes, effects, and criticality analysis) have demonstrated that structural reliability is the most important component of overall grain reliability.

There are two possible approaches in assessing propellant grain reliability: an analytical approach and an experimental approach; both of them are complementary.

5.1. ANALYTICAL APPROACH

This is performed according to the FMECA method [13]. It consists of:

- listing the functions the propellant grain must fulfill;
- describing failure modes;
- assessing probability of failure occurrence for each mode;
- validating assessments by comparing with overtests and analog experimental results.

As mentioned above, this method places emphasis on the structural component of case-bonded grain reliability. This aspect is therefore discussed below. A comprehensive description of the methods used in propellant grain structural reliability assessment would need extensive discussion because of the complexity of phenomena and analytical tools involved. Consequently, the following section provides only an idea of the principles governing structural reliability assessment.

Safety factors are considered in Section 4 as having known values: propellant grain failure occurs when $K = C/S = 1$. K is the structural safety factor, C is capability and S is induced stress/strain. In fact, most of the parameters involved in safety factor prediction are randomly distributed and their statistical distribution law is not always well known. These parameters are related to:

- | | | |
|--|---|--|
| <ul style="list-style-type: none">• grain geometry• boundary conditions• propellant and bond behavior• capability• failure criterion | } | <p>which define induced stress/strain field,</p> <p>which may take aging into account,</p> |
|--|---|--|

When designing a case-bonded grain the distribution law of the parameters defining grains and imposed loads must be known, so that the distribution law of C and S can be known. It is then possible to determine the minimum safety factor ensuring required reliability. In a second stage, taking into account variations due to manufacture (and possibly to aging), it is possible

to define a mean safety factor (higher than the preceding one) that must be the objective at the design phase. Grains designed so as to meet this requirement on K have the desired reliability at a high confidence level.

For a given propellant grain, variations of capability and induced stresses (strains) are due to:

- errors in test measurements of propellant and bond mechanical properties,
- the probabilistic nature of loads imposed to the grain before, and during firing,
- uncertainties related to structural models and to failure criteria determination.

Let C and S be the mean values respectively of capability and of induced equivalent stress (strain) and CV_c and CV_s corresponding deviation factors (which are assumed to be independent of the mean value), then $K = C/S$, and it can be demonstrated that the probability that grain failure does not occur is:

$$\text{Prob}(C > S) = \Phi \left[\frac{\bar{K} - 1}{(\bar{K}^2 CV_c^2 + CV_s^2)^{1/2}} \right]$$

where Φ is the repartition function of normal distribution law. C and S are generally assumed not to be correlated (which is not correct but acceptable). It is possible, however, to take a correlation into account if it is clearly demonstrated.

Minimum safety factor, K_{\min} , ensuring required reliability F , is then obtained by determining the value of K_{\min} which satisfies the relationship:

$$\left[\frac{K_{\min} - 1}{(K_{\min}^2 CV_c^2 + CV_s^2)^{1/2}} \right] = F$$

Taking into account variations due to manufacture, deviation of the safety factor is assessed. It is then possible to calculate a value of safety factor which is the objective of structural design analysis: it ensures that grains accordingly designed have a given probability of meeting the reliability requirement.

5.2. EXPERIMENTAL APPROACH

Safety margin is $C - S$. There is a discrepancy between actual margin of safety $(C - S)_R$ and predicted margin of safety $(C - S)_c$, due to the use of an approximate model. It is possible to write $(C - S)_R = (C - S)_c + \xi$, where ξ is assumed to obey a normal distribution law. The ξ mean value, m_ξ , represents the shift of the model. Deviation σ_ξ represents variations of this shift; m_ξ and σ_ξ must be assessed by performing significant experimental tests. There are two possibilities: either overtests or tests on grain analogs.

5.2.1. Overtest

The first method is to assume that ξ obeys a given normal distribution law and to use overtest results in order to refine this distribution law: this is the Bayesian method [14]. Grain overttests are tests which have a moderate probability (much higher than in a normal motor firing or temperature cycling) that failure does occur. Much information is thus obtained on grain reliability. Overttests are defined by changing thermal cycles applied to the grain (colder temperature, larger cycles number) or firing conditions (reduced nozzle throat diameter) compared to normal conditions.

The most interesting information is obtained when overtest performance does not induce propellant or bond failure: a more accurate definition of distribution law may thus be proposed.

5.2.2. Tests on grain analogs

A second method to quantify the shift of the model consists in performing loading tests on analogs [15]. This analog grain has the following characteristics:

- configuration is simple enough so that analogs may be easily manufactured at low cost;
- two-dimensional geometry induces low-cost computational structural analysis;
- the ratio of maximum stress (strain) to mean stress (strain) induced in the analog is of the same order of magnitude as the one encountered in actual grains;
- maximum induced stress (strain) can be easily adjusted by simply modifying analog manufacture tooling.

The main drawback is that the analog is not ... the grain itself, which means that propellant, liner and bond are not exactly the same, and are not in the same surrounding conditions as those constitutive of the actual grain.

Mechanical testing consists in loading a given number of analogs in identical conditions until failures occur. Analysis of failure results and deviations yields the shift ξ between actual margin of safety and predicted margin of safety. It is then assumed that the shift observed on the analogs is equal to the shift existing in actual grains.

This set of complementary theoretical and experimental methods allows the assessment of structural reliability of case-bonded solid propellant grains.

6. Special Cases

Probably over 90% of cases encountered in practice are included in the preceding discussions. There are, however, some special applications that do

require special configurations or designs, such as: (1) segmented propellant grains; (2) nozzleless grains; and (3) wired, end-burning grains. Finally, an additional special grain, designed to reduce the base drag of shells, is discussed in Chapter 8 and is the special topic of integral boosters in Chapter 12.

6.1. SEGMENTED PROPELLANT GRAINS FOR SPACE LAUNCHERS

The need to launch objects with ever-increasing weight revealed the necessity for rocket motors capable of very high levels of thrust and total impulse at the beginning of the launching operation, to provide the energy needed for lift-off, and to traverse the thick layers of the atmosphere under very precise conditions of acceleration. This has led to the design of special rocket motors. During the first 2 minutes of flight they may deliver a thrust 10 times greater than the thrust of the central rocket motor. The required thrust levels are found within the operating ranges of solid propellant grains, so that solid propellant rocket motors are a basic complement to the classic liquid fuel of these launchers [16].

These rocket motors are positioned on the periphery of the central liquid fuel motors, requiring a very high ratio of length to diameter, that can be as high as 10; the propellant grain may weight over several hundred tonnes.

It is therefore very difficult to manufacture a rocket motor of this type in one single monolithic assembly in classic manufacturing facilities designed usually for the production of propulsion stages for ballistic missiles. The manufacture of these rocket motors turned toward assembling several sections, called segments. Each of these segments consists of several tens of tons of propellant grain case-bonded in a section of metallic case. The segments are then assembled to reproduce the classic configuration of a case-bonded propellant grain [16,17]. Figure 22 shows a four-segment configuration. As a rule, one segment has a star-shaped configuration providing a greater impulse at lift-off, for approximately 20 seconds.

The particular characteristics of these types of propellant grains are the burning areas on the end faces of the segments, resulting in high gas flow rate in the proximity of the joints.

The thrust curve is controlled by working on the star-shaped configuration, the taper coefficient of the central port and the restriction of head-end surfaces by inhibitors.

The general criteria used for the geometry design, and other methods discussed in the preceding sections, are for the most part applicable. A certain number of specific problems must, however, be resolved:

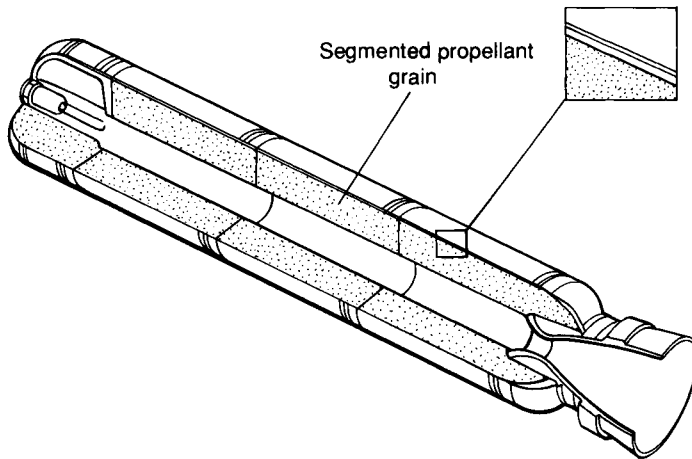


FIG. 2.22. Example of a segmented propellant grain.

6.1.1. Acoustics

The head-end burning areas, at the segments' interface, can produce radial flows disturbing the central gas flow. These disturbances may cause instabilities in the gas flow. This type of situation is similar to axisymmetric propellant grains with radial slots. In addition, the exposure of the inhibitors during the burning process may cause pulsations in the gas flow and be the source of additional acoustic energy [18].

6.1.2. Segment assembly

The segments are connected to each other, and the motor cases are assembled together through a system of clamps and pins.

Sealing of junctions is ensured by flexible seals. These junctions must be protected against the presence of combustion gas in the intersegments during the ignition phase. These junctions are one of the weak points of the rocket motor. The difficulty comes from the stress/strain imposed on the junction during pressure rise at ignition, and from the difficulty of inspecting this area after assembly.

6.1.3. Rocket motor pairs

There are at least two boosters located on the outside of the launcher. Consequently, closely matched thrusts from each specimen are necessary to allow good control of the flight, and particularly to avoid any troubles at separation at burn-out.

Thrust imbalance between boosters is usually the result of variations in the burning rate of the propellant grain, but may also be caused by other factors linked to the nozzle (erosion, etc.).

Control of thrust imbalance is obtained through adjustment of the ingredients, the manufacture process, and control method [1].

6.2. NOZZLELESS BOOSTERS

The nozzleless booster is an early design that resulted from an analysis of a classic rocket motor, demonstrating that the nozzle accounted for a significant portion of the cost, weight and size of a rocket motor.

The propellant grain of a nozzleless booster is usually case-bonded with a generally cylindrical central port, connected at the aft-end to an exit cone tailored in the propellant.

In the absence of a nozzle throat, the operating conditions of the nozzleless rocket motor are governed by an aerodynamic constriction of the gas flow. The exit cone section at the aft-end of the grain is designed to allow gas expansion.

The development of nozzleless rocket motors is linked to composite propellants with high burning rates, because this type of propellant grain requires a minimum flow rate to ensure a stable performance, in turn requiring prohibitive length-to-diameter ratios when other propellant compositions are used.

The main advantages of nozzleless rocket motors are:

- simplicity of the propellant grain geometry,
- greater loading ratio than in a conventional rocket motor,
- weight reduction, due to absence of mechanical parts at the aft-end and absence of nozzle,
- significant decrease of the cost of the rocket motor,
- performance improvement for a given size,
- elimination of a nozzle which otherwise would have to be ejected at the end of the acceleration phase, making this concept very interesting for use as an integral booster for rocket ramjet systems [4].

There are some drawbacks as the price to pay for these advantages:

- loss of approximately 20% of specific impulse in comparison to a conventional system [19];
- the possibility of occurrence of combustion instabilities at low pressure;
- the need to have a thorough knowledge of the normal burning rate and erosive combustion for a very large range of pressures, to enable performance predictions [20];
- the propellant grain mechanical deformation directly reflected in the ballistics of the motor [21].

A highly regressive combustion pressure curve is a characteristic of a nozzleless rocket motor operation, reaching very low pressure (Fig. 23). Because of these particular operational characteristics, the design analysis of a nozzleless rocket motor can be performed only with very specific computer models.

All of these models are monodimensional, a typical code using a single-phase, quasi-stationary description of the flow. The precision of the calculations depends on a very exact knowledge of propellant grain combustion laws, as well as an exact description of the geometry of the structure and the grain's central port, including structural strains.

Before undertaking the computer analysis, and in order to limit computer time, the following method may be used to perform a preliminary design analysis:

- limit the minimum central port diameter for structural integrity reasons;
- in the case of a given diameter, determine the required length of the propellant grain by using I_s of approximately 215 seconds for Butalane and 200 seconds for Butalite.
- determine the diameter of the central port, for a given maximum pressure, using the following simplified formula [22]:

$$D = \frac{4\rho LC^*}{0.8} \cdot \frac{v(p)}{p}$$

p = maximum pressure;

$v(p)$ = burning rate at maximum p ;

ρ = density;

C^* = characteristic burning rate;

L = estimated length of the propellant grain.

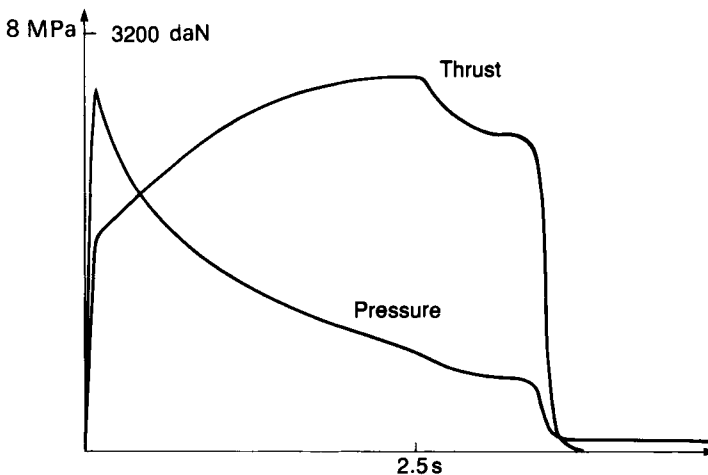


FIG. 2.23. Typical thrust-pressure curves of a nozzleless propellant grain.

These preliminary values for the diameter and the length are used in the computer analyses to optimize the propellant grain.

6.3. WIRE END-BURNING GRAIN

The concept of the wire end-burning free-standing propellant grain first appeared at the beginning of the 1960s. Wire end-burning is one of the means available to increase the effective burning rate of a propellant grain and, in addition, it is particularly well suited for a high loading ratio of the rocket motor. It is based on a simple observation: the burning rate along a wire embedded in the propellant grain is faster than inside the propellant grain itself [24].

Consequently, the burning surface is modified by the formation of a cone whose vertex travels along the wire. Its half-angle at the vertex is solely a function of the ratio between the propellant grain's specific burning rate and the burning rate along the wire. The overburning rate coefficient N is calculated as follows:

$$N = \frac{1}{\sin \alpha} = \frac{V_{\text{wire}}}{V}$$

V_{wire} = burning rate along the wire;

V = propellant burning rate;

α = half-angle of the cone.

This phenomenon is linked to a modification of the thermal field next to the wire, and is a function of the nature and diameter of the wire as well as the nature of the propellant. The principle is used to increase the gas flow rate of front-end burning grains by placing continuous, straight wires, perpendicular to the initial burning surface.

The preliminary analysis of the performance of this type of propellant grain involves two distinct steps that cannot be handled using traditional means:

- The determination of the overburning rate coefficient of a given wire/propellant combination. Currently, this determination is mostly experimental. Theoretical approaches are being developed, requiring the generation of a complete data base for thermal data on wires and on propellant, e.g. diffusivity, conductivity, thermal capacity, etc.
- Determination of the evolution of the wire grain burning surface. When dealing with front-end-burning propellant grains the computational programs are relatively easy to generate, since the evolution of the grain's burning surface involves nothing but cones. The difficulties increase with the number of wires embedded in the propellant grain.

Bibliography

1. DELANOY G. and LOUBERE, B., A physical method for predicting thrust imbalance of solid rocket motor pairs for a satellite launcher AIAA 87-1740, AIAA/ASEE/SAE/ASME 23rd Joint Propulsion Conference, 1987.
2. LEROUX, A. Y., RIBERAU, D. and NAMAH, G., Numerical model for propellant grain burning. Conference on mathematical modeling of combustion and related topics. Ecole Centrale de Lyon, 1987.
3. RAZDAN, M. K. and KUO K. K., Erosive burning of solid Propellants. *Fundamentals of solid Propellant, Combustion Progress in Astronautics and Aeronautics*, Vol. 90, pp. 515-598, 1984.
4. DELANNOY, G., Prediction of antitank solid propellant rocket internal ballistics. AIAA-84-1355. AIAA/SAE/ASME 20th Joint Propulsion Conference, 1984.
5. PHILIPPE, A. and TCHEPIDJIAN, P., Prediction of longitudinal combustion instabilities in axisymmetrical propellant grains. AIAA-84-1358. AIAA/SAE/ASME 20th Joint Propulsion Conference, 1984.
6. FARRIS, R. J., Development of solid rocket propellant nonlinear viscoelastic constitutive theory. AFRPL-TR-75-20, 1975.
7. FRANCIS, E. C. *et al.* Propellant nonlinear constitutive theory extension. Preliminary results. AFRPL-TR-83-034, 1983.
8. LHUILLIER, J. N. *et al.*, Tenue mécanique et fiabilité des chargements à propergol solide. *Sciences et Techniques de l'Armement*, **52**, 11-144, 1978.
9. MEILL, G., DUBROCA, G., PASQUIER, M. and THEPENIER, J., Etude mécanique de chargements moulés-collés en propergol double base composite par une méthode viscoélastique non-linéaire. *Propellants, Explosives, Pyrotechnics*, **7**, 78-84, 1982.
10. TSCHOEGL, N. W., Failure surfaces in principal stress space. *Polymer Science Symposium*, **32**, 239-267, 1971.
11. WANG, D. T. and SHEARLY, R. N., A review of solid propellant grain structural margin of safety prediction methods, AIAA-86-1415. AIAA/ASME/SAE/ASE 22nd Joint Propulsion Conference, 1986.
12. UHRIG, G., DUROURNEAU, B. and LIESA, P., Computer aided design of propellant grains for solid rocket motors. AIAA 87-1734. AIAA/ASME/SAE/ASE 23rd Joint Propulsion Conference, 1987.
13. L'analyse des modes de défaillance, des effets et des probabilités. Cahiers de sécurité de l'Union des Industries Chimiques. Cahier No. 4, Paris, 1981.
14. QUIDOT, M., Méthodes d'incorporation de résultats d'essais à la mesure de la fiabilité. Note technique interne No. 98-77-CRB, 1977.
15. THEPENIER, J., MENEZ-COUTENCEAU, H. and GONDOUIN, B. Reliability of solid propellant grain: mechanical analog motor design and testing. AIAA 87-1987. AIAA/SAE/ASME 23rd Joint Propulsion Conference, 1987.
16. VIDAL, M. and VARI, E. Les chargements à poudre des propulseurs d'accélération d'Ariane 5. *Aéronautique et Astronautique*, **123**, 122, 1987.
17. McDONALD, A. J., Evolution of the space shuttle solid rocket motors—something old or something or something new. AIAA 85-1265. AIAA/SAE/ASME 21st Joint Propulsion Conference, 1985.
18. BROWN, R. S., DUNLAP, R., YOUNG, S. W. and WAUGH, R. C., Vortex shedding as an additional source of acoustic energy in segmented solid propellant rocket motors. AIAA 80-1092, AIAA/SAE/ASME 16th Joint Propulsion Conference, 1980.
19. PROCINSKY, J. M. and SMITH, W. R., Nozzleless Boosters for Integral Ramjet Systems. AIAA/ASEE/SAE/ASME 16th Joint Propulsion Conference, 1980.
20. TRAINEAU, J. C. and KUENTZMANN, P., some measurements of solid propellant burning rates in nozzleless motors. AIAA 84-1469, AIAA/ASME/SAE/ASEE 20th Joint Propulsion Conference, 1984.
21. MUNDAY, J. W., MIKESKA, A. J. and TOMKIN, M. E., N.P.P. Grain deflection model. AIAA 82-1201, AIAA/ASEE/SAE/ASME 18th Joint Propulsion Conference, 1980.
22. NAHON, Nozzleless solid propellant rocket motors. Experimental and theoretical investigations. AIAA 84-1312, AIAA/ASME/SAE/ASEE 20th Joint Propulsion Conference, 1984.
23. ATLANTIC RESEARCH CORPORATION, Perfectionnements aux grains propulseurs. Patent No. 1349125, 26 September 1961.
24. CAVENY, L. H. and GLICK, R. L., Influence of embedded metal fibers on solid propellant burning rate. *Journal of Spacecraft*, **4**, 1, 1967.

CHAPTER 3

Prediction and Measurement of Specific Impulse

JEAN-PAUL BAC

1. Introduction

In the previous two chapters the importance of specific impulse has been noted several times.

All new propellant formulation research, or preliminary design analysis of a solid rocket motor, assumes knowledge of a theoretical value for specific impulse whence it is possible to start the analysis and give a direction to the research.

In most cases, calculations of the theoretical value of the specific impulse are performed with the assistance of thermochemical computations. The principal algorithms which are used throughout the world come from a computer program developed at the Lewis Research Center of NASA [1].

This chapter is a succinct description of the process, to allow the reader to understand the sequencing of the main phases of calculations to create a model for the gas and condensed phase* mixture from the combustion chamber to the exit plane of the nozzle.

Such models lead to solution of a system of equations with partial derivatives as a function of time and spatial coordinates [1-3]. The calculations themselves require access to the JANNAF thermochemical tables. These tables were first issued in 1971 and are periodically updated [4].

The purpose of Section 2 is to present and discuss a very simplified model, based solely on thermodynamics. It is specifically designed to provide an approximate value for the main operating parameters of a rocket motor without having to solve a differential equations system.

The application of the model to obtain predictions, followed by the experimental method for the measurement of the specific impulse, is dealt

* Condensed phase = combustion products in solid or liquid state.

within Sections 3 and 4. The chapter ends with a discussion of special application to performance predictions for solid fuels for ramjets.

N.B. The thermodynamics values used in this chapter are written as follows:

- *Italic capitals*: characteristic values of the overall system.
- *Script capitals*: molar values.
- *Italic lower case*: values per unit of mass.

2. Physical Model

2.1. DESCRIPTION OF THE MODEL

Physical phenomena associated with rocket motor combustion and flow processes are complex; it is therefore necessary to use a model based on an ideal motor, operating under a number of simplifying assumptions, to perform the required calculations.

More specifically, the combustion in the chamber is assumed to be adiabatic, at constant pressure, and yielding to a mixture of ideal gases and condensed phase products that are incompressible with a negligible molar volume in comparison with the gases. In addition, this mixture is in thermodynamic equilibrium at zero velocity. The combustion is followed, in the nozzle, by an isentropic flow, steady and quasi-one-dimensional, during which the condensed phases remain in thermal and kinematic equilibrium with the gas.

The assumption of steady flow allows us to work on the basis of per unit mass values.

The thermodynamic condition of adiabatic equilibrium maximizes entropy while observing the law of conservation of matter. Because we are assuming a transformation under constant pressure and at zero velocity, conservation of enthalpy (h) also occurs. With constant pressure and enthalpy, maximizing entropy is equivalent to minimizing Gibbs free energy:

$$g = h - Ts.$$

The use of the various assumptions given above allows us to progressively build a system of equations which, when solved, provides the values of the major operating characteristics of an ideal rocket motor.

2.1.1. Conservation of mass

For each of the elements of the chemical species included, we can write:

$$b_i = \sum_{j=1}^{ns} a_{ij}n_j = b_i^0; \quad i = 1, \ell \quad (1)$$

where:

- ℓ = number of elements;
- ns = number of species;
- a_{ij} = number of atoms of element i in a species of type j (a species is a given chemical compound or element in a given physical phase);
- n_j = number of moles of these species in the mixture;
- b_i = number of atom-grammes of element i in the propellant grain.

2.1.2. Minimizing free energy

Using the Lagrange multipliers λ_i linked to these equations, this condition is written as:

$$\mu = (\partial g / \partial n_j) T, p, \{n_k; k \neq j\} = \sum_{i=1}^{\ell} \lambda_i a_{ij}; \quad j = 1, ns \quad (2)$$

where g is the free energy per kilogram of mixture, T the gas temperature, and p the pressure.

Writing gases from 1 to m and the condensed products from $(m + 1)$ to ns ($= m + nc$), (where nc stands for the number of condensed species), we have:

$$\mu_j = \mu_j^\circ(T) + RT \ln n_j/n + RT \ln p/p^\circ; \quad j = 1, m \quad (2a)$$

$$\mu_j = \mu_j^\circ(T); \quad j = m + 1, ns \quad (2b)$$

- μ_j is the free molar energy (or thermodynamic potential) of the pure j species, in the same physical state (solid, liquid or gaseous) as the phase where this species is found in the mixture, under standard atmospheric pressure p° and at the temperature of the mixture.
- n is the total number of moles in the gaseous phase:

$$n = \sum_{j=1}^m n_j \quad (3)$$

2.1.3. Enthalpy conservation

With \mathcal{H}_j° as the molar enthalpy of species j and h the enthalpy per unit of mass of the propellant grain, we can write:

$$h = \sum_{j=1}^{ns} n_j \mathcal{H}_j^\circ(T) = h_0 \quad (4)$$

When p is known, we have a system of $(1 + ns + 2)$ eqns (1)–(4) with $(1 + ns + 2)$ unknown $[(\lambda_i), (n_j), n$ and $T]$.

This system is perfectly defined and can therefore be solved, and it is possible to calculate the entropy at equilibrium s .

2.1.4. *Isentropic expansion*

This assumption enables us to write:

$$s = \sum_{j=1}^{ns} n_j \mathcal{S}_j^\circ(T) - R \sum_{j=1}^m n_j \ln n_j p / n p^\circ = s_0 \quad (5)$$

- \mathcal{S}_j° the molar entropy of the pure species j , under standard atmospheric pressure p° , in the same physical state (solid, liquid or gaseous) as the phase where this species is found in the mixture, and at the temperature of the mixture;
- s_0 the entropy per unit of mass in the chamber.

Two types of calculations are performed:

- expansion at thermodynamic equilibrium;
- expansion in frozen composition

In both cases the system is determined by the knowledge of the pressure.

In the first case we have a system of $(1 + ns + 2)$ eqns [(1), (2), (3) and (5)] with $(1 + ns + 2)$ unknowns $[(\lambda_i), (n_j), n \text{ and } T]$, and in the second case one eqn (5) with one unknown T .

Consequently, we can calculate the mass per unit volume $\rho = p/nRT$, the enthalpy $h(T)$ per unit of mass, the coefficient of isentropic expansion $\gamma_s = (\partial \ln p / \partial \ln \rho)_s$ and the velocity of sound:

$$a(T, p) = \sqrt{\gamma_s nRT}$$

2.1.5. *Steady-state expansion*

With v , the combustion gas velocity, we can write:

$$h + \frac{v^2}{2} = h_0 \quad (6)$$

i.e.

$$v = \sqrt{2(h_0 - h)} \quad (6')$$

The sonic throat of the flow is defined by:

$$v = a \quad (7)$$

The throat pressure ratio is determined through iterations on the pressure calculation, starting with the combustion pressure (p_0).

2.1.6. *Assumption of a one-dimensional linear flow in the exit cone*

Indices x , s and t designate, respectively, any cross-section of the divergent part of the nozzle, the section in the exit plane of the nozzle, and the section at

the throat of the nozzle. The equation of the conservation of mass is written as:

$$\rho_s A_s v_s = \rho_x A_x v_x = \rho_t A_t v_t \quad (8)$$

It is therefore possible to:

- either select a value for the ratio of sections $\varepsilon = A_s/A_t$ and calculate the exit conditions with iterations on the pressure;
- or select the exit pressure and calculate the other parameters, including the sections ratio.

Using the various assumptions above, it is possible to write the equations required for the thermodynamic calculations and hence obtain the data that characterize the flow of gases and condensed products.

These data are then used to calculate the parameters characteristic of the operating point of the perfect motor. For example, the value of v_s obtained from eqn (6') can be used for either of the following purposes:

- either the calculation of standard adjusted expansion with $p_o = 7 \text{ MPa}$ and $p_s = p_a = p^\circ = 0.1 \text{ MPa}$, obtaining the standard specific impulse $I_s = v_s/g_0$;
- or the calculation of expansion in a vacuum at given ε and obtaining the specific impulse in a vacuum $I_{vac} = v_s/g_0 + p_s/\rho_s v_s g_0$.

If the values of A_s and A_t are also selected, in addition to the values of ε , we can calculate:

- the mass flow rate: $\dot{m} = v_s A_s \rho_s$
- the thrust: $F = \dot{m} v_s + (p_s - p_a) A_s$

The following are also calculated:

- The flow rate, or discharge coefficient:

$$C_D = \frac{\dot{m}}{p_o \cdot A_t} = \frac{\rho_t \cdot v_t}{p_o}$$

- The characteristic velocity:

$$C^* = 1/C_D = \frac{P_o \cdot A_t}{\dot{m}} = \frac{P_o}{\rho_t \cdot v_t}$$

- The thrust coefficient:

$$C_F = \frac{F}{\rho_o \cdot A_t} = I_s \cdot C_D \cdot g_0$$

2.2. LIMITATIONS OF THE MODEL

2.2.1. *General assumptions*

The thermodynamic model used is concerned only with the area related to the propellant gas volume, whose characteristics are calculated in the combustion chamber and then during the expansion in the nozzle.

We have to apply the laws of macroscopic physics and chemistry: the conservation of mass, the principles of dynamics, the first law of thermodynamics, the law of thermodynamic state, and laws of chemical kinetics and physical kinetics of changes of state. These laws were written for closed systems with the presence of physical equilibrium, which is not the case with the open system to which we are applying them. This is tantamount to considering the gas as closed subassemblies under physical equilibrium, i.e. considering the flow to be much more “orderly” than it really is. The gain in entropy is thereby underestimated; consequently, the mechanical efficiency — i.e. the impulse — is overestimated.

The amount of this overestimation cannot be predicted. This oversimplification must be done, unless all interactions between the atoms were to be written and integrated within the whole motor.

It is assumed that the gas is neither viscous nor heat-conductive (and consequently, that the phenomenon is adiabatic), and that the condensed products stay in thermal and kinematic equilibrium with the gas.

This assumption is not absolutely essential to do the calculation, but it simplifies it greatly. It also results in an overestimation of the impulse, which is particularly significant when the propellant produces condensed products. There is, indeed, a thermal and kinematic disequilibrium between the condensed products and gas, the latter being both more rapid and less hot than the condensed products.

The adiabaticity assumption, a corollary of the non-conductivity of the gas, also leads to an overestimation of the thrust. This is particularly true when the motor is small and not very well insulated.

In spite of the reservations listed above, this set of assumptions allows us to write eqns (1) and:

- The global equation for the conservation of mass:

$$d\rho/dt + \rho \operatorname{div} \vec{v} = 0 \quad (9)$$

- The equation for the fundamental law of dynamics:

$$\overrightarrow{\rho\gamma} + \overrightarrow{\operatorname{grad} p} = 0 \quad (10)$$

- The equation for first law of thermodynamics:

$$\rho \frac{d\left(u + \frac{v^2}{2}\right)}{dt} + \operatorname{div} p \cdot \vec{v} = 0 \quad (11)$$

u = the internal energy per unit of mass of the combustion product.

- The equation of state:

$$\rho = \rho(T, p, \{n_j; j = 1, ns\}) \quad (12)$$

- The kinetic laws:

$$\frac{dn_j}{dt} = \dot{n}_j(T, p, \{n_k\}; k \neq j); j \neq j_i \quad (13)$$

The number of eqns (13) is equal to the number of species, less the number of elements in their standard state, i.e., $(ns - 1)$.

Equation (10) is a vectorial equation that corresponds to three differential equations. We therefore have a system of $(6 + ns)$ differential equations with $(6 + ns)$ unknowns $v_x, v_y, v_z, T, p, \rho$ and $\{n_j\}$.

2.2.2. Assumption related to the combustion chamber

First it is assumed that the gas velocity, and consequently the pressure gradient, is negligible in the combustion chamber. This approximation is reasonably well justified, particularly in the case of a large motor operating at low maximum pressure.

It is further assumed that gases in the entry plane of the nozzle are in thermodynamic equilibrium. This assumption is consistent with the previous one. It is also fairly well justified, particularly in the case of a large, well-insulated motor.

These are the two assumptions used to calculate initially an equilibrium at constant pressure at zero velocity in the combustion chamber.

2.2.3. Assumption related to the gas expansion

The flow is considered to be isentropic. This is not a good assumption since an actual flow is by nature irreversible, and therefore non-isentropic, if it is adiabatic. This particular assumption contributes greatly to an overestimation of the impulse. As for solving the equations, it enables the creation of a relation independent of time and spatial coordinates, between the number of moles, the temperature and the pressure. But it is of no interest if it is not complemented by an assumption which enables us to by-pass equations of

chemical kinetics (13). It explains (but does not justify) the decision to perform two calculations, one in thermodynamic equilibrium and the other in which the composition remains unchanged. *All other assumptions being equal*, the truth lies somewhere in between, closer to equilibrium in the convergent part of the nozzle and closer to frozen composition in the divergent part of the nozzle. Expansion in thermodynamic equilibrium overestimates the impulse, while expansion assuming frozen composition underestimates it.

Using these two complementary assumptions (isentropic flow and thermodynamic equilibrium, or frozen composition), the choice of a pressure determines the temperature and the composition of the mixture.

We then assume a steady-state flow. This assumption is justified by the fact that we are generally looking to obtain an operation which stays quasi-steady during the major portion of its duration. This assumption contributes to an overestimation of the impulse inasmuch as, all other assumptions being otherwise identical, steady-state specific impulse is always greater than specific impulse which is calculated including the pressurization and burnout phases.

Under this steady-state flow assumption (9), the equation reads:

$$\operatorname{div} \rho \cdot \vec{v} = 0 \quad (14)$$

Combining eqns (14) and (11) gives:

$$\frac{d\left(u + \frac{v^2}{2} + \frac{p}{\rho}\right)}{dt} = \frac{d\left(h + \frac{v^2}{2}\right)}{dt} = 0 \quad (15)$$

The quantity $(h + v^2/2)$ is therefore constant along a streamline. Since all flow lines start from the entry section of the nozzle, we can write:

$$h + \frac{v^2}{2} = h_0 \quad (16)$$

2.2.3.1. Analysis of the conditions at the throat of the nozzle

With a steady flow the location of the sonic throat of the flow is stable. It is located at the actual geometric throat of the nozzle.

Equation (14) can then be replaced with

$$v = a$$

to determine, iteratively, the pressure at the throat.

The transformation of propellant into gas is accompanied by an increase in volume. Combustion produces a gas with a velocity v_c , such as:

$$v_c = \frac{dV}{S dt} = \frac{1}{S} \frac{dV}{dm} \frac{dm}{dt} = \frac{1}{S} \left(\frac{1}{\rho_c} - \frac{1}{\rho_p} \right) \dot{m}$$

where:

ρ_c = mass per unit of volume of the gases inside the combustion chamber;

ρ_p = mass per unit of volume of the propellant grain;

v = volume of the propellant grain;

s = burning area of the propellant grain.

Our steady combustion assumption requires that we neglect $1/\rho_p$ before $1/\rho_c$ and write:

$$\dot{m} = \rho_p S v_r = \rho_c S v_c = \rho_t A_t v_t$$

where v_r is the burning rate of propellant grain for a pressure p_o in the combustion chamber.

If velocity v_r is known, the burning area to throat area ratio $K = S/A_t$ can be determined, and by iterations on the pressure of the chamber, the burning rate at which a steady operation should occur can also be determined.

2.2.3.2. *Analysis of the conditions in the divergent part of the nozzle*

Using previous assumptions (adiabatic, isentropic and steady expansion, in equilibrium or with frozen composition), the knowledge of the pressure at one point determines the temperature, the composition of the mixture, and the velocity of the flow at that point.

To simplify calculations an unrealistic approximation is made, for modeling this segment of the nozzle: the pressure is assumed uniform over any nozzle cross-section, and, consequently, that the velocity is everywhere parallel to the axis.

Therefore, the equation for the conservation of matter is written as

$$\rho_s A_s v_s = \rho_x A_x v_x = \rho_t A_t v_t$$

Because of that, the following results are obtained, in a cross-section:

- a pressure and mass per unit of volume which are constant for the entire cross-section rather than increasing from the periphery to the center;
- a velocity which is constant for the entire section instead of decreasing from the center to the periphery (v instead of $v \cos \alpha$, α being the half-angle at the apex of the divergent part).

As a result, this approximation:

- leads to an overestimation (all things being otherwise equal) of the ratio of cross-sectional areas necessary to obtain fixed expansion;
- contributes to the overestimation of the impulse by an amount that cannot be exactly determined, although it is known to be of the order of $(1 - \cos \alpha)$, and therefore of about 1%.

Finally, in order to analyze what occurs in the exit section of the diverging part of the nozzle, it is necessary to research the interaction of the jet with the merging air stream. This problem is far more complex, and resolving it is completely out of the question. The assumptions necessary to bring its complexity down to the level of the preceding assumptions would completely change its characteristics. We therefore limit ourselves to:

- Assuming that $p_s = p_a$ for an expansion at a given ambient pressure, and then calculating the corresponding cross-sectional area ratio. However, p_s is necessarily greater than p_a because the velocity can be different from zero in a given direction only if the pressure diminishes along the corresponding streamline. But this difference is very small, because the ejected gas molecules have an infinite expansion volume, so that they are in an infinitesimal minority compared to the merging air stream and the velocities resulting from intermolecular collisions rapidly become random. This simplification does contribute to an overestimation of the impulse, although to a much less important degree than with the preceding assumptions.
- Calculating p_s regardless of p_a , for a given expansion ratio.

If p_a has been determined to be much greater or smaller than p_s , the impulse calculated will have no significance, because there probably will be no steady operation with such a pressure mismatch.

If p_a is determined to be a little less than p_s , then the entire set of assumptions is self-consistent, and provides a specific impulse with a good indicative value.

2.2.4. Conclusion

In conclusion, the specific impulse calculated using this model is always overestimated. The smaller the rocket motor, the higher mass fraction of condensed phase material elements in the combustion gases and therefore the higher this overestimation. With a propellant producing no condensed phase products the overestimation will be highest if the combustion gas viscosity and thermal conductivity are higher. (For a propellant grain producing condensed products, there are combinations of viscosity and conductivity for which the overestimation is minimal, all other assumptions being equal.) It is necessary to have a value of this overestimation to determine the average specific impulse of rocket motor. A range of values is found in Chapter 1.

The specific impulse determined in this manner provides mainly a comparative value. Even then, great caution is required since, disregarding the size factor, the deviations between the calculated and the actual specific impulses depend on the intrinsic characteristics of the propellant, i.e.

- its physical structure, which plays a major role in the degradation mechanism;
- its basic composition and the molecular structure of the chemical components, which determines its enthalpy, its free energy, its reaction mechanism in the gaseous phase, and the ballistic characteristics (isentropic ratio, viscosity and thermal conductivity) of the combustion gases.

Since each one of these characteristics plays a special role in the deviations between the actual specific impulse and its calculated value, there is no reason to believe that ratio " I_s predicted versus I_s actual" will be identical for all propellants. It is more accurate to state that this model offers the possibility of a valid classification of the propellant within a particular family, and also for propellants with the same molar ratio of condensed products. But caution is advised when comparing two different propellant families. Since the deviation between the actual specific impulse and predicted value is of the order of 10% for any one propellant, a calculated difference of 4–5% between families of propellant is not necessarily meaningful.

3. Predictions

Specific impulse predictions are commonly used in two main areas:

- new propellant formulation research;
- determination of the theoretical performance of a rocket motor.

3.1. NEW FORMULATION RESEARCH

Technical requirements such as guidance and low signature, related to the mission of the missile (particularly in the tactical area), affect the selection of the propellant. In addition to highest performance, the designer must also look for formulations with combustion gases that provide, for example:

- No absorption of electromagnetic waves required for missile guidance. This absorption is caused by the ionization of the gases, particularly alkaline or alkaline-earth.
- No absorption in infrared — another factor in guidance — which supposes aluminum contents lower than 0.5%.
- No absorption in the visible range, to avoid detection of the missile, requiring a plume containing no condensed elements and without any of the HCl-type gases, i.e. gases that can condense when combined with molecules of the atmosphere (H_2O in this case).

The calculated results include the chemical compositions of the plume, allowing its classification according to the established characteristics for operational requirements.

In addition, when identifying the optimum composition from a family of

propellants, a parametric analysis is performed using the three major components (for example, the binder, ammonium perchlorate and aluminum). A ternary diagram is drawn (Fig. 1). Studying the curves I_s , T_c , or $\rho \cdot I_s = \text{constant}$ allows the selection of the highest performing propellant composition. Although a large number of complete calculations are required for these diagrams — approximately 30 for each propellant family — they are very frequently used. They afford substantial savings in cost and research time by limiting the number of experimental tests that would have to be performed for such a selection.

3.2. DETERMINATION OF THE THEORETICAL PERFORMANCE OF A ROCKET MOTOR

Based on the technical requirements of a rocket motor, total impulse: I_{ft} , combustion duration, dimension and on the theoretical specific impulse selected, the calculations related to the ballistics (Chapters 1 and 2) also allow the identification of an average operating point (ε , p_o , p_a).

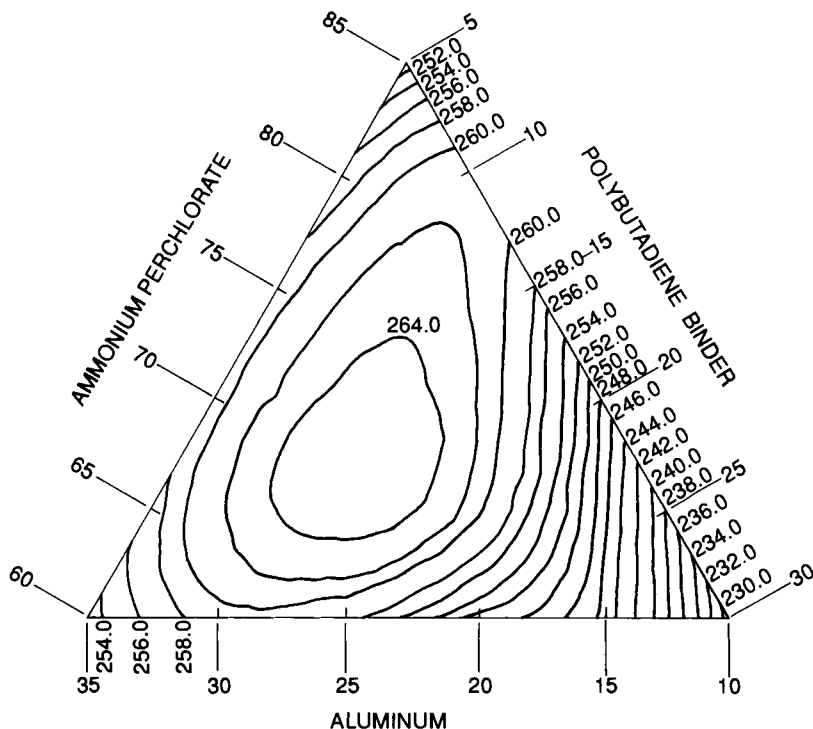


FIG. 3.1. Theoretical specific impulse diagrams (seconds).

The previously defined thermochemical computations are typically programmed for computer solutions. Using results from such a computation, the preliminary analysis designer is able to calculate the theoretical performances of the rocket motor. In addition to the values of the specific impulse (fixed nozzle expansion and expansion to vacuum), he can also obtain the exact composition of the plume as well as the thermodynamic values (C_p , γ , μ , \mathcal{M} , H , S) which characterize the system.

These values will be used as entry data to calculate the flow in the combustion chamber (Chapter 4), or the loss of performance in the nozzles (Chapter 1).

The thermochemical computations are also used to predict the theoretical performance of more complex chemical systems, such as:

- rocket motors using end-burning propellant grains for which the gases from the erosion of the thermal insulation and inhibitors must be taken into account with the combustion gases of the propellant grain [6];
- ramjets using solid fuels for which the mixing of combustion gases with air needs to be calculated (Section 5 of this chapter).

4. Measurement of the Specific Impulse

4.1. INTRODUCTION

Whether determining the value of the specific impulse of a propellant or of any rocket motor, this prediction requires:

- the use of test facilities designed for the purpose (firing stand);
- the acquisition of all data (pressure, thrust, time, mass, etc.) with a maximum of precision;
- a very exact description of the methods used to interpret the results.

The following section describes the equipment necessary to perform the tests, as well as the various operations performed, using as an example the prediction of the standard specific impulse of a propellant.

4.2. THE THRUST STAND

The thrust stand must be capable of withstanding and accurately monitoring the full thrust developed by a rocket motor. There are various types of firing benches, including:

- the blade bed,
- firing beds with sliding plates,
- vertical benches,
- pendulum gun,
- spinning benches.

The blade bed is most widely used to determine the characteristics of a propellant by firing standard configuration propellant grains. It is shown in Fig. 2; the rocket motor is attached to a very rigid frame suspended from rigid supports with a set of flexible blades. The role of the blades is strictly limited to that of a mechanical linkage, having no impact whatsoever on the thrust measurement. They must not be too flexible, to avoid parasite vibrations resulting from ignition of the rocket motor.

The thrust of the rocket motor is transmitted to a load cell.

The continuity of the load cell is completed by a pre-load screw which is attached to a block of solid concrete that absorbs the thrust of the motor.

The bench construction must be done carefully to ensure a perfect alignment between the thrust axis of the rocket motor and the axis of the cell.

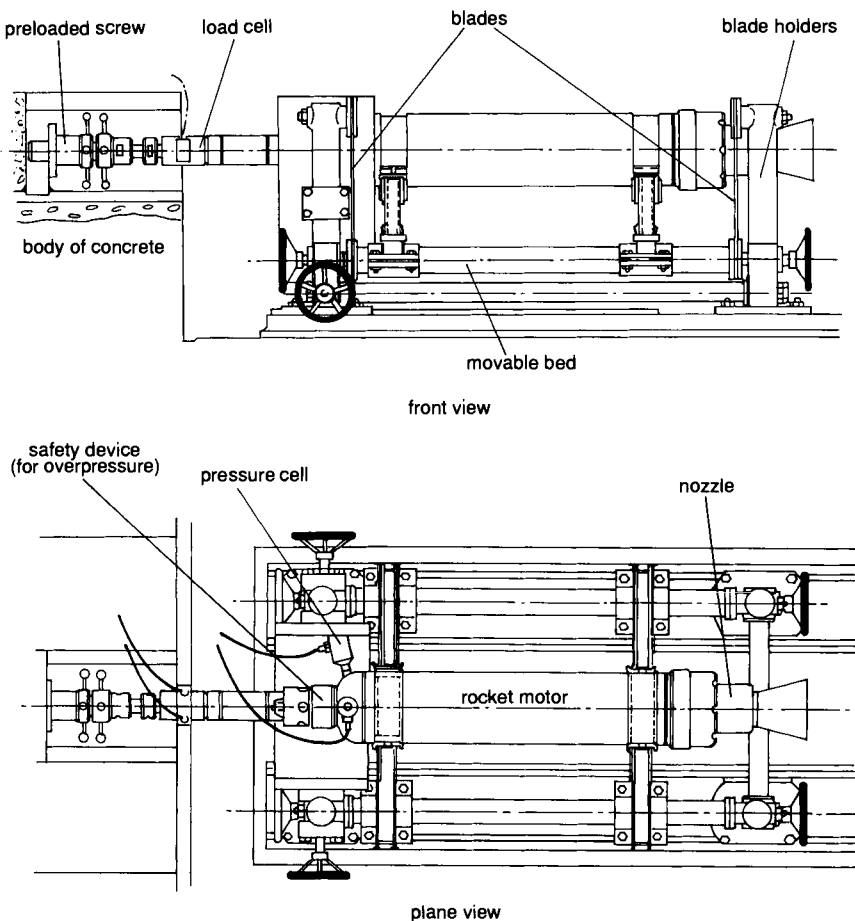


FIG. 3.2. Test bench.

4.3. THE STANDARD MOTOR AND HEAVY WALL MOTOR

This is the test motor configuration used to determine the average standard specific impulse (I_{sm}). The description given in this section is related to the French standard. This equipment is specially designed for repetitive tests necessary when the measurements taken are for the control of industrial production, or for development analysis. For the latter, the metal parts are over-sized, and those parts that have not been heavily exposed to combustion gases (front end and the cylinder) can be reused with a limited amount of maintenance work. On the other hand, because of the importance of their definition for the precision of the measurements, certain subassemblies (nozzle throat, exit cone) are systematically replaced.

The complete assembly includes three major parts:

- (1) An end base, equipped with a rupture disc to limit the pressure in case of a problem during combustion. The pressure and thrust cells are attached to the base. Thermal insulation is placed in the inside of the motor.
- (2) The propellant grain which is contained in a cylinder for cartridge landing (this may also be insulated).
- (3) A cylindrical part, where the free-standing propellant grain is placed. This may also be thermally insulated.
- (4) A rear assembly, made also of three parts: a convergent section, or nozzle, a nozzle throat, and a divergent section (Fig. 3).

Concerning the convergent section of the nozzle:

- it is made of a heat-resistant material (composite or graphite material);
- the half-angle of the convergent section is 45° — the diameter at entry is equivalent to the diameter of the free-standing propellant grain;

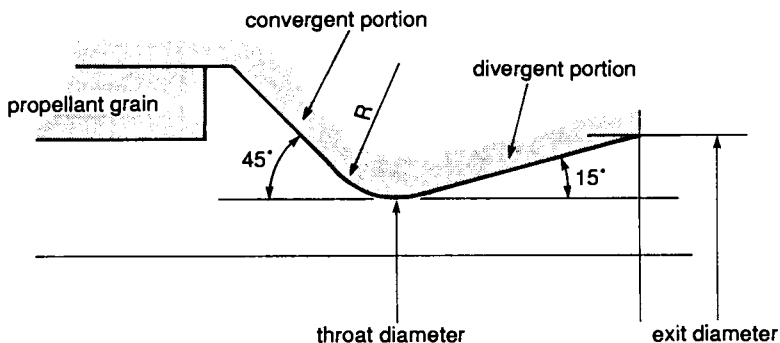


FIG. 3.3. Rear assembly.

- no discontinuity is permitted in the convergent section of the nozzle, including at the junction with the throat the nozzle;
- the surface must be as smooth as possible.

Concerning the throat of the nozzle:

- it is usually made of graphite;
- the radius R of the junction where the convergent and divergent portions meet is such that $R > \varnothing$ throat;
- the diameter of the throat is a function of the size of the free-standing grain, of the composition of the propellant, and of the desired pressure.

Concerning the divergent section:

- it is very often made of composite material;
- the half-angle of the divergent part is 15° ;
- the exit diameter is calculated as a function of the desired expansion.

4.4. THE PRESSURE TRANSDUCERS

- Two types of pressure transducers are used on the motors.
- Piezoelectric sensors with a broad frequency response to allow detection of rapidly changing combustion phenomena.
- Strain gauges to provide very precise measurements of the steady-state pressure curve.

4.5. THE PROPELLANT GRAIN

The selection of the propellant grain configuration is based on the following criteria:

- The burning area should have little dependence on the web burned so that the pressure as a function of time resembles a step function (instant rise, constant pressure plateau, instant pressure drop) as much as possible.
- The evolution of the grain burning surface should be as predictable as possible, which requires:
 - (a) a constant burning rate along the central port, devoid of any interfering phenomena such as erosive burning, or combustion instabilities (Chapter 4), and
 - (b) a very precise knowledge of all configuration characteristics, in particular the thickness of the web and the mass of the propellant grain.
- Fabrication should be simple and reproducible to reduce production costs.
- The mass of propellant should offer a good compromise between a value sufficient to limit errors related to measurement (weight, dimensions, etc.) and a value that respects the previous criterion.

A large number of types of propellant grains fulfilling these criteria are in use throughout the world. The more detailed description that follows is limited to two of the propellant grains often mentioned in this book.

4.5.1. *The star-shaped central port propellant grain*

This propellant grain, called MIMOSA as used in France, has a star-shaped central port with 10 segments. Its outer diameter is 203 mm; its weight is approximately 45 kg for 1 m of length. It has been used for a long time as a control propellant grain for the ballistic properties of composite propellants.

The neutrality of the burning grain surface evolution,

$$\frac{S_{\max} - S_{\min}}{S_{\text{average}}}$$

as a function of web burned, is very good.

The star shape, however, has the drawback of generating a burning surface area evolution which, as it evolves into the final phase (starting at the moment when the burning area is bordering the case), causes a pressure drop with a small combustion tail-off.

For research on new propellants the size of each sample propellant grain is kept small. This minimizes cost and enables evaluation of a large number of compositions. Another propellant grain called CAMPANULE may be used. Its weight is much lower (2.5 kg), with a 90 mm diameter and 300 mm length. It has a star-shaped central port, 10 segments, and provides initial data on the levels of specific impulse. Different companies or organizations use cylindrical smaller grains.

4.5.2. *Perforated grain [7]*

This is a propellant grain with a circular central port with flat, uninhibited end surfaces. This type of propellant grain, used in the United States, is known as the BATES (Ballistic Test Evaluation System). The burning area versus web burned is very constant, with no combustion tail-off: the pressure decrease at burnout is only controlled by the venting of the combustion chamber.

This propellant grain is available in several different sizes, as shown in Table 1. The 7-inch and 12-inch sizes are used in France to determine the characteristics of energetic binder compositions (Chapter 2) because of the very good tail-off curve. This is important for these formulations with high pressure exponent at low pressures which can lead to unburned residual propellant with other initial surfaces.

TABLE 1 *Main characteristics of the various BATES propellant grains*

Outside diameter (inches)	Length (inches)	Approximation propellant mass (kg)
7	12	6.5
12	20	35
28	60	380

4.6. MEANS OF MEASUREMENT

The measurement system must faithfully record the strain/stress signals given by transducers during the motor firing. The analog processing of the signal is not very precise, so a digital processing is usually preferred. A classic measurement system is shown in Fig. 4.1.

4.7. DETERMINING THE PARAMETERS OF A FIRING TEST

(*N. B.*: The exact definition of the parameters, as well as the equations used, are found in Chapter 1.)

This section involves the calculation, for a given propellant grain composition and type, of the three types of parameters discussed below.

4.7.1. *Operating pressure of the firing test*

The ideal, of course, is to reproduce standard operating conditions (expansion ratio 7/0.1, Chapter 1), which alone legitimize comparisons of

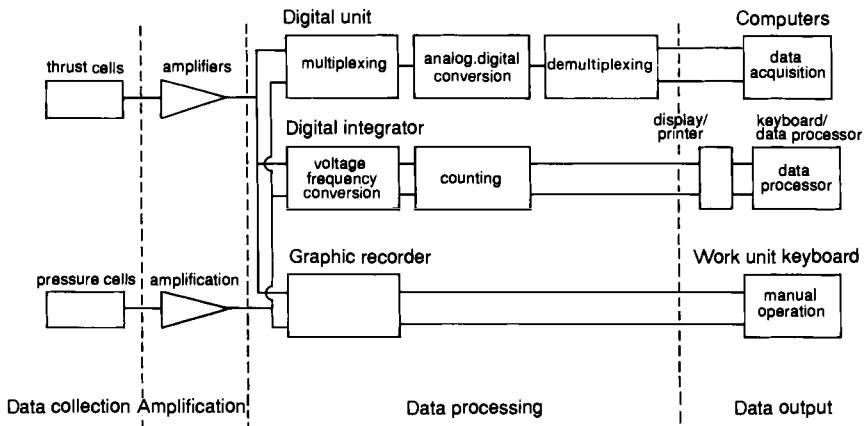


FIG. 3.4. Measurement system.

performance between various propellant grains. Consequently, the average value of pressure obtained during the firing test should be 7 MPa.

This value is representative of the operating range of most of the composite propellants (approximately 3–11 MPa), and will therefore be selected for the firing test parameters used in MIMOSA and BATES configurations.

Some double-base propellants differ, and have an operating range between approximately 15 and 30 MPa. They require a pressure corresponding to the plateau of their burning rate versus pressure curve (Chapter 9). These test conditions necessitate correction of the measurement data to obtain a final value that corresponds to the standard conditions.

4.7.2. Dimensions of the nozzle throat and of the exit plane

The diameter of the throat of the nozzle is calculated as follows:

$$C_D \cdot p_o \cdot A_t = \rho \cdot S \cdot v$$

where:

- C_D = propellant discharge coefficient;
- p_o = combustion chamber pressure;
- A_t = area of the throat,
- ρ = mass per unit of volume of the propellant grain;
- S = burning area of the propellant grain;
- v = burning rate of the propellant grain at pressure p_o .

The diameter of the divergent part of the nozzle (exit plane) is calculated as follows: using the throat diameter, and the section ratio $\varepsilon = A_s/A_t$ (ratio of the area of nozzle exit plane versus the area of the throat), we can determine the diameter of the exit plane. This ratio is a function of pressures p_o and p_s ; it also varies according to the value of γ for the propellant gases (Chapter 1). The thermodynamics calculations done for the propellant yield a value such that the pressure in the divergent exit plane is equal to the ambient atmosphere pressure.

In the case of aluminized propellants, when the test firing occurs with a chamber pressure in the range of 7 MPa (expansion ratio of gases p_o/p_s is 70), that value is of the order 10.

4.7.3. Other parameters

To select the transducers and calibrate the measurement system, the following are also determined:

- firing time: t = web to be burned divided by average burning rate;
- expected thrust: $F = C_F p_o A_t$, where C_F is the thrust coefficient of the nozzle (approximately 1.5 for $p_o = 7$ MPa).

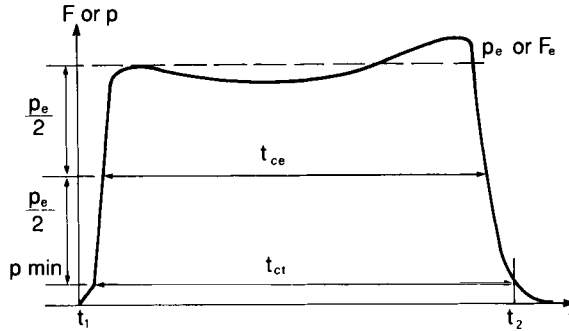


FIG. 3.5. Data analysis.

4.8. ANALYSIS OF THE RESULTING DATA

Figure 5 shows the definition of the parameters which need to be calculated to do a thorough analysis of the firing test, based on the measurements recorded (pressure or thrust versus time).

(1) *Total combustion time, t_{ct}*

Determination of p_{\min} = atmospheric pressure + 1% of the maximum capacity of the pressure cell, gives t_1 and t_2 ; and the $t_{ct} = t_2 - t_1$

(2) *Effective combustion time, t_{ce} and effective pressure, p_e*

Based on the curve $p = f(t)$ obtained, these two parameters are calculated through a series of iterations. They are related through the equation:

$$p_e = \frac{\int_{t_1}^{t_2} p \cdot dt}{t_{ce}}$$

(3) *Discharge coefficient, C_D*

$$C_D = \frac{\text{Weight of propellant burned}}{\int_{t_1}^{t_2} p \cdot dt \cdot A_{tm}}$$

(4) *Average area of the nozzle throat, A_{tm}*

Because the variation as a function of time the throat diameter is not available, it is necessary to calculate the average area of the throat, based on mathematical averaging of the diameter before and after the firing.

(5) *Mass of propellant burned*

The propellant grains used must be carefully weighed during their manufacture.

Usually, the weight of the propellant grain is determined by deducting the weight of the inhibitor from the total weight of the manufactured free-

standing grain. It may, however, be necessary to weigh the inhibitor remaining after firing, particularly in the case of heavy ablation. If it is necessary to take into account the weight of inhibitor burned, its contribution is approximated as half of its weight in propellant.

(6) *Average specific impulse, I_{sm}*

The average specific impulse of the rocket motor tested is calculated using the equation

$$I_{sm} = \frac{\int_{t_1}^{t_2} F \cdot dt}{g_0 \times \text{weight of propellant discharged}}$$

(7) *Standard specific impulse, I_{sm}^s*

The average specific impulse corresponds to average operating conditions that may deviate slightly from the targeted theoretical values (pressure, expansion ratio).

Based on the values actually obtained during a test (ϵ , effective pressure, and atmospheric pressure), corrections are necessary to adjust the average specific impulse to the standard conditions.

To achieve this, we rely on the fact that, with the same propellant grain and similar operational conditions, the specific impulse of a rocket motor is proportional to C_F . This equation takes into account the data presented in Chapter 1 which demonstrated the following:

- the existence of the equation: $I_s = C_F/g_0 C_D$;
- the assumption of the independence of the mass flow rate coefficient C_D from the combustion chamber pressure during firings with a pressure close to standard conditions (7 MPa);
- The dependency of the thrust coefficient, C_F , on the operating pressure, the ambient pressure, and the cross-sectional area ratio (ϵ) of the nozzle.

The standard specific impulse is calculated from the equation:

$$I_{sm}^s = I_{sm} \cdot \frac{C_F \text{ (calculated for standard conditions)}}{C_F \text{ (calculated for the exact operating conditions)}}$$

The values obtained range from approximately 170 s to 255 s, according to the propellant families used.

REMARK: In some cases the operating point of a rocket motor may not be close to the standard conditions (7 MPa). In addition to the above correction it is necessary to include the deviation of the mass flow rate coefficient as a function of pressure. This deviation is calculated using and T_0 (Chapter 1). The equation is written:

$$I_{sm}^s = I_{sm} \cdot \frac{C_F \text{ (standard conditions)} \cdot C_D \text{ (operating point)}}{C_F \text{ (operating point)} \cdot C_D \text{ (standard conditions)}}$$

4.9. ACCURACY OF THE MEASUREMENTS

Many parameters play a role in the quality of the measurement of the specific impulse; they include:

- the accuracy of the pressure and thrust measurements (linked to the firing bench, the sensors, and the measurement system);
- the precision of the calculations done from the firing measurements taken;
- the accuracy of the evaluation of the weight of the propellant discharged (involving the inhibitor, deposits inside the combustion chamber and on the nozzle, and presence of unburned propellant in the inhibitor);
- insufficient knowledge of the variations of the throat area (and possibly of the nozzle exit area) during firing;
- a mismatched nozzle, due to pressure variations in the combustion chamber during firing;
- the presence of transitory phases (ignition phase and burnout phase).

As a result it is necessary to perform several firings under identical conditions so that the evaluation of the specific impulse of a propellant grain may be sufficiently precise (standard deviation $\sigma \approx 0.5\text{--}1$ s).

5. Solid Fuels for Air-breathing Systems

5.1. THE PHYSICAL PHENOMENA

Missiles powered by solid fuel ramjets or ducted rockets use oxygen-deficient propellants. The theory of operation has already been introduced in Chapter 1. These propellants, which are further described in more detail in Chapter 12, are greatly “under-oxidized”, i.e. they contain just enough oxygen for complete gasification. These gases are formed in a primary chamber from which exhaust flow is generally restricted by a nozzle or valve. These gases flow into a secondary chamber, which is the real combustion chamber of the ramjet. Another system, which has already been flight-tested on a missile, did away with the intermediate nozzle by using propellants that burn at the pressure of the ramjet chamber. This type of configuration is called integrated gas generator or unchoked gas generator. For the two-chamber system the fuel-rich gases are injected into the secondary chamber where they mix with air coming through the air inlets located at the front of the missile. The major technical difficulty is the adjustment of the combustion gas flow rate to that of the air, to obtain a homogeneous and inflammable mixture under the actual conditions in the secondary chamber. The theoretical problem is therefore mostly one of dynamics of fluids and chemical kinetics. Thermodynamics helps to determine the upper value for the specific impulse that can be obtained at the exit of the secondary chamber.

5.2. ORGANIZATION OF THE CALCULATIONS

5.2.1. Determination of the properties of the propellant in the primary chamber

This first calculation (following the model described in Section 2 of this chapter) may be performed to obtain data for the thermodynamic parameters and the composition of the combustion gases.

In reality the global performance of the system is more useful. Consequently, the conditions in the secondary chamber are usually determined directly.

5.2.2. Determination of the propellant gas/air mixture in secondary chamber conditions

This calculation is based on the conservation assumption of the total dynamic enthalpy.

The calculation is the same as for a classic propellant grain. The only difference is that the enthalpy in this conservation equation ($h = h_o$) is no longer the propellant's enthalpy alone, but rather the sum of the propellant enthalpy and of the dynamic enthalpy of the air. We should note that the static enthalpy of the propellant has already been actually transformed into the combustion gas dynamic enthalpy, although it makes no difference for this global assessment.

The zero-velocity assumption in the combustion chamber results in even greater deviations than with classic rocket motors. In addition, since the entropy of the mixing of propellant gas and air is not taken into account, the total entropy gain in the chamber is higher than in a classic rocket motor, and the efficiency is overestimated.

However, in spite of this, the value obtained through calculations is very close to the values obtained through experiments.

5.2.3. Calculation of the expansion in the nozzle

This calculation is exactly the same as for a classic propellant grain, and the approximations call for just about the same remarks.

The zero-velocity assumption at the nozzle entrance is even more difficult to control. The additional amount of deviation is very small, however, because the assumption of sonic speed at the throat of the nozzle remains valid.

5.3. PERFORMING THE CALCULATION

5.3.1. Data entry

In standard calculations the data entry consists of the basic composition and the enthalpy of formation of the propellant. In the case of semi-propellant grains the proportions of the mixture, the propellant enthalpy, and the dynamic enthalpy of the air are also needed.

All quantities are expressed in mass, whereby:

f_s is the stoichiometric ratio of propellant combustion gases versus air,
 f is the ratio of propellant gases versus air of the mixture analyzed

$$\varphi = \frac{f}{f_s} \text{ is called the equivalence ratio.}$$

The proportions of the mixture may be determined with:

- either the air and propellant gas flow rates;
- or the equivalence ratio φ of the mixture.

The dynamic enthalpy of the air is calculated with the assistance of a second computer program based on the altitude and the Mach number. This same program is also useful for the calculation of static enthalpy at any temperature and altitude. As a rule the calculations are limited to sea-level altitude, which is a good representation for bench firing.

5.3.2. Results

With the propellant composition and the oxidizing potential, the values of the thermodynamic parameters in the secondary chamber, at the throat, and at the exit plane of the nozzle are obtained. For the various levels of φ selected we therefore obtain the global specific impulse of the mixture which can be expressed as:

- either the fuel-specific impulse (written: I_s);
- or the air-specific impulse (written: $I_{sa} = f \cdot I_s$)

The quantity $f \cdot I_s$ is also known as the air-specific thrust.

In a diagram “ $I_s \cdot \rho - f \cdot I_s$ ”, where ρ is the density of the propellant, the curve plotted for the various equivalence ratios characteristic of that particular propellant.

A comparison is generally made for the performance of the various solid fuels, for the standard conditions (20°C, Mach 2, sea level), and recording the values of $I_s \cdot \rho$ obtained for an identical value of $f \cdot I_s = 50$ s.

The analysis of this diagram provides the values of corresponding $f \cdot I_s$ for a set performance level (I_s). Because these values are directly tied to the air

consumption ($f \cdot I_s = I_{sa}$), the selection of a solid fuel is possible by taking into account the effect it will have on the size of the air inlets of the ramjet (which can be a more or less important factor of drag).

Based on the solid fuel formulation, the specific impulse I_s ranges from approximately 600 to 1300 s. (For comparison purposes only, the specific impulse I_s of the solid fuel alone, calculated under standard expansion conditions (7/0.1), is in the vicinity of 190 s.)

5.4. METHOD OF MEASUREMENT

Measuring the specific impulse of solid fuels for operating conditions of a ramjet is vastly more difficult to do than measuring standard specific impulse of a solid propellant. It requires testing installations which best simulate the overall operation of these motors, and in particular, access to an air-supply system.

Two types of test facilities are used, determined by the goal of the test performed [8].

The direct connect setup: the air inlets of the combustion chamber are directly connected to a hot air supply with a controlled flow rate. Because the pre-heating of the air enables the enthalpy to be brought to the dynamic level intended by simulation, this system offers a good representation of the operating conditions in the combustion chamber. Since it is relatively easy to set up, it is widely used. Unfortunately, because of its design it provides no information whatsoever on the aerodynamic phenomena related to air inlets. It is, however, the only system that allows easy thrust measurement during the performance of the test.

In the free steam setup, the supersonic flow of air necessary to properly simulate the actual supply of air to the air inlets is obtained by putting each of the air inlets within the exit plane of a nozzle. These nozzles are fed by a wind-tunnel system. In addition to the operating conditions in the combustion chamber, this setup has the advantage of providing data on the aerodynamic phenomena (shapes of the shock waves) linked to the actual geometry of the air inlets. It also allows observation of the transition phase between the burnout of the booster propellant grain and the ignition of the sustainer propellant grain when dealing with a ramjet with integral boosters inside the combustion chamber. This setup is much more complex than the previous one, and requires the installation of powerful wind tunnels.

Bibliography

1. GORDON, S. and MCBRIDE, B. J., *Computer Program for Calculation of Complex Chemical Equilibrium Compositions, Rocket Performance, etc.* NASA Lewis, SP, 273. 1971.
2. ZELEZNIK, J. K. and GORDON, S., Calculation of Complex Equilibria. *Ind. Eng. Chem.*, **60**(6), 27-57, 1968.

3. Kinetics and Thermodynamics in High Temperatures Gases. A conference held at Lewis Research Center, Cleveland, Ohio. NASA SP-239, March 1970.
4. STULL, D. R. and PROPHET, H., Project Directors. *JANNAF Thermochemical Tables*. 2nd edition. NSRDS-NRS 37. Catalog Number C13. 48:37. US Government Printing Office, Washington, DC, 1971.
5. CHASE, M. W. *et al.*, *JANNAF Thermochemical Tables*: 1974 supplement, *J. Phys. Chem. Ref. Data* **3**, 311, 1974; 1975 supplement, *J. Phys. Chem. Ref. Data* **4**, 1, 1975; 1978 supplement, *J. Phys. Chem. Ref. Data* **7**, 793; 1978; 1982 supplement, *J. Phys. Chem. Ref. Data* **11**, 3, 1982.
6. BANON, S. and ASTIER, J., The contribution of inert material to end burning propellant grain performances. AIAA 86.1421; AIAA/SAI/ASME; 22nd Joint Propulsion Conference. 1986.
7. COLLINS, R. G., The AFRPL Ballistic Test and Evaluation System (BATES Program). AFRPL Report No. TR-65-7. Air Force Rocket Propulsion Laboratory, Edwards, May 1965.
8. MAHONEY, J. J., Salient characteristics and development status of ramjets for guided missiles with emphasis on air launched tactical configurations. Naval weapons center technical memo, TM4452, October. 1981.

CHAPTER 4

Solid Propellant Combustion and Internal Ballistics of Motors

BERNADETTE GOSSANT*

1. Introduction

The understanding and complete control of combustion are critical areas of research when seeking better performance for solid propellant rocket motors. The purpose of this chapter is to present the current knowledge in internal ballistics of solid propellant rocket motors. Its first part deals with the description of experimental determinations of the burning rate, necessary for any internal ballistics calculations. A description of the combustion of the various propellant ingredients follows. The last two sections of this chapter are devoted to the combustion analysis under actual steady-state or unsteady operation conditions of the rocket motor.

2. Solid Propellant Combustion

2.1. BURNING RATE

2.1.1. Background

The combustion of a solid propellant is characterized by the way its surface regresses once it has begun to burn. The burning rate is the distance traveled by the flame front per unit of time, measured normally to the burning surface. This front is assumed to be regular and, in most cases, progresses in a direction normal to itself. This has been experimentally verified (within the

*With the participation of Paul Tchepidjian.

precision limit of burnt profile measurements) by interrupting the propellant combustion and examining the surface.

The burning rate versus pressure law is usually expressed by the formula given by Saint Robert and Vieille:

$$r = ap^n \quad (1)$$

where:

n is the pressure exponent;
 a is the rate of burning constant.

For a given propellant and a pressure ranging from 3 to 15 MPa, the pressure exponent takes a typical value between 0.2 and 0.7. Some propellants, however, have a different behavior: their pressure exponent is zero (the so-called plateau effect), or even negative (mesa effect). The coefficient a in eqn (1) is known to be dependent on the initial or in-depth temperature of the propellant. An established empirical law is:

$$a = a_0 \exp[\sigma_p(T_i - T_i^0)] \quad (2)$$

where:

T_i^0 = an initial reference temperature;
 T_i = the initial propellant temperature;
 a_0 = the burning rate constant at T_i^0 ;
 a = the burning rate constant at T_i ;

$$\sigma_p = \left(\frac{\partial \ln r}{\partial T_i} \right)_p \left\{ \begin{array}{l} \text{Sensitivity of the burning rate at initial} \\ \text{temperature under constant pressure. As a first} \\ \text{approximation this coefficient may be considered as a} \\ \text{constant.} \end{array} \right.$$

Finally, under certain extreme conditions (violent shock, explosion), the burning rate may considerably increase and become greater than the speed of sound. This catastrophic condition is called a detonation and is not discussed in this chapter.

Tailoring a propellant will always include as major objective to minimize the values of pressure exponent and temperature coefficient (Chapter 1), while ensuring that its mechanical properties will still be sufficient for future applications. There are a large number of physicochemical parameters affecting the burning rate. They will be analyzed in detail when combustion mechanisms of the main propellant families are described.

2.1.2. Experimental determination of the burning rate

Several methods are used. Some of these methods require very small amounts of propellant, and are therefore preferred when performing preli-

minary analyses. The values obtained must later be confirmed at larger scale (control propellant grains).

2.1.2.1. *The strand burner method*

In this method a small sample (standard size) of propellant is fired in a bomb at constant pressure. This method has many advantages, including low cost and quick-and-easy implementation. A disadvantage is that the reduced size of the propellant sample may exaggerate the dependence on propellant inhomogeneities.

(a) Preparation of the samples

The samples used are strands, with a square section (10×10 or $5 \times 5 \text{ mm}^2$) approximately 170 mm long. They are inhibited along their whole length to ensure that combustion occurs perpendicular to the surface. The type of inhibitor depends on the propellant composition. Each strand is perforated with four holes:

- the first hole, close to one end, is used to place the ignition wire;
- the other three, placed at 20, 85 and 150 mm respectively, are used to introduce lead wires which, by melting, allow the electrical detection of location of the flame front with time.

The samples are then placed vertically in a closed vessel, called a firing bomb.

(b) The firing bomb

The firing bomb currently used is made of steel (Fig. 1); its useful volume is 750 cm^3 . A preliminary pressurization is done, usually with nitrogen; the test pressure level is kept constant during the combustion of the strand. Firings at various temperatures are made possible with the use of glycol or oil baths (for respectively low and high temperatures).

(c) Determination of the burning rate

The burning rate is obtained by knowing the burning distance as well as the burning time between two lead wires. These lead wires, acting as fuses, trigger a chronometer. As there are two strands per sample holder, four determinations of burning rate are done per test.

2.1.2.2. *Liquid strand burner method [1]*

This method also uses propellant strands. The strands, however, are shorter (68 mm) and are only equipped with an ignition wire. The firing

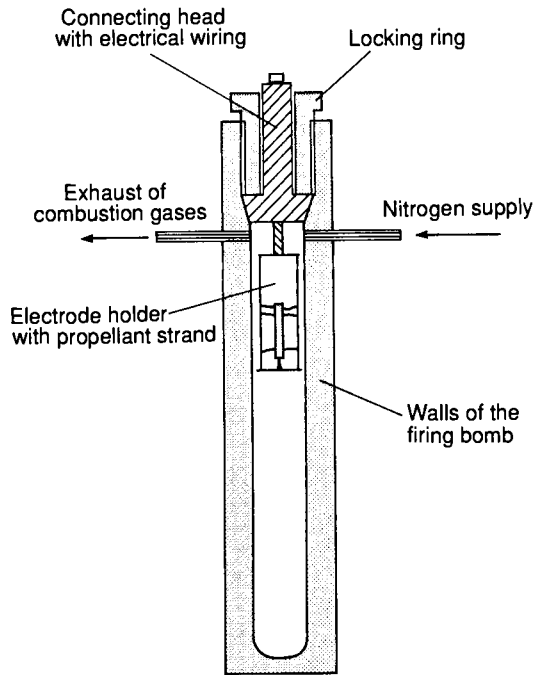


FIG. 4.1. Schematic of a strand burner firing bomb.

bomb is filled with water to ensure lateral restriction of the strand. It is then pressurized to a desired pressure level, using nitrogen. This level, however, is not regulated during firing.

The burning rate is obtained by knowing the strand useful length and the duration of the firing. The latter is determined by monitoring the noise made by combustion. The advantage of this method is that a preliminary lateral restriction of the strand is not necessary.

2.1.2.3. Ultrasonic method [2]

(a) Principle of the method

A mechanical wave is produced by an ultrasonic transducer which works either as transmitter or receiver. The ultrasonic wave travels through the propellant sample and is reflected on the burning surface. Because there is a tremendous difference in acoustic impedance between the propellant grain and its burning products, it is possible to deduce the unburnt propellant thickness by measuring the elapsed time between transmission and reception of the wave. To avoid wave attenuation, the maximum propellant grain thickness is 40 mm; the wave travel time is on the order of a few tens of

microseconds. Changes in the thickness can therefore be monitored by transmitting periodic ultrasonic pulses during firing. Instantaneous values of the steady-state burning rate are obtained by derivation once the recorded signals have been decoded.

(b) Test firing rocket motor

This experimental device consists of a small rocket motor in which a cylindrical, “end-burning” sample of propellant (86 mm in diameter) is mounted. For technical reasons (measurements of small thicknesses, thermal insulation), a material with a similar acoustic impedance, called coupling material, is placed between the receiver (transmission frequency 5–25 MHz) and the propellant grain.

(c) Advantage of the method

This method allows the performance of direct, localized, and instantaneous measurements. Only a small amount of material is used, and a large portion of the burning rate law is obtained from just one firing. The pressure evolution inside the combustion chamber is obtained either through the geometry of the propellant grain, or by using eroding throats. However, the coupling material needs to be tailored to each family of propellant.

2.1.2.4. Standard ballistics test motors

These motors, used to verify the burning rate laws of the various propellant families, are characterized by a low evolution of the grain burning surface. As a result the firing may be done at practically constant pressure, which greatly simplifies results analysis.

Star-shaped or slotted tube propellant grains, used to measure the specific impulse, are discussed in their corresponding implementation in Chapter 3. Some propellant compositions require burning rate measurements to be done through end-burning grains (“cigarette-burning” combustion type). Table 1 provides an overview of the main characteristics of the various SNPE test motors.

The effective burning time t_{ce} is calculated from the pressure–time plot (Chapter 3). Similarly, the same iterative procedure is applied to the burning surface evolution curve versus the burnt propellant thickness; it gives:

- The “effective” surface area S_e ;
- The “effective” burned web e_b , such as:

$$\int_0^{e_f} S(e) \cdot de = S_e \cdot e_b$$

where e_f is the propellant web thickness.

TABLE 1 *Main control propellant grains used at SNPE*

Grain designation	Star grains		Internal burning tube grain				End-burning grain		
	Mimosa	Campanule	Bates		Bates 12"	32 × 16	Flora	Phlox	Panisse
			3"5	7"					
Outer diameter (mm)	203	90	90	177.8	304.8	32	157	90	100
Diameter of propellant (mm)	198	86	86	167.6	298.4	32	151	85	90
Length of propellant (mm)	500	298	157	304.8	508.0	125	100	90	90
Diameter of star wedge (mm)	113.5	50.3	/	/	/	/			
Diameter of central port (mm)	/	/	60	116.8	203.2	16			
Propellant volume (cm ³)	12000	1340	470	3460	19000	75	1790	510	570
Effective web thickness (mm)	43.6	18.6	13.0	25.4	47.6	8	560	90	90

The calculation of the average burning rate is deduced:

$$r = \frac{e_b}{t_{ce}}$$

2.2. COMBUSTION MECHANISMS

Except for the ignition phase, the combustion of a solid propellant is a self-sustained phenomenon. Due to the heat feedback from the flame, the temperature rise of the propellant located very close to the surface causes its decomposition (structure changes, rupture of chemical bonds). Gaseous and reactive chemical products are released, in turn feeding the combustion in the flame zone.

2.2.1. *Description of the burning zone*

Study of the burning zone takes into account, in addition to the flame zone, the thin propellant layer close to the surface area where the temperature is raised. Propellant is a poor heat conductor, and since the flame is very close to the surface, the zone affected by combustion is very small. It is a few hundreds of microns thick.

2.2.1.1. *Description of the phenomenon in the solid material*

With a uniaxial assumption, the integration of the steady-state heat equation, including the following boundary conditions:

$$\begin{aligned} x = 0^- \quad T &= T_s \\ x = -\infty \quad T &= T_i, \quad \frac{dT}{dx} = 0 \end{aligned}$$

gives the evolution of the temperature gradient in the steady-state regime (origin of the axis on the burning surface as it moves). It is expressed by the equation:

$$T = T_i + (T_s - T_i) \exp\left(\frac{r}{d_p} x\right) \quad (3)$$

where:

- r = burning rate of the propellant;
- T_i = initial temperature of the propellant, far from the burning surface;
- T_s = surface temperature of propellant;
- d_p = propellant heat diffusivity.

(a) Decomposition in the solid phase

The following analysis does not take into account the chemical reactions, thermally enhanced, occurring inside the propellant; those are endothermic (decomposition of polymer chains) or exothermic (recombination in the condensed phase of the chemical products resulting from the decomposition). But temperature profiles recorded with very fine thermocouples on homogeneous propellant samples [3] reasonably validate eqn (3). Lengellé *et al.* [4] demonstrated that decomposition reactions practically occur only at the surface.

(b) Kinetics of propellant grain decomposition: pyrolysis laws

• Composite propellants

Experience demonstrates that, for the steady-state regime, the regressive burning rate r_i of each ingredient is related to the surface temperature:

$$r_i = A_i \exp\left(-\frac{E_i}{RT_{s,i}}\right) \quad (4)$$

where:

A_i = constant;

E_i = activation energy decomposition reactions;

$T_{s,i}$ = surface temperature;

R = universal gas constant;

i = stands for each propellant ingredient.

• Homogeneous propellants:

The integration of the conservation equation for the non-decomposed propellant mass, assuming a zero-order reaction, gives:

$$r = \int_{-\infty}^0 B_p \exp\left(\frac{E_p}{RT}\right) dx$$

where:

B_p = constant;

E_p = activation energy of the propellant decomposition reactions.

Taking into account the small thickness where reactions occur, Lengellé [5] shows that:

$$r = \exp\left(-\frac{E_p}{2RT_s}\right) \left\{ \frac{B_p d_p}{\varepsilon_p} \left[1 - \frac{T_i}{T_s} - \frac{Q_s}{2c_p T_s} \right] \right\}^{1/2} \quad (15)$$

where:

d_p = propellant thermal diffusivity;

$$\varepsilon_p = \frac{E_p}{RT_s};$$

T_i = initial temperature;

T_s = surface temperature;

Q_s = heat released by reactions in the solid phase
(breakdown of the N-NO₂ chemical bonds and the
reaction NO₂ + aldehyde in the condensed phase);

c_p = propellant specific heat.

Experiments validate this relationship for this kind of propellant [4].

2.2.1.2. Description of the phenomenon in the gas

Simplified, we may consider that the flame provides sufficient heat flux to maintain the regression of the solid propellant surface through the gaseous layer where the products released by reaction decompositions are hot, although still inactive. In a one-dimensional assumption, resolving the heat equation and assuming boundary conditions:

$$\begin{aligned} x = 0^+ \quad T &= T_s \\ x = x_f^- \quad T &= T_f, \quad \lambda \left. \frac{dT}{dx} \right|_{x_f^-} = \dot{m} Q_F \end{aligned}$$

we obtain the following temperature profile:

$$T = T_f + (T_f - T_s) \left[\exp \frac{\dot{m} c_g x}{\lambda_g} - \exp \frac{\dot{m} c_g x_f}{\lambda_g} \right] / \left[\exp \frac{\dot{m} c_g x_f}{\lambda_g} - 1 \right] \quad (6)$$

where:

T_s = propellant surface temperature;

T_f = adiabatic temperature of the flame;

x_f = flame height;

\dot{m} = mass flow rate of the gaseous reactive products;

c_g = specific heat of the gases, at constant pressure (assumed to be constant);

λ_g = heat conductivity of the gases, assumed to be constant;

Q_F = heat released by the flame.

The value of the flame heat flux (in $x = x_f^-$) allows the computation of the surface temperature T_s :

$$T_s = T_f - \frac{Q_F}{c_g} \left[\exp \frac{\dot{m} c_g x_f}{\lambda_g} - 1 \right] / \exp \frac{\dot{m} c_g x_f}{\lambda_g} \quad (7)$$

Flame system

Kuo [6] presented a synthesis of the knowledge in this field. We will limit ourselves to pointing out that there are two major types of flames that must be considered when studying the combustion of propellants: laminar premixed flames, and laminar diffusion flames.

(a) Laminar premixed flames

In this case the molecules of the reactants are intimately mixed together. The flame height is completely controlled by the kinetics of chemical reactions.

$$x_f = x_r \simeq \frac{\dot{m}}{p^{\delta-2}} B_f \exp\left(-\frac{E_f}{RT}\right) \quad (8)$$

where:

- δ = order of the chemical reaction;
- x_r = height of the reaction;
- E_f = activation energy of the reaction;
- B_f = pre-exponential factor of the reaction;
- p = combustion pressure.

(b) Laminar diffusion flames

Fuel and oxidizer are this time initially separated. The flame height, depending mainly on the diffusion of the products, needed before any chemical reaction, consists of two terms:

$$x_f = x_d + x_r \quad (9)$$

- x_r is the reaction height of the flame due to the intervention of kinetics after the products issued from decomposition have been mixed.
- x_d is this part of the total height which depends on the diffusion; it is estimated from Burke-Schumann analysis [7]. This analysis deals with the case of a Bunsen burner with two separate jets. It is applied by analogy to the case of the reactions between oxidizing products coming from the decomposition of ammonium perchlorate and combustible products coming from the decomposition of the binder. In this section we mention the equation for short flames which allows correlation of analysis and experience [8].

2.2.1.3. Energetic balance at surface

Continuing to assume that the reactions in condensed phase occur at the level of the burning surface, we have:

$$\lambda_g \left. \frac{dT}{dx} \right|_{0+} = \lambda_p \left. \frac{dT}{dx} \right|_{0-} + \dot{m} Q_s \quad (10)$$

where:

- λ_g, λ_p = respectively, heat conductivity of the gas and of the propellant;
 \dot{m} = mass flow rate resulting from combustion;
 Q_s = energy representing the total reactions at the surface; this value is negative if the final result is exothermic.

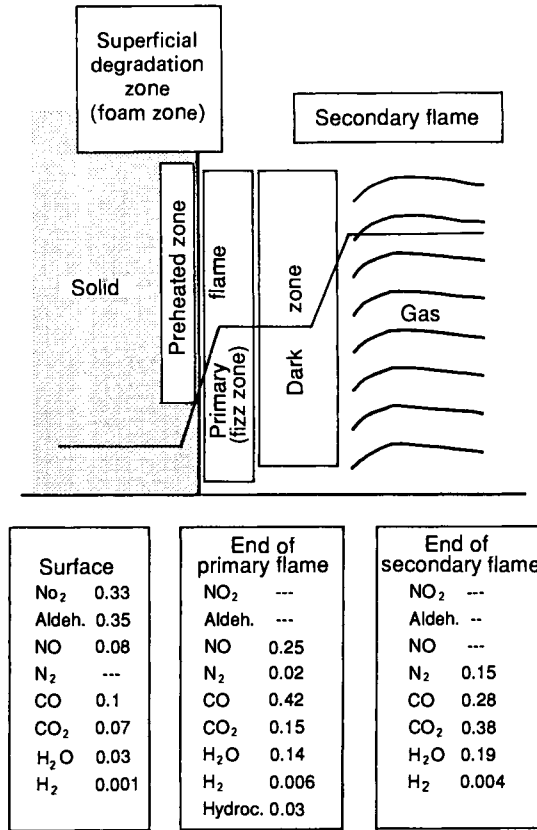
Therefore, using tiny thermocouples to determine the heat gradients on each side of the burning surface [3,9] this makes it possible to calculate the value of Q_s .

2.2.2. Combustion mechanism of extruded double-base propellants (EDB)

2.2.2.1. The various zones of combustion

Several combustion zones are observed (Fig. 2):

- Zone 1 This is the zone where the propellant is not affected by the combustion, although its initial temperature T_i rises until it reaches the value beyond which the reactions in condensed phase are activated.
- Zone 2 The foam zone, because of its foamy aspect. This is the zone where the decomposition processes of the solid phase occur in a very thin layer (10^{-2} to 10^{-3} cm) at moderately high temperature (600 K). Some endothermic transformations produce liquids and gases: they result from the thermal decomposition of nitrocellulose and nitroglycerine. Other reactions, on the other hand, are exothermic (reactions between decomposition products of the various propellant ingredients).
- Zone 3 The fizz zone, because of the fizzing aspect of the combustion. This is the zone where the primary flame lies, resulting from the reactions between the nitrogen peroxide and aldehydes produced by the decomposition of the propellant. The proportions of the gaseous products depend on the propellant composition, and especially when there are specific ingredients controlling burning rate, called ballistic modifiers or burning rate catalysts. In this zone the temperature gradient is high; the adiabatic temperature of the primary flame is about 1300 K.
- Zone 4 The dark zone, because of its color. In this zone the gaseous products produced by the primary flame are mixing; they become hotter because of the heat flux transmitted by zone 5.
- Zone 5 The final flame zone. In this zone combustion is largely completed. The gaseous products produced by the primary flame have reached the concentration and temperature necessary for the chemical



Mass decomposition ratio of the products in the different flame regions

FIG. 4.2. Burning zones of double-base propellants.

reactions to occur (NO/CO, H₂ reactions). The adiabatic temperature of the flame is around 2600 K.

2.2.2.2. Burning rate law and formulation parameters

The burning rate versus pressure law, for these propellants, depends on:

- the flame system;
- the apparition of a carbon deposit on the propellant burning surface.

The first part of this section presents the main trends for reference propellants (without ballistic modifiers). Because they are not interesting for practical use (very high pressure exponents), a second part discusses the behavior of propellants containing ballistics additives.

(a) Effect of pressure

At a specified pressure the intrinsic burning rate of an EDB propellant depends most of all on its composition (Chapter 9). There are:

- so-called “cold” propellants with a heat of explosion around 800 cal/g;
- “hot” propellants, more energetic (approximately 1300 cal/g) and having greater burning rates.

The distance of the flames from the surface is influenced by the pressure:

- Up to approximately 10 MPa, combustion is governed by the primary flame. The NO_2 /aldehyde reaction has an activation energy of approximately 5 kcal/mole, and is distributed over the entire thickness of the fizz zone; in addition, its order of reaction, close to 1, should lead to an n value close to 0.5. The measured temperature of the flame, however, depends on the pressure [11], and is higher than the adiabatic temperature calculated for the NO_2 /aldehyde reactions alone. Lengellé *et al.* [4] suggest that additional reactions between nitrogen monoxide and the surface carbon deposit be taken into account. This increase in primary flame temperature as a function of pressure level explains the high values of pressure exponents (around 0.75) that are observed with uncatalyzed propellants.
- At pressures above 10 MPa, the final combustion flame approaches the burning surface and, because of its tendency to merge with the primary flame, its heat flux also participates to the propellant decomposition. Because of its energy characteristics (order of reaction of 2), the pressure exponent is closer to one in this range of pressure.

(b) Effect of the ballistics modifiers

The introduction during manufacture of ballistic catalysts in the propellant compositions allows the regulation of the burning rate level and a significant decrease in the values of the temperature coefficient and of the pressure exponent. In the pressure range of rocket motors, exponent values close to zero can thus be obtained, thereby “flattening” the burning–pressure curve. The most common additives are:

- lead salts;
- copper salts, mixed with lead salts (copper components alone are not very active).

Their effect, depending on their amount, spreads over a certain range of pressures. They produce an increase in the burning rate of the propellant without catalysts (super-rate) while at the same time allowing the plateau effect. Addition of carbon black permits the displacement of the pressure range where the super-rate occurs.

(c) Initial super-rate

This occurs primarily at low pressure (<15 MPa). Experimental data published by Lengellé and Kubota show that the temperature of the primary flame is increased by the addition of burning rate modifiers. These appear to strengthen the reactions with the carbon deposited on the surface; in this case the deposits become thicker. It seems necessary, however, to invoke other mechanisms to explain the very strong effects observed: in some cases the thick carbon deposit seems to act as a flame-holder, bringing the final flame significantly closer to the surface.

(d) Second super-rate

This appears at high pressure. The carbon deposit on the surface has been eliminated. On the other hand, spots, probably lead monoxide, have been observed at the surface after extinction of strand burner samples.

Little is still known about the mechanisms that cause these super-rates, particularly at high pressure.

2.2.2.3. *The models*

It would not be feasible here to provide a detailed analysis of each model. We limit ourselves to citing the major ones:

- models taking into account, in various manners, the primary flame: Kubota *et al.* [11], Beckstead [12], King [13], and Cohen [14];
- simulations of the complete flame system: Ferreira *et al.* [15].

2.2.3. ***Combustion mechanisms of heterogeneous propellants (inert and active binder propellants)***

Heterogeneous propellants contain a mixture of ingredients; each of them, when decomposing, releases gaseous products whose nature is either oxidizing or reducing. The initial mixture allows a complete combustion, based on the availability of chemical equilibria (Chapter 3). Nitramine molecules and energetic binders both contain combustible and oxidizing agents, ensuring a complete and independent combustion. In the following section we first briefly describe the behavior of each main ingredient when subjected to a significant heat source. This leads to a better understanding of the mechanisms observed in propellants.

2.2.3.1. *Decomposition of the main ingredients of heterogeneous propellants*

(a) Ammonium perchlorate (AP)

Differential scanning calorimetry [16] has shown:

- that solid AP experiences a change of phase that corresponds to a change in the crystal network at 513 K;
- the existence of two exothermic decomposition reactions in the condensed phase at approximately 570 K and 700 K.

Its melting point is 833 K. Linear pyrolysis tests have been performed by Coates and Guinet [10]. Results obtained by Seleznev *et al.* [17], however, who used an optical method to determine the burning surface temperature of strands, also serve as a reference.

AP combustion is sustained by the heat produced by the reactions in the condensed phase and the premixed flame which lies very close to the surface. The reaction between ammonia and perchloric acid, produced by AP decomposition (adiabatic flame temperature is 1205 K, order of reaction 2 and activation energy approximately 15 kcal/mole, as established by Guirao and Williams [18]), occurs at the surface. This reaction provides oxidizing species.

The pressure exponent is high (around 0.77 between 2 and 10 MPa) and there is a pressure threshold below which the combustion is no longer sustained. It corresponds to a surface temperature equal to the melting temperature of this oxidizer.

(b) Cyclic nitramines RDX and HMX

Two cyclic nitramines are used in propellant chemistry. The melting of these ingredients (approximately 477 K for RDX and 553 K for HMX) is a complex phenomenon: it has been observed, for instance, that the large particles liquefy easier than the small ones. Solid HMX comes in four different polymorphic forms, of which form β is the most common. The other forms (α , γ , δ) are successively obtained during a slow temperature rise. It is not known whether they exist under the rapid heating conditions occurring during combustion.

Boggs [19] and Fifer [20] have both written an exhaustive description of the results of decomposition studies of these nitramines. The decomposition reactions in the condensed phase lead to the rupture of the C-N and N-NO₂ chemical bonds. Analysis of pyrolysis gases shows the presence of N₂, N₂O, NO, CO₂, CO, H₂, HCHO, H₂O, and HCN. According to Fifer, the reaction controlling the combustion is the reaction between aldehyde and NO₂, very

rapid at the temperature reached. The flame temperature, contrary to the AP flame, is very high (3286 K for RDX and 3278 K for HMX).

The burning rate law for HMX was determined using monopropellant crystals or pressed strands [21]. Sample observation after extinction shows the presence of a melted layer on the surface during combustion, with a thickness depending on the pressure.

(c) The binder

In this section we only describe the case of inert binders, because the combustion mechanisms of energetic binders are identical to homogeneous propellant ones.

An inert binder is a polymer where C–C or C–H chemical bonds prevail. Under the effect of heat these bonds break down. This reaction may occur in the solid or the liquid phase, depending on the nature of the polymer. This heat-related degradation results in the appearance of hydrocarbons that are:

- polymerized at the surface in the form of a charcoal residue or “char”, in some cases;
- gaseous, and, when placed in an oxidizing atmosphere, burn with diffusion flames.

The binder pyrolysis law can also be evaluated by thermogravimetry.

(d) Aluminum

Its introduction in compositions containing ammonium perchlorate allows a significant increase of their adiabatic combustion temperatures. This effect is due to the additional reaction for the formation of metal oxide. Since the melting temperature of aluminum is 933 K, the micron-size particles contained in the propellant melt at the surface where the temperature is generally higher, and they gather into aluminum droplets. A detailed description of the combustion of aluminum has been done [10]. In order to facilitate the comprehension of the models, we shall only state that:

- the liquid droplets leave the surface and are oxidized at a significant distance from the surface;
- the alumina particles formed in the combustion chamber of the propellant grain are very small (approximately a few microns) and liquid (Al_2O_3 melts at 2318 K); they agglomerate or burst before they solidify inside the nozzle, which ensures the gas expansion;
- Aluminum combustion is usually fairly well completed inside the chamber. Some configurations, however, may decrease its efficiency when aluminum residence time in the combustion chamber is too short.

2.2.3.2. Combustion mechanisms of inert binder propellants

The following solid particles are dispersed in the binder matrix:

- oxidizer particles with large particle size distribution (1–400 μm);
- and possibly, aluminum particles.

The following occurs during combustion:

- In the gaseous phase: all of the combustion reactions resulting in the appearance of a complex flame system (Fig. 3): reactions involving AP;
- In the gaseous phase: all of the combustion reactions resulting in the appearance of a complex flame system (Fig. 3):
 - premixed AP flamelets, considered as monopropellant. AP adiabatic temperature, at a realistic operation pressure in the range of 7 MPa, is approximately 1230 K;
 - diffusion flames between the oxidizing products resulting from AP decomposition or from AP premixed flame and the hydrocarbons produced by the binder; the adiabatic temperature of the final diffusion flame, for a non-metallized propellant containing 80% AP, is in the range of 2300 K.

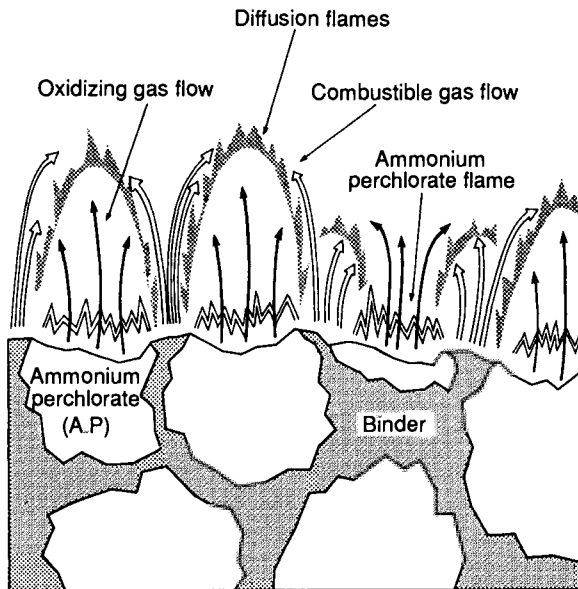


FIG. 4.3. Flame structure of heterogeneous propellant with inert binder.

(a) Burning rate law and composition parameters

For these propellants the burning rate law is a function of:

- the pressure range;
- the AP size distribution.
 - At very low pressure, the burning rate is low and the heated thickness of propellant is large compared to the size of AP particles. Because the gaseous reactants produced by the various ingredients have had time to mix, combustion is controlled by chemical kinetics. The influence of the AP particle size is weak and the pressure exponent is high.
 - At medium pressure (1–15 MPa), the thickness of heated propellant is less than above, and the diffusion phenomena between the reactive gaseous products become controlling phenomena. Premixed and diffusion flames are simultaneously observed, and the pressure exponent value is moderate (0.3–0.4). In this pressure range the burning rate is closely tied to the AP particle size: the finer the ammonium perchlorate, the greater the burning rate.
 - At very high pressure ($p \geq 15$ MPa), a new regime appears, with a higher pressure exponent (0.6–0.7). The current models do not predict this. It could be explained by a modification of the AP pyrolysis law at high pressure. We may also think that under the effect of the increase of velocity of the exhaust gases coming out of the surface, or caused by the high pressure level, the heat transfers are increased, in turn increasing the flux transmitted to the propellant.

(b) Influence of ballistics additives

The additives used contain metallic atoms. Their action results less from chemical reactions than from modifications of the thermal properties of the burning surface:

- Some additives cause the formation of a very thin residue on the surface. They must be well dispersed inside the propellant to ensure the most efficient effect. Liquid additives are, for this reason, vastly preferable (particularly for small oxidizer particle sizes), which explains the good results obtained with ferrocenic additives.
- Other additives induce an increase of heat transfers as the diffusion flame stands closer to the burning surface. In this particular case, metallic oxides with sufficiently large particle size are used as flame-holder.

(c) The models

From the various existing models [22], we would like to point out that:

- The first model developed by Summerfield *et al.*, the GDF model (granular diffusion flame), studies the combustion reaction of oxidizing gaseous “pockets” in the gaseous flow of binder decomposition gases. Assuming that the size of these pockets is equal to the size of the solid AP particles, there are two burning regimes:
 - a low-pressure, premixed flame regime,
 - a high-pressure, diffusion flame regime.

The resulting law is usually verifiable, up to approximately 15 MPa:

$$\underbrace{\frac{1}{r} = \frac{a}{p}}_{\text{premixed regime}} + \underbrace{\frac{b}{p^{1/3}}}_{\text{diffusion regime}}$$

where a and b (linked to AP particle size) are constant.

- Hermance calculates the mass flow rates of the binder and of the oxidizer, and introduces the notion of delayed ignition of the AP particles as well as a binder/oxidizer reaction at the surface. He takes into account the possibility of a “turbulent regime” caused by the heterogeneity of the combustion at the propellant surface. This regime modifies the thermal characteristics of the gases and causes an increase of the pressure exponent when the flow rate is significant.
- The BDP Model (Beckstead *et al.* [8]) takes into account a complex and more realistic flame system: a control parameter is used to adjust the flame’s relative importance in accordance with the pressure range. At low pressure the primary flame is prevalent (HClO_4 /hydrocarbon). At high pressure it is replaced by the AP premixed flame and the final diffusion flame (oxidizing products produced by the AP/hydrocarbon flame). Binder and AP surface temperatures are assumed to be the same. A statistical analysis using pyrolysis laws and taking into account the AP size distribution, reputed to be unique, allows calculation of the binder and AP mass flow rates.
- The PEM model (Petite Ensemble Model) offers the possibility of performing a more detailed analysis of the heterogeneities of the surface, coming from a better modeling of oxidizer particle size distribution. By supposing that each flamelet is linked to a particle surrounded by a thin binder coating, and that all these small flames do not interact among themselves, the propellant can be regarded as a collection of simpler propellants (one particle size log-normal distribution) called pseudo-propellants. The description of the combustion of each pseudo-propellant uses the same flame system as the BDP model. Its mass flow rate is calculated on the basis of AP particle combustion as a function of time.

As in the case of BDP, mathematical formulae allow for evaluating geometry of the pseudo-propellant burning area. The PEM model assigns an identical value to the surface temperature for the binder and the oxidizer of each pseudo-propellant. The burning rate of the entire propellant is determined by averaging the burning rates of each pseudo-propellant.

- In France, the method developed by ONERA [23] is similar to the last two models. The flame system is the BDP system, with the exclusion of the primary flame. The calculation of the mass flow rate is also done as a function of the combustion time of a particle. But the pyrolysis of the ingredients is determined by using two different surface temperature values, one for AP and the other for the binder. Like the PEM model this method allows computations for several different values of the filler particle size.

2.2.3.3. *Combustion mechanisms of advanced energetic binder propellants*

RDX or HMX, which significantly increase the specific impulse, are introduced in the EDB-type binder. These are the so-called composite modified double-base propellants. They are divided into two families (CMCDB and XLDB), based on their manufacturing process and resulting different ballistics characteristics (Chapter 11). Because their combustion mechanisms are very similar, the following section discusses only those related to XLDB propellants. Their performance level may be further increased by adding ammonium perchlorate and aluminum to their ingredients (NEPE propellants). The preceding discussion on the various ingredients behavior of homogeneous and heterogeneous propellants will now help to understand better the combustion mechanisms of these two major families of solid propellants.

(a) Combustion mechanisms of XLDB propellants

Observation of the burning area

By observing the combustion of samples, we see that nitramine particles melt at the surface, under the effect of heat flux. Therefore an intimate mixture, close to the surface, of the various gaseous species takes place, facilitating reactions led by premixed flames. We know that the nitramine molecule has a balanced amount of oxidizer and reducer. In addition, the combustion products are mostly N_2 , CO, and H_2O . Since the products of the primary flame are mainly NO, CO, and H_2 , we may safely assume that there is no interaction between the various flame systems.

Burning rate law and formulation parameters

The burning rate law of a polyester binder is shown in Fig. 4. It is close to that of a “cold” extruded double-base propellant. We also see, in this figure,

that it is slightly modified by the addition of nitramine. The propellant burning rate realizes a compromise between the burning rate of the binder and that of the nitramine. Experience has also shown that the size of the particles has no effect on burning rate: this is explained, at least at low pressure, by the nitramine melt layer at the surface. Finally, we see that the exponent remains very high, regardless of the pressure level.

Influence of the ballistic catalysts

Fifer [20] has summarized the main results already known concerning the catalysis of these propellants. When researching ballistic catalysts it is necessary to act either on binder or on nitramine.

- Catalysts of binder decomposition

Catalysts used with homogeneous propellants (lead salts) develop a carbonized layer at the surface, leading to a strengthening of the NO-C reactions. They cannot, however, all be used with a polyester binder, because they catalyze the cross-linking reaction, resulting in an unacceptable rise of propellant viscosity during processing. Some of these catalysts induce super-rates, although less spectacular than with homogeneous propellants: the thickness of the carbon deposit at the surface is, in this case, certainly less than with nitroglycerine- and nitrocellulose-based propellants.

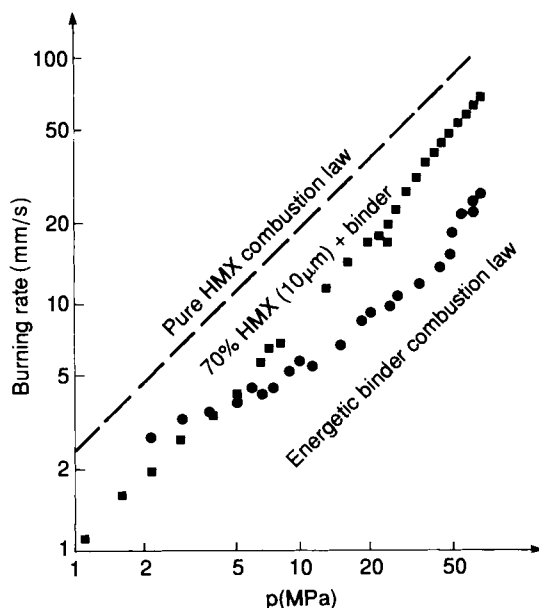


FIG. 4.4. Burning rate laws for propellant and basic ingredients.

- Additives facilitating nitramine decomposition

Because of the large quantities of nitramines added to the propellant, another possibility consists in facilitating the decomposition of the filler. Today, part of the research efforts are oriented to the development of products that would have such effects.

(b) Combustion mechanism of NEPE propellants

Observation of the burning area

Current compositions use a polyether binder, more heavily oxygenized than a polyester binder. In addition to the nitrated plastifier and the nitramines already contained in the XLDB propellants, NEPE propellant performance is increased by adding ammonium perchlorate and aluminum.

By introducing ammonium perchlorate, the structure of the flame zone is significantly modified. Oxidizing species resulting from AP decomposition and hydrocarbons produced by the binder form diffusion flames leading to the disappearance of the very characteristic dark zone. The flame of a NEPE propellant is very much like the flame of a heterogeneous inert binder propellant.

Burning rate law and composition parameters

- Behavior of the binder

Although the burning rate laws of polyether and polyester binders are very close, when ammonium perchlorate is added the polyether binders show very peculiar behavior. Experience has shown that it is capable of dissolving a non-negligible quantity of AP; saturation was seen at a 6% mass ratio value of $AP/(AP + \text{binder})$. The portion of dissolved AP brings about the appearance of a premixed flame with the gaseous products of the binder. The burning rate of the so- "filled" binder increases rapidly and its pressure exponent is high.

- Propellant burning rate law

Due to the formation of diffusion flames, the propellant burning rate depends on the AP particle size. While keeping constant AP content in a formulation, the burning rate can be improved by using micron-size particles. The addition of increasing quantities of AP promotes the formation of diffusion flames, particularly in the cases of medium or large particle sizes; lowering of pressure exponent is subsequently observed.

3. Steady-State Combustion in a Solid Propellant Rocket Motor

The causes of the modification of propellant burning rate law are studied in this section which also deals with methods used to predict the steady-state operation of a rocket motor.

3.1. MODIFICATIONS OF THE BURNING RATE LAW INDEPENDENT OF THE INTERNAL AERODYNAMIC FIELD

3.1.1. Modifications caused by involved materials

3.1.1.1. Modifications occurring at the propellant/insulator interface

In the case of an end-burning combustion mode, the solid propellant grain is particularly susceptible to this phenomenon. An analysis of the burning front after quenching often shows a surface deformation, easily explained by a modification of the burning rate in the immediate vicinity of the thermal insulator (Fig. 5).

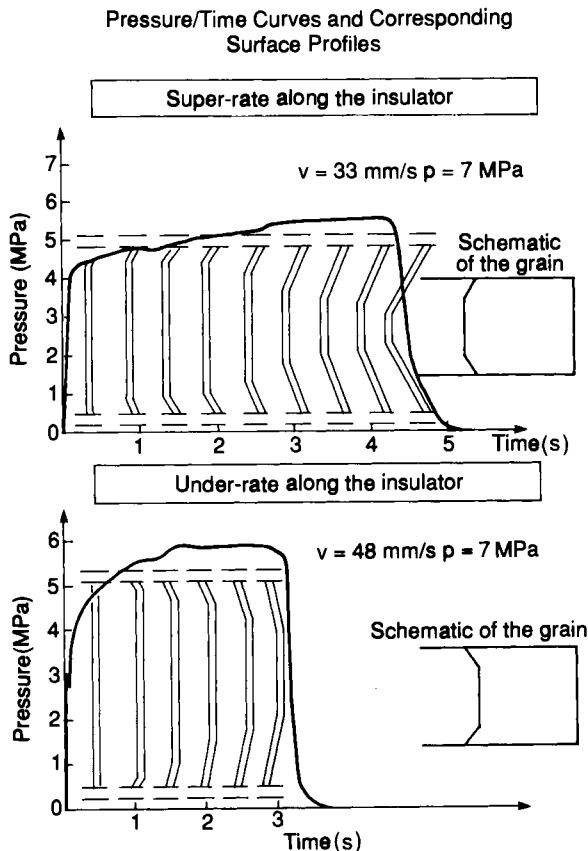


FIG. 4.5. Visualization of the regression front of an end-burning grain.

(a) Origin of local burning rate modification

- Large concentration of fine particles in the area close to the inhibitor, or peculiar distribution of the particles in that area

These particles may be ammonium perchlorate, anti-instability additives, or ballistics catalysts used in solid form. If finely divided, all these ingredients increase the burning rate values. Messner [24] indicates that super-rate values of 70% have been obtained with compositions containing iron oxide. Smith [25] comments on tests demonstrating the accumulation of AP close to an interface. Jolley *et al.* [26], however, believe that this behavior does not systematically occur.

- Migration of propellant liquid ingredients at the interface

During curing, when the propellant is still a dough, and to a lesser degree during aging, the migration of the plasticizer and/or of the ballistic additive may occur. Any displacement of the plasticizer in the inhibitor leads to a local increase in the propellant filler content as well as to a growth in the burning rate. Conversely, a local thinning in ballistic additives content of the propellant decreases the burning rate, but the progression of the flame front in parallel layers tends to counteract this effect.

- Conduction heating of the material near the interface

This phenomenon, resulting from the heat transfer to the motor walls caused by gas flow inside the combustion chamber, occurs consecutively to the temperature rise of the propellant in immediate contact with the heated materials. This situation is more likely to happen during the firing of solid free-standing end-burning grains. The flow of heated gases in the gap between the case and the grain may induce local heating of the insulator and of the propellant in contact.

(b) Remedial measures

- In the case of active binder propellant grains

Here we are concerned with the absorption of nitroglycerine by the thermal insulator: the propellant heat of explosion locally decreases, but the percentage of ballistic additives is clearly increased. The use of highly cross-linked inhibitors or silicones is recommended. A primer (polyisocyanate) may also be interposed, which, delaying ingredients migration, provides the insulator with sufficient time to acquire mechanical strength. When thermal heating of materials occurs near an interface, the addition of an ingredient with endothermic decomposition may prove useful to limit the super-rate.

- In the case of inert binder heterogeneous propellant grains

The super-rate decreases by slowing down migration of the plasticizer

in the bonding resin, usually of a polyurethane type. This can be done by using high cross-linked polyurethanes or primers acting as barriers against migrating species.

3.1.1.2. Controlling the burning rate

(a) Technology used

There have been a large number of studies to evaluate the advantage of end-burning propellant grains with locally controlled burning rates. Two techniques were examined.

- The first technique consists in incorporating strands of propellant perpendicular to the surface, these strands having a higher burning rate than the matrix propellant. No heat exchange occurs between the two propellants because they are good heat insulators, and the angle of resulting cones in the slower composition depends on the ratio between burning rates at the specified operating pressure [27];
- With the other technology, the super-rate effect is obtained by incorporating metal wires inside the propellant grain. These wires melt at a relatively low temperature, conduct the heat very well, and transmit a heat flux to the adjacent propellant, raising its initial temperature and therefore its local burning rate. The wires used are typically made of copper or silver. The design of these wired grains is discussed in Chapter 2.

3.1.2. The hump effect

3.1.2.1. The phenomenon

The hump effect — also called BARF, BRAF, SBRE or RAINBOW when used to indicate the effects due to mechanical stresses in composite propellant grains — refers to an overpressure during firing that may reach 8% of the planned value. This overpressure is not constant during operation. The corresponding time depends on the propellant grain geometry. In a BATES grain, for instance, it corresponds to the point where approximately half the web is burned. This phenomenon may occur in many internal configurations: it has also been observed on star-shaped grains.

The result analysis of such a firing is based on internal ballistics laws, assuming that the burning rate law of the propellant is the same in any point

of the grain. This analysis then provides the evolution of the burning area, becoming an equivalent area, as a function of the burnt thickness. When the hump effect occurs during a firing, comparison of the previous analysis with the theoretical curve of the evolution of the burning area clearly demonstrates the presence of differences (Fig. 6). Those primarily depend on AP, its ratio and size distribution in coarse and fine particles [27,28], and on the presence of aluminum in the composition.

3.1.2.2. Influence of processing

An analysis of results obtained after extinction of a BATES propellant grain at the maximum value of overpressure, shows that hump effect is caused by a burning rate law change as a function of the propellant thickness. Friedlander and Jordan [28] offer the same interpretation. The explanation may be a peculiar distribution of the propellant solid fillers, induced by the manufacturing process.

3.1.2.3. Taking the hump effect into consideration for ballistics predictions

Currently, it is only through accumulating results analyses from firings that an average and empirical law of burning rate deviations for a specific propellant grain may be obtained, of the form:

$$\frac{r_r}{r_0} = f(e)$$

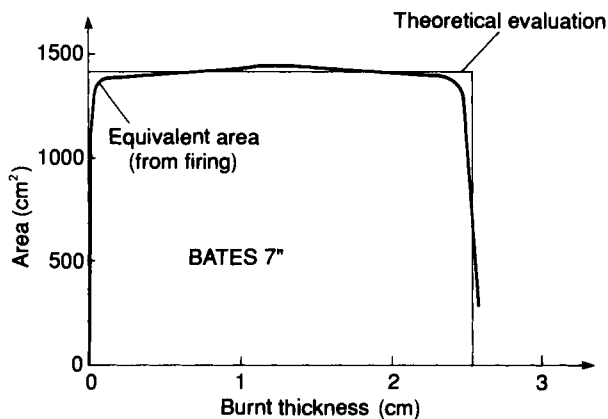


Fig. 4.6. Comparison of burning area evolutions of a BATES grain.

where:

- r_r is the actual burning rate of the propellant during firing;
- r_0 is the known burning rate of the propellant, excluding the hump effect;
- e is the burnt thickness.

As a rule, the ratio r_r/r_0 varies by 5% in a range from 0.95 to 1.05. For some grain shapes (tubular, star) with a mainly radial burning the above law exhibits a hump when plotted. For more complex shapes (FINOCYL type) with a combination of several types of combustion (in R , Z and θ), the curve has the shape of a sinusoid.

Currently, precise ballistics predictions presuppose a sufficient number of results from experiments the analysis of which helps estimating the $r_r/r_0 = f(e)$ law which has to be considered in the computations.

3.1.3. Mechanical stresses

Mechanical stresses occur in case-bonded propellant grains:

- during the cooling period after propellant curing;
- during operation, when the combustion chamber is pressurized.

In some cases these stresses modify the burning rate law.

3.1.3.1. At the bonding interface

Kallmeyer *et al.* [30] demonstrate the increase of the super-rate at the propellant/inhibitor interface as a function of the bonding stress level; this stress level is a function of the difference between curing and firing temperatures.

3.1.3.2. Inside the propellant

Internal stresses cause dewetting to occur between the various fillers and the binder; dewetting increases with load intensity. As a result the propellant acquires a certain internal porosity and becomes compressible. An increase in the burning rate is then observed [31]. Figure 7 illustrates this effect on a strand which has been first strained, then inhibited with a stiff agent strong enough to maintain elongation. The burning rate change does correspond to the beginning of the strand volume variation.

3.1.4. Acceleration

The motor operation, in flight, may be modified by the acceleration of the rocket. This modification is particularly clear with aluminized propellant grains.

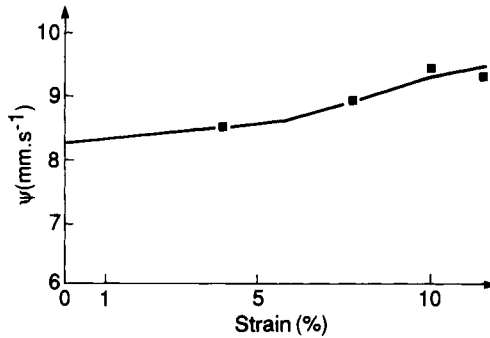


FIG. 4.7. Influence of propellant elongation on the burning rate law. Burning rate vector parallel to the tensile stress.

Extinguishments have shown that the burning surface of this type of propellant, when submitted to a normal acceleration directed toward the propellant, exhibits a large number of small conical craters. They are caused by amounts of aluminum droplets which contribute to heat conduction at the surface and consequently significantly increase the burning rate at the point of contact. When an aluminum droplet becomes larger (and probably oxidizes), the burning rate at the bottom of the crater slows down (though remaining greater than the burning rate without acceleration). The bottoms of the craters flatten themselves out.

Based on studies done on this subject, and illustrated by Fig. 8, we note that this type of phenomenon occurs when:

- the acceleration exceeds a threshold value which is a function of the size of the aluminum particles and of the burning rate (approximately 10 g for

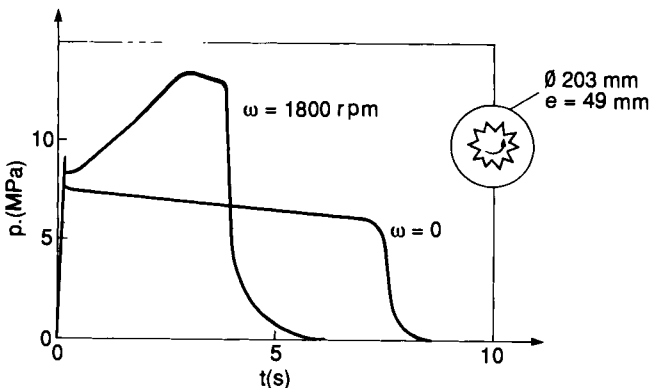


FIG. 4.8. Effect of acceleration on motor operation.

propellant grain burning at 5 mm/s and containing aluminum particles measuring 5 μm);

- the angle between the acceleration and the burning surface normally does not exceed a threshold value (of about 20°); beyond that value, the influence of acceleration on the burning rate is negligible.

3.2. DETERMINATION OF THE FLOW FIELD

3.2.1. Background and fundamentals

The simplified analysis [33] of the motor stationary operation is based on the possibility of realizing equilibrium between:

- the mass flow rate produced by the burning surface of the propellant grain;
- the mass flow rate the nozzle can eject.

The steady-state regime resulting when the two are matched, and related specific fundamental equations, were discussed in Chapter 1. Continuing to assume that combustion and expansion of burned gases form two separate phenomena, respectively taking place in the combustion chamber and in the nozzle, we are able to analyze the transient regime associated with grain ignition and burn-out phases.

3.2.1.1. Transient regime

While we disregard the volume variation of the central port resulting from combustion (rather small since transient phases are short), we do include the term representing internal gaseous mass variations, which stands for the filling (or emptying) of the central port, and is tied to gas compressibility. Therefore the exhaust mass flow rate coming out of the nozzle corresponds to the mass flow rate emitted by the propellant burning surface less the build-up term. The continuity equation is written:

$$t_s \frac{dp_c}{dt} + p_c = \frac{\dot{m}}{C_D A_t} \quad (11)$$

where:

- $t_s = V/(r T_c C_D A_t)$ = the residence time;
- V = volume of the chamber;
- p_c, T_c = pressure and temperature of the chamber;

- A_t = area of the nozzle throat;
 \dot{m} = mass flow rate of the propellant grain;
 C_D = propellant discharge coefficient;
 $r = R/M$ where R is the ideal gas constant, M is the gas molecular weight.

(a) Pressurization

Assuming the validity, under these conditions, of the steady-state burning rate law as well as instantaneous ignition of the entire surface of the propellant grain, the pressure evolution is given by:

$$p_c = p_{c0} \left\{ 1 - \exp \left[1 - (1 - n) \frac{t}{t_s} \right] \right\}^{1/1-n} \quad (12)$$

where p_{c0} is the chamber pressure corresponding to stationary operation.

(b) Depressurization

Assuming a sudden extinction of the entire surface, we have:

$$p_c = p_{c0} \exp \left(-\frac{t}{t_s} \right) \quad (13)$$

3.2.1.2. Requirements when designing a propellant grain

The steady-state regime assumption of Chapter 1 and the simplified reasoning above turn out to be insufficient, for several reasons:

- It only gives an average value for the pressure. This pressure level is uniform in the entire combustion chamber. Its evolution, as a function of propellant thickness, is known as long as the operating point can reasonably be approximated by a succession of discrete equilibria.
- The pressure variations inside the combustion chamber are not determined; they must be known to assess the structural integrity of the propellant grain, particularly at the onset of the firing. They also must be determined in conjunction with the local burning rate expressions (e.g. eqn (1)).
- The gas velocity inside the combustion chamber being assumed to be zero, risks connected with heat transfer increase, as well as erosive burning, cannot be taken into consideration.

- There is no modeling of the non-steady phenomena: eqns (12) and (13) hold a limited validity for the transient sequences. In addition these assumptions do not include variations of the propellant discharge coefficient.

More complete models should include unsteady phenomena and are therefore necessary for a precise knowledge of the internal aerodynamics.

3.2.2. Conservation equations in fluid mechanics

The fluid domain consists of the combustion chamber and nozzle. Some of the boundaries are inert ones, i.e. inert parts of the combustion chamber and of the nozzle. The burning surface, on the other hand, is an injecting boundary which, over time, moves along its normal at a velocity r (propellant burning rate law).

SNPE computer codes solve the fluid mechanics equations while respecting the conservation conditions relative to the mass, momentum and energy, within a framework of restrictive assumptions concerning the nature of the fluid and its heat exchanges with the case walls:

- The fluid produced by the propellant combustion is a gas assumed to be ideal and heated at a high temperature.
- The fluid is non-viscous, non-reacting and non-conductive. There is no heat exchange with the walls. The boundary with the burning propellant occurs at the end of the flame; the flame height is assumed to be negligible.
- The fluid is single-phased. There is no need to introduce the condensed phase because neither the pressure fields nor the burning rate are basically modified by its presence. It should, however, be taken into consideration in any realistic performance prediction (Chapter 3).

3.2.3. Solving the one-dimensional equations

3.2.3.1. Local equations

Each term of the conservation equations will be assessed in the fluid sector shown in Fig. 9. This sector has two stationary boundaries (A_1 and A_2) and a moving boundary S .

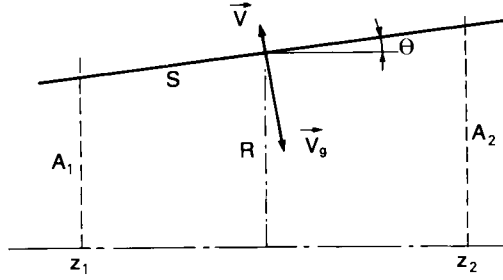


FIG. 4.9. Element of fluid. One-dimensional assumption.

(a) Absolute velocity of the gases at the combustion wall

The fluid velocity at the wall is assumed to be the exhaust gas velocity released at the wall. Here, the equation of mass conservation requires:

$$\rho \vec{v}_r = \rho_p \vec{v} \quad (14)$$

where:

- ρ, ρ_p = density of, respectively, the gases and the propellant;
- \vec{v}_r = velocity of the gases relative to the wall;
- \vec{v} = absolute velocity of the wall.

Therefore:

$$\vec{v}_r = \vec{v}_g - \vec{v} \quad (15)$$

where \vec{v}_g is the absolute velocity of the gases at the wall.

Taking into account the respective orientation of each of the vectors, we find:

$$v_g = v \left(\frac{\rho_p}{\rho} - 1 \right) \quad (16)$$

(b) Continuity

With:

- \vec{u} = flow velocity vector
- \vec{n} = vector perpendicular to the surface. The term of the exhaust flow is calculated for A_1 , A_2 , and S (the normal directed outside the field)

from:

$$[\vec{u} - \vec{v}] \cdot \vec{n} \Big|_{A_1} = \vec{u} \cdot \vec{n} = -u(z_1) \quad (17)$$

$$[\vec{u} - \vec{v}] \cdot \vec{n} \Big|_{A_2} = \vec{u} \cdot \vec{n} = u(z_2) \quad (18)$$

$$[\vec{u} - \vec{v}] \cdot \vec{n} \Big|_S = \vec{v}_g \cdot \vec{n} - \vec{v} \cdot \vec{n} = -(v_g + v) \quad (19)$$

knowing that:

$$dS = 2\pi R \frac{dz}{\cos \theta}; \quad \frac{\partial A}{\partial t} = 2\pi R \frac{v}{\cos \theta}$$

and for a small dz increase, we have:

$$\frac{\partial}{\partial t}(\rho A) + \frac{\partial}{\partial z}(\rho u A) = \rho_p \frac{\partial A}{\partial t} \quad (20)$$

(c) Momentum

Assuming a uniaxial flow along the z axis, the projection on z of the tensorial product of the equation below must be calculated:

$$\frac{\partial}{\partial t} \int_{V(t)} \rho \vec{u} dV = - \int_{S(t)} \rho [\vec{u} \otimes (\vec{u} - \vec{v})] \vec{n} dS - \int_{S(t)} (p I + T) \vec{n} dS$$

where:

T = deviator of the tensor of the second order, representative of viscous tensions;

I = identity matrix;

$V(t)$ = moving volume limited by the surface $S(t)$

We obtain:

$$\text{Proj on } z [\vec{u} \otimes (\vec{u} - \vec{v})] \vec{n} \Big|_{A_1} = [\vec{u} \otimes \vec{u}] \vec{n} \Big|_{A_1} = -u^2(z_1) \quad (21)$$

$$\text{Proj on } z [\vec{u} \otimes (\vec{u} - \vec{v})] \vec{n} \Big|_{A_2} = [\vec{u} \otimes \vec{u}] \vec{n} \Big|_{A_2} = u^2(z_2) \quad (22)$$

$$\text{Proj on } z [\vec{u} \otimes (\vec{u} - \vec{v})] \vec{n} \Big|_S = -v_g(v_g + v) \sin \theta \quad (23)$$

Taking into account that $\partial A/\partial z = 2\pi R \tan \theta$, and by making z_1 approach z_2 , we obtain:

$$\frac{\partial}{\partial t}(\rho u A) + \frac{\partial}{\partial z}(\rho u^2 A) + A \frac{\partial p}{\partial z} = \rho_p v^2 \frac{v_g}{v} \frac{\partial A}{\partial z} \quad (24)$$

(d) Energy

When it is integrated over the volume $V(t)$, the local conservation equation for energy gives:

$$\begin{aligned} \frac{\partial}{\partial t} \int_{V(t)} \rho \left(e + \frac{\tilde{u}^2}{2} \right) dV = & - \int_{S(t)} \rho \left(e + \frac{\tilde{u}^2}{2} \right) (\tilde{u} - \tilde{v}) \tilde{n} dS \\ & - \int_{S(t)} (p \cdot \tilde{u} + T \cdot \tilde{u}) \tilde{n} dS - \int_{S(t)} \tilde{q} \cdot \tilde{n} dS \end{aligned}$$

The various terms are assessed as above, and the local expression is written:

$$\frac{\partial}{\partial t}(\rho \varepsilon A) + \frac{\partial}{\partial z}(\rho \varepsilon u A) + \frac{\partial}{\partial z}(p u A) = \frac{\partial A}{\partial t} \left[p \frac{v_g}{v} + \rho_p \cdot \varepsilon_b \right] \quad (25)$$

where:

- ε = total internal energy of the gaseous discharge, $e = u^2/2$, where e represents the internal energy of the fluid;
- ε_b = total internal energy of burned gases as they are created
 $= e_b + v_g^2/2$, where e_b represents the internal energy of the burned gases.

3.2.3.2. Computer codes for calculations of one-dimensional equations

There are several codes, because the one-dimensional assumption is fairly well justified for propellant grains with a high “length versus diameter” ratio and a gas flow section area that evolves slowly. This assumption allows rapid executing times. We will limit ourselves to one example: PROCNE 1 [34], which is very widely used for preliminary propellant grain design analyses.

The unsteady terms of the conservation equations are taken into account. The fluid domain is shared into discrete sections along the axis of the propellant grain: it includes the combustion chamber and the nozzle. The

numerical procedure selected for this code is the fractional two-steps method, proposed by Yanenko [35]. PROCNE 1 code is used to calculate the evolution of the internal aerodynamic field while taking into account the geometry evolution as a function of time. Figure 10 compares predicted pressure and thrust levels to experimental results for a nozzleless motor.

3.2.4. Calculation of conservation equations for complex geometries

Improved ballistics performances of rocket motors are obtained through propellant volumetric loading fraction enhancement, typically realized with complex geometrical shapes. Such configurations entail the presence of significant variations in the pressure and fluid velocity, as well as the possibility of couplings between the propellant burning rate law and the local

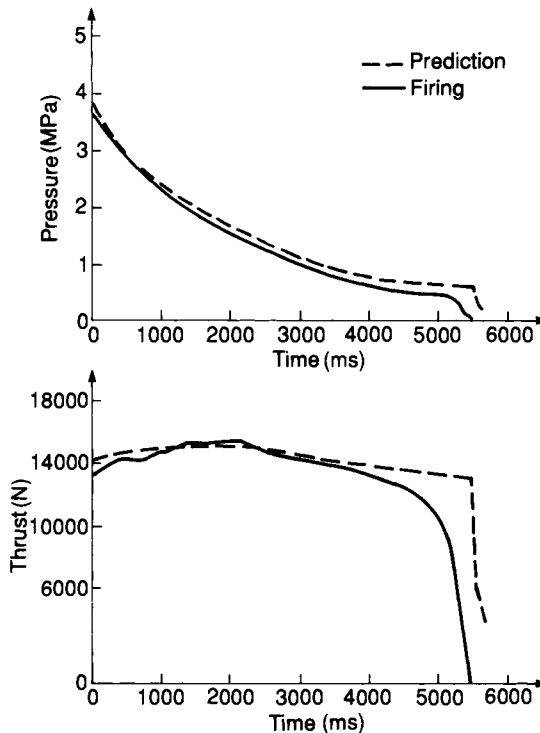


FIG. 4.10. Comparison between prediction (PROCNE) and experiment (nozzleless motor).

aerodynamic field. Consequently, the fluid mechanics equations must be resolved in a situation which is as representative as possible.

3.2.4.1. Fundamentals of the two- and three-dimensional codes

The numerical scheme used to solve the governing equations was created by Godunov *et al.* [36]. A few reminders on shock waves and discontinuity decomposition are necessary before discussing this procedure.

(a) Shock waves

First, some fluid mechanics notions: given a source S of small perturbations in a motionless fluid or in a uniform motion (Fig. 11):

- Motionless fluid: $u = 0$
A perturbation occurring at time $t = 0$ propagates at the speed of sound a in all directions and occupies at time t a spherical surface with a radius value of at .
- Fluid in uniform translation, with $u < a$
In a subsonic flow the perturbation spheres are inside each other, and surround the source. With sufficient time the perturbations reach every point of the fluid.
- Fluid in uniform translation, with $u > a$
In a supersonic flow the perturbation waves occur within an envelope. Only the areas within that envelope are affected by the perturbations.
- Formation of a discontinuity

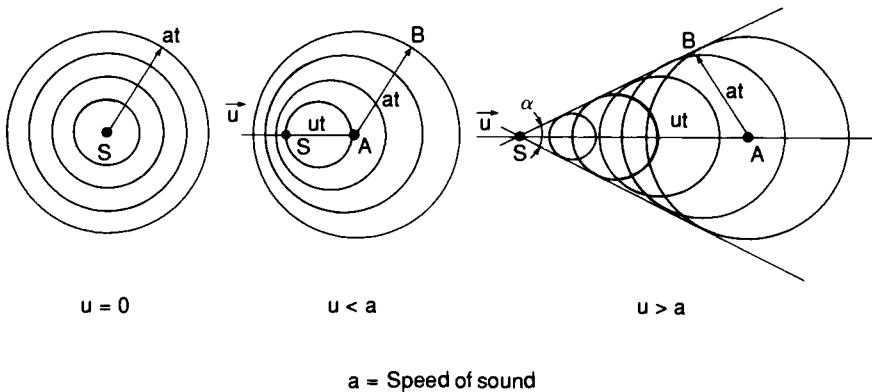


FIG. 4.11. Propagation of small perturbations in a uniform flow fluid.

In a fluid activated by a slight compression the successive waves will propagate faster and faster because of the rise in temperature of the medium, finally catching up to each other and forming a compression wave. In the opposite case, when the fluid is subjected to a slight expansion, the waves no longer catch up with each other because of temperature decay: a discontinuous expansion wave does not occur in most gases, although it may occur in some computational methods.

- Evolution through a flat discontinuity surface (Fig. 12)

When going through a discontinuity surface a compressible fluid is subjected to finite pressure and temperature variations, but its velocity suddenly varies in magnitude as well as in direction. The conservation equations on the ABCD volume are written as follows:

- Mass conservation

$$\rho_1 u_{1n} = \rho_2 u_{2n} \quad (26)$$

- Momentum conservation

$$p_1 + \rho_1 u_{1n}^2 = p_2 + \rho_2 u_{2n}^2 \quad (27)$$

where $u_{1t} = u_{2t}$

- Energy conservation assuming adiabaticity:

$$\frac{u_{1n}^2}{2} + \frac{\gamma}{\gamma - 1} \frac{p_1}{\rho_1} = \frac{u_{2n}^2}{2} + \frac{\gamma}{\gamma - 1} \frac{p_2}{\rho_2} = \frac{\gamma + 1}{2(\gamma - 1)} \left[c^2 - \frac{\gamma - 1}{\gamma + 1} u_{1t}^2 \right] \quad (29)$$

where $c = \sqrt{\frac{2(\gamma - 1)}{\gamma + 1} c_p T_c}$

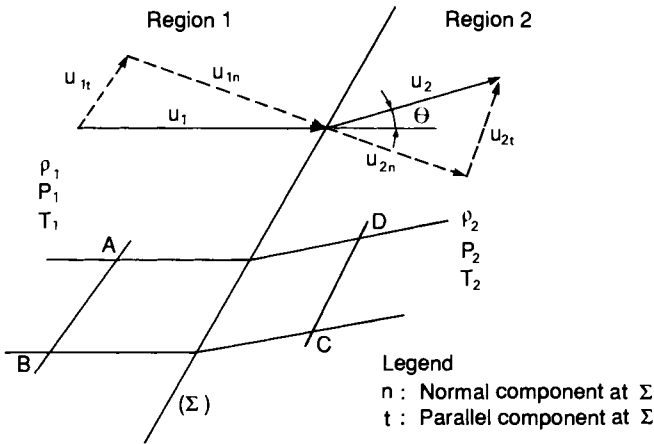


FIG. 4.12. Flow field evolution through a discontinuity surface (Σ).

to which the equation of the ideal gas state is added:

$$p_1 = \rho_1 r T_1; \quad p_2 = \rho_2 r T_2$$

where $r = R/M$ = specific gas constant

Hugoniot/relationship

This determines the relationship between p_1 , ρ_1 , p_2 and ρ_2

$$\frac{\rho_2}{\rho_1} = \frac{1 + \frac{\gamma + 1}{\gamma - 1} \frac{p_2}{p_1}}{\frac{\gamma + 1}{\gamma - 1} + \frac{p_2}{p_1}}$$

This relation is definitely different from the isentropic:

$$\left(\frac{\rho_2}{\rho_1} \right)^\gamma = \frac{p_2}{p_1}$$

Through a shock wave, the fluid therefore undergoes an irreversible evolution. The entropy for an ideal gas is given by:

$$s = c_v \ln \left(\frac{p}{\rho^\gamma} \right) + \text{constant}$$

The Hugoniot relationship expresses an actual physical evolution only when it corresponds to an increase of entropy.

(b) Process for discontinuities analysis

Godunov *et al.* [36] propose the following method: when two masses of the same gas, assumed ideal and compressed at different pressure levels, come into contact, the contact surface forms a discontinuity surface within the initial pressure distribution. The physical values on each side of the surface may undergo any sort of jump. Discontinuity, however, can exist as a stable formation only if it satisfies certain conditions; if not, it breaks down into several discontinuities becoming distant from each other with time. Consequently, several configurations may occur. Pressure and velocity values on each side of the contact discontinuity are identical; density and internal energy differ, on the other hand. These two fields are themselves separated from the non-perturbed area by either a shock wave or an expansion wave.

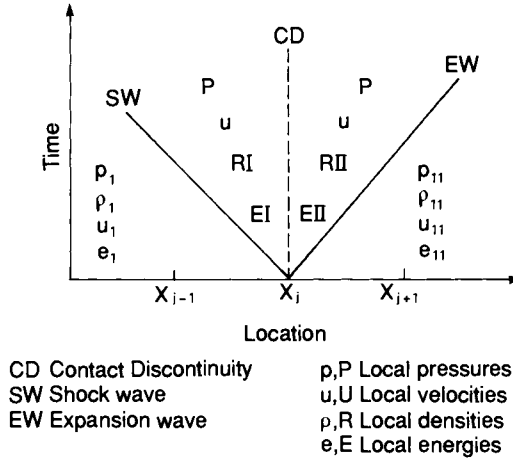


FIG. 4.13. Discontinuity splitting between two gaseous masses.

Figure 13 illustrates the one-dimensional case of a shock wave to the left and an expansion wave to the right. These are usually expressed as follows:

- Left-hand wave:

$$U - u_I + \frac{P - p_I}{\beta_I} = 0 \quad (31)$$

- Right-hand wave:

$$U - u_{II} - \frac{P - p_{II}}{\beta_{II}} = 0 \quad (32)$$

For a shock wave

$$\beta_i = \sqrt{\rho_i \frac{\gamma + 1}{2} P + \frac{\gamma - 2}{2} p_i} \quad (33)$$

where $i = I$ or II , depending on whether the wave is to the left or to the right.

For an expansion wave:

$$\beta_i = \frac{\gamma - 1}{2\gamma} \rho_i a_i \frac{1 - \frac{P}{p_i}}{1 - \left(\frac{P}{p_i}\right)^{\frac{\gamma - 1}{2\gamma}}} \quad (34)$$

where:

$$a_i = \text{the sonic speed of the medium } i = \sqrt{\frac{\gamma p_i}{\rho_i}}$$

$i = \text{I or II}$, depending on whether the expansion wave is to the left or to the right.

Consequently, the configuration appearing when two gaseous masses come into contact can be determined. Elimination of U between eqns (31) and (32) allows the determination of P solving:

$$F(P) = u_I - u_{II} = \frac{P - p_I}{\beta_I} + \frac{P - p_{II}}{\beta_{II}} = f(P, p_I, \rho_I) + f(P, p_{II}, \rho_{II}) \quad (35)$$

with:

$$f(P, p_i, \rho_i) = \begin{cases} \frac{P - p_i}{\sqrt{\rho_i \left(\frac{\gamma + 1}{2} P + \frac{\gamma - 1}{2} p_i \right)}} & \text{where } P \geq p_i \\ \frac{2}{\gamma - 1} a_i \left[\left(\frac{P}{p_i} \right)^{\gamma - 1/2\gamma} - 1 \right] & \text{where } P < p_i \end{cases} \quad (36)$$

The analysis of the function $F(P)$ reveals several possibilities. Assuming that $p_I < p_{II}$ and writing:

$$F(p_I) = U_{\text{exp}} = -\frac{2a_{II}}{\gamma - 1} \left[1 - \left(\frac{p_I}{p_{II}} \right)^{\gamma - 1/2} \right] \quad (37)$$

$$F(p_{II}) = U_{\text{shock}} = \frac{p_{II} - p_I}{\sqrt{\rho_I \left(\frac{\gamma + 1}{2} p_{II} + \frac{\gamma - 1}{2} p_I \right)}} \quad (38)$$

- If $0 < P \leq p_I$, two expansion waves propagate, one to the left and one to the right. We have:

$$u_I - u_{II} \leq U_{\text{exp}}$$

- If $p_I < P < p_{II}$, a shock wave develops to the left and an expansion wave develops to the right. In which case:

$$U_{\text{exp}} < u_I - u_{II} < U_{\text{shock}}$$

- If $P \geq p_{II}$, two shock waves propagate, one to the left and the other to the right. In which case:

$$u_I - u_{II} \geq U_{\text{shock}}$$

The value of P is determined by resolving eqn (35), proceeding by successive iterations using Newton's tangent method which, as indicated by

the authors, ensures a rapid convergence from an initial value. The other parameters are calculated using the P value at convergence [36].

(c) Numerical procedure

Looking at the difference scheme for the unsteady one-dimensional equations of the fluid dynamics developed by Godunov *et al.*, we are provided with a simple illustration of the method. Assuming density ρ , impulse ρu , and total energy $\rho(e + u^2/2)$ constant on each elementary part of the field, the conservation equation laws (described in section 3.2.2) although simplified in terms of the fluid behavior and applied to grid $j - 1/2$ (part $[x_{j-1}, x_j]$) for the period of time from t to $t + \Delta t$, are written as follows:

$$\begin{aligned} (\rho^{j-1/2} - \rho_{j-1/2})(x_j - x_{j-1}) + \Delta t([RU]_j - [RU]_{j-1}) &= 0 \\ ([\rho u]^{j-1/2} - [\rho u]_{j-1/2})(x_j - x_{j-1}) + \Delta t([P + RU^2]_j - [P + RU^2]_{j-1}) &= 0 \\ \left(\left[\rho \left(e + \frac{u^2}{2} \right) \right]^{j-1/2} - \left[\rho \left(e + \frac{u^2}{2} \right) \right]_{j-1/2} \right) + \Delta t \left(\left[RU \left(E + \frac{U^2}{2} \right) + PU \right]_j \right. \\ &\quad \left. - \left[RU \left(E + \frac{U^2}{2} \right) + PU \right]_{j-1} \right) = 0 \end{aligned}$$

Indices in lower position stand for the values at time t while indices in upper position stand for those at time $t + \Delta t$.

The extension of the calculations to three-dimensional configurations can be done: the method used is a finite volume explicit method. The calculations have to be run over a three-dimensional fluid domain discretized in small elementary cells. Within each cell i (volume V_i , surface Σ_i), the conservation equations can be generalized:

$$\frac{\partial}{\partial t} \int_{V_i} (\text{F.F.C.}) dV = \int_{\Sigma_i} (\text{F.F.C. flux}) d\Sigma \quad (39)$$

where F.F.C. (for flowfield characteristics) is either gas mass density, momentum or energy.

In order to obtain the left-hand term in (39), F.F.C. is assumed to be constant on each basic cell, leading to the following approximation:

$$\frac{\partial}{\partial t} \int_{V_i} (\text{F.F.C.}) dV = \frac{V_i}{\Delta t} \left[\text{F.F.C.}_{t+\Delta t, i} - \text{F.F.C.}_{t, i} \right]$$

where $\text{F.F.C.}_{t, i}$ represents F.F.C. at time t over cell i .

To calculate the second term of equality (39) which corresponds to F.F.C. flux through the boundaries of the grid cell, we resolve the contact discontinuity problem with each cell adjacent to cell i using the method described in the previous section.

These calculations are performed in a direction normal to each face of cell i . The tangential components of the velocity are then not modified by crossing a shock or an expansion wave.

This gives the characteristics of the fluid at that boundary: pressure, normal velocity, tangential velocity, mass density and energy. The amplitudes of various fluxes can then be explicitly computed at time $t + \Delta t$ and in cell i using:

$$\text{F.F.C.}_{t+\Delta t, i} = \text{F.F.C.}_{t, i} + \frac{\Delta t}{V_i} \int_{\Sigma_i} (\text{F.F.C. flux}) d\Sigma$$

Equation (39) being completed with the ideal gas state equation, the F.F.C. values at time $t + \Delta t$ can be explicitly calculated, based on the known values at time t and on the “major values” (P , U , R , E) obtained from the discontinuity analysis:

- in two-dimensions, to each of the four faces;
- in three dimensions, to each of the six faces of cell i .

The values of u_I and u_{II} which are taken into account for the calculation at this point are the normal components of the velocity vectors over the boundary selected.

(d) Boundary conditions

The scheme description (eqn 39) shows that boundaries need to be introduced in the form of mass, momentum, and energy fluxes crossing the faces located at the boundary of the computational domain. Further data, depending on the type of boundary met, are necessary to determine these fluxes:

- In the case of an impermeable wall the velocity of the gases penetrating into the cell must be zero at the boundary, i.e. $U = 0$. The determination of P then requires the creation of a phantom cell characterized by the values (u_I , p_I , ρ_I) satisfying the above condition. If (u_{II} , p_{II} , ρ_{II}) are the values of the boundary cell, we see that the selection $u_I^N = -u_{II}^N$ (where the upper index N stands for the component of the velocity vector perpendicular to the face), $p_I = p_{II}$, and $\rho_I = \rho_{II}$ is a solution of the problem.
- If the boundary corresponds to a symmetry plane of the propellant grain, the calculations are handled in the same manner as for the impermeable wall.
- In the case of an injecting wall two steps are necessary to determine the various fluxes. First, the reaction of the wall is calculated as for the inert wall. Second, the fluxes obtained are increased by the mass and energy

fluxes resulting from the propellant combustion; the momentum flux related to propellant combustion is assumed to be zero.

- If the boundary is located at the exit plane of the nozzle in the supersonic jet zone, the simplest solution consists in extending the fluid domain a little beyond this plane, and assigning to the phantom cell the same F.F.C. values as those computed for the boundary cell. At the beginning of the calculations, before the nozzle plays its full role, the condition is identical, and consequently not very strict. Care must be taken that the induced error is not spread in the whole internal fluid flow domain.

3.2.4.2. *Examples using the two- and three-dimensional programs*

In Fig. 14 a comparison between the calculated and experimental results is shown for a two-dimensional plane case. The experimental set-up developed by ONERA reproduces a configuration close to the combustion chamber of a nozzleless rocket motor. Its porous walls are fed by a cold air flow (260 K) sufficient to initiate a supersonic regime in the expansion region. Figure 15 illustrates the calculated results for a forehead FINOCYL type of propellant grain.

3.2.5. *Experimental determination of the flowfield*

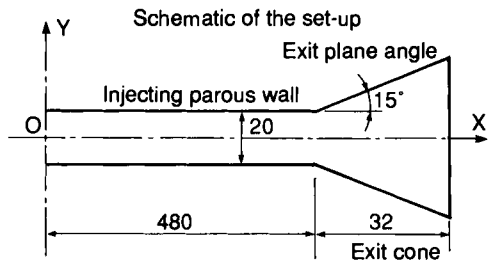
The tests are performed to:

- determine the flowfield pattern in actual geometries;
- confirm results obtained through predictions. These tests are done on models the geometry of which sometimes differs from the actual propellant grains configurations; nevertheless they have the advantage of an easier control of input parameters and of less complex boundary conditions.

3.2.5.1. *Flowfield measurements*

(a) Pressure measurements

Tests on steady flows do not require the use of transducers having a very wide bandwidth. But to obtain correct measurements of the pressure level in various locations in the flowfield, these pressure gages must be accurate even for fairly high average levels.



Evolution of the pressure P/P_o ratio along the symmetry axis

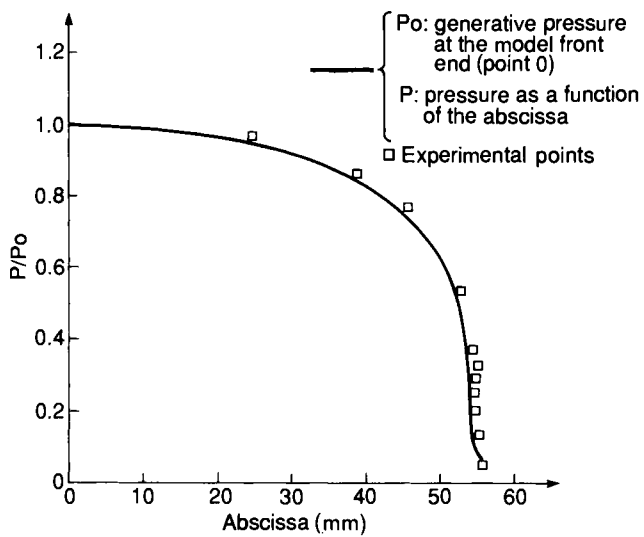


FIG. 4.14. Procne code. Comparison between prediction and experiment.

(b) Velocity measurements

The hot-wire technique [37] used to determine both the average value of the velocity and its fluctuations (needed when evaluating the Reynolds tensor components) is interesting for “clean” flows of cold gases (without particles). Laser anemometry (used by ONERA) allows to examine the local velocity field in cold gases, but it necessitates seeding the fluid with very fine particles.

(c) Temperature measurements

A manufacturing technique for thermocouples of short response time has also been developed. This provides the possibility of measuring temperature in the hot and corrosive gaseous environment of the combustion chamber.

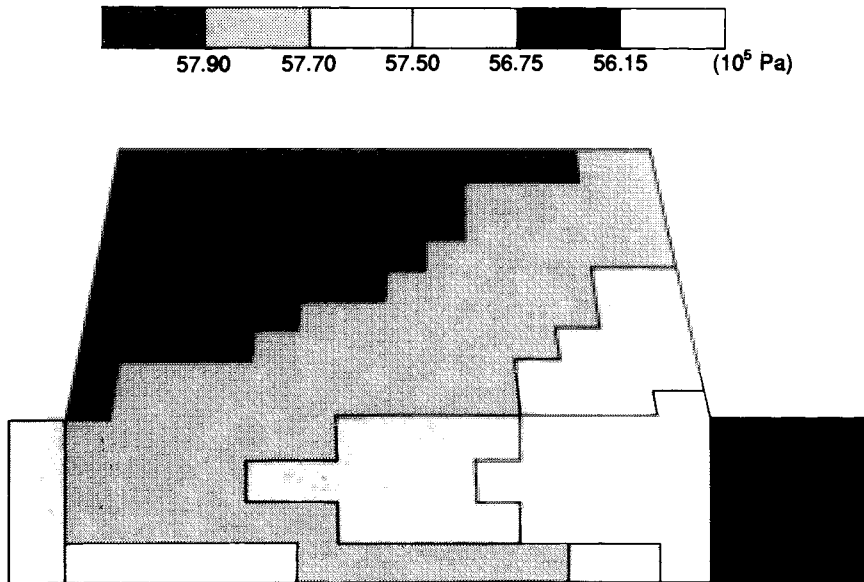


FIG. 4.15. Pressure distribution in a Fin.

(d) Visualizations

Visualization consists of providing a transparent viewport on an experimental set-up in order to observe the flowfield during a test. This process is used with cold and hot gases as well. At very high temperatures it is necessary, however, to make sure that the viewport ablation is not able to distort both the observation of the phenomenon and its progress.

3.2.5.2. Models for the determination of flowfield pattern

(a) Models for analysis of gap pressurization

Free-standing propellant grains exhibit a gap between the thermally insulated metal case and the insulator surrounding the propellant grain. During ignition the pressure inside this gap is not in equilibrium with the pressure in the combustion chamber. Because of this pressure difference, the propellant grain flattens against the case wall, causing an elongation of the propellant grain and the appearance of non-isotropic compression stresses which may affect its structural integrity, particularly in the case of cold firing.

The experimental model is made of a case in which a cylindrical center port propellant grain is placed. The whole assembly is pressurized through an external tank. This is a cold gas test. Numerous gages (pressure, gap

thickness) distributed along various generatrices, describe the model behavior when it is subjected to a pressure rise at a given rate.

(b) Model for streamlines visualization

Several types of geometry can be tested. Figure 16 shows an example of an axisymmetric model. A half-cylindrical propellant grain with axisymmetrical slots, modeling the actual propellant grain configuration, is glued to a viewport. Photographs reveal streamlines issuing from the slots: they experience a significant deviation when meeting the main central spout. In addition, photographs show the occurrence of a burning rate faster at the downstream bottom of the slots than anywhere else in the propellant grain.

(c) Analysis model for pressure field

The propellant grain for these models is axisymmetric, or three-dimensional (FINOCYL). The locations of the various transducers are selected to allow a local measurement of the pressure along the symmetry axes and the burning surface.

The geometry of the chamber is specifically designed so that there are significant pressure differences between the various measurement points. This

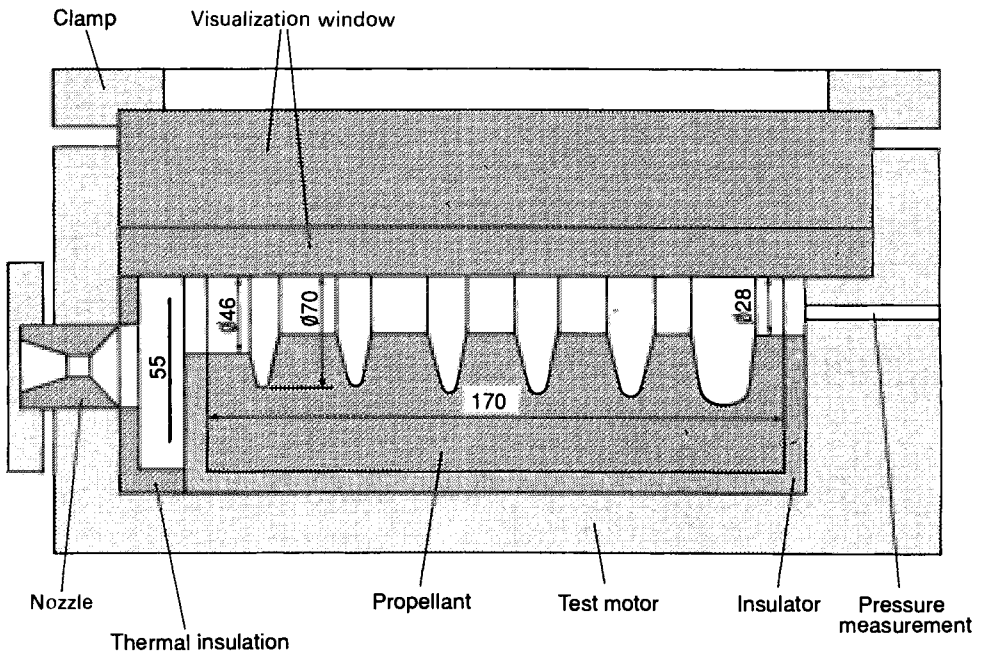


FIG. 4.16. Fluid flow lines visualization during firing of an axisymmetrical test motor. Schematic of the experimental set-up.

also explains why the model is fired under relatively high pressure (approximately 10 MPa), and why, in some cases, it is equipped with a central rod used to increase the pressure differences in the chamber.

3.3. BALLISTICS MODIFICATIONS TIED TO THE INTERNAL AERODYNAMIC FIELD

Performance increases of rocket motors have led to the development of grains with high volumetric loading fractions. The resulting geometries often have the disadvantage of reducing the port areas which, as a consequence, increases the mass flow in the combustion chamber, particularly at the beginning of firing. Experience has shown that, under these conditions, a local increase in the propellant burning rate, causing a deviation from the theoretical evolution of the grain burning surface, occurs at the beginning of the firing. Figure 17 illustrates the evolution of the pressure obtained at the front end of a long star-shaped propellant grain. It clearly shows the existence of an over-pressure at ignition. This phenomenon, which is nowadays better controlled, is sometimes desired to obtain the specified pressure envelope. Considered for a long time to be undesirable, it must be precisely quantified in order to determine its consequences on the structural integrity and the evolution of the propellant burning area.

3.3.1. *Erosive burning phenomena*

3.3.1.1. *Determination of formulation sensitivity*

A great number of researchers have developed testing equipment to determine the burning rate of a propellant subjected to a hot mean flux

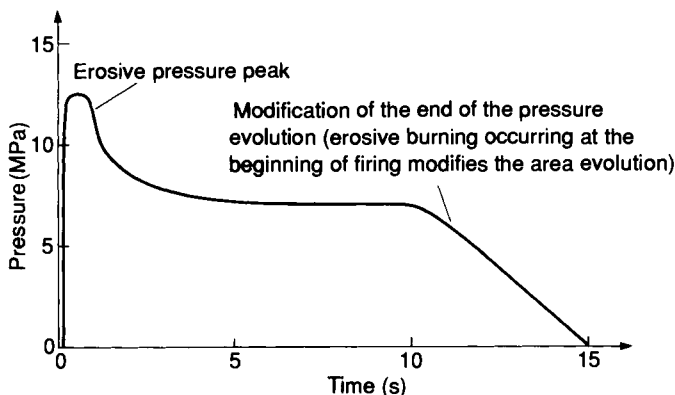


FIG. 4.17. Erosive burning of a star-shaped grain, diameter 203 mm, length 1000 mm.

parallel to its burning surface. Most of them used small test samples, shaped like small thin plates, placed in the hot gas flow released by a gas generator located upstream.

Various methods have been used to determine the burning rate of the sample: X-ray photography, detection of the burning time through a photo-multiplier, extinction to pattern the new surface of the partially-burned sample, and high-speed photography through a transparent viewport.

Published research describes various set-ups. Razdan and Kuo [38], and King [39] used a gas generator, placed upstream. In France, at ONERA and SNPE, interesting test systems have been developed, based on the use of the ultrasonic method. This method allows a direct and local measurement of the burning front location and therefore, by differentiation, the rate of propellant burning rate without perturbing the phenomenon. This system is illustrated in Fig. 18; it includes a viewport making it possible to use several ultrasonic transducers, as well as the use of large quantities of propellant. The latter characteristics offer the advantage of conditions closer to the actual combustion of propellant grains, without having to resort to a gas generator.

3.3.1.2. *Experimental results*

The most important observations are [38]:

- The occurrence of an erosive phenomenon related to a threshold value of the main flow. It is possible, for a large number of compositions, to

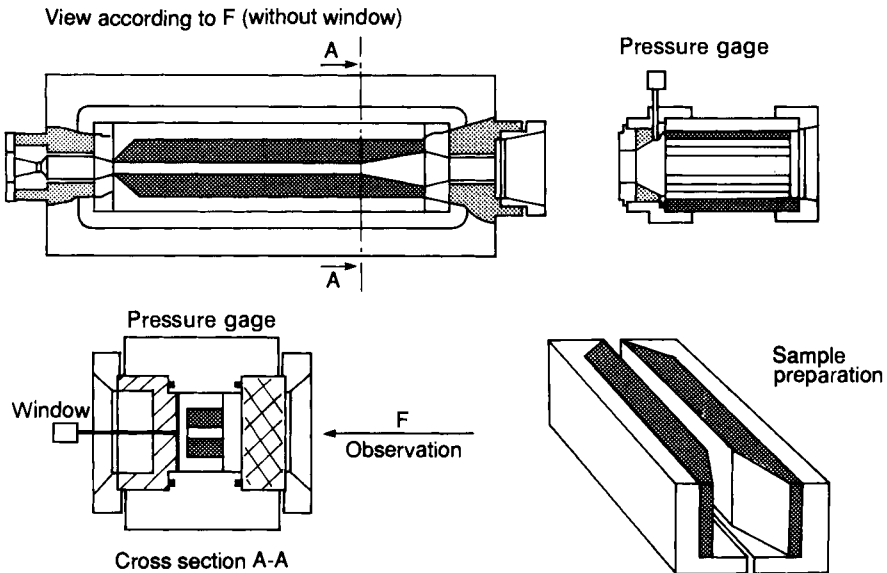


FIG. 4.18. Erosive burning experimental arrangement.

determine one velocity threshold (or specific mass flow rate) beyond which the propellant burning rate increase occurs. The lower the reference burning rate (value determined when there is no mean flow) the greater its sensitivity to the main flow will be.

- For a given flow velocity the propellant sensitivity depends on the pressure level. The experiments performed by Marklund and Lake [40] show that, for the same flow velocity at the walls, the relative burning rate increase grows with the pressure level. But if we consider the specific mass flow rate instead of the flow velocity, we still find the trends previously noticed with the variation of the propellant reference burning rate. The higher the pressure, the faster the reference burning rate of the propellant which then becomes less sensitive to the specific mass flow rate.
- Typically, the main flow temperature and chemical species have no effect:
 - the sensitivity of a propellant composition is independent of the nature of gases produced by the generator when the combustion gases are non-reactive;
 - the burning rate increase seems basically independent of the temperature of the hot gases sweeping the propellant surface.
- The presence of certain formulation parameters may lead to a negative erosive effect: this effect (burning rate decrease instead of increase) is clearly observed with active binder compositions the basic burning rate of which has already been increased by a ballistic modifier. Several possible explanations are offered:
 - decrease of the heat transfer at the surface caused by a “blowing” of the chemical reactants in the boundary layer that modify the transmission coefficients and the reaction rates;
 - formation of a melt binder coating on the surface, caused by the shear stress in the fluid;
 - in some cases, destruction of the carbonized residue due to the addition of ballistic modifiers in the propellant composition.

3.3.2. Modeling of the phenomenon

3.3.2.1. The basic models

To relate the value of the local burning rate to the gas flow characteristics in the combustion chamber, various empirical or theoretical laws have been advanced.

(a) The multiplicative law

$$r = r_b(1 + ku) \quad \text{or} \quad r = r_b(1 + kG) \quad (40)$$

where:

- $r_b = ap^n$ = reference burning rate of the composition;
- k = constant;
- u = average velocity of the main flow, assumed to be one-dimensional;
- $G = \rho_g u$ = specific mass flow rate of the main flow;
- ρ_g = density of the gases.

Likewise, with the introduction of a G^* threshold of flow rate:

$$r = r_b[1 + k(G - G^*)] \quad (41)$$

Green and Vilyunov proposed similar equations [40].

(b) The additive law

This type of law, expanded from research work done by Corner and Geckler, was proposed by Boisson [41]:

$$r = r_b + ku \quad (42)$$

3.3.2.2. Detailed models

(a) Lenoir and Robillard model

Lenoir and Robillard [42] propose a description of the erosive mechanism where the burning rate increase results from the heat transfer from the flow to the burning surface. For a given pressure and an external flow, the new propellant burning rate is calculated by adding an erosive component to the reference burning rate. It is obtained from the energy equilibrium at the surface:

$$\alpha(T_f - T_s) = \rho_p r_e [L + c_p(T_s - T_i)] \quad (43)$$

where:

- r_e = erosive burning component;
- L = heat resulting from the decomposition of solid into gas, assumed null by Lenoir and Robillard;
- T_f, T_s, T_i = respectively, flame, surface and initial temperature of the propellant;
- c_p = propellant specific heat;
- ρ_p = propellant density.

The coefficient of heat transfer α is the Chilton–Colburn coefficient modified by Rannie [41]. It accounts for the surface injection:

$$\alpha = 0.0288 \cdot c_g \cdot \rho \cdot u \cdot R_{ex}^{-0.2} \cdot P_r^{-2/3} \cdot \exp \left[-\beta \frac{\rho_g \cdot v_g}{\rho u} \right] \quad (44)$$

where:

- c_g = specific heat of the gases at constant pressure
- R_{ex} = Reynolds number, based on the axial position
- ρ, u = respectively, density and velocity of the main flow
- ρ_g, v_g = respectively, density and velocity of the gases emitted at the injecting wall
- β = constant
- P_r = Prandtl number

Taking eqns (43) and (44) into account, the new burning rate is implicitly expressed by:

$$r = ap^n + r_e \quad (45)$$

Some researchers [38] have modified this law:

- using a Reynolds number based on the diameter rather than on the axial location;
- introducing a term representing the mechanical erosion (Osborn and Burick);
- introducing, for catalyzed EDB formulations, an additional component due to the plateau effect when it exists (constant burning rate whatever the pressure level): Jojic and Blagojevic.

(b) Analytical models for boundary layer including the burning mechanisms

Lengellé's model [43]

The basic burning model used is Summerfield's GDF model, which is representative of composite propellant containing ammonium perchlorate. With this model, which only takes into account a diffusion flame between the oxidizing products (AP decomposition) and the combustible gases (binder decomposition), and assuming the Lewis and Schmidt numbers to be close to one, the burning rate is given by:

$$r = \left[\frac{c_g(T_f - T_s)}{Q} \right]^{1/2} \cdot \frac{\rho_g}{M^{1/3}} \cdot \frac{\mu}{\rho_p} \left(1 + \frac{\rho \cdot \varepsilon}{\mu} \right) \quad (46)$$

where:

- c_g = specific heat of gases;
- T_f, T_s = respectively, flame and surface temperatures;
- Q = energy necessary to heat the propellant and transform it into gas;
- ρ_g, ρ_p = respectively, gas and propellant density;
- M = mass of a pocket of combustible gas;

μ, ε = coefficients representing, respectively, viscosity and turbulent diffusion in the main flow.

Expression (46) was established taking into account the modification of the transport properties of the fluid by the main flow. Consequently, the GDF model leads to add to the reference burning rate of the composition, a term related to the local flow pattern, as the height of the flame itself is not affected.

The term $\rho \cdot \varepsilon / \mu$ in (46) is calculated from the integration of the equations within a Couette flow boundary layer assuming a constant external velocity independent of the downstream location. Based on the work of Marxman, Lengellé writes the equation that gives the velocity profile (inside the boundary layer) above a plane plate with a constant injection velocity at the wall. Based on this profile, on the calculation of the momentum thickness, and on the friction coefficient, Lengellé calculates the turbulent diffusion term using Prandtl's mixing length assumption. This term changes within the boundary layer. Lengellé suggests using its average value for the entire flame height L . The relationship providing the propellant burning rate is written as follows:

$$r = \frac{c_g (T_f - T_s)}{\rho_p Q} \left[\frac{\mu}{L} + \frac{8.3}{10^2} \frac{\rho_e \cdot \mu_e}{R_{ex}^{0.1}} \left(\frac{L}{\delta} \right)^m \psi \right] \quad (47)$$

where:

$$\psi = \frac{\ln(1 + B)}{B} \left[1 + B \left(\frac{L}{\delta} \right)^\alpha \right] \frac{1}{\alpha + 2}$$

King's model [44]

The mechanisms considered in this model are also representative of composite propellants combustion, containing ammonium perchlorate. Two flames are included:

- the premixed flame of the ammonium perchlorate, considered as a monopropellant;
- the diffusion flame between the gaseous species produced by AP and binder decompositions.

The burning rate, determined by the energetic balance at the surface, is then given, without external flow by:

$$r = \frac{I}{\rho_p \cdot Q} \left[\frac{\lambda_1 (T_{fox} - T_s)}{L_1} + \frac{\lambda_2 (T_f - T_s)}{L_{diff} + L_{kin}} \right] \quad (48)$$

where:

- ρ_p, Q = same definitions as for (46);
- λ_1 = thermal conductivity of the $\text{HClO}_4/\text{NH}_3$ gaseous phase;
- λ_2 = thermal conductivity of the oxidizers/fuels mixture issued from AP and binder decomposition;

T_{fox} = AP flame temperature;

T_f = diffusion flame temperature;

T_s = propellant surface temperature;

L_1 = AP flame height;

$L_{\text{Diff}}, L_{\text{Kin}}$ = parameters related to diffusion flame, respectively: height due to the diffusion and to kinetics of reactions.

When expressing the various heights, King writes:

$$r = A_1 p \left\{ 1 + \frac{A_2}{1 + A_3 p^2 d_{\text{AP}}^2} \right\} \quad (49)$$

where:

A_1, A_2, A_3 = constants depending on propellant and gases thermal properties and on the propellant surface temperature and heights corresponding to the various flames types;

p = pressure;

d_{AP} = diameter of AP particles

In this model the action of the flow is taken into account through the diffusion flame bending under the effect of fluid velocity; eqn (48) becomes:

$$r = \frac{1}{\rho_p \cdot Q} \left[\frac{\lambda_1 (T_{\text{fox}} - T_s)}{L_1} + \frac{\lambda_2 (T_f - T_s)}{L_{\text{Diff}} \cdot \sin \theta + L_{\text{Kin}}} \right] \quad (50)$$

where $\theta (< \pi/2)$ is the angle formed between the diffusion flame axis and the burning surface.

The various physical properties used in eqn (50) keep the same value in the case of an injecting wall. Angle is calculated from the velocity profile in the boundary layer using a simple iterative process. Empirical equations, based on Mickley and Davis' experimental results, make it possible to express the local fluid velocity as a function of transverse location above the propellant surface, main flow velocity and velocity of the injected gases.

(c) Recent models

These models (Sviridenkov and Yagodkin in 1976, Razdan and Kuo [38], Beddini [45]) solve the conservation equations for simple two-dimensional configurations (plane plates, cylindrical channels) of constant port area. Far from the wall, simplifying assumptions are considered [38]: the two-dimensional flow is isentropic and the fluid is non-viscous, though this assumption was not invoked in ref. [45].

Close to the wall the fluid behavior is more complex; terms related to viscosity are included (taking into account the Reynolds tensions). These researchers use the assumption that a turbulent flow field, when averaged, is

steady: each physical parameter consists of an average steady value and of a term representing the fluctuation from the average value over time.

3.3.2.3. *Practical applications*

The so-called “standard grain” SNPE method was developed for the purpose of a quick determination of the propellant erosive burning sensitivity. It consists of firings at fixed pressure of small star-shaped grains. These tests are performed on grains of various length, therefore corresponding to an evolution of the burning surface area to the port area ratio. Approximate values of the erosive burning parameters of the composition tested (slope k and threshold G^* of eqn 41) are worked out applying King’s model [44], when the propellant is a composite containing ammonium perchlorate. The values are later refined to match as best as possible the pressure evolution (Fig. 19).

4. Transient and Unsteady Burning Phenomena

In the previous sections the mechanisms involved during steady burning or slowly evolving operation sequences of a solid propellant rocket motor were discussed. On the contrary, the following section deals with phenomena observed during transient or unsteady burning: ignition and burn-out periods, unexpected development of pressure oscillations in the combustion chamber or thrust modulation.

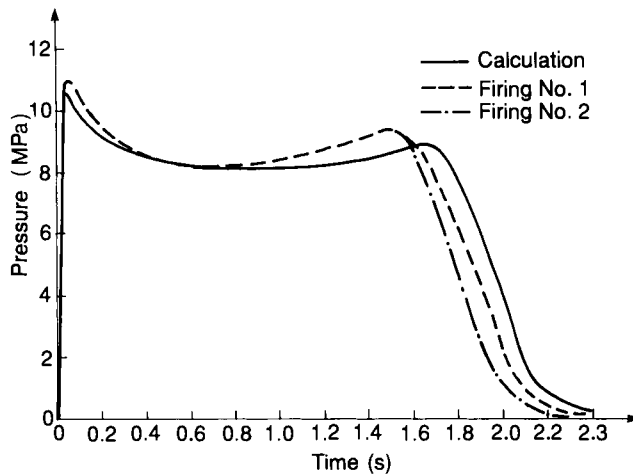


FIG. 4.19. Comparison between prediction and experiment. Using the first King’s model.

4.1. TRANSIENT BURNING

4.1.1. Origin

Transient burning occurs when the pressure level in the combustion chamber changes very rapidly with time. Assuming a stationary regime (Section 2.2), the heat flux transmitted by the gaseous phase creates a thermal gradient in the propellant close to the burning surface. The equilibrium displacement caused by any pressure variation requires an adjustment of thermal gradients in the gaseous and condensed phases. Characteristic times are associated with each zone:

for the propellant:

$$\tau_p = \frac{d_p}{r^2} \quad (51)$$

for the gaseous phase:

$$\tau_g = \frac{\lambda_g \cdot c_p \cdot \rho_g}{\lambda_p \cdot c_g \cdot \rho_p} \cdot \tau_p$$

where:

- λ_i, c_i, ρ_i are, respectively, thermal conductivity, specific heat, and density of the propellant (index p) and of gas (index g) at constant pressure
- d_p is the propellant heat diffusivity

The typical residence time associated with the gaseous phase is much smaller than the corresponding time for that associated with the solid propellant. Consequently, several cases may occur, depending on the time during which the pressure level is changed.

- if $\tau \ll \tau_p$ no unsteady effect;
- if $\tau \approx \tau_p$ the thermal gradient evolution in the propellant is delayed while the gaseous phase instantaneously adjusts itself to pressure changes;
- if $\tau \approx \tau_g$ each burning mechanism is affected by the fast pressure evolution.

4.1.2. Models

Kuo *et al.* [46] have done a very clear presentation of the conservation equations that need solving to deal with the general problem of unsteady burning. Various types of models have been developed. They significantly differ from each other by:

- the terms excluded or included in the conservation equations;
- the method selected to solve the governing equations.

4.1.2.1. Models of dp/dt type [47,48]

The gaseous phase of these models is assumed to be steady and the unsteady heat equation resolution is simplified. These models provide the following relationship for the instantaneous burning rate:

$$r = r_b \left[1 + \psi \left(\frac{n \cdot d_p}{p \cdot r_b^2} \right) \right] \frac{dp}{dt} \quad (52)$$

where:

- $r_b = ap^n$ = steady-state burning rate;
- d_p = propellant thermal diffusivity = parameter which depends upon instantaneous pressure and propellant characteristics.

4.1.2.2. Zel'dovich–Novozhilov model

Zel'dovich [49] assumes that during the unsteady regime the gaseous phase instantly reacts. The heat flux at the propellant surface is found from the steady analysis of propellant regression, avoiding a detailed and tricky modeling of the gaseous flame zone.

Equation (3) gives the expression of the steady-state temperature profile occurring in the propellant assuming no condensed phase reaction. The value of the surface heat flux is then:

$$\Phi_{p,s} = \lambda_p \left. \frac{dT}{dx} \right|_{x=0^-} = \frac{r_b \cdot \lambda_p}{d_p} (T_{s,s} - T_i) \quad (53)$$

where:

- $\Phi_{p,s}$ = heat flux at the propellant surface;
- λ_p = propellant thermal conductivity;
- d_p = propellant thermal diffusivity;
- $T_{s,s}$ = propellant surface temperature for the steady-state regime;
- r_b = propellant stationary burning rate.

In addition, the steady-state propellant pyrolysis and burning rate laws (eqn 4), are assumed to be valid and the convenient relationship between surface temperature, initial temperature, pressure and burning rate is then established. The heat conservation equation relative to unsteady events can now be solved by including the steady-state thermal flux expression at the propellant surface using stationary data. Due to assumptions involved, this method is not suitable for homogeneous propellants.

4.1.2.3. Models with flame zone description

These models [47,50] solve the conservation energy equations for the gaseous zone to determine the heat flux value at the propellant surface. Simplifying assumptions are used; combustion, in particular, is represented by only one reaction. Assuming a uniform production rate for the flame products, the KTSS model [47], used for heterogeneous propellants containing AP (diffusion flame), gives the following value for the unsteady heat flux at the propellant surface:

$$\Phi_{g,s} = -\lambda_g \left. \frac{dT}{dx} \right|_{x=0^+} = \frac{1}{r} \cdot \rho_p \cdot r_b^2 \left\{ c_p \left[\frac{r_b}{b} \right]^{1/k} - Q_s \right\} \quad (54)$$

where:

- r = instantaneous burning rate;
- r_b = stationary burning rate = ap^n ;
- c_p, ρ_p = respectively, propellant specific heat and density;
- b, k = steady-state pyrolysis law coefficients written as $r_b = b(T_{s,s} - T_i)k$;
- Q_s = heat released by the superficial decomposition reactions.

4.2. IGNITION

4.2.1. Propellant grain ignition—flame spreading

A pyrotechnical device is used to ignite the propellant. Hot gases and particles supplied by the igniter heat the propellant surface by conduction, convection and thermal radiation. This heat flux is sufficient for the propellant surface to ignite in some scattered spots. Then the flame propagates, the combustion reactions begin to be self-sustained, and the entire surface is soon burning.

Equation (12) under certain assumptions expresses the pressure rise due to the central bore gas filling, consequence of the propellant surface ignition. When written as:

$$\ln \left\{ \left[1 - \left(\frac{p_c}{p_{co}} \right)^{1-n} \right]^{-1} \right\} = \frac{1-n}{t_s} \cdot t \quad (55)$$

the left-hand side term becomes a linear function of time t . This offers the possibility, together with pressure recordings to determine the flame propagation time [51]. It also allows one to calculate the maximum pressure rise in the chamber,

$$\left. \frac{dp_c}{dt} \right|_{\max} = \frac{p_{co}}{t_s} (1-n)n^{n/(1-n)} \quad (56)$$

This equation demonstrates that, theoretically, the smaller n , the greater the pressure rise.

The rate of flame speed is particularly important when the propellant grain is very long, or when the internal configuration is complex. Barrère [52] has worked out an equation for convective heat transfer to the propellant surface.

4.2.2. Experimental methods for ignition study

The ignition characteristics of the various propellant families are usually determined by performing tests on small samples. Hermance [53] has reviewed the various methods used.

(a) Ignition through conductive heat transfer

As a reminder, numerous experiments are conducted in a shock tube. In this technique the propellant sample ignites under the sudden pressure and temperature rise resulting from the shock wave.

(b) Ignition through convective heat transfer

Lengellé *et al.* [54] describe a set of results obtained by submitting a sample to hot gases produced by either an arc generator or a small motor using a polybutadiene solid propellant.

(c) Ignition through radiative flux

At present the laser beam method is widely used. A CO₂ laser, emitting a 10.6 μm coherent beam and about 200 W cm⁻² flux, is well suited for the propellant ignition studies. This technology offers the possibility of selecting a flux level independent of pressure level, chemical nature of ambient gases and moisture level. In addition, the laser can be operated in a pulsed mode. It is then possible to differentiate the self-sustained combustion sequence occurring after ignition from possible dynamic extinguishment. However, the laser ignition method has several drawbacks:

- absence of hot gases at the sample surface;
- sometimes deep beam penetration inside the propellant;
- a relatively slow increase of the surface temperature in comparison with actual ignition events.

4.2.3. Thermal flux measurement [56]

The flux received by a surface can be total or selective:

- to determine the total incident flux, the fluxmeter emissivity is, as much as possible, close to one;
- to determine the flux actually received by the surface, the fluxmeter emissivity matches the propellant one;
- to select radiative flux, a viewport is placed between the fluxmeter and the heat source: its spectral characteristics are chosen to allow a good transmission of the source radiant component and it also plays the role of a protection against convective flux.

4.2.4. Characterization of the various propellant families

4.2.4.1. Ignition delay—flux charts

Before ignition, the unsteady heat equation can be solved if the initial temperature $T(x, 0)$ or flux $\Phi(x, 0)$ fields are known. This equation is written:

$$\frac{\partial T}{\partial t} = d_p \frac{\partial^2 T}{\partial x^2} \quad (57)$$

$$x \leq 0, \quad 0 \leq t \leq t_{\text{ign}}$$

where t_{ign} is the ignition delay under constant flux.

In the particular case where a propellant (initial uniform temperature T_i) is ignited, and assuming that its thermal properties are independent of the instantaneous local temperature, the following equations are obtained:

$$T_s(t) - T_i = \frac{1}{\sqrt{\Gamma\pi}} \int_0^t \Phi(\tau) \frac{d\tau}{\sqrt{t-\tau}} \quad (58)$$

$$\Phi(t) = \sqrt{\frac{\Gamma}{\pi}} \int_0^t \dot{T}_s(\tau) \frac{d\tau}{\sqrt{t-\tau}} \quad (59)$$

where:

T_s = propellant surface temperature;

$\dot{T}_s = dT_s/dt$;

Φ = flux incident to the propellant surface = $\lambda_p dT/dx|_0$;

t = time;

Γ = propellant thermal effusivity;

T_i = propellant initial temperature.

When the tests are performed under constant flux level, eqn (58) becomes simpler:

$$T_s(t) - T_i = \frac{2}{\sqrt{\Gamma\pi}} \Phi \cdot t^{1/2} \quad (60)$$

Representing surface temperature rise of the heated propellant, eqn (60) is further verified during ignition:

$$T_{s,\text{ign}} - T_i = \frac{2}{\sqrt{\Gamma\pi}} \Phi \cdot t_{\text{ign}}^{1/2} \quad (61)$$

where $T_{s,\text{ign}}$ is the propellant surface temperature at ignition.

If, for a given propellant, ignition occurs at the same surface temperature ($T_{s,\text{ign}}$), regardless of the flux level, experimental results must align in the ($T_{s,\text{ign}} - \ln \Phi$) axis with a (-1) slope value. Figure 20 shows that eqn (61) is clearly verified, whatever the propellant family; but it must be pointed out that the higher the ignition delay the lower the ignition temperature.

4.2.4.3. Modification of the ignition delay—flux charts

(a) Definition of the ignition delay (Fig. 21)

Under an external heat flux the propellant starts to decompose. The regression of its surface is observed. This event sometimes occurs simultan-

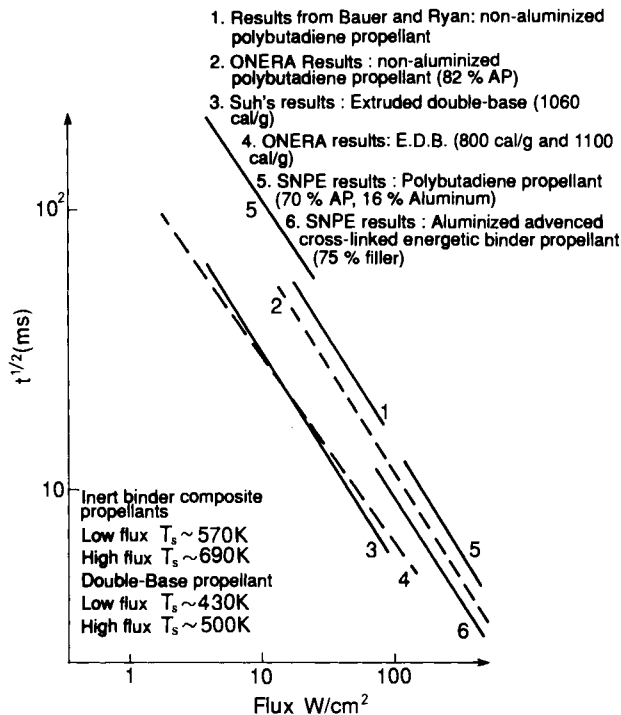


FIG. 4.20. Ignition chart for different propellant families. Tests performed with CO_2 laser under continuous radiation.

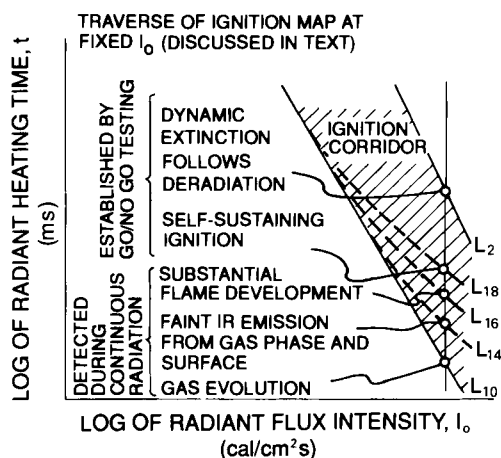


FIG. 4.21. Different events occurring during ignition.

eously with a luminous reaction taking place even before the conditions for sustained ignition are met (concentration of reactants, thickness of the propellant heated zone). At this moment a sudden suppression of the external flux leads to drastic extinguishment.

Flux pulses of variable duration are used with the “go/no go” technique to obtain ignition maps and delimit the self-sustained burning region (L_{1d} point) on the delay-flux chart.

(b) Definition of a dynamic extinction region

Experiments performed on double-base propellants containing no ballistic catalysts [58] have shown that, a long time after ignition, the propellant may be extinguished by suppressing the external flux. These experiments demonstrate the existence of a dynamic extinction limit, thereby determining a region on the “ignition delay-flux” map where the combustion is self-sustained after flux suppression (Fig. 21). They also show that this extinction limit greatly depends, as opposed to the ignition limit, on the pressure level: the higher the pressure, the larger the self-sustained combustion region. De Luca [59] believes that this behavior can be generalized to all propellants.

(c) Effect of flux source

Several authors have published experimental results showing that the nature of the flux has no noticeable influence on ignition events, provided that:

- an effective flux is taken into account during tests performed under convective flux, because of the flux level variation during propellant heating;
- radiation penetration in the propellant is limited during radiative flux tests.

(d) Effect of optical properties

Because propellant is not entirely opaque, a portion of the incident radiation is absorbed deep inside the solid, thereby increasing the ignition delay [60].

(e) Effect of pressure level

Although it does not influence the ignition delay value when the flux intensity is low ($< 10 \text{ W} \cdot \text{cm}^{-2}$), pressure variations significantly modify the previous charts under high thermal fluxes: whatever the propellant family, the higher the pressure, the lower the ignition delay.

(f) Effect of oxygen partial pressure

Experiments reported by Hermance [53] show that the ignition delay decreases when the oxygen partial pressure increases. It appears that, with low concentrations of oxygen, the binder nature has a significant influence.

4.2.5. Numerical simulations

Under a forced constant flux, and considering an initial temperature field evenly distributed, numerical models can predict the surface temperature profile before and after ignition, until a steady-state combustion regime has been reached. The propellant surface regression is introduced into the governing equations as soon as its surface temperature reaches a critical value.

One of these codes, developed by ONERA, has been adapted for extruded double-base propellants. A description of condensed phase reactions and stationary primary flame is included. Another code has also been developed for polybutadiene propellants. The Zel'dovich–Novozhilov method is used to compute the incident flux at the propellant surface.

4.3. INSTABILITIES IN SOLID ROCKET MOTORS

4.3.1. Background

Combustion instabilities during a rocket motor operation are detected as oscillations superimposed to the average pressure. Their amplitude depends

on the firing conditions and they are always undesirable, even if they do not all have catastrophic consequences:

- average pressure shifts modify the motor performance, including exceeding specified limits; they sometimes lead to motor failure;
- heat transfers are intensified by pressure oscillations and induce such a rapid degradation of inner parts (thermal insulation, nozzle) that in some cases they are destroyed before burn-out.
- pressure oscillations create vibrations which are transmitted to the whole motor case causing greater stress on it than expected.

4.3.1.1. Origin of motor instabilities

The existence of numerous perturbation sources inside a combustion chamber (small solid pieces ejected by the nozzle, inner jets confluence, etc.) may be at the origin of the combustion instabilities. These perturbations affect propellant combustion. The burning rate adjustment to the instantaneous pressure value triggers an oscillatory phenomenon, the frequency of which may be close to one of the acoustic modes of the central port acting as a resonant cavity. They can also be close to frequencies specific to the internal flow pattern. Instabilities occurrence and feeding in a rocket motor are due to the energetic balance between amplifying (combustion) and damping (condensed phase in gases, case vibrations, etc.) phenomena.

4.3.1.2. Classification of instabilities

Two sets of phenomena are referred to as “instabilities.”

(a) Irregular combustion phenomena

Pressure oscillations, even extinction and reignition are observed. These oscillations, of a few hertz, are in phase throughout the whole combustion chamber. They are called “chuffing” or “ L^* ”, or “non-acoustic low frequency” instabilities (NALF). They occur under very specific operating conditions: at low pressure and small characteristic length L^* (combustion chamber volume to throat nozzle area ratio).

(b) Pressure oscillations matching cavity acoustic modes:

Two families of instabilities are observed:

- Longitudinal instabilities, matching the longitudinal modes of the cavity. They are characterized by frequencies of a few hundreds of hertz and moderate peak-to-peak amplitudes, sometimes associated to average pressure shifts. They are typically observed on large rocket motors.

- Transverse instabilities, following the transverse modes of the cavity (in a cross-section of the cavity); these are characterized by frequencies of a few tens of kHz, high peak-to-peak amplitudes and generally sudden and important average pressure shifts. They occur on small rocket motors using non-metallized propellants.

4.3.1.3. Determination of acoustic modes

Acoustic pressure field description is needed to predict instabilities occurrence. The wave equation is solved using classical acoustics assumptions [33]:

- oscillation p' has a low amplitude compared to average pressure p ;
- absence of average flow;
- walls are rigid (the nozzle is acoustically closed):

$$\frac{\partial^2 p'}{\partial t^2} - \bar{a}^2 \cdot \Delta p' = 0 \quad (\text{where } \bar{a} = \text{average speed of sound})$$

with the following boundary conditions:

$$\vec{\nabla} p' \cdot \vec{n} = 0$$

Computations in the case of simple geometries

When considering a closed tube as a first approximation of a simple motor cavity, the solution is expressed by:

$$p' = p(r, \theta, z) \cdot \cos(\omega t + \psi)$$

where $p(r, \theta, z)$ represents the spatial distribution of the mode (now shortened as \hat{p}).

For a stationary mode, we have:

$$\hat{p} = A \cdot J_m \left(\frac{\pi \cdot \alpha_{mn} \cdot d}{D} \right) \cdot \cos(m \theta + \varphi) \cdot \cos \left(\frac{\pi q z}{L} \right) \quad (62)$$

and

$$f = \frac{\omega}{2\pi} = a \sqrt{\left(\frac{\alpha_{mn}}{D} \right)^2 + \left(\frac{q}{2L} \right)^2};$$

L = length of the cavity;

D = port diameter;

d = considered diametral position;

a = average speed of sound in the gases;

m, n, q = arbitrary integers;

J_m = Bessel function of m th order;

α_{mn} = roots of $dJ_m/dr = 0$ (tabulated values);

φ, ψ = phase angles;

A = amplitude known with a multiplicative constant.

Modes can be classified depending on m , n and q values:

$m = 0$	$n = 0$	$q \neq 0$	pure longitudinal mode
$m \neq 0$	$n = 0$	$q = 0$	pure tangential mode
$m = 0$	$n \neq 0$	$q = 0$	pure radial mode

Computations in the case of complex geometries

In the case of actual more complex propellant grain configurations (machined grains or FINOCYL), longitudinal and transverse modes are obtained by specific computer programs solving the wave equation in the combustion chamber. Figure 22 illustrates this type of resolution for a grain with axisymmetric slots; longitudinal acoustic modes are determined using a finite elements procedure.

4.3.2. Unsteady combustion models

4.3.2.1. Definitions

The purpose of this section is to identify the sensitivity of the propellant combustion to the acoustic field ("pressure-coupling" effects) and to the aerodynamic field ("velocity-coupling" effects).

Pressure-coupling

The propellant pressure-coupled response involves two major effects:

- (a) mass flow rate response to pressure fluctuations:

$$R_{MP} = \frac{m'/\bar{m}}{p'/\bar{p}}$$

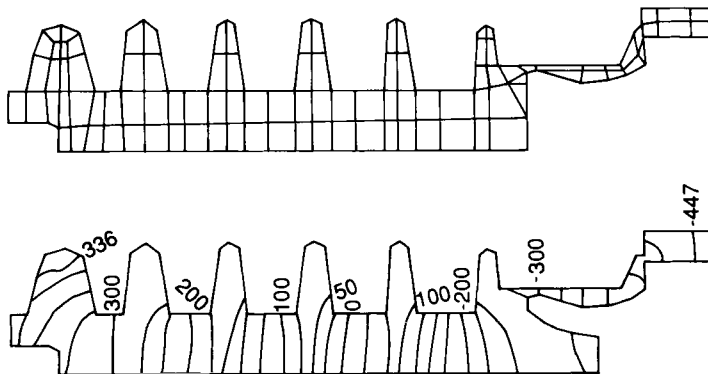


FIG. 4.22. Axisymmetric propellant grain analysis. Grid and isopressure values.

(b) mass flow-rate response to temperature fluctuations:

$$R_{TP} = \frac{T'/\bar{T}_f}{p'/\bar{p}}$$

where:

m', p', T' are respectively maximum specific mass flow rate, pressure and temperature fluctuations;
 $\bar{m}, \bar{p}, \bar{T}_f$ are respectively average values of specific mass flow rate, pressure and flame temperature.

Fluctuations are mainly dependent on frequency and average pressure. If the frequency is very low, specific mass flow rate response term is equal to the pressure exponent of the steady-state burning rate law.

Velocity-coupling

In the linear range the specific mass flow rate response is defined by:

$$R_{MV} = \frac{m'/\bar{m}}{u'/\bar{a}}$$

where:

u' = unsteady normal component of gas velocity;
 \bar{a} = average speed of sound.

The velocity-coupling phenomenon is complex, depending on the average velocity of combustion gases and acoustic velocity fluctuations. Unlike pressure-coupling, the velocity-coupled response is not only a propellant characteristic, since it also depends on the gas flow pattern inside the chamber.

4.3.2.2. Models

Current models are one-dimensional and based on a description of the combustion zone. Simplifying assumptions especially involve a homogeneously heated solid phase, a very small interface where the decomposition reactions occur and a gaseous phase where combustion products react. The following expression for the specific mass flow rate response has been proposed by Culick [61]:

$$R = \frac{n \cdot A \cdot B}{\lambda + (A/\lambda) - (1 + A) + A \cdot B}$$

where:

λ = complex function of frequency f ;
 n = exponent of the steady-state pressure law $r = ap^n$;
 A and B = constants, worked out from physicochemical analysis (activation energies, surface temperature).

4.3.3. “ L^* ” instabilities

This chuffing phenomenon is characterized by pressure oscillations at very low frequencies (a few hertz). Large pressure peaks and depressions are generally observed:

- the amplitudes of pressure oscillations are inversely proportional to the frequency;
- frequency increases with pressure;
- an increase of the motor characteristic length (L^*) leads to a decrease of frequency and of oscillations magnitude.

For the moment, only experimental methods enable the designer to predict motor L^* instabilities occurrence.

4.3.4. Prediction of instabilities

4.3.4.1. Background

Due to the complexity of phenomena, the methodology of instabilities prediction has been split in two major steps:

- The first step is devoted to predict instability risks; it consists in determining whether a perturbation will tend to grow (unsteady operation) or damp (steady-state operation); this analysis must be made for each potential mode.
- The second step is run for each unstable mode. It consists in computing limiting cycles amplitude as well as the magnitude of average pressure shift. Theoretical approaches account for non-linear phenomena that, in this case, drive instabilities growth.

4.3.4.2. First step: linear acoustic balance

Linear acoustic balance theory

Linear acoustic balance is the most widely used approach. The principles of this method have been given and developed by Culick [62].

The fluid mechanics equations, written for the combustion chamber, and the ideal gas state equation are linearized: small quantities, called “perturbation parameters” such as the Mach number and the amplitude of the pressure oscillations, are the new unknowns. The problem consists of seeking solutions expressed in the following form:

$$p' = \hat{p} \cdot \exp i(\omega - i\alpha)t = \hat{p} \cdot \exp(i \cdot a \cdot k \cdot t) \quad (63)$$

where k is related to the frequency of oscillations ($\omega = 2\pi f$) and to the coefficient α characterizing amplification or damping.

Mechanisms considered in the acoustic balance assessment will either amplify the initial mode perturbation (combustion, turbulent flow) or will tend to damp it (nozzle, two-phase flow, mechanical vibrations).

Consequently, various terms are summarized which form coefficient α and express the contribution of each mechanism i :

$$\alpha = \sum_i \alpha_i$$

Detail of linear acoustic balance terms

(a) Gain resulting from pressure-coupling

This is written as follows:

$$\alpha_{cp} = \frac{\bar{a} \int_S \gamma \cdot M_b \cdot R \cdot \hat{p}_n^2 \cdot dS}{2 \int_V \hat{p}_n^2 \cdot dV} \quad (64)$$

where:

- R = real part of the pressure-coupled propellant response;
- M_b = Mach number of the gases leaving the burning surface;
- \hat{p}_n = shape of mode n (acoustic calculations).

Integrals are computed over the whole propellant burning surface S (numerator) and the whole chamber volume V (denominator).

(b) Gain resulting from velocity-coupling

Culick expresses the gain resulting from velocity-coupling, in the linear range, as follows:

$$\alpha_{cv} = \frac{\bar{a} \int_S R_v \cdot \hat{p}_n \cdot \nabla \hat{p}_n \cdot dS}{2 \int_V \hat{p}_n^2 \cdot dV} \quad (65)$$

where R_v is the imaginary part of the propellant velocity-coupled response.

(c) Gain resulting from the average flow rate and its perturbations (vortex shedding)

Especially devoted to segmented configurations (propellant grains independently mounted in a motor), Brown *et al.*'s research [63] shows the

nature of interactions between flow and acoustic fields. Vortices detach from the aft end of one segment and impact on the following downstream segment. A perturbation travels back through along the flow and can reinforce vortex shedding effects. These experiments performed in cold gas channels revealed the importance of Strouhal number S_t , defined as:

$$S_t = \frac{f \cdot d}{\bar{u}}$$

where:

f = vortex shedding frequency;
 d = characteristic distance;
 \bar{u} = average flow velocity.

These experiments have demonstrated that coupling between chamber acoustics and flowfield occurs when $0.2 < S_t < 1$. This law seems to be correctly proven on actual rocket motors. The formulation of this contribution to acoustic balance has yet to be properly expressed and verified.

(d) Particulate damping

Because of their dynamic and thermal drags, particles distributed in gases induce attenuation and dispersion of the pressure waves in the combustion chamber. Culick [64] proposed the following expression describing the damping capacity of spherical particles of diameter d :

$$\alpha_p = -\frac{1}{2} \frac{C_m}{1 + C_m} \left[\frac{\omega^2 \cdot \tau_d}{1 + \omega^2 \cdot \tau_d^2} + (\gamma - 1) \frac{c_s}{c_g} \frac{\omega^2 \cdot \tau_t}{1 + \omega^2 \cdot \tau_t^2} \right] \quad (66)$$

where $\tau_d = \rho_s \cdot d^2 / 18 \mu$ and $\tau_t = (3/2) (c_s / c_g) P_r \cdot \tau_d$

are, respectively, the dynamic and thermal relaxation times, and

ω = pulsation;
 C_m = particles mass ratio;
 ρ_s, c_s = respectively, density and specific heat of the particles;
 μ, γ, c_g = respectively, viscosity, specific heat ratio and gas specific heat at constant pressure;
 d = particles diameter;
 P_r = Prandtl number.

A very detailed knowledge of the particle size distribution in the combustion chamber remains one of the main difficulties in making an accurate particulate damping prediction. At present, calculations are done only on rough estimations of this particle size distribution.

(e) Losses associated with nozzle impedance

These are written as follows:

$$\alpha_t = -\frac{\bar{a} \int_S (A_t + M_e) \hat{p}_n^2 \cdot dS}{\int_V \hat{p}_n^2 \cdot dV} \quad (67)$$

where:

M_e = Mach number in the nozzle entrance plane;

A_t = admittance of the nozzle in the same plane. The absolute value of the upper integral is computed over this reference plane; the absolute value of the denominator is calculated for the whole chamber volume.

With longitudinal modes and short nozzles (entrance cone length \ll wavelength) and assuming isentropic oscillations, we have:

$$A_t = \frac{\gamma - 1}{2} \cdot M_e$$

In complex cases the nozzle admittance is numerically calculated.

(f) Visco-acoustic losses

The initial linear acoustic balance model does not take into account viscous phenomena, which are of primary importance for the particles behavior and appear close to the burning surface.

Culick suggested introducing the so-called “flow turning” effect for the first time in 1973. Flandro’s approach [65] is based on a detailed analysis of the fluid layer located near the burning surface. His method uses the notion of admittance correction. Both approaches give very similar results when used for simple propellant grains under strong flow conditions.

(g) Losses caused by the solid grain

This contribution requires additional calculation: the acoustic analysis of the cavity is coupled with a vibration analysis of the propellant grain. At the gas/solid interface, displacements are set to the same value, so that continuity is ensured. Using experimental results for the propellant complex modulus it becomes possible to evaluate structural damping.

4.3.4.3. *The second step: evaluation of oscillation amplitudes and average pressure shifts—non-linear analyses*

There are two kinds of approach:

- Exact methods, which strive to solve complete equations, are using numerical procedures that are, at this time, very difficult to apply to actual motors [66,67].
- Approximate methods which simplify the problem: the system of partial derivative equations representing the motor operation is cast into a differential equations system. This approach, proposed by Culick [68], is the so-called “averaging” method, which has been successfully applied to rocket motors with simple geometry.

4.3.5. *Longitudinal instabilities*

4.3.5.1. *First step: linear acoustic balance*

- (a) Characterization of the propellant pressure-coupled response

Indirect Methods

These methods are based on the propellant response determination from a model and on the unsteady analysis of a test motor firing. Two types of motors are widely used: self-excited or pulsed center-vented burners and rotary valve or modulated exhaust burners.

T-Burner. The T-burner (Fig. 23) is a tube at the end of which two propellant samples are placed (end-burning slabs or small slotted tubes) [64].

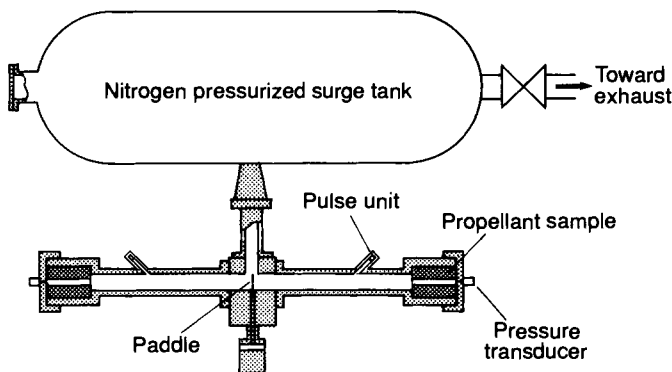


FIG. 4.23. T-burner schematic of the set-up.

The frequency is determined by T-length and average gas temperature. The combustion products are flushed outside through a non-sonic center vent toward a surge tank which maintains the T-average pressure roughly constant during firing. The whole set-up is nitrogen pressurized before firing in order to simulate the actual motor operating pressure. Various longitudinal modes can be observed:

- self-excited operation mode: the term corresponding to pressure oscillations increase, α_1 , is determined during firing, and after burn-out the α_2 term related to damping phenomena becomes available.
- pulsed operation mode: pressure oscillations are triggered during firing by pulsers. They allow determination of the α_i terms describing the rate of amplitude change of the driven oscillations. The difference $\alpha_c = \alpha_1 - \alpha_2$ gives the combustion contribution related to the propellant pressure-coupled response.
- Variable area T-burner: in this mode, obtained by using hollow cylindrical sample with variable combustion area, the T-burner may exhibit oscillations even with highly aluminized compositions.

ONERA modulated exhaust motor [69]. In his technique (PEM burner), oscillations are driven in the combustion chamber during the whole firing. The test motor includes an end-burning propellant grain, and a nozzle limited to its entrance cone. A cog-wheel rotates in front of the throat area, producing a partial modulation of the throat nozzle area and of the ejected flow.

The propellant response is obtained by analyzing the pressure oscillations, the throat modulation oscillations, and using an operational model of the test motor. Figure 24 shows the pressure-coupled response of a propellant tested in the SNPE T-burner and ONERA PEM motor.

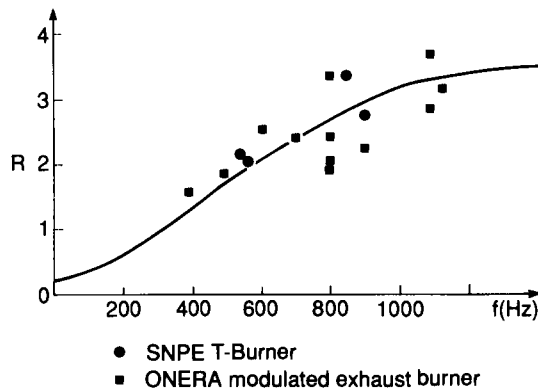


FIG. 4.24. Propellant pressure-coupled responses measured with modulated exhaust and center-vented burners.

Direct methods

Results obtained with the previous indirect methods are not very accurate. This lack of accuracy is mainly related to model deficiencies as well as to technical difficulties involved in test implementation.

To overcome these difficulties, studies have been undertaken in the United States [70] and in France (at ONERA) in order to directly determine fluctuations of specific mass flow rate induced by transient pressure fluctuations. Fluctuation measurements in this case are based on the analysis of the changes in the characteristics of a microwave frequency electrical wave traveling through the propellant and reflecting on the burning surface.

(b) Velocity-coupling characterization

This is a delicate determination because of the difficulties met in designing a test device in which the propellant would be affected only by acoustic velocity oscillations. This phenomenon being always associated with pressure-coupling, the intricate aspect of this characterization is enhanced by the fact that the velocity-coupled response is very closely linked to internal aerodynamics. It is necessary to make sure that the considered testing device gives a valid reproduction of the internal flowfield pattern of the actual motor.

(c) Linear acoustic balance assessment

Philippe and Tchepidjian [71] have developed a computer code based on an analysis of linearized equations which performs the acoustic balance for axisymmetrical motors. The input data are the parameters related to the pressure coupling α_c , average flow rate α_e , nozzle impedance α_t , particulate α_p , and structural vibrations.

Parametric studies performed with this code demonstrate that the most significant terms correspond to pressure-coupling and particulate damping. In order to account for experimental discrepancies and simplified assumptions (in particular, particle size distribution), the authors have defined the following criteria:

- damping of considered acoustic mode when $\alpha \leq -0.1 f$;
- occurrence of the considered acoustic mode when $\alpha \geq +0.1 f$;
- "critical" acoustic mode when $-0.1 f < \alpha < 0.1 f$.

4.3.5.2. Second step: non-linear aspect—limiting amplitudes and average pressure shifts

Test results are obtained by firing star-shaped grains with a constant burning area. When half of the web is burned, an impulse is triggered by

igniting a load of black powder located at the front-end of the propellant. Under low average pressures, pressure oscillations damp: the rocket motor is in a steady configuration. Under higher average pressures the pressure perturbation grows and reaches a limiting cycle. In this case the chamber average pressure is most of the time largely increased.

Tests performed at various pressures allow the determination of a threshold pressure p_s . Applied to a large number of polyurethane and polybutadiene propellants [72], they help to draw a pressure-burning rate diagram in which pressure thresholds are located along a line that separates steady and unsteady regions (Fig. 25).

This is a useful test for the classification of various compositions according to their instability tendencies from a non-linear point of view. It is also used to characterize the motor sensitivity to high-amplitude pressure and velocity perturbations.

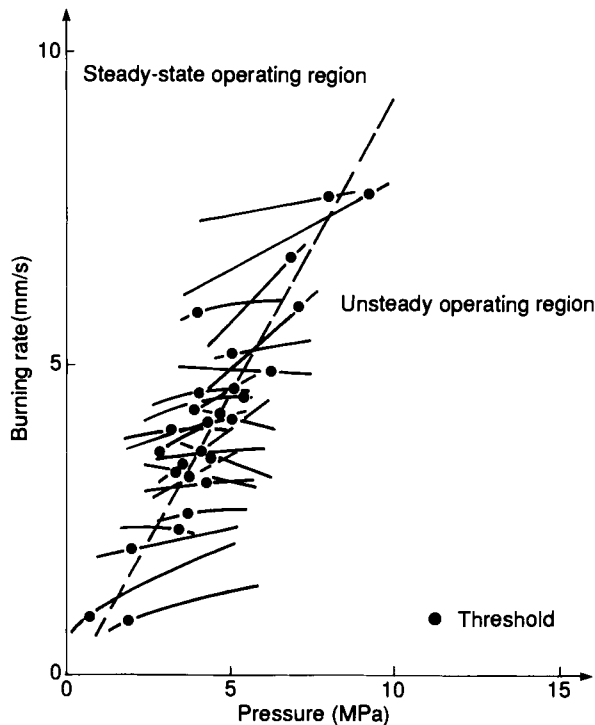


FIG. 4.25. Determination of steady-state and unsteady regions in a velocity versus pressure plot.

4.3.6. *Transverse instabilities*

4.3.6.1. *Experimental studies*

Firings exhibiting transverse instabilities (generally tangential) are characterized by high-frequency pressure oscillations and significant average pressure shifts.

A special burner equipped with a viewing port has been designed in order to observe combustion phenomena. The pressure level in the cylindrical combustion chamber is recorded at several locations in one cross-section. Tests performed demonstrate that the observed acoustic modes are unsteady modes. Furthermore, random motions of nodal lines are observed: strong rotations correspond with high pressure peaks.

4.3.6.2. *"L/D" Method*

At the origin of this method, a series of investigations [72] have been done on simple grain geometries, and researchers varied the firing conditions to determine an acceptable operation range (Fig. 26). They proposed a non-linear criterion to compare the severity of the observed acoustic modes. This criterion is defined as the ratio of the amplitude of the first pressure shift (Δp) to the stabilized pressure level p just before the shift. The motor operation is said to be steady when $\Delta p/p$ is zero or small (a few per cent) and unsteady when $\Delta p/p$ is high (several tens of per cent). It is a non-linear criterion.

(a) Effect of burning to throat area ratio K

With a given propellant, it can be noticed that pressure oscillations are first driven by K growth. Then these oscillations rapidly diminish, becoming non-existent beyond a threshold value K_s (or threshold pressure p_s).

(b) Effect of length

While keeping a constant K value, increase of the propellant grain length (without varying its port section) leads to unsteady effects beyond a threshold length L_s .

(c) Effect of initial diameter

By varying the propellant grain length for different values of the initial diameter, we observe:

- The existence of an L/D threshold, beyond which pressure oscillations occur. This threshold value varies from 5 to 10 depending on the propellant composition.

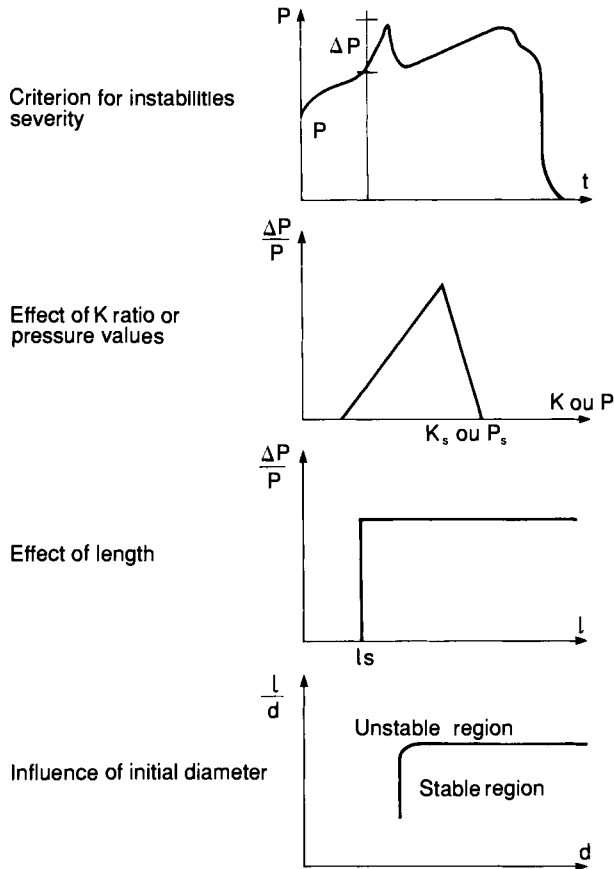


FIG. 4.26. Research of a steady-state operation range.

- In some cases the existence of a critical diameter, below which motor firings are always instability-free.

4.3.6.3. Acoustic balance

Few studies have been done on this method in the field of transverse instabilities, because of the lack of experimental evaluation for the propellant response function at these high frequencies.

Lovine [74] has described a slotted T-burner. Its small dimensions make it possible to obtain frequencies up to 13 kHz. Kuentzmann *et al.* [75] have developed a motor with a partially modulated nozzle throat. Response measurements between 3 and 15 kHz are obtained within one firing, which is due to the geometrical evolution of the propellant grain.

4.3.7. *Suppression of instabilities*

There are two ways to cancel instabilities:

- the first consists of adjusting the propellant grain shape;
- the other consists of tailoring the propellant (production of particles that damp oscillations during combustion).

Implementation of these solutions is never easy. The solutions require design testing, and improvements are always obtained at motor performance expense.

4.3.7.1. *Propellant grain geometry*

(a) Helmholtz resonator

This is a small cavity linked to the combustion chamber through a throat. It must be located at a vibrational antinode and tuned to the frequency that needs to be damped. This device has been used several times to stabilize longitudinal modes.

(b) Resonance rod

This device is widely used. It consists of a rod embedded at the forward end of a rocket motor; it fills a portion of the central port length. Rods with rectangular or cruciform sections are the most efficient. They prevent gas rotation and suppress pressure peaks, particularly at the beginning of firing.

(c) Longitudinal baffles

These are small plates placed lengthwise inside the propellant grain. During combustion, they emerge inside the combustion chamber and create obstacles that block the rotation of the gases.

4.3.7.2. *Propellant composition*

The addition of a low particle content, as ingredients in the propellant, is a method often successful in stabilizing motor combustion. This is particularly true in the case of tangential instabilities. Once the frequency that needs to be damped is known, it is possible to theoretically predict, depending on the particulate nature, the most efficient particle diameter [76]. This first estimation is very helpful in selecting size distribution of commercial products.

The actual problem is in fact much more complex, because there is often not one frequency, but a large frequency range that needs to be stabilized, and

the products used never exhibit a single diameter. Aluminum has been used for quite a long time; because of the lack of control on the alumina particles diameter that are produced in the combustion gases it is impossible to reach a maximum damping. Therefore, researchers have made new attempts with inert products, the high melting point of which gives the possibility of damping effect optimization with low particle amounts. This solution has the additional advantage of not affecting the rocket motor signature.

With an average particle size ranging from 1 to 2 μm , these products provide good damping for frequencies of the order of 15 kHz.

Bibliography

1. CHRISTENSEN, W. N., Development of an acoustic emission strand burning technique for motor burning rate prediction. AIAA 78-984, AIAA/SAE/ASME, 14th Joint Propulsion Conference, 1978.
2. TRINEAU, J. C. and KUENTZMANN, P., Some measurements of solid propellant burning rates in nozzleless motors. AIAA 84-1469, AIAA/SAE/ASME, 20th Joint Propulsion Conference, 1984.
3. KUBOTA, N., OHLEMILLER, T. J., CAVENY, L. H. and SUMMERFIELD, M., The mechanism of super-rate burning of catalysed double-base propellants. AIAA 74-124, AIAA/SAE/ASME, 10th Joint Propulsion Conference, 1974.
4. LENGELLÉ, G. *et al.*, Steady-state burning of homogeneous propellant. *Fundamentals of Solid Propellant Combustion*, Vol. 90, Progress in Astronautics and Aeronautics, pp. 361-403, 1984.
5. LENGELLÉ, G., Thermal degradation kinetics and surface pyrolysis of vinyl polymers, *AIAA Journal*, 8, 1989-1996, November 1979.
6. KUO, K. K., *Principles of Combustion*. Wiley Interscience, 1986.
7. WILLIAMS, F. A., *Combustion Theory*. Addison-Wesley, 1965.
8. BECKSTEAD, M. W., DERR, R. L. and PRICE, C. F., A model of composite solid propellant combustion based on multiple flames, *AIAA Journal*, 8(12), 2200-2207, 1970.
9. ZENIN, A. A., Structure of temperature distribution in steady-state burning of a ballistic powder, *Combustion, Explosion and Shock Waves*, 2(3), 1966.
10. WILLIAMS, F. A., BARRERE, M. and HUANG, M. C., *Fundamental Aspects of Solid Propellant Rockets*, Agardograph 116, Technivision, 1969.
11. AOKI, Y. H. and KUBOTA, N., Combustion wave structures of high and low energy double-base propellants. AIAA 80-1165, AIAA/SAE/ASME, 16th Joint Propulsion Conference, 1980.
12. BECKSTEAD, M. W., Model for double-base propellant combustion. AIAA 80-4079, AIAA/SAE/ASME, 16th Joint Propulsion Conference, 1980.
13. KING, M. K., A model for prediction of effects of pressure, cross-flow velocity and heat of explosion on double-base propellant burning rate. AIAA 81-1555, AIAA/SAE/ASME, 17th Joint Propulsion Conference, 1981.
14. COHEN, N. S., Analysis of double-base combustion. AIAA 81-0120, AIAA/SAE/ASME, 17th Joint Propulsion Conference, 1981.
15. FERREIRA, J. G., BIZOT, A. and LENGELLÉ, G., Model for double-base propellants combustion, with and without additives. AIAA 83-1197, AIAA/SAE/ASME, 19th Joint Propulsion Conference, 1983.
16. KISHORE, K., PAI VERNECKER, V. R. and KRISHNA-MOHAN, V., Differential scanning calorimetric studies on ammonium perchlorate, *Thermochimica Acta*, 13, 277-292, 1975.
17. SELEZNEV, V. A., POLHIL, P. F., MALTSEV, V. M. and BAVYKIN, I. B., An optical method of measuring the burning surface temperature of condensed systems, *Combustion and Flame*, 13(2), 139-142, 1969.
18. GUIRAO, C. and WILLIAMS, F. A., A model for ammonium perchlorate deflagration between 20 and 100 Atm, *AIAA Journal*, 9(7), 1345-1356, 1971.

19. BOGGS, T. L., The thermal behavior of cyclotrimethylene trinitramine (RDX) and cyclotetramethylene tetranitramine (HMX) *Fundamentals of Solid Propellant Combustion*, Vol. 90, Progress in Astronautics and Aeronautics, pp. 121-168, 1984.
20. FIFER, R. A., Chemistry of nitrate ester and nitramine propellants, *Fundamentals of Solid Propellant Combustion*, Vol. 90, Progress in Astronautics and Aeronautics, pp. 177-225, 1984.
21. BOGGS, T. L., PRICE, C. F., ZURN, D. E., DERR, R. L. and DIBBLE, E. J., The self-deflagration of cyclotetramethylene tetranitramine (HMX). AIAA 77-859, AIAA/SAE/ASME, 13th Joint Propulsion Conference, 1977.
22. RAMOHALLI, K. N. R., Steady-state burning of composite propellants under zero cross-flow situation, *Fundamentals of Solid Propellant Combustion*, Vol. 90, Progress in Astronautics and Aeronautics, pp. 409-472, 1984.
23. GODON, J. C., Modélisation de la combustion normale et érosive des propergols composites. Thèse de Docteur d'Etat es-sciences physiques, Université Pierre et Marie Curie, Paris 6ème, Soutenue le 24 novembre 1983.
24. MESSNER, A. M., Transient coning in end-burning solid propellant grains. AIAA 80-1138, AIAA/SAE/ASME, 16th Joint Propulsion Conference. 1980.
25. SMITH, R. E., End burning technology program: interim report. Task A: laboratory effort. Task B: subscale motor tests. Aerojet Solid Propulsion Company, Sacramento, Calif., Report AFRPL-TR-71-38, AD-891 362, October 1971.
26. JOLLEY, W. H., HOOPER, J. F., HILTON, P. R. and BRADFELD, W. A., Studies on coning in end-burning rocket motors, *Journal of Propulsion*, 2(3), 223-227, 1986.
27. BRONGNIART, C., DAMIEN, M. and FRÈCHE, A., Chargements propulsifs à combustion frontale a forte vitesse de combustion, mis en oeuvre par le procédé Epictète (Casting process). ICT, *International Jahrestagung, Technologie des Poudres et Explosifs*, Karlsruhe, pp. 361-374, 1984.
28. FRIEDLANDER, M. P., III and JORDAN, F. W., Radial variation of burning rate in center perforated grains. AIAA 84-1442, AIAA/SAE/ASME, 20th Joint Propulsion Conference, 1984.
29. BECKMAN, C. W. and GEISLER, R. L., Ballistic anomaly trends in subscale solid rocket motors. AIAA 82-1092, AIAA/SAE/ASME, 20th Joint Propulsion Conference, 1984.
30. KALLMEYER, T. E. and SAYER, L. H., Differences between actual and predicted pressure-time histories of solid rocket motors. AIAA 82-1094, AIAA/SAE, ASME, 18th Joint Propulsion Conference, 1982.
31. BOGGS, T. L., ZURN, D. E. and DERR, R. L., The effects of strain on the burning rates of high energy solid propellants. 13th JANNAF Combustion Meeting, September 1976.
32. PLANTIF, B., Influence of acceleration on the combustion of solid propellants, measurement and prediction of the effects. *Problems and Methods of Simulation of the Environment*. ICT Jahrestagung, Karlsruhe, pp. 409-451, 1972.
33. BOISSON, J., *La propulsion par fusée*. Cours de l'Ecole Nationale Supérieure des Techniques Avancées, Vol. 1, 2, 1981.
34. DELANNOY, G., Prediction of antitank solid propellant rockets internal ballistics. AIAA 84-1355, AIAA/SAE/ASME, 20th Joint Propulsion Conference, 1984.
35. YANENKO, N. N., *The Method of Fractional Steps*. Springer-Verlag, Berlin, Heidelberg, New York, 1971.
36. GODOUNOV, S., ZABRODINE, A., IVANOV, M., KRAIKO, A. and PROKOPOV, G., *Résolution numérique des problèmes multidimensionnels de la dynamique des gaz*, Editions Mir-Moscou, 1976.
37. ASCH, G., CHARNAY, G. and SCHON, J. P., Capteurs de vitesse, débit et niveaux de fluide. *Les capteurs en instrumentation industrielle*, Dunod, pp. 535-572, 1982.
38. RAZDAN, M. K. and KUO, K. K., Erosive burning. *Fundamentals of Solid Propellant Combustion*, Vol. 90, Progress in Astronautics and Aeronautics, pp. 515-592, 1984.
39. KING, M. K., Erosive burning of composite solid propellants: experimental and modeling studies. AIAA 78-979, AIAA/SAE/ASME, 14th Joint Propulsion Conference, 1978.
40. MARKLUND, T. and LAKE, A., Experimental investigation of propellant erosion, *ARS Journal*, 3, 173-178, February 1960.
41. BARRÈRE, M. and LARUE, P., Contribution à l'étude de la combustion érosive des poudres composites, *La Recherches Aérospatiale*, No. 95, pp. 25-36, July-August 1963.

42. LENOIR, J. M. and ROBILLARD, G., A mathematical method to predict the effect of erosive burning in solid propellant rocket. *Sixth International Symposium on Combustion*, Reinhold Publishing Co., pp. 663-667, 1957.
43. LENGELLÉ, G., Model describing the erosive combustion and velocity response of composite propellants, *AIAA Journal*, **13**(3), 315-322, March 1975.
44. KING, M. K., A model of the erosive burning of composite propellants. AIAA 77-930, AIAA/SAE/ASME, 13th Joint Propulsion Conference, 1977.
45. BEDDINI, R. A., Analysis of injection-induced flows in porous walled ducts with application to the aerothermochemistry of solid propellant motors. Thesis of the Graduate School of Rutgers, New Jersey, October 1981, See also BEDDINI, R. A., Injection induced flows in porous-walled ducts, *AIAA Journal*, **24**(11), pp. 1766-1773, 1986.
46. KUO, K. K., GORE, J. P. and SUMMERFIELD, M., Transient burning, *Fundamentals of Solid Propellant Combustion*, **90**, 599-653, 1984.
47. KRIER, H., T'EN, J. S., SIRIGNANO, W. A. and SUMMERFIELD, M., Non-steady burning phenomena of solid propellants: theory and experiments, *AIAA Journal*, **6**(2), 278-285, 1968.
48. KRIER, H., Solid propellant burning rate during a pressure transient, *Combustion Science and Technology*, **5**, 69-73, 1972.
49. SUMMERFIELD, M., CAVENY, L. H., BATTISTA, R. A., KUBOTA, N., GOSTINTSEV, YA. and ISODA, H., Theory of dynamic extinguishment of solid propellants with special reference to non-steady heat feed-back law, *Journal of Spacecraft and Rockets*, **8**(3), 251-258, 1971.
50. DE LUCA, L., GALTETTI, L., RIVA, G. and TOBACCO, U., Unstable burning of thin solid propellant flames. AIAA 80-1126, AIAA/SAE/ASME, 16th Joint Propulsion Conference, 1980.
51. SUMMERFIELD, M. and PARKER, K. H., Interrelations between combustion phenomena and mechanical properties in solid propellant rocket motors; mechanics and chemistry of solid propellants. *Proceedings of the 4th Symposium on Naval Structural Mechanics*, Pergamon Press, pp. 75-116, 1967.
52. BARRÈRE, M., L'allumage des propergols solides, Considérations générales, *La Recherche Aéronautique*, No. 123, pp. 15-28, March-April 1968.
53. HERMANCE, C. E., Solid propellant ignition theories and experiments, *Fundamentals of Solid Propellant Combustion*, Vol 90, Progress in Astronautics and Aeronautics, pp. 239-295, 1984.
54. LENGELLÉ, G., MENTRÉ, P. G., GUERNIGOU, J., BIZOT, A. and MAISONNEUVE, Y., Allumage et extinction des propergols solides. Paper submitted at the 53rd Symposium of the AGARD Commission "Propulsion et Energétique sur la Technologie des moteurs fusées à propergols solides", OSLO, 2-6 April 1979.
55. DE LUCA, L., Solid propellant ignition and other unsteady combustion phenomena induced by radiation. Ph.D. thesis, Dept. of Aerospace and Mechanical Sciences, Princeton University, N.J. AMS Rept 1192-T, November 1976.
56. GUERNIGOU, J., INDRIGO, C., MAISONNEUVE, Y. and MENTRÉ, P. G., Mise au point de fluxmètre à température superficielle, *La Recherche Aéronautique*, No. 3, pp. 159-168, 1980.
57. DE LUCA, L., CAVENY, L. H., OHLEMILLER, T. J. and SUMMERFIELD, M., Radiative ignition of double-base propellants, I — Some formulation effects, *AIAA Journal*, **14**(7), pp. 940-946, July 1976.
58. OHLEMILLER, T. J., CAVENY, L. H., DE LUCA, L. and SUMMERFIELD, M., Dynamic effects on ignitability limits of solid propellants subjected to radiative heating. Contract AFOSR-69-1651-BRL, *14th International Symposium on Combustion*, Combustion Institute, Pittsburgh, Pa. pp. 1297-1307, 1973.
59. DE LUCA, L., Extinction theories and experiments, *Fundamentals of Solid Propellant Combustion*, Vol. 90, Progress in Astronautics and Aeronautics, pp. 661-726, 1984.
60. FLEMING, R. W. and DERR, R. L., The use of non-reactive coatings in solid propellant arc-image ignition studies. *Proceedings of the 7th JANNAF Combustion Meeting*, CPIA Publication 204, Vol. 1, pp. 379-389, 1971.
61. CULICK, F. E. C., A review of calculations for unsteady burning of solid propellant, *AIAA Journal*, **6**(12), pp. 2241-2255, 1968.
62. CULICK, F. E. C., Stability of high-frequency pressure oscillations in rocket combustion chambers, *AIAA Journal*, **1**(5), pp. 1097-1104, May 1963.
63. BROWN, R. S., DUNLAP, R., YOUNG, S. W. and WAUGH, R. C., Vortex shedding as an additional source of acoustic energy in segmented solid propellant rocket motors. AIAA 80-1092, AIAA/SAE/ASME 16th Joint Propulsion Conference, 1980.

64. CULICK, F. E. C. (Editor), T-Burner testing of metallized solid propellants. AFRPL.TR. 74-28, 1974.
65. FLANDRO, G. A., Solid propellant acoustic admittance corrections, *Journal of Sound and Vibrations*, **36**, pp. 297-312, 1974.
66. KOOKER, D. E. and ZINN, B. T., Numerical solution of axial instabilities in solid propellant rocket motors, *10th JANNAF Combustion Meeting*, CPIA Publication 243, Vol. 1, pp. 389-415, 1973.
67. KUENTZMANN, P., Etudes récentes à l'ONERA sur les instabilités de combustion dans les moteurs fusées à propergol solide. AGARD CPP No. 259, Solid Rocket Motor Technology, 1979.
68. CULICK, F. E. C., Non-linear behavior of acoustic waves in combustion chamber, *Acta Astronautica*, **3**, 715-757, 1976.
69. KUENTZMANN, P. and NADAUD, L., Réponse des propergols solides aux oscillations de pression et de vitesse, *Combustion Science and Technology*, **11**, 119-139, 1975.
70. STRAND, L. D., SCHULTZ, A. L. and REEDY, G. K., Microwave Doppler shift technique for determining solid propellant transient regression rates, *Journal of Spacecraft and Rockets*, **11**, 75-83, February 1974.
71. PHILIPPE, A. and TCHEPIDJIAN, P., Prediction of longitudinal combustion instabilities in axisymmetrical propellant grains. AIAA 84-1358, AIAA/SAE/ASME, 20th Joint Propulsion Conference, 1984.
72. TISSIER, J. P. and LHUILLIER, J. N., Etude récentes des instabilités de combustion dans les fusées à propergol solide. *Colloque sur la combustion des propergols solides*, Poitiers, 1972, Cahiers de la Thermique, No. 4, Série B, pp. 35-40, May 1974.
73. BROWNLEE, N. G. and MARBLE, P. B., An experimental investigation in solid propellant rocket motors. Solid Propellant Rocket Research Conference, ARS Paper 1067, 1960.
74. LOVINE, R. H., High frequency propellant response measurements. AIAA 77-976, AIAA/SAE/ASME, 13th Joint Propulsion Conference, 1977.
75. KUENTZMANN, P. and LAVERDANT, A., Détermination expérimentale de la réponse d'un propergol solide aux oscillations de pression de haute fréquence, *La Recherche Aérospatiale*, No. 1, pp. 39-55, 1984.
76. EVANS, G. I. and SMITH, P. K., The suppression of combustion instability by particulate damping in smokeless solid propellant motors, AGARD CPP No. 259, *Solid Rocket Motor Technology*, pp. 27.1-27.10, 1979.

CHAPTER 5

Plume, Signal Interference and Plume Signature

GÉRARD PRIGENT

1. Introduction

The presence of a plume with attendant radiation and smoke at the aft end of a missile, due to the combustion and pyrolysis products of the rocket motor exhausted through the nozzle, may cause a missile to fail in its mission.

The plume or smoke may reveal the launch location of a missile and allow the missile to be located in flight. In the case of missiles guided optically (at visible or infrared wavelengths), the transmission of commands through the plume or smoke trail may be substantially attenuated, leading to the loss of control of the missile. Intense flames at the rear of the missile, caused by combustion of the motor exhaust products with air (afterburning), may also reveal the launcher location and trajectory of the missile.

The flames may also cause saturation of the instruments used for optical tracking of the missile or of the target. The flames increase the temperature of the plume, resulting in increased emission of infrared radiation. In addition, the transmission of radar frequency electromagnetic waves is generally very weakened by absorption by these flames that contain ionized species. The flames have also been known to cause engine flameout of jet aircraft that launch the missiles, and also damaging impingement effects on launcher surfaces.

Finally, the nozzle exhaust products may often cause a disturbance of the thrust vector control components because of slag or erosion.

The principal methods used to guide and control missiles [1,2] new ref usually require links between:

- the firing station and the missile;
- the firing station and the target;
- the missile and the target.

The nature of these links may vary:

- optical links (visible or infrared), the wavelengths most used in infrared are 0.9, 1.06, 10.6 μm ;
- electromagnetic links (radar);
- electrical links with conductive wires.

As for the detectability (or signature) of a missile, there are several factors intervening, such as the contrast of the plume and smoke trail [3] against various backgrounds and under various types of lighting, and the emission of visible and infrared radiations by the gases and hot particles that make up the plume.

The purpose of this chapter is to describe (1) plumes and plume phenomena, (2) interactions of plumes with the links necessary for guidance and the means of detection, and (3) means to diminish or suppress these interactions. Therefore this chapter includes:

- a physicochemical analysis of the plumes and smoke trails;
- a description of the methods available to determine the physicochemical characteristics;
- a presentation of the methods available to predict the properties of the plume and smoke trail;
- an examination of the influence of the characteristics of the rocket motor (operating conditions, nature of the propellant, inhibitor, liner, and insulation materials, etc.) on the nature and the properties of the plume and smoke trail;
- methods to eliminate or minimize some of these undesirable characteristics in terms of guidance and signature.

2. Description of the Flow Exiting from a Nozzle

2.1. BACKGROUND

The flow at the exit plane of the nozzle of a solid propellant rocket motor in operation is supersonic, with an average temperature of the mixture of gases and solid or liquid particles generally over 1000 K. The local pressure may be greater, lower or equal to the atmospheric pressure, and the flow is said to be, respectively, under-expanded, over-expanded or matched (optimum expansion).

Downstream from the nozzle, the hot portion of the flow is commonly called the plume. Various phenomena, such as turbulence, electronic excitation, ionization, and most important, afterburning, occur in the plume.

The plume gas dynamic structure, as shown in Fig. 1, must take into account not only the existence of discontinuities both in the velocity (slipline) and the pressure (straight or oblique shocks), but mixing with the ambient air.

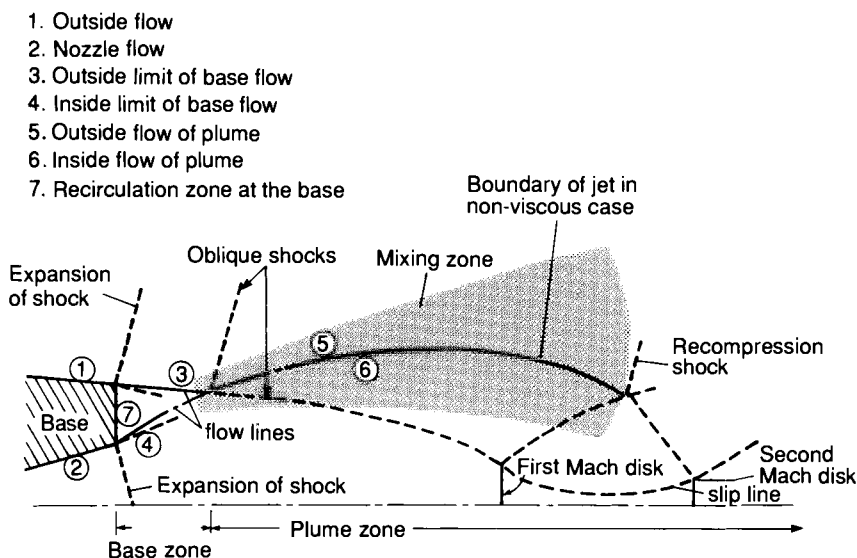


FIG. 5.1. Diagram of the zones of the plume of missile in flight.

Condensed exhaust products, solid or liquid, may be present downstream of the nozzle exit plane, leading to the presence of plume smoke, called primary smoke. Secondary smoke may develop, further downstream and in external regions of the plume, depending on the atmospheric conditions, caused by the condensation of water vapor from both the plume and the atmosphere.

The attenuation of radar waves and infrared emissions are more important in the plume, and the absorption and scattering of visible light are more important in the smoke trail.

Most of the chemical products in the plume come from combustion of the propellant. Additional contributions to the exhaust gases and particles come from thermal and mechanical erosion, pyrolysis and combustion of the inhibitors, liners and insulators, and from ablation of nozzle and blast-tube materials.

2.2. THE GASEOUS PRODUCTS

The major gaseous products contained in the combustion residue mixture are nearly always CO , CO_2 , H_2 , H_2O and N_2 . Propellants containing ammonium perchlorate produce, in addition, hydrochloric acid HCl (Table 1).

The reducing power or fuel index of a gaseous mixture is usually characterized by the sum of molar fractions of hydrogen H_2 and of carbon monoxide CO .

$$P = N_{\text{CO}} + N_{\text{H}_2}$$

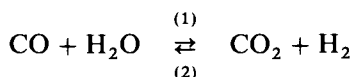
TABLE 1 *Major combustion products from typical propellants calculated*

Composition	N% ^a						Condensed products ^c	T ^b (K)
	HCl	CO	CO ₂	H ₂	H ₂ O	N ₂		
EDB	0	38	13	10	23	12	1.5	2630
Smokeless EMCB (NC, NgI, RDX)	0	34	12	10	23	19		2775
Butalite (HTPB + AP)	17	18	8	12	36	9	0.2	2798
Butalane	16	22	1.3	31	11	8	10	3620

^a Molar fractions inside the chamber.^b Combustion temperature inside the chamber.^c Total fraction of the condensed particles at the exit plane of the nozzle after equilibrium expansion.

This value, always somewhere between 0 and 1, is obtained by analyzing the composition of the gases inside the combustion chamber (Chapter 3).

Assuming that the gaseous mixture in the combustion chamber is in thermodynamic equilibrium, the reaction



is sufficient to provide an initial approximation to the respective amounts of the mixture's principal ingredients. The reducing power of the few propellants used as examples in Table 1 ranges from 0.3 and 0.55. With composite propellants it decreases when the ammonium perchlorate level increases, and it increases with the level of HMX and aluminium. With EDB and CMDB propellants it usually varies conversely with the combustion chamber temperature. When the mixing of the combustion residual products with air is accompanied by afterburning, the level of CO₂ and H₂O and the temperature, increase significantly.

2.3. PRIMARY SMOKE

Primary smoke consists of a mixture of liquid and solid particles usually exhausted at the exit plane with the combustion gases. It is easily detected because it exhibits the triple capacity of, at the same time, absorbing, emitting and scattering ultraviolet visible, or infrared radiation. The corresponding optical magnitudes depend on the number, size and nature of the particles.

The smoke may come from the pyrolysis of the inhibitor, the thermal insulation, or from any other parts of the motor that come into contact with the combustion gases, as well as from the propellant itself, which may contain

ballistic catalysts, anti-instability additives, and flash suppressors with mineral elements or reducing metallic fuel solids. It may also sometimes originate directly in the combustion chamber as in the case of alumina, which is liquid at a temperature over 2315 K, or of zirconium oxide, which solidifies as soon as the temperature drops below 2990 K.

Other chemical products condense further beyond the throat of the nozzle. Lead, copper, potassium and their oxides, for example, produce submicron-size particles. From an attenuation point of view, these particle sizes result in absorption and scattering of visible and infrared light which are very notable.

Carbon and soot particles constitute a special case. They are primarily caused by the pyrolysis of materials of the chamber (liners, insulators, etc.). Their size increases as a function of the residence time in the combustion chamber [4]. Their size at the nozzle exit remains small, between 10^{-1} and 10^{-2} μm , contributing significantly to the signature of the plume, particularly at shorter wavelengths.

End-burning grains that are inhibited on the lateral face produce a significant amount of this type of primary smoke. It has been demonstrated that the polyester inhibitor, having lost 3% of its mass due to heating by the combustion gases of a CDB propellant (reducing power 0.6, combustion temperature 2000 K) is enough to produce 1% (in mass) of soot in the smoke. This quantity is sufficient to make the smoke trail of a missile detectable.

2.4. SECONDARY SMOKE

The combustion of propellant containing ammonium perchlorate (Buta-lite, reduced smoke Nitramite) produces hydrochloric gas. Under specific atmospheric conditions of temperature and humidity (Fig. 2) the combination with air results in the formation of a mist of azeotropic liquid drops of H_2O and HCl .

It is observed that it usually takes several seconds for the secondary smoke cloud to reach maximum opacity (Fig. 3). Increases of the absorption and scattering of the visible and infrared light occur simultaneously, due to the growth both in number and size of the drops.

In the case of composite propellants, with ammonium perchlorate contents greater than 60%, the secondary smoke forms a very dense fog.

In contrast, the smoke observed during the firing of a XLDB (high-energy binder + HMX) propellant with a low ammonium perchlorate percentage is translucent, and difficult to differentiate from the primary smoke due to some additives.

The importance of the secondary smoke depends on the operational climatic environment of the missile. Table 2 compares the frequency of the occurrence of secondary smoke for two propellants based on climate variations (according to statistics provided by the French National Weather Bureau).

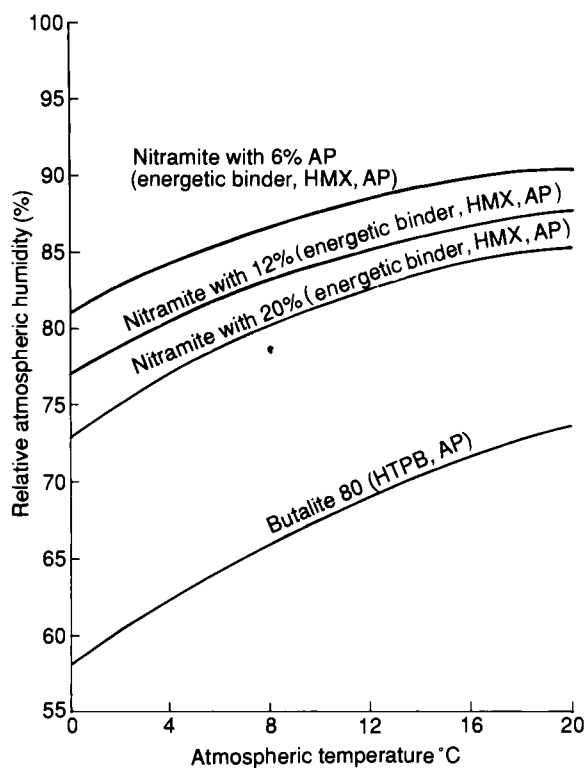


FIG. 5.2. Range of occurrence of secondary smoke.

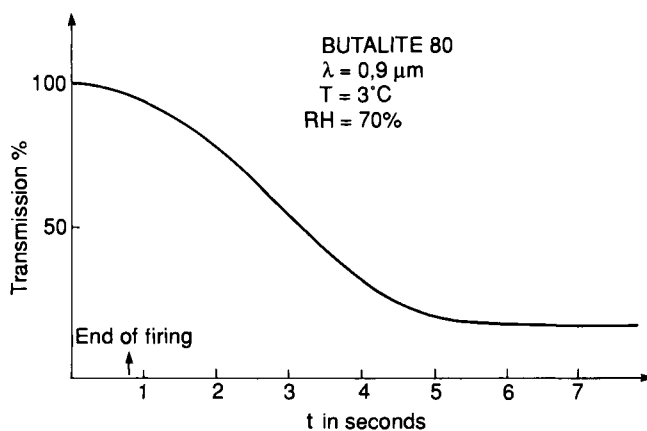
FIG. 5.3. Growth kinetics of a trail of secondary smoke in a climatic chamber (600 m³). Transmission versus time.

TABLE 2

Season	Frequency of occurrence of secondary smoke in Paris Montsouris (percentages)	
	82% AP composite	15% AP XLDB
Spring	30	17
Summer	19	4
Fall	50	25
Winter	64	40
Annual average	40	21

2.5. PLUME AFTERBURNING

Since the specific impulse of a propellant is inversely proportional to the square root of the molecular weight of the gases, it is more efficient, from the standpoint of thrust, to select a fuel-rich propellant whose combustion produces an underoxidized (less than stoichiometric) gaseous mixture with more carbon monoxide molecules than carbon dioxide, and more hydrogen than water, and thus a relatively high reducing power. Theoretically, we note the reducing power varies relatively little during the expansion through the nozzle, so that downstream of the exit plane the gases are likely to burn again when they mix with atmospheric oxygen. This phenomenon is called afterburning or secondary combustion of the plume.

The motor exhaust flow, the design of the base of the missile, the speed of the missile, the altitude, the pressure of the combustion chamber, and the expansion ratio of the nozzle exit plane are some of the variables that, like the reducing power and the temperature of the gases, affect the probability that afterburning will occur, and at the same time, influence the ignition point and the position of the flame in the exhaust flow downstream of the nozzle.

Afterburning is a complex phenomenon, and its parametric study is made very difficult because the influence of the various parameters is not additive, and because of their interactions within a complicated flowfield, typified by Fig. 1.

Afterburning causes a temperature increase in the plume with resulting increases in luminosity, infrared emission, concentration of ions and free electrons (which increases radar attenuation and radar cross-section). Afterburning also increases the turbulence of the plume and, consequently, the interference and defocusing of guidance laser beams, and the noise imposed on radar guidance signals. The acoustic noise of a rocket motor is also increased by afterburning. Afterburning may also modify the nature and quantity of primary and secondary smoke.

Because of the very high temperatures and high flow velocities in the areas where afterburning is triggered, validation of theoretical values of these two parameters by experiments presents serious technical difficulties.

It is easier, although somewhat uncertain, to validate theory by measuring effects induced using the methods described below.

3. Description of the Methods Used to Measure the Characteristics of the Plume and Smoke

The experimental methods developed have as a main objective the study of phenomena induced by the flow of the gas-particle mixture of the plume and smoke.

Firings generally take place on static benches, and projecting the measurement values to the real case of a missile in flight involves risky extrapolation. The static test results therefore most often serve to classify the propellants tested for the optical phenomenon under study. Greatly different results may occur in flight, as predictable with appropriate computer programs.

3.1. MEASUREMENT OF THE RADAR ATTENUATION

The presence of alkaline or alkaline-earth metal vapors, often just as traces (a few tens of ppm) in the combustion gases, causes significant ionization of the medium when the temperature is sufficiently high ($T > 2000$ K). This situation occurs in the combustion chamber of the rocket motor and in the afterburning region of the plume.

Free electrons subjected to the excitation of a radar wave with a frequency of several gigahertz traversing the medium begin to vibrate. A portion of the energy picked up is later dissipated in the plume through collisions with the more massive gas molecules in the plume (N_2 , such as HCl, O_2). The energy lost from the wave, known as attenuation, is measured in decibels, using the formula:

$$A = -10 \log \frac{I_r}{I_e}$$

where I_e is the intensity of the incident wave and I_r the residual intensity of the wave after absorption by the plume.

The attenuation value depends not only on the frequency of the radar wave, but also on the characteristics of the ionized medium traversed (electronic density, collision frequency, etc.) [5].

For the purpose of simply comparing propellants, the attenuation is usually measured transversely (that is perpendicular) to the axis (Fig. 4). This measurement is not directly comparable with the measurements obtained by a control station when the missile is in flight. For this reason a second type of

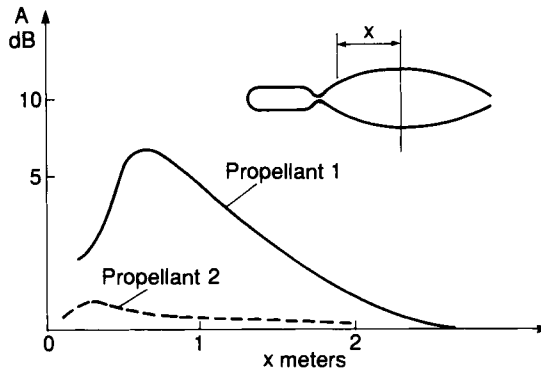


FIG. 5.4. Attenuation measured perpendicularly to the axis of a rocket motor for two different propellants.

device is used to measure the attenuation as a function of the sighting or aspect angle θ (Fig. 5), known as a longitudinal or diagonal measurement.

For any specific propellant there usually is a ratio of 6 to 10 between the maxima of attenuation obtained by longitudinal and transverse methods unless the plume electron density is so high that non-linear effects, such as refraction and diffraction, modify the longitudinally measured radiation.

3.2. OPTICAL TRANSMISSION IN THE VISIBLE AND INFRARED RANGES

As examples, two methods of measurements used to study the optical phenomena related to the occurrence of smoke will be described:

- measurement made with a “smoke meter”;
- measurement on a free plume.

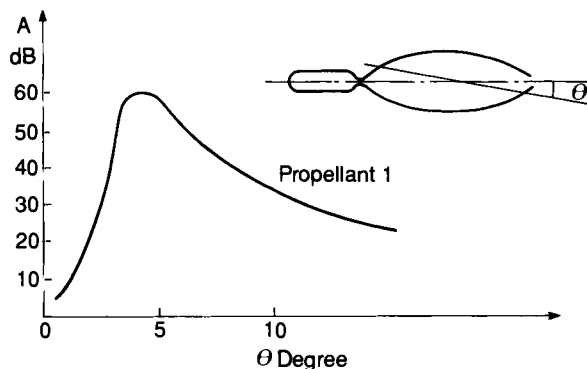


FIG. 5.5. Attenuation measured longitudinally.

3.2.1. The smoke meter

The smoke meter is a subsonic wind tunnel, 10 m long and 1 m in diameter, in which static motor firings are made to compare various propellants under standard conditions by measuring the transparency of their primary smokes. The optical measurements are made at the exit of the wind tunnel (Fig. 6), with dilution of the exhaust flow between 10^{-1} and 10^{-2} expressed by the ratio of the respective flow rates of the motors and the air drawn into the wind tunnel.

The major drawback is that the device is not very representative of the real conditions under which smoke is formed. Furthermore, it does not allow the study of firing with a short burning time (less than 2 s). But the measurements are little influenced by the perturbations of outside climatic conditions, and therefore are easily reproduced.

3.2.2. Free jet measurements

The test site for free jet firings must be protected from wind, and be sufficiently spacious so as not to disturb the shape of the smoke trail.

A stationary measurement of the transmission is made, perpendicular to the axis of the trail, in an area located downstream from the exit plane where all primary smokes are usually condensed. A non-stationary (source and sensor moving parallel to the trail axis) measurement allows estimation of the rate of build-up, settling, and dissipation of the smoke trail behind the motor of a missile versus time. A longitudinal measurement may be made instead.

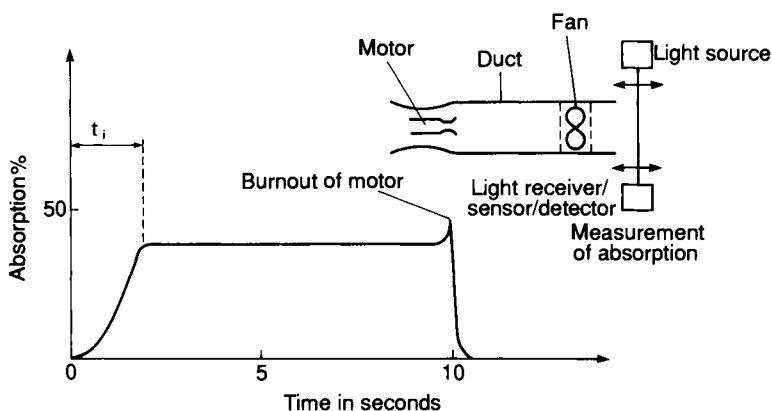


FIG. 5.6. Absorption measurement at exit of smoke measurement device. (t_i) is the time needed to reach a stationary flow in the duct).

3.2.3. *Optical instruments*

The instruments used to measure the transmission, through the smoke trail, consist of an emitting source and a detector. The transmission level is given as the ratio of the intensity received by the detector during the firing to that before or after the firing.

The selection of the source and the detector depends on the range of wavelengths in which the measurements are to be made. The range is always located within the limits where the atmosphere is transparent.

3.3. MEASUREMENT OF INFRARED EMISSION BY A PLUME

The plume of a rocket motor is a source of heat, similar to an infinite number of point sources emitting a radiation characteristic of the temperature and of the local concentration of chemical products, either gaseous or condensed.

The resulting total emission is not the sum of the point sources because for each emitting point a portion of the radiation is partially absorbed or scattered by the other points in the vicinity.

The emission spectrum of a plume, whose maximum intensity is in the short to mid-infrared wavelengths, is the superposition of a continuum of particle radiation and radiation manifesting the vibration-rotation or rotation-only types of radiation transfer (emission, absorption and scattering) phenomena, of the gas molecules thermally excited.

An increase in the temperature in a plume, and chemical changes of the mixture such as occur with afterburning, cause a corresponding increase of the total intensity and a change in the spectrum of the radiation.

The use of an infrared camera (thermal imager) has allowed assessment of afterburning; in particular, the verification of the efficiency of some flash suppressors compounds in a smokeless propellant, by comparing the intensity radiated by the plume from a modified propellant composition to that of a propellant containing no such additive.

4. Description of the Methods of Analysis

The modeling of the physicochemical phenomena occurring downstream of the exit plane of the nozzle required the development of computer programs to simulate both the flow and chemistry of the gas-particle mixture, and the optical phenomena tied to the plume or the smoke trail.

4.1. THE FLOW PROGRAMS

4.1.1. Analysis of the flow of a plume

The results of the analyses of the properties of a plume depend on the simplifying assumptions used to solve the Navier-Stokes equations, as well as on the types of measurements on which the comparisons with theory are based. Two types of models and computer programs are generally used when there is a possibility of afterburning.

In the zone close to the base of the missile where there is a confluence of the nozzle flow and the flow of external air behind the nozzle exit plane, and up to a distance of 10 nozzle radii, the program used will calculate the three characteristics (Fig. 7): pressure, temperature and velocity, as well as the chemical composition. This program can be used for the large pressure gradients that occur in this region. To reduce computer run times, simplified chemical reaction schemes are often used; for example, use of reactions involving only five gaseous products (CO , CO_2 , H_2 , H_2O , O_2) is often adequate.

Further from the nozzle exit plane, a satisfactory description of the plume can be obtained by using a computer program [6] assuming a constant pressure in the plume, thereby allowing the use of a more sophisticated set of chemical reactions. In particular, it is accepted that, in spite of the notorious imprecision of some values of the rate constants in reactions that give rise to free radicals, only a flow model using a chemical reaction system, such as the system recommended by Jensen [7], affords the possibility of correctly assessing the afterburning phenomenon [8]. More complex computer programs calculate pressure fluctuations of the plume with a full reaction set [9].

The ability to predict the plume with a computer program is fairly limited in the case of weak afterburning [10,11]. The discrepancy between the computer model and reality is probably related to imprecisions in the kinetic model used in the computer programs, as well as to the fact that the fluctuations due to turbulence are not taken into account in the calculations of the chemical reactions in the plume. These two points are currently the subject of many studies.

4.1.2. Analysis of a flow in a smoke trail

Much further downstream from the nozzle exit plane, the combustion products have cooled down, the gases are diluted, and all chemical products likely to condense in the ambient temperature form a trail of smoke which shows the flight trajectory of the missile. The trail of condensed water vapor left behind by a jet plane is caused by the same phenomenon.

A computer program can calculate temporal evolutions of the temperature, the velocity, and the dilution in each location of the trajectory, taking into

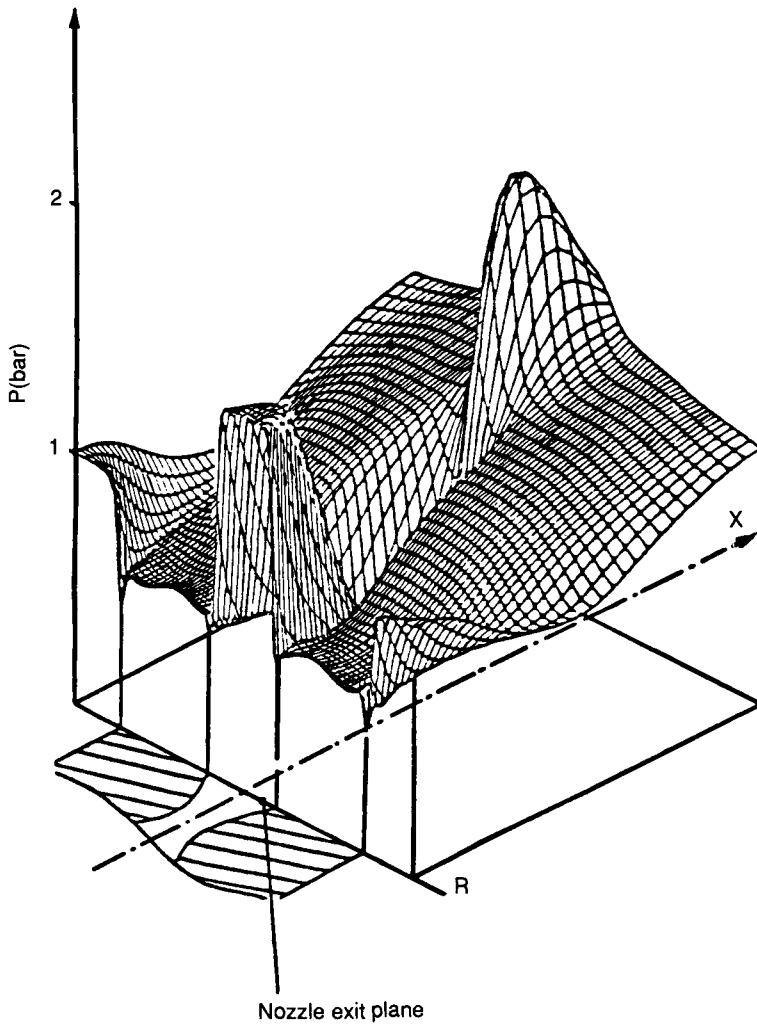


FIG. 5.7. Pressure field in a plume..

account the flight characteristics of the missile (direction, speed), the atmospheric conditions affecting the rapidity with which the trail dissipates (wind velocity, ambient temperature), and the characteristics of the residual products ejected by the nozzle (temperature, velocity, condensable fraction).

As an example, the modeling of the smoke trail may be based on the one-dimensional flow, using an empirical law of dilution of the combustion gases with the air along a specific trajectory of a missile [12]. The input data include the velocity, the temperature and the composition of the gases and size and number distribution of particles exiting the nozzle.

4.2. THE OPTICAL PROGRAMS

Calculations of physical values such as the emission, absorption, transmission, and visible, infrared or radar scattering, is done using computer programs whose input data are specific to the phenomenon being studied, and use the results obtained with the flow programs described in Section 4.1.

4.2.1. Calculation of radar attenuation

Absorption is the major cause of radar attenuation. On the line-of-sight of the radar link that intercepts the plume, the attenuation is the sum of the local discrete values of absorption expressed in decibels/cm according to:

$$\alpha = 0,08686 \left(\frac{\omega}{c} \right) \left[-\frac{1-A}{2} + \frac{1}{2} \sqrt{(1-A)^2 + A^2 \left(\frac{\vartheta}{\omega} \right)^2} \right]^{1/2}$$

where $A = \omega_p^2 / (\vartheta^2 + \omega^2)$ and $\omega_p^2 = 3.181 \times 10^3 n_c \text{ (rad/s)}^2$

ω , ϑ , ω_p and n_c representing, respectively, the signal frequency, collision frequency, plasma frequency and local electronic concentration of the plasma environment. The signal frequency data are supplied by the missile designer; the other data are obtained by calculations of the plume flowfield, using the computer programs in Section 4.1.1.

Refraction, diffraction, and scattering are phenomena that are often neglected, but may be very important in operational situations with high electron concentrations in the plume. The effect of diffraction is to change the polar distribution of radar energy in the far field of the plume. The result is that the maximum attenuation (signal loss) value may be much less than would be caused by line-of-sight absorption alone [5,13]. Refraction and diffraction by the plume may also cause guidance errors by ducting around the plume radar energy to and from the target, with a resulting shift in the apparent target location.

Another radar interference effect is manifested as noise on the radar carrier frequency, presumably due to scattering of the radar wave by large refractive index gradients associated with high-velocity turbulent eddies in the plume. This noise can interfere with and mask missile control information coded into the radar wave [14-16]. The same scattering phenomenon causes backscatter of the radar wave, manifested as the plume radar cross-section.

4.2.2. Calculation of optical transmission

According to the Beer-Lambert law, the transmission factor is expressed by:

$$T = e^{-(N\sigma_a + N\sigma_d)Z}$$

with

$$\sigma_a = \frac{Q_a}{\pi r_0^2} \text{ and } \sigma_d = \frac{Q_d}{\pi r_0^2}$$

N , r_0 , σ_a , σ_d are, respectively, the number of particles in the environment, their average radius, the effective absorption and scattering cross-section, and Z , the thickness of the medium traversed.

Q_a and Q_d are complex functions that provide the values of the absorption and scattering coefficients, as a function of the optical refractive index n of the particles, their radius, and the wavelength λ of the signal. Electron microscope measurements of the diameter of particles from samples taken from the plumes and smoke trails of motors with variable flow rates resulted in particle sizes ranging from $1/100 \mu\text{m}$ to several tens of μm .

The theory of scattering of light [17,18], enables us to calculate the various Q_d for each of the following three cases:

- (1) where the radius of the particle is small in comparison with the wavelength (Rayleigh scattering);
- (2) where the radius of the particle and the wavelength are similar (Mie theory);
- (3) where the radius of the particles is very large in comparison with the wavelength (the domain of geometrical optics).

Because the calculations in the Mie range are complex, a computer program [19] is used to obtain the Q_a and Q_d coefficients for a population of particles (in this reference, obeying a log-normal law of particle size distribution). The last calculation to determine the light intensity scattered in all directions θ by this cloud of particles is done according to:

$$I_\theta = \frac{I_0 \lambda^2}{8} \frac{(I_1 + I_2)}{r_0^2 \pi^2}$$

with

$$I_i = \frac{\pi^2 r_0^2}{\lambda^2} Q_d P_i$$

P_i = the function values tabulated by Deirmendjian [20].

The calculations of the coefficients of transmission through primary smokes, based on experimental data on the nature and the size of the particles ejected by the nozzle, provide a certain amount of useful guidelines for the design of rocket propulsion propellants:

- Carbon soots are highly absorbing, regardless of the wavelength.
- As a rule, as long as the radius of the particles is not too great, transmission in infrared is usually better than transmission in the visible range.

- The scattering indices of copper and carbon are fairly similar. Both are high in terms of the signature of the plumes and smoke trails. Figure 8 shows, based on the size of the particles ejected by the nozzle, the maximum mass fraction for a number of materials that cannot be exceeded in order to keep a transmission through a given smoke trail (1 m thick, 5×10^{-2} dilution) equal to at least 95%.

We observe that only a very small amount of carbon is required to degrade the transmission in infrared at $10.6 \mu\text{m}$, and that zirconium oxide is found to be better than aluminum oxide in the visible range.

4.2.3. Calculation of infrared emission

The first models for infrared emissions in plumes appeared in 1967, in the work of Rochelle [21]. They were followed by the NASA models and Lockheed in 1973, Aerodyne in 1974, and finally Grumman in 1976 [22]. In

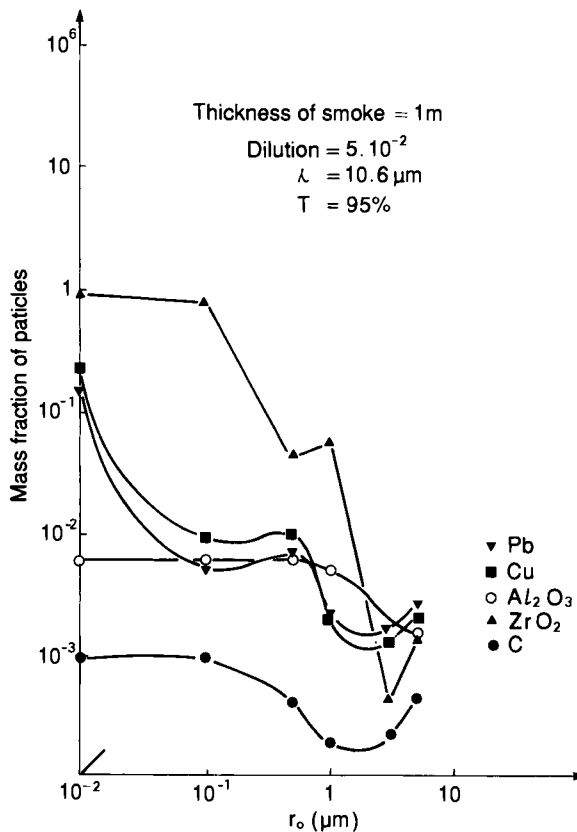


FIG. 5.8. Influence of the type, density and the radius of the particles, on the infrared transmission at $10.6 \mu\text{m}$.

1978 the JANNAF Exhaust Plume Technology Subcommittee undertook to develop a standard model that included a standard plume flow model (SPF), and a standard infrared radiation model (SIRRM) [23].

A typical simple model calculates the infrared radiation of a gas particle mixture containing the main gaseous products (H_2O , CO_2 , CO , HCl) and one condensed species, alumina.

Results from calculations of the infrared radiation in the plume of a motor burning aluminized propellant show that the infrared radiation is highest in the afterburning region, and in its absence it is highest just behind the first Mach disk.

4.3. PREDICTION MODEL FOR THE OCCURRENCE OF SECONDARY SMOKE

Under specific temperature and humidity conditions, atmospheric water vapor may condense into pure water drops and create fog. The combustion of a propellant containing ammonium perchlorate leads to the mixing of hydrochloric acid and water vapors. At a given temperature, and in the presence of an azeotrope, the saturating vapor pressure of the mixture is lower than that of pure water. This phenomenon results in condensation and the formation of a secondary smoke trail in the operational range when such propellants are used [24,25].

For a given temperature and humidity level, the quantity of condensed water versus the dilution ratio of the combustion products in the air can be determined. The mixing of these two vapors is assumed to be homogeneous, without any chemical reaction, and its enthalpy assumed equal to the sum of their total enthalpies. The conditions of thermodynamic equilibrium liquid/vapor are calculated from tabulated experimental data. Two possibilities emerge:

- the results of the calculations indicate that a complete lack of condensation is expected regardless of the dilution ratio of the combustion products in the air: secondary smoke will never occur;
- the results of the calculations indicate that there is a dilution ratio for which condensation is possible: this means there is a possibility that secondary smoke will form.

The results are plotted for each propellant, in a curve of the type shown on Fig. 2, that provides the minimum humidity level versus the ambient temperature of the air above which secondary smoke may occur.

5. Influence of Propellant Formulation on Transparency and Low Signature

At the start of a new program for a tactical or strategic missile, based on the requirements of the missile manufacturer for transmission on through the

plume and low plume or trail signature, the propellant designer is often led to make a selection of the various ingredients that can be part of the formulation.

5.1. FLASH SUPPRESSORS

The addition of potassium salts in the formulation of homogeneous EDB and CDB propellants and Nitramites with high energy binder and HMX or RDX makes it possible to suppress the afterburning. Because these additives, for the most part, generate primary smoke, their percentage in the so-called smokeless propellants, as described in Table 3, must be limited to the exact amount required.

5.2. PARAMETERS AFFECTING THE RADAR TRANSMISSION

In composite propellants the K (potassium) equivalent content (K equivalent \approx ppm of K + ppm \times 1/10 of Na) is usually between 15 and 300 ppm. In homogeneous or Nitramite propellants, containing no ballistic additives, the level is often between 5 and 30 ppm.

Potassium in composite propellants is an impurity contained in the ammonium perchlorate, and in homogeneous or Nitramite propellants, an impurity contained in the nitrocellulose.

The K content of some insulation materials may reach 5000 ppm.

When there is afterburning in the plume, these amounts may cause very

TABLE 3 *Classification of the propellants^a based on their signature*

Class	Primary smoke	Secondary smoke	Restrictions place on the formulation
Smokeless	Very little	None	No aluminum No AP Very low level of condensable species
Minimal smoke	Very little	Low density and not frequent	Little or no aluminum, Little AP (< 20%) Very low level of condensables species
Reduced smoke	Little	Yes	AP permitted Very low level of condensable species
High signature	Yes	Yes	None

^a This classification cannot yet be considered as an international classification.

A working group of NATO/AGARD is now trying to define a standard international classification.

high levels of transverse attenuation (see Table 4) and unacceptably high signal loss in flight.

Other specific additives included in composite propellants exhibit anti-attenuation characteristics (tin, chromium or lead molybdenum). The mechanism of their action in the plumes remains, for the time being, rather poorly defined. It is thought, however, that they have the power to inhibit the occurrence of the OH radicals that initiate the afterburning.

5.3. PARAMETERS AFFECTING THE PRIMARY SMOKE

Propellant metal fillers included as fuels, ballistic burning rate modifiers, and the metal fillers of the insulation materials included as additives to improve their heat resistance and structural integrity, are the main sources of primary smoke.

Consequently, a compromise must be sought between the increased plume signature and the gain in impulse due, for example, to aluminum.

Tests with a smoke meter show that the transmission in the visible range through smoke produced by an 82% ammonium perchlorate Butalane drops from 80% to 11% when the percentage of aluminum is from 0.5% to 8% (rocket motor flow rate around 500 g/s).

The same type of measurements performed at $\lambda = 2 \mu\text{m}$ give two corresponding transmission values of 95% and 30%.

Aluminum-free propellants, in spite of the possible presence of ballistic additives, usually exhibit a very high level of transmission in the visible and infrared ranges. To avoid degrading these qualities it becomes necessary to optimize the nature and content of anti-instability additives included in the formulation, particularly in the case of radial burning, and to use an inhibitor producing little smoke for an end-burning propellant grain. In the last case, even when the best inhibitors are selected, the transmission drops by several percent. It is further necessary to optimize the igniter and the various rocket motor materials that come into contact with the combustion gases.

TABLE 4 *Transverse attenuation in a plume; function of the ratio of alkaline impurities*

Propellant	K Equivalent ppm	Afterburning	Attenuation dB	Frequency GHz
CDB	21	yes	16	10
Nitramite 1905 (minimum smoke CMDB)	150	yes	16	16
Nitramite 1903 (minimum smoke CMDB)	3720	no	0.2	16
EDB	2635	yes	11	16
Butalite (HTPB/AP)	45	no	1	10

5.4. PARAMETERS AFFECTING SECONDARY SMOKE

To obtain a total suppression of secondary smoke, on the ground and in a temperate climate, halogen, and therefore perchlorate, must be left completely out of the propellant. A very significant reduction in the frequency of occurrence and the opacity of the secondary smoke can be obtained—in Butalites—by limiting the proportion to less than 20%, as is the case for Nitramites G (see Section 2.4, above).

Bibliography

1. CARPENTIER, R., Le Guidage des missiles tactiques. Bilan et évolution pour les années 90. Armement No. 84, 16–38, 1985.
2. RAMSAY, D. A., The evolution of radar guidance. *GEC J. Res.*, 3(2), 92–103, 1985.
3. JARMAN, R. T. and TURVILLE, C. M., The visibility and length of chimney plumes. *Atmos. Environ.* 3, 257–280, 1969.
4. JENSEN, D. E., Prediction of soot formation rates: a new approach. *Proc. Roy. Soc. London, Series A*, 338–375–396, 1974.
5. VICTOR, A. C., Plume signal interference. Part 1, Radar attenuation. NWC China Lake, California. NWC TP 5319 Part 1, 1975.
6. MIKATARIAN, R. R., KAW, C. J. and PERGAMENT, H. S. Air Force Rocket Propulsion Laboratory. A fast computer program for non-equilibrium rocket plume predictions. Aerochem Research Laboratories AD 751984 Aerochem-TP-282; AFRPL-TR-72-94. August 1972.
7. JENSEN, D. E. and JONES, G. A., Reaction rates coefficients for flame calculations. *Combust. Flame*, 32, 1–34, 1978.
8. PRIGENT, G. and DERVAUX, M., Prédiction de l'atténuation électromagnétique de propergols solides composites. Processus de combustion et de détonation. ICT Internationale Jahrestagung, Karlsruhe, 713–728, June 1979.
9. DASH, S. M., Analysis of exhaust plumes and their interaction with missile airframes. *Tactical Missile Aerodynamics*. Progress in Astronautics and Aeronautics, Vol. 106, AIAA, New York, 1986.
10. MACE, A. C. H., Exhaust signature predictions for rocket motors. AGARD Conference Proceedings No. 391 (Confidential) Smokeless Propellants, 1985.
11. AJDARI, E., Méthodologies et moyen d'étude de la discrétion des moteurs à propergols solides. AGARD Conference Proceedings No. 391 (Confidential). Smokeless Propellants, 1985.
12. VICTOR, A. C. and BREIL, S. H., A simple method for predicting rocket exhaust smoke visibility. *Spacecraft J. Rockets*, 14(9), 526–533, 1977.
13. SENOL, A. J. and ROMINE, G. L., Three-dimensional refraction/diffraction of electromagnetic waves through rocket exhaust plumes. *Spacecraft J. Rockets*, 23(1), 39–46, 1986.
14. VICTOR, A. C., Plume signal interference. Part 2, Plume-induced noise. NWC, China Lake, California. NWC TP 5319 Part 2, 1972.
15. WILLIAMS H., WILSON A. S., and BLAKE C. C. Scattering from a Turbulent Rocket-Exhaust Jet Illuminated by a Plane Wave. *Electron. Lett.*, 7(19), 595–597, 1971.
16. CLARRICOATS, P., SENG, L. M., TRAVERS B. and WILLIAMS, H., Scattering from a turbulent rocket-exhaust jet illuminated by a focused microwave beam. *ibid*, pp 597–600.
17. KERKER, M., *The Scattering of Light and Other Electromagnetic Radiation*. Academic Press, New York, 1969.
18. VAN DER HULST., *Light Scattering by Small Particles*. John Wiley and Sons, New York, 1967.
19. GREHAN, G., GOUESBET, G. and RABASSE, C., The computer program SUPERMIDI for Lorenz MIE theory and the research of one to one relationship for particule sizing. ISL-R-117, 1980.
20. DEIRMENDJIAN, D. *Electromagnetic Scattering on Spherical Polydispersions*. American Elsevier, New York, 1969.

21. ROCHELLE, W. C., Review of thermal radiation from liquid and solid propellant rocket exhaust. N.67.31300. NASA-TM. 53579, 1967.
22. VANDERBILT, D. and SLACK, M., A model for emission and scattering of infrared radiation from homogeneous combustion gases and particles. Grumman Research, AD-A027 576/8. Department Memorandum RM-621, 1976.
23. LUDWIG, C. B., MALKMUS, W., WALKER, J., SLACK, M. and REED, R., The Standard Infrared Radiation Model A-81-039063. American Institute of Aeronautics and Astronautics, Thermophysics Conference. (U.S.), Vol. 16, pp 81-1051, 1981.
24. MILLER, E., Smokeless propellants. *Fundamentals of Solid Propellant Combustion*. Progress in Astronautics and Aeronautics, Vol. 90, AIAA, New York, 1984.
25. VICTOR, A. C., Computer codes for predicting the formation of rocket exhaust secondary smoke in free jets and smoke chambers. NWC, China Lake, California. NWC TM 3361, 1978.

CHAPTER 6

Structural Analysis of Propellant Grains

BERNARD GONDOUIN

1. Introduction

Causes of operational failures of solid rocket motors are varied, but the major causes are tied to the structural integrity of the propellants. During their entire service life propellants are subjected to stresses which, in some cases, cause cracks in the propellant grain or separation between the propellant and the inhibitor or the liner. During firing, there are a large number of possible consequences from one of these structural failures.

1.1. PROPELLANT STRUCTURAL FAILURE

A crack in the propellant grain results in additional burning surface. The increase in pressure resulting from this accidental increase of the burning surface may lead to either the destruction of the motor, if the pressure is greater than the burst pressure of the motor case, or operation outside of the specifications (modification of the thrust, the burning time, etc.).

1.2. BONDING SEPARATION

A bondline separation, when it results in an increase of the burning surface, triggers the same occurrences as described above. Another type of failure may occur, however. The bonding of the propellant with the other materials (inhibitor or thermal protection) is usually located somewhere close to the wall of the case; burning in the debonded area may cause a significant heating for the structure with a risk of burnthrough that would result in an abnormal, and possibly catastrophic, operation of the rocket motor.

There are two very distinct stages in the operational life of a propellant grain:

- the stage before firing: this includes manufacturing followed by various transportation and storage phases. The duration of this stage varies, and could last from a few months to several years.
- the firing, which lasts from a few milliseconds to several seconds, depending on the function expected from the motor.

The mechanical design problem that needs to be solved is the assessment of the risk of a structural failure occurring in the propellant grain and that of debonding during the two stages mentioned above.

An initial method of handling this problem would consist in taking a number of samples during the manufacture of the propellant grains and performing a variety of tests under well-defined conditions. This experimental method requires a large number of tests. It can be contemplated for small objects, with short and easy-to-implement operational conditions. In the case of propellant grains for rocket motors, where dimensions can be quite large and operational conditions difficult to reproduce, a large number of tests are not feasible.

An analytical method allowing the determination, *a priori*, of the structural integrity of the propellant grains seems better indicated. The principle is simple, and consists of determining two values for each loading condition (corresponding to the various phases of the service life). These values are the induced stress or strain resulting from induced loads in the propellant grains, and the allowable stress or strain.

In general, the induced stress or strain in a propellant grain is the maximum stress or strain developed in the propellant. It is found at the location where the propellant is the most mechanically constrained, known as the “critical point.” The assumption is as follows: the level of stress/strain at points surrounding the critical point does not influence the structural failure risk of the propellant.

The location of the critical point and corresponding stress and strain are generally determined using a numerical method (finite element method).

The “capability” or allowable stress or strain is the structural stress or strain that must be induced in a propellant grain to cause a structural failure. This value is determined through tests; it is a function of the stress and/or strain measured at the point of structural failure of the test specimens during the various mechanical properties tests performed on the propellant.

The ratio of the capability versus the load gives the factor of safety:

$$K = \frac{C}{S} \quad \text{with} \quad \begin{array}{ll} K > 1 & \text{no structural failure} \\ K < 1 & \text{structural failure} \end{array}$$

where:

C = capability of the propellant;

S = induced stress or strain in propellant grain.

If C and S have exact values, this factor must always be greater than 1 to ensure proper mechanical performance of the rocket motor. The variable nature of physical phenomena involved requires a probabilistic approach. The probability of the capability being greater than the induced stress/strain is assessed: it is the structural reliability F :

$$F = Pb(K > 1) = Pb(C > S)$$

The analytical method used for this purpose is discussed in this chapter. An overview is provided in Fig. 1. The following questions will be addressed:

- description of the mechanical loads found in propellant grains;
- mechanical properties of the bonding;
- determination of the stress/strain in propellant grains;
- determination of the grain structural integrity.

Note: When assessing the grain structural integrity, another value is sometimes determined: the margin of safety, MS . It is written as follows:

$$MS = \frac{C - S}{S} = K - 1$$

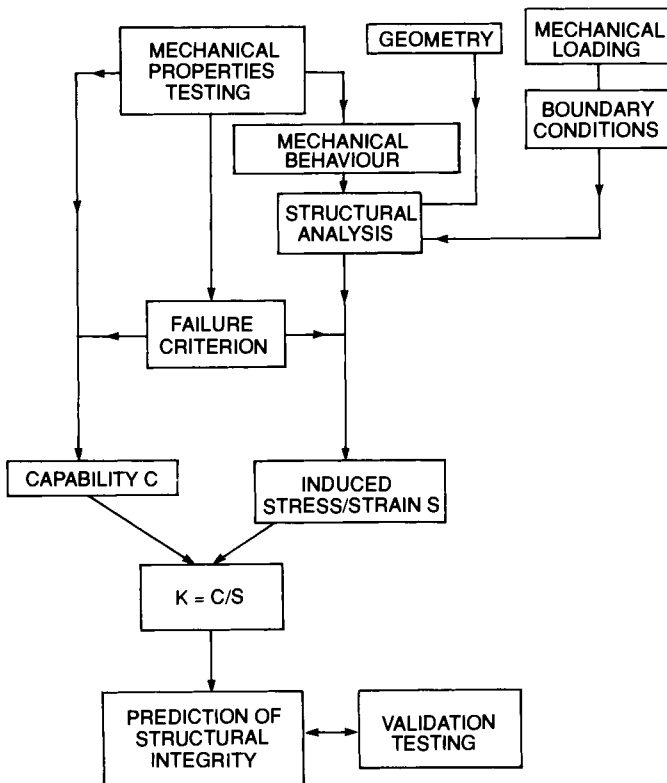


FIG. 6.1. Determination of the structural integrity.

Therefore, the reliability is the probability that the margin of safety is greater than zero:

$$F = Pb(MS > 0)$$

2. Description of the Mechanical Loads

The service life of a propellant grain before firing consists of a succession of transport and storage phases, under conditions that are contingent upon the mission of the missile.

The transport of a space missile to the launching site, for example, happens only once. The propellant is subject to low magnitudes of vibrations, and the temperature variations are often controlled.

Repeated transports of tactical missiles stored or carried beneath an aircraft subject the propellant grain to major accelerations, vibration, and temperature variations. Furthermore, storage of all rocket motors causes creeping due to the effect of the gravity; and because of repeated and various handling, the risks of falls or shocks are certainly not negligible. Lastly, at the time of firing, the pressure rise in the combustion chamber and the acceleration resulting from the induced thrust impose loads on the propellant grain, in addition to those already induced during the pre-firing phase.

To analyze the effect of these various environments on the stress/strain imposed on the propellant, it is necessary to make a distinction between the two major families of propellant grains:

- case-bonded grains;
- free-standing or cartridge-loaded grains.

2.1. CASE BONDED GRAINS

2.1.1. *Temperature changes*

At the time of its manufacture the propellant grain is cast in the insulated case. The propellant hardens and bonds with the case or its thermal protection with the help of a liner at a temperature which is typically greater than 40°C, known as the cure temperature. Following the curing phase the propellant, subjected to temperatures that are lower than the curing temperature, induces a change in its volume. This change is bound to induce stress/strain in the propellant because it is bonded to a rigid structure with a lower thermal expansion coefficient. A field of thermal stress occurs. The sketches in Fig. 2 illustrate this phenomenon on a cylindrical propellant grain.

In addition to the thermal stresses caused by temperature changes evenly throughout the propellant grain, there are the stresses from thermal gradients occurring during transient phases. These stresses play a greater role in the propellant grain contained in tactical missile motors, where the temperature changes are sometimes very quick.

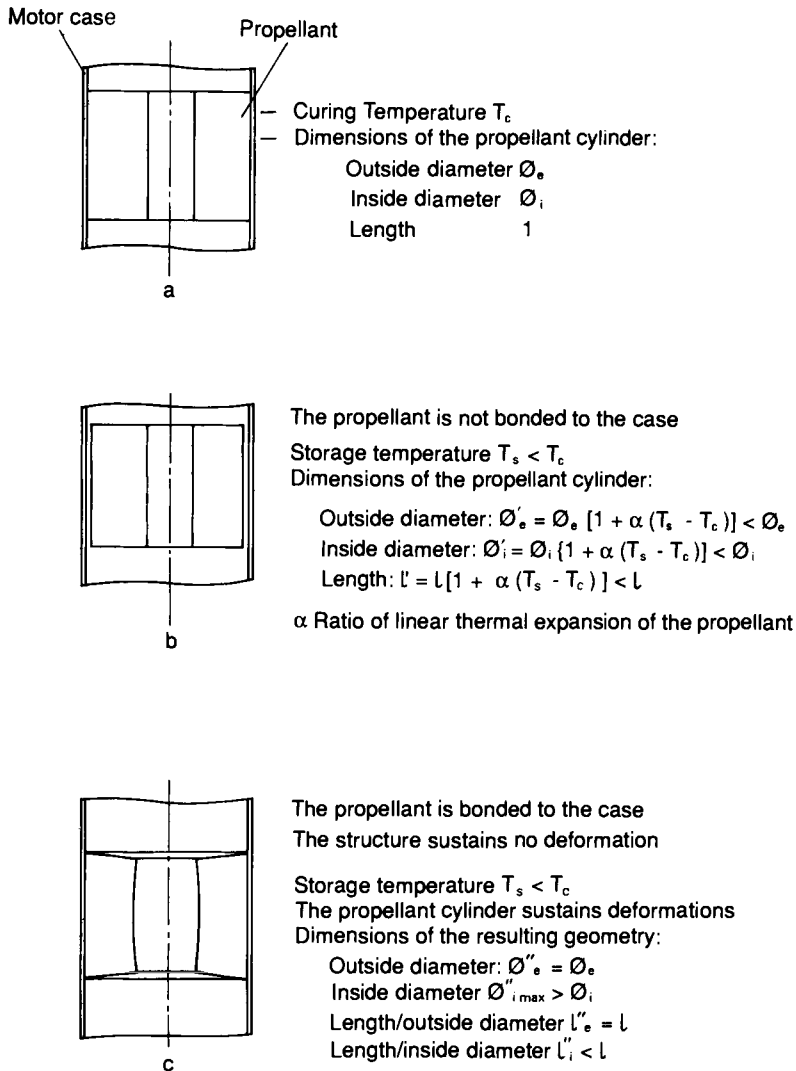


FIG. 6.2. Diagram of the effect of thermal shrinkage.

2.1.2. Force of gravity

Long-term storage of a case-bonded propellant grain brings on a creeping of the propellant grain due to the force of gravity. The motor case is usually sufficiently rigid to keep its original shape. The strains observed on a cylindrical case-bonded grain due to the effect of gravity are illustrated in Fig. 3.

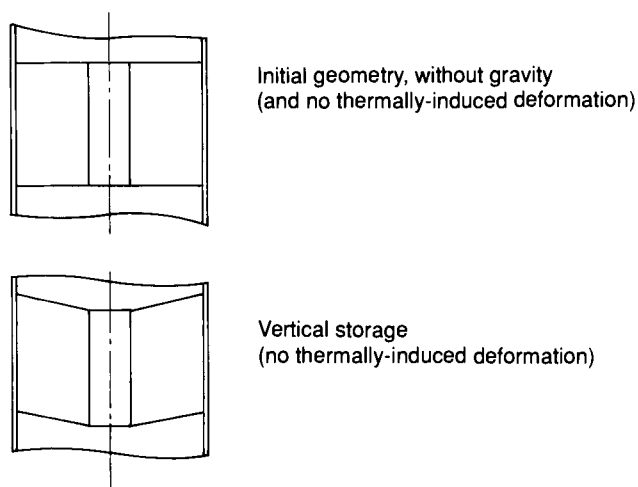


FIG. 6.3. Diagram of the effects of gravity.

2.1.3. *Pressure rise at firing*

When a case-bonded propellant grain is fired, the pressure in the combustion chamber increases within a few milliseconds to reach maximum operating pressure. Through the entire time the pressure is transmitted through the propellant to the motor case. The deformation of the case induces a strain field in the propellant and stresses at the bondline.

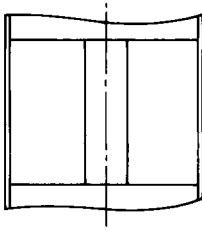
The strains occurring in a cylindrical propellant grain at the time of pressure rise in the combustion chamber are shown in Fig. 4.

The combustion chamber pressure, at the time of firing, is not steady. There may be significant variations, resulting in a deformation of the combustion chamber, and as result all of the propellant grain faces are subjected to different pressures.

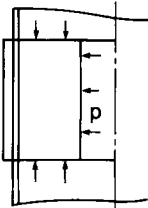
Finally, eventual combustion instabilities may trigger a vibration state in the propellant grain.

2.1.4. *Curing under pressure*

In Section 2.1.1 the effects of temperature changes on a case-bonded grain are described. In a case where, during its entire service life, a motor is stored after curing under controlled temperature conditions, the only thermal loads intervening are due to the difference between curing and storage temperatures. If it were possible to compensate for the variation in geometry due to the thermal shrinkage with an equivalent change of geometry, the thermally induced strain would decrease: it is the principle of curing under pressure. A cylindrical case-bonded grain cured under pressure is described in Fig. 5.

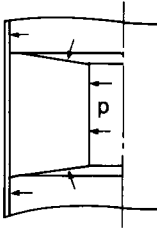


Zero pressure in the motor case



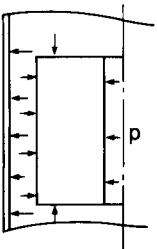
Pressure p

Without the case when the propellant cylinder is subjected to internal pressure only, it has the tendency to sustain significant deformations.



Pressure p

The propellant is bonded to the case and presses against it.

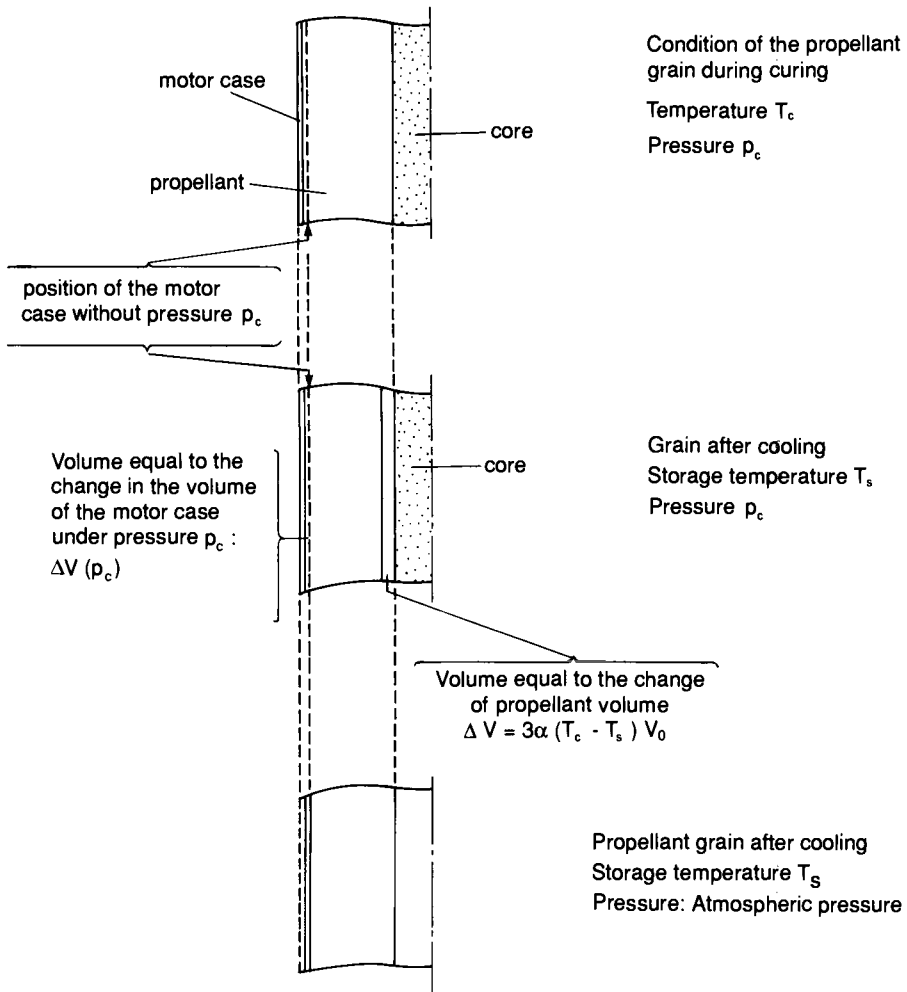


Pressure p

The propellant is not bonded to the case the pressure causes deformations in the case. The pressure is exerted on all surfaces of the propellant cylinder which sustains no deformation if it is incompressible.

FIG. 6.4. Diagram of the pressure rise induced by firing.

Because in modern motor cases the deformations are small in the cylindrical part, the pressures that should be induced to compensate completely for the thermal shrinkage would simply be too great. Nevertheless, even a partial compensation for the thermal shrinkage permits a reduction of the stresses along the bondline and a decrease in the damage to the propellant grain before its firing.



If $\Delta V(p_c) = \Delta V$ the deformations in the propellant cylinder are zero

FIG. 6.5. Diagram of the principle of curing under pressure.

2.2. FREE-STANDING GRAINS

The major differences between the mechanical loads induced in case-bonded grains and free-standing grains occur during propellant temperature changes and pressure rises at firing. Theoretically there should not be any stress/strain in a free-standing grain under thermal and pressurization loads. (Figs 2b and 4d). In fact, there are transient phases for these two types of loading conditions that eventually could create significant stress/strain.

2.2.1. Temperature changes

When a change in temperature occurs that is even throughout the propellant grain, a free-standing grain deforms freely, and no strain results. This is the case illustrated in Fig. 2b.

In transient phases, during which the temperature is different in each point of the propellant grain, thermal stress/strain is created. In any type of thermal cycle these thermal stresses are non-existent at the initial and final stabilized temperatures; they can be measured only during the cycle (Fig. 6).

The maximum stress/strain value of a cycle depends on the distribution of the temperatures in the propellant. Consequently, this particular stress/strain is a function of the thermal properties of the material (thermal conductivity of the propellant), of the boundary thermal conditions (convective heat transfer, radiating heat transfer), and of the geometry of the propellant grain.

2.2.2. Pressure rise at firing

In the steady phase at firing, if the pressure is applied on all faces of the propellant, the resulting stresses/strains are those occurring when a motor case is subjected to an even pressure: it is known as an isostatic state of the stress/strain.

During the unsteady phase the pressure in the combustion chamber and the pressure taking place in the gaps between the propellant grain and the case may increase at a different rate. The grain is thus subjected to pressure gradients causing stress/strain in the propellant. At least two different possibilities have been observed.

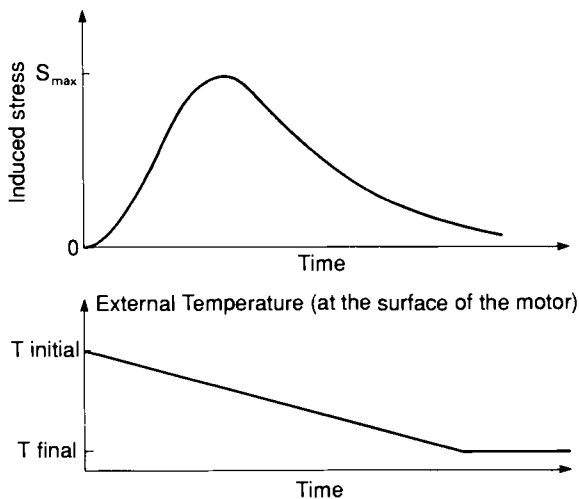


FIG. 6.6. Effects of a temperature change in a free-standing grain.

(a) *Regular pressure increase in the gaps*

The maximum pressure gradient to which the propellant grain is subjected depends on the manner in which the pressure increases in the gap. Figure 7 illustrates the pressure evolutions for a cylindrical propellant grain with a central port.

The question then consists in determining whether the propellant grain can withstand the evolution of the pressure difference $\Delta p(t)$.

(b) *Oscillating pressurization in the gaps*

The dimensions of the gaps and the nature of the gases may cause an oscillating pressurization, such as illustrated in Fig. 8.

Hence, in addition to the problem of a propellant grain subjected to a pressure gradient $\Delta p(t) = P_c(t) - P_i(t)$ —identical to case (a)—there is a

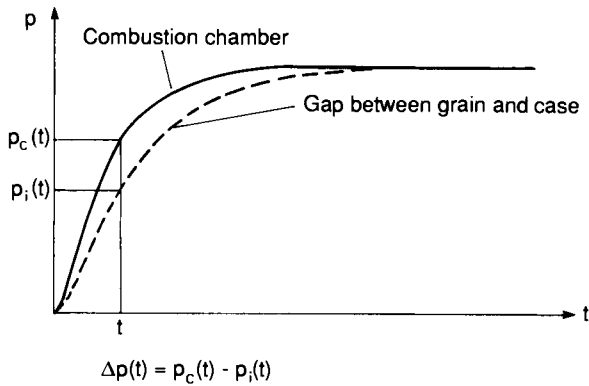


FIG. 6.7. Pressure rise induced by firing in a free-standing propellant.

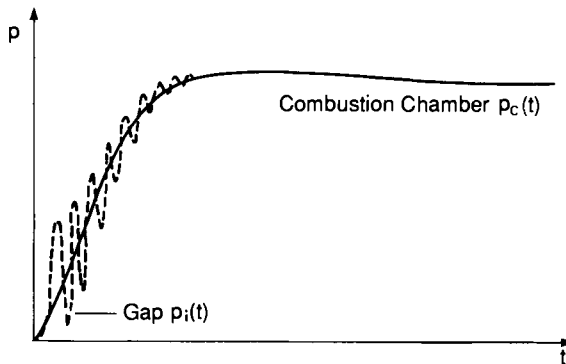


FIG. 6.8. Oscillating pressure rise induced by firing in a free-standing grain.

dynamic coupling between the propellant grain and the gases in the gap. This is a very complex problem to resolve because the dimensions of the gap evolve continuously, modifying the pressure rise conditions. An initial approach consists in making sure that a natural frequency of the grain does not correspond to the oscillation frequency of the pressure in the gap.

The mechanical loads described in the preceding section are usually the most significant factors in the structural design analysis. Yet, during the service life of rocket motors, other stresses/strains may appear that influence the structural integrity of the propellant grains. These include dynamic loads, typically shocks. These mechanical stimuli are not included in this chapter.

The grain structural analysis allows the clear identification of the parameters necessary to determine the margin of safety. These are:

- the temperature of the propellant;
- the pressure in the combustion chamber;
- the loading rate;
- the loading time.

They are used to calculate the boundary conditions, the behavior laws, and the capability of the materials.

3. Some Generalities and Definitions

3.1. STRESSES AND STRAINS

An object which is subject to mechanical loading (stresses or displacements applied to the external surfaces) finds a new state of equilibrium after the deformation has taken place. In each point M of this object, there is an infinity of forces applied to the infinity of planes traversing this point (Fig. 9a).

In relation to a P_1 plane, on a dS_1 surface element, a $d\vec{F}_1$ force is applied; in relation to a P_2 plane, on a dS_2 surface element, a $d\vec{F}_2$ force is applied.

For each of the planes, the $d\vec{F}$ forces are the sum of a component $dF_n \cdot \vec{n}$, normal to the plane, and a component $dF_t \cdot \vec{t}$, contained in the plane:

$$d\vec{F} = dF_n \cdot \vec{n} + dF_t \vec{t}$$

The stresses applied to each plane are defined by the following equations:

$$\sigma_n = \lim_{dS \rightarrow 0} \frac{dF_n}{dS}, \quad \tau = \lim_{dS \rightarrow 0} \frac{dF_t}{dS}$$

Consequently, there is an infinity of stresses at each point of an object subjected to mechanical loading. The stress state is defined by a matrix composed of nine components expressed in a given perpendicular axis system. We use the term "stress tensor."

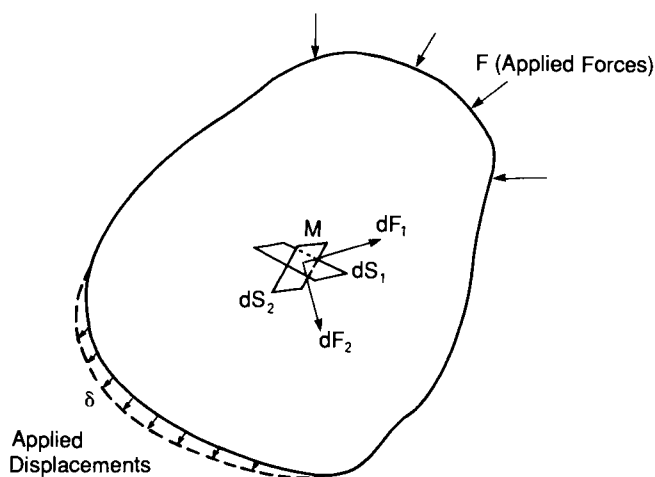


FIG. 6.9a. Description of forces in one point of a body at equilibrium.

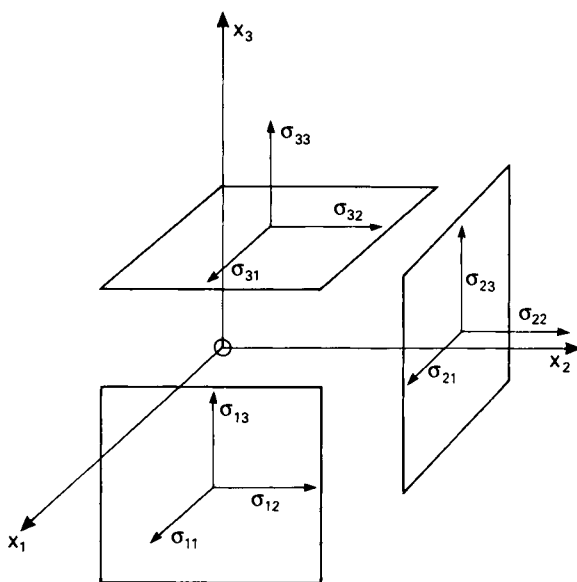


FIG. 6.9b. Description of the tensor component at one point of a body in equilibrium.

Similarly, a strain tensor is defined for each point; if u_1 , u_2 and u_3 are three components in a reference system (Ox_1, x_2, x_3) of the displacement of the M point, the nine strain components expressed in the reference system are written:

$$\varepsilon_{ij} = \frac{1}{2} \left(\frac{\partial u_i}{\partial x_j} + \frac{\partial u_j}{\partial x_i} \right) \quad i, j, 1 \text{ to } 3$$

3.2. BEHAVIOR LAW: THE NECESSARY COEFFICIENTS TO BE DETERMINED

To know the behavior of a material is to determine the law relating the stress tensor to the strain tensor when the material is subjected to mechanical loading. For each point, there is a relation:

$$\sigma_{ij} = \mathcal{E}_{ijkl} * \varepsilon_{kl}$$

stress tensor = behavior * strain tensor.

In its general form the behavior of a material is rather complex; it has been demonstrated, however, that in a material that is homogeneous, elastic and isotropic, the definition of the behavior is limited to two coefficients, which are:

- the Lamé coefficients λ, μ ;
or
- Young's modulus and Poisson's ratio, E and ν ;
or
- the shear modulus and the bulk modulus, G and K .

For infinitesimal strains there are equations between these three pairs of coefficients (Table 1).

TABLE 1

		Function of		
		λ and μ	E and ν	G and K
Lamé's coefficients	λ		$\frac{E\nu}{(1+\nu)(1-2\nu)}$	$K - \frac{2}{3}G$
	μ		$\frac{E}{2(1+\nu)}$	G
Young's modulus	E	$\frac{\mu(3\lambda + 2\mu)}{\lambda + \mu}$		$\frac{9KG}{3K + G}$
Poisson's ratio	ν	$\frac{\lambda}{2(\lambda + \mu)}$		$\frac{3K - 2G}{2(3K + G)}$
Shear modulus	G	μ	$\frac{E}{2(1+\nu)}$	
Bulk modulus	K	$\lambda + \frac{2}{3}\mu$	$\frac{E}{3(1-2\nu)}$	

One or the other of these pairs of coefficients can be used indifferently. In any Cartesian coordinates (x_1, x_2, x_3), the stress tensor and the strain tensor at an M point are expressed by the following six components:

for the stress tensor (Fig. 9b):

$$\sigma_{11}, \sigma_{22}, \sigma_{33}, \sigma_{12} = \sigma_{21}; \sigma_{13} = \sigma_{31}; \sigma_{23} = \sigma_{32}$$

for the strain tensor:

$$\varepsilon_{11}, \varepsilon_{22}, \varepsilon_{33}, \varepsilon_{12} = \varepsilon_{21}, \varepsilon_{11} = \varepsilon_{31}, \varepsilon_{23} = \varepsilon_{32}$$

The equations between stress and strain are then written as:

with E and ν :

$$\left\{ \begin{array}{l} \varepsilon_{11} = \frac{1}{E} (\sigma_{11} - \nu(\sigma_{22} + \sigma_{33})) \\ \varepsilon_{22} = \frac{1}{E} (\sigma_{22} - \nu(\sigma_{11} + \sigma_{33})) \\ \varepsilon_{33} = \frac{1}{E} (\sigma_{33} - \nu(\sigma_{11} + \sigma_{22})) \\ \varepsilon_{12} = \frac{1+\nu}{E} \sigma_{12}; \varepsilon_{13} = \frac{1+\nu}{E} \sigma_{13}; \varepsilon_{23} = \frac{1+\nu}{E} \sigma_{23} \end{array} \right. \quad (1)$$

with λ and μ :

$$\sigma_{ij} = 2\mu\varepsilon_{ij} + \delta_{ij}\lambda e \quad i \text{ and } j \text{ vary from 1 to 3} \quad (2)$$

with

$$e = \varepsilon_{11} + \varepsilon_{22} + \varepsilon_{33}$$

$$\delta_{ij} = \begin{cases} 0 & i \neq j \\ 1 & i = j \end{cases} \quad \text{the Kronecker symbol}$$

with G and K :

Any condition of stress, expressed by one of the equations described above, can be written as follows:

$$\sigma_{ij} = \sigma'_{ij} + \delta_{ij}\bar{\sigma} \quad i \text{ and } j \text{ vary from 1 to 3} \quad (3)$$

with

$$\bar{\sigma} = \frac{1}{3}(\sigma_{11} + \sigma_{22} + \sigma_{33})$$

δ_{ij} Kronecker symbol

$\bar{\sigma}$ is the mean stress or mean pressure

σ'_{ij} are the deviatoric stresses.

In parallel, the strain can be written under the same form, i.e. the equation:

$$\varepsilon_{ij} = \varepsilon'_{ij} + \delta_{ij} \frac{e}{3}$$

The stress-strain equations are therefore written as:

$$\begin{aligned} \sigma'_{ij} &= 2G\varepsilon'_{ij} & 6 \text{ equations for the deviatoric components} \\ \bar{\sigma} &= Ke & 1 \text{ equation for the isotropic component} \end{aligned} \quad (4)$$

The isotropic component represents the behavior of material subjected to a uniform load. For example, an isotropic object subjected to hydrostatic pressure shows a uniform strain. The deformation of the object is the same in all directions, and there is no shear effect.

The equations for the deviatoric components represent the behavior in the case of a non-uniform loading, where shear effects occur.

These two types of behavior involve different physical mechanisms. It is for that particular reason that during the behavior analysis of propellants, as well as for the stress/strain analysis in a propellant grain, this formulation is sometimes called upon, even though Young's modulus and Poisson's ratio are traditionally used.

General comment. The components of the stress tensors and strain tensors are expressed within the coordinate system. It is obvious that an object subjected to mechanical loading is in equilibrium with a stress and strain state which is independent of the coordinate system by which the components are expressed. The notion of a tensor invariant is used in this case. The first three invariants of the stress tensor and of the strain tensor are S_1 , S_2 and S_3 for the stress, and I_1 , I_2 and I_3 for the strain.

$$S_1 = \sigma_{11} + \sigma_{22} + \sigma_{33}$$

$$S_2 = \sigma_{11} \cdot \sigma_{22} - \sigma_{12}^2 + \sigma_{22} \sigma_{33} - \sigma_{23}^2 + \sigma_{33} \sigma_{11} - \sigma_{13}^2$$

$$S_3 = \text{the determinant of the matrix of the stress tensor coefficients.}$$

These values are independent of the coordinate system selected; only a function of these values can be used to represent the stress or strain states of an object.

3.3. TESTS DESIGNED TO DETERMINE THE COEFFICIENTS

All that is needed to know the behavior of a material is the determination, through simple tests, of one of the three coefficient pairs described above. In practice, relations (1) and (4) alone are used.

3.3.1. Determination of E and ν

In the following example we assume a parallelepipedic object with one dimension greater than the other two (Fig. 10).

When this object is subjected to a force \vec{F} in the direction of its greatest dimension (Ox_1 in Fig. 10), the stress and strain induced in the material are:

$$\begin{aligned}\sigma_{11} \text{ and } \varepsilon_{11} & \text{ in the } Ox_1 \text{ direction} \\ \sigma_{22} \text{ and } \varepsilon_{22} & \text{ in the } Ox_2 \text{ direction} \\ \sigma_{33} \text{ and } \varepsilon_{33} & \text{ in the } Ox_3 \text{ direction.}\end{aligned}$$

The only measurable physical values are the force applied and the deformation of the object.

On a surface that is free to deform itself the stress is equal to zero. Since the dimension of the object in the Ox_2 and Ox_3 directions is very small, the following can be written: $\sigma_{22} = \sigma_{33} = 0$.

Calling Δl_1 , Δl_2 , and Δl_3 the variations of the dimensions of the specimen, the stress and strain are written as follows:

$$\begin{aligned}\sigma_{11} &= \frac{F}{S_0} & \varepsilon_{11} &= \frac{\Delta l_1}{l_1} \\ \sigma_{22} &= 0 & \varepsilon_{22} &= \frac{\Delta l_2}{l_2} \\ \sigma_{33} &= 0 & \varepsilon_{33} &= \frac{\Delta l_3}{l_3}\end{aligned}\tag{5}$$

Equation (1) enables us to write:

$$\begin{aligned}\varepsilon_{11} &= \frac{1}{E} (\sigma_{11} - \nu(\sigma_{22} + \sigma_{33})) = \frac{\sigma_{11}}{E} \\ \varepsilon_{22} &= \frac{1}{E} (\sigma_{22} - \nu(\sigma_{11} + \sigma_{33})) = \frac{\nu\sigma_{11}}{E} = -\nu\varepsilon_{11} \\ \varepsilon_{33} &= -\nu\varepsilon_{11}\end{aligned}$$

E (Young's modulus) is obtained directly from the equation:

$$E = \frac{\sigma_{11}}{\varepsilon_{11}} = \frac{F}{l_2 l_3} * \frac{l_1}{\Delta l_1}\tag{6}$$

and similarly, Poisson's ratio ν is written:

$$\nu = -\frac{\varepsilon_{22}}{\varepsilon_{11}} = -\frac{\Delta l_2}{\Delta l_1} \times \frac{l_1}{l_2}\tag{7}$$

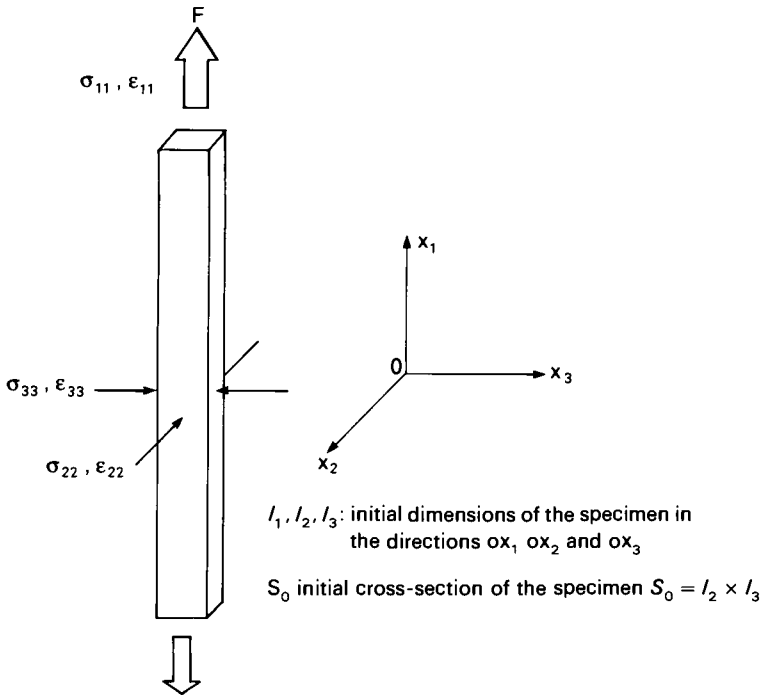


FIG. 6.10. Uniaxial tensile test specimen.

This parallelepipedic object is a unidimensional specimen. Its dimensions may vary. In Fig. 11 several unidimensional specimens used to analyze the behavior of propellants are described.

Comment. When analyzing the results of tests performed on propellant grains which show a great deal of deformation, the use of eqns (5) to predict the stress and strain is no longer valid. Indeed, when the changes of the dimensions of the specimen are no longer small compared to the initial dimensions themselves, the assumption of infinitesimal deformation is no longer valid. It becomes necessary to use a specially designed mechanical model [22]. Using a model adapted to large-scale deformation is a very complex task; it requires a coherence between the methods of analysis of the tests and the methods of structural analysis. Among the many ways of performing the test analysis, the most widely used is as follows:

If σ_{11} and ϵ_{11} are the stress and the strain determined according to eqns (5), the corrected stress and strain are to be written as follows:

$$\begin{aligned}\sigma_{11}^c &= \sigma_{11}(1 + \epsilon_{11}) \\ \epsilon_{11}^c &= \frac{\epsilon_{11}}{1 + \epsilon_{11}}\end{aligned}\tag{8}$$

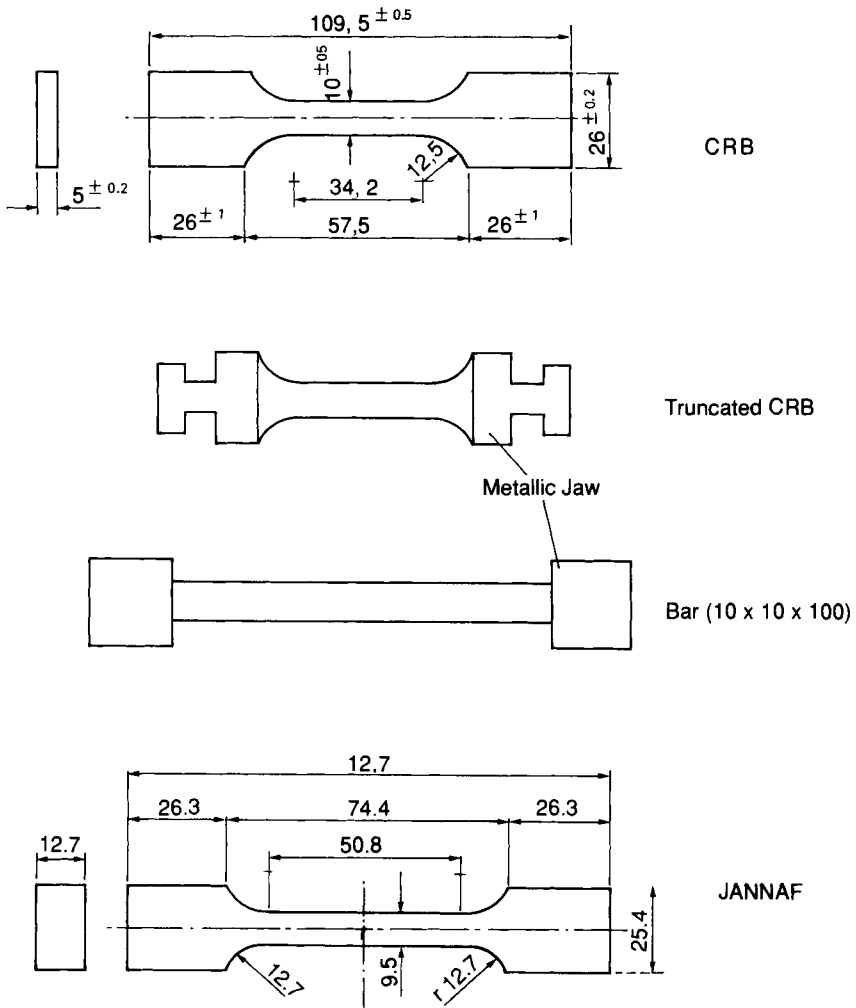


FIG. 6.11. Widely used uniaxial specimens.

3.3.2. Determination of K

The measurement of the bulk modulus is done simply by measuring the variation in the volume of an object of any shape subjected to hydrostatic pressure. Based on eqn (4):

$$\bar{\sigma} = Ke$$

for a material that exhibits little strain, e corresponds to the change in volume.

$\bar{\sigma}$ is equal to the pressure applied.

3.3.3. Determination of G

Knowing E , ν and K makes it possible to calculate G using the relations existing between the various coefficients. There are, however, specific specimens with which the shear modulus G can be directly determined. These are the torsional stress or shear specimens shown in Fig. 12.

Uniaxial specimens (Fig. 11) are widely used for a variety of tests (Fig. 13):

- tensile tests (induced displacements);
- relaxation tests (constant strain);
- creeping tests (constant stress load);
- combined tests: (a) loading-relaxation-loading (LRL); (b) loading-unloading-loading (LUL)

Torsion test specimen



Shear test specimen

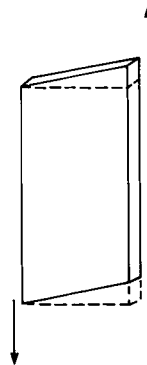


FIG. 6.12.

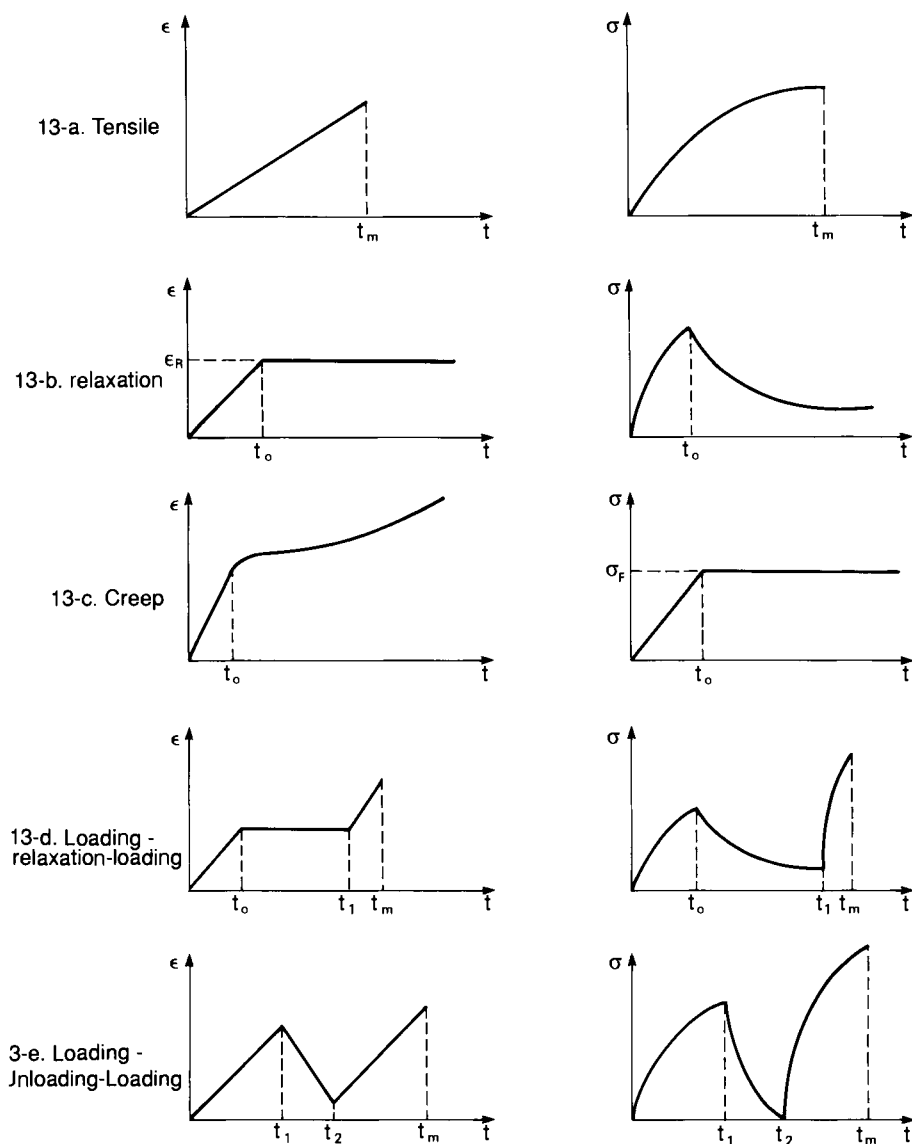


FIG. 6.13. Description of the various types of tests.

These tests are performed under various:

- temperatures;
- pressures;
- loading rates for the tensile tests, and durations for the relaxation and creeping tests.

3.4. VARIOUS TYPES OF BEHAVIORS OF THE MATERIALS

To determine the behavior law of a material, it is necessary to perform combined tests, such as loading-relaxation-loading or loading-unloading-loading types of tests. Tensile tests alone are not sufficient to draw conclusions on the behavior type of a material. For example, the results of a tensile test listed in Fig. 14 can be obtained from materials whose structural integrity is different, which can only be discovered through combined tests (Fig. 15).

In solid mechanics there are only two types of behavior:

- elastic or elastoplastic, where the rate of loading and the duration play no role;
- viscoelastic or viscoplastic, where the rate of loading and the duration modify the response of the material.

The behavior, for each of these families, may be either linear or non-linear, since linearity satisfies the rules of homogeneity and additivity.

Homogeneity

$$\begin{aligned} \text{if } \varepsilon_{ij}(t) &\rightarrow \sigma_{ij}(t) \\ \text{then } k\varepsilon_{ij}(t) &\rightarrow k\sigma_{ij}(t) \end{aligned} \quad (9)$$

where k is any constant.

Additivity

$$\begin{aligned} \text{if } \varepsilon_{ij}^1(t) &\rightarrow \sigma_{ij}^1(t) \\ \text{and if } \varepsilon_{ij}^2(t) &\rightarrow \sigma_{ij}^2(t) \\ \text{then } \varepsilon_{ij}^1(t) + \varepsilon_{ij}^2(t) &\rightarrow \sigma_{ij}^1(t) + \sigma_{ij}^2(t) \end{aligned}$$

To determine the response of a material under induced stress and strain, it is desirable first to determine the structural behavior type (elastic, plastic, viscoelastic, and linear or non-linear); and second to select the tests best suited for the future applications of the material and for the measurement of its mechanical coefficients.

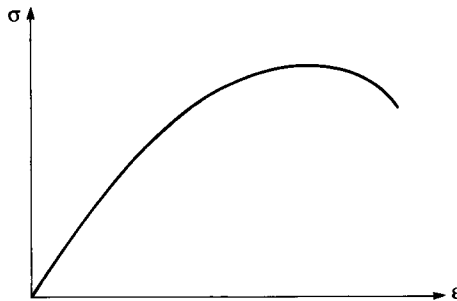


FIG. 6.14. Result of a classic tensile test.

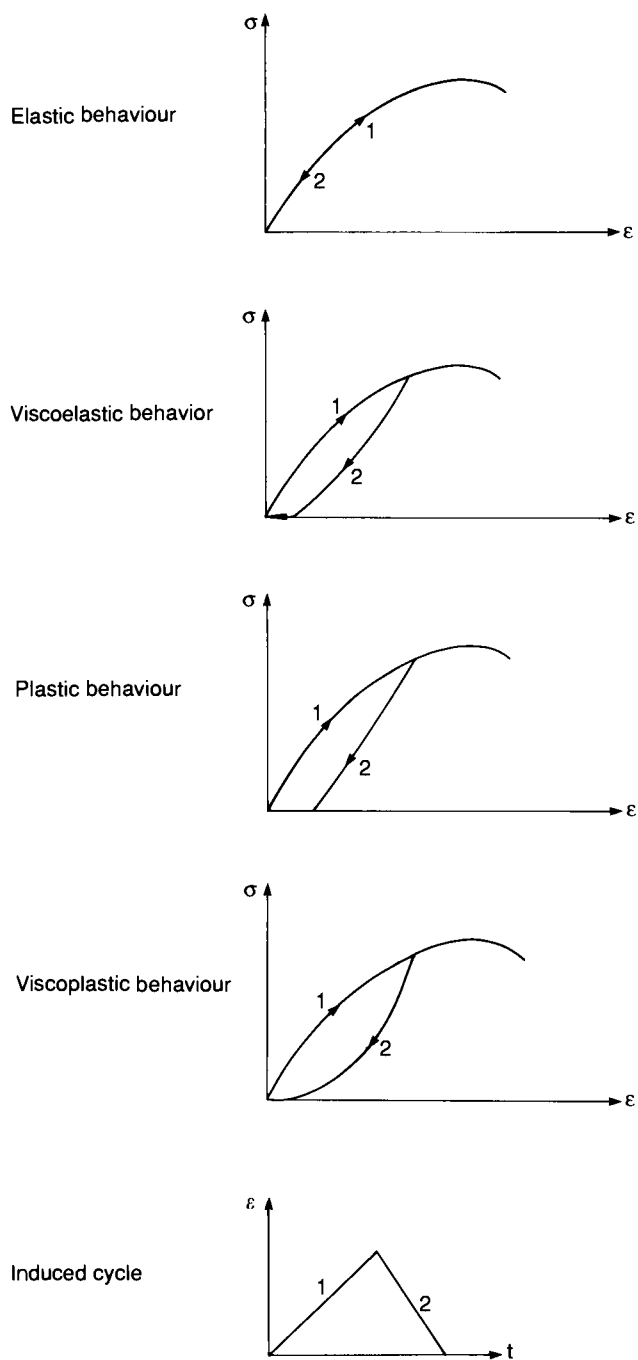


FIG. 6.15. The various types of behavior for the same tensile curve.

4. Structural Properties of Propellants and Their Bonding

4.1. PHYSICAL DESCRIPTION OF PROPELLANT

4.1.1. *Composite and composite modified double-base propellants (Chapters 10 and 11)*

Composite propellants consist of small-particle-size solids in a polymeric matrix. The loading ratios are, typically, very high (sometimes greater than 70% of the volume). The bonding surfaces between the binder and the fillers are very important. When relatively low rate structural loading is induced ($\dot{\epsilon} < 1 \text{ s}^{-1}$), there is failure of the bonding between some fillers and the binder, or failure of the binder close to a solid particle. Vacuum holes are created, and their size increases with the stress/strain. This phenomenon generates a dissipation of energy resulting in a viscous behavior, at a macroscopic scale to which is eventually added the viscous nature inherent to the binder.

When these vacuum holes reach a significant size (several microns) they act as microfailures initiating small cracks in the binder, and causing failure of the propellant grain.

These phenomena correspond to two clearly distinct phases (Fig. 16).

- *Stress/strain of the bonding between the binder and the fillers.* It is the structural properties of the binder and of the bonding that govern the mechanical behavior of the propellant. The total solids content, their

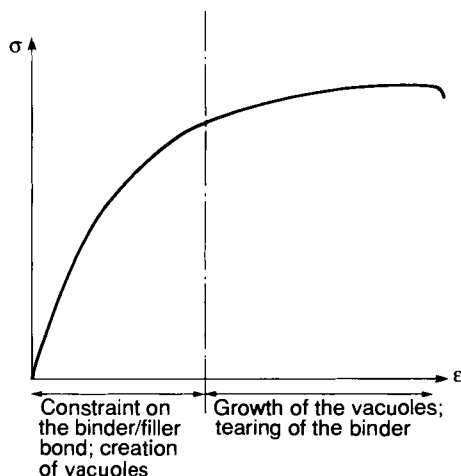


FIG. 6.16. Tensile test on a composite propellant.

shape, and particle size distribution influence the propellant behavior by affecting the bonding properties.

- *Growth of the microfailures (vacuum holes).* It is the tearing characteristics of the binder, as well as the total solids content and their size distribution which rule the structural behavior up to the failure of the propellant grain.

The behavior type of these propellants is determined by performing the LRL or LUL tests. The aspect of the curves obtained (Fig. 17) indicates a non-linear viscoelastic behavior.

Comment. Some composite propellants have a perfectly elastic binder. Since the fillers themselves are also elastic, their viscous structural behavior is due solely to the dissipation of energy at the bonding level between the binder and the solids.

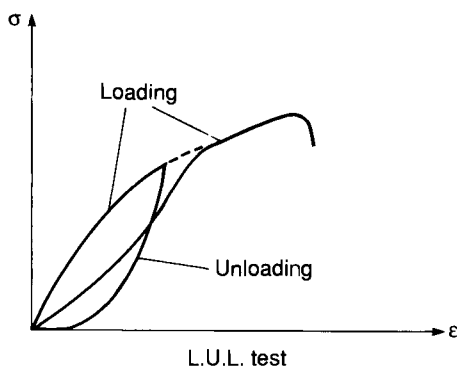
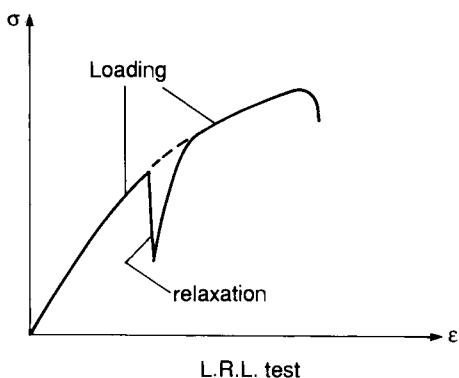


FIG. 6.17. L.R.L. and L.U.L. tests on composite propellant.

4.1.2. Double-base propellant grains

The double-base propellant grains are gels containing at least two main ingredients: nitrocellulose and nitroglycerine. According to the various manufacturing methods, there are two main families (Chapter 9):

- solventless double-base propellants (also called extruded double-base propellant EDB);
- cast double-base propellants (CDB).

These are homogeneous propellants from the aspect of structural mechanical properties; but their production process may cause anisotropies, for instance in EDB propellants.

Their physical structure looks like a solid phase (nitrocellulose), consisting of a continuous tridimensional network inside of which there is a liquid phase (nitroglycerine).

Usually, this structure leads to materials which are more rigid than the composite propellants, but when mechanical loading is imposed, the presence of the two distinct phases causes energy dissipations resulting in a more or less pronounced viscous behavior.

Comment. Crosslinked double-base propellants (Chapter 11) have some of the characteristics of the double-base propellants: the binder has the physical structure of a gel, which is crosslinked. They are, nevertheless, ranked as composite propellants insofar as the solids content ratio is such that the bonding phenomena between the binder and the solids are the predominant factors and govern the behavior of the propellant.

4.2. MECHANICAL BEHAVIOR OF THE PROPELLANTS

Each type of propellant has its own specific mechanical characteristics. Still, the methods used to determine their behavior are identical for every one of them, and the influence of the various parameters (temperature, pressure, loading rate) is the same overall for all propellants. Consequently, distinctions will no longer be made between each type of propellant in the following sections of this chapter.

4.2.1. Tensile behavior

The tensile tests are widely used for the fine analysis of the propellants' behavior as well as for the manufacturing controls of these propellants. Because their behavior is not linear elastic, it is necessary to define a certain number of parameters that allow a better representation of the aspects of the experimental curves. These parameters, shown in Fig. 18, are:

- E Young's modulus, or tangent modulus, or initial modulus;
- σ_m maximum stress;

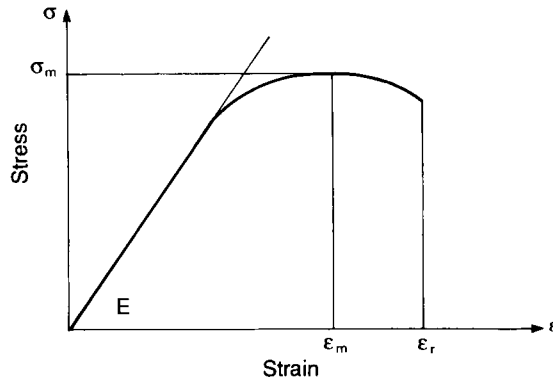


FIG. 6.18. The various parameters describing a typical curve.

- ε_m strain at maximum stress;
- ε_r strain at rupture.

The capability, as defined above in Section 1, for a tensile test is expressed by the maximum stress σ_m , and the strain ε_m , or by any other function taking these two parameters into consideration.

When the aspect of the tensile curve differs from the curve shown in Fig. 18, other values need to be determined.

The values for the parameters defined above vary with each propellant type, and with the pressure, temperature, and loading rate parameters for each propellant. Age and humidity are also common factors which affect these parameters.

When it is used in the case-bonded form, the propellant must exhibit the greatest possible ε_m during the thermal cycle and at the time of firing. On the other hand, maximum stress, σ_m must be high for the stress induced by acceleration (gravity and flight of the missile).

The problem is different in the case of a free-standing grain, and in fact this type of configuration is selected for highly rigid propellants (high modulus E), with high σ_m and low ε_m . For example, this is the case with double-base propellants.

During a tensile test the physical nature of the propellant (described in Section 4.1.) results in an increase of the volume of the specimen, caused by the occurrence of vacuum holes around some crystalline fillers, or by the increase of micro-cracks in double-base propellants. Knowledge of these phenomena contributes greatly to the determination of the behavior of the materials.

The simultaneous measurement of the volume dilation during a tensile test is done with a gas dilatometer developed by Farris [4]. The method consists in measuring the pressure variation in an enclosure where the specimen is

placed. The change of the pressure is directly linked to the volume dilation of the specimen.

The general aspect of the curves obtained is shown in Fig. 19.

Phases I, II and III of the behavior illustrated in Fig. 19 can be understood in the following manner:

Phase I The zero relative volume dilatation corresponds to an incompressible behavior.

Phase II Creation of vacuum holes or micro-cracks.

Phase III Size increase of the vacuum holes and micro-cracks.

The ε_d value is also called dewetting strain; it identifies the threshold above which the propellant is no longer incompressible. For composite propellants, the higher its value, the better the bonding between the binder and the oxidizers will be. It is a characteristic indicative of good structural integrity of the propellants. ε_d depends on temperature, loading rate, and pressure imposed.

As a rule, ε_d increases with the temperature, or when the loading rate decreases, or again when the pressure increases.

It is difficult to assign values to the dewetting elongation, since this parameter may take different values for each propellant with the pressure (p) temperature (T) and loading rate ($\dot{\varepsilon}$) parameters. For composite propellants with a 20°C temperature, at atmospheric pressure, and a $\dot{\varepsilon}$ loading rate of the order of 10^{-2} s^{-1} , ε_d is usually comprised between 7 and 12%.

α , the angle formed by the asymptote with the axis of the strains, corresponds to the quantity of vacuum holes or micro-cracks present in the propellant. The smaller the number of cavities in the propellant, the smaller $\tan \alpha$ is (a favorable characteristic). As in the case of ε_d , $\tan \alpha$ varies with the three p , T , and $\dot{\varepsilon}$ parameters. As a rule, $\tan \alpha$ decreases when the pressure increases, when the temperature increases or when the loading rate decreases.

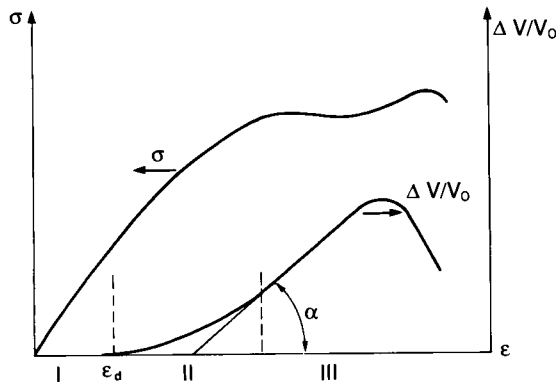


FIG. 6.19. The three behavior phases of a propellant. During a tensile test with measurement of the volume dilatation.

In composite propellants $t g \alpha$ must be as low as possible, but the selection of the propellants must be primarily based on a dewetting strain that is as high as possible.

A particularly interesting test, which is derived from the tensile test, consists in varying the temperature of the propellant specimen during a low-speed tensile test. This test corresponds to the stress imposed on the propellant in a case-bonded propellant subjected to a temperature drop.

The stress response is illustrated in Fig. 20.

Given T_f as the temperature at rupture of the specimen; the elongation at break obtained during a tensile test with simultaneous cooling is much higher than for a tensile test performed at a constant T_f temperature and identical loading rate.

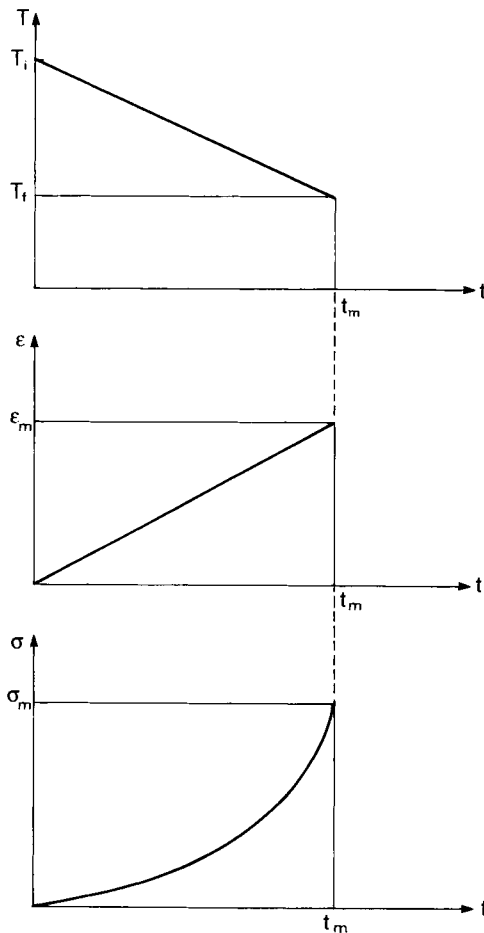


FIG. 6.20. Tensile test with simultaneous cooling of the specimen.

Results of tests performed with propellants under various testing conditions are given in the table and diagram in Fig. 21. Of great interest is the fact that when a case-bonded propellant is cooled down, the e_m elongation capability depends on the way the cooling-down is handled. Figure 21 shows the evolution of this parameter as a function of the ratio of the loading rate to the cooling-down rates. For a given propellant, subjected to a cool-down, there is a corresponding value of the $\Delta\epsilon/\Delta T$, and a maximum allowable elongation value corresponds to that ratio.

4.2.2. Stress relaxation and creep

The viscous nature of the mechanical behavior of a propellant is demonstrated by relaxation and creep tests.

The relaxation test, which consists in subjecting a specimen to a constant elongation and in measuring the evolution of the stress, corresponds to the mechanical load existing in a case-bonded propellant stored at a constant temperature, below the curing temperature.

T in °C/h	V_T in mm/min	T_i °C	E_m in %	σ_m in MPa	$ \frac{\Delta\epsilon}{\Delta T} $ %/°C
-10	0,05	-72	55	13,5	0,6
-10	0,1	-67,5	105	6,3	1,2
-5	0,05	-70,8	109	7,8	1,2
-20	0,1	-70	54	9	0,6
-7	0,1	-65,8	147	4,5	1,71

T = - 60°C	0,1	11,4	12	isothermal tensile test	
------------	-----	------	----	-------------------------	--

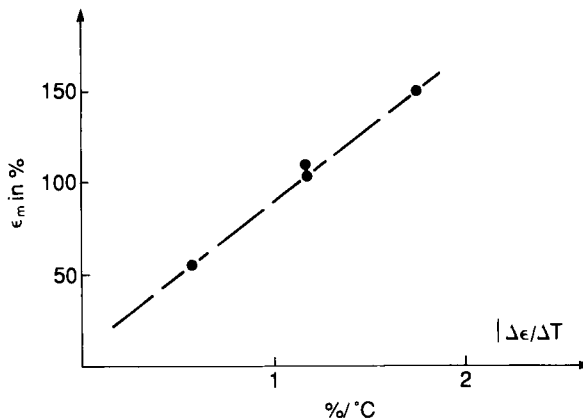


FIG. 6.21. Results of tensile test with simultaneous cooling.

The creep test consists of subjecting a specimen to a constant load and in measuring the evolution of the elongation. This test corresponds to the mechanical loading induced into propellants subjected to a constant acceleration.

(a) Relaxation

In a relaxation test performed on an uniaxial specimen, if ε_i is the constant elongation prescribed during the test, and if $\sigma(t)$ is the evolution of the stress versus time which is measured, the relaxation modulus $E_R(t)$ is expressed by:

$$E_R(t) = \frac{\sigma(t)}{\varepsilon_i} \quad (11)$$

Similarly, in a creeping test, the compliance $J(t)$ is expressed by:

$$J(t) = \frac{\varepsilon(t)}{\sigma_i} \quad (12)$$

The compliance is the inverse of a modulus.

The shape of the relaxation modulus $E_R(t)$ looks like the illustration in Fig. 22.

For the propellants, the relaxation modulus usually depends on the temperature and the strain level. For an identical amount of time, the relaxation modulus decreases when the temperature increases, or when the strain level increases (Fig. 23).

When the variation in the relaxation modulus versus the strain level is small, a linear viscoelastic law can be used. At a given temperature, the curve plotted on Fig. 22 can be written using one of the following forms:

Homographic form

$$E_R(t) = E_1 + \frac{E_2}{\left(1 + \frac{t}{\tau}\right)^n} \quad (13)$$

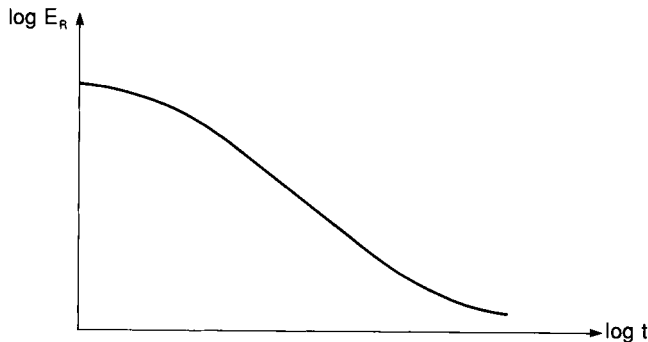


FIG. 6.22. Aspect of the relaxation modulus of composite propellants.

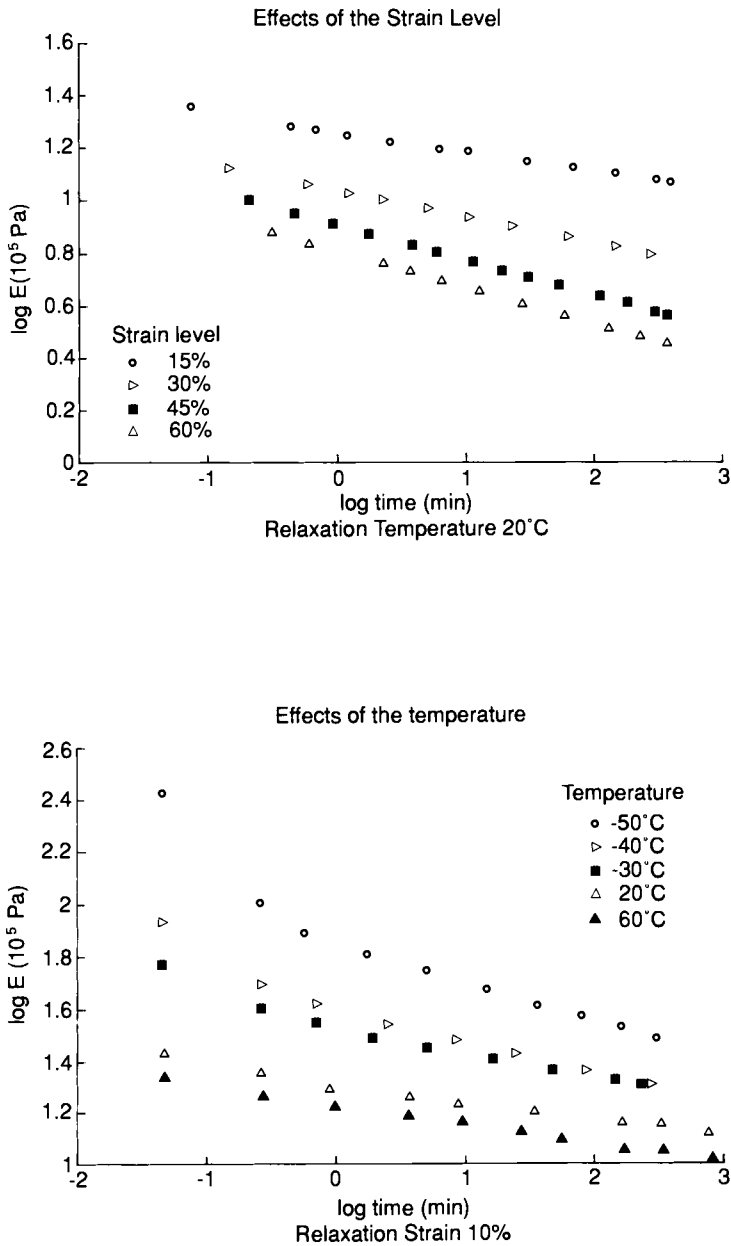


FIG. 6.23. Effects of the temperature and of the level of elongation on the relaxation modulus.

E_1 , E_2 , τ and n are characteristic constants of the material that are determined experimentally.

Prony series

$$E_R(t) = E_0 + \sum_{i=1}^N E_i e^{-t/\tau_i} \quad (14)$$

E_0 , E_i and τ_i are characteristic constants of the material that are determined experimentally.

When tests are performed on an uniaxial specimen, the stress is expressed by the relation [2,3]:

$$\sigma(t) = E_R(t)\varepsilon(o) + \int_0^t E_R(t-\tau) \frac{\partial \varepsilon}{\partial \tau} d\tau \quad (15)$$

This form is valid only for a linear viscoelastic behavior.

In the case of non-linear behaviors, some authors propose using the same form as (15) by expressing the relaxation modulus into the product of two terms.

$$E_R(t, \varepsilon) = E_{R1}(\varepsilon)E_{R2}(t) \quad (16)$$

$E_{R1}(\varepsilon)$ may take the form of a polynomial.

Other authors propose laws that are better suited to propellants [9]; Francis has done a comparison of the laws developed by various authors for solid propellants [13]. No model appears completely satisfactory, and major research work is still being done in this area [23].

(b) *Creeping*

The creep test is used only to determine the failure characteristics of solid propellants. A constant load σ_F is applied on a specimen; the time to failure t_R is recorded (Fig. 24).

4.2.3. *The effect of the temperature; time-temperature equivalence*

When relaxation tests are performed (at a given elongation) at various temperatures, the curves representing the evolution of the relaxation modulus for each temperature are deducted one from the other by a shift factor versus time (Fig. 25). This observation is generally true in the case of polymers. There is an equivalence between time and temperature. In the case of the relaxation, we can write:

$$E_R(t_0, T_0) = E_R(t_1, T_1) = E_R(t_2, T_2)$$

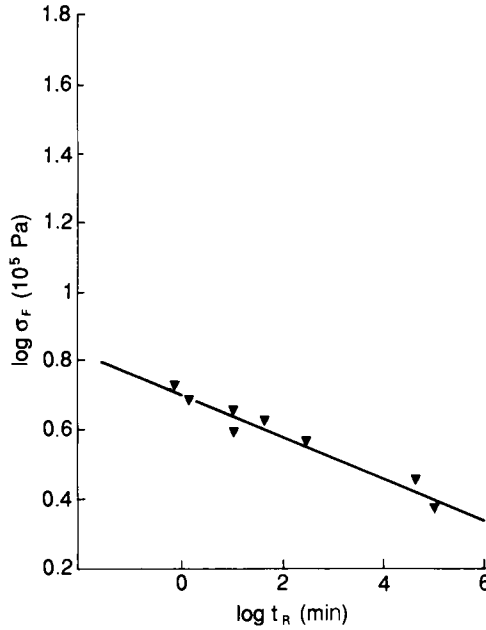


FIG. 6.24. Creep test: time to failure versus stress level.

where:

$$\log t_1 = \log t_0 + \log a_{T_1}^{T_0}$$

$$\log t_2 = \log t_0 + \log a_{T_2}^{T_0}$$

where $a_{T_1}^{T_0}$ and $a_{T_2}^{T_0}$ are the shift factors, in relation to the T_0 reference temperature.

A sole curve can be identified, called the “master curve,” which gives the value of the relaxation modulus versus a reduced time $t/a_T^{T_0}$ for various temperatures. The corresponding time, called reduced time, is written as follows:

$$\xi = \int_0^t \frac{d\tau}{a_T^{T_0}(T(\tau))}$$

The shift function is determined experimentally. Williams, Landel and Ferry [10] have developed an analytical form with two coefficients, C_1 and C_2 , usually known as W.L.F. equation:

$$\log a_T^{T_0} = \frac{-C_1(T - T_0)}{C_2 + T - T_0}$$

The reference temperature T_0 is often the ambient temperature, and the corresponding shift factor is written: a_T .

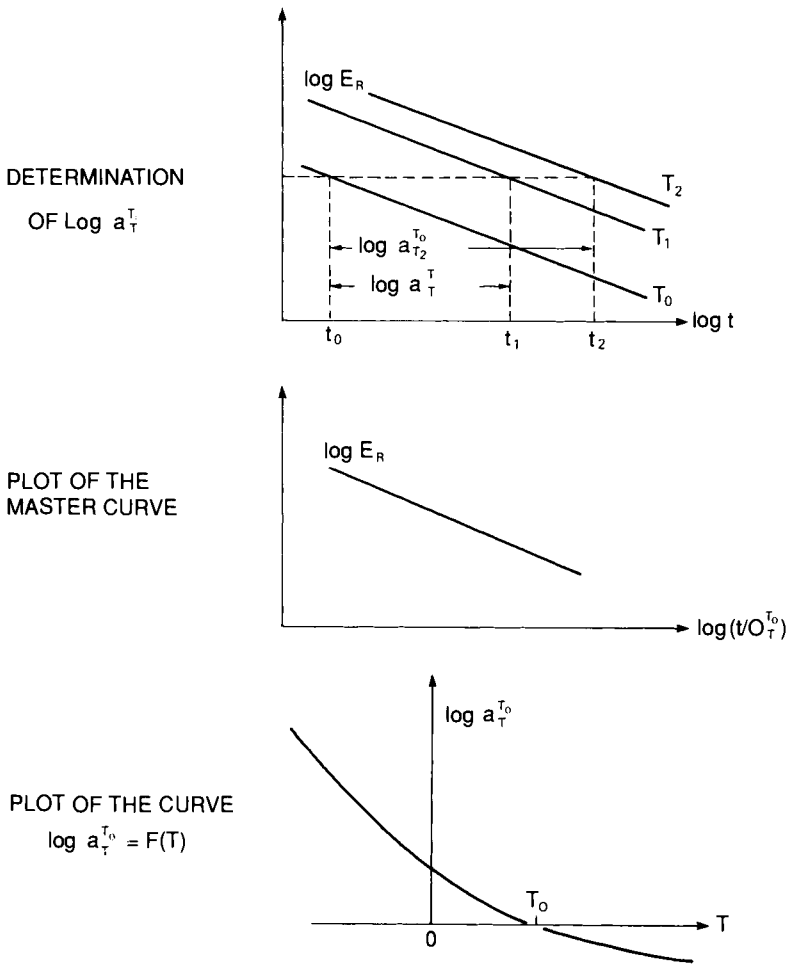


FIG. 6.25. Time-temperature equivalence.

Extending the concept, the principle of time-temperature equivalence is used on all characteristics measured experimentally during tensile tests:

- tangent modulus E ;
- maximum stress σ_m ;
- strain at maximum stress ε_m .

In the case of tensile tests it is an equivalence loading rate ($\dot{\varepsilon}$) - temperature that is used. The master curves are defined with the reduced variable $1/\dot{\varepsilon}a_T$.

$$\log E = f(\log 1/\dot{\varepsilon}a_T)$$

$$\log \sigma_m = g(\log 1/\dot{\varepsilon}a_T)$$

$$\log \varepsilon_m = h(\log 1/\dot{\varepsilon}a_T)$$

Time to failure at maximum stress σ_m is:

$$t_m = \varepsilon_m / \dot{\varepsilon}$$

It becomes possible to plot the master curve under another form (Fig. 26).

$$\log \sigma_m = g'(\log t_m / a_T)$$

For some number of propellants, the shift factors measured on the moduli and on the maximum stresses are identical.

The time-temperature equivalence concept is empirical. Consequently, it must be determined for each propellant.

4.2.4. Effect of the pressure

It is necessary to know the effect of the pressure on the mechanical behavior of propellants as well as on their capability because, at the time of firing, the propellant grains operate under pressure. This pressure varies according to the propellant grains from 4 MPa to 15 MPa, and possibly higher.

Tests performed under pressure on specimens are done at constant pressure; the strain imposed on the propellant in a case-bonded grain is different, because the evolution of the stress and strain is due to the evolution of the pressure. To obtain the best possible simulation of the firing phenomena, it would be necessary to perform tensile tests with simultaneous pressure variation.

Qualitatively, during a tensile test, the effect of the pressure is to delay the occurrence of micro-cracks and vacuum holes. The relative variation in the

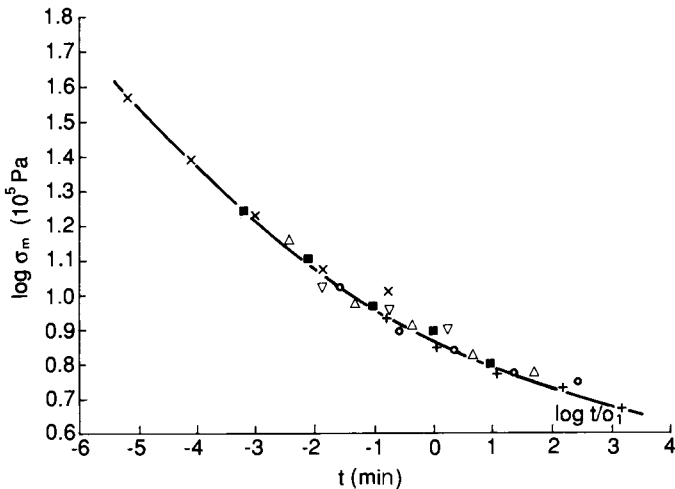


FIG. 6.26. Master curve of the maximum tensile stress.

volume that is measured during the test reveals an increase in the dewetting elongation and a decrease in $tg\alpha$.

The values of the maximum stress and corresponding strain are significantly increased in comparison with the values obtained at atmospheric pressure under the same temperature and strain rate conditions (Fig. 27, upper). For any common incompressible portion where the relative volume variation is zero, at atmospheric pressure and under pressure the propellant behavior is, of course, unchanged.

In the case of composite propellants with large elongations, and with a significant Phase III (shown in Fig. 19), the effect of pressure is generally described as follows (Fig. 27, lower).

Phase I. The propellant is incompressible, the amount of vacuum holes around the charges is low, possibly zero; the pressure has no effect on the behavior, and the tensile curves are identical for all pressures.

Phase II (of a test performed at atmospheric pressure). The number of vacuum holes increases and reaches maximum value at stress σ_1 . The effect of the pressure is to delay the occurrence of the vacuum holes and to significantly decrease their number. With pressures of the order of 7 MPa, the number of vacuum holes stays very low until stress σ_m^p . Stress σ_m^p and the corresponding elongation ε_m^p must be compared to the strain at the end of Phase II, σ_1 , and the corresponding elongation ε_1 . The tensile behavior of highly filled composite propellants often exhibits only Phase I and II at atmospheric pressure. As a result, the comparison between the maximum stress and corresponding elongation presents no problem (Fig. 27, upper).

Phase III (of a test at atmospheric pressure). All vacuum holes have appeared; their number remains constant until stress σ_m . Their size increases between ε_1 and ε_m and the difference between ε_m and ε_1 is characteristic of the resistance to tearing of the binder. Under pressure, this phase may completely disappear. When micro-cracks appear in the binder, at a stress close to the maximum stress σ_m^p , which is much greater than the corresponding stress at atmospheric pressure (σ_1), the propagation of the cracks in the binder is much more rapid under pressure. Phase III is greatly reduced, sometimes practically nonexistent. It is therefore important to compare the corresponding stress and strain, respectively, because although the maximum stress of tests performed under pressure is typically greater than any stress experienced under tests at atmospheric pressure ($\sigma_m^p > \sigma_1$ and $\sigma_m^p > \sigma_m$), it is not true for elongations ($\varepsilon_m^p > \varepsilon_1$ and $\varepsilon_m^p < \varepsilon_m$).

The following question needs to be answered: which capability is to be taken into consideration? The effects described above increase when the pressure increases, up to a threshold pressure, after which the effects remain constant.

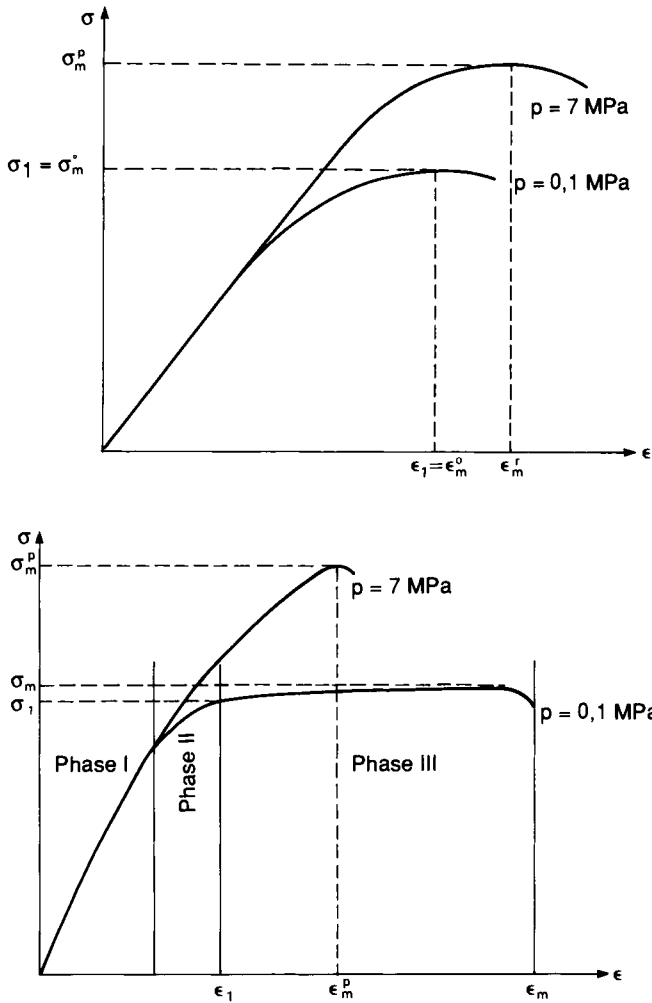


FIG. 6.27.

That threshold pressure depends on the materials, and for each propellant it depends on the rate of stress and the temperature. In fact, the higher the stiffness of the specimen, the greater the threshold pressure will be (Fig. 28).

4.2.5. Behavior law of solid propellants

Section 3.2 describes the coefficients that must be determined to know the mechanical behavior of the propellants.

All of the tests described above reveal a non-linear viscoelastic behavior, tricky to represent in a single model.

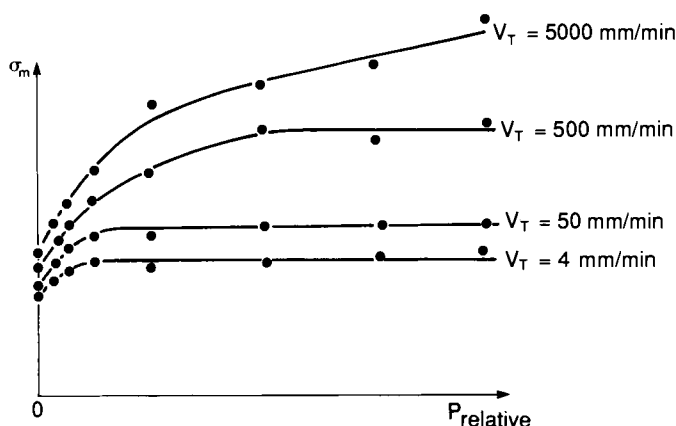


FIG. 6.28. Effect of the pressure on the maximum tensile stress.

The first important result is obtained during the tensile test with the simultaneous measurement of volume dilation. The volume dilation is zero up to elongation ϵ_d , which corresponds to incompressible behavior of propellants under small strains. Incompressibility, in the equations of mechanics, is a discontinuity which expresses itself by the fact that it is not possible to determine stress field from the strain field. The average stress $\bar{\sigma}$ depends on the geometrical confinement of the propellant.

Returning to the definition of the coefficients characteristic of the behavior, incompressibility is expressed by:

$$E(\text{any}) \quad \nu \rightarrow 0.5$$

$$\text{or} \quad G(\text{any}) \quad K \rightarrow \infty$$

In fact, the bulk modulus has a finite value, but it is much greater than the shear modulus.

For that reason, relations (4) are used. In the case of a viscoelastic behavior, the formulation becomes:

$$\begin{aligned} \sigma'_{ij}(t) &= 2G(t)\epsilon'_{ij}(0) + 2 \int_0^t G(t-\tau)\epsilon'_{ij}(\tau)d\tau \\ \bar{\sigma}(t) &= k\bar{e}(t) \end{aligned} \quad (17)$$

where:

$\sigma'_{ij}(t)$ and $\epsilon'_{ij}(t)$ are the deviatoric stress and strain tensors;

$\bar{\sigma}(t)$ is the average stress;

$e(t) = 3\bar{e}(t)$;

$\bar{e}(t)$ is the average strain.

For infinitesimal strain, the volume dilatation is equal to $e(t)$. For an incompressible mechanical behavior, the relations between coefficients E , ν and G , K , become:

$$E = 3G; \quad \nu = \frac{1}{2} \quad (18)$$

Therefore, the relaxation modulus identified in Section 4.2.2 allows us to calculate easily the G modulus, and the relation between the deviatoric tensors will be established simply. The relation between the average stress and the average strain is more complicated because, as a rule, $e(t)$ is very small and K is very large. The methods used most widely to handle this problem are described in Section 5.

Propellants generally have a non-linear viscoelastic behavior. The laws used to model this type of behavior are mentioned in Section 4.2.2.

Starting with relation (17), which is valid for a linear behavior, an extension can be done by writing:

$$\sigma'_{ij}(t) = 2 \int_0^t G(\varepsilon, t - \tau) \dot{\varepsilon}'_{ij}(\tau) d\tau + 2G(\varepsilon, t) \dot{\varepsilon}'_{ij}(0) \quad (19)$$

There have been other formulae proposed to model propellant behavior [13]. Farris [4], in particular, developed a theory that applies to composite propellants. This law is written:

Deviatoric stress tensor

$$\sigma'_{ij}(t) = \exp\{\beta I_\gamma - \beta'(\Delta V/V_0)/I_\gamma\} \left\{ \left[G_1 + G_2 \left(\frac{I_\gamma}{\|I_\gamma\|_{p_1}} \right)^{m_1} \right] \dot{\varepsilon}'_{ij}(t) + G_3 \left[1 - \left(\frac{I_\gamma}{\|I_\gamma\|_\infty} \right)^{m_2} \right] \int_0^t (t - \xi)^{m_3} \dot{\varepsilon}'_{ij}(\xi) d\xi \right\} \quad (20)$$

σ'_{ij} = deviatoric stress tensor

$\dot{\varepsilon}'_{ij}$ = deviatoric strain tensor

$\Delta V/V_0$ = volume dilatation

if $\varepsilon_1, \varepsilon_2, \varepsilon_3$ are the principal strains

$$I_\gamma = \frac{1}{3}((\varepsilon_1 - \varepsilon_2)^2 + (\varepsilon_2 - \varepsilon_3)^2 + (\varepsilon_3 - \varepsilon_1)^2)^{1/2} \|I_\gamma\|_{p_1} = \left\{ \int_0^t \frac{(I_\gamma)^{p_1}}{\mathbf{a}_T} d\tau \right\}^{1/p_1}$$

\mathbf{a}_T = shift factor of the time-temperature equivalence

$$\xi = \int_0^t \frac{d\tau}{\mathbf{a}_T} \text{ is the reduced time}$$

$$\|I_\gamma\|_\infty = \max |I_\gamma|$$

$$G_1, G_2, G_3, \beta, \beta', m_1, m_2, m_3, p_1$$

are constants that are dependent on the material.

Isotropic part

$$\Delta V/V_0 = \frac{\bar{\sigma}}{K} \left[\exp \left\{ \left[\chi_1 + \chi_2(T - T_0) \right] \bar{\sigma} - 1 \right\} \right] + A I_{\dot{\gamma}}^r \exp \left\{ \left[\lambda_1 + \lambda_2(T - T_0) \right] \bar{\sigma} \right\} \quad (21)$$

$\bar{\sigma} = (\sigma_{11} + \sigma_{22} + \sigma_{33})/3$ is the average stress;

$K, A, r, \chi_1, \chi_2, \lambda_1, \lambda_2$ are constants of the material.

In most cases this law can be simplified. It allows us to represent, with a fairly good level of accuracy, the behavior of the propellant as a function of various physical parameters: temperature, pressure, and strain rate (Figs 29–32).

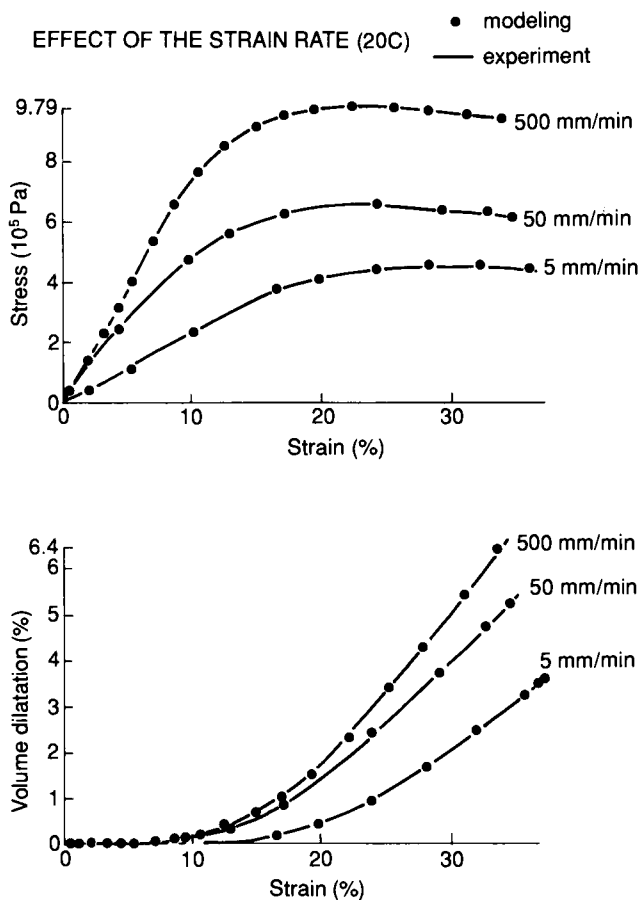


FIG. 6.29. Model of the Farris law behavior.

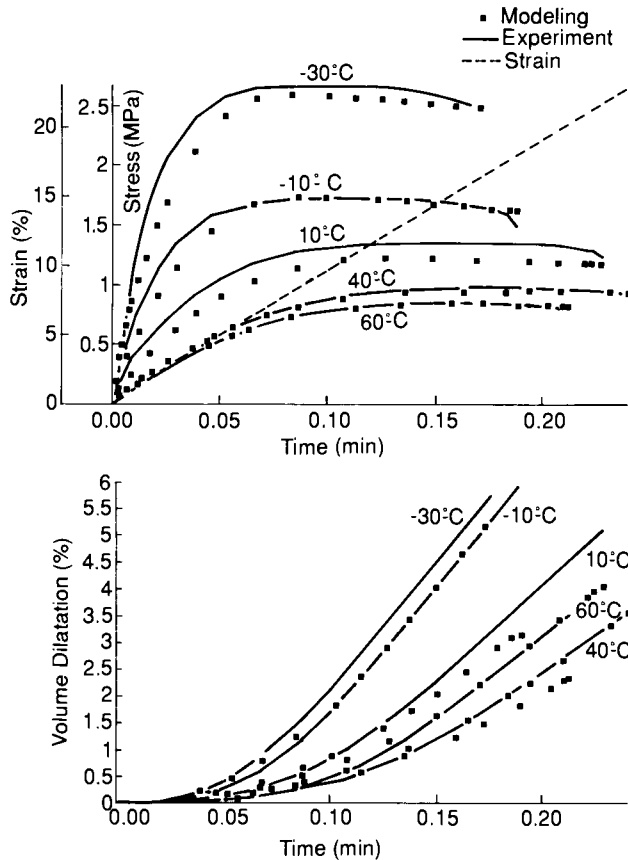


FIG. 6.30. Influence of the temperature.

Some points of the field are modeled with a great lack of precision, which is a serious disadvantage when used systematically. This remark seems to have been justified for most of the models proposed by various authors [13].

In fact, the modeling of a behavior law can be done according to two methods:

- (a) Experimental results are written into models according to various mathematical expressions (polynomials, power laws), which are not necessarily supported physically. In this case the precision of the model selected depends on the quantity of tests performed to explore the experimental field.
- (b) The choice of a constitutive law to approximate the behavior based upon the modeling of the physical phenomena involved during the tests (for example, with composite propellants, the dissipation of energy

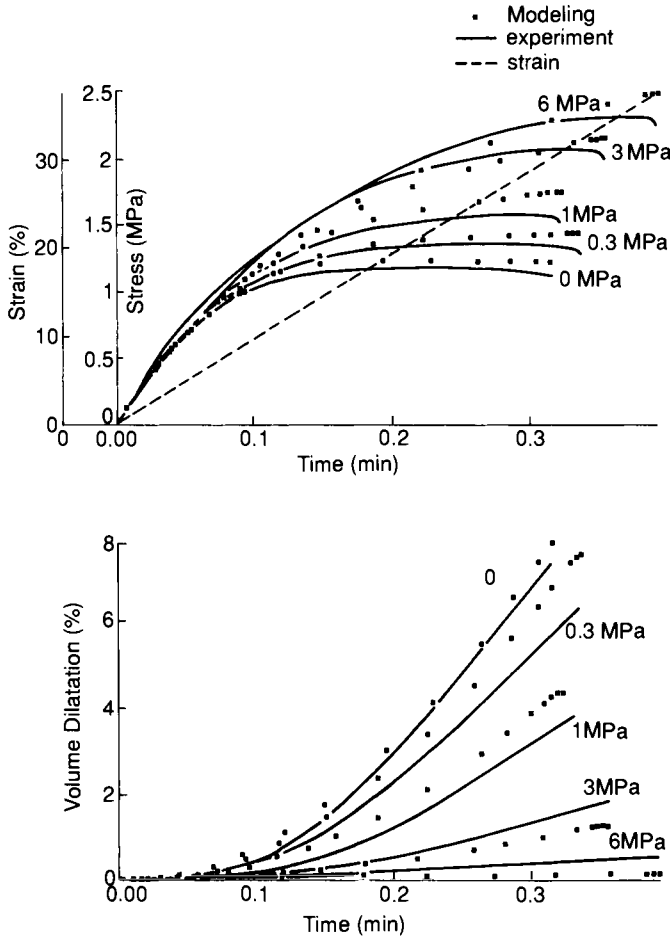


FIG. 6.31. Influence of pressure.

through the creation of vacuum holes, growth of cracks and ripping of the binder until a break occurs). This method, based predominantly on physics, and therefore more real, should allow us to obtain a global modeling of the behavior of propellants, with a good level of accuracy over a fairly extensive experimental field. In fact, the physical phenomena taken into consideration do not correspond to all physical phenomena involved. The simplified assumptions used to create the models do not have the same degree of validity for the whole field examined. For some conditions of utilization, some phenomena that have not been taken into consideration may modify the behavior, and the modeling used will be imprecise.

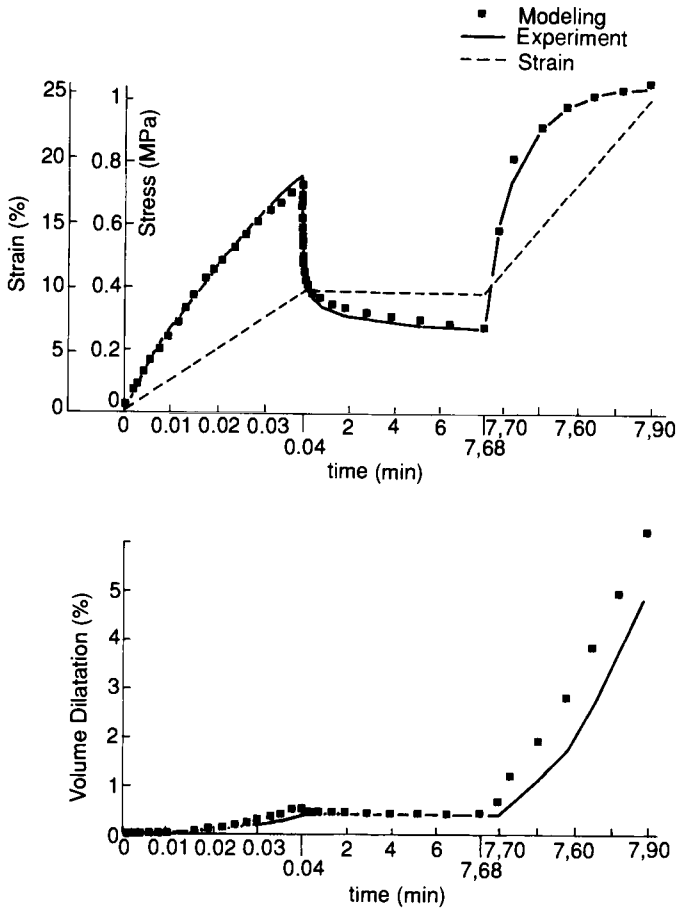


FIG. 6.32. L.R.L. test..

These slightly pessimistic comments do not prevent research activities from continuing, which is a good thing. Even though it seems improbable that we will be able in the short term to use a constitutive law expressing the complex behavior of propellants, the development of modeling, even if it can never be completed, increases considerably our knowledge of propellants and gives us the possibility of improving their structural integrity.

4.2.6. *Capability: failure criterion*

4.2.6.1. *Capability (allowable stress or strain)*

The propellant capability is the induced maximum stress or strain necessary to cause failure of the material.

The propellant capability, under tensile load, may be expressed either by the maximum stress σ_m , or by the corresponding maximum elongation. If cracks appear at elongation ϵ_m and propagate throughout the specimen up to ϵ_r (Fig. 18), the propellant cannot be used for an elongation ranging between ϵ_m and ϵ_r .

The capability of a propellant is determined experimentally. It is expressed by using master curves (Fig. 33).

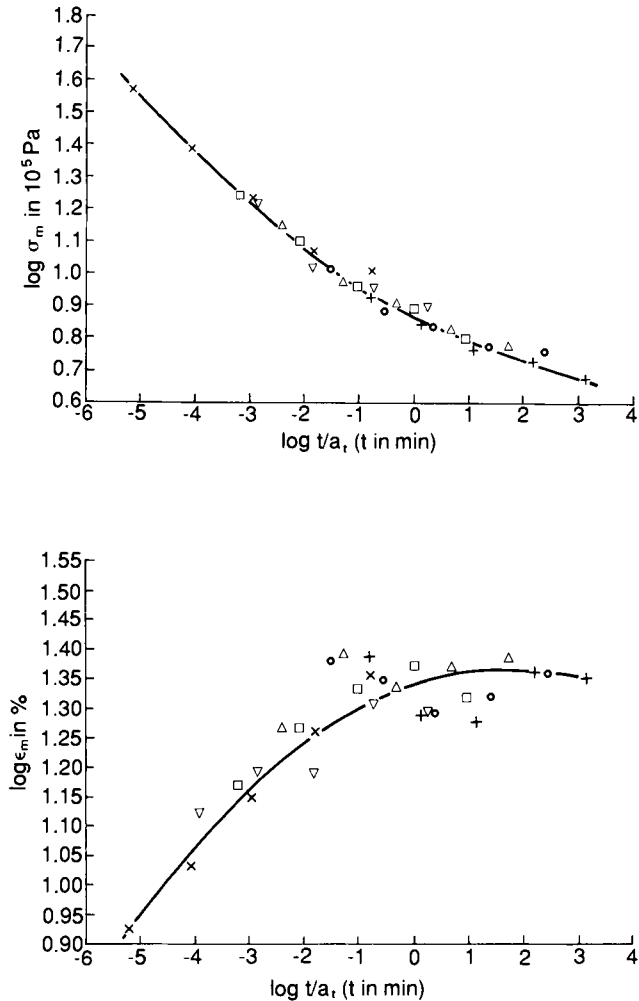


FIG. 6.33. Tensile master curves σ_m and ϵ_m .

4.2.6.2. Failure criterion [14]

The propellant capability, as defined in Section 4.2.6.1., corresponds to a monodimensional test. The stress tensor is reduced to a single component.

$$\bar{\sigma} = \begin{bmatrix} \sigma_m & 0 & 0 \\ 0 & 0 & 0 \\ 0 & 0 & 0 \end{bmatrix}$$

In a propellant grain the stress tensor has, at each point, more than one non-zero component. Consequently, it is not possible to do a direct comparison between the capability obtained by monodimensional tests and a three-dimensional stress field.

When inducing a mechanical load, there is at each point of the propellant a stress tensor and a strain tensor. These tensors can be characterized by their three principal components and the corresponding invariants (as defined in Section 3). The stress tensor (or strain tensor) for each point of the propellant grain is represented by one point in the principal stress space (or principal strain space). In that space there exists a volume where the propellant keeps its structural integrity, where there is a little damage, and a volume where the propellant is made worthless by significant damage, even possibly a crack. It is sufficient to ensure that the points representative of the stress tensor in the propellant are located in the volume where the propellant keeps its structural integrity.

Generally, the propellant is considered worthless when it is ruptured. The two areas are separated by an assumed continuous surface, called the failure surface. It is defined only in stress, and it is obtained with different tensile tests under different hydrostatic pressures, different temperatures, different tensile rate, and biaxial and triaxial tests.

Several authors have proposed different equations for these surfaces [14]. For propellants in general, it seems that the best-suited equation corresponds to a mixed formula:

- the Stassi formula for the area where the stresses are positive or slightly negative;
- the Von Mises formula for the area where the stresses are negative (Fig. 34).

These two formulae correspond to revolution surfaces centered on the axis Δ where $\sigma_1 = \sigma_2 = \sigma_3$. Figure 35 shows the intersection of that surface with a plane containing the Δ axis. Axes Δ and Y of this new space are related to values using invariants of the stress tensors:

Δ is the axis of the average stresses $\sigma_{oct} = \frac{1}{3}(\sigma_1 + \sigma_2 + \sigma_3)$ Y is the axis of the octahedral shear stress

$$\tau_{oct} = \frac{1}{3}[(\sigma_1 - \sigma_2)^2 + (\sigma_2 - \sigma_3)^2 + (\sigma_3 - \sigma_1)^2]^{1/2}$$

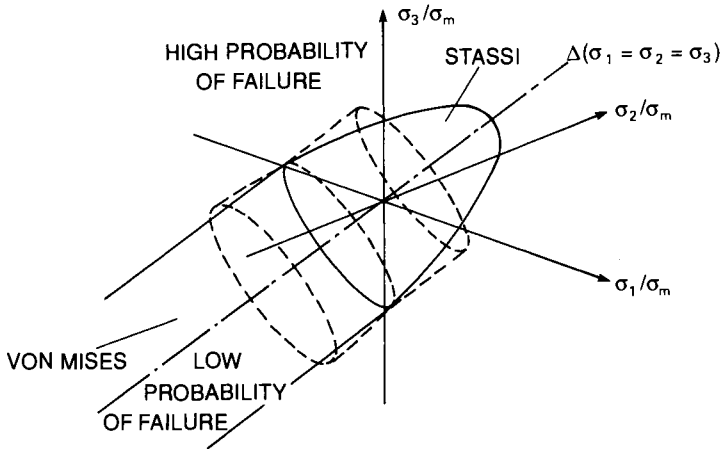


FIG. 6.34. The failure criterion.

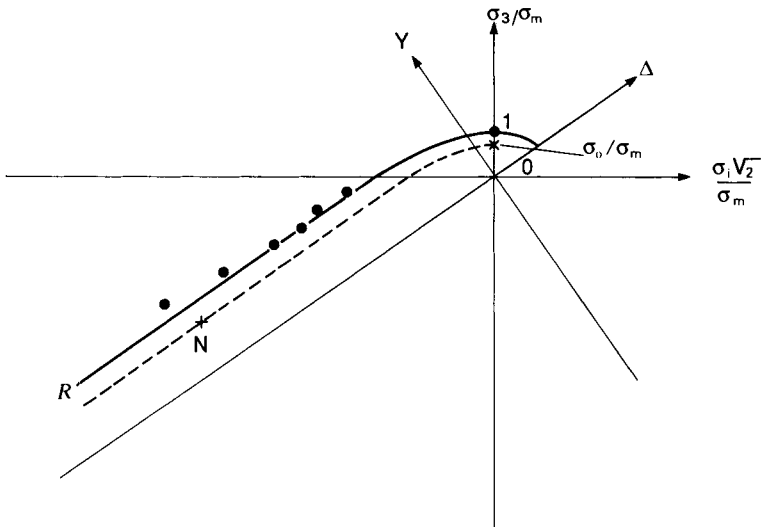


FIG. 6.35. The failure criterion shown in a two-dimensional axis system.

All points representative of the stresses in a propellant grain are located within that plane. Taking a point M in this plane, the homothetic curve to the curve \mathcal{R} (representative of the failure surface) passing through M cuts the axis σ_3/σ_m at a point whose measurement on this axis is σ_o/σ_m ; σ_o is called the equivalent stress. It allows us to compare directly the three-dimensional stress state represented by the point M to the maximum stress obtained in a tensile test.

For the Von-Mises part, this equivalent stress is defined by:

$$\sigma_o = [[(\sigma_1 - \sigma_2)^2 + (\sigma_2 - \sigma_3)^2 + (\sigma_3 - \sigma_1)^2]/a]^{1/2}$$

and for the Stassi part:

$$\sigma_o = [(\sigma_1 + \sigma_2 + \sigma_3) + \{(\sigma_1 + \sigma_2 + \sigma_3)^2 + b[(\sigma_1 - \sigma_2)^2 + (\sigma_2 - \sigma_3)^2 + (\sigma_3 - \sigma_1)^2]\}^{1/2}]/c$$

a , b , and c are coefficients that depend on the material.

Comment. The use of this failure criterion implies that the effects of the pressure observed on the stress capability are identical to the effects on the strain capability. It is therefore necessary to verify, experimentally, that the gain contributed by the pressure to the stress is at least equal to the gain contributed to the corresponding strain.

Furthermore, if the failure surface of a propellant is not identical for all stress rates and temperatures tested, the failure criterion defined in this section does not exist. When this occurs, the propellant capability must be determined experimentally under conditions similar to the operating conditions (stress rate, temperature and pressure), using multiaxial specimens.

4.2.7. Damage

The capability defined in the preceding section corresponds to an elementary mechanical load, i.e. one rate of load, one temperature and one pressure.

Propellant grains are subjected to various loading conditions whose effects are cumulative in time. It is therefore necessary to introduce the notion of damage, which represents the ability of the material to be subjected to a cumulation of various elementary loads.

Several models have been suggested. Currently, the most widely used model for propellants is the Bills model, based on the Miner model, and defined as follows: [4,23-25]

$$\mathcal{D} = \sum_{i=1}^N \frac{t_i}{t_{Ri}} \quad (22)$$

where:

i represents the various elementary loads;

t_i represents the time spent under elementary loads i ;

t_{Ri} represents the failure time corresponding to the elementary load i ;

\mathcal{D} is the damage which, by definition, must be less than 1 for the propellant to be used.

When the creep failure curve is written in the form of:

$$\sigma_F \left(\frac{t_R}{a_T} \right)^{1/m} = 1/\mathcal{D}_O \quad (23)$$

where:

- σ_F is the applied load in creeping;
- t_R is the failure time for applied load σ_F ;
- m and \mathcal{D}_0 are the coefficients depending on the material.

The damage can be expressed as follows:

$$\mathcal{D}(t) = \mathcal{D}_0 \left[\int_0^t (\sigma_0(\tau))^m \frac{d\tau}{a_T} \right]^{1/m} \quad (24)$$

In this manner the entire history of the stress is taken into account, regardless of the nature of the mechanical loads that are applied.

The creep failure curves cannot always be written in the form of eqn (23). In that case, a more general form to express damage is:

$$\mathcal{D}(t) = \mathcal{D}_0 (\|\sigma_0\|_m)^{\mathcal{D}_1} + \mathcal{D}_2 (\|\sigma_0\|_\infty)^{\mathcal{D}_3} \quad (25)$$

\mathcal{D}_0 , \mathcal{D}_1 , \mathcal{D}_2 , \mathcal{D}_3 and m are constants of the material.

4.2.8. Tearing

Cracks may occur in the propellant as a result of certain manufacturing or handling operations without necessarily compromising the operation of the rocket motor.

To assess the severity of a crack it is necessary to determine the manner in which it propagates itself under the effect of mechanical load.

There are three modes in which a crack propagates itself (Fig. 36).

A stress intensity factor at the tip of the crack is determined for each propagation mode (K_I , K_{II} , K_{III}). It is typically dependent on the initial length a_0 of the crack and on the stress that would exist in the area at the bottom of the crack if the crack were not there. As a rule, the propagation rate of cracks obeys a power law for the stress intensity factor.

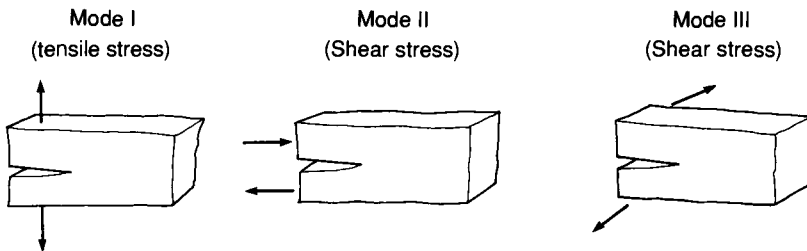


FIG. 6.36. The three modes of propagation of a crack.

Mode I, for example:

$$\frac{da}{dt} = AK_I^n$$

$\frac{da}{dt}$ is the propagation rate of the crack;

K_I the stress intensity factor in Mode I;

A and n constants of the material.

In a propellant grain, when cracks exist, they propagate themselves primarily in Mode I and II.

The tests designed to determine the propagation in Mode I are performed on special specimens (biaxial notched strip specimen) which are subjected to tensile stress in a direction perpendicular to the crack (Fig. 37).

During the test, the length of the crack does not evolve in a continuous manner [26]. But, by proceeding to an integration of the phenomenon, it is possible to obtain an average evolution of the propagation rate of the crack (Fig. 38), as well as the intensity coefficient of the stress.

Crack propagation tests give results that are very scattered. The laws describing the phenomenon can be only an approximation of that phenomenon.

Nonetheless, the law described below [15,16] permits a global representation of the crack propagation phenomenon in propellants (Fig. 39).

$$\frac{da}{dt} = A \frac{K_I^2}{\sigma_m^2 t_m};$$

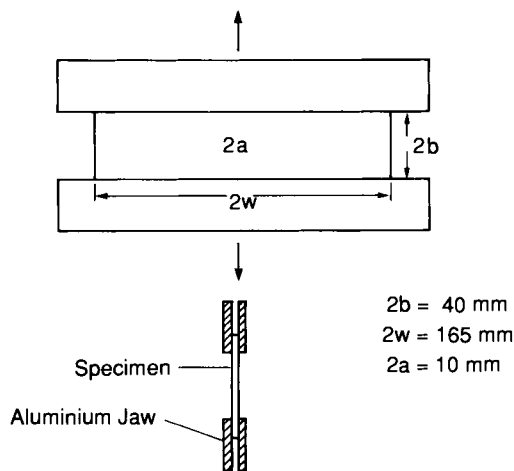


FIG. 6.37. Notched biaxial strip specimen.

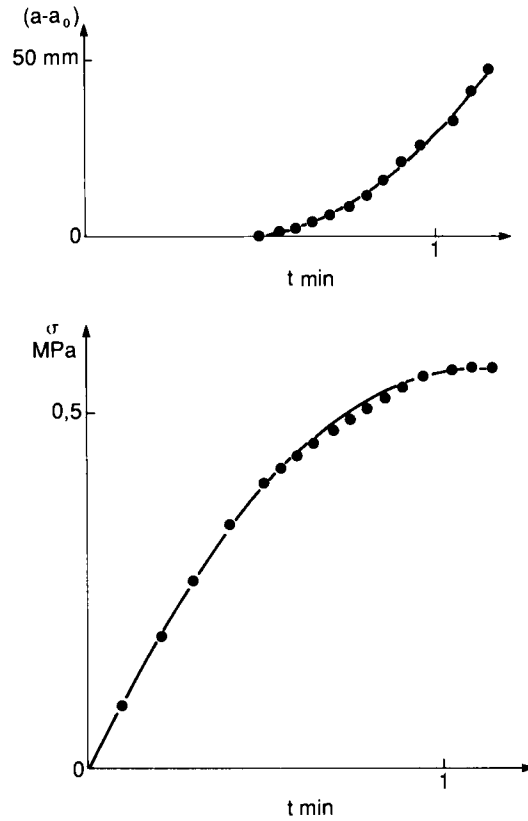


FIG. 6.38. Evolution of the length of a crack and of the stress during a test.

A material constant;

$\frac{da}{dt}$ propagation rate of the crack;

σ_m tensile capability of the material for the corresponding mechanical load (same tensile rate);

t_m time to failure corresponding to σ_m ;

K_I stress intensity factor in Mode I.

There are other authors proposing laws for viscoelastic materials [17–19]. A significant amount of research is being done currently in this area; crack modeling in solid propellant grains continues to be done with simple models.

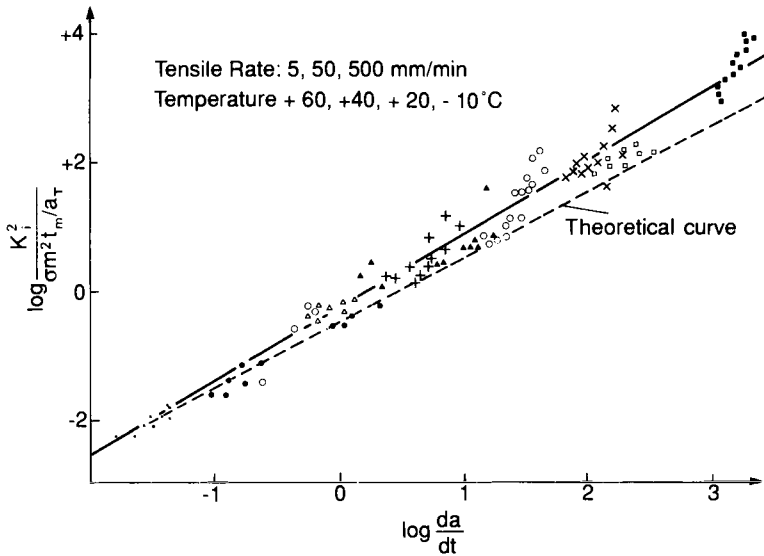


FIG. 6.39. Law of crack propagation.

4.3. BONDS (BONDING BETWEEN THE LINER AND THE PROPELLANT)

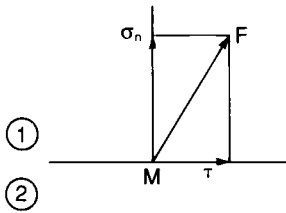
4.3.1. *Physical and mechanical nature of the bonds*

The bonds represent physically the adhesion occurring during the propellant curing phase, between the propellant and the liner. This adhesion takes place by the migration through the surface of various products that allow the creation of physicochemical bonds. A detailed analysis of the material in the vicinity of the bonds reveals that there is no bondline, geometrically speaking, but rather a significant gradient of the mechanical properties.

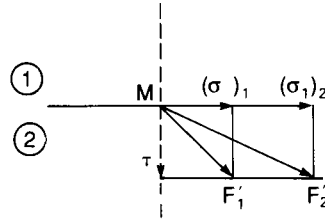
Mechanically, the bonding is represented by a surface separating two homogeneous materials. Consequently, there is a discontinuity of the stress tensor and of the strain tensor through the bondline. From a mechanical point of view there is a continuity of the displacement of all surface points belonging both to the liner and to the propellant, and of the force applied to the surface. All other components are discontinuous.

On the bondline, the force per unit surface is the sum of an elongation component σ_N , called normal stress, and a sliding component called shear stress (Fig. 40).

$$\vec{F} = \sigma_N \cdot \vec{n} + \tau \vec{t}$$



F Applied Force at M
relating to bonding plane



F'_1 et F'_2 Applied Forces at M
relating to the plane
normal to the bonding plane

At the point M , there are 2 stress tensors

relating to material ①

$$\begin{bmatrix} \sigma_n & \tau \\ \tau & (\sigma_1)_1 \end{bmatrix}$$

relating to material ②

$$\begin{bmatrix} \sigma_n & \tau \\ \tau & (\sigma_1)_2 \end{bmatrix}$$

There is continuity of σ_n and τ

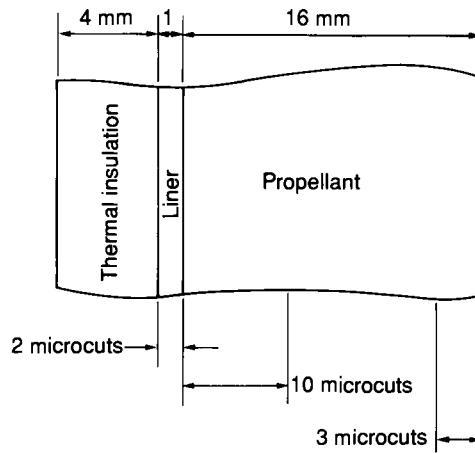
FIG. 6.40. Discontinuity in the vicinity of a bondline.

The continuity of the force is expressed by the continuity of the normal stress and of the shear stress applied to the bondline. These components are therefore the components that globally characterize the capability of the bonds.

4.3.2. Behavior of the bonds

4.3.2.1. Micromechanical analysis

The micromechanical analysis of the behavior of the material in the plane area of the bonding is conducted by taking microspecimens on which the mechanical characteristics under tensile test are determined (Fig. 41). Additional microhardness tests make it possible to confirm the results obtained on the small specimens. There is, in some propellant compositions, an increase in Young's modulus in the vicinity of the bondline, as well as an increase in hardness (Figs 42 and 43).



Dimension of the specimens for the micromechanical study
 Length = 25 mm Width = 5 mm Thickness = 0,5 mm

FIG. 6.41. Removal of microspecimen in the vicinity of the bondline.

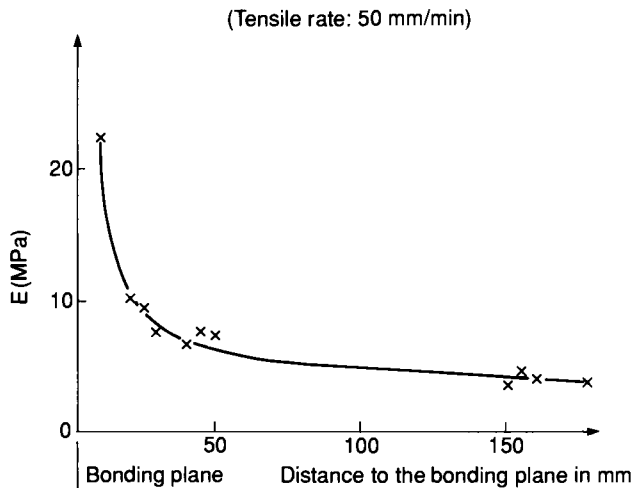


FIG. 6.42. Evolution of the modulus in the vicinity of the bonding plane.

4.3.2.2. Global analysis

The complex nature of the bonding area having been revealed by the micromechanical analysis, it is therefore possible to mechanically characterize the entire bonding area by assuming that the liner-propellant whole is an

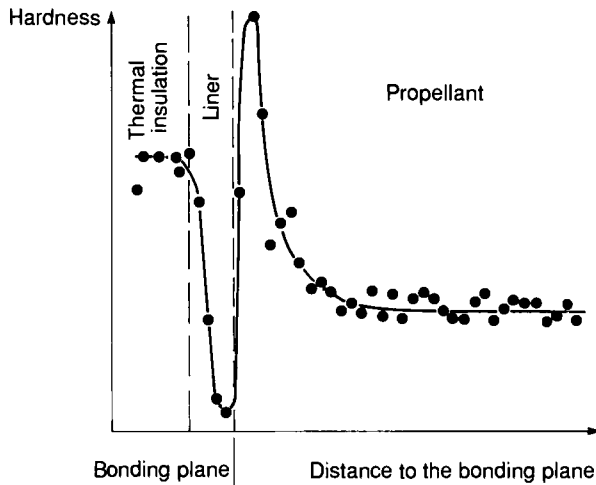


FIG. 6.43. Evolution of the hardness in the vicinity of the bonding plane.

orthotropic material. The symmetry of the superposition of the various materials reduces to five the number of coefficients that need to be determined to characterize the behavior (Fig. 44).

4.3.3. Capability of the bonds

The capability of the bonds is obtained by applying increasing load until failure of the specimen occurs.

4.3.3.1. Micromechanical analysis

This particular analysis, performed on microspecimens described in Section 4.3.2.1, allows us to discover a variation of the maximum stress at break and the corresponding strain in the vicinity of the bonding area (Fig. 45).

4.3.3.2. Global analysis

There are two ways of performing the global analysis of the capability:

- by assimilating the bonding area to an orthotropic material;
- by measuring the maximum force applied to the bonding plane.

The first method is simply a prolongation of the method described in Section 4.3.2.2.

The second method consists of measuring the maximum force applied to the bonding plane for different application angles. The specimens used are those described in Fig. 46.

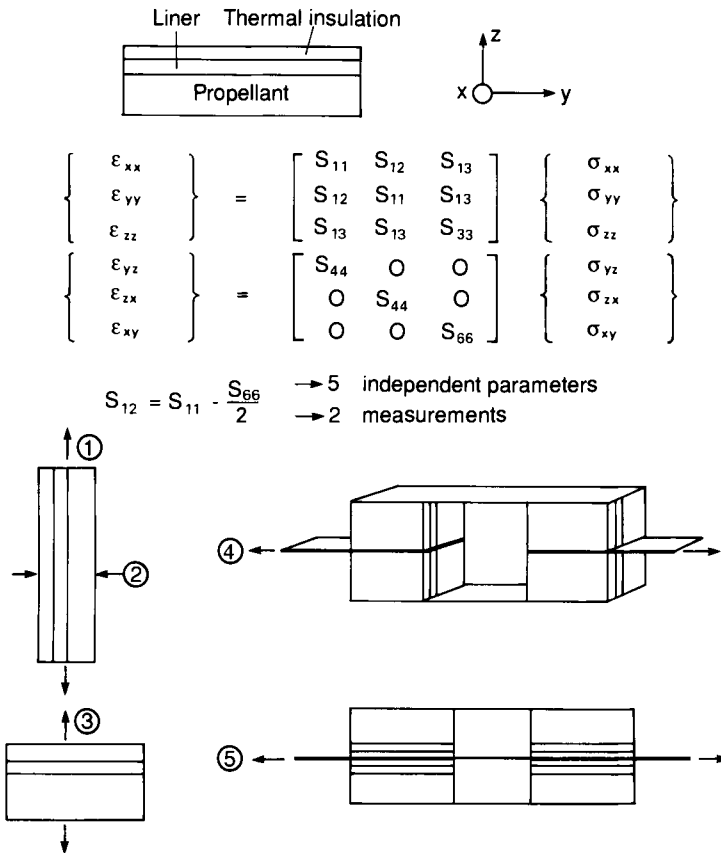


FIG. 6.44. The bonding area is an orthotropic material.

One can identify, in a plane (σ_N, τ) a curve that limits a high probability failure area and a low probability failure area (Fig. 47).

The scattering observed in these tests is important.

In most cases the failure in the propellant occurs in the vicinity of the bonding plane.

The tensile stress specimen used to characterize the bonds (Fig. 46) is not a monodimensional specimen. The maximum stress obtained at the failure of the specimen, in the propellant, in the vicinity of the bonding plane, is lower than the maximum stress obtained on propellant alone from a monodimensional specimen. A tensile test performed on propellant alone with a cubic specimen used for bonding is sufficient to verify the influence of the geometry of the specimen.

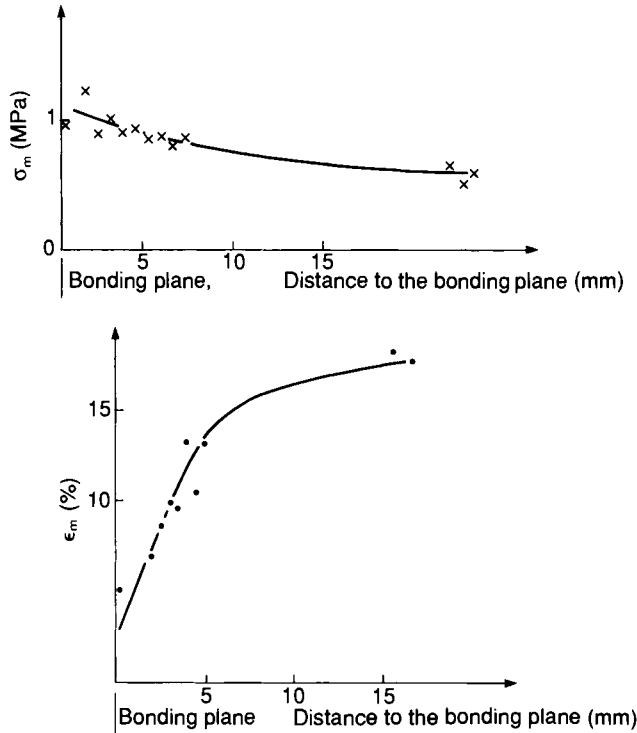


FIG. 6.45. Evolution of σ_m and ϵ_m in the vicinity of the bonding plane.

4.3.4. Propagation of the debondings; peeling

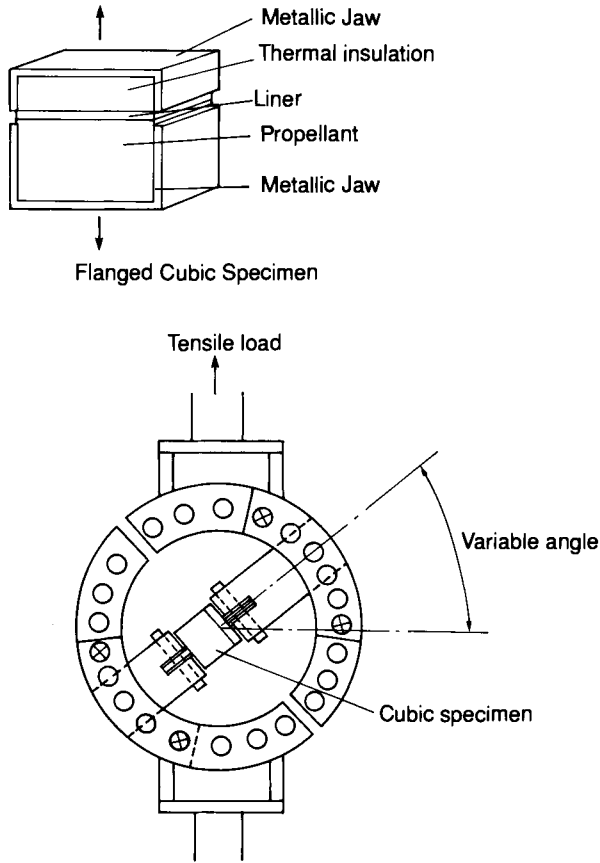
The characterization of the ability of an initial debonding to propagate is determined by performing a peeling test. This test is described in Fig. 48. This test is used to categorize, for various liner-propellant assemblies, the force necessary for the debonding to propagate itself, for a given loading rate. The greater the peeling force versus the width of the specimen, the better the structural integrity of the specimen will be, all other things being equal.

As the debonding propagates itself in the propellant, the results of tearing in the corresponding propellant can be used to perform a qualitative correlation.

5. Determination of the Induced Stress-Strain (Requirement)

5.1. BRIEF BACKGROUND

The determination of the stress existing in a propellant grain subjected to a mechanical load is vital to assess the safety coefficient of this propellant grain.

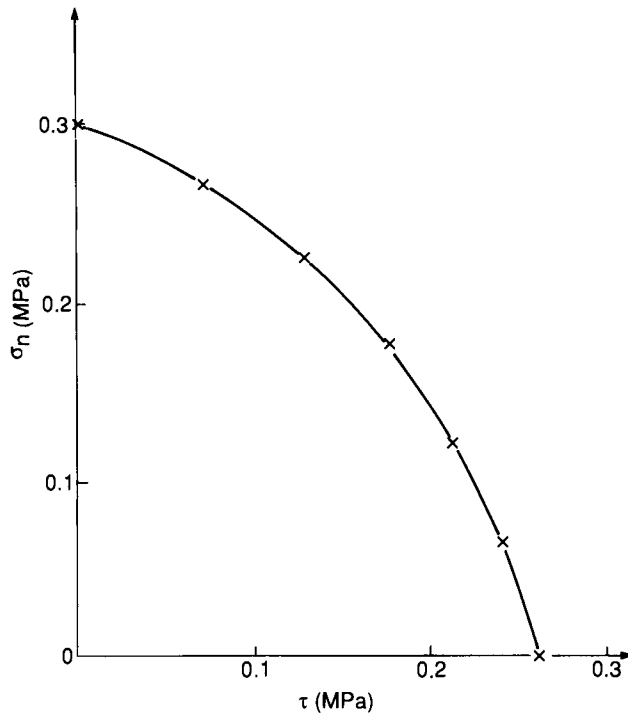


Device used to determine the failure criterion

FIG. 6.46. Specimens for bonding tests.

This problem has always been, and continues to be, a constant source of concern. The methods used to resolve it change with the discovery of new technology.

Until the 1960s experimental methods were widely used. Then, with the progress made by numerical methods and computers, numerical analysis became the preferred method. Currently, they are the primary tool, and their use has modified considerably the steps followed to analyze propellant grains. Experimental methods did not allow the analysis of geometries that were too complex. These geometries were the results of the experience — often very extensive — of the designers, but the optimization from the point of view of structural integrity was not always possible (because the experimental methods used were very cumbersome). Computerized methods allow us, on

FIG. 6.47. Failure criterion (σ_n , τ).

the contrary, to analyze a great number of geometries and to select the one geometry that is best suited to solve the problem at hand. The experimental methods are, nevertheless, still used and developed parallel to the computerized methods to validate experimentally the theoretical analyses.

5.2. THE EXPERIMENTAL METHODS

When a direct measurement of stress/strain in a propellant grain is used, it usually involves measurements of strains. The analysis of stresses is more difficult because the gages are for the most part larger and can mechanically disturb the environment where they are implanted.

The indirect method most widely used to perform indirect measurements is photoelasticimetry [5]. This allows an experimental determination of the stress. Some transparent materials have the characteristic of becoming birefracting when subjected to a stress field. Polyurethane and some of the epoxy resins have that property. When specimens made of these materials are subjected to a mechanical loading, interference fringes are revealed when the specimens are placed between two polarizing and analyzing filters in the path of a light ray. These fringes are caused by the existence of stresses in the

Sketch of the testing equipment

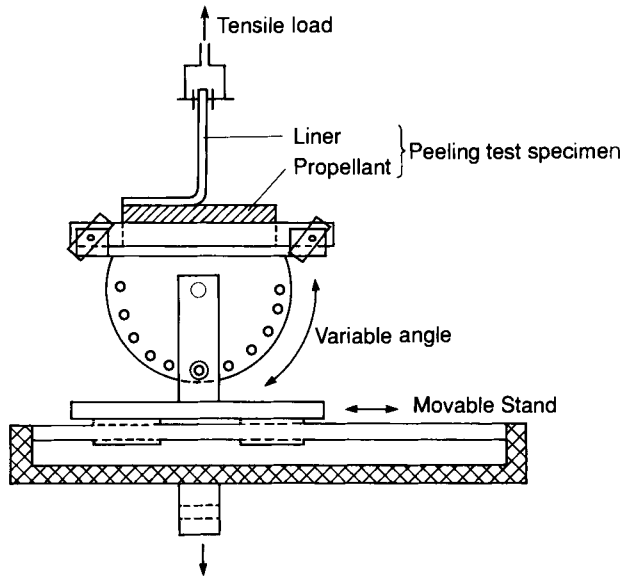


FIG. 6.48. Peeling test.

sample under study. This method consists of preparing samples made of resin shaped like the propellant grain or the portion of the propellant grain under analysis. Reduced scale may possibly be used. A mechanical load is applied to the sample to obtain stresses identical to those present in the propellant grain.

The stress state modifies the optical properties of the sample; these properties are frozen in that particular state by the appropriate thermal cycle. After this, thin slices are cut—they have kept their birefracting state corresponding to the mechanical stress field—and analyzed with a two-dimensional method.

The main difficulties encountered with this method are to obtain the proper geometry and to apply the stress conditions within realistic boundary limits. Moreover, the analysis of the stress field is performed in a material that typically exhibits an incompressible linear elastic behavior.

5.3. NUMERICAL METHODS

The subject discussed in this section has been by itself the object of a tremendous number of studies for many years. Today, a significant number of studies continue to be performed. It is therefore not necessary to provide here a detailed description of numerical methods, since there is a large quantity of

good-quality literature on the subject. Their practical use is discussed in Chapter 2. Only special aspects of the structural integrity analysis of propellant grains are listed below.

All mechanical analyses are defined by (Fig. 1):

- a precise description of the geometry to which the mechanical load is applied;
- the boundary conditions depicting the loading conditions;
- the mechanical behavior law of the materials.

The geometry involved in propellant grain is three-dimensional; the mechanical loads applied are static, dynamic, and with or without thermal effects, and the behavior laws are non-linear viscoelastic.

Dealing with the mechanical analysis involves resolving the conservation equations (of the mass, the energy, and the volume for an incompressible material) and the equilibrium equations of the forces and the vectorial moments, taking into account the boundary conditions applied. All of these equations are expressed, in the end, in differential equations for the displacements. The numerical method used is the finite element method. Without going into great details about this method, the subject of an abundant specialized literature ([6] and [7] among many others), the principle may be succinctly described as follows:

The geometry is decomposed into a finite number of small areas (called finite elements) where the function to be determined (the displacement field) is expressed by a function of the coordinates of the points of the areas. This function is usually a polynomial of the first or second degree.

When dealing with propellant grains there is the additional problem of incompressibility. Let us consider the formulation expressed by equations (4)

$$\begin{cases} \sigma'_{ij} = 2G\epsilon'_{ij} \\ \bar{\sigma} = 3K\bar{\epsilon} \end{cases}$$

The volume conservation equation (incompressibility assumption) in the case of infinitesimal deformations is expressed by $\bar{\epsilon} = 0$.

Consequently, the mechanical problem is solvable only to determine the deviatoric tensor, the average stress is indeterminate. There have been a number of methods proposed to determine the average stress. Some iterative methods do not give satisfaction in all cases studied. There is, however, one method particularly well suited for structural analysis of propellant grains. This was developed by Herrmann [20] and consists of assuming the average stress $\bar{\sigma}$ to be an unknown in the problem. There are therefore two types of unknown to determine: displacement unknowns and average stress $\bar{\sigma}$ unknowns.

With the finite element method, the structural analysis is generally performed with linear behaviors of the propellant. The methods that include nonlinear behaviors take an inordinate amount of time for the calculations. In Section 2, however, the description of the mechanical loads imposed on

propellant grains shows that, in the worst conditions (temperature changes and pressurization at firing) and because the propellant is an incompressible material, the strain field in the propellant depends little on the mechanical behavior law. Consequently, the analysis can be performed in the following manner (Fig. 49):

1. calculations are done using the linear and incompressible behavior law to determine the strain field;
2. at the point where the elongation is the greatest, the stress tensor is recalculated, using a behavior law that is more representative for the propellant.

Nowadays, the finite-element computer programs that allow a correct handling of the problems of propellant linear behavior are the programs that have the following characteristics:

- programs dealing with the propellant incompressibility with the Herrmann method;
- types of solid elements:
 - in two-dimensional, elements with eight nodes with the Herrmann formula;
 - in three-dimensional, elements with 20 nodes with Herrmann formula;
 - skin elements to determine stress tensor at free surface.

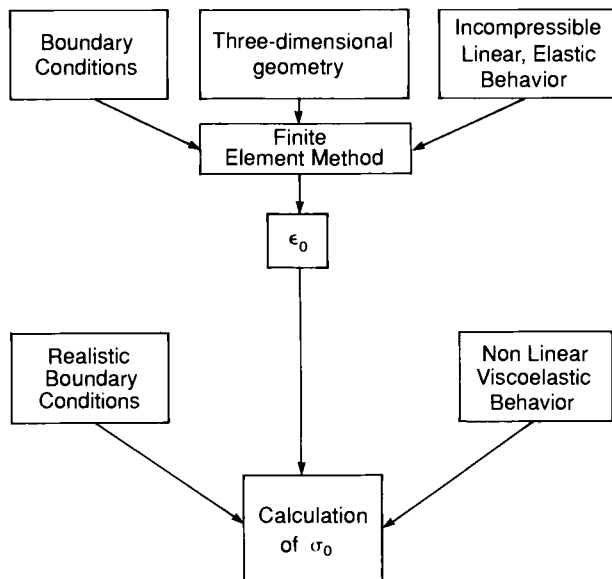


FIG. 6.49. Calculation of the induced load for a non-linear viscoelastic behavior.

The quality of a computer program depends on the structural analysis itself, but also, and most particularly, on the quality of the tools used to prepare and analyze the calculations. These tools are called pre- and post-processors. There is no particular interest in describing these tools here, except for saying that they are extremely useful. They have a great value for a rapid implementation and rational utilization of computer programs for mechanical analysis. The level of professionalism of the designers is often dependent on the quality of these tools.

Figures 50 to 54 provide a summary of the possibilities offered by these analysis methods, without which today's advanced mechanical analysis could not be done.

5.4. SIMPLIFIED ANALYTICAL METHODS

For preliminary design analysis, analytical methods are useful when the geometry of the propellant grains can be likened to a specific one-dimensional geometry: the infinite-length hollow cylinder.

The stress/strain and displacements are expressed in a cylindrical coordinates reference system (r, θ, z). The mechanical state of a cylinder under a specific mechanical load is described by 15 quantities.

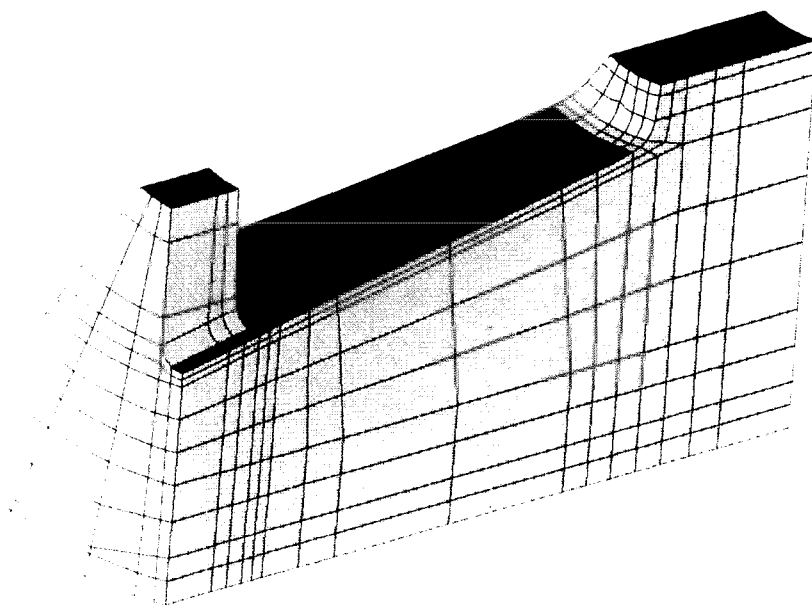


FIG. 6.50. Determination of the induced load. Three-dimensional mesh I.

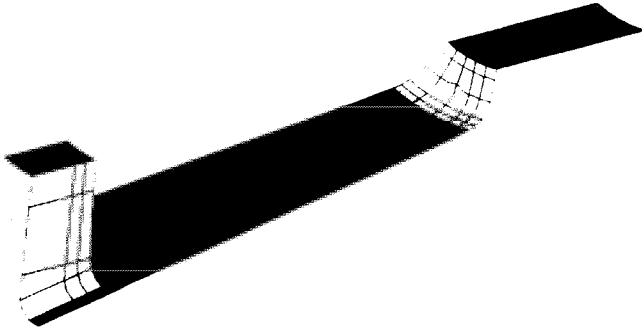


FIG. 6.51. Three-dimensional mesh II. (Skin elements.)

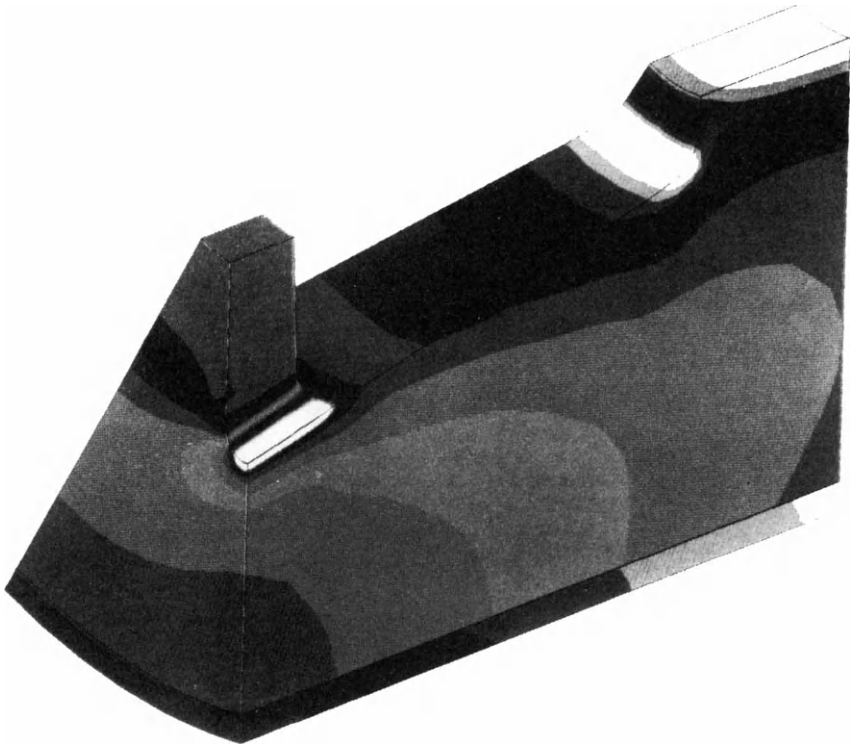


FIG. 6.52. Iso-stresses I. (On skin elements.)

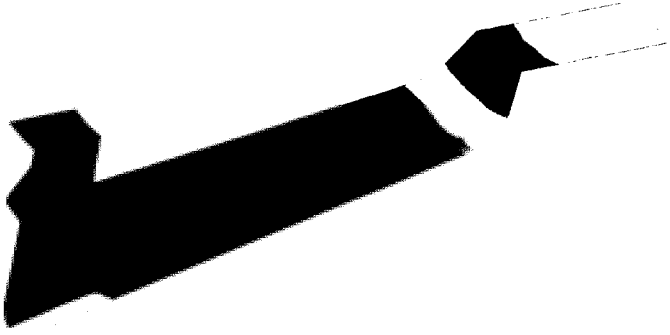


FIG. 6.53. Iso-stresses II. (On a section plane.)

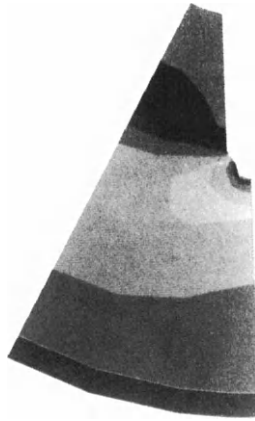


FIG. 6.54. Iso-stresses III.

- six stress components: σ_{rr} , $\sigma_{\theta\theta}$, σ_{zz} , $\sigma_{r\theta}$, σ_{rz} , $\sigma_{\theta z}$
- six strain components: ε_{rr} , $\varepsilon_{\theta\theta}$, ε_{zz} , $\varepsilon_{r\theta}$, ε_{rz} , $\varepsilon_{\theta z}$
- three displacement components: u_r , u_θ , u_z

In an infinite-length cylinder, the displacement at each point is expressed by only one component u_r ; it is a plane strain assumption:

$$u_\theta = 0, u_z = 0 \text{ and } u_r = u_r(r)$$

$$\Rightarrow \varepsilon_z = 0, \varepsilon_r = \frac{\partial u_r}{\partial r}, \varepsilon_\theta = \frac{u_r}{r}$$

and for axisymmetric boundary conditions:

$$\varepsilon_{r\theta} = \varepsilon_{\theta z} = \varepsilon_{rz} = 0$$

$$\sigma_{r\theta} = \sigma_{\theta z} = \sigma_{rz} = 0$$

When the material is assumed to be incompressible, Hooke's thermoelastic law is written as:

$$\begin{aligned}\varepsilon_{rr} &= \frac{3}{4E} (\sigma_{rr} - \sigma_{\theta\theta}) + \frac{3}{2} \alpha \Delta T \\ \varepsilon_{\theta\theta} &= \frac{3}{4E} (\sigma_{\theta\theta} - \sigma_{rr}) + \frac{3}{2} \alpha \Delta T\end{aligned}\quad (26)$$

where:

E = Young's modulus;

α = linear thermal expansion coefficient of the material;

$\Delta T = T - T_0$;

T = temperature at which the stress occurs;

T_0 = equilibrium temperature (at which stress is zero).

The equation of equilibrium is written:

$$\frac{\partial \sigma_{rr}}{\partial r} = \frac{\sigma_{\theta\theta} - \sigma_{rr}}{r} \quad (27)$$

and the strain-displacement relation

$$\frac{\partial \varepsilon_{\theta\theta}}{\partial r} = \frac{\varepsilon_{rr} - \varepsilon_{\theta\theta}}{r} \quad (28)$$

From eqns (26), (27) and (28), we can write:

$$\frac{3}{4E} \frac{\partial (\sigma_{\theta\theta} - \sigma_{rr})}{\partial r} + (\sigma_{\theta\theta} - \sigma_{rr}) \left[\frac{3}{4} E \frac{\partial (1/E)}{\partial r} + \frac{3}{2E} \frac{1}{r} \right] + \frac{3}{2} E \frac{\partial \alpha \Delta T}{\partial r} = 0 \quad (29)$$

For a hollow circular cylinder with

a : inside radius

b : outside radius

the general solution is written:

$$\sigma_{rr}(r) = \int_a^r -\frac{2E}{r^3} F(r) dr + F(a) \int_a^r -\frac{2E}{r^3} dr + \zeta_1 \int_a^r \frac{E}{r^3} dr + \zeta_2 \quad (30)$$

$$\sigma_{\theta\theta}(r) = -\frac{2E}{r^2} \int_a^r r^2 \frac{\partial \alpha \Delta T}{\partial r} dr + \zeta_1 \frac{E}{r^2} + \sigma_{rr}(r) \quad (31)$$

ζ_1 and ζ_2 are integration constants determined by the boundary conditions.

$F(r)$ is the primitive of $r^2 (\partial \alpha \Delta T / \partial r)$.

When the temperature is uniform and the modulus constant in the entire geometry, the general solution will be:

$$\sigma_{rr}(r) = C_1 - \frac{C_2}{r^2} \quad (32)$$

$$\sigma_{\theta\theta}(r) = C_1 + \frac{C_2}{r^2} \quad (33)$$

C_1 and C_2 are determined by the boundary conditions.

5.4.1. *Uniform thermal shrinkage in a case-bonded cylinder*

When the propellant is bonded to an non-deformable, rigid motor case, with a very small linear thermal expansion coefficient when compared to that of the propellant, the boundary conditions will be expressed by:

$\sigma_{rr}(a) = 0$, because the inside surface of the cylinder is a free surface;
 $u_r(b) = 0$, $\varepsilon_{\theta\theta}(b) = 0$, because there is no displacement of the propellant points bonded to the case.

Consequently:

$$\begin{cases} \sigma_{rr}(r) = E \frac{b^2}{a^2} \alpha \Delta T \left(1 - \frac{a^2}{r^2} \right) \\ \sigma_{\theta\theta}(r) = E \frac{b^2}{a^2} \alpha \Delta T \left(1 + \frac{a^2}{r^2} \right) \\ \varepsilon_{\theta\theta}(r) = -\frac{3}{2} \alpha \Delta T \left(\frac{b^2}{r^2} - 1 \right) \end{cases} \quad (34)$$

- The circumferential strain $\varepsilon_{\theta\theta}$ is maximum in the central port at $r = a$.

$$\varepsilon_{\theta\theta}(a) = -\frac{3}{2} \alpha \Delta T \left(\frac{b^2}{a^2} - 1 \right)$$

- The normal stress σ_{rr} is maximum at the propellant/case bonding at $r = b$.

$$\sigma_{rr}(b) = -E \alpha \Delta T \left(\frac{b^2}{a^2} - 1 \right)$$

With this type of geometry and a mechanical load corresponding to a uniform thermal shrinkage, strains are independent of the propellant Young's modulus and stresses are directly proportional to that modulus. Stress at the free surface and at the bonding, in addition, is dependent on b^2/a^2 . The

volumetric loading fraction expressed by the ratio b^2/a^2 , will have an important effect on the stress.

Propellant grains have a finite length. There are corrective factors [27] allowing the determination of the stress tensor in a finite-length circular cylinder. These factors are given in diagrams (Parr diagrams).

All stresses/strains for this type of mechanical load are proportional to the $\alpha\Delta T$ product. That is why α , the linear thermal expansion coefficient of the propellant, must be well determined.

5.4.2. *Internal pressure p on a case-bonded cylinder*

When the motor case in which the propellant grain is located is a thin one, the boundary conditions are written as:

$$\alpha\Delta T = 0$$

$$\sigma_{rr}(a) = -p$$

$$\varepsilon_{\theta\theta}(b) = -k\sigma_{rr}(b)$$

where k is the flexibility coefficient of the case

$$k = \frac{(1 - \nu_c^2)b}{E_c \cdot h}$$

ν_c = Poisson's ratio of the motor case;

E_c = Young's modulus of the motor case;

h = thickness of the motor case.

For a motor case showing little deformation (k is very small), simplifications allow us to obtain:

$$\begin{cases} \varepsilon_{\theta\theta}(r) = -\varepsilon_{rr}(r) = kp \frac{b^2}{r^2} \\ \sigma_{rr}(r) = \frac{2}{3} kpE \left(\frac{b^2}{a^2} - \frac{b^2}{r^2} \right) - p \\ \sigma_{\theta\theta}(r) = \frac{2}{3} kpE \left(\frac{b^2}{a^2} + \frac{b^2}{r^2} \right) - p \end{cases} \quad (35)$$

As with the thermal load, strains are independent of the propellant Young's modulus, and stresses are proportional to that modulus. The loading ratio, when it grows, increases the level of the stresses in the propellant. Finally, the induced stress/strain depends greatly on the flexibility coefficient of the motor case. The smaller the flexibility coefficient, and consequently the higher the Young's modulus of the motor case, the lower the induced stress/strain will be.

5.5. COMMENTS ON THE NECESSITY OF INCOMPRESSIBLE ANALYSES

The mechanical analysis of incompressible materials involves a discontinuity which is expressed with a special formula. A material is considered incompressible when it sustains a deformation while maintaining its constant volume under the effect of applied mechanical load. Based on this definition, the particularity of the incompressibility characteristic does not seem evident. But a deformation under constant volume implies that the material has been provided with a shape that allows such a deformation. The amount of free surface has a determining impact on the rigidity of the object. For example: a viscous liquid has no rigidity; a flexible polyethylene bottle has a low rigidity when it is empty. When that same bottle is completely filled with viscous liquid, the combination exhibits a rigidity under pressure that allows an integral transmission of loads. This is the basic principle which allows hydraulic systems to transmit significant energy quantities.

Incompressible materials are, therefore, sensitive to confinement, which can be defined by the ratio of the volume of the object versus the surfaces free to sustain deformation. An infinite confinement corresponds to an infinite rigidity of the object. This is the meaning of the discontinuity mentioned at the beginning of this section.

- What is the effect of incompressible behavior on the equations?

Based on eqns (1) and (4), assuming infinitesimal deformations, constant volume deformations imply the following relation:

$$\frac{\Delta V}{V_0} = \sum_{i=1}^3 \varepsilon_{ii} = 0$$

which, in terms of the behavior parameters, is expressed by:

$$\nu = 0.5 \text{ or } K \rightarrow \infty \text{ as } \frac{G}{K} \rightarrow 0$$

therefore the stress deviator is determined directly by the existing strain field, but the average stress is mathematically undeterminate.

$$\bar{\sigma} = K e \text{ with } K \rightarrow \infty_{e=0}$$

This average stress is determined physically by the geometry and the confinement.

- In fact, the measurement of the bulk modulus of a propellant gives a finite value; this value is very high in comparison with the value of the shear modulus. It is that significant difference between the compressibility modulus and the shear modulus that confers the incompressible property to propellants.
- What is the behavior of a propellant in the shape of a grain?

Consideration of the incompressibility is of concern only with case-bonded propellant grains. Typically, this type of propellant grain has a higher volumetric loading fraction. All of the propellant surfaces are bonded to the motor case; the only free surfaces are those in the combustion chamber. The higher the volumetric loading fraction, the greater the confinement of the propellant will be.

In general, stresses induced by thermal shrinkage and by pressure rise at the beginning of firing are the most severe.

The average level of strain is often lower than the strain at which vacuum holes occur (i.e. at which the propellant becomes compressible).

Only a small volume of the propellant has a significant strain level, making it compressible. This low volume of compressible propellant (with vacuum holes) does not modify the incompressible behavior of the major portion of the propellant. Simple calculations (Fig. 55) show that because the volume of propellant with vacuum holes is low, the maximum induced stress/strain can be determined by assuming that the entire propellant is incompressible. This is particularly applicable to the stress/strain induced by thermal shrinkage; at the time of firing, the behavior of propellant under pressure likens it to an incompressible material, whatever the level of applied load.

It is therefore necessary to take into account the incompressible nature of the propellant to evaluate induced stress/strain in case-bonded grains, and it is the determination of average stress at each point which allows an accurate mechanical analysis. The average stress is not dependent on the propellant behavior, and a mechanical analysis taking into consideration the incompressible elastic linear behavior of the propellant is sufficient. The viscoelastic properties may be introduced to calculate the stress deviators.

Some calculations based on a simple geometry allow us to summarize the importance of incompressibility.

The geometry used is an infinite length cylinder with an inner diameter of 100 mm and an outer diameter of 400 mm. A temperature change of -100°C is induced. The external surface of the cylinder is bonded to a rigid, non-deformable case. The calculations are done with a finite element program including Herrmann's formulation to treat incompressible behavior. This program also includes classic elements, allowing it to process compressible materials. In addition, the elements with the Herrmann formula allow the processing of materials with any Poisson's ratio, including $\nu = 0.5$.

First analysis. The impact of Poisson's ratio on the infinite-length cylinder is indicated in Fig. 56.

The induced stress is represented by an equivalent stress (Stassi stress), which takes the average stress into account; it is at a maximum on the free surface and is heavily dependent on the value of Poisson's ratio (Fig. 57).

Second analysis. The propellant is considered to be very compressible (Poisson's ratio equal to 0.33), and the analysis is done with two types of element: the classic element and the Herrmann formula element. The results,

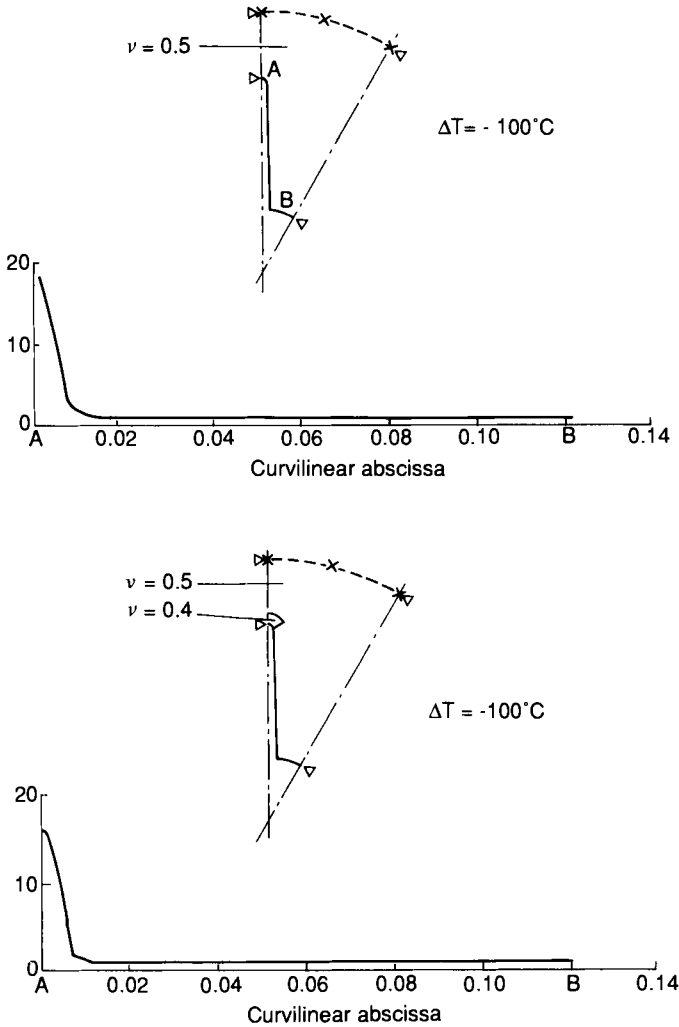


FIG. 6.55. Calculation without and with compressible volume. (Plane strain assumption.)

when compared to the analytical solution, reveal a high level of correspondence between the numerical analysis and the analytical solution (Fig. 58).

Third analysis. Finally, a third analysis is performed, for propellants exhibiting a low compressibility ($\nu = 0.495$).

A low-compressibility element can be analyzed with a classic element. The results listed in Fig. 59 show good agreement between the analytical solution

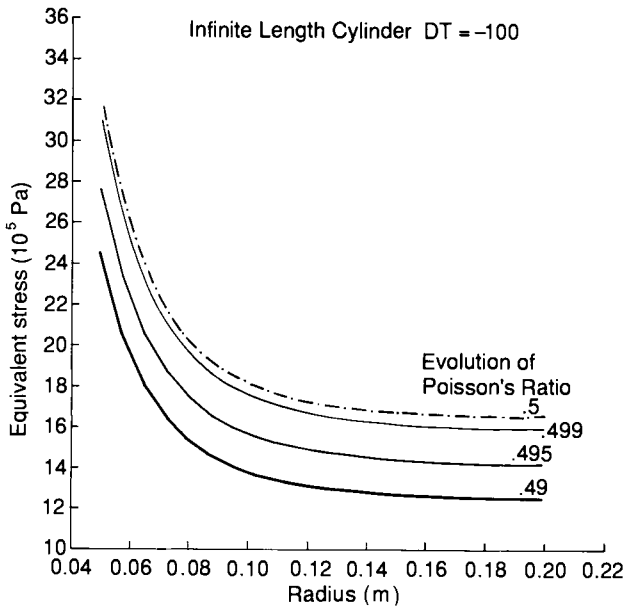


FIG. 6.56. Influence of Poisson's ratio on the equivalent stress.

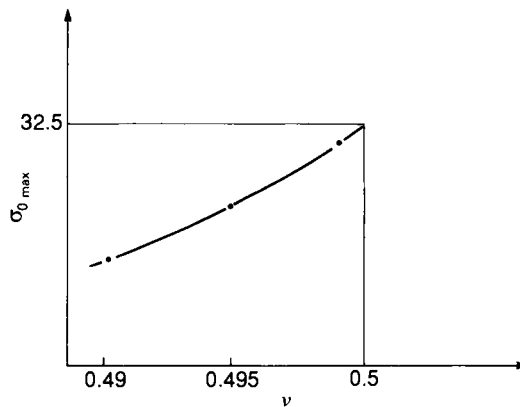


FIG. 6.57. Influence of Poisson's ratio on the equivalent stress on the free surface.

and the analysis done with the Herrmann's formulation. Results obtained with the classic elements are completely erroneous.

The Von-Mises stress, which depends solely on the stress deviators and not at all on the average stress, is analyzed with two types of elements:

- the classical element formulated in displacement;
- the Herrmann formula element.

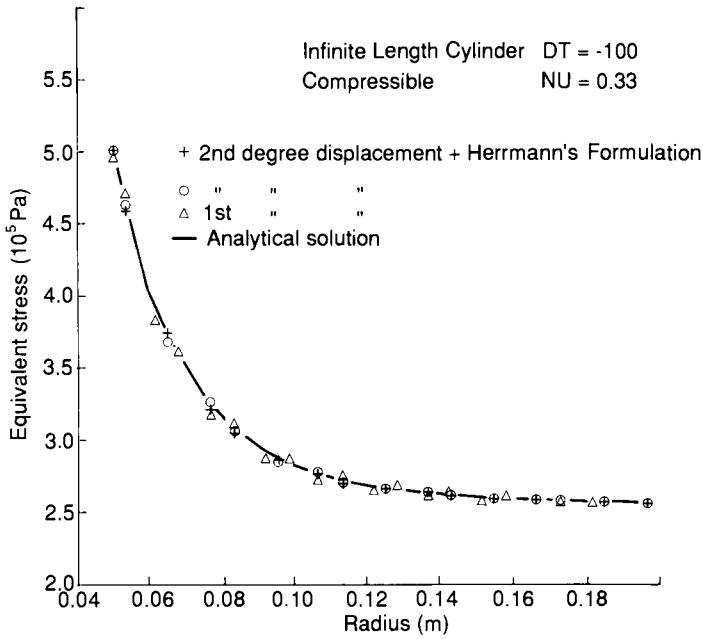


FIG. 6.58. Comparison of Herrmann's formulation and classical formulation applied to a compressible material.

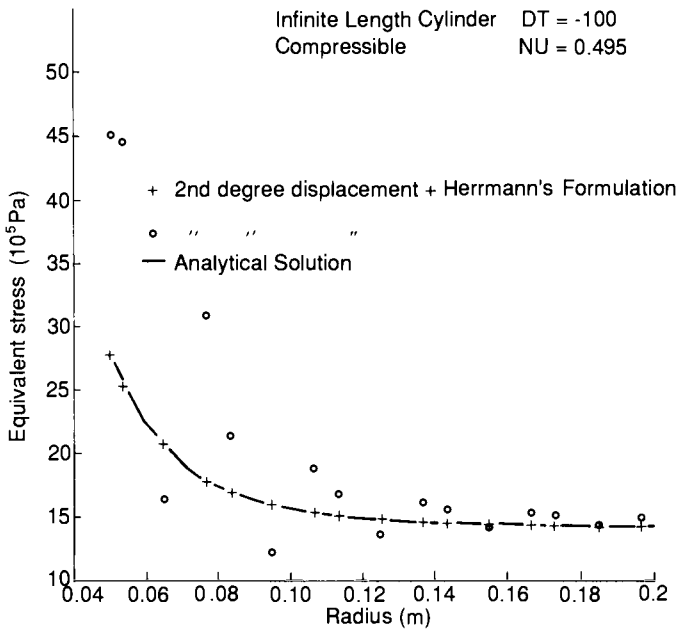


FIG. 6.59. Comparison between Herrmann's formulation and classical formulation applied to a quasi incompressible material.

The good agreement between both numerical analysis and analytical solution (Fig. 60) demonstrates that correctly solving an incompressible problem consists in determining the average stress at each point.

6. Determination of the Factor of Safety

Following the description in the preceding sections of the methods used to determine the capability and the induced stress/strain, the next logical step is the determination of the structural factor of safety:

$$K = \frac{C}{S}$$

In fact, the problem is really complex, because a propellant grain is subjected to very varied mechanical loads, and the cumulation of the corresponding induced stress/strain complicates the determination of a factor of safety. The capability of the propellant of a case-bonded grain which experiences temperature changes from 50°C to 20°C in a few days, which is then subjected to the force of gravity over a period of several months, and which finally is subjected at the time of firing to a pressure rise in a few milliseconds, is difficult to determine.

With a cumulation of mechanical stresses, the difficulty resides in the definition of the capability that should be taken into consideration. The

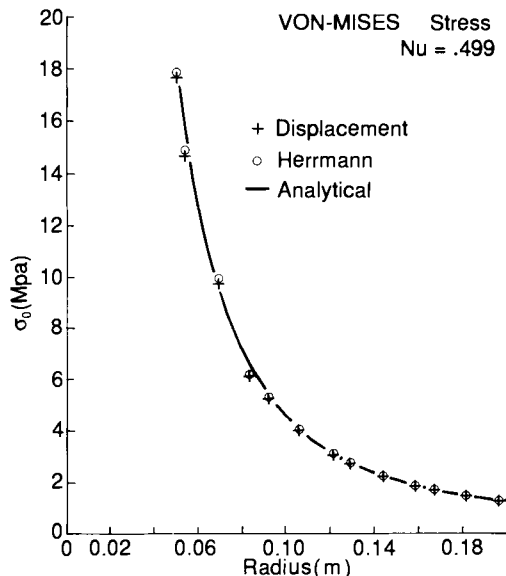


FIG. 6.60. Comparison of the deviatoric stresses obtained by the Herrmann's formulation and the classical formulation in a quasi incompressible material.

induced stresses/strains can be combined using the classic additivity laws (making sure that the components of the stress and strain tensors are added only when they are expressed in the same coordinates system).

One method used to assess the capability resulting from the cumulation of mechanical loads consists in submitting a propellant specimen to a succession of mechanical loads experienced by the propellant, under identical temperature, pressure, and loading rates. This highly experimental method does not always permit the determination of real operation conditions of a propellant, because it would require the use of very heavy and costly test facilities. A low-speed tensile stress, for example, applied while simultaneously varying the temperature, and followed by a rapid and progressive increase of pressure from 1 to 10 MPa, is not a simple operation to carry out!

Another method consists of defining the factor of safety of each of the basic mechanical loads, such as temperature changes, the force of gravity, the pressure rise at firing, and others, after which the resulting factor of safety will be a function of each basic factor of safety. Nevertheless, whatever the method used, the factor of safety calculated from stresses or strains must be equal to 1 at grain rupture and, similarly, the reliability calculated using each of the methods must be identical. It is therefore of prime importance to verify each of the methods on reduced-size objects subjected to various mechanical loads leading to failure.

The methods used to calculate the factors of safety are described below. Tests are performed on simple geometries to compare these methods, and eventually improve them. They are described at the end of this section.

6.1. FACTOR OF SAFETY OF PROPELLANT GRAINS

6.1.1. *Factor of safety in cumulative damage theory*

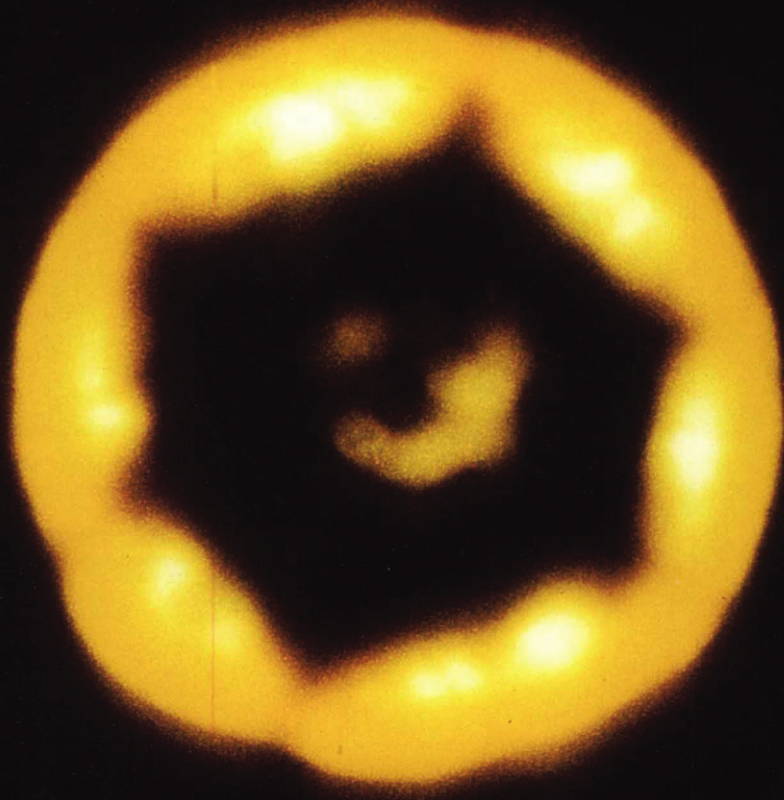
Damage, described in Section 4.2.7, characterizes the damage done to propellant during its useful life. By definition, it varies over time from 0 to 1:

- $\mathcal{D}(0) = 0$ Corresponds to sound propellant grain after its manufacture;
- $\mathcal{D}(t_R) = 1$ Corresponds to the failure of the propellant (failure time t_R).

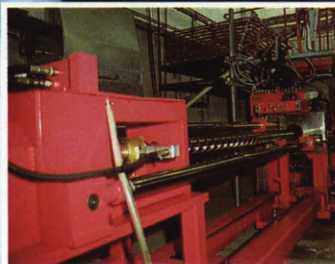
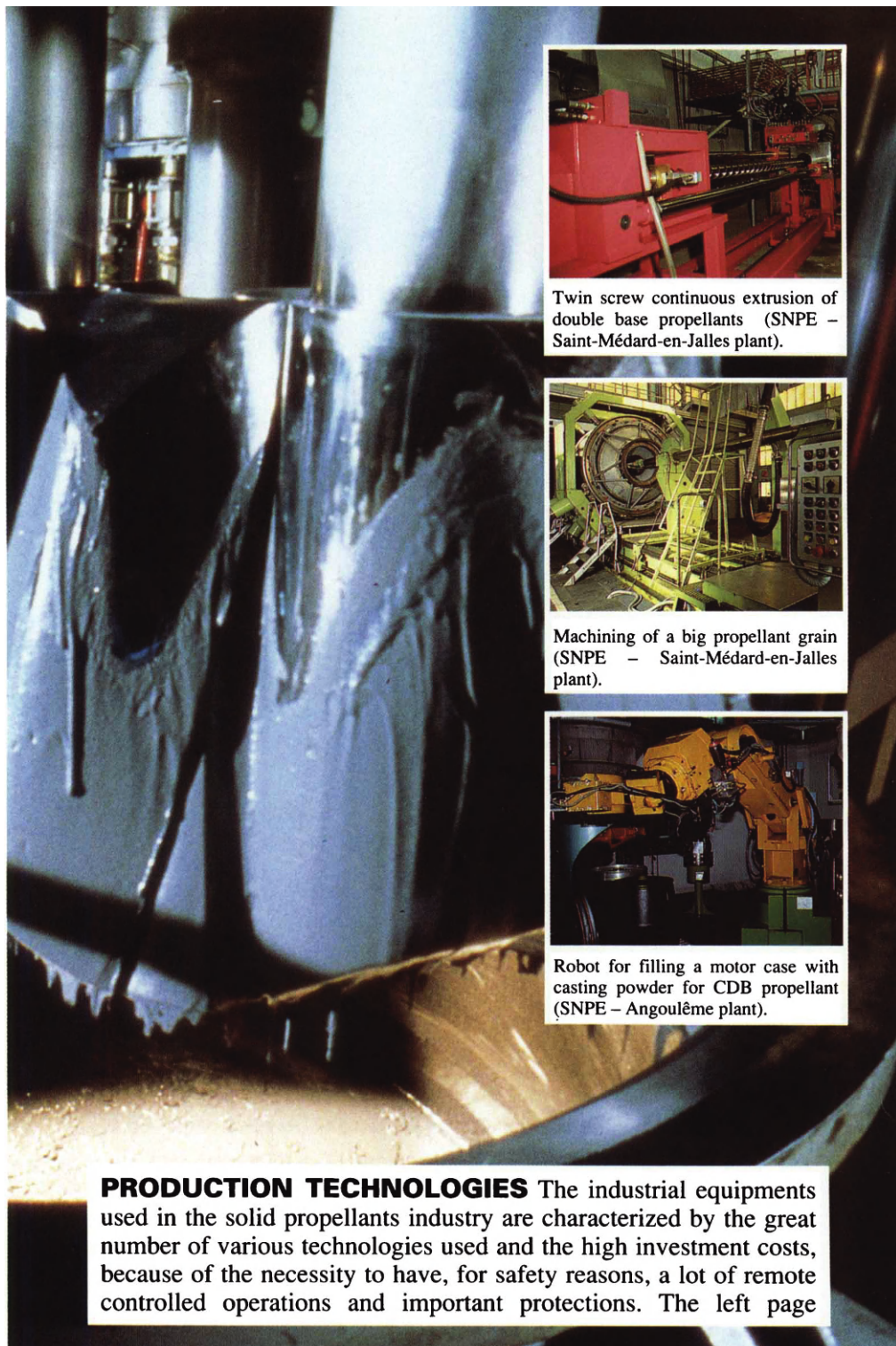
The factor of safety is simply deduced from damage $\mathcal{D}(t)$ using the relation

$$K_{\mathcal{D}}(t) = \frac{1}{\mathcal{D}(t)} \quad (36)$$

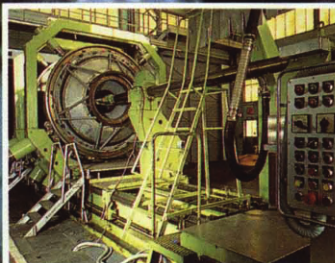
Defined in that manner, the factor of safety varies over time from infinity to 1.



Fundamental studies on propellants combustion requires sophisticated hardware because of the very extreme conditions of temperature, pressure, gas velocities existing in the combustion chambers of solid rocket motors. The photograph shows the observation of tangential acoustic instabilities – mode 3 – in the section of a star-shaped grain.



Twin screw continuous extrusion of double base propellants (SNPE – Saint-Médard-en-Jalles plant).

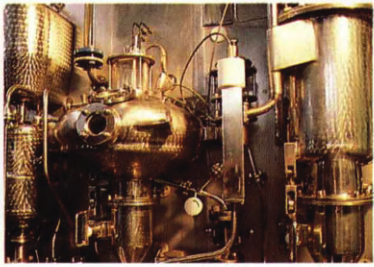


Machining of a big propellant grain (SNPE – Saint-Médard-en-Jalles plant).



Robot for filling a motor case with casting powder for CDB propellant (SNPE – Angoulême plant).

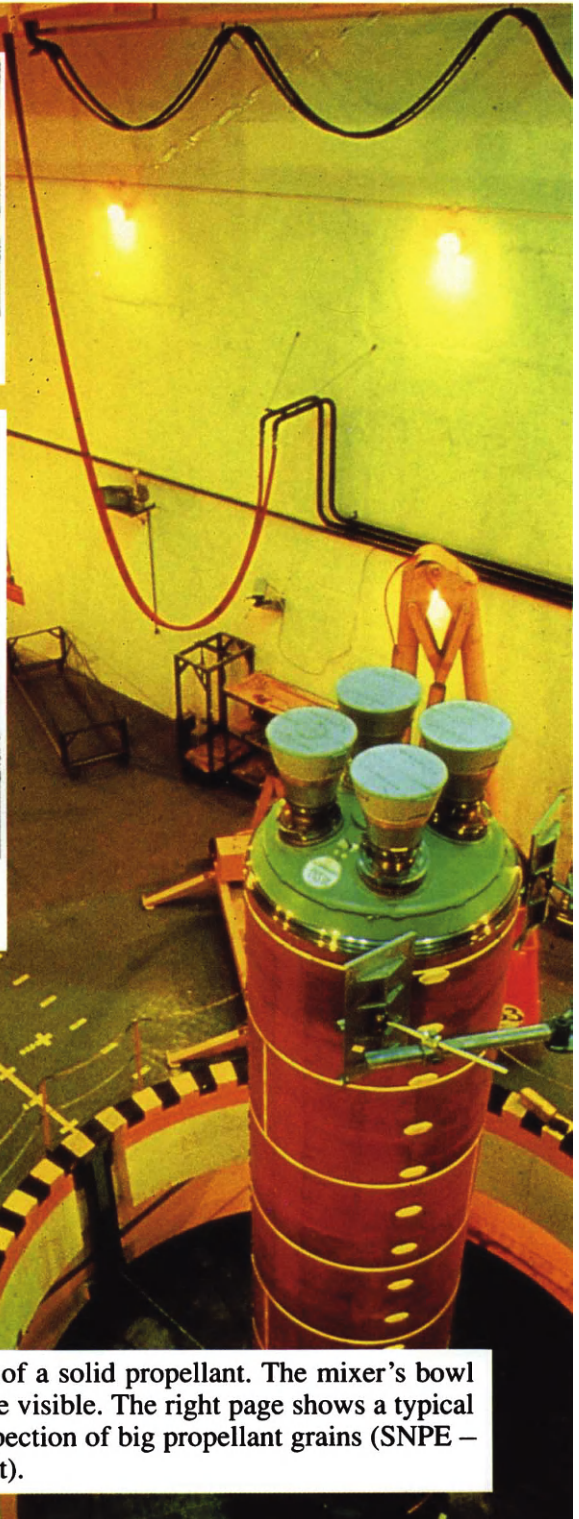
PRODUCTION TECHNOLOGIES The industrial equipments used in the solid propellants industry are characterized by the great number of various technologies used and the high investment costs, because of the necessity to have, for safety reasons, a lot of remote controlled operations and important protections. The left page



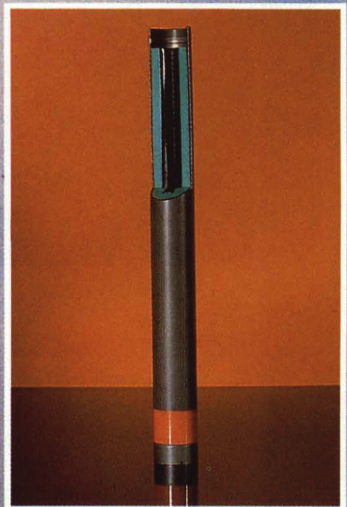
Nitric esters production plant (SNPE – Angoulême).




UDMH (unsymmetrical dimethyl hydrazine) production plant for Ariane Viking motors (SNPE – Toulouse plant).



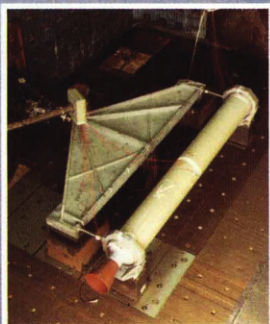
illustrates the batch mixing of a solid propellant. The mixer's bowl is lowered and the blades are visible. The right page shows a typical radiographic facility for inspection of big propellant grains (SNPE – Saint-Médard-en-Jalles plant).



Composite propellant case-bonded motor for an air to ground rocket.



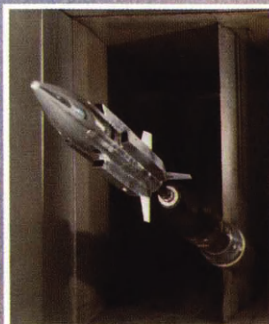
INNOVATION Constant requirements for the improvement of missiles and space boosters performances lead to the necessity of progress on every subsystem, and specifically on propulsion systems. While the very successful EXOCET antiship missile



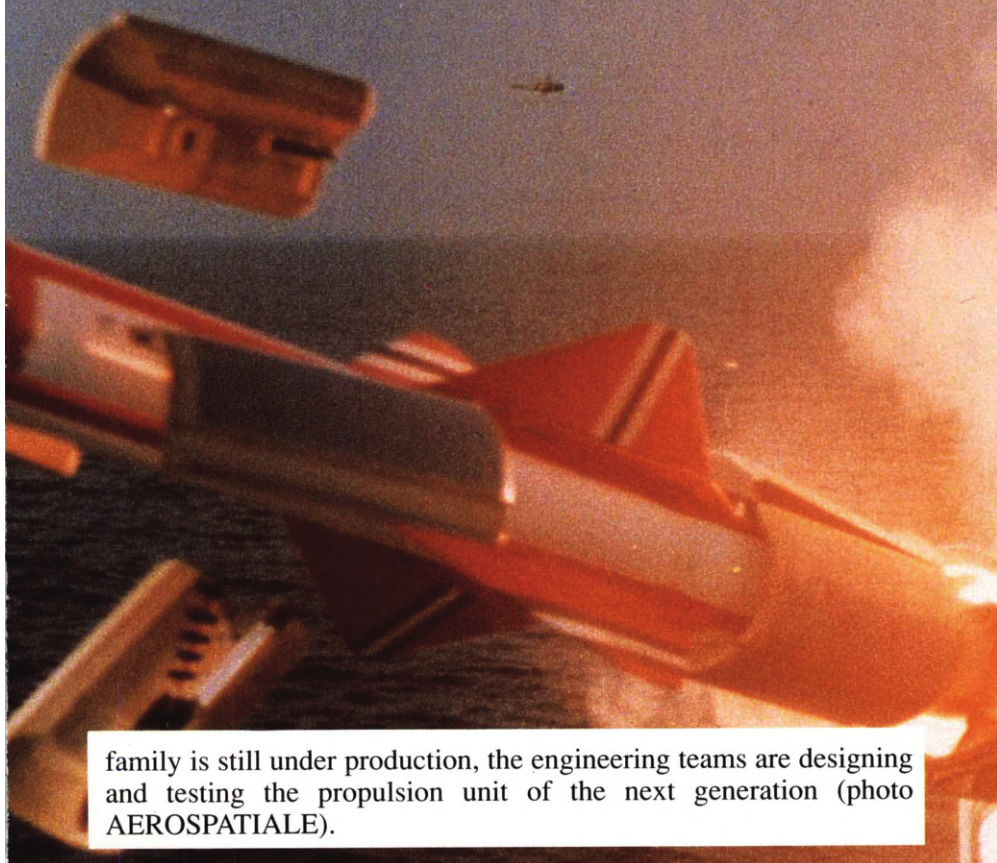
Vibration testing of a new ballistic missile motor.



Computer assisted design of static test hardware.

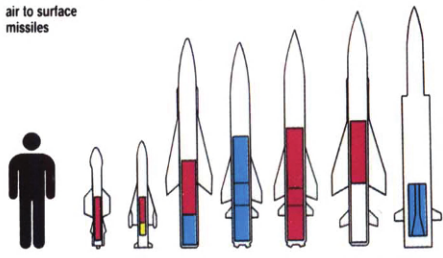
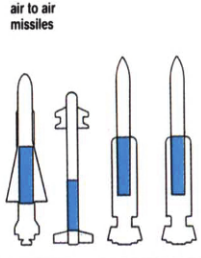
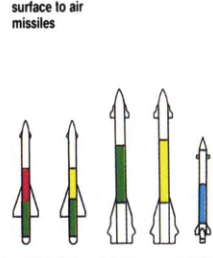
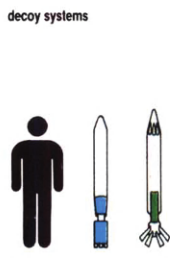
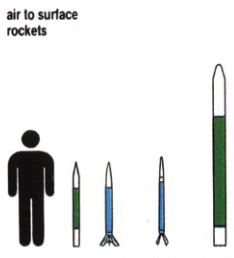
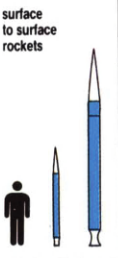


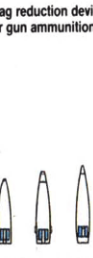

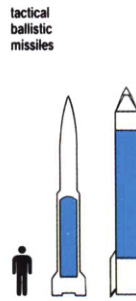

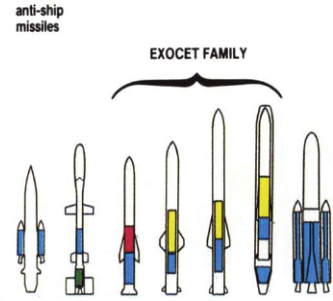

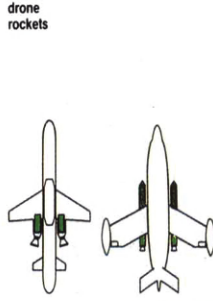


Wind tunnel testing of a model of a new antiship supersonic missile with integral booster and ramjet sustainer (photo ONERA).

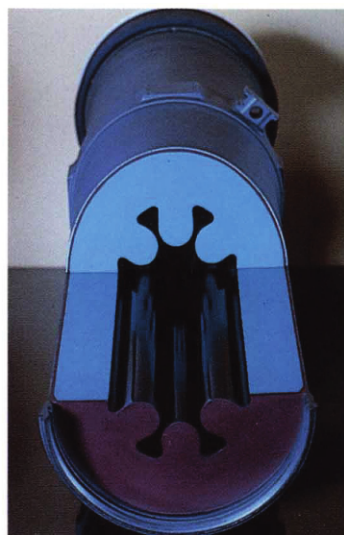
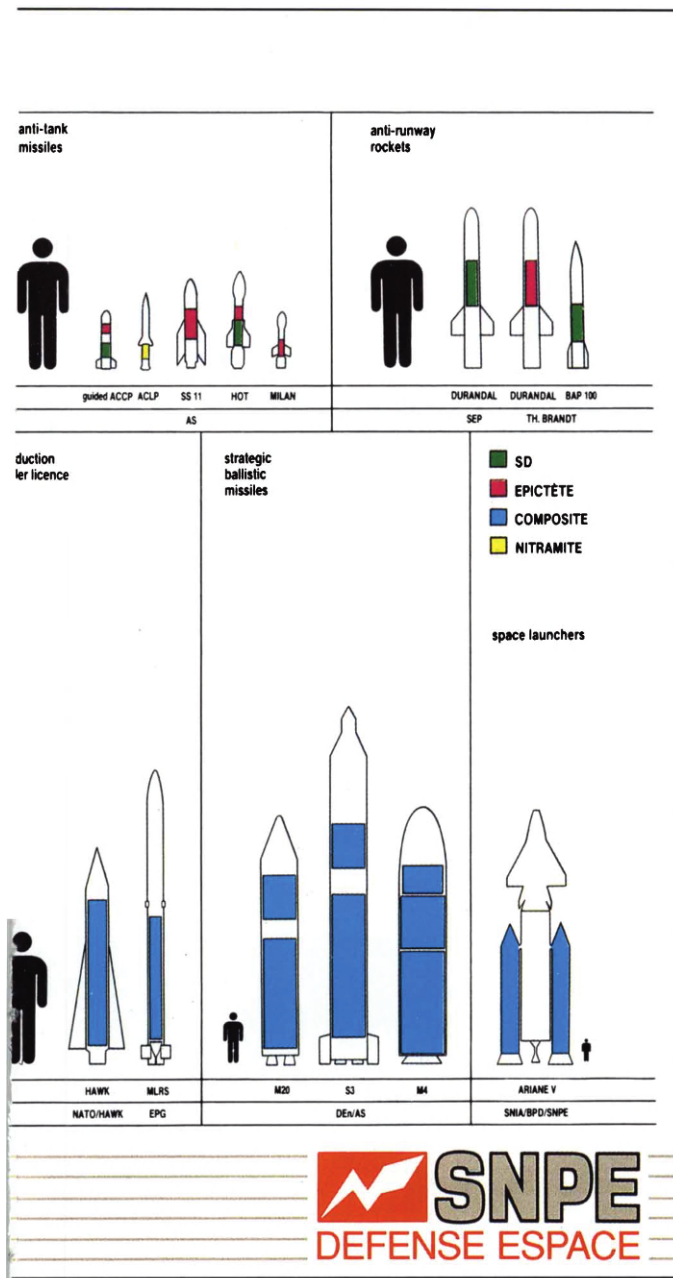


family is still under production, the engineering teams are designing and testing the propulsion unit of the next generation (photo AEROSPATIALE).

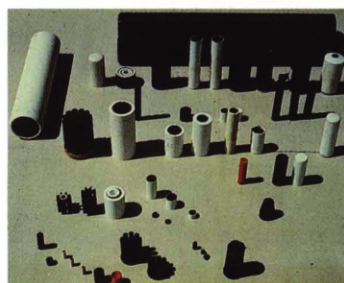
SNPE Production

air to surface missiles							air to air missiles				surface to air missiles					
																
name of weapon							R 530				ROLAND					
AS 12							R 550				ROLAND III					
AS 15 TT							SUPER 530				CROTALE					
AS 30 L							SUPER 530 D				SHAHINE					
MARTEL AR											SATCP					
MARTEL TV																
KORMORAN II																
ASMP																
contractor							MATRA				AS					
AS											TH-CSF					
											SEP					
decoy systems			air to surface rockets				surface to surface rockets		anti-tank rockets		additional propulsion for motors ammunitions		drag reduction device for gun ammunition		precision munitions	
																
name of weapon			68 mm				122 mm		APILAS		PRPA		130 mm		precision munitions	
SAGAIE			68 mm				310 mm		89 mm		PEPA LP		155 RTC		precision munitions	
SIBYL			70 mm										155 DTC		precision munitions	
contractor			TH BRANDT				SAKR		MMD		TH BRANDT		LUCHAIRE		precision munitions	
LACROIX			FORGES ZEEBRUGGE						LUCHAIRE/GIAT				GIAT		precision munitions	
			BRANDT												precision munitions	
tactical ballistic missiles			anti-submarine missile		EXOCET FAMILY						sea-air missile		drone rockets			
																
name of weapon			MALAFON		OTOMAT						MASURCA		C 22			
PLUTON					MARTE								CT 20			
HADES					MM38						DCN/EAN RUELLE		AS			
contractor			DCN		MATRA/OTOMELARATIS						AS		AS			
DEN/AS					SISTEL/SEP								DCN/AS			

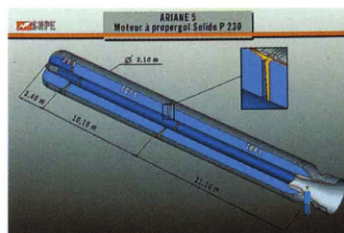
INDUSTRIALIZATION Solid propellant grains are designed according to requirements for various different missions. These designs use a great variety of shapes,. masses, dimensions and propellant formulations. This page illustrates the main propellant



Air to air missile motor.

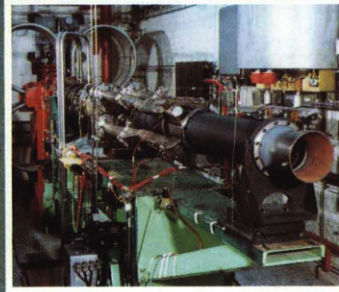


EDB solid propellant grains.

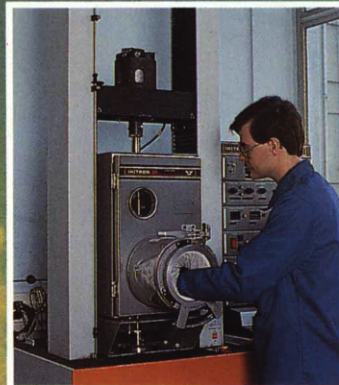


Internal view of a segmented space launcher booster.

grains under development and production at SNPE in 1988. The scale of propellant masses involved goes from a few grams (thrusters) to a few hundred tons (ARIANE 5 solid boosters).

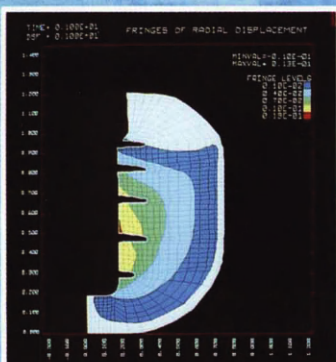


Static test hardware for a solid propellant ramrocket (photo ONERA).



Solid propellant mechanical behaviour testing at extreme temperatures.

SOPHISTICATION The methodologies, éqúipement, R and D work used in the solid propulsion industry have always used the higher performing technologies of the time... The importance and cost of its applications, the constant requirement for improved

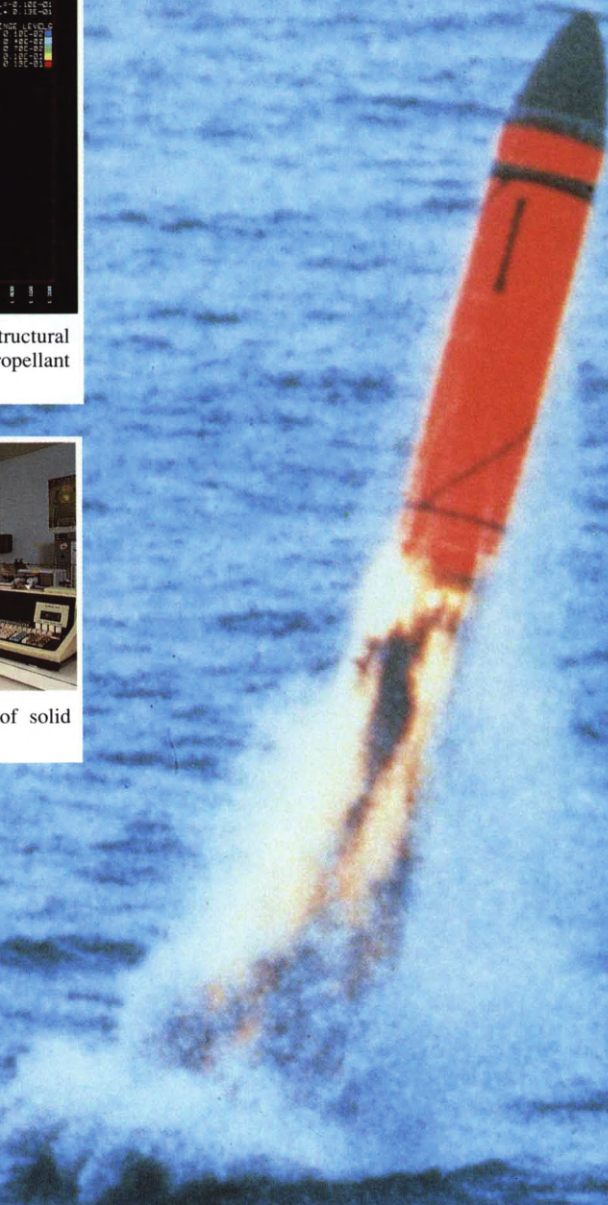


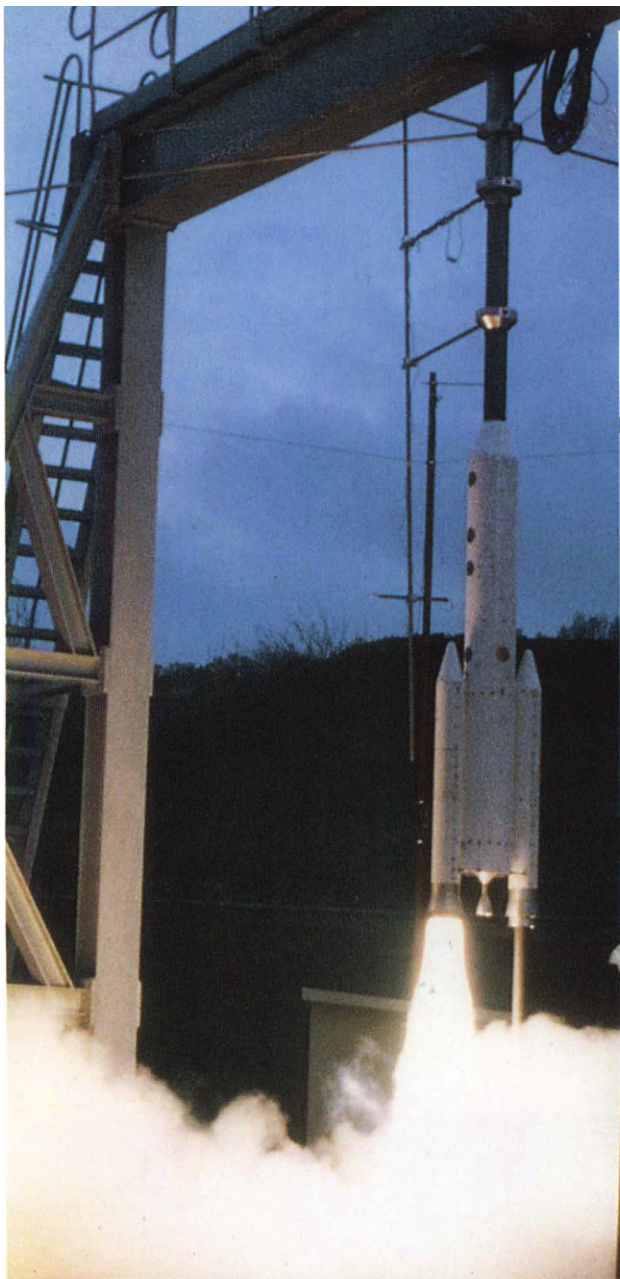
Graphic display of the structural analysis of a case-bonded propellant grain.



Physico chemical analysis of solid propellants.

performances, justify the use of the most sophisticated equipments. This is particularly illustrated by the Submarine Launched Ballistic Missiles.





Centrifuge for acceleration testing of solid rocket motors (SNPE – Saint-Médard-en-Jalles).

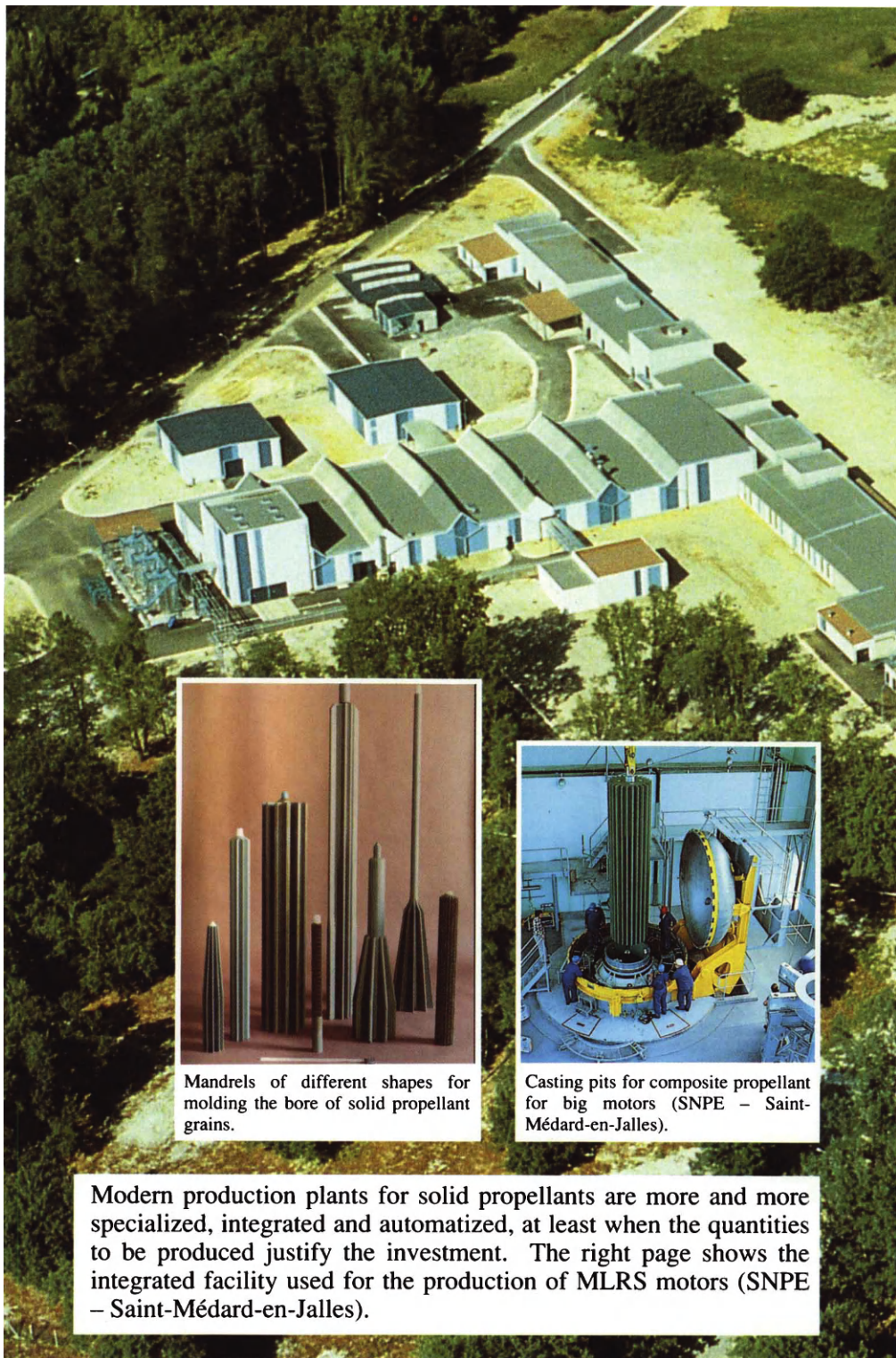


Environment testing centre for rocket motors (SNPE – Saint-Médard-en-Jalles).

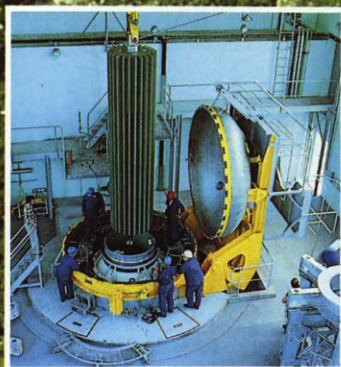


Ramrocket missile ready for a flight test (photo ONERA).

SOPHISTICATION Because of the great cost of real testing and particularly of flight tests, experimental and numerical simulations are very important for the design of new solid rocket motors. The left page shows the subscale testing at ONERA of models of the solid boosters for ARIANE 5. This test is designed to evaluate the interaction between the rocket exhausts and the launch pad.

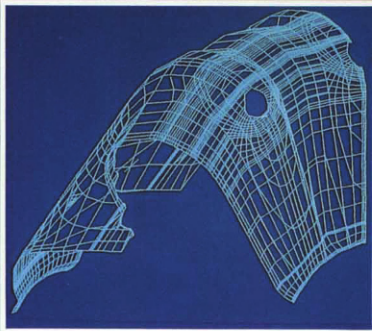


Mandrels of different shapes for molding the bore of solid propellant grains.

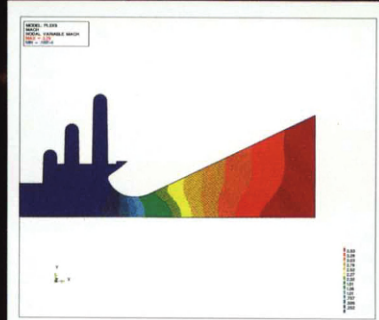


Casting pits for composite propellant for big motors (SNPE – Saint-Médard-en-Jalles).

Modern production plants for solid propellants are more and more specialized, integrated and automatized, at least when the quantities to be produced justify the investment. The right page shows the integrated facility used for the production of MLRS motors (SNPE – Saint-Médard-en-Jalles).



Evolution of a surface in combustion from a tridimensional initial geometry.



Internal flowfield in the propellant cavity and nozzle of a solid rocket motor.



Observation of the combustion of an end-burning solid propellant grain. The “coning” resulting from a higher combustion rate along the inhibitor interface can be observed (SNPE – Le Bouchet Research Center).

In Section 4.2.7 an expression was suggested for the damage from experimental results obtained from creeping tests (eqn 24):

$$\mathcal{D}(t) = \mathcal{D}_0 \left(\int_0^t [\sigma_0(\tau)]^m d\tau \right)^{1/m}$$

This equation calls for several remarks:

Remark 1. The factor of safety defined from eqn (24) is written:

$$K_{\mathcal{D}}(t) = \frac{1}{\mathcal{D}_0} \times \frac{1}{\left(\int_0^t [\sigma_0(\tau)]^m d\tau \right)^{1/m}} \quad (37)$$

In this relation: $1/\mathcal{D}_0$ represents the capability of the propellant; it is an experimental datum.

$$\left(\int_0^t [\sigma_0(\tau)]^m d\tau \right)^{1/m}$$

stands for the induced stress in the propellant grain; it is a value obtained by calculations.

$K_{\mathcal{D}}$ is, in fact, the ratio of a capability to an induced stress.

Remark 2. Equation (24), providing a damage type, can also be written in the following manner:

$$[\mathcal{D}(t)]^m = D(t) = \mathcal{D}_0^m \int_0^t [\sigma_0(\tau)]^m d\tau \quad (38)$$

$D(t)$ varies from 0 to 1, and therefore corresponds to another expression of the damage that has the same definition.

In fact, eqn (38) is the equation that corresponds to the initial definition of the damage, and best expresses the physical phenomenon. For example, in a tensile test during which the stress varies in a linear fashion over time, the two types of damage are written:

$$\mathcal{D}(t) = \mathcal{D}_0 \dot{\sigma}_0 \left(\frac{1}{m+1} \right)^{1/m} t^{m+1/m}$$

$$D(t) = \mathcal{D}_0^m \dot{\sigma}_0^m \frac{1}{m+1} t^{m+1}$$

The plotting of these two forms of expression is given in Fig. 61 for a realistic value of parameter $m(m = 10)$ $D(t)$, representing a linear cumulation of the damage, and demonstrates the fact that the damage sustained by the propellant is very low up to a fairly high value of the stress, relative to the maximum stress σ_m .

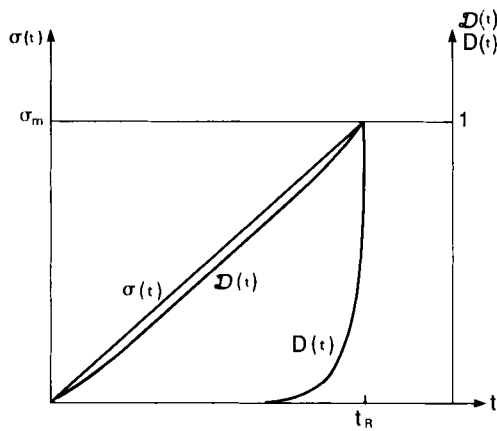


FIG. 6.61. Damage for a linear evolution of the stress.

For example, if the propellant is to be subjected to stress cycles, illustrated in Fig. 62, during which the stress varies between 0 and $\alpha\sigma_m$, where σ_m is the maximum stress for the tensile test at the same stress rate, and α the coefficient ranges from 0 to 1, the number of cycles N it can withstand is dependent on the value of the coefficient α and is given, based on eqns (24) or (38), by:

$$N = \left(\frac{1}{\alpha}\right)^{m+1}$$

With a realistic value for $m(m = 10)$, the values obtained are indicated in Table 2.

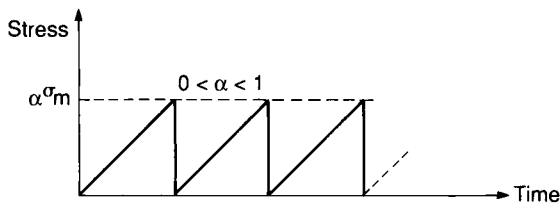


FIG. 6.62. Stress cycles imposed on a specimen.

TABLE 2

α	Number of cycles
0.5	2048
0.8	~ 11
0.9	~ 3

Under these conditions the damage sustained by the propellant for a $0.5 \sigma_m$ cycle is negligible in comparison with the damage sustained at a $0.9 \sigma_m$ cycle.

Remark 3. Strain damage can be defined based on experimental results obtained from relaxation tests, for various strains, up to failure. Typically, the formula is very close to that given by eqn (24) but the value of exponent m is greater ($m > 30$).

Similarly, the factor of safety is given by the inverse of the damage.

Remark 4. The cumulation of induced stresses/strains presents no problem when the factor of safety is calculated in terms of damage, because the induced stress/strain is integrated over time, and the capability, represented by $1/\mathcal{D}_o$, is representative of multiple tests performed under very varied conditions. The use of the factor of safety in terms of damage seems, therefore, to resolve all cumulation problems. Although it is certainly the factor that deals best with the problem, it should not be forgotten that eqn (24) is a simple equation applied only when the creep failure curve is a straight line ($\log \sigma_F = A \log t_R + B$). In propellants, the equations expressing the damage are usually more complex (eqn 25) and, in any case, they must be experimentally determined and verified for each propellant.

6.1.2. Factor of safety defined with strains

For an elementary mechanical load, this is defined by:

$$K_\epsilon = \frac{\epsilon_m}{\epsilon_o} \quad (39)$$

where:

ϵ_m = strain under tensile stress relative to the maximum stress, for the parameters of loading rate and temperature corresponding to the applied mechanical load;

ϵ_o = strain corresponding to the point where the induced strain is maximum; it is determined from the equivalent stress, assessed with the failure criterion, for a Young's modulus E that corresponds to parameters of loading rate and temperature of the mechanical load:

$$\epsilon_o = \frac{\sigma_o}{E}$$

This definition of equivalent strain implies that the multidimensional effects are the same for stresses as for strains. In particular, the effect of pressure must be identical for the stress capability as for the strain capability (see Section 4.2.4.).

One method for the cumulation of basic factors of safety determined for strain is obtained from remarks 2 and 3 of the preceding section. When m is

very large ($1/m$ close to 0), the initial definition of damage can no longer be used because, during a relaxation test, the failure time tends to be infinite.

Damage, in this situation, is written in other forms, including:

$$\mathcal{D} = \max\left(\frac{\varepsilon_{oi}}{\varepsilon_{mi}}\right) \quad (40)$$

where:

ε_{oi} = equivalent strain sustained by the propellant grain for an elementary mechanical load i ;

ε_{mi} = strain at failure of the propellant grain for the elementary mechanical load.

$$K = \frac{1}{\max\left(\frac{\varepsilon_{oi}}{\varepsilon_{mi}}\right)} = \min\left(\frac{\varepsilon_{mi}}{\varepsilon_{oi}}\right) \quad (41)$$

This relation is correct in the case where, after each basic load, the induced strain returns to a zero value (Fig. 63).

But in the case of mechanical load increments (Fig. 64) this relation is not applicable. In this case, the damage could be expressed by:

$$\mathcal{D} = \sum_{i=1}^N \frac{\Delta\varepsilon_{oi}}{\varepsilon_{mi}} \quad (42)$$

$\Delta\varepsilon_{oi}$ = Equivalent strain increment resulting from mechanical load i ;

ε_{mi} = strain capability at mechanical load i .

Therefore, the factor of safety is written as:

$$K = \frac{1}{\sum_{i=1}^N \frac{\Delta\varepsilon_{oi}}{\varepsilon_{mi}}}$$

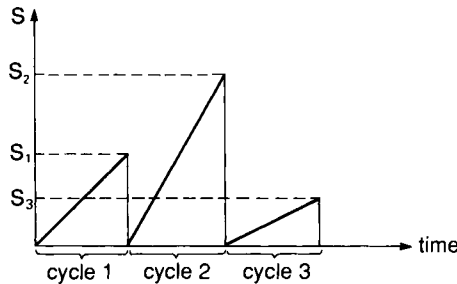


FIG. 6.63. Cumulation of mechanical loading.

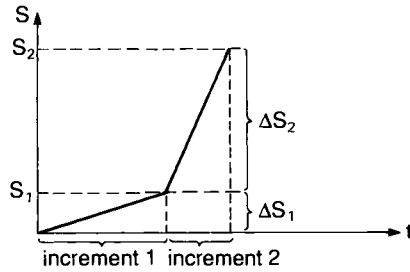


FIG. 6.64. Loading increments.

The calculation of the factor of safety based on the strains presents a very distinct advantage for case-bonded grains. In these grains the two important mechanical loads are due to temperature changes and pressure rise at firing. For these mechanical loads the strains are not dependent on the behavior of the propellant when it is used in its incompressible portion.

That is why research continues, so that a relation can be determined which takes the cumulation of strains into consideration, specifically in the case of tensile stress with simultaneous temperature changes [34].

6.1.3. Factor of safety defined with stresses

For an elementary mechanical load, this is defined by:

$$K_{\sigma} = \frac{\sigma_m}{\sigma_o}$$

where:

- σ_m = maximum stress for the loading rate and temperature parameters corresponding to the applied mechanical load;
- σ_o = equivalent stress at the most stressed point, assessed through calculations using the failure criterion.

The cumulation of induced stresses presents the same problem, whether the basic factors of safety were determined from the stresses or the strains.

It is possible, however, to establish empirical rules based on observations made in the course of simple tests, provided that these rules constantly remain subject to revision.

The following rule can be proposed

$$K_{\sigma} = \frac{\sigma_o(t)}{\sigma_m(t)}$$

where:

- $\sigma_o(t)$ = stress cumulation existing in the propellant grain at time t ;
- $\sigma_m(t)$ = stress capability of the propellant under the total load conditions at time t .

Unfortunately, with a case-bonded grain, the induced stresses are often dependent on the behavior of the propellant; consequently, to obtain a reliable factor of safety, it is important to know that behavior.

6.2. BONDING FACTOR OF SAFETY

The assessment of the safety factor of the bonding is always done using stress. Several failure criteria can be used for bondings:

- normal stress criterion;
- shear stress;
- surfacic force applied at the bondline (σ_N, τ).

In every case the factor of safety is defined by the ratio between the capability (obtained experimentally as described in Section 4.3.3) and the induced stress using one or the other failure criteria.

The failure criterion expressed in force seems to be best suited.

In every case the factor of safety in relation to the propellant is calculated at the critical point of the bonding. When it is found to be smaller than one of the factors of safety obtained from the bonding failure criteria, it is used to characterize the bonding.

In the case of the induced stress resulting from firing, the importance of the effect of the pressure varies, based on whether the grain has been stress-relieved (prepared debonding), or completely bonded. For a stress-relieved grain the most stressed point of the bonding is located fairly far from the burning surface. Should debonding occur during pressure rise, the propellant is pressed again against the liner and the risk of propagation is rather low. In addition, since the flame reaches the debonding at the end of the firing, the operation of the motor is not affected.

But in the case of an entirely bound grain, the critical point is located very close to the free surface, i.e. the combustion chamber. A debonding in that area has a high level of probability of opening into the combustion chamber creating at the time of firing an additional burning surface, and therefore a faulty operation of the motor (Fig. 65). In this case the effect of the pressure on the normal stress must be taken into account.

Comment. As with propellant (Section 6.1.1.) there is the problem of damage cumulation for the propellant–liner bonds. Research is being done in that area [28]. The cumulative damage laws described in Section 6.1.1 can, however, be used for the propellant–liner bonds, even though the bond failures always occur in the propellant.

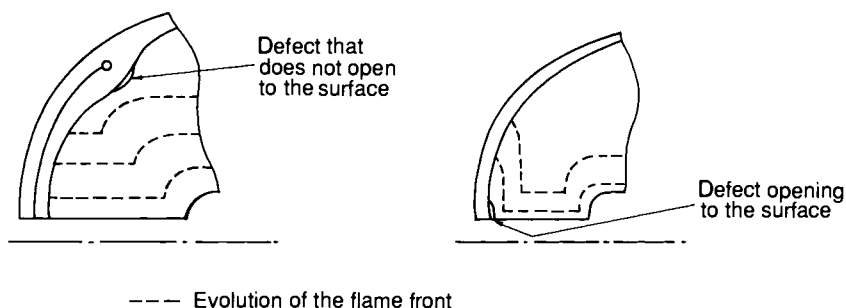


FIG. 6.65.

6.3. VERIFICATION AND ADJUSTMENT OF VARIOUS METHODS OF ANALYSIS OF FACTORS OF SAFETY

Verification of the methods cannot be done on a large number of propellant grains when these are either expensive or of large size.

It is therefore desirable to design objects that are small in size, inexpensive, simple to use, and allow the creation in the propellant of induced stresses/strains identical to those occurring in propellant grains. Several objects, of varying geometry, have been proposed, including the SEC model developed in the United States [29], and the PHI model from France [30] (Figs 66 and 67).

These objects are subjected to various thermal cycles or to pressurizations until the propellant fails. These are used to evaluate the various methods used to calculate the factor of safety in the case of cumulative mechanical stresses.

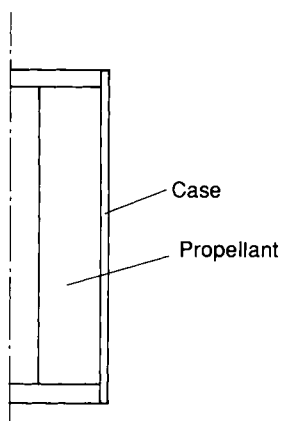


FIG. 6.66. S.E.C. model.

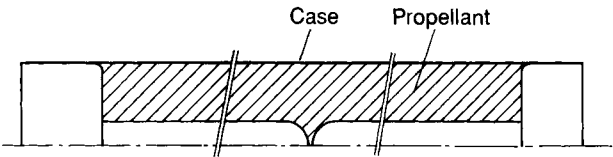


FIG. 6.67. PHI model.

The PHI model offers the distinct advantage of very different induced load levels simply by modifying several geometrical parameters (Fig. 68):

- inside diameter;
- diameter of the hole in the membrane;
- thickness of the membrane;
- length of the model.

In addition, as it is the case for many propellant grains, the location of the most stressed point in the PHI model is clearly known, and the volume of propellant heavily stressed around that point is small in comparison with the total volume of the propellant. On the other hand, in the SEC model, the volume of propellant heavily stressed is much larger.

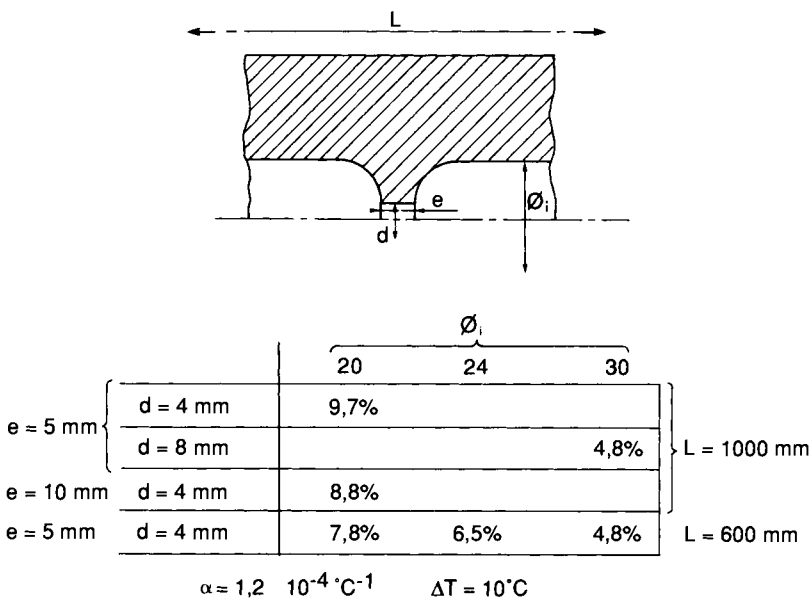


FIG. 6.68. Maximum strain as a function of the geometry of the PHI model.

6.4. SEMI-EXPERIMENTAL DETERMINATION OF THE FACTOR OF SAFETY

When dealing with propellant grains with a complex geometry, subjected to induced stresses/strains for which it is difficult to develop models (thermal cycles, for example), semi-experimental methods can be used to calculate the factor of safety.

Phase 1. A finite element analysis is done on the three-dimensional geometry with an incompressible linear elastic behavior, for a simple mechanical load (uniform temperature change, for example), and the strain field is determined.

Phase 2. A PHI model is selected (Fig. 67). Its geometrical dimensions are such that they allow the same strain level under the same analysis conditions: same behavior law, same boundary conditions.

Phase 3. The PHI model is made with the propellant that needs to be tested. It is subjected to the same cycles as the propellant grains being analyzed.

If the specimen breaks during the cycling, the factor of safety propellant grain is lower than 1. It will therefore be necessary to modify either the propellant or the geometry of the grain.

If the specimen does not fail, it is subjected to a N number of cycles, identical to the preceding one, until failure occurs.

If the propellant obeys a damage law of the form (24), one can write, for a cycle:

$$D = \left(\frac{1}{N} \right)^{1/m}$$

and

$$K = N^{1/m}$$

This allows us to determine the order of magnitude of the factor of safety.

The steps involved in this method are shown in Fig. 69.

7. Propellant Behavior Under Dynamic Loads

7.1. LOW AMPLITUDES

Propellant grains are subjected to this type of load during transport or during a defective operation of the rocket motor (combustion instabilities, for example). The loads, in these conditions, can be written in terms of Fourier

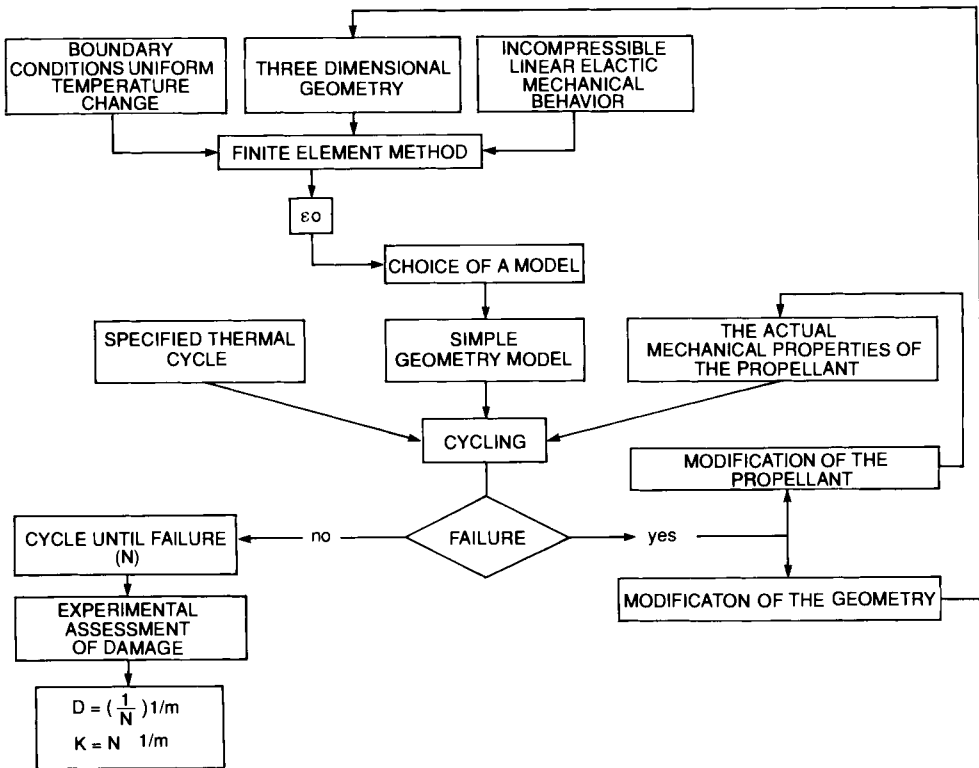


FIG. 6.69. Semi-experimental determination of the factor of safety.

series, and the propellant behavior is determined as a function of the frequency. Two methods are used:

- viscoanalyzer (1–1,000 Hz);
- ultrasounds (0.5–2.5 MHz).

The expression of the modulus of a propellant under harmonic stress loading takes the form of a complex number.

$$E^* = E' + iE''$$

$$\operatorname{tg} \delta = \frac{E''}{E'} \quad \text{expresses the damping of the material.}$$

Figures 70.1 and 70.2 illustrate the aspect of the master curve of the dynamic modulus with which the time–temperature equivalence principle can be applied.

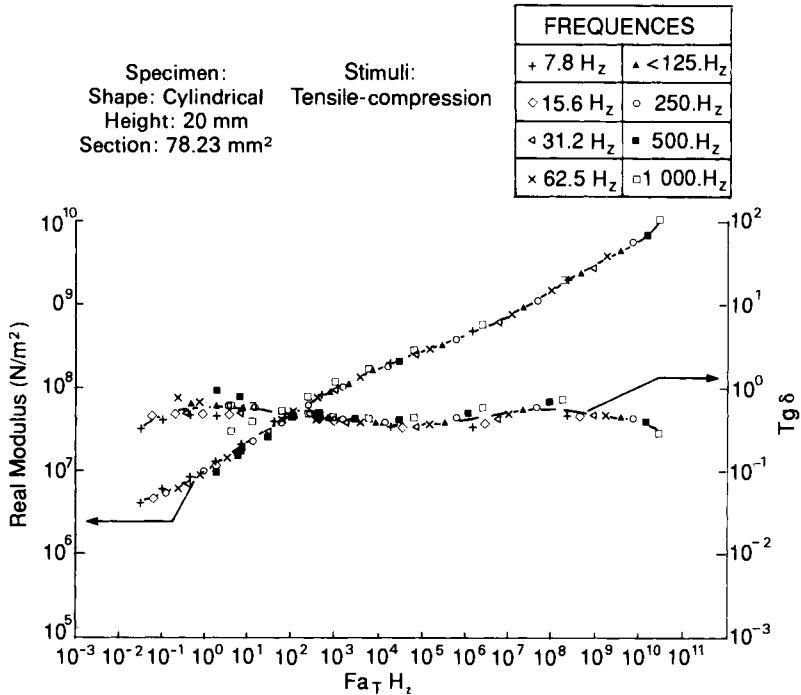


FIG. 6.70(1). Dynamic tests. Viscoelasticimeter.

7.2. HIGH AMPLITUDES

The propellant grains may be subjected to rapidly varying loads, usually considered as shocks. These are loads that could have a dynamic impact, very high amplitudes, rendering Fourier series analyses useless because behavior non-linearity occurs. These loads may cause a fragmentation of the propellant. When these fragments are smaller than a critical size, a transition phase may occur in the combustion regime for some propellants, leading to a mass detonation of the rocket motor.

These studies are all concerned with the safety of the motors; they are discussed in Chapter 7. The experimental methods that help characterize the propellant behavior are as follows:

- rapid tensile loading machine with a displacement rate of 20 m/s;
- Hopkinson bars;
- impact against flat wall;
- shock Hugoniot measurements with a light gas gun.

The study of the impact behavior on a propellant is discussed in many research papers ([31–33], among many others), and could fill an entire

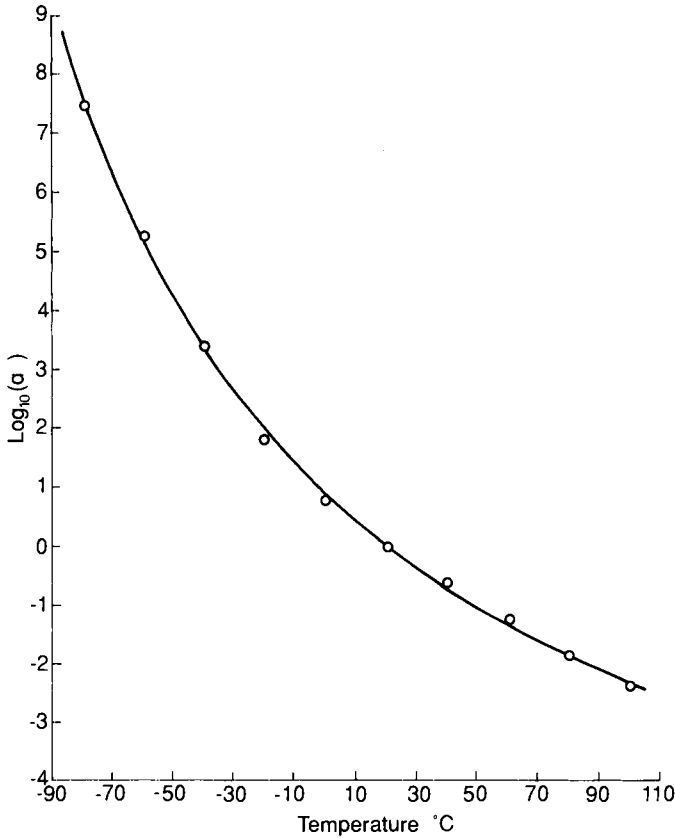


FIG. 6.70(2). Time-temperature equivalence factor.

chapter. A detailed description of the result of these studies cannot be given here. It is important, however, to indicate that in the case of composite propellants, the behavior of the crystalline oxidizers has a major effect on the behavior of the propellant, while in the case of static loads, whose rates are much lower, the propellant behavior is mostly dependent on the bonding between the binder and the crystalline oxidizer.

8. Conclusions and Future Prospects

With a method which would allow a precise determination of the factor of safety of a propellant grain it would be possible to optimize the performance of rocket motors through a potential increase in the volumetric loading fraction of the grain.

The methods used nowadays are still somewhat imprecise in some cases, and need to be improved. They have, however, made it possible to improve propellant grain designs. Even though there is no perfect model of the propellant behavior, the research work has helped us obtain a better understanding of the phenomena and, indirectly, assisted in the formulation of new compositions.

A high level of activity must be continued in this area to model the behavior of propellants and their fracture mechanisms. At the same time, numerical analysis techniques must evolve further to take the actual propellant behavior into account, at the lowest possible cost.

Finally, all of the research must be based on many experimental results obtained from tests performed on propellant grains or models.

Bibliography

1. PERSOZ, B., *Introduction à l'étude de la rhéologie*. Dunod.
2. CHRISTENSEN, R. M., *Theory of Viscoelasticity: An Introduction*. Academic Press.
3. FERRY, J. D., *Viscoelastic Properties of Polymers*. Ed. J. Wiley, 1970.
4. FARRIS, R. J., Development of Solid Rocket Propellant Non-Linear Viscoelastic Constitutive Theory. AFRPL-Tr-75-20, May 1975.
5. PARASKEVAS, Etude théorique et expérimentale de la photoélasticimétrie tridimensionnelle. Rapport CETIM No. 15 G 151.
6. ZIENKIEWICZ, O. C., *La méthode des éléments finis* (traduit de la 3ème édition anglaise). McGraw-Hill.
7. TOUZOT, G., Une présentation de la méthode des éléments finis. Presse de l'Université Laval (Quebec).
8. MARTIN, Ch., RACIMOR, P., LE ROY, M. and QUIDOT, M., Représentation par des lois de Farris du comportement viscoélastique non linéaire d'un matériau chargé. Groupe Français de Rhéologie. December 1980.
9. MELI, G., THEPENIER, J., PASQUIER, M. and DUBROCA, G., Mechanical design of case bonded C MDB grains by a non linear viscoelastic method. AIAA, SAE, and ASME Joint Propulsion Conference, Vol. 16, No. 80-1177, 1980.
10. WILLIAMS, M. L., LANDEL, R. F. and FERRY, J. D., The temperature dependence of relaxation mechanisms in amorphous polymers and other glass-forming liquids. *J. Am. Chem. Soc.*, **77**(3), 701, 1955.
11. BOLEY, B. A. and WEINER, J. H., *Theory of Thermal Stresses*. 1st edition. John Wiley, New York. 1960.
12. REISMANN, H. and PAWLIK, P. S., *Elasticity Theory and Applications*. John Wiley and Sons.
13. FRANCIS, E. C. et al., Propellant Non-Linear Constitutive Theory Extension: Preliminary Results. UTC/CSD-2742-AFRPL-TR-83-034, August 1983.
14. TSCHOEGL, N. W., *Failure Surfaces in Principal Stress Space*. Polymer Science Symposium No. 32, 239-267. John Wiley and Sons. 1971.
15. LANGLOIS, G. and GONARD, R., New law for crack propagation in solid propellant material. *J. Spacecraft Rockets*, **16**, 357, 1979.
16. NOTTIN, J. P., GONDOUIN, B. and LUCAS, M., Experimental investigation of cracks growth in composite propellants. AIAA 85-1437. AIAA/SAE/ASME/ASEE 21st Joint Propulsion Conference. Monterey, California, 1985.
17. SCHAPERY, R. A. *Int. J. Fracture*, **11**, 141, 1975; *International Journal of Fracture*, **11**, 369, 1975; *Int. J. Fracture*, **11**, 549, 1975.
18. KNAUS, W. G., On steady propagation of a crack in a viscoelastic sheet: experiments and analysis. *Deformation and Fracture of High Polymers*, edited by J. Henning Kausch, Hohn A. Hassel and Robert K. Jaffee. Plenum Press, 1974.

19. BECKWITH, S. W. and WANG, D. T., *Crack Propagation in Double-Base Propellants*. Hercules Incorporated Bacchus Works, Magna, Utah.
20. HERRMANN, L. R., Elasticity equations for incompressible and nearly incompressible materials by a variational theorem. *AIAA Journal*, 3, 1886-1900, 1965.
21. SHAPERY, R. A., *A Micromechanics Model for Non-Linear Viscoelastic Behavior of Particle-Reinforced Rubber with Distributed Damage*. Texas A & M University, College Station, Texas. MM 4867-86-1, January 1986.
22. GREEN, A. E., and ZERNA, W., *Theoretical Elasticity*. Clarendon Press, Oxford, 1968.
23. WANG, D. T., and SHEARLY, R. N., A review of solid propellant grain structural margin and safety prediction methods. AIAA/ASME/SAE/ASEE 22nd Joint Propulsion Conference. AIAA Paper No. 86-1415, 1986.
24. BILLS, K. W., Jr., *et al.*, Non-linear fracture mechanics. Final Report. NWC-TP-5684. February 1975.
25. MINER, M. A., Cumulative damage in fatigue. *J. Appl. Mech., Trans. ASME, Series E*, 67, 1945.
26. LIU, C. T., Crack growth behavior in composite propellant with strain gradient. AIAA/ASME/SAE 20th Joint Propulsion Conference, June 1984.
27. PARR, C. H., End effect due to shrinkage in solid propellant grains. *Bulletin of the 20th JAN-AF Panel on Physical Properties of Solid Propellants*, Vol. 1, November 1961.
28. BILLS, K. W., Jr *et al.*, A cumulative damage concept for propellant-liner bonds in solid rocket motors. *J. Spacecraft*, 3, 3, 1966.
29. ICRPG, *Solid Propellant Mechanical Behavior Manual*, CPIA Publications, 1963.
30. THEPENIER, J., GONDOUN, B., and MENEZ-COUTENCEAU, H., Reliability of solid propellant grains: mechanical analog motor design and testing. AIAA/SAE/ASME/ASEE 23rd Joint Propulsion Conference, AIAA-87, 1987.
31. STANKIEWICZ, F., HUMBERT, P. and BOULE, P., Effect of dynamic loading on fracture behavior of filled polymers. *Impact Loading and Dynamic Behavior of Materials*. DGM Information Gesellschaft Verlag, Vol. 1, 1988.
32. QUIDOT, M., Dynamic fragmentation of compact energetic materials. *Impact Loading and Dynamic Behavior of Materials*. DGM Information Gesellschaft Verlag, Vol. 2, 1988.
33. Mechanical Properties at High Rates of Strain, Conference, Oxford, edited by J. Harding, March 1979.
34. RACIMOR, P. and NOTTIN, J. P., Mechanical behavior of solid propellants during tensile test with variable temperature. AIAA/ASME/SAE/ASEE, 25th Joint Propulsion Conference No. 89-2645.

CHAPTER 7

Safety Characteristics of Solid Propellants and Hazards of Solid Rocket Motors

JACQUES BRUNET*

1. Introduction

The rapid growth of performance requirements and the new missions now performed necessitate:

- the use of increasingly larger rocket motors;
- the use of, and search for, increasingly powerful propellants, or propellants with increasingly faster combustion rates;

as well as finding propellants that remain very energetic while presenting a lower level of vulnerability.

Because of these trends, and of the evolution of safety regulations, it is now necessary to take safety issues into account at the beginning of any project.

2. Overview of Solid Propellant Rocket Motor Hazards

During the course of their entire life cycle, from production to utilization, solid propellant rocket motors can be found in many varied environments, and subjected to stresses corresponding to a series of various activities. Safety, under these conditions, is not only a function of the rocket motor *per se*, but of the environment in which the rocket motor finds itself.

During the life of the motor, various undesirable events are likely to occur:

* With the participation of Michel VIDAL.

- propulsion caused by untimely ignition: untimely operation;
- inadvertent initiation, with thermal and mechanical effects:
 - explosion, with thermal, blast and projection effects;
 - detonation of the propellant grain, with blast and projection effects;
- faulty performance, that may also result in the undesirable events listed above.

These events are linked to the energy stored inside the propellant, and cause the following physical effects:

- thermal fluxes;
- active or inert projections, which can be characterized in terms of density, kinetic energy, and caloric energy:
 - propulsion,
 - projection of inert materials (fragments),
 - projection of energetic materials (propellants);
- blast, accompanying:
 - the mechanical explosion,
 - the detonation of a portion of the motor or the entire motor.

These are the primary threats from the solid propellant rocket motors; but, beyond these primary hazards, any active projection may lead to a secondary hazard (other than kinetic or calorific) caused by the impact of energetic material against walls or other objects against a wall.

In the case of a violent event, the blast causes an overpressure in the surroundings, which may remain modest in the case of an explosion (several kPa), or become very important (several MPa) in the case of a detonation.

3. Pyrotechnic Behavior of Solid Propellants

The pyrotechnic behavior of solid propellants can be characterized by:

- an evaluation of their various modes of decomposition;
- a knowledge of their reactions (threshold of reaction and type of reaction) when exposed to certain types of stimuli.

A full knowledge of the solid propellant behavior is very valuable because it allows us to:

- identify the modes of decomposition;
- know the level of stimuli that will cause a pyrotechnic reaction;
- compare the solid propellants with each other, and assess the general behavior of a solid propellant grain or of a rocket motor by comparing it against a reference solid propellant grain or rocket motor for which the behavior is well known, and based, in particular, on past experience.

3.1. DECOMPOSITION MODES OF SOLID PROPELLANTS

Propellants may, like any other explosive substance, exhibit various modes of decomposition.

3.1.1. *Definition of the modes of decomposition*

The major modes of decomposition are as follows:

- conductive combustion;
- convective combustion;
- detonation;
- thermal explosion.

Let us examine the propagation of decomposition into a solid propellant (Fig. 1). The “reaction zone” is the zone existing at any time between zone I — the propellant in its initial physical state, and zone II — the products of the decomposition.

- When the reaction zone travels inside the initial matter (zone I), through thermal conduction, we say that there is “deflagration.”

In that case, volume, pressure, temperature and material velocity vary in a continuous manner from zone I to zone II inside of the reaction zone. The propagation velocity is lower than the sound velocity in the solid propellant and is called “deflagration velocity” (often called “the burning rate” of the propellant). Solid propellants deflagrate in a linear “cigarette burning” mode with slow propagation velocities up to high pressures.

- This steady propagation of the deflagration front into the unreacted solid propellant is often called conductive combustion. The propagation

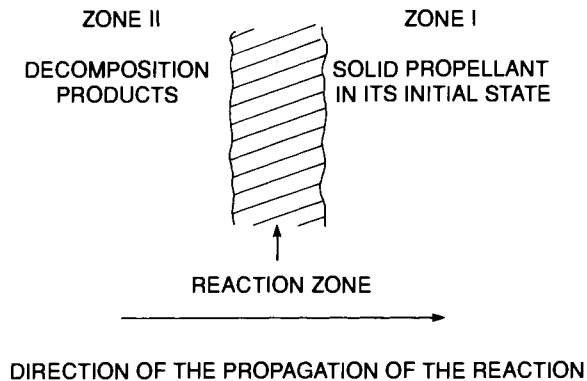


FIG. 7.1. Sketch of the propagation of the decomposition in a solid propellant.

velocities (burn rates) are in the range of several to tens of centimeters per second.

- When the reaction zone travels through the unreacted propellant (zone I) via a shock wave, we say that there is “detonation.”

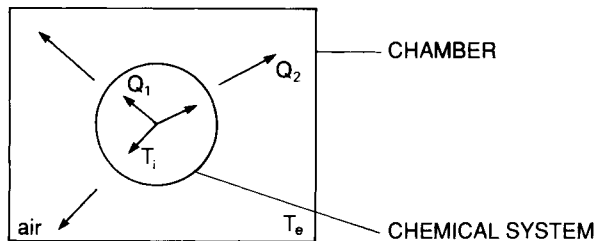
Across this detonation wave, the volume, the pressure and the material velocity of the matter experience a discontinuity. The typical propagation velocity of a detonation ranges between 2000 and 9000 m/s. The detonation is the functional decomposition mode of explosives. It is one of the accidental and feared decomposition modes for propellants.

- The term “convective combustion” is often used in the case of porous materials (a gunpowder layer, for example). In this case the reaction zone travels via the penetration of heated gases in the spaces existing between the grains. The propagation rates are in the 100–1000 cm/s range, and because of the increased burning area and subsequent compaction of the porous bed and accelerating pressure can lead to a deflagration to detonation transition (DDT).
- The thermal explosion (cook-off), as described by Frank Kamenetski [2], is a violent and somewhat peculiar reaction: it indicates a chemical decomposition in the core of the matter.

Let us consider a chemical system, likely to react to thermal stress, which is placed in a heated chamber at constant temperature T_e (Fig. 2).

There may be a critical temperature T_m such that:

- if $T_e \leq T_m$: then the heat produced per unit of time is lower or equal to the heat dissipated: $Q_1 \leq Q_2$. In this instance the state is steady and there is no self-heating inside the system;
- if $T_e > T_m$: then the heat produced is greater than the heat dissipated per unit of time: $Q_1 > Q_2$. Here the condition is unsteady. Because the heat



Where T_i = Initial temperature of system, such as $T_i \ll T_e$

Q_1 = Heat resulting from the reaction per unit of time inside the system

Q_2 = Heat dissipated by the system per unit of time toward the outside.

FIG. 7.2. Sketch of a chemical system subjected to constant thermal stimuli T_e .

produced cannot escape, the substance self-heats and can ignite, explode and eventually even detonate.

The closer the temperature T_e is to T_m , the greater the likelihood for the reaction to occur within the bulk of the propellant. It is in the vicinity of T_m that the “thermal explosion” phenomenon occurs.

3.1.2. *Main characteristics of solid propellant decomposition*

3.1.2.1. *Combustion*

Conductive combustion occurs, in solid propellants, in a very broad range of pressures (1 Pa to 1000 MPa). Studies have particularly concentrated on operational pressures, i.e. of the order of several MPa. Safety studies, however, are also interested in the other pressures regimes (“ambient” pressure and high pressures). The major methods used to characterize the combustion of propellants are as follows:

- determination of the regression rate, measured at atmospheric pressure on solid propellant grains;
- determination of burning rate versus pressure, using the classic “strand burner” method (a small amount of propellant in a large vessel to give essentially a constant-volume, constant-pressure burn. Each run determines the burn rate at a given pressure and many runs are required to give the burn rate pressure curve);
- combustion under high pressure that might represent situations of high level of confinement. This test is performed in a closed bomb with a static resistance to rupture in the area of 1000 MPa. (A larger amount of propellant is burned in the closed vessel giving a varied pressure–time history. Reduction of the pressure–time curve gives a range of burn rates versus pressure from one run.)

Figure 3 and Table 1 provide some samples of measurement results.

TABLE 1 *Burning rate versus the pressure range in mm/s*

Solid propellant type	Pressure			
	Atmospheric	7 MPa	100 MPa	400 MPa
Classic butalane*	1.6	10	/	/
Butalane, high burning rate	3 to 8	20 to 80	/	/
Butalane with HMX	1.5	13	108	356
Double-base	0.5 to 1	7	66	334
High energy	0.5 to 1.5	8 to 30	/	/

* Aluminized polybutadiène composite propellant.

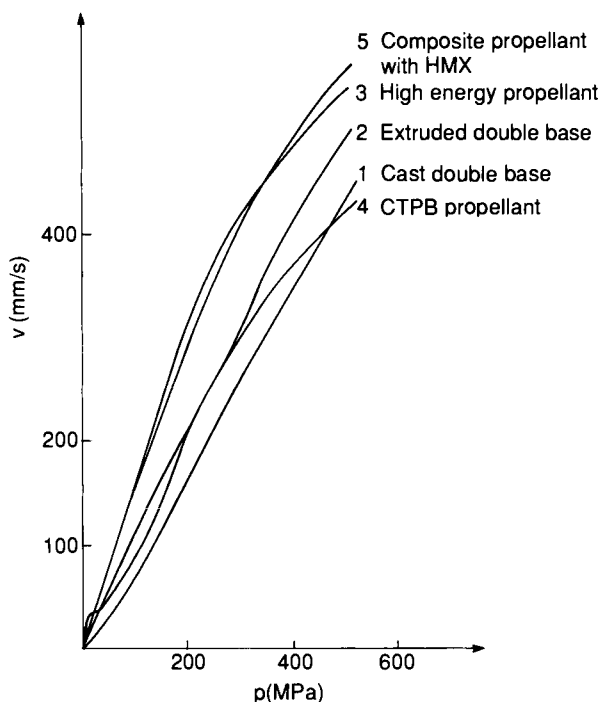


FIG. 7.3. Burning rate versus the pressure of typical propellants.

The monotonic character of these curves indicates that there is no abnormal burning (burning into cracks, or sample deconsolidation). In some instances, with certain high explosives, abnormal combustion occurs. This abnormal combustion may lead to convective combustion and in the extreme to deflagration to detonation transition.

3.1.2.2. Detonation

(a) Detonation in the classical sense of the term

The main detonation properties of propellants are characterized by:

- the detonation critical diameter;
- the pressure required to initiate a given diameter of propellant often measured by various gap tests;
- the TNT equivalency in terms of the blast effect.

Detonation critical diameter. The critical diameter is that diameter below which a steady-state detonation induced by a violent plane shock wave is no longer able to propagate. That is, the shock wave “dies out.” In explosives

this happens in a relatively sharp manner. For example if a cone of explosive is initiated at the base, the detonation will propagate toward the apex of the cone until the critical diameter is reached, at which point the detonation will die out. The stepped cylinder method (cylinders with decreasing diameter) is often used (see Fig. 4). In this test the diameter where the detonation stops is recorded by reading the witness lead plate. This diameter is called the detonation critical diameter.

Card gap test. This test consists of determining how many cards, made of cellulose acetate stacked to form a barrier, are necessary to prohibit the transmission of the detonation from the donor explosive (320 g) to the confined acceptor sample. The setup for this test is shown in Fig. 5.

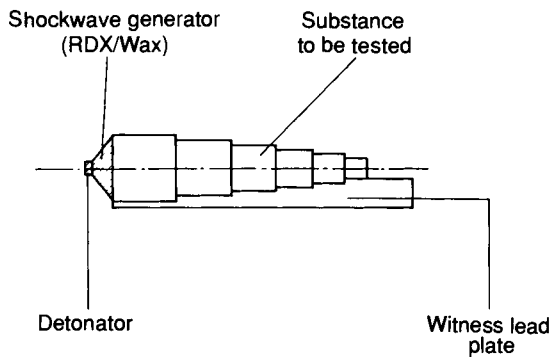


FIG. 7.4. Determination of the detonation critical diameter; SNPE test no. 10.

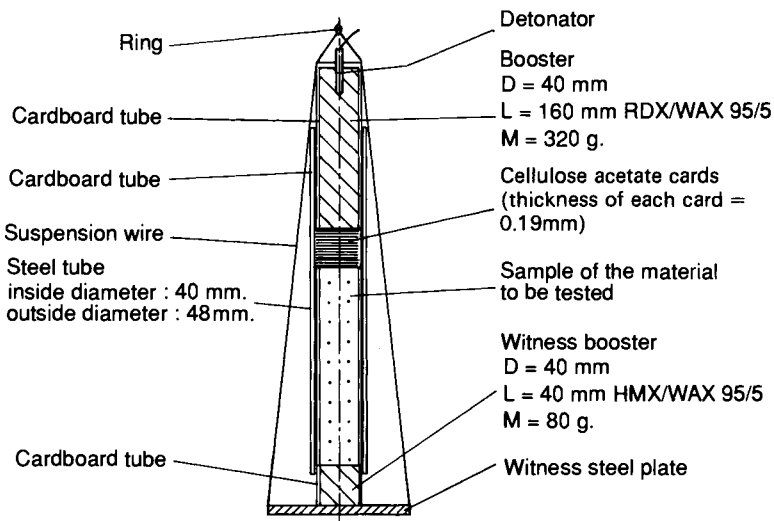


FIG. 7.5. French card gap test.

TABLE 2 *Detonic characteristics of solid propellants*

Propellant type	Critical diameter (mm)	CGT (number of cards)	TNT equivalency in blast effect
"Classic" composites	from 80 to 1000 ^a	< 1	1.4
Butalane with HMX	from some mm to 100 mm ^b	from < 1 to 105 ^b	1.4
Double-base	2 to 25	from 55 to 100	1.2
High energy	2 to 10	from 100 to 200	1.4 to 1.7

^a Function of the solid loading ratio.

^b Function of the ratio and quality of the HMX.

TNT equivalency in terms of the blast effect. This is the ratio of the TNT and propellant weight having the same effect at the same distances. Typical results are shown in Table 2.

We discover that the detonation characteristics of propellants are as varied as the formulas are different, but that the blast effect is about the same magnitude.

(b) New mechanisms for transition to detonation

We saw that the transition between deflagration and detonation caused by convective combustion cannot happen in an undamaged propellant grain with correct mechanical properties.

Nevertheless, several detonations occurred in the 1970s in the United States, during the development of the Trident missile [3–6]. It became necessary to explain these accidents, to imagine other mechanisms. Figure 6 presents, as a scheme, this new approach.

This scenario, which includes damage of the solid propellant leading to the creation of convective combustion conditions, reveals, on one hand, that correct design of the rocket motor is a key to operational safety, and on the other hand, that this DDT process can be eliminated by using propellant with a low propensity to fine fragmentation, therefore with good mechanical properties.

The most common test used to characterize the propensity of the propellant to this type of failure is the "friability or toughness" test, also known as the "shotgun" test. This consists of determining the condition of a piece of propellant grain fragmented through impact against a plane wall, by burning it in a closed bomb. The test principle is illustrated in Fig. 7.

The derivatives of the maximum pressure obtained on fragments of propellant grains, after impact, are recorded for each manometric chamber

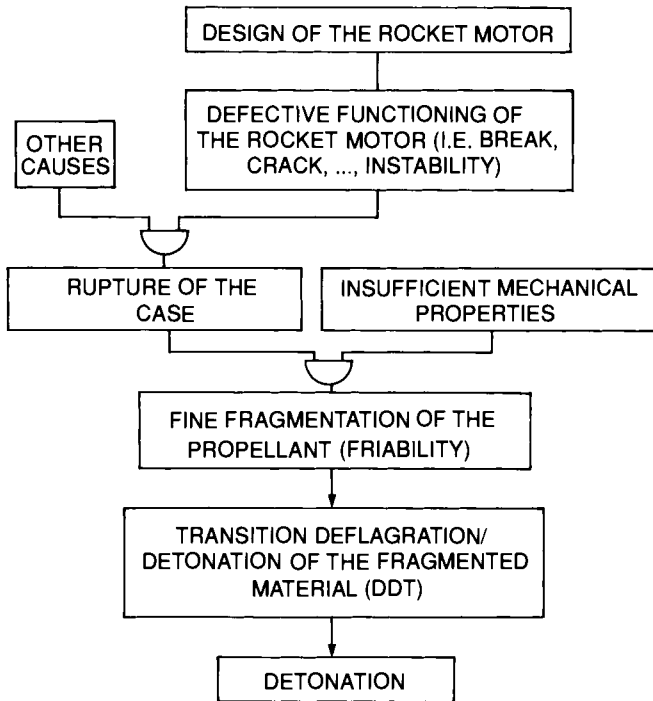


FIG. 7.6. Scenario of the DDT transition of a propellant grain.

test. These tests permit to plot the curve:

$$\left(\frac{dp}{dt}\right)_{\max} = f(\text{impact velocity})$$

This curve is useful because ancillary experiments showed that when the propellant was damaged sufficiently to give 18 MPa/ms in the 90 cm³ closed bomb, it was sufficiently damaged to produce DDT in a DDT tube experiment. Thus the impact velocity that causes damage sufficient to produce this 18 MPa/ms dp/dt in the 90 cm³ closed bomb, is called the critical impact velocity or CIV. Values of CIV of 200 m/s are considered good, that is a tough propellant which is not very friable, while 100 m/s is indicative of poor, friable propellant.

These accidents have led to the analysis of the failure mode of the firing operation. The experiments carried out revealed, in particular, the so-called "XDT" phenomenon (delayed detonation through shock). J. F. Kincaid [7] has put together a study combining all of these tests and their results.

The delayed detonation occurs at a time later than the normal transit time of the shock through the material. These reactions not only occur at times

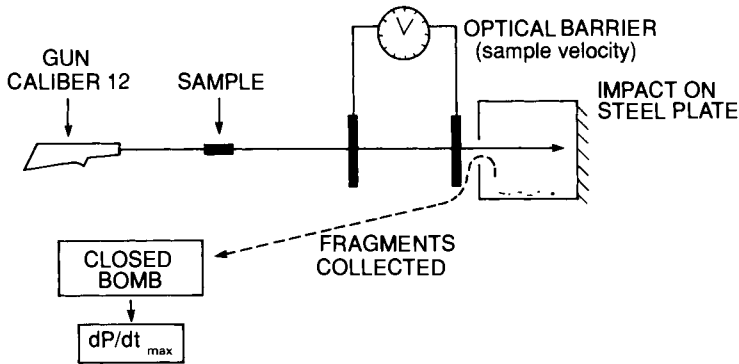


FIG. 7.7. Resistance to dangerous fragmentation.

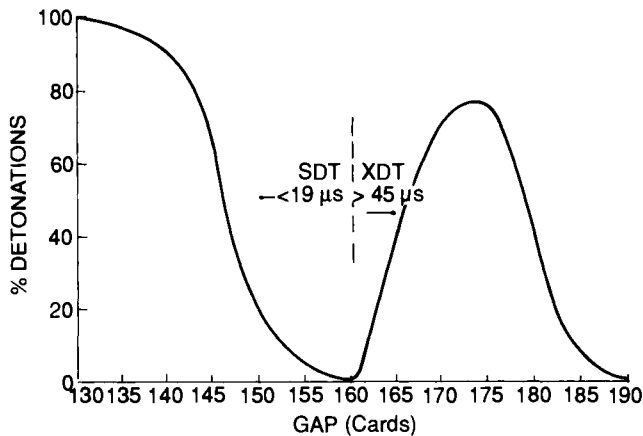


FIG. 7.8. NOL card gap test results showing SDT and XDT (from ref. [8]).

longer than characteristic of SDT, they also require a lower stimulus, for example an increased number of cards in the card gap test as shown in Fig. 8.

Sample size and mechanical properties also determine the initiation threshold as seen in Fig. 9.

So, detonation initiation by shock can be resumed in the following manner:

- high shock → SDT 1 D initiation;
- low shock → XDT 2 D and 3 D initiations.

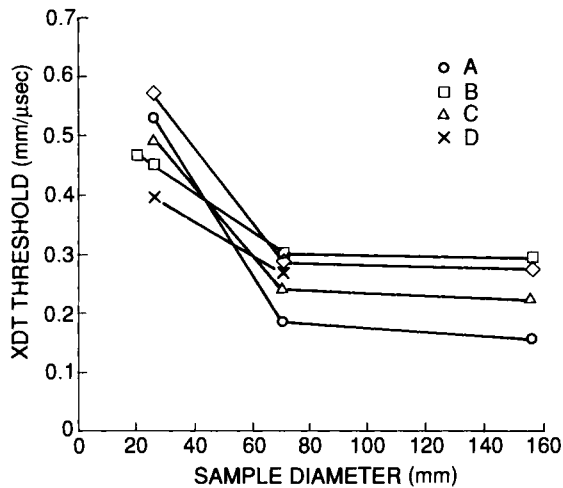


FIG. 7.9. Dependence of the velocity threshold for observation of XDT on sample diameter for various propellants A through E (from ref. [9]).

3.2. SENSITIVITY OF PROPELLANTS TO VARIOUS STIMULI

3.2.1. Impact sensitivity

Traditionally, at SNPE the Julius Peters drop-hammer test was used to determine the sensitivity to impact of high explosives. Initially, it was also used for solid propellants. Its major drawback is the very small quantity of

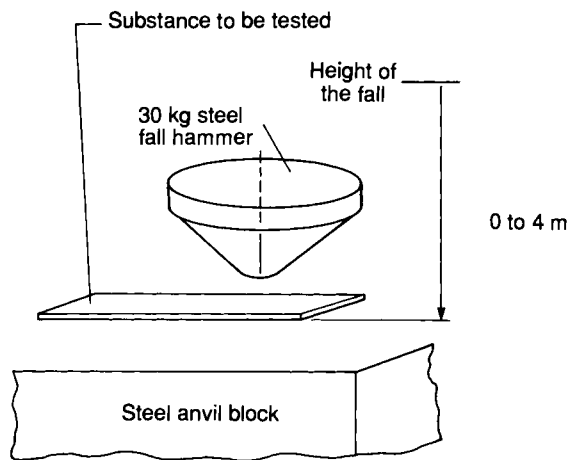


FIG. 7.10. Sensitivity test with a 30 kg fall-hammer; SNPE test no. 17.

material that is used to perform the test: 20 mm³. The “30 kg fall-hammer test” is now preferred; its major advantage resides in the capability of testing 100 g of material.

This test is, in addition, very interesting because it allows us to make a distinction between the types of reaction of the explosive substance:

- violent reaction with propagation (detonation);
- local reaction or ignition.

Generally, there is no propagation of violent reaction in the specimen of any solid propellants, up to an impact stimulus from 4 m high. However, local reactions, ignitions with or without propagation are observed.

3.2.2. Sensitivity to friction

As for the impact sensitivity testing discussed above, the sensitivity to friction test is carried out with the Julius Peters testing device. The principle of this device is illustrated in Fig. 11. It allows classification of the friction sensitivity of the solid propellants, but the safety margin in relation to the stimuli cannot be determined. Typical results obtained are given in Table 3.

To determine the safety margin of an operation performed on the solid propellant, this test can be complemented by other selective tests. These consist of rubbing propellant specimens, weighing several grams on surfaces

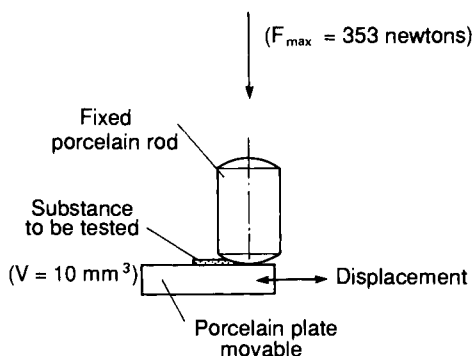


FIG. 7.11. Device for the friction sensitivity test “Julius Peters”—SNPE test no. 16.

TABLE 3 Sensitivity to friction of solid propellants

Composite	80 to 150 N
Composite with burning rate modifier	50 to 90 N
Double-base and high energy without ammonium perchlorate	50 to 353 N
Ammonium perchlorate high energy	60 to 150 N

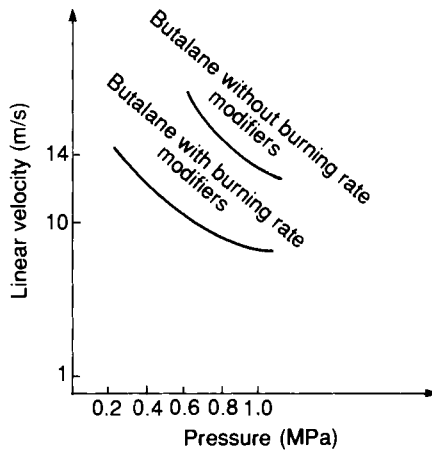


FIG. 7.12. Results of linear friction tests; SNPE test no. 76.

selected according to the data required, for periods of time lasting eventually up to several tens of seconds. By performing a series of tests a curve can be plotted from which safety margins can be obtained for pyrotechnic events considered as likely to occur during an operation inducing this type of stress. Figures 12 and 13 provide examples of such curves.

The solid propellant itself can be a surface that is selected, in which case an increase in sensitivity was noticed when moving from a steel surface to a propellant surface.

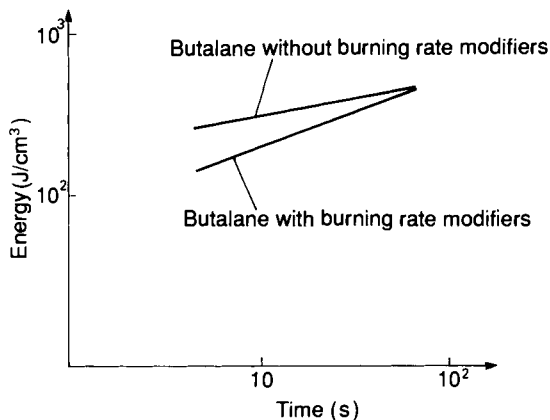


FIG. 7.13. Results of rotary friction.

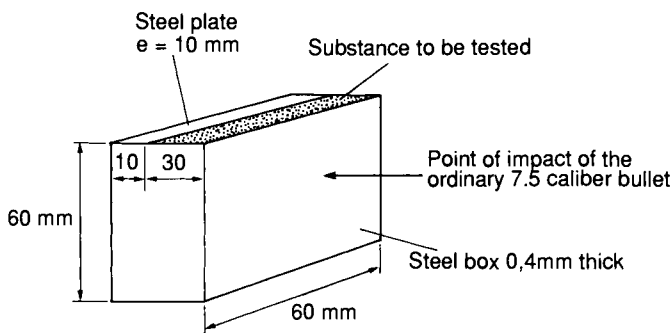


FIG. 7.14. Sensitivity to 7.5 mm caliber bullet impact; SNPE test no. 32.

3.2.3. Sensitivity to projectiles and fragments

It is, in fact, the sensitivity to impact from bullets that is usually determined. A test currently performed is shown in Fig. 14.

Generally, the results obtained at ambient temperature are as follows:

- ignition in all solid propellants;
- no violent reaction up to impact velocity of 930 m/s.

This systematic ignition, which we see in all composite propellants regardless of the velocity (beginning at 385 m/s), occurs in double-base propellants beginning at 555 m/s.

In Nitrargols the ignition threshold velocity decreases when the ammonium perchlorate content increases. These results have been confirmed by tests performed with rocket motors.

Nevertheless for rocket motors using solid propellant with small critical diameter of detonation we have to perform tests on more realistic models. In fact it is necessary to take into account that the vulnerability of a rocket motor is the vulnerability of a system. Some new results show that detonation can be obtained essentially due to a bore effect [10].

In this work detonation occurred when the bullet passed through the center bore in the motor, while detonation did not occur when the same caliber bullet with the same velocity passed through just propellant web (impact off-center so that the path of the projectile does not pass through the bore).

3.2.4. Sensitivity to temperature increase

3.2.4.1. Temperature of ignition

The ignition temperature of a solid propellant is the temperature at which ignition of the solid propellant occurs when the temperature of a small-size

specimen is raised; it is dependent only on the composition when the weight, the shape and other aspects of the specimen are given.

This characteristic varies with the temperature gradient. Two tests are commonly performed using 200 mg of shredded product:

- progressive heating with a standard gradient of $5^{\circ}\text{C}/\text{min}$;
- Sudden heating, which is achieved by plunging the product suddenly into an environment at a specific temperature. The ignition temperature is the temperature at which the propellant ignites within 5 s.

3.2.4.2. *Temperature of thermoinitiation of an unconfined solid specimen*

In the preceding sections we gave a brief description of the thermal explosion phenomenon. This phenomenon is different from that of ignition.

A composite propellant with ammonium perchlorate that does not contain any burning rate modifier, for example, can react very violently at a temperature of 175°C after several hours. This is the case of an accelerated chemical reaction at the core of the sample. A summary of the situation is given in Fig. 15.

The sensitivity to thermal explosion is determined through the cook-off test. The principle of this test is given in Fig. 16.

The specimen is contained in a cylinder made of steel or aluminum. The results of this test can be influenced by the environment and the size of the specimen [11]. The results obtained from progressive heating and thermoinitiation tests are indicated in Table 4.

Whenever we have seen the thermal explosion phenomenon occur, it always is within a narrow range of temperatures (approximately 10°C).

Nitrargols G containing ammonium perchlorate have no temperature

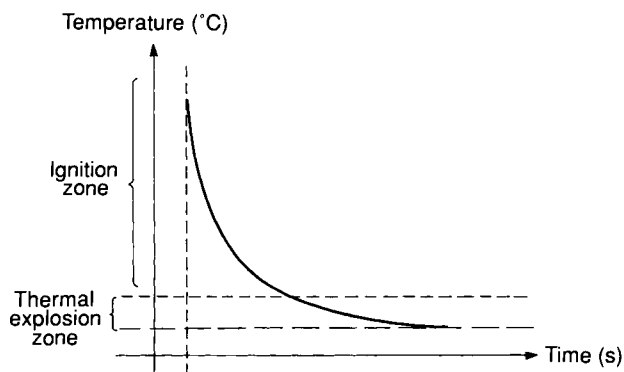


FIG. 7.15. Diagram of the evolution of the reaction temperature versus time.

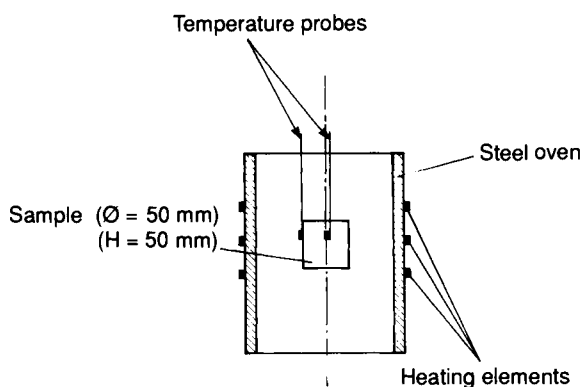


FIG. 7.16. Principle of the cook-off test.

TABLE 4 *Experimental results from thermal stimuli*

Propellants	Ignition temperature (progressive heating)	Results	
		Cook-off — Ø 50 mm, h 50 mm (at constant temperature)	
		Result	Maximum pyrotechnic event
“Classic” composites	270 to 320	Approx. 175°C	Thermal explosion
High burning rate composites	280 to 170	Decreases until 120°C when the catalyst ratio increases	Same
Epictète (CDB)	165 to 185	100 – 110°C	Same
Nitrargols (high-energy propellant)			
without perchlorate	160 to 180	110 – 110°C	Same
with perchlorate	170 to 180	No critical values	Ignition

limits or cook-off phenomenon. Decomposition occurs through burning. Test results that are now available demonstrate that their decomposition is directly controlled by the consumption of the nitric ester stabilizers of the formulation. The reaction temperature is independent of the size of the specimen.

3.2.4.3. *Fast cook-off and slow cook-off*

These terms describe thermal stimuli observed, typically, in munitions in an operating environment.

- Fast cook-off corresponds to a munition exposed to an intense and direct fire. The munition is engulfed within the flames.
- Slow cook-off corresponds to a munition subjected to a relatively low heat flux. Under these conditions it is understandable that the temperature of the munition increases very slowly.

The tests discussed in Sections 3.2.4.1. and 3.2.4.2. can also be used to study this type of slower thermal stimulus.

3.2.5. Sensitivity to static electricity

3.2.5.1. Background

Until 1975, France, like most other countries, performed a test using around 100 mg of propellant to determine its electrostatic sensitivity. This test is comparable to the Picatinny Arsenal test [12] and is shown in Fig. 17. In this test, propellants in the shape of compact discs were always found insensitive. Occasionally, after some tests, the propellant discs were found to have a very small axial hole.

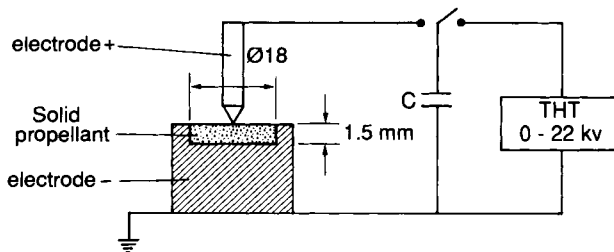


FIG. 7.17. Sketch of initiation by electrical spark.

3.2.5.2. Recommended operational method for the tests

During the 1970s, ignitions of composite propellant grains occurred in manufacturing facilities. Investigations demonstrated that these ignitions could only have been caused by static electricity.

Additional tests were then performed, leading to the adoption of a new testing method that proved to be more representative of the accidents that had occurred [13]. The principle of this new method is shown in Fig. 18.

Using a pointed electrode, the propellant grain ($\varnothing = 90$ mm, height = 100 mm) is subjected to the discharge measuring 34.7 nF, charged at 30 kV. Thirty successive discharges are released into the grain. The result is considered as negative when there are no cracks and no ignition. A composition is declared electrostatic-insensitive when negative results have

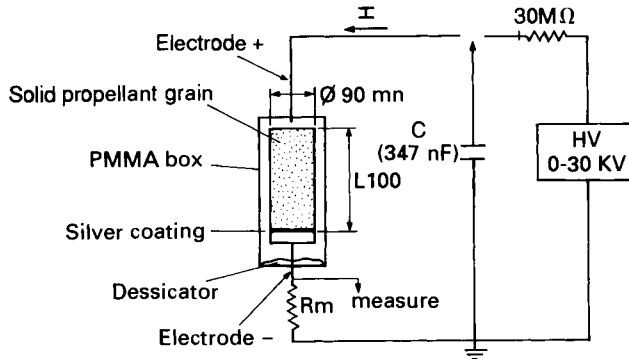


FIG. 7.18. Sketch of the testing setup for electrostatic.

been obtained on three grains of that propellant composition, at the specific temperature. Further details can be found in the chapter on composite propellants (Chapter 10).

4. Assessment of the Risks Presented by Propellant Grains

A risk assessment consists of assigning a probability of occurrence to each potential hazard, for each phase of the life of propellant grain. There are two traditional methods used:

- the regulatory approach;
- the analytical study.

4.1. THE REGULATORY APPROACH

4.1.1. Major regulations

The propellant industry is subject to the application of various regulations. The most general in its scope of these regulations is the UN Recommendation [15].

Generally speaking, these regulations establish hazard categories or sections for the various explosive substances, solid propellants in this case, corresponding for the most part to the pyrotechnic effects likely to be encountered.

Table 5 provides, for example, the definitions of the hazards divisions of the French Labor Regulation (almost the same definition as UN).

They also provide data for a decision chart, based on tests or experiments whose results have been quantified and compared with criteria or sanctions

TABLE 5 *Classification of hazards of explosive substances and objects*

Class number	Division number	Characteristics of the substances or articles in this section
1	1	Substances or articles essentially involving a mass explosion hazard, i.e. affecting almost the entire load virtually instantaneously.
	2	Substances or articles involving a projection hazard but no mass explosion hazard.
	3	Substances or articles involving a fire hazard with a minor blast or projection hazard, and no mass explosion hazard. This division includes the following two subdivisions: Subdivision 3a, consisting of substances or articles whose combustion gives rise to considerable radiant heat; Subdivision 3b, consisting of substances or articles that burn fairly slowly, or burning one after the other with minor blast and projection effects.
	4	Substances or articles involving no significant hazard, designed or packed so as to exhibit only relatively minor hazard or whose effects, in case of ignition or initiation, do not give rise to the projection of fragments of appreciable size, and remain in any case small enough not to significantly hinder fire-fighting operations and the application of emergency measures.
	5	Substances that are, when they explode, as hazardous as those of Section 1, but that are relatively insensitive. These substances display a very low probability of initiation and transition from combustion to detonation except when in large amounts in a small and confined space. They may not explode when exposed to outside fire.

allowing the classification of the product into one or another of the hazards divisions defined in Table 5.

Finally, they provide a general definition of the dispositions, precautions and facility designs for the established classes of products.

National or international regulations on transport, storage, possession, and use of hazardous substances are being or have been revised in accordance with the UN recommendations.

The differences existing between the procedures are explained by the fact that these regulations take implicitly into account the probability of the occurrence of a stimulus. It is therefore understandable, for instance, that stimuli considered in the case of storage are different from those in the case of transport.

The only regulation that explicitly considers the probability of the occurrence of pyrotechnic events is the French Labor Regulation [16].

The test most widely used for all regulations is the card gap test. There are, however, various versions of this test, and the criteria followed by the various regulations differ, possibly resulting in making comparisons difficult. The test used in France and related results are described in Section 2. The determination of whether a product should be upgraded from Hazard Division 1.3 to 1.1 is based on card gap tests greater than 240 French cards in France and 70 American cards in the United States, the latter being equivalent to approximately 95 French cards, because the thickness of the cards is different. The positions on this criterion seem to be very far apart. It would be necessary, however, in order to judge the validity of either regulation, to compare them in their entirety and not on that particular point only.

4.1.2. Labor regulations

The assessment of threats and the corresponding assignment to a hazard class in accordance to French labor regulations is particularly applicable to small propellant grains rather than large grains for various reasons, including the significant number of specimens required (i.e. cost and space limitations). The assignment to a hazard class is done based on a procedure which includes a series of tests, and is applied to new explosive substances or articles (such as free-standing grains, rocket motors, and others).

The procedure involves five steps:

The first step involved in this classification consists of determining whether the rocket motor or the propellant grain is a new type or “insufficiently known”.

Of course, when the design of the rocket motor, or the propellant grains, shapes or compositions, is in fact very new, it is *ipso facto* insufficiently known. But this case is a very rare one, and what is termed as new is the result, in practice, of more or less extensive modifications to existing, known propellant grains.

In practice, to be able to avoid having to perform all required tests, it is necessary to provide proofs that a new propellant or motor can be placed in the same category as existing propellants or motors.

These studies and analyses, which make up the first step of the procedure, can be summarized as follows:

- acquire the technical elements of the definition of the type of propellant grain or motor under consideration;
- identify the differences;
- analyze these differences;
- conclude whether the analogy is reasonable — if it is not, proceed to the second step.

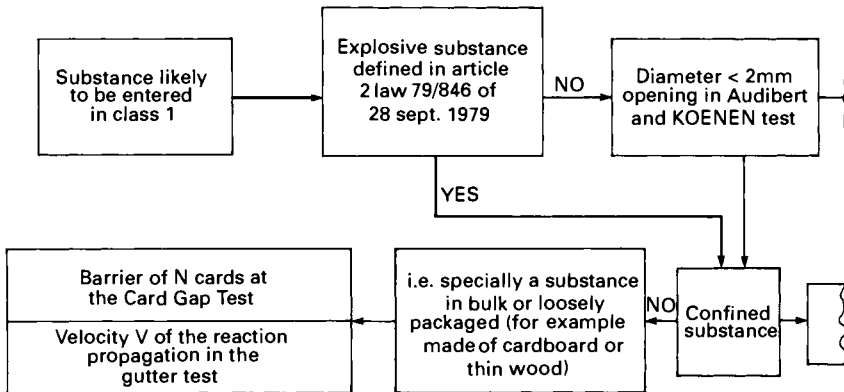


FIG. 7.19. Procedure to include propellant grains in hazards divisions—right part of the decision flow-chart.

When in doubt, the higher hazard class is selected, as described above. Tailoring of the procedure to the case of propellant grains is discussed below. The beginning of the path is shown by the thicker line in Fig. 19, within a general decision flow-chart.

The second difficulty involved in the classification, based on the flow-chart, is coming to a conclusion about the meaning of the word “confinement.” Consequently, the second step consists of qualifying the confinement of a propellant grain.

One possible method is:

The “decision chart” indicates that the substances in bulk, or loosely packed (i.e. in a cardboard box, or a thin wood box) are considered to be “not confined,” or “in an object that provides no confinement”.

This confinement concept aims essentially at ensuring that the risks of transition from deflagration to detonation are taken into account. Furthermore, we know that a propellant will not transit to detonation unless it has been previously finely fragmented after, for example, an early-damaged material.

As long as the constituent material of the grain is undamaged and solid, the propellant grain itself becomes in some ways like an open container. We are able, then, to consider that the confinement is tied only to the Klemmung of the propellant grain and to the probable effects of the bursting of the motor, whether it acts as a container under pressure or it is case-confined in the case of accidental burning. A technical equivalence of the confinement concept may then be suggested for the rocket motor.

The technical equivalence of the definition for the expected confinement is specific to the particular object that a solid propellant motor constitutes.

When the four following conditions are satisfied simultaneously, it is said that there is no confinement.

- *First condition.* This concerns the propellant constituting the solid propellant grain.

This propellant must burn in a normal layerwise manner up to very high pressure levels.

- *Second condition.* This requirement is related to the violence of the eventual bursting of the container under pressure, which is the propellant grain itself in the case of accidental burning.

Precise specifications related to the characteristics of the propellant and its case are used to determine these two conditions.

- *Third condition.* The propellant grain is loosely packaged, or not at all (absence of confinement from packaging).
- *Fourth condition.* The storage condition of a number of rocket motors does not create any significant additional confinement (absence of confinement in storage).

When all four conditions are satisfied we may say that there is no confinement and the left portion of the decision chart is used. If even one of these conditions is not satisfied, the right side of the decision chart is used.

The following steps consist of characterizing the situation and following the applicable procedure for classification.

Finally, the fifth and last step consists of ensuring that the quality assurance of the program guarantees that each propellant grain or rocket motor will have the same characteristics of the specimens used to perform the classification tests.

4.2. ANALYTICAL ASSESSMENT

This method is much more general and complete than the preceding one [17]. It is better suited for large rocket motors.

Three steps are involved:

The first step consists of preparing an exhaustive list of all possible stimuli. By stimuli, we mean both a stimulus proper, i.e. coming from the outside, and possible failures of the system, in particular, a defective operation. The list created must show, for each stimulus:

- the probability of the stimulus;
- the gravity of the stimulus (such as among other things, intensity and duration).

The second step consists of creating a general scenario of the behavior of the rocket motors under the various stimuli identified in the first step. A typical scenario is shown in Fig. 20. The goal of this type of scenario is to assess the

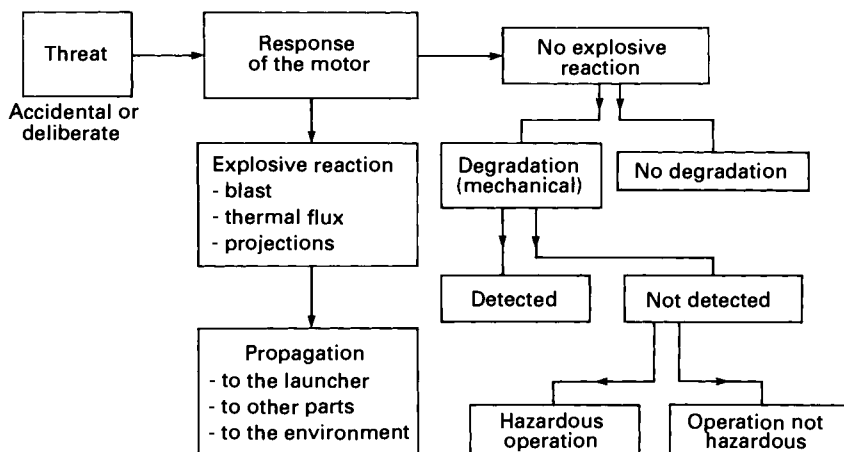


FIG. 7.20. General scenario of the behavior of a rocket motor faced with a threat.

explosive hazards and to discover eventual degradations and their consequences.

The third step involves the analysis of the possible behavior of the rocket motor for a specific stimulus. A sample of an analysis is given in Fig. 21, for the case of a threat resulting from a shaped charge.

The result of this analysis is the probability of an undesirable pyrotechnic event.

For the third step, the following are indispensable to be able to quantify the probability:

- the performance of basic tests;
- the use of computer codes;
- the performance of tests on models.

For instance, the example in Fig. 21 requires, among other things:

- knowledge of the critical detonation diameter of the composition, which is a basic test;
- determination of the fragmentation condition due to the stimuli, which requires the use of a code.

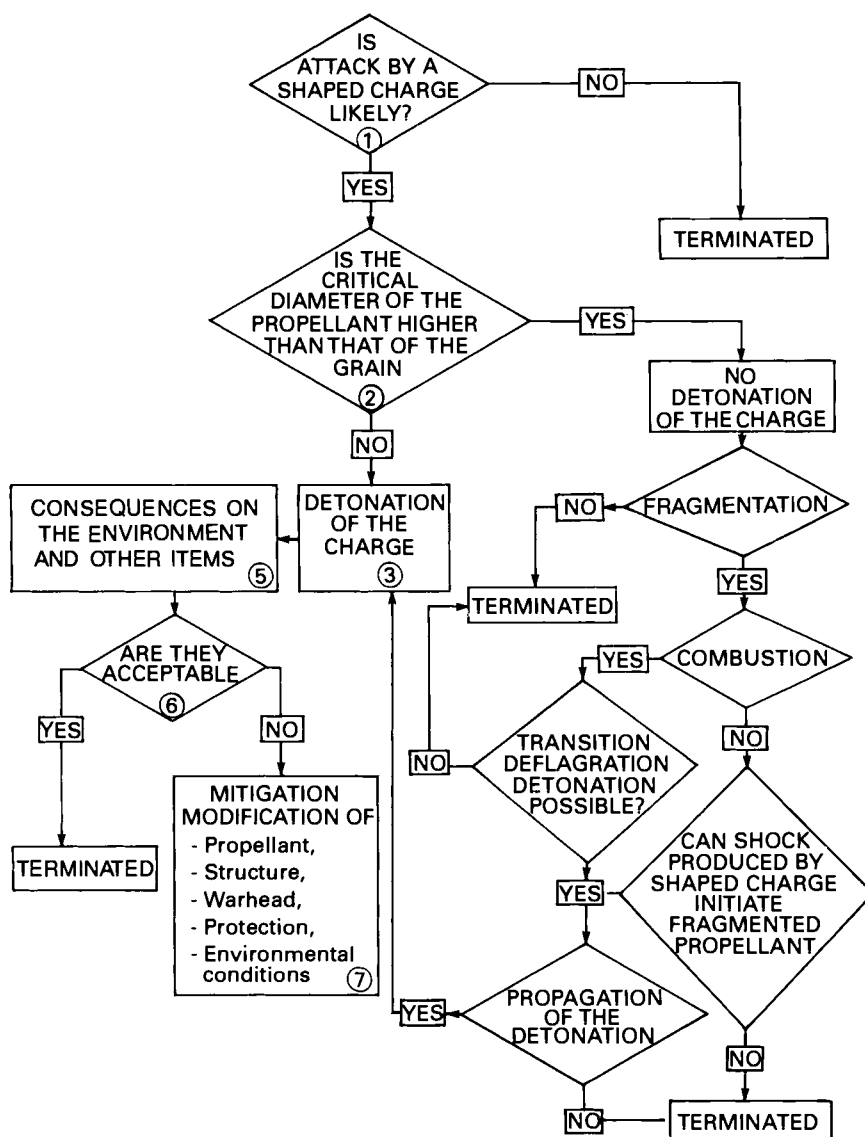


FIG. 7.21. Analysis of an attack by a shaped charge jet.

Bibliography

1. MÉDARD, L., *Les Explosifs Occasionnels*, vol. 1. Propriétés—Collection Technique et Documentation, 1978.
2. KAMENETSKY, F., *Diffusion and Heat Transfer in Chemical Kinetics*. Translated from the Russian edition by N. Thon. Princeton University Press, 1955.

3. PANNINGTHON, F., MAN, T. and PERNOM, B., *Rocket Propulsion Hazard Summary: Safety Classification, Handling Experience and Application to Space Shuttle Payload*. May 1977.
4. WEISS, R. R., VANDERHYDE, N. and MERRILL, C., *Review of USAF Treatment of Solid Propellant Rocket Motor Hazards*. AGARD Conference Proceedings No. 367, 1984.
5. BRUNET, J. and PAULIN, J. L., *Etude de la transition de la déflagration à la détonation des propergols préalablement fragmentés*. AGARD Conference Proceedings No. 367, 1984.
6. LEE, E. L., JAMES, E., GREEN, L., VON HOLLE, W. and TARVER, C., Lawrence Livermore National Laboratory. Curran, D., Murri, W. and Seaman, D., Contributors. Stanford Research International. *Response of Propellants to High Dynamic Stresses. The Uses of Gun Launch Techniques*. AGARD Conference Proceedings No. 367, 1984.
7. KINCAID, J. F., *The Determination of the Propensity for Detonation of High-Performance Propellants*. ICT Jahrestagung, pp. 155–168. Karlsruhe, Germany, 1982.
8. KEEFE, R. L., *Delayed Detonation in Card Gap Tests—7th Symposium on Detonation*, pp. 233, 240, 1981.
9. BLOMMER, E. J., *Delayed Detonation of Propellants in the 25 mm Instrumented Shotgun Test—19th JANNAF Combustion Meeting*, vol. II, pp. 225–246, 1982.
10. NOUGUEZ, B., BERGER, H., GONDOUIN, B. and BRUNET, J., *An Odd Bore Effect on Bullet Induced Detonation of High Energy Propellant Grains*. ADPA symposium, 23–25 October 1989, Virginia Beach.
11. KENT, R. and RAT, M., *Explosion thermique (cook-off) des propergols solides*. *Propellants and Explosives*, 7, 129–136, 1982.
12. WESTGATE, C. R., POLLOCK, B. D. and KIRSHENBAUM, M. R., *Electrostatic Sensitivity Testing for Explosives*. Technical Report 4319. Picatinny Arsenal, Dover, New Jersey, USA.
13. KENT, R. and RAT, M., *Phénomènes d'électricité statique dans la fabrication et la manipulation des propergols solides*. ICT Jahrestagung, 423–438. Karlsruhe, Germany, 1981.
14. KENT, R. and RAT, M., *Static Electricity Phenomena in the Manufacture and Handling of Solid Propellants*. 20th DDESB, Norfolk, Virginia, USA, 1982.
15. *Recommandations relatives au transport des matières dangereuses*. Nations Unies ST/SG/AC.10/1 Rev. 5 and ST/SG/AC 10/11, 1988.
16. *Sécurité pyrotechnique*. Journal officiel de la République Française. 26 Rue Desaix 75727 Paris Cedex 15. No. 1196 ISBN 2 11.0702082.6, 1981.
17. LIEVENS, C., *Sécurité des Systèmes*. Cepadues Editions, Toulouse, 1976.

CHAPTER 8

The Main Families and Use of Solid Propellants

ALAIN DAVENAS

1. Background

The recent and spectacular development of rocket propellants is in sharp contrast to the slow, even non-existent development of materials for propulsion purposes during previous centuries, when the single basic product, black powder, was not sufficient to propel objects by gas jets, in spite of numerous attempts. At the end of the 18th century the main application of this type of propulsion was for entertainment purposes: fireworks. It was not until the beginning of the 19th century that the military began again to take an interest in rockets.

The great industrial growth of that period promoted their development, and it is clear that the history of propulsion is closely linked to the history of the chemical industry which, in a very short time, offered scientists possibilities for research of new products. The 19th century saw the discovery of new basic molecules, such as nitrocellulose and nitroglycerine, followed by much research designed to master their usage as explosives as well as propellants. The end of that century and the beginning of the 20th century witnessed the emergence of the first modern propulsive powders, today's double-base extruded or cast propellants.

The development of propellants is not, however, linked solely to the development of chemistry; ballistics development was a second essential factor. For 150 years the experts doing research in these specific areas judiciously combined their knowledge and efforts to make rocket propulsion what it is today. In the course of time, other research areas were applied to rocket propulsion: mechanics, thermodynamics, fluid mechanics and industrial technologies, etc.

While the second half of the 19th century witnessed the beginning of the development of today's double-base propellants, known in France as "homogeneous propellants," the second half of the 20th century was characterized

by the development of composite propellants containing aluminum and ammonium perchlorate.

Here again, the development was linked to the progress made in chemistry, and in particular to the development of plastic materials, which was very rapid during the Second World War. From 1950 on, polyurethane chemistry found in propellants an ideal area of application. This outlet continues to appear the most significant in industrial terms, as emphasized by Klager [1]. But other systems had been researched before that, and some of their applications are still in existence today, for example the polystyrene-polyesters and polysulfide systems [2], and polyvinyl chlorides [3]. These formulations were developed by large companies, mostly American, who at the time were interested in rocket propulsion. Polystyrene-polyesters, followed by the polyurethanes, resulted from the activities of Aerojet General Corporation and General Tire and Rubber Company. The polysulfides, then polydienic structure products, came from Thiokol Chemical Company and the Jet Propulsion Laboratory. Atlantic Research Company was responsible for PVCs, while Hercules was mostly interested in single and double-base propellants and the possibilities of improving them [4]. Even though, during the past 30 years, the activities of each of these various companies were mainly a function of the sectors of applications they were assigned, they continuously looked for ways to improve performance and link the qualities and advantages of the two basic families. This slowly led to the creation of a new third family of high-energy products, implemented following the typical composite propellant methods, which are known today as composite double-base propellants [4]. Both families were combined and gave birth to high-performance products at the end of the 20th century. Figure 1 gives an

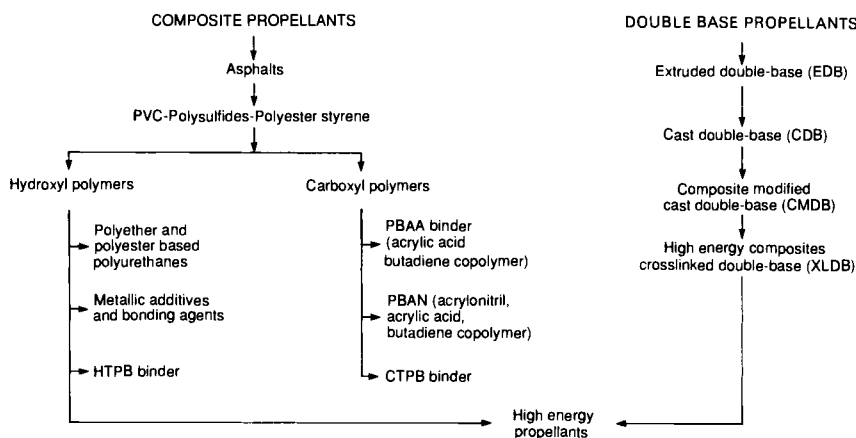


FIG. 8.1. Chronological development of double base propellants and composite propellants.

overview of this evolution through the major improvements brought to the various families of materials.

The development of solid propellants was also accompanied by the development of insulation materials. The research on complementary properties in areas as varied as combustion control, thermal protection of structures, propellant case-bonding, signature, and mechanical behavior, has required the involvement of all sectors of chemistry.

Simplified in the extreme, the development of research in the area of solid propellants has led, as a result, to the existence of two separate major families:

- double-base or homogeneous propellants;
- composite propellants.

Figure 2 provides a basic diagram of their formulation and manufacturing processes.

For more information than is provided by this very quick historical presentation, it will be useful to read the very interesting article published by Lindner [5] in the *Encyclopedia of Chemical Technology*, and in French, the work of Quinchon and Tranchant [6].

2. Utilization in the Propulsion Stages for Missiles or Space Launchers

A color photograph in this book shows the range of industrial grains manufactured by one propellant company, with the various families of propellants grouped according to applications. For each specific application

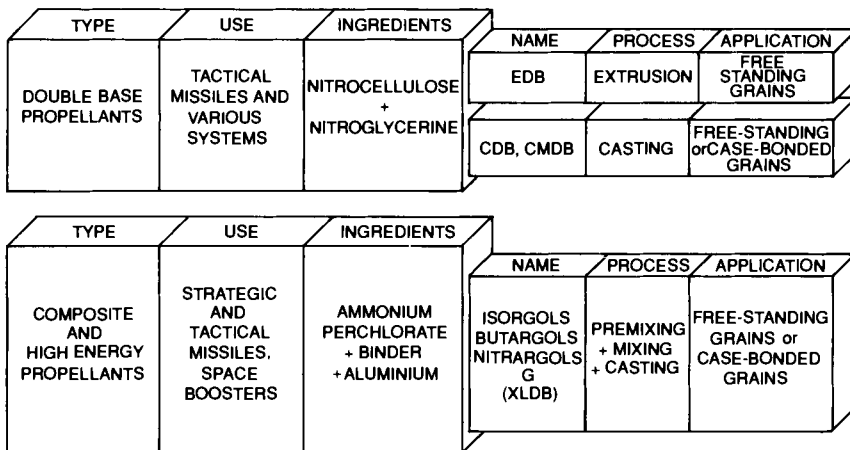


FIG. 8.2. Propellants: use-composition-process.

the technical or industrial specifications dictated the selection of a particular type of grain, through design work, as explained in Chapter 2. However, general trends do emerge: high-mass grains are made with composite propellants or composite double-base (CMDDB) and are case-bonded and those of very low mass are more often made of a homogeneous propellant or smokeless CMDDB or XLDB. So we can see that there are some general principles and criteria that guided their selection.

We shall now look at the manner in which the various propellants respond to the general requirements for the propulsion stages of a missile: requirements for performance, physical and mechanical characteristics, signature, manufacturing processes, cost, safety, and vulnerability.

2.1. PERFORMANCE COMPARISON OF INDUSTRIAL PROPELLANTS

2.1.1. Energy performance

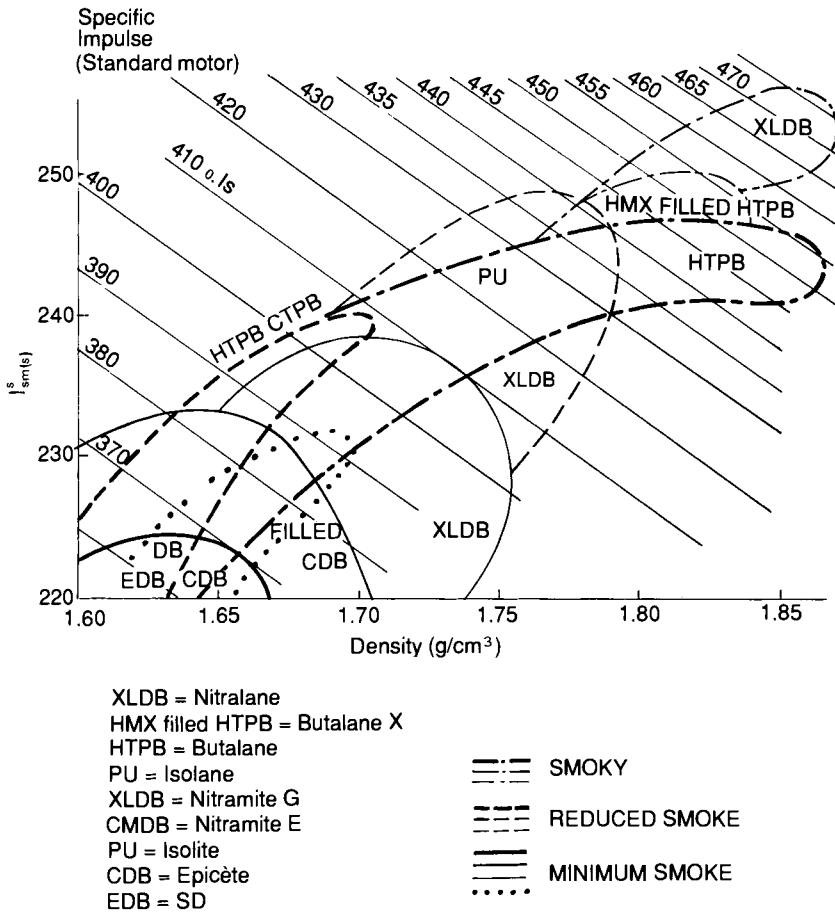
Figure 3 shows the two major energy characteristics of a propellant: the standard specific impulse I_{sm}^s , and density ρ . Very roughly: the greater the product ρI_{sm}^s , volumetric specific impulse, which we are using as the energy index, the better-performing the family being investigated.

On the diagram are the family of "low signature" propellants within the visible range, inside which the Nitramites (smokeless XLDB) perform better than the classic homogeneous EDB and CDB and the family of aluminized propellants with approximately 15% greater performance?

To the non-expert an energy difference of 15% might seem insignificant. In real applications, however, its significance becomes much clearer. Take for example a three-stage ballistic missile with a 10,000 km range and typical range differential coefficient, indicated in Table 1 for stage I and II, carrying respectively a 24.5 and 10 ton propellant grain. The related range increase resulting from the higher performance of the first two stages will be 3370 km;

TABLE 1 *Range differential coefficients for the first two stages of a three-stage missile with a 10,000 km range [7].*

First stage		Second stage
$\frac{\partial P}{\partial M_p}$ (km/kg)	0.4	0.5
$\frac{\partial P}{\partial I_s}$ (km/s)	40	70

FIG. 8.3. Propellant characteristics ρ , I_s .

i.e. a 40% range increase will be gained by this performance increase on all three stages.

Consequently, whenever greater propulsion performance is the primary goal, as is the case for long-range ballistic missiles, space launch boosters, and apogee motors, aluminized composite propellants are preferable.

In the case of tactical missiles a trade-off must be found between performance and signature. It is a delicate trade-off. The search for a reduced signature to prevent early detection of the missile without performance loss has, of course, been the major factor behind the important research done on the nitramite propellants (smokeless propellants based on a nitramine and energetic, nitroplasticized, binder). This criterion might in the future play an

increasing role also for ballistic missiles, with the objective of decreasing the possibility of detecting and destroying these missiles.

2.1.2. Burning rate characteristics

Limitation of propellant burning rates available for a specific project is one of the most frustrating difficulties for the designer who would prefer the use of the greatest possible range of burning rates.

Figure 4 shows the burning rate range, at a given pressure of 7 MPa for the most commonly used propellants. When seeking the highest burning rates the answer lies with composite propellants for the usual burning times for missile propulsion stages (several seconds to several tens of seconds). However, for very short burning times, on the order of a few tens of milliseconds, which are often used for light anti-tank missiles where a low signature is generally required, EDB (extruded double-base) propellants (solventless) are a prime

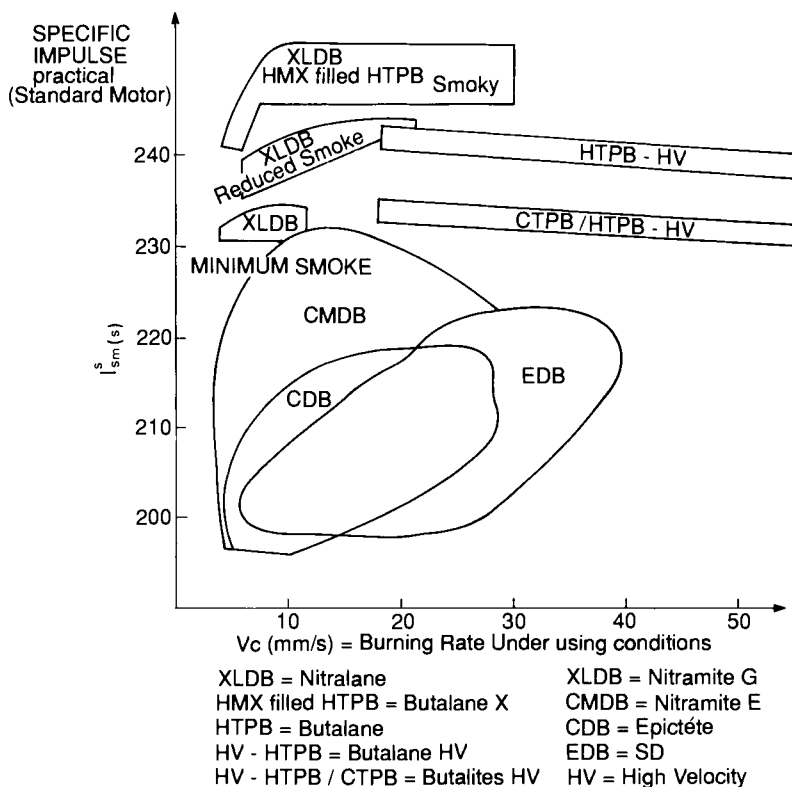


FIG. 8.4. Propellant characteristics.

solution because of their physical properties lending themselves particularly well to designs with thin webs (fraction of a millimeter).

For very long burning times, solutions can be found in every family, although they are always accompanied by a significant decrease in the energy characteristics.

“Average” burning rate ranges can be obtained with every type of propellant. It is useful to know, however, that EDB propellants offer greater burning rates than the CDBs for an equal level of energy. This is a characteristic inherent in the product (Chapter 9). And again, in applications where a large range of operating temperatures is required, the lower temperature coefficient of the homogeneous propellants may compensate for low rates of specific impulse per unit volume. As a matter of fact, with an identical burning time at 20°C, the propellant with the highest temperature coefficient results in a higher maximum working pressure of the grain at high temperatures, necessitating a thicker structure for the motor, resulting in a weight increase. Similarly, the decreased flow rate at low temperatures can have negative effects because of the resultant reduction in thrust.

2.1.3. *Ducted rocket or ramrockets*

Based on energy performance, the choice between a conventional propellant engine or a ramrocket appears obvious for a tactical missile. But taking into consideration the overall constraints, that choice is no longer as clear, as is demonstrated by the relatively limited number of modern applications (missiles with integrated boosters) in existence today: the Soviet SAM 6 and the French ASMP* with liquid ramjet. But there are some cases where the advantages are obvious [8], as demonstrated in Fig. 5 by a plot of the weight

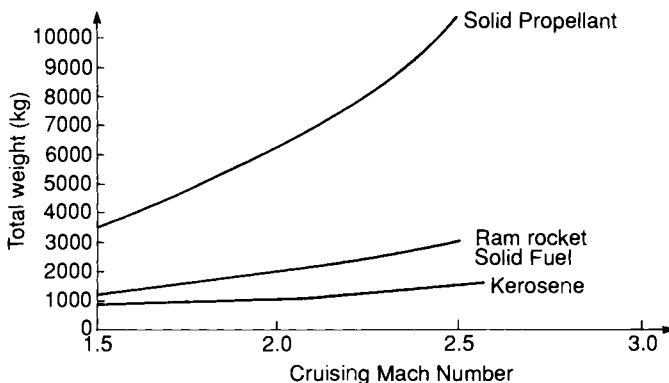


FIG. 8.5. Comparison of propulsion systems.

* Air, Sol, Moyenne Portée: air-to-ground medium range.

of a missile for a zero-altitude mission with a 100 km range, as a function of the cruising Mach number.

2.2. COMPARISON OF PHYSICAL AND MECHANICAL CHARACTERISTICS

These characteristics very often dictate the feasibility of a given architecture, directly influencing performance (volumetric loading ratio, evolution of grain burning surface versus time) and cost.

2.2.1. Mechanical behavior

The mechanical properties of solid propellants are given by the master curves of the parameters S_m , e_m , E_{tg} , and ϵ , which are explained in Chapter 6 and illustrated in Fig. 6.

These curves reveal three distinctive zones, each related to a specific behavior of the material:

- the glassy zone (Zone 1), characterized by a constant modulus in the short time range, indicating a fragile linear elastic behavior;
- the transition zone (Zone 2), in the interim time range, emphasizing the viscoelasticity of the material;
- the rubber-like zone (Zone 3), in the long time range, with stable behavior of the propellant, which can be represented by a law of the type:

$$E_r(t/a_T) = E \cdot (t/a_T)^{-n}$$

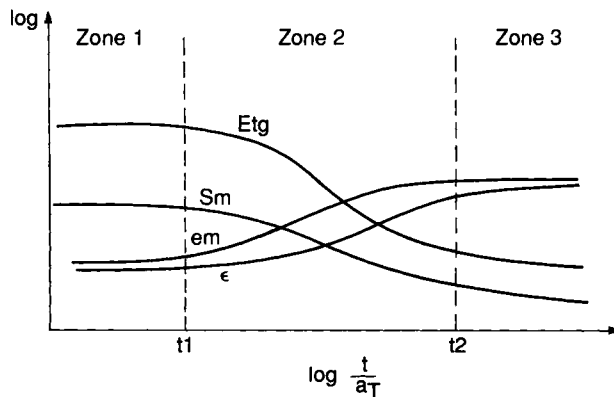


FIG. 8.6. Mechanical behavior of solid propellants.

These three zones are found in all propellant families:

- CDB and CMDB;
- XLDB;
- composites with polyurethane and polybutadiene (HTPB and CTPB) binders.

This allows us to define the following specific parameters:

- width of the transition zone;
- glassy modulus;
- rubber-like modulus.

Width of the transition zone

The transition zone is the zone where the propellant's viscous mechanisms are activated.

The width of the glass transition zone attests to the variety of viscous mechanisms that can be activated. Typical values are given in Table 2, for the various materials.

The glass transition zone of composites and XLDB is reached during load times that are shorter than the usual pressurization times at low temperature. These propellants are therefore very rarely stressed in the glass states.

All propellants show a relatively stable behavior, significant strain at rupture, and a time of relaxation under constant load stress/strain for equivalent times greater than 10^5 min, which corresponds to long-term storage (over 1 year).

Glassy modulus-rubbery modulus

The glassy transition zone is characterized by the values of the elasticity modulus.

The behavior for long times specific to each propellant can be represented by the following type of equation:

$$E_r\left(\frac{t}{a_T}\right) = E \cdot \left(\frac{t}{a_T}\right)^{-n}$$

It is therefore impossible to establish a rubber-like modulus as described for classic linear viscoelastic materials ($E = \text{constant}$). For comparison purposes

TABLE 2 *Width of the glass transition zones of the main propellants*

	Propellant					
	EDB	CDB	PU	HTPB	CTPB	XLDB
t_1 to t_2 (in mn)	10^{-4} to 10^5	10^{-6} to 10^0	10^{-12} to 10^0	10^{-8} to 10^0	10^{-9} to 10^2	10^{-14} to 10^{-2}
Width (tens of mn)	8	5	11	7	10	11

TABLE 3 *Relaxation modulus of propellants for long-term storage*

	Propellant					
	EDB	CDB	PU	CTPB	HTPB	XLDB
E_{glass} (MPa)	2000	1000	3000	300	200	2000
$E_{\infty}(10^7)$ (MPa)	3	1.5	2	0.7	0.5	1.5

between the various propellant families, the modulus at $t/a_T = 10^7$ min is used in Table 3.

The family of propellants we are looking at shows two types of behavior:

- high glassy modulus materials: EDB, CDB, PU, XLDB;
- low glassy modulus materials: CTPB and HTPB composites.

In addition, the transition is much more pronounced for materials that are very stiff at low temperatures than for polybutadiene propellants.

- $E_{\text{glassy}}/E_{\infty} \sim 1000$ for polyurethanes, EDB, CDB and XLDB;
- $E_{\text{glassy}}/E_{\infty} \sim 500$ for polybutadiene composite propellants.

The various behavioral criteria examined above provide a glimpse at the behavior of propellants during the various loading zones (firing, storage, etc.). However, to be able to judge the capability of a family of propellants to handle a given load, we will have to analyze the result of a parameter characterizing its behavior.

2.2.2. Mechanical resistance

2.2.2.1. Analysis of the most severe loads

(a) Long-term storage, thermal cycles, firing/ignition

In long-term storage and thermal cycles, strains inside the grain caused by volumetric variations of the propellants are constant over time for a specific range of temperatures.

This type of loading is similar to a relaxation test (constant strain), and the behavior at relaxation is the parameter that must be studied.

Through experiments we have discovered that the maximum strain during tensile test (e_m) is representative of that behavior.

In the firing of a case-bonded grain, strains are caused by the deformation of the case resulting from pressurization occurring during ignition. This phenomenon is comparable to a tensile test performed under temperature and stress rates corresponding to firing conditions.

Assuming a linear elastic behavior, the resistance parameter will be the pseudo-elastic deformation:

$$\varepsilon = \frac{S_m}{E_{tg}}$$

Four operating zones will be selected from the master curve of the propellants investigated.

- Firing of a grain for tactical missile at low temperatures:
temperature, $\theta = -30^\circ\text{C}$ (for example),
Ignition time: $t_i = 30$ ms.
- Firing of a ballistic or space missile grain at ambient temperature:
temperature, $\theta = 20^\circ\text{C}$,
Ignition time, $t_i = 200$ ms.
- Thermal cycles of a grain for a tactical missile:
minimum temperature, $\theta = -30^\circ\text{C}$,
storage time, $t = 200$ h.
- Long term storage of a ballistic or space missile grain:
storage temperature, $\theta = 20^\circ\text{C}$,
storage time, $t = 10$ years.

The pseudo-elastic deformation at firing and the strain at maximum stress are indicated in Table 4, for all four zones described above.

Cold-temperature firing

The propellants best suited for firing at low temperature, using case-bonded grains, are CTPB and HTPB, and XLDB.

Propellant types EDB and CDB, as well as the polyurethane composite of Table 6, show insufficient deformation capability to withstand the case deformation during firing.

TABLE 4 *Propellant mechanical capability at firing and under thermal stress*

	Propellant					
	EDB	CDB	PU	CTPB	HTPB	XLDB
Low-temperature firing $\varepsilon(\%)$	4.3	2.8	2.4	5.6	6	8.1
Ambient-temperature firing $\varepsilon(\%)$	4.3	10.5	16.5	12.5	13	13.5
Cold cycle $e_m(\%)$	18.5	42	40	35	38	80
Long-term storage $e_m(\%)$	24	60	20	35	42	60

From a mechanical point of view they can be used only for free-standing grains which are subjected to less stress at low temperatures.

Ambient-temperature firing

The HTPB, CTPB, polyurethane, CDB and XLDB propellants have a greater capability than the EDB. Therefore, they will show a better mechanical behavior at ambient temperature firing of case-bonded grains.

Cold thermal cycle

The CDB, polyurethane, CTPB and HTPB and XLDB propellants have maximum strain above 35%, and consequently good mechanical resistance to thermal cycles.

The elongation capability of EDB is definitely smaller ($e_m \sim 18\%$), and could, as a result, lead to some risks of rupture during severe thermal shock, even for a free-standing grain structure.

Long-term storage (Fig. 7)

In this stress-strain situation typical of case-bonded grains HTPB, CTPB, CDB and XLDB the best mechanical capability.

Even though CDB has a great deformation capability we cannot place it ahead of the other propellants for this type of load, because the thermal expansion coefficient plays a significant role, leading to an increase of the thermal stress in the grains:

$$\begin{aligned}\alpha_p &\sim 1 \times 10^{-4} \text{ } ^\circ\text{C}^{-1} \text{ for composites} \\ \alpha_p &\sim 2 \times 10^{-4} \text{ } ^\circ\text{C}^{-1} \text{ for CDB}\end{aligned}$$

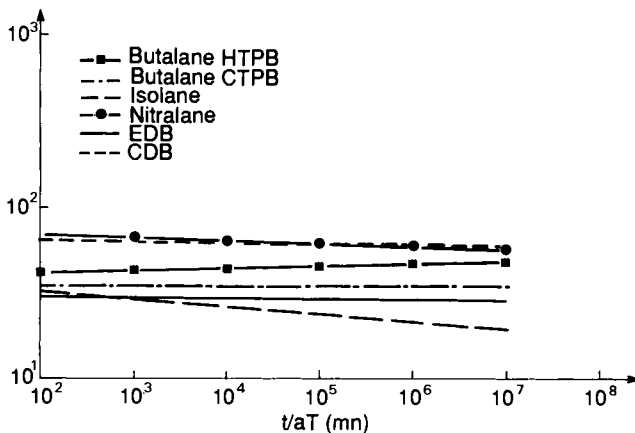


FIG. 8.7. Long term storage behavior of various propellants.

2.2.2.2. Conclusions

Analysis of the various parameters of the behavior and strain capabilities of the main propellant families provides us with the following conclusions:

- *Propellant grain for tactical missiles.* From a strictly mechanical point of view, only the polybutadiene and XLDB propellants can be used for case-bonded grains, because of their good mechanical resistance during firing at low temperatures. EDB and CDB propellants, as well as the polyurethane propellant discussed above, can be used only for free-standing grain, because of their high modulus and their low capability for deformation under this particular stress. In this type of design, mechanical resistance to thermal shocks is greater for CDB than for EDB propellants.
- *Propellant grain for ballistic motors/missiles: $= 20^{\circ}\text{C}$.* The CTPB, HTPB, polyurethane, CDB, XLDB propellants can be used in case-bonded grains. However, CDB demonstrates the lowest mechanical resistance to firing, as well as to long-term storage, due to its high thermal expansion coefficient. The capability of the polyurethane tends to decrease under long-term storage: therefore the HTPB and CTPB and XLDB propellants are preferable.

2.3. COMPARISON OF SIGNATURES AND SIGNATURE CHARACTERISTICS

The most dramatic aspect is, of course, the visible signature which marks the launching of a ballistic missile or the space shuttle with a huge plume of white smoke. That visible smoke is characteristic of propellants with aluminum (primary alumina fumes). More generally, it is characteristic of metallized propellants and in the case of ammonium perchlorate composites without aluminum of the recondensation of hydrochloric acid when the suitable ambient temperature and humidity conditions are present (secondary smoke).

Figure 8 shows the smoke occurrence, and illustrates its intensity for various propellants under average climatic conditions in Europe.

In the case of a missile target that is followed visually, these smokes completely mask the target and are absolutely unacceptable. As a result the first generations of anti-tank or ground-air missiles were forced to use homogeneous propellants. Today, these could be replaced by Nitramites (minimum smoke XLDB propellants).

Today's guidance systems rely mainly on the interaction of the plume with laser beams within the infrared frequencies, requiring low absorption by the combustion gases in the corresponding frequencies. Similarly, the infrared signature resulting from the plume emission is often related to afterburning in the atmosphere, which should be decreased or eliminated. The related criteria

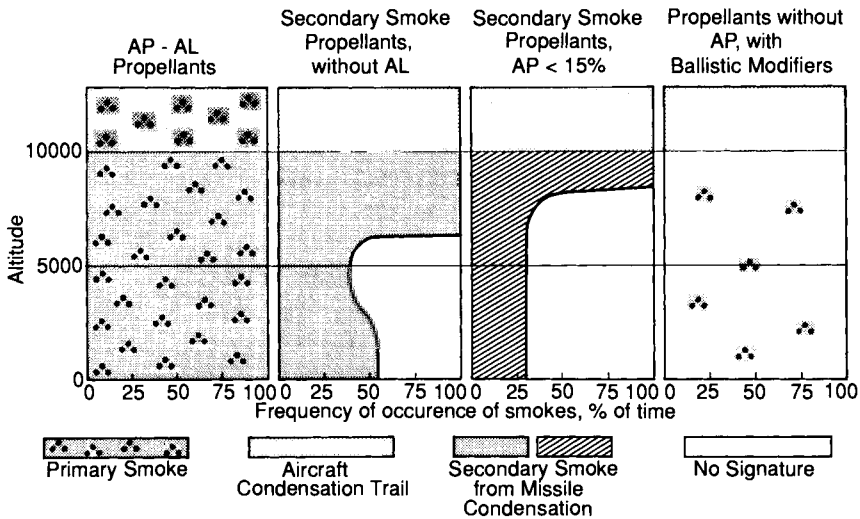


FIG. 8.8. Appearance of visible signature of missiles in a European climate.

are more subtle. Some of the characteristics of plume emissions of propellant gases are indicated in Chapter 5, and can provide initial direction.

2.4. COMPARISON OF MANUFACTURING PROCESSES AND COSTS

Figure 2 gave an overview of the flow-chart for the production of propellants.

EDB grains obtained by extrusion are clearly limited in their mass and size. These limitations are mainly due to the size and the performance of the presses that can be used. Diameters are generally limited to 250 mm in the Western world.

Similarly, only cylindrical grains simple to manufacture, and therefore inexpensive, can be produced.

The EDB process, on the other hand, lends itself particularly well to industrial production as well as to high production rates. It is therefore particularly suited for the production of small ammunitions, and for various non-military applications. The homogeneity of this product and its high degree of rigidity, allowing the production of very thin webs as well as the possibility of machining within very precise limits (a few hundredths of a millimeter), makes it very useful when seeking high-precision impulses. In addition, the combination of rigidity and very thin webs is attractive for grains combining short combustion times with high accelerations — useful for light anti-tank missiles.

Finally, processes such as continuous screw extrusion and stamping may well give new impetus to this product by contributing to a decrease in costs or improvements in working conditions, production rates, or geometry (see Chapter 9).

The CDB and CMDB propellants have the advantage of allowing the production of free-standing grains in any type of shape with performances that are comparable to that of the EDBs. Free-standing grains weighing several tons manufactured by this process were used on propulsion stages of US missiles. In France, free-standing grains weighing several hundred kilograms are used in the sustainer motors of the Exocet missile family.

2.4.1. *The industrial cycles*

The length of the production cycle is of critical importance for the client. It is, of course, determined not only by the type of propellant but also by the production capability available and by the number of specific tools and equipment required for production.

All things being equal, a classification of the length of production cycles would be in the following increasing order: EDB, composites or XLDB, CDB (or CMDB).

The production of EDB grains with selected raw materials is almost instantaneous as they are thermoplastics shaped directly. The length of the cycle is controlled by finishing and quality control operations.

At the other end of the scale, the production of CDB is very slow, requiring various intermediate production steps, as well as ballistic adjustment of the casting powder, requiring firing test controls on specially cast specimens.

The decision to select a free-standing grain or a case-bonded grain is, of course, greatly dependent on the industrial production of the motors. In the case of free-standing grains the production of the cases and of the grains can be done separately, allowing the creation of buffer stocks in case of production difficulties in one of the other production lines.

2.4.2. *Costs*

The issue of the cost of propellants is important both for the client and the manufacturer; it is also the object of many controversies.

Without pretending to do an in-depth analysis of this problem, it may be useful to look at the subject and to determine several major factors. The cost of a propellant grain is linked to four main parameters:

- cost of the raw material;
- manufacturing process;
- quantities required and delivery schedules stipulated;
- technical specifications, including conditions for acceptance and control.

Of course, there is an interaction between the selection of the propellant grain (and its manufacturing process) and the specifications requested by the client. A constructive dialog is necessary to avoid certain specifications unnecessarily increasing the complexity and thereby the cost of the propellant grain.

- When the volume and the duration of the manufacturing process allow the organization of a specific production facility (as in the case of the MLRS), the cost may decrease significantly.
- The cost of raw material may also be an essential factor, e.g. XLDB using HMX of very specific particle size, or special nitrate esters (BTTN) are intrinsically more expensive than a simple composite propellant.

Cost comparisons between various supplies in various countries are difficult for at least two reasons:

- the quantities required and production schedules are rarely the same;
- the rules followed to determine cost (e.g. amortization rules, raw material sometimes supplied free by the Government, investments that are or are not compensated by the client) vary greatly.

Finally, the calculations are often expressed in terms of the cost of the complete motor, and not of the propellant grain.

This raises the very interesting issue of the relative costs of various services involved in the production of a rocket motor.

Gaunt has done an analysis of that issue [9] for ballistic missiles and motors for space launchers. Figure 9 shows that the grain averages approximately 27% of the total cost. This ratio is very similar to observations made in France. In these two specific cases, nozzles and the thermal protection are especially expensive; that ratio is usually much smaller for tactical missile

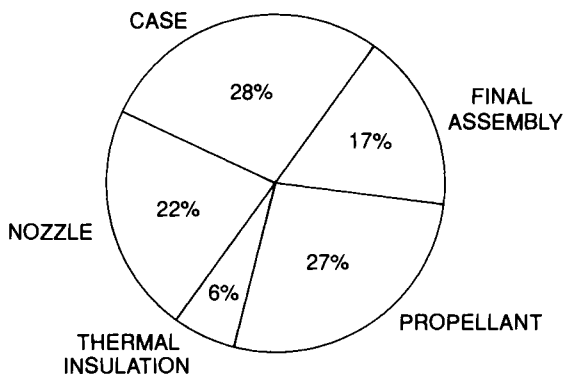


FIG. 8.9. Breakdown relative costs for a large motor.

motors with a less sophisticated rear assembly, in which case the grain cost can be as high as 50% of the total.

The same analysis demonstrates that the principal component of the production cost for today's rocket motors is labor (an average of 55% of the total cost). Cost reduction is obtained through intensive automation, requiring heavy investments that can only be amortized if very large programs are launched.

Finally some simple things can be said for the cost of the different propellant families:

- For composite propellants, the mass of propellant has a very important effect on the price of propellant per kilogram.
- A precise comparison can only be obtained on a specific project. For instance, for a small propellant grain (a few kilograms) for an anti-tank system, we compared the cost of an EDB and CDB solution, both compatible with the specifications, and discovered that their predicted cost was so close that it was impossible to consider this parameter for the final choice.

2.5. SAFETY AND VULNERABILITY CHARACTERISTICS

The client, whether the integrator or the end-user, is particularly interested in these characteristics because they are the determining factor for size of final assembly facilities, storage areas, conditions for transport, and handling and operations. The operational risks vary with the setting: for example, the use of missiles under war conditions, or for space launchers, the risk of lightning strikes on the launch pad, etc.

Here again, we must emphasize the relative and somewhat arbitrary nature of individual national regulations that complicate attempts to establish comparisons at an international level. Although the regulations tend to be similar in their hazard classification of explosive substances, the classification methods are not the same. An identical propellant or grain — CMDB, for instance — can be found in a class 1.1 in the US (liable to detonate), and class 1.3 in France (see Chapter 7).

In addition, these classification tests were established for production, storage and transportation purposes. Reactions to stimuli in operational conditions are not necessarily well characterized by these tests.

For several years, in the wake of serious incidents, or accidents that took on catastrophic proportions such as those on the American aircraft carriers *Forrestal* and *Nimitz*, emphasis has been placed on the concept of “lower sensitivity munition”. Missiles conforming to this designation will be considered as “reduced risk ammunitions” (Munitions à Risques Atténués — MURAT — in French) and “insensitive ammunition” in English.

2.5.1. *Pyrotechnic threats from munitions*

All munitions containing any energetic material (the term “munitions” refers to armament devices of any caliber and includes mines, torpedoes, missiles, and rockets) present pyrotechnic threats. Any munition that has been subjected to unplanned stimuli (e.g. from a bullet or a shaped charge) is not only likely to have been damaged, but its energetic material (gunpowder, propellant, explosives) will probably also deteriorate or react. The reaction of the munition generates thermal fluxes, a release of debris and shock overpressures in its surroundings. The detonation of the first munition can induce a reaction in other munitions nearby. The ensuing disaster may result in the loss of the carrier, known as the combat platform (e.g. tank, helicopter, aircraft, warship, aircraft carrier) with munitions aboard.

2.5.2. *Survivability of the combat platform*

Today, these platforms are extremely expensive, and as a result are limited in number. Defense organizations in various countries are greatly concerned with the improvement of their survivability. Such an improvement involves:

- diminished detectability;
- diminished probability of being hit, once detected;
- reduced severity of the damage, once the platform has been hit.

The general improvement in the survivability of land, air, and sea platforms is a major aspect of armament modernization. It requires a minimization of the effects of explosive hazards from munitions subjected to unplanned stimuli, contributing to the reduction of the vulnerability of the platform by limiting the severity of the reaction and subsequent damage in a credible event.

2.5.3. *Basic corrective measures*

These are as follows:

- protection with materials designed to reduce the impact of the stimuli, barriers to slow down or prevent the propagation of the disaster, and adapted storage configuration;
- intervention devices, including flooding, more or less automatic;
- modification of the cases containing the energetic material (for example, pressure relief systems).

2.5.4. *Need for improvements*

The above measures have the advantage of being rapidly implementable. Unfortunately, their application is not always practical. Protective materials are often heavy, cumbersome, and they hinder the operation of the munition.

Worse yet, these remedies can, over time, turn out to be useless. The great variety of scenarios of credible events makes it particularly difficult to demonstrate the efficiency of these measures.

As a result, the expected minimization of severity could prove entirely misleading. Recognizing this, various defense organizations and industry leaders began to consider the possibility of lowering the sensitivity of munitions, the third step in this process. Progress made in the area of chemical explosives for nuclear warheads and explosives for mining and demolition suggests the possibility of having munitions that reliably fulfill their performance and operational requirements, but which are designed to minimize their sensitivity.

2.5.5. Lower sensitivity munitions or insensitive munitions

The design of these new munitions, particularly at the research stage, must be based on the following conditions:

- specially designed cases;
- revised inner configuration;
- energetic materials with limited reaction.

The last of these conditions, alone, could provide a satisfactory solution to the problem, provided, however, that the survivability is not adversely affected.

Specifications have already been introduced by the US Navy, the prime force behind this activity. The related tests and criteria are shown in Table 5. For propellants, the following data must be determined and provided:

- Test results for:
 - slow cook-off,
 - fast cook-off,
 - sympathetic detonation,
 - impact from multiple bullets,
 - impact from multiple fragments;
- Critical diameter data.

The threat of fire, alone, is generally considered acceptable if thermal explosions, and particularly detonations, are prevented.

TABLE 5 *Tests and criteria for lower-sensitivity munitions*

Slow cook-off	No reaction greater than fire
Fast cook-off	No reaction greater than fire
Bullet impact	No reaction greater than fire
Sympathetic detonation	Unacceptable for storage
Sensitivity to electromagnetic radiation	No explosive reaction

Systematic research has been undertaken in various countries with the purpose of establishing or completing the characterizations of existing energetic materials. This research sometimes leads to unexpected results, and the meaning or consequences of those results remain to be determined. An example is significant variations in the critical diameter of polybutadiene-AP-Al propellants according to the percentage of ferrocene derivative in the formulation [10]. All composites with ammonium perchlorate propellants show very poor results in the slow cook-off tests.

It is too soon yet to have formed any conclusions on the respective merits of existing propellants. A new perspective must be gained, and it will take several years. Most likely, no existing propellant providing sufficient energy will ever satisfy all requirements. For example: a sub-critical detonation geometry requirement for double-base grains or XLDB could lead to a considerable energy loss for smokeless propellants. However, various labs are working on the development of lower-sensitivity high-energy smokeless propellants, based on logical decisions such as those illustrated by Fig. 10.

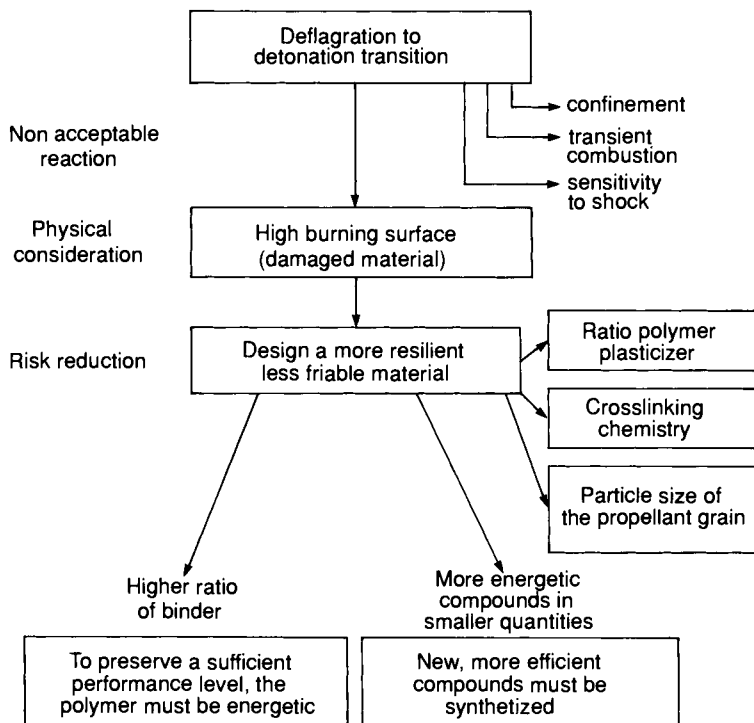


FIG. 8.10. Demonstration of how the formulation of an energetic material can reduce the threats.

3. Additional Propulsion for Artillery

Increase in range and improvement of the accuracy of impact are two major concerns in the design of artillery munitions. A technical solution to satisfy these requirements consists of the injection, at low rate, of gases in the vicinity of the base of the shell, to compensate partly or entirely for the aerodynamic drag of the base.

The location of the ejectors will determine the selection of the configuration:

- The systems with ejectors located at the very base of the projectile are commonly known by the English term “base-bleed” [13]. This configuration is illustrated in Fig. 11.
- The systems with ejectors located over the perimeter of the afterbody, ejecting gases in the outer supersonic flow area, are termed external combustion.

A description of the base-bleed system follows:

3.1. PRINCIPLE FOR THE DECREASE OF BASE DRAG

In modern artillery, base drag is 30–50% of the projectile total drag. It is represented by the nondimensional coefficient, C_x base, expressed by the

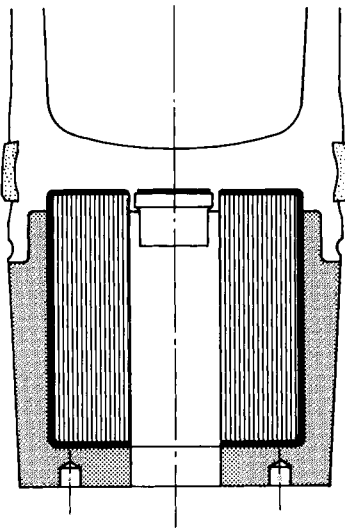


FIG. 8.11. Aft-end of a shell equipped with a base-bleed generator.

formula:

$$C_x \text{ base} = \frac{p_\infty - p_{\text{base}}}{\frac{1}{2} \rho_\infty V_\infty^2}$$

where p , ρ , and V stand for pressure, density and speed of supersonic outer flow, base, base pressure.

By ejecting gases at a low rate directly into the low-pressure zone, the base pressure can be raised, thereby decreasing the C_x base drag coefficient.

The model of drag correction selected for combustion of a base-bleed grain is taken from the works of the Swedish scientist, Hellgren [14].

C_x corrected: $C_x \text{ total} - C \text{ dec. } C_x \text{ base}$
 with $C_x \text{ total}$: Total drag coefficient without base-bleed
 $C_x \text{ base}$: Drag coefficient without base-bleed
 $C \text{ dec.}$: Decrease factor for the base-bleed effect.

The $C \text{ dec.}$ parameter is, essentially, a function of flight conditions, rate of exhaust gases, and the shape of the afterbody.

The drag reduction effects increase with the V_0 initial speed of the projectile. The increased range of a maximum range firing is estimated at:

$$\begin{aligned} &+20\% \text{ for } V_0 = 800 \text{ m/s;} \\ &+25\% \text{ for } V_0 = 900 \text{ m/s.} \end{aligned}$$

3.2. OPERATION SPECIFICATIONS FOR A BASE-BLEED GAS GENERATOR

The base-bleed gas generator is designed to satisfy the following specifications:

- The internal configuration of the grain allows a highly regressive burning surface versus web burnt, in order to obtain conditions of ejection during the combustion while the missile is on its trajectory, so that the characteristic or reduced flow rate is close to $q = 5 \times 10^{-3}$.
- The effect of mass injection at the base is defined by this adimensional coefficient, called the characteristic flow rate:

$$q = \frac{m_b}{\rho_\infty V_\infty A_b}$$

m_b = mass flow rate of the combustion gases injected to the base;

V_∞, ρ_∞ = speed and density of the surrounding air;

A_b = surface of the base.

- To maintain the subsonic flow of the combustion gases, the pressure generated inside the chamber must stay in the subatmospheric pressure range. The composition used must offer satisfactory combustion stability

at this pressure range. Based on the firing conditions, the burning rate level will be situated between the range of 1 and 1.5 mm/s at 0.1 MPa.

- The reducing combustion gases mix with the air of the outside flow and cause a re-ignition phenomenon. This addition of weight and energy close to the base reinforces the pressure increase effect.

The mechanical properties of the propellant are optimized so that the generator can survive the stress induced in the cannon bore, where the pressure and acceleration levels are very high.

The propellant selected allows operation within a wide range of temperatures: -45 to $+60^{\circ}\text{C}$.

- As a rule, the materials and the implementation process are selected with the idea of using industrial capabilities that are compatible with large series production, with costs known to be acceptable in the artillery sector, i.e. costs that are lower than those acceptable in the case of missiles.

This type of production satisfies therefore two major criteria:

- limited cost and production time;
- manufacturing process easily adjustable to the various calibers used in the artillery sector.

An acceptable solution that satisfies all of these specifications is a gas generator made of a composite propellant (Butalites, i.e. reduced smoke HTPB).

3.3. ROCKET-ASSISTED PROJECTILES

Another solution to increase the speed of the projectile on path is to apply a thrust provided by the combustion of a rocket motor. These are known as rocket-assisted projectiles: RAP.

The rocket motors necessary for an effect comparable to base-bleed are very large and heavy, limiting the amount of explosive in the shell.

Finally, various countries are researching ramrocket or ramjet shells, with the purpose of either increasing the range of classic artillery [15], or propelling anti-tank arrow-piercing projectiles. This is expected to be fairly long-term research.

4. Gas Generators and Their Various Applications

The first systems moved by gas generated by propellants or powders made their appearance during the Second World War, in German combat aircraft with ejection seats in 1944.

Propellant cartridges had also been successfully used to help in the starting of piston-engine aircraft. A propellant cartridge with a high burn rate was ignited in the engine combustion chamber, resulting in the starting of the entire device.

Since that time the use of gas generators has greatly expanded, and today they have numerous applications in the aeronautics and space sectors, in military missiles, and in some commercial activities [11,12].

These gas generators can be used in conjunction with many other existing energy sources, such as:

- gas turbines;
- internal-combustion engines and electric motors;
- compressed gases and hydraulic accumulators;
- flywheels;
- batteries and fuel cells;
- solar cells.

These energy sources provide relatively varied application times, working power levels, and density of stored energy.

The gas generators are classified in four major categories, based on the type of propellants used:

- solid propellant gas generator;
- hybrid gas generator;
- liquid monopropellant gas generator;
- liquid propellant gas generator.

Further in the text, we cover only the solid propellant gas generators capable of producing energy only once, for periods of times ranging from fractions of seconds to several minutes at the most. These generators can nonetheless be controlled, regulated, and in some cases even stopped and started several times, although these latter types of generators are much more complex.

There are several types of solid propellant gas generators, based on their application:

- Highly reducing gas generators used to produce gases to be burned in a second step with the oxygen in the air. This class of generators include essentially solid fuel generators used on ramjets.
- Hot gas generators designed to produce gases used to activate power units such as hydraulic turbines, alternators, pumps, cylinders actuators, etc. or to ensure auxiliary propulsion. In systems of this kind, the exhaust gas temperatures of the generators are generally higher than 900–1000°C.
- Cold gas generators designed to supply gas to pressurize or inflate systems incapable of handling high temperatures; in such cases the temperature of the gas when it is used must always be lower than 300°C, sometimes even below 100°C, requiring the use of cooling devices for the initial gases.

The propellants used for these various generators have a formulation similar to the classic solid propellants. Either homogeneous propellants or composite propellants can be used, but the use of the latter is more prevalent these days.

The technology and materials used determine the performance of each of these various energy sources. Table 6 gives a list of energies that can be produced by gas generators and by various competing systems.

We see here that gas generators are perfect choices for short operation times of less than several minutes. According to the sort of energy required, compressed gas and flywheel can also be used. Since the use of a gas generator does not require the use of any valve, and it can be ignited by a pyrotechnic device, the gas generator can be smaller, lighter, and offer quicker reaction

TABLE 6 *Comparison of various energy sources in terms of applications and available energy*

Energy source	Applications	Available energy (in kW) range
Gas generator	Auxiliary propulsion Inflation Liquid propellant tank pressurization Thrust vector control	0.5 to 1000
Gas generator with turbine	Hydraulic energy Engine starter Fuel pump	0.5 to 100,000
Gas generator with turbine generator	Auxiliary energy units for aircraft, missiles or space shuttles	0.5 to 1000
Gas turbine	Transportation (ground, air, sea) Auxiliary power units Stationary energy	50 to 10,000
Internal combustion engine	Transportation (ground, air, sea) Stationary energy Leisure vehicles Portable tools	5×10^{-3} to 1000
Pressure gas	Auxiliary propulsion Inflation Propellant pressurization	0.05 to 100
Flywheel	Toys Public buses Machines	5×10^{-3} to 100,000
Batteries	Lighting Toys Engine starter Emergency power	5×10^{-8} to 10 (per unit)
Fuel cell	Energy for astronautics Stationary energy	0.05 to 10 (per unit)
Electric motor	Hand tools Toys Vehicles	5×10^{-4} to 100,000
Photovoltaic solar cell	Energy for astronautics	5×10^{-3} to 20

times than a compressed gas system. The problems caused by exhaust pressure, temperature, and chemical composition can constitute, however, an obstacle to their use.

When compared to a flywheel (rotating energy), the gas generator coupled with a turbine has the advantage of always being ready to use.

The gas generator is a serious competitor to the gas turbine for utilization times greater than 1 min, provided the total power required is less than 150 kW and the total operating time does not go beyond a few minutes.

When operation takes place without atmospheric oxygen, gas generators are superior to all other systems, regardless of the operating time requirements.

The advantages over batteries can be demonstrated in the case where the power required is relatively high (several hundreds of watts). It would include the following uses, for example:

- composite propellants for power generators for ballistic or tactical missiles;
- EDB propellant to propel submarine missiles out of their containers;
- EDB propellant, or CDB, for pressurization of liquid propellant tanks;
- composite propellants supplying very low CO contents for inflatable airbags used in case of collision in some automobiles (generally based on NaN_3 propellants).

5. Pyrotechnic Compounds and Propellants for Ignition Systems

The various pyrotechnic elements forming an ignition system for a propulsion grain were introduced in Chapter 1: primary initiator, ignitor initiator, and main ignition grain. For a detailed description of these components, consult a pyrotechnics dictionary [16]. Table 7 provides a description of the composition of an ignition system, and a typical igniter is shown on Fig. 12.

The function of the main grain is to deliver a significant amount of hot gases or a large number of hot particles in a very short time, a few tens of milliseconds.

This rapid generation must satisfy two requirements necessary for the ignition of the propulsion grain [17], as follows:

- creation in the volume surrounding the grain of thermodynamic conditions (constitution of the gaseous phase, pressure, temperature), close to the conditions of the grain's steady combustion state;
- ignition by heat transfer of the igniter toward the propellant through convection (transmission of heat flow), radiation (solid particles), or conduction through solid or condensable particles;

TABLE 7 Constitution of an igniter: most commonly used components

Grain type to ignite	Initiators	Increments or main grain initiators	Main grain igniter
Large	Electric with high energy level and ignition threshold; operated by shock-wave or laser and pyrotechnic compounds.	Easily ignited pyrotechnic composition, powder or pressed, and usually generating a gas rate adapted to the main grain.	Free-standing case-bonded grain with high burning rate composite or EDB propellant.
Small	Usually electric.	Same type, although often integrated with the initiator.	<p><i>Either:</i> same principle as for large grains: ignition with a micro rocket EDB propellant or fast-burning composite.*</p> <p><i>Or:</i> pyrotechnic compound for ignition generally compacted.</p>

* In such cases, the ability of the propellant to ignite is so high that it is possible to do without the increment grain.

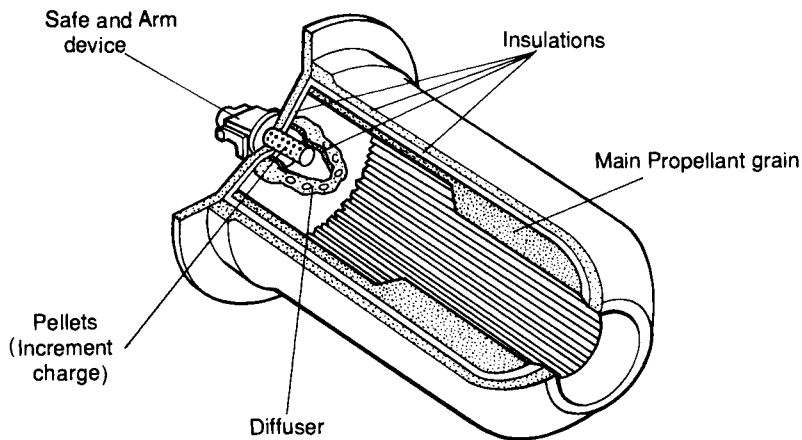


FIG. 8.12. Typical ignition system.

- component selection and design of the igniter can be done on the basis of operating specifications (volume, ignition time, position in the motor, safety, and cost).

Propellants

When the main ignition charge needs to be significant (ignition of large grain), it will take the form of a small propellant grain. This grain must present a large combustion surface which, coupled with a high burn rate, will deliver a high flow rate. Composite or EDB propellant are particularly well suited for this function.

Granulated or pelletized pyrotechnic compositions

These are used for initiator, increments and main charge in the case of small grains, for which the volume to be pressurized is small. They are discussed in Section 5.1 below.

For each of the pyrotechnic materials, the following information is necessary:

- combustion temperature;
- flame temperature;
- nature of the combustion materials, and related gaseous volume;
- ignitability;
- safety characteristics.

5.1. FORMULATION, COMPOSITION AND CHARACTERISTICS OF THE PYROTECHNIC MIXTURES

The powder or compact mixtures are composed of a fuel (metal) and an oxidizer (oxide or fluoride) [18]. Once initiated, they are subject to a very exothermic oxidation–reduction reaction.

The combustion translates itself into the progression of a reaction zone which separates the reacting elements from those which are not reacting yet. The burning rate, i.e. the pressure rise time, is a function of the particle size and of the reactivity of the oxidizer and the fuel.

Ignition mixture families and their main characteristics

Six major families exist today, with two or three elements each, and differentiated by the fuel and oxidizers that are used. The first family (black powder) is very old; the others were developed in conjunction with the propellants.

The elements and major characteristics of these six families are as follows:

(a) Black powder

Black powder is a mixture of three ingredients: potassium nitrate (75%), sulfur (12.5%) and charcoal (12.5%). It dates from antiquity and is still used today as a powder or pellet ignition powder.

It is not very powerful (775 cal/g), highly gaseous, and easily ignited (except in a vacuum).

(b) Aluminum and ammonium perchlorate mixtures

A powder mixture of aluminum flakes (40%) and ammonium perchlorate (60%) powder. It is a very energetic composition (2500 cal/g), with a high rate of gas generation, good ignitability, highly sensitive characteristics, and a burning rate greatly affected by confinement.

(c) Aluminum, potassium perchlorate mixture

A mixture of two aluminums in flakes, with different reactivity (35%), with potassium perchlorate (64%), and aluminum stearate (1%). This mixture can be used in a powder form, although it is more often compressed into pellets, 1 to 6 mm thick. The aluminum stearate acts as a binder.

It is a very energetic composition (2500 cal/g), highly gaseous, possesses very good safety characteristics, but is difficult to ignite, and its burning rate is very dependent on pressure.

By modifying the ratio of the two types of aluminum it is possible to modify the powder's burning rate, and consequently the ignition characteristics (time and pressurization).

(d) Zirconium-oxide mixtures

These are primarily binary mixtures of zirconium (37%), with copper oxide (63%), or quadruple mixtures of zirconium (45%), with barium chromate (34%), ammonium perchlorate (14%), and ammonium bichromate (7%).

These mixtures are used in the form of powders. They are moderately energetic (700 to 1000 cal/g), but offer very good ignitability. They are, however, very sensitive to electrostatic discharges.

The mixtures including CuO produce little gas but a large number of hot particles. Mixture with barium salts and potassium yields a high volume of generated gas.

(e) Boron and potassium nitrate mixtures [19]

These are essentially boron and potassium nitrate mixtures used in the form of powder, or pellets or compact mixtures of nitrocellulose, boron and potassium nitrate used in the form of micro-rockets.

These mixtures are moderately energetic (1500 cal/g), highly gaseous, have very good ignitability and excellent safety characteristics. Their main drawback is their hygroscopicity.

(f) Magnesium-teflon-viton mixtures [20]

These powerful mixtures (2200 cal/g) can be compressed or extruded. Not very gaseous, and with a moderate flame temperature, they offer very good safety characteristics but are difficult to ignite.

The main performance and safety characteristics of these four typical compositions are shown, respectively, in Tables 8 and 9.

5.2. MANUFACTURING PROCESSES

5.2.1. Powders

The homogeneity of the powder mixtures is obtained by using a mixer of solids which consists of, for example, two containers and a rotation system outside of the mixing zone. After drying has occurred, the oxidizers are placed in one container, and the fuel in another. The whole is rotated for approximately 1 hour to ensure good homogeneity of the products. For safety reasons all operations, including dividing into small quantities, weighing, and closing of the containers, are done remotely with the use of a mechanical remote control device.

5.2.2. Compacting

After homogenization the powder mixture can be compacted into pellets of different sizes.

This operation is done with an automatic pellet machine with mold plate. The various operations, including filling of the mold, molding, compression, and ejection of the pellet, are done remotely and continuously.

The quality of the compacting is controlled through a crash resistance test of the pellets.

TABLE 8 *Performance of four powder mixtures*

Mixture	Flame temperature (K)	Energy (Cal/g)	Volume of gases released (l/g)
Aluminum and ammonium perchlorate	4500	2500	6.0
Aluminum and potassium perchlorate, and aluminum stearate (compacted)	4500	2500	4.0
Zirconium and copper oxide	2500	700	0.4
Zirconium and barium chromate, and ammonium perchlorate and dichromate	3400	950	3.0

TABLE 9 *Safety characteristics of four powder mixtures*

Mixture	Index of detonation sensitivity cards*	Sensitivity to friction (Newtons)	Ignition Temperature (°C)	Sensitivity to static electricity
Aluminum and ammonium perchlorate	350	171	250	very sensitive
Aluminum and potassium perchlorate, and aluminum stearate (compacted)	300	26% of ignition at 353 N	400	low sensitivity (> 726 mJ)
Zirconium and copper oxide	< 1	150	520	very sensitive (< 1 mJ)
Zirconium and barium chromate, and ammonium perchlorate and dichromate	< 1	52	280	very sensitive (3 mJ)

* Card gap test—French test, see Chapter 7.

6. Laboratory to Industrial Production: Development Programs, Service Life, Research Programs

6.1. GENERAL INFORMATION

The development of a modern weapon system, or of a space launcher, is characterized by the simultaneous and interdependent development of complex subsystems, whose production in conformance with the initially determined specifications and schedule spells the success or failure of the entire program.

In addition, the technologies involved demand, as a rule, a very high degree of development: high performance and reliability are usually the primary characteristics.

Consequently, it is necessary to reduce to a minimum contingencies and uncertainties at the beginning of the program, from a technical point of view as well as from a financial one. This implies the use of proven technologies and methods. Because the programs involved are long-term, complex, and costly programs, and because many disciplines, professional specialities, and industrial capabilities must be involved in a coordinated manner to reach the goal, special program management methods and specific organizational rules must be applied.

Under these conditions it is understood that, at the beginning of the development of the propellant grain or of the motor, the products, processes and methods to be used in the implementation of the program must be sufficiently proven.

The terms research and development are used in the solid propellant industry with a specific meaning.

The goal of the research is, generally, to develop and qualify materials, processes, and measurement processes which will be used later in the development of a motor or a propellant grain when the decision is made, by a company or by government authorities, to develop a new system.

Propellant research, for example, must go from the laboratory phase, involving several grams of the substances, to "Scale 1" at industrial facilities capable of using several tons of the product. In the case of materials used in a motor, research includes "exploratory development." At this stage, however, research is not immediately finalized. It will only be finalized through its direct application in a system.

6.1.1. *Definition of the term "development" and general organization of development programs*

According to the official definition, development is: "all activities with the purpose of developing devices, processes or materials responding to well-

defined specifications, and which can be built or implemented in a reproducible manner”.

To use more precise terms, the purpose of engineering development is:

- to design and define the propellant grain responding to a specific need;
- to justify the design through tests, and if necessary, overtests, and by simulated use;
- to establish mandatory production and control methods to ensure overall quality of future industrial production;
- to prepare the industrial documentation for future industrial production and quality control of the product;
- to determine, with the client, the conditions for acceptance of the future series production.

6.1.2. Determination of the requirements, setting of the specifications

The determination of the requirements must, however, be as detailed and exhaustive as possible; it involves:

- a detailed look at the operational requirements of the future motor;
- expressing them in specifications for the grain.

The major types of specifications are described in Chapter 2.

Frequently, the determination of these specifications will require repetitive steps. At this particular time, a joint review with the client of the impact of the various specifications on the cost and final product quality for industrial production, is of major importance. The techniques of functional or value analyses applied at this stage provide a very efficient means of achieving the optimization of cost and quality.

6.1.3. The program

The technical proposal forms the basis of the commitment of the company or organization in charge of the development.

This technical proposal includes a development program, divided into various phases. The logic of the activities planned within each phase, and the sequencing of the successive phases, have to demonstrate that the objectives of the program will be reached without major obstacles.

In France, as an example, the phases usually planned in a program are:

- development, tailoring, and manufacturing, testing to reach a final design (“MAP 1”);
- qualification by the contractor (“MAP 2”);

- official qualification of the grain (called certification when done by governmental action);
- the industrial phase: implementation of the industrial facilities and qualification of the production line.

The content of the program, in particular the number of tests performed, will naturally vary as a function of the complexity of the grain and the degree of innovation of the project. The length of the program will depend both on the number of tests, and on the industrial cycle of the product considered.

Purely as an example, the number of tests necessary for a grain used in a tactical application which requires to perform within a large range of temperatures can vary from 10 to 20 (in a simple case), and 30 to 40 for the development phase (MAP 1). The number of tests performed during the internal qualification or certification phase is, of course, contingent on the requirements of the client. The number of tests can also be determined by requirements related to demonstration of reliability requiring overtests (more stringent conditions) and to the performance of safety and vulnerability tests. The duration of the development may vary from 2 years in exceptional cases to approximately 4 or 5 years for tactical systems, and up to around 10 years for strategic or space systems.

6.1.4. Role of value analysis in the clarification of the requirement during the preliminary project and the project

This technique is designed to assist in finding the best compromise for the definition of the product in terms of its performance and its cost. Briefly described, a value analysis consists in giving responsibility to a group of individuals, having various roles in the project, who together perform a functional analysis of the product with the objective of finding a means of reducing the production cost. It is a collective effort that should, to the extent possible, include the client and the subcontractors, in order to arrive at a functional expression of the requirement, the determining factor of the product's competitiveness.

6.1.5. Design to cost

This is the implementation of methods designed to control recurrent industrial production costs for the product under development. This method involves:

- identifying objectives for the recurring costs right at the beginning of the development program;

- encouraging, through the inclusion of contractual incentives, the search for and selection of technical solutions for both the cost objectives and development requirements (quality, performance, schedule);
- managing the recurring costs during the development, the same as for performance, quality and schedule.

6.2. PROGRAM MANAGEMENT

The methods described above, although included within the propellant grain development, are not specific to propellants. They are, for the main part, identical for the development of a motor, a missile, even an armament system. However, with a growing number of sub-assemblies or basic operations, strict program management becomes increasingly complex, even for propellant grains.

The program director needs to rely on increasingly complicated planning and information tools.

The first activity consists in a breakdown of the program into basic tasks and the creation of detailed flow-charts, known as the “work breakdown structure” (WBS).

This allows decreasing the complexity of the project, identifying its main components, and laying down a base for budgetary, scheduling and assignments planning and control.

At the technical level, the use of relatively sophisticated planning tools (for example, GANTT diagrams and critical path methods such as PERT), offers the possibility of emphasizing the logic and the critical interfaces, and of seeing whether the planning has been realistic. It results in a better appreciation of the principal difficulties, and the possibility of analyzing fall-back solutions or alternatives.

At the program cost and budget control levels it provides the possibility of having available, in real time, information necessary to evaluate the economic performance by comparing expenses with work performed, and the remaining expenses and work.

Nowadays, software systems for program management that integrate this type of services are available commercially, and their use is becoming increasingly frequent, particularly in the space industry.

6.3. SERVICE LIFE

This is one of the most difficult questions that will face the individuals in charge of the development of a new motor or a new grain.

The client or prime contractor usually wishes to know the estimated service life or—a direct consequence—the replacement cycle of the motors.

Unfortunately, that question can only be answered with great caution at the beginning. As we will see later, it is therefore advisable to accumulate a

maximum of relevant information, starting at the time of the research phase. Similarly, it is necessary to use the greatest possible amount of information that can be provided by results from the operational behavior of existing motors and grains, whose designs are as similar as possible.

During the development, although at a time when the designs are sufficiently determined (at the end of MAP 1, for example), it is possible to start what is commonly known as “accelerated aging,” which will provide the opportunity of estimating the potential life at the end of the development phase. Ideally, to have the best estimate, the development phase would have to last at least as long as the projected service life, and provided that the impact of the various “treatments” the missile is subjected to when in use can never be entirely simulated, have a limited impact. The principle of these accelerated agings usually consists in using an increase in temperature to increase the rate of the chemical phenomena responsible for the evolution of the materials that make up the grain. Extreme caution is recommended, however, because the failure processes can be of different natures, and the temperature can impact differently on each of them, so that, in the worst case, it is possible to create a failure that would not occur in the real application. There have been such instances.

General recommendations in this regard are as follows:

- The temperature increases and accelerated aging must remain within modest ranges to be representative.
- The samples, subjected to aging, must be as representative as possible of the propellant that will be industrially manufactured.
- Not only non-destructive and firing tests must be performed on the aged samples, but also detailed and analytic evaluations. It is these evaluations alone that provide the capability of creating models of the evolution of the safety ratio throughout the service life, as various properties of the propellant change.

6.4. IMPORTANCE OF THE RESEARCH PHASE

We have determined that the teams responsible for the development of a new grain must have access to proven technological tools, materials and propellants, so that they may propose development programs that are short and without contingencies.

The mission of the research teams is to supply these elements, and in particular:

- create and validate methods to design the grains, estimate their service life and estimate their operation under all types of working conditions;
- formulate, identify the characteristics, and implement up to the industrial feasibility stage any new materials that are necessary for the progress of the technology and the needs of the development.

Industrial considerations should be present very early during the research. As much as possible they should be the principal factor in major decisions concerning the various possible routes to reach the objectives selected for density, specific impulse, burning rate, etc. This is particularly true for the considerations of process costs and of raw material availability.

The last point is of particular importance for the continuity of the industrial production, which in some cases can last for over 20 years, and for systems which, when they are modified, require new certifications which are extensive and expensive because of the interaction between the sub-assemblies. The company supplying the propellant is rarely the manufacturer of all, or even most, of the raw materials included in his products. The company is, as a result, totally dependent on the industrial and commercial strategy of its suppliers, or on official authorizations for imported products. It is therefore advisable to ensure that the raw materials selected have solid long-term guarantees, and to undertake, at the beginning of the research, actions such as surveying substitute products, certifying second sources, preparing supply agreements and so forth.

It is also necessary, when developing a new propellant, to test a sufficient number of samples of those raw materials that have the greatest impact on the quality of the propellant, to determine reproducibility and to have control capabilities at a later time. Of course, these activities must be completed during the development *per se*. Specific technical adjustment must be made during the development phase, although the assessment of particular propellants or materials for a new development must use this raw material information base as much as possible.

Finally, it will be necessary to have, already at this stage, as much information as possible concerning the aging of the propellant and related materials under conditions similar to the future conditions of usage. This requires that very early, during the research phase, programs be initiated to learn about the mechanisms of degradation and the laws of evolution of the products over time.

Based on the service life required for today's propulsion systems, and the limitations of accelerated aging methods in standard environmental conditions, it is unfortunately rather rare to have a thorough knowledge of those characteristics at the onset of the development of a grain. It is true that, for older materials, their service life characteristics are well known, but these materials do not have the performance characteristics now required. To gain a better appreciation of grain life it is necessary to:

- strengthen the initial selection by using as much aging data as possible, gathered from similar products under research, or from older grains with practical experience that has been accumulated through monitoring programs;
- perform, during the development phase, the evaluation programs described previously.

This discussion emphasizes the importance of the role of the development activity for the orientation of the research, and the inclusion of the research within a broader perspective, which can be considered as being particular to this type of industry.

6.5 ADVANCED DEVELOPMENTS AND EXPLORATORY DEVELOPMENT MODELS

When very advanced technology is involved, an exploratory phase is often included between the research phase and the development phase. Its purpose is to confirm, at "Scale 1," that the right combination has been made of design method equivalents, processes, and materials in a new type of propellant. This advanced development can be considered as the furthest culmination of the research, and the surest way of having a shorter development phase (because of the reduction of the number of tests required) without any unpleasant surprises.

Bibliography

1. KLAGER, K., Polyurethanes, the most versatile binder for solid composite propellants. AIAA 84-1239—AIAA/SAE/ASME 20th Propulsion Conference, 1984.
2. SUTTON, E. S., From polysulfides to CTPB binders—a major transition in solid propellant binder chemistry. AIAA 84-1236—AIAA/SAE/ASME 20th Propulsion Conference, 1984.
3. MARTIN, J. D., Polyvinylchloride plastisol propellants. AIAA 84-1237—AIAA/SAE/ASME 20th Propulsion Conference, 1984.
4. STEINBERGER, R. and DRECHSEL, P. O., *Manufacture of cast double base propellant. Propellants, manufacture, hazards and testing*, pp. 1-28. American Chemical Society, Washington, 1969.
5. LINDNER, V., Propellants. *Encyclopedia of Chemical Technology* (Kirk-Othmer), 9, 620, 3rd edn., 1980.
6. QUINCHON, J. and TRANCHANT, J., Poudres, propergols et explosifs—La nitrocellulose et autres matières de base des poudres et propergols. *Technique et Documentation*, Paris, 1984.
7. CALABRO, M. *et al.*, Reverse forward dome for a missile first stage. AIAA 87-1989—AIAA/ASME/ASEE 23rd Propulsion Conference, 1987.
8. MARGUET, R., ECARY, C. and CAZIN, P., Studies and tests of rocket ramjets for missile propulsion. 4th International Symposium on Airbreathing Engines, Orlando, 1-6 April 1979.
9. GAUNT, D. C., Understanding costs of solid rocket motors. AIAA 86-1638—AIAA/ASME/SAE/ASEE, 22nd Propulsion Conference, 1986.
10. BRUNET, J., Detonation critical diameter of modern solid rocket propellants. ADPA, JISC, New Orleans, 1988.
11. CUTLER, H., Gas generators—perspective. AIAA 73-1168—AIAA/SAE 9th Propulsion Conference, 1973.
12. SUTTON, E. S. and URIESEN, C. W., Gas generators for aerospace applications. AIAA 79-1325—AIAA/SAE/ASME 15th Propulsion Conference, 1979.
13. MAGNUSSON, A. I., GUNNERS, N. E., AX, L. and LUNDAHL, K., Brevet suédois 76 104 8217.
14. HELLGREN, R. V., Range calculation for base-bleed projectiles. 6th International Symposium on Ballistics, 1981.
15. MERMAGEN, W. H. and YALAMANCHILI, R. J., Design and development of a ramjet tank training round. 8th International Symposium on Ballistics, 23-25 October 1984.
16. GROUPE DE PYROTECHNIE SPATIALE, *Dictionnaire de pyrotechnie*, 3rd edn. CEDOCAR, Paris, 1985.

17. HERMANCE, C. E., Solid propellant ignition theories and experiments. *Progress in Astronautics and Aeronautics*, **90**, 239, 1984.
18. CALZIA, J., *Les substances explosives et leurs nuisances*. Dunod, Paris, 1969.
19. VOLK, E. *et al.*, Innenballistische Bewertung der Wirkung von Anzündmitteln. 10th International Pyrotechnics Seminar, Karlsruhe, 2-5 July 1985.
20. PERETZA, and COHEN, J., Development of a magnesium-teflon-viton composition for propulsion system igniters. *Israel Journal of Technology*, **18**, 112-114, 1980.

CHAPTER 9

Double-base Propellants

HERVÉ AUSTRUY

1. Introduction

Propellants in which the binder consists of an energetic polymer plasticized with a nitric ester, more particularly nitrocellulose plasticized with nitroglycerine, are commonly called double-base propellants. The oxidizing and reducing elements that are involved in the release of energy through combustion are combined in the same molecule. In fact, nitrocellulose and nitroglycerine bring together the carbon, hydrogen and oxygen necessary for the chemical reaction. As a result these are known as homogeneous propellants, in contrast to the composite propellants. And depending on whether the manufacturing process is by extrusion or casting, they are also known in France either as “SD” (solventless or extruded double-base propellants or EDB), or as “Epictetes” (cast double-base propellants or CDB).

Double-base propellants are one of the oldest propellant families. Their development is connected to the development of propulsion. At the end of World War One, gun propellants were essentially colloidal powders with a nitrocellulose base. The incorporation of nitroglycerine made it possible to increase the energy level, and although the simultaneous increase of combustion temperature limited their use as gun propellants, they became usable for rocket motor propellants.

The applications for such rocket motors require tailoring of the combustion pressure, burning time, over a wide operating temperature range, which is activated by means of additives to the propellant. For the past 40 years, propellant compositions have continued to evolve. The number of additives has increased, and in some compositions where they represent 5–10% of the total weight there are as many as 10 additives. These developments have allowed a considerable increase in the quality, performance and reliability of motors using double-base propellants.

Today, their development and use are linked to the economics of their production and to some of their inherent characteristics such as:

- good mechanical properties including stiffness which is particularly well suited for free-standing grains and for the manufacture of various geometries with close dimensional tolerances;
- good aging capabilities, particularly under humid conditions;
- operational characteristics that are well suited to some specific applications such as:
 - little or no solid particles in the gas jet, i.e. little or no primary smoke,
 - little or no chemical elements likely to recombine with the atmosphere to create secondary smoke,
 - burning rates that are well under control and generally show little sensitivity to the operational temperature.

2. Compositions and Raw Materials

2.1. FUNCTIONS OF THE CONSTITUENTS

The constituents of double-base propellants can be classified in five large groups of products, based on their functions:

- energetic base constituents,
- additives for easier manufacture,
- chemical stability additives,
- burning rate additives,
- other additives for specific operations.

2.1.1. *The energetic base*

The energetic base of double-base propellants is mainly composed by nitrocellulose (40–70%) and nitroglycerine (15–41%). Other nitrated products are also sometimes used, such as nitroguanidine.

The manufacture of these propellants involves combining these two products homogeneously, using a gelatinization process [1] which is based on the mechanism of interaction between the nitroglycerine molecules introduced in the network of the nitrocellulose macromolecules, and the atoms or groups of atoms of these polymers. These mechanisms are numerous, complex and governed, at a microscopic scale, by means of attractive forces, ranging from Van der Waals forces (relatively weak attractive forces), to hydrogen bonds whose energy may reach 12 kcal per bond, and including dispersion forces, interaction forces between dipoles and others.

The behavior of nitrocellulose in relation to solvents with a basic nature has been the object of many studies [2]. These solvents include ketones, esters and alcohols. The oxygen (basic) of carboxyl groups can interact with the hydrogen (acid) of the secondary nitrated groups (CH-O-NO_2). This

phenomenon is a function of a large number of parameters such as the degree of nitration of the cellulose (referred to as percentage nitrogen in the NC), the crystallinity, and the degree of polymerization.

As far as nitroglycerine is concerned it is to be considered as a poor solvent which does not form a true solution with the polymer. It does not penetrate the organized zones of the polymer and swells only the amorphous interstitial spaces according to a solvation process. One of the explanations is considered to be the presence of oxygen links in the nitrocellulose molecule. Because of the rigidity of the chains and their spatial organization, these oxygens have a weak interaction with the nitrated groups of the nitrocellulose molecules.

The introduction of mobile solvents such as nitroglycerine permits bringing nitrate groups closer to the vicinity of the oxygen links. This allows an interaction to occur between the oxygens of the nitrocellulose and the acid hydrogen of the CH-O-NO_2 group of the nitroglycerine. As a result a portion of the nitroglycerine (30%) is used to solvate the nitrocellulose, the remainder being more or less mobile within the network. At the macroscopic level the beginning of the gelatinization process is often marked by a swelling of the nitrocellulose fibers. The continuation of the process must be promoted by a mechanical, thermal or chemical intervention, such as the addition of another volatile solvent.

2.1.2. Additives for easier manufacture

These additives are necessary to facilitate the manufacture of the material. These are essentially inert plasticizers designed to promote the gelatinization phenomenon. They represent typically 0–10% of the propellant, and phthalates or triacetate types are commonly used to desensitize the nitroglycerine for safer handling. Mechanical properties may also be modified.

Other additives, such as graphite, are used in very small amounts (below 0.1%) to facilitate some operations; for example, the flowing of the casting powders (Xenon powders) used for the production of CDB propellants.

2.1.3. Stability additives

The nitric esters of double-base propellants decompose at rates dependent on time and temperature. This decomposition corresponds to the rupture of the O-NO_2 bonds, and releases nitrogen oxides. Without a stabilizer, the products resulting from the decomposition have a catalytic effect on the decomposition reaction rate. The reaction is controlled when stabilizers are included, which usually have a benzene nucleus capable of fixing the nitrogen oxides by substitution.

An uncontrolled decomposition of the nitric esters could have serious disadvantages:

- From a safety point of view: since the decomposition is exothermic, there could be a risk of ignition of the propellant when the energy released becomes greater than the heat loss through exchange with the environment.
- From a quality point of view: there could be a risk of gas cracking of the propellant when the decomposition kinetics of gas generation is faster than the gas diffusion. This phenomenon is observed beyond a certain thickness of the material. The critical size corresponds to the dimensions where cracks appear at a given storage temperature.
- From a performance point of view: because the decomposition is exothermic, the propellant energy — that is, the energy available for use — would decrease with time.

The above emphasizes the importance of the selection of stabilizers in the formulation of double-base propellants.

2.1.4. Ballistic additives

The burning rate of double-base propellants varies greatly with pressure, so that during their combustion in a rocket motor, small fluctuations in the combustion are translated into significant pressure variations. As a consequence, an accidental increase of the burning surface may result in an overpressure that could lead to the explosion of the rocket motor.

Ballistic additives are added to the propellant to reduce the sensitivity of the burning to pressure fluctuation, as well as to catalyze burning rates to the higher regimes.

Some of these additives permit a burning rate independent of the pressure, within a given range of pressures (the plateau effect). The plateau effect was given its name because the burning-rate-versus-pressure curve has the shape of a plateau. When the burning rate decreases with increased pressure the phenomenon is called mesa effect. In the absence of such additives the burning rate increases with pressure according to an exponential law. Accordingly such additives are commonly referred to as ballistic modifiers or burning rate catalysts, or sometimes as platonization agents.

The advantage of propellants with such plateau curves is obvious. Random fluctuations of the burning area to throat area ratio result only in minimal variations of the burning rates, and in very weak pressure variations. This in turn enhances control, predictability and reliability of the motor performance.

Furthermore these burning rate additives usually reduce the temperature coefficient of variation of burning rate, enabling reduced motor performance variability over a wide temperature range.

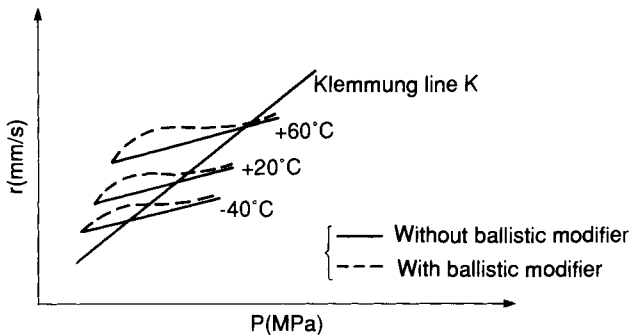


FIG. 9.1. Diagram burning rate-pressure of a double-base composition.

2.1.5. Operational additives

Some characteristics peculiar to the use of a specific rocket motor or its design may need some other additives.

Regardless of the configuration of the combustion chamber, the burning rate must be stable, and this may require the presence in the combustion gases of solid particles, such as refractory products to attenuate acoustic combustion instability effects.

Special needs in terms of guidance or plume signature may require the absence of re-ignition of the gaseous jet; flash suppressant additives may be used to satisfy such requirements.

2.2. RAW MATERIALS CHARACTERISTICS

This section describes some of the characteristics of the principal ingredients of double-base propellants with respect to their influence on processing and final properties.

2.2.1. Energetic raw materials

2.2.1.1. Nitrocellulose

Cellulose nitrate, commonly called nitrocellulose, is obtained by action of sulfonitric mixture (sulfuric and nitric acids) on cellulose. Such nitrate esterification is in a heterogeneous phase reaction of mixed sulfuric and nitric acids on cellulose fibers, in the course of which all three hydroxyl functions of the cellulose may be nitrated to a greater or lesser degree.

The nitrogen content of the nitrocellulose represents the degree of nitration of the available hydroxyls in the cellulose chains. Accordingly it indicates the energetic level of the product.

In France the nitrocelluloses are classified following a nomenclature connected to the nitrogen content (in mass percentage). The more usually used in a double-base production, are the following grades: CP₁D, CP₂L and CP₂U (13.1 N–12.6 N–11.7 N).

(a) Solubility

The nitrocellulose solubility in polar solvents varies in accordance with the nitrogen content.

The nitrocellulose grades insoluble in a given mixture of ether and alcohol at 56° Baume are called type 1 (CP₁). The soluble grades are called CP₂.

(b) Viscosity

An important characteristic of the nitrocelluloses is the degree of polymerization or molecular weight, which is equal to the number of anhydroglucose structural units forming the cellulose chain. This parameter principally determines the viscosity of the nitrocellulose in a given solvent.

(c) Calorimetric value in calories per gram

The energetic properties of the nitrocelluloses are a function of their percentage of nitrogen. Table 1 lists the major characteristics of nitrocellulose, based on the French nomenclature.

2.2.1.2. Nitroglycerine

Nitroglycerine or glycerol trinitrate resembles a colorless oil. It is obtained through nitration of glycerine by a sulfonitric mixture. Its very high calorimetric value (1750 cal/g) has led to its generalized use in double-base propellants [4].

2.2.1.3. Other energetic ingredients

Beside nitrocellulose and nitroglycerine, other energetic products may be used when special applications are involved. Nitroguanidine, for instance, is used as a cooling agent or as a combustion moderator.

Other nitrate esters may be used either wholly or in part in substitution for nitroglycerine. In particular the use of triethylene glycol dinitrate or butanetriol trinitrate is noteworthy.

TABLE 1 *Major characteristics of different nitrocellulose qualities*

Type	N%	Calometric value (cal/g)
CP ₁ D	≥ 13.35	1060
CP ₁ E	13 to 13.35	1040
CP ₂ L	12.60 to 12.80	970
CP ₂ P	12.40 to 12.59	940
CP ₂ S	12.20 to 12.39	910
CP ₂ T	11.80 to 12.19	870
CP ₂ U	11.60 to 11.79	830

2.2.2. *Process additives*

2.2.2.1. *Plasticizers*

The most commonly used are:

- diethyl phthalate, a phthalic ester employed as a plasticizer for EDB propellants;
- dioctyl phthalate, a plasticizer for CDB propellants;
- and particularly, in the CDB process glycerol triacetate or triacetin, as an inert liquid mainly used in association with nitroglycerine in the casting solvent. In this way the impact and friction sensitivity are reduced and the gelatinizing behavior reinforced.

Other plasticizers sometimes used are:

- saccharose acetoisobutyrate, also acts as a burning rate modifier;
- ethyl phenyl urethane, a plasticizer for EDB propellants;
- sucrose octoacetate;
- adipates such as ethyl, octyl, etc.

2.2.2.2. *Other additives*

Graphite is often used as a coating agent for the casting powder in the cast double-base process. In low quantities (less than 0.1 %) it reduces electrostatic charges and facilitates the powder flow into the casting molds.

Waxes (Candellila, Montant) in very small amounts, on the order of 0.5 %, facilitate the extrusion process of solventless propellants. Some stearates, magnesium stearate for example, have a similar role to the waxes.

2.2.3. Stabilizers

The molecular structure of stabilizers consists of aromatic benzene rings suitable for reaction with nitro groups NO_2 arising from the decomposition of the NC/NG nitric esters. The most common stabilizers are:

- Diethyl diphenyl urea or centralite acts as a stabilizer and also a plasticizer for nitrocellulose. It is not suitable in charge grains of large web thickness because the products of its stabilization reaction are gases of poor solubility and diffusivity in the propellant. This can result in gas cracking or fissures in the propellant.
- 2-Nitrodiphenylamine, which can act on the ballistic properties of the propellant by increasing the burning rate and temperature coefficient. On the other hand, diphenyl amine, a basic stabilizer for single-base powders, cannot be used because of its reaction with nitroglycerine.
- *N*-methyl-*para*-nitro-aniline, with its very high capability of fixing the nitrogen oxides, has an efficient stabilizing action, but also a more rapid consumption and, consequently, quicker utilization of the stabilizer. Its use is recommended for applications with high thermal stresses, or for large size-grains. It is generally associated with one of the other stabilizers, which ensures a longer lasting complementary effect.
- Resorcinol, which has a weaker stabilizing effect.

A certain number of other substances with aromatic cores compatible with nitroglycerine can also be used, including, for example, 2-methoxynaphthalene and trimethoxybenzene.

2.2.4. Ballistic additives

For double-base propellants the ballistic catalyst effect is obtained by using metallic compositions [5,6], in particular lead salts or oxides.

The most widely used ballistic modifiers are lead salts such as dibasic stearate, neutral stearate, salicylate, octoate, resorcyate, basic oxide (PbO), and saline oxide (Pb_3O_4).

These products affect the energetic level of the propellant, its burning rate, the operational pressure range, and the manufacturing process. Consequently their use and amount are dependent on the properties required, and vary from one composition to another.

Copper-based products can be added to the propellant to strengthen the effect of the other catalysts. Salicylate, octoate, oxides, and chromite are among the most common copper compounds used.

Finally, although alone it has a non-catalytic action, acetylene black is widely used, because its efficiency becomes very high when associated with other catalysts such as lead or copper salts.

2.2.5. Operational additives

The major particulate damping agents are zirconium oxide, zirconium silicate, and silicon carbide. Various other products may also be used, including tungsten and boron carbide.

After burning flash suppressant additives are potassium-based; they are selected based upon:

- their efficiency in flash suppression;
- their chemical compatibility with the propellant;
- their influence on the propellant properties, in particular, the ballistic properties.

Among the potassium salts used are, for example, cryolite, sulfate (the oldest), bitartrate, and oxalate.

3. The Manufacturing Process

3.1. REMINDER OF THE FUNCTIONAL ROLE OF THE PROCESS

The role of the manufacturing process is to ensure the transformation of the raw materials into a finished product which is as close as possible to the desired grain shape and size. Therefore, the manufacturing process provides for a number of essential functions, such as the homogenization of the product, its gelatinization, and its shape.

3.1.1. Homogenization

The various ingredients exist in very different physical states: floss for nitrocellulose, liquid for nitroglycerine, and amorphous powder or crystalline state for the ballistic catalysts. An intimate mixture must be ensured. There are various techniques to be used, including kneading, screw extrusion, and laminating between rollers.

All three of these techniques are used with solventless propellants. Solvent kneading is used for the first phase of the production of CDB propellants.

3.1.2. Gelatinization

Nitrocellulose gelatinization by nitroglycerine results in the swelling and partial solution of the fibrous structure of the nitrocellulose.

A temperature increase facilitates the gelatinization. The rolling of EDB propellants, for instance, is done at high temperature (100°C); the kneading of casting powders at a temperature between 30 and 40°C; CDB propellants are cured at a temperature close to 60°C.

Gelatinization is also facilitated by mechanical action during the mixing of the casting powders and particularly, during the rolling of EDB propellant. Finally, it is further facilitated by the use of the solvent system with an acetone and alcohol base, or ether and alcohol, during the preparation of the casting powders. These will modify the state of the nitrocellulose and the absorption kinetics of the nitroglycerine by the nitrocellulose.

3.2. MANUFACTURING PROCESS OF EXTRUDED DOUBLE-BASE PROPELLANTS (EDB)

3.2.1. The conventional process

3.2.1.1. *Manufacture of the paste: impregnation of the nitrocellulose with nitroglycerine*

Since the transport of nitroglycerine was forbidden, the mixing of nitrocellulose and nitroglycerine has been done at the facility where the nitroglycerine is manufactured. The process used, called "impregnation", consists of placing nitrocellulose in suspension in water agitated by compressed air, and of pouring nitroglycerine, which disperses itself into droplets suspended in the water medium under the effect of the agitation. These droplets are absorbed by the nitrocellulose fibers with which they come in contact. The resulting product, called a paste, is then homogenized and drained of excess water, leaving a water content of 30% as required by law for transportation.

3.2.1.2. *Drying of the paste*

Too wet to be used in the manufacturing process, the paste is dewatered by spin centrifuge for several minutes, reducing the water content to approximately 20%.

3.2.1.3. *Kneading*

The water content of the paste is neither accurately known, nor is it perfectly constant throughout the entire mass. A further mixing operation is

necessary to obtain a homogenized product. The water content is also measured, which allows calculation of the weight of dry nitrocellulose, and therefore deduction of the amounts of constituents that need to be added during the kneading operation. These other ingredients are added successively during the kneading, in small amounts for the solids and by spraying for the liquids. At the end of approximately 30 min, the premixed paste obtained is unloaded from the kneading machine. This paste constitutes a homogeneous unit, identified and used as such for the remainder of the manufacturing process.

3.2.1.4. *Gelatinization: rolling operations*

The removal of water from the paste and the gelatinization of the nitrocellulose by the nitroglycerine is obtained by the dual effect of pressure and heating, in two rolling phases.

During approximately 6 min, the agglomeration rolling is an essential step for the gelatinization of the propellant and for the creation of the ballistic properties. Because the rollers are rotating at various speeds, this operation is also called differential lamination.

The sheets produced by differential rolling still contain too much water. A further rolling, during approximately 15–20 min, perfects the gelatinization and eliminates the residual amount of water. It is done with rollers rotating at identical speeds, called a finish rolling.

3.2.1.5. *Carpet rolling of milled sheets*

Before they can be put into the barrel of the extrusion press the laminated sheets must be rolled up to have a diameter slightly smaller than the diameter of the barrel of the press involved. It is very important during this operation to prevent heat losses.

3.2.1.6. *Extrusion*

Whether horizontal or vertical, an extrusion press for double-base propellants always includes a barrel with a heating jacket, where very hot water is circulated (70–80°C) and a piston moving inside the barrel. This is fitted with annular air outlets. It is absolutely necessary to avoid blocking air into the propellant rolls being compressed, because the air could become heated through adiabatic compression, and cause ignition.

The press barrels have various sizes; they may measure up to 380 mm diameter and hold up to 90 kg of propellant. The bottom of the barrel consists of a sort of filter with holes, the “sieve plate” through which the material is forced into a second barrel located just before the extrusion device. The extrusion device consists of a die that determines the outside shape of the free-standing grain or the propellant (cylinder, star, square, rectangle, etc.)

and of one or several needles to create perforations within the required shape.

When manufacturing large grains there is only one die per extrusion press; but for small or mid-size diameters the extrusion press may be equipped with up to 12 dies. The operations are performed in the following order:

- introduction of the roll into the press barrel;
- the piston is lowered to the surface of the propellant (approach of the piston);
- vacuum process takes place to remove occluded air;
- the piston is set in motion, at a specific speed to effect the extrusion process.

To guarantee a good stability of the dimensions of the sections extruded, precise heat control is necessary to maintain the die at a uniform temperature. Manufacturing quality depends on strict control of the extrusion operations. Rheology studies have been done to determine the thermal and mechanical mechanisms involved in the extrusion process [7]. A model reproducing the thermomechanics of the flow inside the die has been developed that takes into account the variations of viscosity as a function of the temperature and the shear stress to which the propellant is subjected. The thermal phenomenon, however, does not occur inside of the product, but at its surface. A boundary layer is created, and its characteristics govern the flow and/or defects caused by ripping. The conventional laws applied to molten polymers are not capable of taking this boundary layer into consideration. Consequently, even if its modeling is rather complex, the knowledge of the boundary layer occurrence guides the choice of the geometry of the dies. For example, profiles that have a propensity to break or disturb this boundary layer should be avoided.

On exit from the extrusion press the strand or section of propellant swells, because of the release of pressure. The higher the extrusion pressure, the greater the swelling will be. To ensure the reproducibility of the swelling, the extrusion pressure is set for the specific compositions, and the rate curve of the descending piston is also controlled.

Typically the hydraulic pressures that are being exerted are approximately 18 MPa, resulting in a pressure on the material that may reach 70–100 MPa.

Safety rings limit the exerted pressure, and can be cut in case of fire.

3.2.1.7. Cutting

The extruded sections are roughly cut to be somewhat longer than the final dimension.

3.2.1.8. Machining

The propellant strands or sections, which undergo swelling to a larger or smaller extent depending on the extrusion conditions, shrink during cooling.

This phenomenon makes it difficult to obtain dimensions of close tolerances without including a final machining.

Cutting to the final length is done after cooling has been completed, sometimes even after an aging period. The cutting is usually done with a milling saw. With the use of lathes, mills and drills, the outside and the inside of the grain can be precisely shaped, according to requirements.

For the most part the cutting tool is cooled with fluid during the machining operation, and the propellant machining swarf is removed from the vicinity by vacuum exhaust.

3.2.1.9. *Inhibiting*

Most of the grains for rocket propulsion must be inhibited on their outside surface, as well as inside, in some cases. There are various techniques available that depend on the size and the shape of the grains. They also depend on the nature of the inhibition material. Typical materials are:

- filled or unfilled polyester cast inhibitors from prepolymers, with low viscosity, and applied by a casting process;
- silicone polymer resins, applied by injection into molds surrounding the propellant grain;
- polyurethane inhibitors, currently becoming increasingly popular, which are injected around the propellant grain whose surface has been coated with a primer.

3.2.2. *Other processes*

The process described above is the process most widely employed for the manufacture of solventless propellant grains. A significant amount of energy is put into the material, giving propellants manufactured in this manner excellent ballistic and mechanical properties. However,

- there are some variations in the manufacture of the propellant material (calendering and stamping);
- new technologies, such as screw extrusion, already widely used for the production of plastic materials, are replacing the conventional processes.

3.2.2.1. *Calendering*

Calendering permits the production of sheets or strips with a very regular thickness, varying from 0.075 to 2 mm, and a textured surface, including ribs, ridges, barbs, grids, and others variations.

The propellant sheets from the finishing extrusion rollers previously described are passed through calender rolls. The latter is a powerful rolling machine in which the rolls have a surface tailored to the propellant manufacture. The rolls are also heated and have variable rotation speeds.

3.2.2.2. *Stamping (or hot forming)*

Stamping is a hot forming process, or thermoforming, of propellant pieces obtained by press or screw extrusion. These pieces are first cut to have approximately the weight and size of the future grain [8]. The operation is carried out in several phases:

- the propellant piece is placed in the mold, which consists of a die with the desired outside profile and a stamp with the complementary geometric profile required;
- the mold is closed, the temperature is raised to 80–90°C, the forming temperature, and limited pressure is applied (3 kPa);
- the stamp is moved inside the die cavity to compress and force the softened propellant to obtain the final shape desired;
- the stamp is removed from the die.

The advantage of this process resides mainly in the fact that it allows the production of geometrical shapes that cannot be obtained by extrusion, such as full head-end grains (where the central bore opens at only one end) and elaborate and complex patterns which are difficult to obtain by extrusion.

3.2.2.3. *Screw extrusion*

The production process for EDB propellants involves a large number of successive phases, which are an economic handicap for the production of a large number of parts.

Various attempts have been made to replace the EDB process with a more continuous and economically more advantageous process (using solvents and production in a non-solvent-liquid phase [9,10]).

The most complex attempts have sought to use the technology widely employed for the production of plastic materials, i.e. the screw extrusion process [11,12]. After a considerable period of adaptation this process is currently used for the industrial mass production of EDB propellant grains [13].

Two extruders are used successively; they are designed to perform the following operations: agglomeration rolling, final rolling, and extrusion. Kneading is the only separate operation that is retained, owing to the critical importance of precise measurement of the quantities of the various ingredients in the propellant composition. These screw extruders include:

- a variable-rate feeding system;

- a temperature control system for the screw and the die;
- a set of exhaust ducts to allow removal of water and gases;
- a die placed at the end of the extruder, used to shape the material.

The first extruder is fitted with an adjustable screw; this ensures the gelatinization of the wet mixture. The mixture, transformed into granules, is fed continuously to the second extruder. These granules can also be obtained through a continuous rolling process. The second extruder, which is fitted with two parallel screws, completes the homogenization of the mixture and ensures the shaping of the material.

In addition to the economic advantages, this process is also a safer one, inasmuch as the work can be done at a certain distance, does not require any contact between the operator and the material, and reduces the amount of handling and transfers.

3.2.3. *Current products*

There is a very wide selection of double-base extruded propellants. The size range extends from very thin sticks (outside diameter 1.5–5 mm) to very large diameter grains (around 500 mm).

Many extrusion profiles have been created, including end-burning grains, multiperforated, and external star grains with cylindrical or star-shaped central bores.

The weight of the grains varies from several grams, in the case of ignition increments, for example, to a few tens of kilograms for ground-to-air missile boosters.

The propellant manufacturing cycle is relatively short. The mixing, rolling and extrusion operations can be done in just 1 day. This rapid production feature of the solventless process makes it attractive for large-scale industrial production.

3.3. MANUFACTURING PROCESS OF CAST DOUBLE-BASE PROPELLANTS (CDB)

This process involves two main phases:

- Manufacture of the casting powder, which contains all of the nitrocellulose and the solid ingredients, as well as a portion of the inert plasticizers and, sometimes, nitroglycerine. This powder comes in the shape of small cylinders with a diameter and length close to 1 mm.
- The casting and curing phase. The casting powder is placed in a mold. A casting solvent — consisting mainly of desensitized nitroglycerine — fills the interstices between the grains. Heating at moderate temperature leads to a penetration of the casting solvent into the grains, resulting in the creation of a homogeneous propellant grain [14].

3.3.1. *Manufacture of the casting powder*

3.3.1.1. *Preparation of the raw materials*

The raw materials are generally used without any special treatment. The nitrocellulose, however, stored in a wet condition, undergoes a dehydration by ethyl alcohol before it is used.

When the casting powder contains nitroglycerine, a premixing operation is necessary. This consists of impregnating the dehydrated nitrocellulose with a nitroglycerine solution in acetone. This operation is carried out in a mixer equipped with one vertical blade slowly rotating.

3.3.1.2. *Kneading*

All ingredients are mixed together with the suitable solvents in order to obtain an extrudable dough. Although various solvents can be used for this operation, the most common ones selected are mixtures of ether and alcohol or acetone and alcohol.

The kneading, which takes place in a horizontal mixer with Z blades, produces a uniform mixture of all of the powder ingredients and allows the beginning of the gelatinization of the nitrocellulose in the presence of volatile solvents and plasticizers. Various parameters govern this gelatinization:

- The amount of solvent is adjusted according to the compositions used and, in particular, to the quality of nitrocellulose. The solvent to dough ratio or percentage has a significant influence on the solvation/gelation of the nitrocellulose and, as a result, on the ballistic and mechanical properties of the final propellant.
- The composition of the gelating solvent, i.e. the relative proportions of ether and alcohol, or acetone and alcohol.
- The introduction order of the ingredients. The nitrocellulose, if necessary premixed with the nitroglycerine, is introduced first, and the mixing operation is begun with the solvent so as to prepare a dough which will be ready for the subsequent homogenization of the various ingredients: plasticizers and ballistic catalysts.
- The temperature, generally maintained below the boiling point of the solvent, at approximately 30–40°C.
- The duration of the mixing operation, usually less than 4 h.

3.3.1.3. *Extrusion*

After the mixing, the dough is compacted into the barrel of an extrusion press which, unlike the presses for the solventless propellants, does not require a fine heat control or vacuum system. The operation is controlled to

ensure a constant extrusion speed, because this speed has a direct effect on the size of the extruded sticks (diameter close to 1 mm). The behavior of the dough at extrusion is largely a function of its composition and of its gelatinization state [15].

3.3.1.4. *Removal of solvents*

The cords produced by the extrusion press are placed in an oven in order to remove most of the residual solvents. As a result the sticks get a certain hardness, which makes them easier to cut.

3.3.1.5. *Cutting*

The quality of the cutting, typically using a guillotine technique, is important, because it directly influences the bulk or packing density of the powder. Typically, the length of cut is equivalent to the diameter of the sticks, i.e. 1 mm.

3.3.1.6. *Final drying*

Most of the solvents have been removed in the course of the previous operations; however, residual solvents are caught in the nitrocellulose fibers, and a simple heat conditioning may not be sufficient to remove them completely. Consequently, the next step may involve soaking the product for several days in hot water (60–80°C). This hot water medium facilitates removal of the solvents. Water has little chemical affinity with nitrocellulose, and can easily be removed by hot air drying (60°C). The proportion of volatile material in the powder is reduced to a value close to 1%.

3.3.1.7. *Finishing*

After the drying phase, the casting powder is often coated with graphite. This reduces the powder electrostatic charges and facilitates its flow properties. This operation also permits a deburring of the grains, i.e. a removal of the surface roughness, increasing the bulk or packing density of the powder. This operation is carried out either in a batch process in a mixing tower or a coating machine, or in a continuous process in a hopper with an endless screw.

The powder sub-batches obtained are mixed together to form a large homogeneous blended lot of casting powder. This operation is an essential one, because the uniformity of the properties of the cast propellant are largely determined by the properties of the casting powder.

3.3.1.8. Control of properties

A certain number of the characteristics of the casting powder are systematically controlled:

- the water and volatile material contents in the finished powder are limited respectively to 0.7 % for water and 1.8 % for the volatile materials;
- the apparent density or gravimetric density, which determines the packing or volume loading of the grains in a column of powder, and is consequently directly related to the final composition of the propellant;
- the chemical composition and, in particular, the amount of stabilizers, ballistic catalysts and graphite;
- the thermal stability, which is monitored by a sample heat test, where the temperature is raised up to 108.5°C or 120°C — the time required for the emission of nitrogen oxides is determined;
- the heat of explosion, which determines the final energetic properties of the propellant.

3.3.2. Manufacture of the casting solvent

The casting solvent is a mixture of nitrate esters and inert plasticizers. The latter are called desensitizers because they decrease the sensitivity to shock and friction of the nitrate esters.

The most commonly used solvents are obtained by mixing nitroglycerine and triacetin, which is a good desensitizer of nitroglycerine (Fig. 2).

Values for the following parameters are chosen to meet the requirements of particular applications and the desired performance:

- percentage of desensitizer (between 21 % and 27 % in most cases),
- percentage and the nature of the stabilizer (between 0.5 % and 1 %).

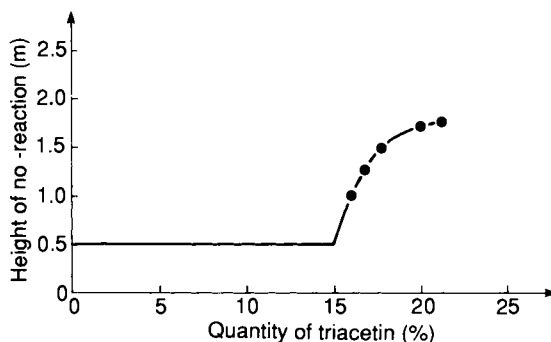


FIG. 9.2. Sensitivity to 30 kg fall-hammer test of casting solvent as a function of the quantity of triacetin.

The casting solvent is produced by introducing the nitroglycerine into a premix containing triacetin and the stabilizer. A dehydration process is carried out by heat treatment — under vacuum accompanied by pappling or bubbling dry air through the mix. A water content of less than 500 ppm is attained.

3.3.3. *Manufacture of the cast double-base propellants*

The objective is to obtain a homogeneous product by gelatinizing the casting powder with the casting solvent.

3.3.3.1. *Filling of the molds*

The casting powder is loaded into a casting mold that consists of the following parts:

- a base to allow the positioning of the casting corset and ensure a good distribution of the casting solvent;
- a metal casting corset or tube which will give the propellant blank grain its outside shape;
- a metal core to shape the central bore of radial burning grains;
- a top assembly to seal the mold, which includes a vacuum system and a sighting system allowing a check on the casting solvent injection.

The powder packing density generally reached is around 65%. This is a function of:

- the size of the casting powder grains — theoretical calculations reveal that the grain arrangement is optimum when the length versus diameter ratio is close to 1.
- the method by which the casting powder is introduced — various methods have been used to best fill the molds: vibrations, successive sieves with cross mesh and bars set in a spiral along the filling funnel;
- the characteristics of the casting powder itself: apparent density and also the surface condition, which in turn depends on manufacturing conditions, quality of the nitrocellulose, and powder nitroglycerine content.

Once the mold has been filled with powder a degassing phase, carried out under reduced pressure at ambient or moderate temperature and lasting a few hours, removes the residual volatile solvents and the air contained in the mold.

3.3.3.2. *Casting*

The casting consists of injecting the casting solvent into the base portion of the mold serving as a distribution chamber, and subsequent passage through the powder bed.

The interstices between the casting powders are filled with the casting solvent or gelatinizing liquid. Modeling studies of this phase [16,17] have revealed significant behavior variations, depending on the state of gelatinization and the nature of the casting powders.

3.3.3.3. *Curing*

Following casting the mold contents are subject to a curing process. This accelerates the gelatinization of the nitrocellulose by the casting solvent. The diffusion of the solvent is assisted by the presence of the triacetin molecules, which have a significant affinity for nitrocellulose. This phenomenon corresponds to more or less active interactions between the plasticizer and the nitrocellulose polymer, and causes a slight exothermic effect [18].

The curing process varies within different countries; it includes either one curing phase or two distinct steps:

- A precuring of 24–72 h, at a temperature of approximately 40–45°C, letting the grains absorb the maximum quantity of solvent necessary to make them swell. During this precuring phase the casting powders are already sufficiently gelled and coalesced to each other to allow the removal of excess casting solvent. This is necessary to avoid a risk of decomposition of the nitroglycerine in the surplus liquid during the second curing operation.
- The curing itself, which completes the migration of the solvent to the core of the nitrocellulose fibers.

As the curing progresses, the core of the granules becomes increasingly translucent and, after a few days, the entire grain is transformed into a homogeneous substance. The propellant has then attained its finished mechanical and ballistic properties. The entire operation requires periods of more than 72 h and temperatures ranging from 50 to 65°C (Fig. 3).

During the curing phase the propellant undergoes variations of volume whose magnitude depends on the degassing conditions of the powder and the solvent. These variations correspond mainly to the filling of the microporosities of the granules of the casting powder (Fig. 4).

3.3.3.4. *Mold disassembly*

Disassembly consists of removing the core from the propellant grain and drawing the grain from the casting tube.

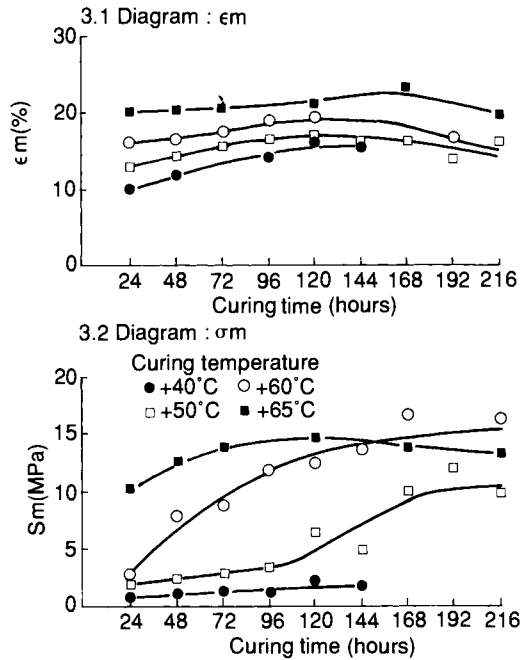


FIG. 9.3. Diagram of mechanical properties set up of a cast double-base propellant as a function of the curing conditions (time-temperature).

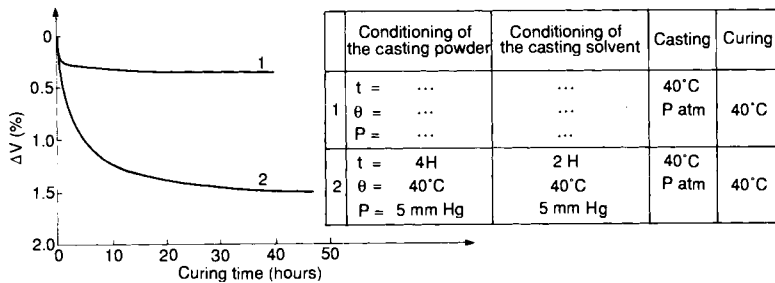


FIG. 9.4. Diagram of the volume variations of a cast double-base propellant as a function of the conditioning of the casting powder and of the casting solvent.

3.3.3.5. Machining

The ends of the propellant grain must be removed because their composition is slightly different due to the fact they were in proximity to the excess solvent during the precuring operation.

The grain is then cut to the proper dimensions using the same techniques as for extruded propellant grains (Section 3.2.).

3.3.3.6. *Inhibiting*

The process used to inhibit double-base cast propellants is the same as the process described for extruded propellants (Section 3.2.).

In some instances there are advantages for other techniques when application allows it (small or medium-size grains with fairly regular external profile). These techniques involve casting the propellant into the inhibitor by using an insulator as a casting mold. This operation offers the two following advantages:

- the machining operation is no longer necessary because the grains are cast directly in the dimensions required (except for the length of the grain);
- the final inhibiting operation is not necessary.

3.3.4. *Other processes*

The evolution of double-base cast composition toward increasingly energetic propellants has imposed some modifications to the process. For instance, the search for high contents of nitrate esters (nitroglycerine, for example) led to partly incorporating them into the casting powder, requiring, as a result, two modifications:

- the addition, already mentioned, of nitroglycerine to the nitrocellulose in a premixing phase;
- the exclusion of the water steeping phase, since the presence of high amounts of plasticizers facilitates the elimination of the volatile solvents.

The screw extrusion technique can simplify the process of obtaining casting powder. The performance characteristics of propellants made from such a casting powder are similar to that of propellants obtained by the conventional process.

3.3.5. *Current products*

The casting technique permits the production of propellant grains with virtually no limitations as far as shape is concerned, except for the height of product cast, although these can be as high as 2 m.

Many varied types of propellant grains are produced, such as end-burning grains, grains with cylindrical or star-shaped center bore, with variable profile such as partially slotted tubes, or dual propellant grains.

Their size may vary from a few grams to several hundreds of kilograms.

Because the cast double-base propellant technique has been thoroughly mastered, it allows the production of large industrial quantities; for example, sustainer propellant grains for anti-tank missiles.

4. Characteristics of Double-base Propellants

4.1. PHYSICOCHEMICAL CHARACTERISTICS

4.1.1. *Density*

The density of double-base propellants results from the density of their raw materials: nitroglycerine (1.60), nitrocellulose (1.650–1.662). However, it is also influenced by the density of the additives: lower-density non-energetic plasticizers and higher-density ballistic modifiers. Typically:

- 1.55 to 1.66 for EDB propellants;
- 1.50 to 1.58 for CDB propellants.

4.1.2. *Linear thermal expansion coefficient*

The coefficient determines the geometrical changes to the grains as a function of temperature, and consequently, permits assessment of the tolerances required inside the combustion chambers. This coefficient is characteristic of the nitrocellulose, nitroglycerine and plasticizer mixture, and is approximately 1.2×10^{-4} .

4.1.3. *Specific heat capacity*

Characteristic of the nitrocellulose–nitroglycerine matrix, the specific heat capacity is approximately 0.350 calorie per gram per degree for all double-base propellants.

4.1.4. *Thermal capacity*

Derived from the previous characteristics (specific heat, density) this is in the range of 0.570 calorie per gram per cubic centimeter.

4.1.5. *Thermal conductivity*

This property governs the heat exchanges inside a grain subjected to varying thermal environmental conditions. The reference value of 10×10^{-4} watt per centimeter per degree means that these propellants are a relatively insulating material.

4.1.6. *Heat of explosion*

The heat of explosion of the propellant is directly tied to its energetic level. Based on the respective ratios of the various ingredients, the two double-base propellants cover the following ranges:

- from 700 to 1100 cal/g for EDB propellants;
- from 500 to 900 cal/g for CDB propellants. The low values correspond to compositions with high contents of inert plasticizers, used as gas generators.

The heat of explosion of a propellant is equal to an additive value characteristic of each of its constituents. Table 2 gives the theoretical values for the major constituents of double-base propellants.

TABLE 2 *Heat of explosion of the main ingredients of double-base propellants*

	Potential (cal/g)
<i>Slabs</i>	
Nitrocellulose	+ 800 to 1080
Nitroglycerine	+ 1750
Nitrocellulose/nitroglycerine paste: 74/26	+ 1070
66/34	+ 1180
62/38	+ 1250
60/40	+ 1190
59/41	+ 1270
58/42	+ 1280
50/50	+ 1350
<i>Additives</i>	
Centralite	− 2440
2 Nitrodiphenyl amine (2NDPA)	− 1548
Diethylphthalate	− 1765
Dibutylphthalate	− 2070
Triacetin	− 1253
Neutral lead stearate	− 2103
Basic lead stearate	− 1264
Lead salicylate	− 915
Lead octoate	− 1331
Pb ₃ O ₄ minium	+ 139
Lead oxide (PbO)	+ 68
Copper octoate	− 1941
Copper chromite	+ 245
Potassium cryolite	− 14
Potassium sulfate	+ 222
Potassium nitrate	+ 1428
Acetylene black	− 3395
Magnesium stearate	− 2806
Aluminum	+ 3656
Candelilla wax	− 3277
Magnesium	+ 3214
Copper oxide (CuO)	+ 367
Dinitrotoluene 2-4	− 150
Dinitrotoluene 2-6	− 72
Ethylphenylurea	− 2236

4.2. MECHANICAL CHARACTERISTICS

Over the course of their service life, solid rocket motors are subjected to various stress factors (such as acceleration, vibration, shock, thermal effect, and others) which need to be compared with the mechanical capability of the propellant. A certain number of characteristics determines the propellant mechanical capability, including those discussed in the following paragraphs.

4.2.1. Hardness

Hardness is a quick and simple way of assessing the mechanical properties of a material. The values usually obtained at 20°C are about 55 shore A.

4.2.2. Tensile and compression behavior

Double-base propellants are characterized by high elastic moduli and mechanical properties suited to use in free-standing grains, sometimes with a very thin web.

These characteristics are most commonly determined by performing uniaxial tensile tests. The JANNAF specimen, dumbbell type, is most widely used. A complete mechanical characterization of the properties of a propellant needs the performance of a large number of tensile tests in order to test the behavior of the material within a wide range of times and temperatures. A sample of the master curve (S_m , E , ϵ , e_m) of an EDB propellant is given in Fig. 5. Table 3 is a mechanical characteristics example of an extruded and cast composition.

TABLE 3 Comparison of the mechanical properties of an EDB propellant and a CDB propellant

	-40°C	+20°C	+60°C
<i>EDB Propellant</i>			
S_m (MPa)	51	11	2
ϵ (%)	2.8	2.5	8.0
E (Mpa)	1835	439	21
e_r (%)	3.4	15.7	31.8
<i>CDB Propellant</i>			
S_m (MPa)	33	11	3
ϵ (%)	1.0	2.0	10.7
E (MPa)	3279	555	27
e_r (%)	1.2	24.5	66.8

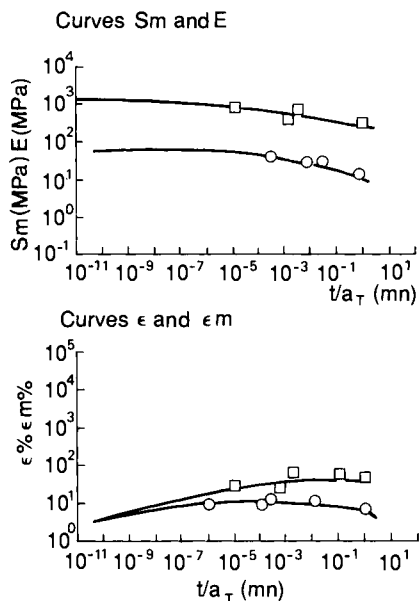


FIG. 9.5. Master curves for an E.D.B. propellant.

4.3. KINETIC CHARACTERISTICS

4.3.1. *Burning rate*

The burning rate of homogeneous propellants depends primarily on the ballistic modifiers in the composition.

Figure 6 and 7 show the performance currently available. The range of burning rates of EDB propellants, at 20°C, is between 5 and 40 mm/s, while the range of CDB propellant is narrower, from 3 to 20 mm/s.

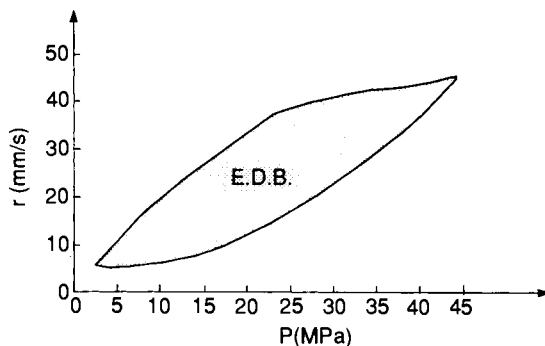


FIG. 9.6. Range of burning rate-pressure available to E.D.B. propellant.

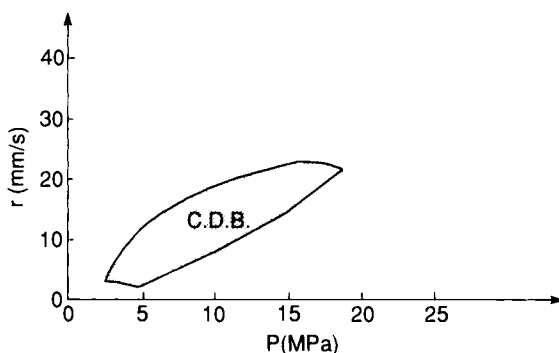


FIG. 9.7. Range of burning rate-pressure available to C.D.B. propellant.

The plateau effect is found in a pressure range which depends on the burning rate. Consequently, at 5 mm/s the plateau pressure is around 5 MPa, while at 40 mm/s it is approximately 30 MPa.

4.3.2. *Temperature coefficient*

The temperature coefficient expresses the sensitivity of the propellant burning rate to its temperature before combustion. Where homogeneous propellants are concerned the values obtained vary greatly, depending on the composition:

- $\pi_k = 0$. The burning rate is independent of the temperature. This phenomenon is observed, in particular, for EDB propellants with low energetic levels (lower than 900 cal/g).
- $\pi_k < 0$. As the temperature before combustion goes up, the burning rate decreases. This type of value is found mainly with CDB propellants with low energetic levels (of the order of 700 cal/g).
- $\pi_k > 0$. This is the most frequent case with these propellant families. The values obtained are in the range of 0–0.3% per degree; a few higher values can be found with highly energetic propellants (higher than 1100 cal/g).

4.3.3. *Parameters affecting the burning rate*

The burning rate depends mainly on the nature of the catalytic system. Besides this major factor, there are other parameters worthy of notice.

4.3.3.1. *Adjustment*

Certain elements such as acetylene black, by varying very slightly the amounts used, can significantly change the burning rate. This property is

used to guarantee a perfect reproducibility of a specific composition, regardless of the various raw materials lots.

4.3.3.2. Ballistic modifiers particle size

Some of the catalysts can influence the burning rate with their particle size. This effect is of relatively modest importance; it has been seen with certain oxides (CuO, for instance). The particle size of the catalysts typically is of the order of a few microns.

4.3.3. Manufacturing process

The processing may also have an impact on the ballistic properties of double-base propellants, inasmuch as they influence the homogeneity of the catalysts' distribution and the gelatinization of the product. This effect was demonstrated with both propellant families.

(a) Extruded double-base propellants

The duration of the agglomeration rolling operation (done in the presence of humidity) can be significant in some cases to the level of the final ballistic performance. There is a decrease in the pressure exponent and the creation of a plateau effect by prolonging the duration of this rolling operation [19].

(b) Cast double-base propellants

The gelatinization phenomenon is, for this family, mostly due to the chemical action of the solvent used to manufacture the casting powder. As such, the amount of solvent introduced in the mixer and, in particular, the quantity of acetone, are likely to have an influence on the characteristics of the final propellant. A large quantity of acetone promotes the gelatinization and makes the fibrous structure of the nitrocellulose disappear. Casting powder, in an advanced state of gelatinization, has less affinity for the casting solvent, which will have more difficulty in penetrating inside the casting powders. The final propellant, as a result, will be more heterogeneous and the ballistic properties, which are related to the homogeneity and the state of gelatinization, will therefore be modified.

(c) Comparison of EDB and CDB processing techniques

Both processing techniques have been tested for the manufacture of double-base propellants. The EDB process leads to a better-gelatinized and more homogeneous product, because of the efficiency of the mechanical and

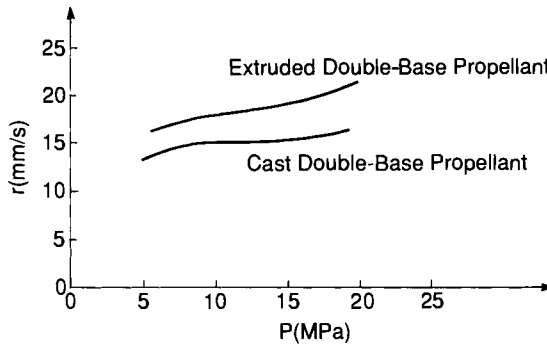


FIG. 9.8. Influence of the manufacturing process on the ballistic characteristics of a double-base propellant.

thermal actions of rolling. A comparison of the ballistic properties (Fig. 8) reveals a higher burning rate for the EDB propellants.

4.3.3.4. Energetic level

The plateau effect of the double-base compositions is obtained by using catalytic systems tailored to the energetic level of the composition.

The plateau burning rate is related to the super-rate effect caused by the ballistic modifiers. The result is that a high energetic level leads naturally to a high burning rate.

The energetic level also has a significant impact on the temperature coefficient, which generally increases with the energy of the compositions.

4.4. ENERGETIC CHARACTERISTICS

The energetic characteristics are usually expressed in terms of specific impulse (in seconds). As an alternative to the necessity of systematic experimental measurements on standard grain, various simplified approaches have been used to determine the energy characteristics of a propellant:

- the theoretical specific impulse, derived from thermodynamic calculations;
- the heat of explosion, corresponding to the measurement of the calorific value during the combustion of the propellant.

4.4.1. Theoretical performance

The theoretical performance of a given composition may be calculated by taking various parameters into account, such as:

- atomic composition of the propellant (C, H, O, N and others);
- chemical equilibrium in the combustion chamber;
- combustion conditions (gas expansion).

4.4.2. Heat of explosion

The heat of explosion, expressed in calories per gram, permits a simple measurement of the energetic level. The operation is carried out in a calorimetric closed vessel, and consists of measuring the rise in temperature of a specific quantity of water during the combustion of a specific amount of propellant.

The value of the heat of explosion of a composition may also be determined through calculations. It is the result of the weighted algebraic sum of the calorimetric values of its constituents (Section 4.1.).

4.4.3. Available range

This is primarily a function of the amounts of the major constituents (nitroglycerine: 1750 cal/g, nitrocellulose: 920 cal/g, inert plasticizer: –1300 cal/g), as well as of the possibility of having a plateau effect. An increase in the energetic level leads, in fact, to a decrease of the plateau effect, because of a loss of efficiency of the combustion catalysts.

Today, the highest performances with acceptable ballistic characteristics are approximately 1100 cal/g for EDB propellants and 900 cal/g for CDB propellants.

An increase of the energetic level, significantly higher than these values, may be obtained by adding nitramines (Chapter 11).

4.4.4. Correlation between the specific impulse and the heat of explosion

There exists a linear relationship between the specific impulse and the calorimetric value (Fig. 9). The difference between the theoretical specific impulse and the delivered specific impulse for a reference rocket motor weighing approximately 2 kg is about 15 s.

The weight of the reference grain is also an important parameter in terms of influence. For instance, a difference of 2 s in specific impulse is found depending on whether the measurement is made on a standard motor equipped with a star-shaped central bore grain 203 mm in diameter, 500 mm long, and weighing 19 kg; or with a grain measuring 90 mm in diameter, 300 mm in length, and weighing 2 kg.

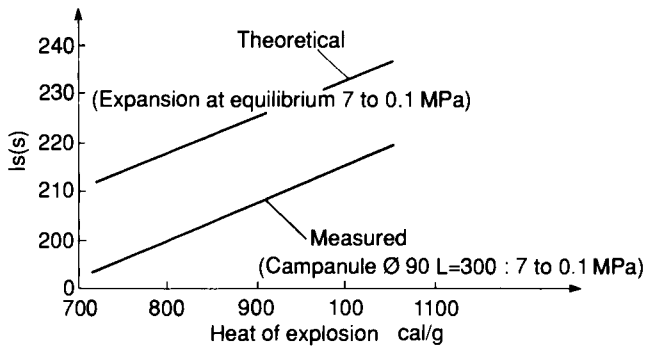


FIG. 9.9. Correlation diagram between the measured specific impulse, the theoretical specific impulse, and the heat of explosion of double-base propellants.

5. Operating Characteristics

5.1. SIGNATURE

5.1.1. Smoke

Propellant combustion and the decomposition through pyrolysis of the inert materials of the rocket motor (inhibitors and thermal insulation, for example) generate smoke in the rocket exhaust which may have a detrimental consequence, either by interference with the missile guidance or by permitting the missile or its firing location to be revealed. A distinction must be made between:

- primary smoke, which is generally the result of metallic particles contained in the propellant; and
- secondary smoke, which may result from the condensation of the combustion gases (H_2O , for example) or of the combination of atmospheric water vapor with certain combustion products (HCl , HF , and others).

Various approaches, more or less quantitative, allow evaluation of the amount of smoke produced by a propellant:

- thermodynamic calculation, used to determine the chemical products resulting from the combustion;
- visual assessment; and
- optical measurements taken in the visible or the infrared wavelengths.

Homogeneous propellants produce no secondary smoke and little primary smoke, since they contain no reducers and have only a small amount of metallic particles from their additives [20] such as:

- ballistic modifiers, generally consisting of organic salts and copper or lead minerals;
- particulate damping, generally consisting of refractory oxides, limited to the necessary amount because they remain as solids in the jet and their particle size can be optimized to reduce their interaction with light;
- Flash suppressant additives, which as alkaline-ion-based products (usually potassium) may also include other metallic-type elements (aluminum, for instance).

5.1.2. Secondary flame

Besides smoke, another element considered when assessing the signature is the presence of flames in the exhaust. The combustion gases may re-ignite downstream from the exit plane of the nozzle. This is known as the afterburning phenomenon, which corresponds to an oxidation by the air of the reducer products (H_2 and CO) produced by combustion of the propellant.

Similar to the smoke, the measurement of the exhaust during propellant combustion gives an indication of the intensity of the flash produced. The signature is not limited to the visible spectrum, but occurs also in the infrared region.

Many studies in this field have determined that the principal parameters are:

- composition of the propellant (energetic level, combustion temperature, nature of the gases, amount of reducing products, and presence of flash suppressants);
- combustion conditions;
- performance of the missile.

To prevent secondary afterburning it is necessary to seed the exhaust with particles likely to block the reactive mechanisms of re-ignition [22].

Many studies have been made to identify the additives that would be effective and the best manufacturing processes. Among the products most often mentioned in publications, and most widely used industrially, we find products with an alkaline metal base (usually potassium), such as nitrate, cryolite, sulfate, and potassium hydrogenotartrate, but also barium-based and tungsten-based products. The selection of an additive is made by taking into account not only its efficiency, but also the consequences resulting from its introduction on the propellant performance, in particular:

- energetic level,
- chemical stability,
- aging properties,
- creation of primary smoke and
- ballistic performance.

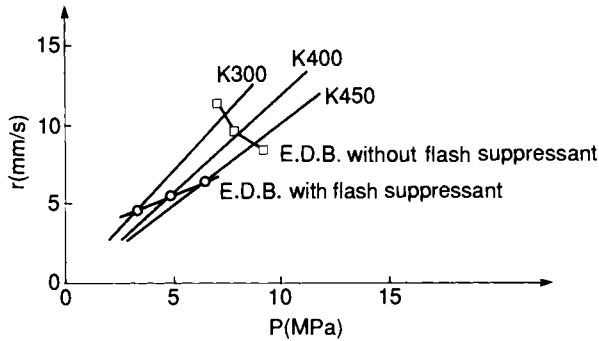


FIG. 9.10. Diagram of burning rate-pressure of an E.D.B. propellant with and without flash suppressant.

The direct introduction in manufacture during mixing of a flash suppressant is likely to significantly modify the ballistic performance of EDB or CDB propellants (Fig. 10); it is therefore necessary to modify the propellant manufacturing process to avoid this problem.

In the case of EDB propellant it suffices to incorporate the flash suppressant late in the process. This prevents it from mixing intimately with the ballistic catalysts. By introducing the suppressant at the time of the final rolling operation it is possible to obtain propellants with ballistic performances which are not adversely affected by the presence of this additive.

In the case of cast double-base propellant the process modification consists of separating the flash suppressant from the ballistic modifiers by using two casting powders, only one of which contains the suppressant additive. This allows the content of suppressant to be adjusted to the relative amounts of the casting powders. The best trade-off needs to be determined between the amount of additive in the special casting powder, and the amount of that casting powder to be used in the composition.

5.2. COMBUSTION INSTABILITIES

5.2.1. Theoretical data

Under certain internal configurations and firing conditions, radial burning grains may exhibit combustion instabilities that will translate into pressure fluctuations. These instabilities may belong to two types:

- longitudinal instabilities, whose frequency is a function of the geometrical dimensions of the grain (a few hundred hertz);
- high-frequency transverse instabilities, which may have two different modes, radial or tangential, or possibly a mixture of the two.

These instabilities cause:

- perturbations in the nominal pressure, triggering oscillations of the thrust delivered by the propellant grain;
- a possible pressure shift that may, in some cases, result in the extinction of the grain;
- the risk of re-igniting the gas jet, leading to an afterburning phenomenon.

These instabilities are more frequently triggered in propellants with a high energy level or a fast burning rate.

5.2.2. *Effect of the configuration of the propellant grain and of the firing conditions*

The frequencies of the instabilities are related to the geometrical dimensions of the central bore of the grain. For instance, there usually is, for a given diameter, a length above which combustion instabilities will occur (Fig. 11). This length depends on the nature of the propellant. Conversely, for a specific grain length these instabilities appear at a diameter smaller than a certain limit value. We must also consider that, in addition to the length and the diameter values, certain geometrical configurations of the central bore may also be more prone to trigger instabilities. In the case of a star-shaped central bore, for example, an even number of branches is a factor likely to trigger instabilities (perfect symmetry of the grain).

While the firing conditions are a significant triggering factor, pressure is still the essential parameter. While they do not occur at high operating pressures, instabilities appear toward the lower pressure, generally corresponding to the lower limit of the plateau effect. It is, as a matter of fact, possible to identify a threshold pressure below which instabilities are started.

Similarly, low temperatures are more likely to trigger instabilities [22]. The

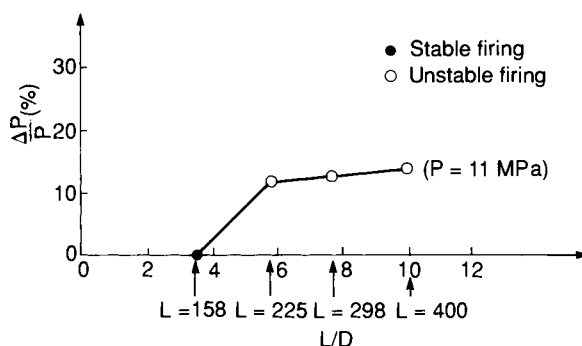


FIG. 9.11. Influence of the length of a 90 mm diameter star grain on the severity of the combustion instabilities.

combination of a low pressure and low temperature (-40°C) creates a high likelihood of instabilities.

Finally, this phenomenon does not appear to be related to the chemical nature of the propellant but rather to its ballistic characteristics (such as burning rate), and its energetic characteristics (such as heat of explosion).

5.2.3. *Function of the refractory additives*

The presence of solid particles in the gas exhaust from the combustion chamber permits damping of the pressure oscillations. A judicious selection of their quality and quantity allows complete suppression of the combustion instabilities (Fig. 12). There are several possibilities:

- a source, outside of the propellant, such as the inhibitor or the thermal insulations, which, through degradation caused by the combustion, seeds the gas exhaust with particles;
- the inclusion in the propellant of aluminum, zirconium, or tungsten particles which, during combustion, produce liquid or solid products (Al_2O_3 , W_2O_3 , for example);
- the presence of refractory additives in the propellant, which is the most widely used technique.

The products used are selected on the basis of the smallest possible needed quantity. Among the selection criteria are:

- The melting temperature, which must be greater than the flame temperature; the most widely used compositions are oxides (ZrO_2 , SiO_2 , B_2O_3), carbides (Si, Zr, Ti) and silicates (ZrSiO_4) [23].

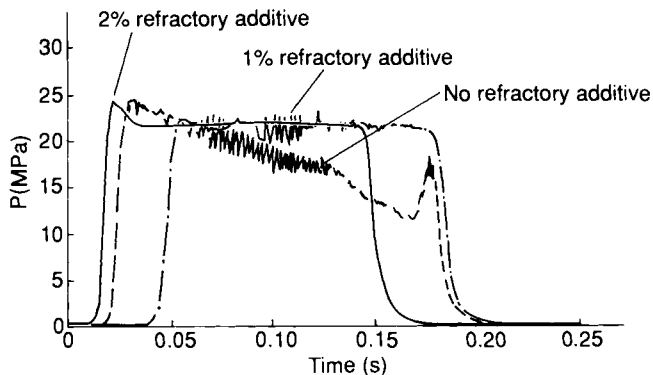


FIG. 9.12. Evolution of the combustion instabilities recorded on an E.D.B. standard ballistic grain (32×16 Type) as a function of the quantity of refractory additive.

- The particle size, selected in accordance with the formula:

$$R = \frac{3}{2} \left(\frac{\mu}{\rho \pi F} \right)^{1/2}$$

where:

R = optimal radius of the particles,
 μ = viscosity of the combustion gases,
 ρ = density of the particles,
 F = frequency of the instabilities.

In practice, the optimal radius is smaller than a micron.

- Finally, since these additives may have a detrimental effect on the other characteristics of the propellant, they are chosen for the minimum negative impact on:
 - the chemical stability of the propellant and its energetic performance,
 - the burning rate and the temperature coefficient, and
 - the signature.

5.3. EROSION COMBUSTION

Erosive combustion occurs when a solid propellant grain is exposed to a gas flow, parallel to its surface and with a high flow rate (Q). We see a significantly increased burning rate for the propellant (V) compared with the normal burning rate (V_o), related by a formula of the type:

$$V = V_o [1 + k(Q - Q_s)]$$

where k is the erosivity coefficient of the composition (which depends on the burning rate, the catalytic system used, etc.) and Q_s the threshold of the flow above which the erosive phenomenon occurs.

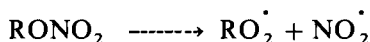
Firing of the propellant grain, followed by quenching, permits the analysis of the contours, and determination of the erosivity coefficient. The erosivity coefficient of EDB propellants is of the order of 4×10^{-4} and the threshold flow rate varies from 500 to 100 g per second per square centimeter.

6. Chemical Stability

6.1. BACKGROUND

The nitrate esters used with double-base propellants are molecules that are not very chemically stable. In the usual ambient conditions of temperature, pressure and hygrometry their decomposition is slow. However, in more severe environments (high temperatures, acid chemical environment), the

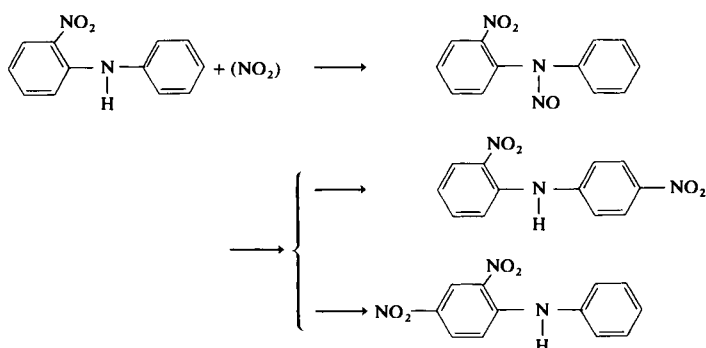
decomposition of nitric esters becomes autocatalytic. These reactions give rise to radical thus:



The free radicals attack the nitrate esters not yet decomposed; this is followed by a complex succession of secondary reactions producing gaseous products such as CO, N₂, and mainly, nitrogen oxides NO and NO₂.

The function of stabilizers introduced into the propellant is to remove a portion of the nitrogen oxides by fixing them chemically. The autocatalytic procedure is thereby slowed down.

The stabilizer reactions involved correspond to a succession of nitrosation and nitration reactions. In the case of 2-nitrodiphenylamine, it is of the type:



In these conditions the use of a double-base propellant is based on knowledge of:

- the intrinsic chemical stability of the composition, assessed at the time of its development and controlled during its manufacture;
- the preservation of sufficient stability for the entire service life of the propellant, which is generally determined through the performance of accelerated aging tests.

Consequently, the manufacturing controls are based mainly on two principles:

- the inclusion of stabilizer in the propellant;
- the kinetics of emission of nitrogen oxides.

6.2. TESTS

6.2.1. Stabilizer quantity

The inclusion of stabilizers is checked on standard samples that are representative of the various batches. In the case of CDB propellants this control is also made, on the casting powder.

The analyses are done using chromatographic techniques (chromatography during the gaseous phase, or high-performance liquid chromatography).

The values obtained usually correspond to a theoretical percentage, ranging from 1 % to 3 %. A drop in this percentage reveals a variation in the manufacturing process such as, for example, a rolling temperature that is too high.

6.2.2. Stability test at 120°C

The high-temperature stability tests measure the rate of nitrogen oxide output of a propellant standard specimen (2.5 g) placed in a test tube inside a temperature-regulated enclosure. A methyl purple reactive paper is placed in the tube. The color of the paper changes in the presence of nitrogen oxides. This change of color marks the first release of nitrous vapors that are not trapped by the stabilizer. The test usually takes place at 120°C in order to accelerate the decomposition phenomenon and shorten the time necessary for the paper to change color (a few tens of minutes). This type of test is also done for CDB propellants, on the casting powder at 108.5°C.

The results obtained from these tests are a function of the composition and may vary for the double-base propellant family from 30 to more than 100 min. However, when testing a given propellant composition, industrially manufactured, the values obtained are highly reproducible.

The results of these tests may not be directly related to the service life of the propellant, but yet they allow us to assign each manufactured propellant a reference value which is characteristic of the composition, thereby giving a basis for detecting possible changes caused by foreign bodies in the propellant, variation in manufacturing conditions, or quality of the raw material.

A significant difference in comparison to an average value indicates a manufacturing deviation.

6.2.3. Chemiluminescence

This technique has been recently developed to assess the chemical stability of propellants and to avoid some of the drawbacks of the test done at 120°C, i.e.:

- 120°C is a very high temperature that is not related to the normal storage temperature of propellant;
- the 120°C test is a global analysis of the phenomenon of the generation of nitrogen oxides, without any distinction between the various types: NO, NO₂ and others.

The chemiluminescence technique relates the amounts of NO and NO_x to the intensity of a luminous radiation that accompanies the chemical reaction

(NO_x: mixture of NO and NO₂) of NO in the presence of ozone.



The quantity of light given out is directly proportional to the number of nitrogen molecules contained in the gas being analyzed.

The propellant sample, when heated, gives off an amount of gaseous nitrogen oxides. This gaseous sample is separated into two parts, one which goes directly into a chamber containing ozone where the reaction takes place, in front of a photomultiplier, and the other first going through a catalytic convertor that reduces NO_x to NO.

The analysis of the data obtained in this manner allows us to measure by deduction the amounts of NO, NO_x and NO₂. With this method the emission of the various nitrogen oxides can be continually recorded.

A quantitative interpretation of this test for manufacturing control may be done by specifying:

- the shape and weight of the reference sample;
- the temperature of the test;
- the duration of the test.

Finally, by comparing the NO and NO₂ levels, an indication of the degree of the material alteration is obtained; the degree increases with the level of NO.

6.2.4. Other tests

The stability of propellants can also be measured by performing a number of other gaseous evolution tests. These are generally done when there is a need to determine the characteristics in a special environment. There is, for example, the vacuum test designed to quantitatively measure the gaseous volume released after a 200 h exposure to a specified temperature.

6.3. PARAMETERS AFFECTING THE CHEMICAL STABILITY [24]

Much work has been done to determine the parameters that have an influence on the chemical stability of propellants. As a result, the following parameters were identified:

- *The heat of explosion*: the increase in the energetic level results in an acceleration of the kinetics of nitrogen oxide generation.

<i>Heat of explosion</i>	<i>CDB Composition</i>	<i>Stability at 120°C (mn)</i>
900 cal/g	Paste 1 + 2 NDPA	100
1100 cal/g	Paste 2 + 2 NDPA	80

● *The nature of the stabilizers:*

Stabilizer level 2%	Centra- lite	2 NDPA	MNA	Resor- cinol	2 NDPA 1% MNA 1%	2 NDPA 1% Resorcinol 1%
Stability at 120°C (mn)	60	80	100	80	90	65

- *The amount of stabilizers:* with a 1100 cal/g composition the stabilizer does not have much effect at an amount above 2%.
- *The nature of the additives:*
 - potassium salts are usually detrimental to chemical stability;
 - refractory additives have no influence;
 - the effect of burning rate additives (Pb and Cu salts) depends on the nature of the salt. Aromatic salts have the capability of fixing nitrogen oxides, and are therefore generally favorable to chemical stability.

7. Aging

The decomposition of the nitrate esters described above leads to an aging of the propellant, depending on environmental conditions (temperature, humidity, presence of inhibitor, etc.), resulting in the progressive consumption of the stabilizer, which can culminate in a cracking of the propellant, an alteration of the mechanical properties, and a change in the ballistic properties.

7.1. CONSUMPTION OF THE STABILIZER

In order to assess the service life of a propellant in terms of its chemical stability, samples are subjected to accelerated aging at temperatures ranging between 60 and 80°C. The amount of stabilizer is measured over time. Based on usual kinetic laws (Arrhenius or Berthelot), a stabilizer consumption law can be deduced for the storage temperatures of the propellants.

With EDB and CDB propellants the service life that corresponds to a consumption of less than 50% of the stabilizer is on the order of several tens of years at ambient temperature.

7.2. AGING-RELATED CRACKING

The gaseous products from the decomposition of the nitrate esters are soluble in the propellant through which they diffuse to atmosphere. When the kinetics of gaseous generation exceeds the rate of diffusion, the gases created exert a pressure which may cause a physical breakdown of the material (cracks, vacuum holes), particularly in the case of thick propellant grains.

Several formulas have been proposed to determine the critical pressure in terms of the mechanical properties (S_m , e_m) of the propellant [25].

The cracking phenomenon can be modeled, based on the laws:

- of Arrhenius for gas generation;
- of Henry for solubility of gases in propellant;
- and of Fick for gas diffusion.

The experimental studies may be done with propellant cubes, of different sizes, subjected to high temperatures (on the order of 60–80°C). X-rays of the cubes can detect the occurrence of defects such as vacuum holes and cracks. This is known as the cube test. It can be used to determine the critical edge length: the largest cube which, when subjected to a test of specified duration at a specified temperature, exhibits no degradation [26].

The analysis of these results, extrapolated to normal temperatures, makes it possible to determine the critical diameters of the grains of a given propellant composition.

7.3. MECHANICAL AND BALLISTIC AGING

Providing that the environmental conditions are such that the chemical stability of the propellant is preserved, double-base propellants do not have any significant change of their mechanical or ballistic properties. However, a substantial loss of nitroglycerine could lead to a hardening of the propellant.

8. Safety Characteristics

Propellant grains for rocket motors are designed and manufactured to be used according to a well-defined decomposition mode: combustion burning. This is a slow phenomenon that propagates itself through parallel layers. The initiation of the phenomenon can be obtained through various types of induced stress: thermal, mechanical, or electric.

However, propellant may, under certain conditions best avoided, adopt a different mode of decomposition, even a different regime of decomposition.

8.1. SAFETY AND TOXICITY OF THE INGREDIENTS

The various ingredients used in propellants are indexed in toxicity lists which indicate the various and particular precautions that must be observed during the manufacture.

As far as the pyrotechnic safety characteristics are concerned, the nitrocellulose is usually desensitized through the addition of water — manufacture of pastes — or alcohol. (A propellant conditioned with alcohol belongs in the hazard class 1.4.)

On the other hand, taking into account its characteristics (Table 4) nitroglycerine is never used pure, but in association with nitrocellulose (EDB propellant pastes) or with triacetin, a casting solvent for CDB propellants.

The crystallization of nitroglycerine, likely to occur at temperatures below 12°C, must be prevented, although the crystallized product is no more sensitive than the liquid product. The hazard lies in the fact that the crystallization is likely to produce frictions between the crystals, and thus in turn may lead to a decomposition by detonation.

In addition to the pyrotechnic risk, nitroglycerine is also toxic. Its vapors cause migraines and nausea because it is a cardiac hypotensor.

TABLE 4 *Comparison of safety characteristics between nitroglycerine and casting solvent*

Test	Results expressed in	Nitroglycerine	Casting solvent (78% Nitroglycerine)
Card gap test	Number of cards	> 340	75
Sensitivity to 30 kg fall hammer	Height of no reaction (m)	0.5	> 4
Critical thickness	mm	< 0.1	4
Steel tube-drop test	Height of no reaction (m)	< 0.25	1

8.2. APTITUDE TO IGNITION

8.2.1. Heat sensitivity

The heat sensitivity tests are designed to determine the temperatures at which a propellant specimen ignites. These tests may be performed with specimens broken into small pieces (autoignition test) or compact (cook-off test).

8.2.1.1. Autoignition test

This test is used to measure the temperature of spontaneous ignition of the propellant:

- either by progressive heating, regularly increasing the temperature by 5°C every minute;
- or by sudden heating.

These tests tell us exactly the maximum temperatures to which the propellant can be subjected during its manufacture or its use.

In the progressive heating test, 180°C is a reference temperature used for all double-base propellants.

8.2.1.2. Cook-off test

This test is used to determine the lowest temperature of spontaneous ignition after extended exposure to that temperature.

This temperature is around 110°C for all double-base propellants.

8.2.2. Mechanical sensitivity

The combustion of the propellant may also be triggered by the mechanical stimuli of impact or friction. Various tests have been devised to quantify the level of stimulus necessary to cause ignition, including:

- friction sensitivity: the average recorded value is of the order of 20 Newton;
- impact sensitivity.

Several tests have been developed to characterize the impact behavior of propellants. Two of these are most widely used:

- the 30 kg fall hammer test: the principle involves dropping a 30 kg weight onto a plate of propellant; the height of the drop determines the amount of energy involved;
- the impact sensitivity test: steel fall hammers of various weights are dropped from varying heights onto a propellant sample held between two steel clamps.

The values obtained in these tests identify the level of impact that are prohibited for the propellant (dropping propellant grains, shocks, etc.).

8.2.3. Electric sensitivity

Double-base propellants have been found insensitive to electric energy up to about 600 mJ.

8.3. DETONABILITY

Detonation is an exothermic chemical decomposition reaction which, coupled to a shock wave, propagates itself through the material. This

accidental rate of decomposition is a risk for all solid propellants, and in particular for double-base propellants. A certain number of criteria exists that permits us to characterize the detonability:

- the detonability index. When compared to the results obtained with composite propellants — one card — the values corresponding to double-base reveal a significantly increased aptitude for detonation: 90–100 cards.
- the critical diameter. They are significantly smaller than those of composite propellants.

Table 5 provides an overview of the major safety characteristics of double-base propellants.

TABLE 5 *Main safety characteristics of double base propellants (typical cases)*

Tests	1000 cal/g EDB	800 cal/g CDB
<i>Ignition</i>		
Autoignition through progressive heating	173°C	176°C
Autoignition through sudden heating	268°C	277°C
Cook-off	110°C	
Friction sensitivity	210 N	210 N
30 kg hammer fall sensitivity (no reaction)	greater than 4 m	greater than 4 m
Impact sensitivity	4.9 J	5.9 J
Static electricity sensitivity	600 mJ	600 mJ
<i>Detonability</i>		
Card gap test	100 cards	90 cards
Critical diameter	2 mm	14 mm

Bibliography

1. DUBAR, J., Thèse de Doctorat d'Etat ès Sciences Physiques. Faculté des Sciences de Paris. Contribution à l'étude des interactions entre les nitrocelluloses et la nitroglycérine. Comparaison de cette dernière avec différents solvants. 1969.
2. COSGROVE, J. D., HURDLEY, T. G., LEWIS, T. J. and PERME, W. A., The diffusion of acetone and isopropyl nitrate into nitrocellulose and nitrocellulose/nitroglycerin in films. Conference on Nitrocellulose Characterisation and Double-Base Propellant Structure. Waltham Abbey, Essex, England, 1980.
3. QUINCHON, J. and TRANCHANT, J., *Les Poudres, propergols et explosifs*. Tome 2: *Les Nitrocelluloses et autres matières de base des poudres et propergols*. Editions Lavoisier, Technique et Documentation, 1984.
4. CAIRE MAURISIER, M., Thèse de Docteur Ingénieur: La Nitroglycérine dans les propergols: Conformation — Stabilité thermique — Recherche de stabilisants et de modificateurs de combustion — Migration à travers les vernis polyesters. Université de Bordeaux I., 1976.
5. CAMP, A. T., CSANADY, E. R. and MOSER, P. R., Plateau propellant compositions. United States Patent 4-239-561, 1980.
6. ALLEY, B., DAKE, J. D. and DYKES, H. W. H., Ballistic modifiers and synthesis of the ballistic modifiers. United States Patent 4-202-714, 1980.
7. SORNBERGER, G., DELEGLISE, P. M. and AGASSANT, J. F., Etude théorique de filières améliorées pour extrusion de propergols S. D. CEMEF — Contract Dret, 83/406.

8. GOUGOUL, P., DOIN, B. and HISS, A., SNPE. Brevet Français no. 76 39455. Procédé de moulage à chaud des blocs de propergol double-base, 1976.
9. CRAIG-JOHNSON, C. E. and DENDOR, P. F. No roll process for manufacture of double-base and composite modified double-base extrusion compositions. 19th Explosive Safety Seminar, Los Angeles, 1980.
10. GIMLER, J. R., Solventless extrusion of double-base propellant prepared by a slurry process. United States Patent 4-298-552, 1981.
11. MULLER, D. and STEWART, J., Twin screw extrusion for the production of stick propellants. *Journal of Hazardous Materials*, 9, 47-61, 1984.
12. OLSSON, M., *Screw extrusion of double-base propellants*. ICT Jahrestagung, Karlsruhe, 1981.
13. AUSTRUY, H., RAYMOND, J. P. and CANIHAC, J., Utilisation d'une boudineuse à vis pour la production industrielle d'un bloc de propergol double base pour autopropulsion. ICT Internationale Jahrestagung, 1984.
14. STEINBERGER, R. and DRECHSEL, P. D., Manufacture of cast double-base propellant. *Advances in Chem. Serv.* (88), 1-28, R. F. Could, Ed., 1969.
15. CARTER, R. E., Extrusion properties of propellant doughs. Conference on Nitrocellulose Characterisation and Double-Base Propellant Structure, Waltham Abbey, Essex, England, 1980.
16. CHARRE, J. M., LONGEVIALLE, Y. and NAIDEAU, P., Test de pertes de charges. Application à la caractérisation des poudres à mouler. Internationale Jahrestagung, ICT, 1978.
17. HARRIS, D. and IRLAM, G., A study of mechanism of the casting process for the manufacture of double-base propellants. Internationale Jahrestagung, ICT, 1978.
18. RAT, M., HERMANT, I. and LONGEVIALLE, Y., Application de la microcalorimétrie à la caractérisation de la cuisson des propergols double base et double base composites moulés. Internationale Jahrestagung, ICT, 1986.
19. LEWIS, T. J., The effect of processing variations on the ballistics of fast-burning, extruded, double-base propellants. AIAA 14th Joint Propulsion Conference, AIAA 78 1014, 1978.
20. DERR, R. L. and BOGGS, T. L., Hazard/performance tradeoffs for smokeless solid propellant rocket motors. AGARD Propulsion and Energetics Panel. 66th Meeting, Florence, Italy, 1985.
21. EVANS, G. I. and SMITH, P. K., The reduction of exhaust signature in solid propellant rocket motors. AGARD Propulsion and Energetics Panel, 66th Meeting, Florence, Italy, 1985.
22. NUGEYRE, J. C., DAUGA, P. and PHILIPPE, P., An example of failure by acoustic coupling of a free-standing double-base propellant grain. AIAA/SAE/ASME 17th Joint Propulsion Conference. AIAA 81 1525, 1981.
23. EVANS, G. I. and SMITH, P. K., The suppression of combustion instability by particulate damping in smokeless solid propellant motors. AGARD 53rd Meeting on Solid Rocket Technology, Oslo, 1979.
24. RAYMOND, J. P., AUSTRUY, H. and RAT, M., Evaluation de la stabilité thermique et du vieillissement fissurant des propergols homogènes double base. Internationale Jahrestagung, ICT, 1986.
25. COST, T. L., WEEKS, G. E. and MARTIN, D. L., Service Life Analysis of Rocket Motors with Internal Gas Generation. AIAA/SAE/ASME 17th Joint Propulsion Conference, AIAA 1546, 1981.
26. AUSTRUY, H. and RAT, M., Gas Generation in Double-Base and Crosslinked Double-Base Propellants. ADPA Symposium, Long Beach, Ca. 27 — 29, 1986.

CHAPTER 10

Composite Propellants

ALAIN DAVENAS

1. Introduction

Composite propellants are made of a polymeric matrix, loaded with a solid powder oxidizer, and possibly a metal powder that plays the role of a secondary fuel component.

In composites the oxidizing and reducing atoms are not in the same molecule, as is the case with double-base propellants, thereby creating a microscopically homogeneous phase, but are rather juxtaposed with a composite structure. A certain number of properties, such as burning rate, rheology, and mechanical behavior, are directly related to this composite character.

The first composite propellants used thermoplastic binders such as asphalt, polyvinyl chloride, and polyisobutylene. Their use required softening or melting obtained through a temperature increase. Around 1950, the first liquid binders allowing crosslinking appeared. Because these binders allowed high ratios of oxidizing and fuel charges, they led to the considerable development of composite propellants in large case-bonded grains (several tens of tons, even several hundreds of tons of propellant) that were impossible to manufacture with other types of propellants.

This development era can be broken down into two major periods:

- From 1950 until 1965, when composite propellants were made with polysulfide binders (“thiokols”) and with polyurethane polyethers.
- From 1965 on, new binders emerged, with a functional polybutadiene basis: acrylonitrile-acrylic acid-butadiene, acrylic acid-butadiene copolymers, and homopolymers with functional ends called telechelics. These new polymers led to increasingly better-performing elastomer binders, since they offered higher solids loadings and a wider operating temperature range, especially at low temperatures.

Clearly the significant events in the history of composite propellants are tied to the emergence of high-performance binders and not to new oxidizers.

Indeed, although ammonium perchlorate was not used right away — first potassium perchlorate and ammonium nitrate were used — it rapidly became the oxidizer of choice.

2. Formulation of Composite Propellants

Like all solid propellants, a composite propellant must produce hot gases which create a thrust by expanding in the nozzle, and include an oxidizer–fuel couple with a reaction capable of releasing sufficient energy to ensure the burning of the grain.

Oxidizing and fuel products come in the form of solid powders, which must be incorporated into a binder to give cohesion and homogeneity. This binder must exhibit very specific properties:

- It must be in liquid form during the preliminary phase of the preparation of the intimate mixture of the oxidizer and the fuel charge, although its elements must have sufficiently low volatile characteristics to withstand the high vacuum used during the mixing of the slurry and the casting into a grain.
- It must be chemically compatible with the oxidizer, which means that it will not cause even a slight temperature increase that would result in an exothermal reaction causing an unwanted autoignition of the propellant.
- It must be capable of accepting very high solid loading ratios (up to 80% in volume). The mixing operation must remain feasible, and the resulting slurry must be easily cast into a molding system or into the case of a rocket motor with molding devices with shapes that are often complex and include some fairly narrow sections.
- After the slurry is in the mold, crosslinking must ensure its transformation into a solid through a chemical reaction obeying the following criteria:
 - It must be a polyaddition reaction. Any elimination reaction producing more or less volatile products would result in the creation of cracks or “bubbles” in the crosslinked mass. Additionally, the mixing of the slurry must be done under vacuum to eliminate the gas present in soluble form in the binder. The decrease of the solubility of the gases during the crosslinking would lead to cracks in the propellant during cure.
 - This reaction must have on one hand a sufficiently slow cure kinetic to allow for the casting operations — this useful reaction time of several hours is also known as “pot-life” — and on the other hand must set sufficiently rapidly so as not to require lengthy crosslinking or curing times.

The curing temperature cannot be too high, so as to prevent severe mechanical loads in case-bonded propellants.

- It must also be athermic, or not very exothermic, to avoid the release of heat inside the grain, resulting in an increase of temperature inside this material, which is a poor heat conductor. This temperature increase could lead to mechanical loading conditions, possibly leading to cracks and autoignition of the propellant.
- Finally, once it is cured, the binder must lend its mechanical properties to the propellant.

Case-bonded grains are used in most of the composite propellants applications, i.e. the propellant forms one piece with the structure through the use of a bonding material, the liner. During its service life the propellant is subjected to major thermal stresses, resulting in significant strains because the thermal expansion coefficient of composite propellants is approximately ten times greater than that of the metals or composite materials used to make the cases. At firing, the propellant is, in addition, subjected to a range of important stresses and strains due to the deformation of the case under pressure.

The cured propellant must be able to withstand these strains without rupture, requiring it to have elastic type properties, viscoelastic to be more precise. These properties can only be provided to the propellant by the binder, which, taking into account the high proportion of solid loading, must therefore be an excellent elastomer. It is not unusual to require strains of 50% from the propellant, which means that the strains are more than ten times greater for the binder.

In Fig. 1 the tensile strength of a binder is compared to that of a propellant with a solid loading ratio of 88%. This figure demonstrates the effect of the loading ratio on the tensile strength (multiplied by 5) and on the strain at rupture (divided by 8) for a polybutadiene-AP-Al propellant.

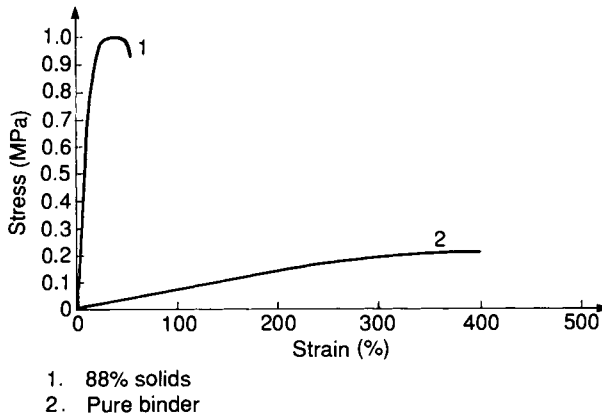


FIG. 10.1. Stress-strain curves.

2.1. THE BINDER

The binder is essentially composed of a liquid prepolymer, with chemical capability to react with a crosslinking system designed to ensure the dimensional stability of the product after the reaction has taken place.

In simplified terms, a prepolymer is a molecule formed by the repetition (several tens of times) of a monomer form (butadiene, polypropylene oxide, etc.), generally ending with reactive functions (telechelic prepolymers).

The crosslinking system may in its most simple state be a polyfunctional molecule (at least trifunctional) with a low molar weight, or a mixture of difunctional molecules, called chain extenders, whose role is to increase the length of the chain of prepolymers and of at-least-trifunctional molecules in order to ensure an average functionality (number of reactive functions, divided by the total number of molecules) greater than 2 for the whole crosslinking system.

After the polyaddition, chemical reaction has occurred between the prepolymer and the crosslinking system and the three-dimensional links are created. If they are in sufficient number — in the areas where it is not glassy — the resulting binder has a vulcanized elastomer type of behavior.

The crosslinked density of a binder, as well as the molecular mass between two links, are the essential characteristics of the network that constitutes the binder. These characteristics determine, in particular, its mechanical properties.

Many attempts have been made to link the mechanical properties (represented by the elasticity modulus) of the crosslinked polymer to the structure of the network defined by the crosslinking density and the molecular mass between two links (from 10,000 to 100,000 in usual composite propellants). They all derive from the statistical theory of rubber elasticity which links strain and stress according to:

$$\text{where: } \sigma = kT(\alpha - \alpha^{-1})$$

σ stress;

k Boltzman constant;

T absolute temperature in K;

α relative deformation of the specimen;

ν number of segments between links

where $\nu = \rho/M_c N$ and $E = \nu kT$

ρ mass per unit volume of the polymer;

N Avogadro number;

M_c molecular mass between two links;

E elastic modulus.

In reality this formula does not apply very well, because the binders of propellants are viscoelastic. It is useful only after long periods of relaxation, when there is equilibrium or quasi-equilibrium.

To be freed from this complication, M_c measurements are done on specimens swollen in a solvent. The Flory-Rehner theory [1] allows us then to determine the mass between links.

Finally, it is necessary to discuss the kinetics of crosslinking in order to describe the formation of the network on which the development of the rheologic characteristics of the slurry will depend.

Theories have been formulated based on the observation of the probability of reaction at the reactive sites [2]. Unfortunately, all of these theories come up against the complexity of the reactional system, whose exact characteristics are difficult to assess, such as: distribution of molecular masses and functionalities of the prepolymer; reactivity of the reaction sites which change during the formation of the network, and in particular, difficulty in measuring the development of reactive functions after the gel point where, through the formation of the first "infinite" molecule, the reacted group becomes partially insoluble. The use of these theories is nevertheless essential in guiding propellant designers.

2.1.1. Prepolymers

Prepolymers are the main element of the binder of composite propellants (70–80%). It is the prepolymer that confers on the binder its essential properties. These can be derived from the nature of the polymeric chain or the properties of the functional ends.

2.1.1.1. Characteristics related to the chain

Several examples are given in Table 1.

(a) ΔH_{fo} Enthalpy of formation

The higher this quantity is, the more energetic it will help make the propellant (in fact, less negative, because for all usual binders ΔH_{fo} is negative).

This enthalpy is directly related to the nature of the links between the atoms of the chain, which typically are C, H, O and N.

We will see, later in this chapter, that the binder must consist of light atoms which, through their combustion, will produce gases leading to a high specific impulse.

(b) Oxygen content

It would actually be better to talk about the ratio of the oxidizing valences (O, F, Cl) versus the reducing valences (C, H). In practice, the binders used so far contain, with a few exceptions, only C, H, O and N. Under these

TABLE 1 *Properties of the polymers used in composite propellants*

Polymers	Chain	Density (g/cm ³)	ΔH_{fo} (kcal/kg)	T_g^* °C	M_p^\dagger	Amount of oxygen mass (%)
Polyisobutylene	$\left(\begin{array}{c} \text{C}-\text{CH}_2 \\ \quad \diagup \\ \text{CH}_3 \quad \text{CH}_3 \end{array} \right)_n$	0.91	-375	-65	> 100,000 (thermoplastic)	0
Polybutadiene (20% of 1-2)	$(\text{CH}_2-\text{CH}=\text{CH}-\text{CH}_2)_n$	0.92	+5	-80	1500/5000	5
Polyether	$\left(\begin{array}{c} \text{CH}_2-\text{CH}-\text{O} \\ \\ \text{CH}_3 \end{array} \right)_n$	1.05	-895	-60 -70	1500/3000	26
Polyester	$\left(\begin{array}{c} \text{O}-\text{C}-(\text{CH}_2)_x-\text{C}-\text{O}-(\text{CH}_2)_y \\ \quad \\ \text{O} \quad \text{O} \end{array} \right)_n$	1.19	-1070	-50 -30	1000/2000	35
Polysiloxane	$\left(\begin{array}{c} \text{CH}_3 \\ \\ -\text{O}-\text{Si}- \\ \\ \text{CH}_3 \end{array} \right)_n$	0.87	-1890	-120	30,000	21

* T_g = Glass transition temperature measured by performing a differential enthalpic analysis.† M_p = Weight average molecular weight.

conditions it seems logical to assume that only the oxygen present in the binder counts as oxidizing valences, and it is customary to consider the mass percentage of the oxygen in the binder. The higher this percentage, the less necessary it is to use high levels of oxidizer to obtain the maximum specific impulse. We must note, however, that the optimum does not correspond to a complete combustion of the reducing valences, as we will see later.

However, the incorporation of high ratios of oxygen in the binder through ether, ester, or carbonate functions is accompanied by a decrease of the enthalpy of formation. This is the reason why there is little interest in these types of binders, except for special applications, such as "cold" propellants or when plasticized by energetic molecules. This is especially true since other parameters intervene adversely: increasing glass transition temperature, and decreasing capability to withstand high solid loading when the amount of oxygen increases.

In practice the polybutadiene chain offers a good energetic compromise in spite of a density somewhat lower than that of oxygenated binders (Fig. 2).

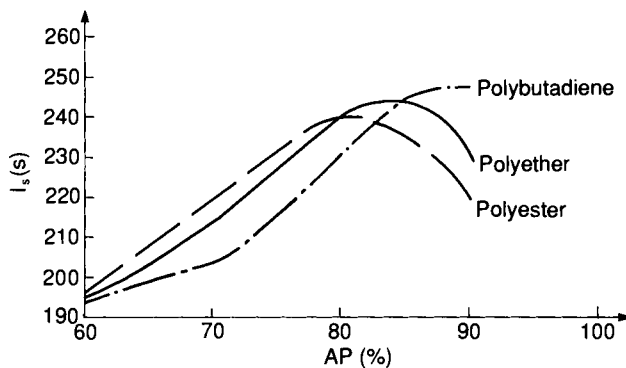


FIG. 10.2. Theoretical specific impulse as a function of AP concentration for three types of prepolymers.

(c) T_g , Glass transition temperature

This transition point of the second order corresponds to an important modification of the mobility of the polymeric chain that occurs when the temperature decreases and goes through a phase called "glass transition", which spreads over approximately 10 degrees Celsius. The physical properties of the polymer are greatly modified. Its elasticity modulus, in particular, increases significantly, and the capability of elongation becomes very small: the polymer has lost the specific qualities for which it was used. Table 1 shows, again, the advantage of using polybutadiene, at least for structures including no more than 20% of vinyl groups.

(d) Average molecular weight

The average molecular weight is tied to the number of monomer units which make up the prepolymer chain — a few tens of units for the polyethers and polybutadienes — and therefore to the length of the segments of the macromolecular network. Therefore, it plays an important role in:

- The average molecular weight between links in the binder, i.e. its mechanical properties (low masses lead to a highly crosslinked and very rigid network).
- The viscosity of the propellant slurry. The slurry may not exceed a certain viscosity of the order of 15,000 to 20,000 poises if the filling of the molds is to occur under good conditions using classic processes. The viscosity of the prepolymer, which is the main element of the binder, may not exceed certain values. In practice it varies from a few tens of poises to a few hundreds at 25°C.

Beyond that, it is virtually impossible to do the mixing under good conditions without using extremely large quantities of plasticizer, which may lead to undesirable changes in aging properties.

Below several poises the molar mass of the prepolymer is usually too low, and the resulting network will be too rigid.

(e) Polydispersity index, $I = M_p/M_n$

Ratio of the weight average molecular weight versus number average molecular weight, this characterizes the distribution of the molecular weights around the average weight and is, consequently, related to the structure of the network (distribution of the molecular weight between the links). In Fig. 3 the

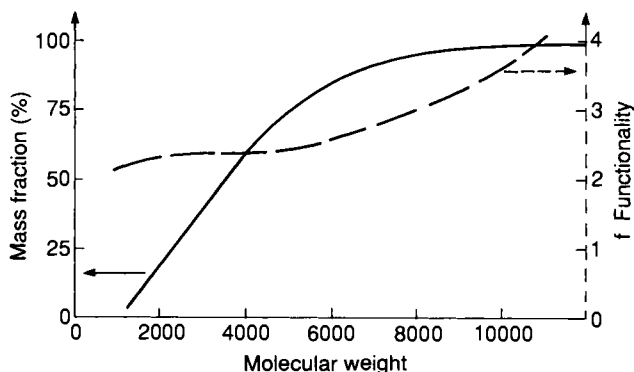


FIG. 10.3. Molecular weight and functionality distribution of an HTPB prepolymer.

distribution curve in weight of a hydroxytelechelic polybutadiene (HTPB) is given as an example.

2.1.1.2. *Characteristics related to the functional ends*

We have already seen that the functionality — the number of reactive functions per molecule — should be at least two to ensure a good formation of the network. This condition has been proven correct for many of the polymers in Table 1.

We must however mention the average functionality of 2.2 to 2.4 for HTPB R45M, which indicates a mixture of molecules with variable functionalities (from 0 to 7). This is related to the synthesis process of this polymer [3], and it has not been an obstacle to its development since 1970.

Ideally, the reactive functions should be located at the end of the chain to take advantage of its entire length and mobility.

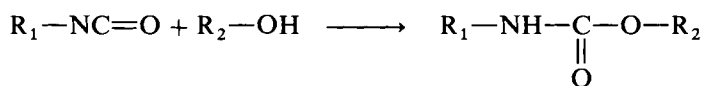
In practice, the ends most widely used are the hydroxyl and carboxyl (hydroxy or carboxytelechelic polymers) whose methods of crosslinking are indicated in Table 2.

2.1.2. *The crosslinking agent*

As discussed, the function of the crosslinking agent is to bind the prepolymer molecules and is, when the functionality of the prepolymer is 2, to lead to the crosslinking nodes of the network. Therefore it plays a critical role in the crosslinking kinetic and in the mechanical properties of the propellant.

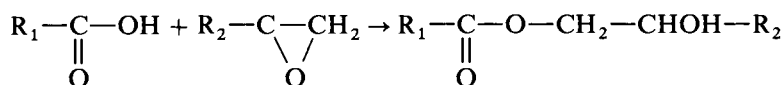
There are three types of polyaddition reactions used for solid propellants:

- Addition of an alcohol to an isocyanate. Isocyanates $R_1-N=C=O$ react with most of alcohols R_2-OH according to the reaction:

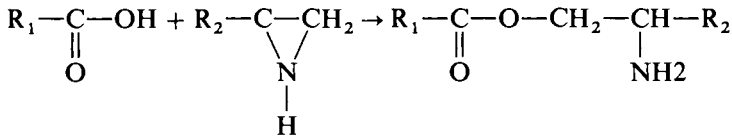


The link $NH-\underset{\underset{O}{\parallel}}{C}-O$ is called urethane.

- Addition of an organic acid to an epoxide



- Addition of an organic acid to an aziridine



(a) Effect on the mechanical properties

Figure 4 gives an example of the important effects of the stoichiometry, and of the percentage of crosslinking agent on the mechanical properties of a polybutadiene-AP-Al propellant. We must note that below a certain level of crosslinking (in this case, 0, 94 for the curing ratio), the propellant is not sufficiently crosslinked. Beyond this limit, maximum strains and stresses increase, which is a very general behavior of these compositions.

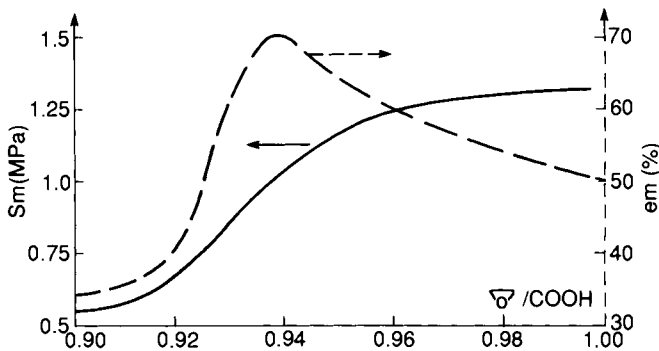


FIG. 10.4. Effect of the cure ratio on the mechanical properties of a CTPB propellant.

(b) Influence on the kinetic of polymerization

The reactivity of the crosslinking functions versus the prepolymer functions must be properly selected. Polyoxypropyleneglycol with secondary hydroxyl functions, for instance, requires an aromatic isocyanate that is fairly reactive (such as TDI), while R45M with primary hydroxyl ends is to be crosslinked with an aliphatic or cycloaliphatic diisocyanate that is less reactive, isophorone diisocyanate (IPDI), for example.

2.1.3. Plasticizer

Plasticizer plays the essential role of complementary element to reduce the viscosity of the slurry, therefore facilitating production, and to affect the mechanical properties by lowering T_g and the modulus of the binder.

Typically, it is an oil that is non-reactive with the polymer, a true diluting agent whose function is to separate the polymer chains, thereby reducing their interaction in the liquid state as well as in the crosslinked state. Table 3 lists the major plasticizers (polyesters for the most part) and Table 4 shows the effect of a plasticizer on T_g . Plasticizers contribute to lowering the mix viscosity and extending the elastic range at low temperatures. However, they have the drawbacks of being able to migrate, particularly at the propellant-liner and/or propellant-inhibitor interfaces, thereby modifying the properties of the propellants in those areas.

TABLE 3 Major plasticizers for composite propellants

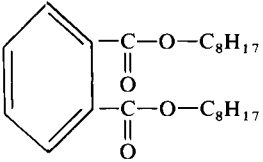
Diisooctyl azelate	$ \begin{array}{c} \text{COO}-\text{C}_8\text{H}_{17} \\ \diagup \\ (\text{CH}_2)_7 \\ \diagdown \\ \text{COO}-\text{C}_8\text{H}_{17} \end{array} $
Diisooctyl sebacate	$ \begin{array}{c} \text{COO}-\text{C}_8\text{H}_{17} \\ \diagup \\ (\text{CH}_2)_8 \\ \diagdown \\ \text{COO}-\text{C}_8\text{H}_{17} \end{array} $
Isodecyl pelargonate	$\text{CH}_3-(\text{CH}_2)_7-\text{COO}-\text{C}_{10}\text{H}_{21}$
Polyisobutylene	$\text{C}_n\text{H}_{2n+2}$
Diocetyl phthalate	

TABLE 4 Influence of the percentage of plasticizer on T_g of a polyether + diisooctyl azelate binder

Plasticizer/polyether (%)	0	10	30	50	70	100
$T_g^\circ\text{C}$	-68	-75	-80	-85	-101	-107

2.1.4. Additives

These are liquid or solid products added at a few percent of the binder. Their function is to modify at will the characteristics of the propellant to improve them, except specific impulse, which they often decrease due to secondary adverse effects. This decrease does not exceed 1-2%.

2.1.4.1. Burning rate modifiers

These are used to modify the propellant burning rate — beyond what can be done with variations of the particle size of the solids — and to adjust the exponent “*n*” of the burning rate–pressure curve in the pressure zone where the propellant grain will be operating.

There are two types of burning rate modifiers: accelerators and moderators.

(a) Burning rate accelerators

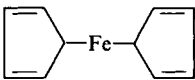
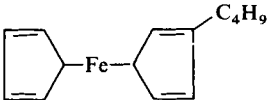
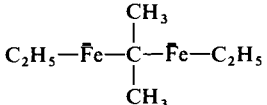
These are products that accelerate the decomposition of the perchlorate, or that lower its decomposition temperature. Virtually all burning rate accelerators are mineral or organic metallic by-products of copper, iron, chromium, or boron.

For many years only solids, iron oxides, and copper chromite were used. Liquid derivatives from iron (ferrocene derivatives) and boron (carboranes) are also used because their incorporation as plasticizers to the binders facilitates the high amounts necessary for high burning rates without lowering the loading ratio of energetic solid charges. The major ferrocene derivatives in use are listed in Table 5.

Unfortunately, because they are not linked with the network, these products, like the plasticizers, have a tendency to migrate at the interfaces. That is why we are now trying to graft the useful functions to the basic polymer chain. Prepolymers resulting from the addition of sililferrocene onto functional polybutadiene vinyl groups are currently being developed [4].

The curves shown in Fig. 5 illustrate the effect of a solid burning rate

TABLE 5 Major ferrocene derivatives used as burning rate accelerators

Ferrocene (Fe)	
<i>n</i> -Butylferrocene	
Di <i>n</i> -butylferrocene	$\text{C}_4\text{H}_9\text{—Fe—CH}_2\text{—Fe—C}_4\text{H}_9$
“Catocene”	

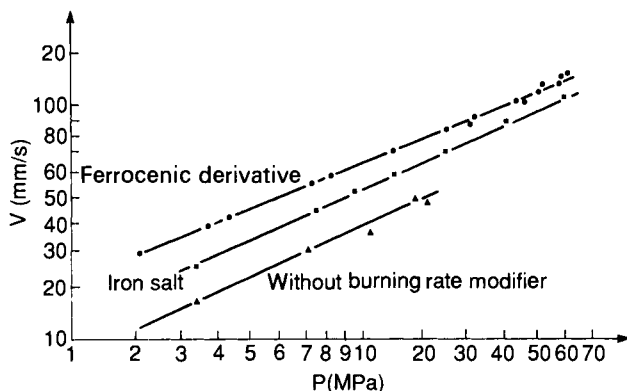


FIG. 10.5. Burning rate vs pressure curves for propellants with burning rate accelerators.

accelerator (copper salt) and a liquid one (ferrocene derivative) on polybutadiene-AP-Al propellants.

The efficiency of burning rate accelerators is highly dependent on the nature of the oxidizer. While there is a large number of burning rate modifiers for ammonium perchlorate and ammonium nitrate propellants, they are rather rare for potassium perchlorate composite propellants, or composite propellants that use organic energetic solids such as HMX or RDX.

(b) Burning rate moderators

There are two types of moderators, based on their mode of intervention.

Additives modifying the kinetic of decomposition of ammonium perchlorate. These generally are alkaline salts, or alkaline-earth solids added in low proportions, not exceeding 1–2% of the propellant.

Like the burning rate accelerators, although to a lesser degree, their efficiency varies as a function of the pressure, and is also associated with a decrease of the pressure exponent. Figure 6 gives an example of the effect of lithium fluoride on an ammonium perchlorate propellant. Although the effect of these additives could be significant (lowering of the burning rate by 50%), very slow burning rates cannot be obtained. Furthermore, they have no effect on aluminized propellants. As a result, “coolants” are preferred.

Coolants, also called “cold oxidizers,” are products that also lower the propellant burning temperature, and unfortunately, its specific impulse as well, by:

- a lowering of ΔH_{f_0} , while maintaining a high content of oxygen;
- enriching the combustion gases with nitrogen which, since it takes no part in the combustion, acts as a diluter.

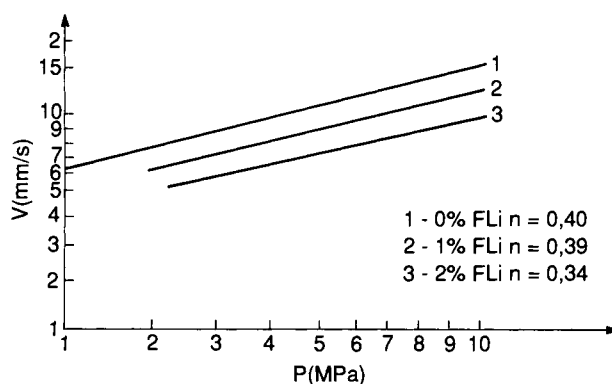


FIG. 10.6. Effect of lithium fluoride on the burning rate of an AP composite propellant.

The more commonly used coolants are:

- oxamide $\text{NH}_2-\text{C}(=\text{O})-\text{C}(=\text{O})-\text{NH}_2$;
- nitroguanidine $\text{NH}_2-\text{C}(=\text{NH})-\text{NHNO}_2$;
- ammonium nitrate.

Their main properties are listed in Table 6.

Oxamide has the most severe adverse effect on the specific impulse, but it is also the most efficient of the coolants. In practice, ammonium nitrate is used mainly as the major oxidizer for propellant with very low burning rates (but not very energetic) ranging from 1 to 2 mm/s at 7 MPa.

These products make it possible to reduce by half the burning rate of

TABLE 6 Some characteristics of the major coolants

Coolant	O (%)	N (%)	Density (g/cm ³)	ΔH_{fo} (kcal/kg)
Nitroguanidine	30.7	54	1.76	-217
Ammonium nitrate	60	35	1.72	-1090
Oxamide	36	31.8	1.67	-1355

ammonium perchlorate propellants, including those that are aluminized, with a drop in specific impulse up to 10 s.

2.1.4.2. *Surface agents and binder-charge bonding agents*

For many years the only role of these additives, used in low quantities not exceeding 1% of the binder, was to help the manufacturing of the propellant by decreasing the viscosity of the slurry. In this capacity all surface agents that decrease the surface energy of the solid charge, to permit better “wetting” of the surface by the binder, can be used.

However, it was quickly noticed that these agents, as valuable as they may have been in terms of the production, had a detrimental effect on the mechanical properties of the propellant by preventing the adhesion of the binder to the solids, thereby decreasing its tensile strength. Consequently, products called bonding agents have been developed, which through a judicious adaptation of their molecules, of the formulation of the binder, and of the mixing process of the ingredients play a double role, serving as wetting agent for the solids and increasing the cohesion between the binder and the solids [5].

A good bonding agent must satisfy the following criteria:

- Be efficient at very low levels (less than 1%).
- Be capable of bonding itself on a solid (generally the oxidizer, because it is the most important ingredient in terms of quantity). As a result, a bonding agent is specific to the type of solid.
- Be capable of incorporating itself with the binder through a chemical reaction which must be compatible with the crosslinking system.
- Reinforce the mechanical properties of the binder in the vicinity of the solids where the highest mechanical stresses appear in the area close to the surface of the charges [6].

Triethanolamine is a good example of a bonding agent for ammonium perchlorate in polyurethane-type binders through:

- Reaction on the surface of the perchlorate by displacing the ammonia and forming triethanolamine perchlorate.
- Integration in the binder through the highly reactive primary alcohols.
- Trifunctionality of the molecule, ensuring a good crosslinking density in the area close to the ammonium perchlorate particles.

Because of the release of ammonia with amine-type bonding agents, polyaziridine-type additives are often preferred. Several of these additives are listed in Table 7. A good example of this family of additives is MAPO, which polymerizes on contact with ammonium perchlorate by opening aziridine rings. This layer becomes reactive to isocyanates, as illustrated in Fig. 7.

TABLE 7 *Binder–solid bonding agents: imine or aziridine type*

MAPO	Tri (2-methyl-1-aziridinyl) phosphine oxide
HX 752	Bis-isophthaloyl-1-methyl-2-aziridine
MT4	Product resulting from the reaction of 2 MAPO moles: 0.7 adipic acid moles and 0.3 tarttric acid moles
Methyl BAPO	Methylamino-bis (2-methyl-1-aziridinyl)-phosphine-oxide

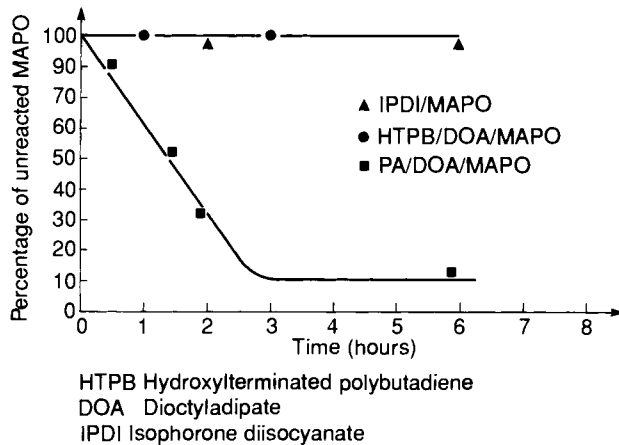


FIG. 10.7. Reaction of MAPO with IPDI and HTPB.

A number of additives featuring nitrile groups are also fairly widely used [8].

2.1.4.3. Catalysts

Catalysts are often necessary to reduce the curing time of the propellant.

Besides the kinetic aspect they may have a significant impact on the mechanical properties by facilitating some favorable reactions, thereby giving direction to the formation of the polymer network.

They are usually organic salts of transition metals (iron, chromium, tin). Several examples are provided in Table 8. Very detailed research is being performed because their nature and the amounts used must result in a trade-off between the workability of the mixture (viscosity of the slurry, pot life), curing time, and mechanical properties.

Complex systems with two or three chemical products such as triphenyl-bismuth, maleic anhydride, and magnesium oxide have emerged, and allow excellent compromises between pot life and curing time [9].

TABLE 8 Catalysts for polyurethane binder propellants

Iron acetyl acetonate	$\text{Fe}(\text{C}_5\text{H}_7\text{O}_2)_3$
Copper acetyl acetonate	$\text{Cu}(\text{C}_5\text{H}_7\text{O}_2)_2$
Lead octoate	$\begin{array}{c} [\text{CH}_3-(\text{CH}_2)_3-\text{CH}-\text{COO}]_2^{\text{Pb}} \\ \\ \text{C}_2\text{H}_5 \end{array}$
Ditubyl tin dilaurate	$\begin{array}{ccc} \text{CH}_3-(\text{CH}_2)_{10}-\text{COO} & & \text{C}_4\text{H}_9 \\ & \diagdown \quad \diagup & \\ & \text{Sn} & \\ & \diagup \quad \diagdown & \\ \text{CH}_3-(\text{CH}_2)_{10}-\text{COO} & & \text{C}_4\text{H}_9 \end{array}$
Lead chromate	Pb CrO_4

2.1.5. Various additives

Based on the various properties required from the propellants, specific additives are included. These usually are solids and their amount rarely exceeds a few percent of the binder.

2.1.5.1. Antioxidant

These are essential to ensure satisfactory aging of the propellant in various ambient conditions.

The binder, an organic material, is subject to degradations that are reflected by changes in the network and consequently, in the mechanical properties of the propellant. Generally, the combustion properties are little affected.

The aging may be:

- Oxidizing: this occurs with either the oxygen in the surroundings of the propellant grain, or gases occluded inside the propellant. Antioxidants are added, usually phenols or aromatic amines. This occurs particularly in the case of propellants with polybutadiene binder, whose $\text{C}=\text{C}$ links are particularly sensitive to oxidation, in accordance with mechanisms that have been extensively studied for high molecular mass rubber. Antioxidants, well known in the rubber industry, are used, phenols in particular (di tertiary butyl paracresol, diamino *n*-phenyl-*n'*cyclohexyl-paraphenylene, 2,2. methylene bis (4-methyl-6-tertiary-butyl phenol), among others).
- Hydrolytic: this occurs with polyesters, where the ester links may hydrolyze and lead to a depolymerization of the binder.

2.1.5.2. Burning rate stabilizing agents

The pressure-time curve of a propellant grain may be considerably disturbed by inopportune local variations in the burning rate of the propellant. This is often the case with non-metallized propellants.

Based on the origin of these disturbances, the grain designer uses stabilizing additives of a varying chemical nature:

- Opacifiers (carbon black): these are found to be necessary in non-metallized propellants to block the radiation of the burning front, which has a tendency to heat the propellant below the burning surface, accelerating its combustion and creating low pressure fluctuations.
- Anti-instabilities and damping additives: these additives are discussed in Chapters 4 and 5. Their use may eventually adversely affect the polymerization of the propellant.

2.2. SOLIDS

There are two types:

- Oxidizers: the primary ingredient of the propellant (60–80%).
- Fuels: generally used in amounts not exceeding 25%.

These are powder solids whose shape and particle size determine the maximum amounts that can be included in the binder [11]. Figure 8 shows the influence on the relative viscosity (ratio of the viscosity of the suspension versus the viscosity of the interstitial liquids) of several particle size distributions of spherical particles whose diameters range between a 5 to 10 ratio. For a given viscosity limit (imposed by manufacturing capabilities), the accept-

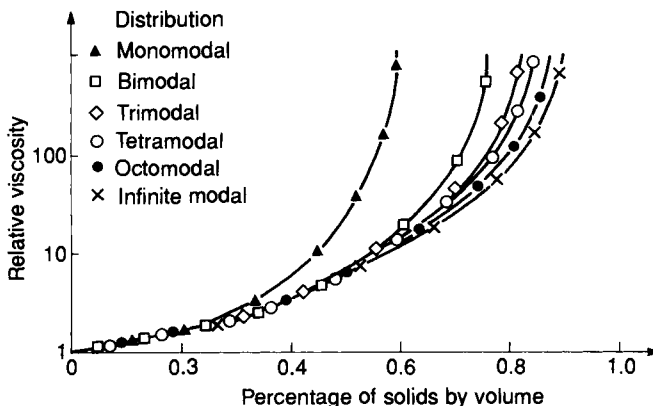


FIG. 10.8. Comparison of relative viscosities calculated for multimodal optimum systems.

able amount of charges by volume increases with the number of particle sizes, each particle size settling in the gaps formed by the larger sizes.

Three or four particle sizes are commonly used in propellants; it is sufficient to come close to a viscosity optimum for a specific solid loading. However, it is not always possible to use the particle size distribution best suited to obtain a high solid loading. This is due to the fact that particle size has a considerable effect on the burning rate of the propellant, and often it is this parameter which predetermines the size of the particles that will be used.

The nature of these solids is, of course, the major parameter influencing the energy of the system, although it also affects the burning rate, as already discussed.

In Chapter 1 we saw that the specific impulse can be expressed in a very simple manner:

$$I_s = K \sqrt{\frac{T_c}{M}}$$

where:

T_c = combustion temperature in the chamber;

M = average molecular weight of the exhaust gases.

The selection of an oxidizer-fuel couple is consequently a compromise between seeking to obtain a high burning temperature (related, in preliminary analysis, to the enthalpy of the formation H_{fo} of the propellant), a low molecular weight for the combustion products, a high propellant density and, naturally, the required burning rate.

2.2.1. *Oxidizers*

The characteristics of a good oxidizer are:

- The capability of supplying oxygen (or fluorine) to burn the binder and the other fuel, with the maximum heat of combustion.
- The highest possible formation enthalpy. Figure 9 shows the formation enthalpies of the major kinds of oxidizer products that include the groups: ClO_3 , ClO_4 NO_3 in the solid products.

The advantage of using NF_2 and NO_2 is revealed by the good location in the graph of CH_3NO_2 , N_2F_4 :

- The highest possible density.
- A sufficient thermal stability. Decomposition temperatures exceeding 100°C are required to permit the manufacturing operations and to safeguard the propellant.
- A good chemical compatibility with the other ingredients contained in the propellant, in order to avoid any undesirable exothermic reaction.

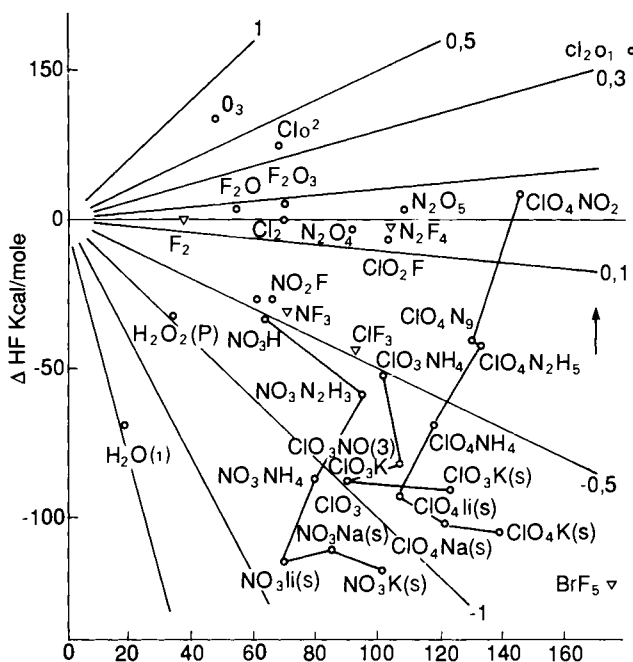


FIG. 10.9. Enthalpy of formation for major oxidizers as a function of the molecular weight.

- The availability of different particle sizes in order to obtain high solid loading and required burning rates.

In practice, the number of oxidizers used in composite propellant is rather small: ammonium perchlorate (AP) covers most of the cases. Next, ammonium nitrate, HMX and nitroguanidine are used the most. The characteristics of these products are given in Table 9.

2.2.1.1. NH_4ClO_4

By looking at Table 9 one easily understands why the use of this compound is so prevalent: it is dense, thermally stable (much more so than the chlorates) and its decomposition produces only gases of which a large proportion is oxygen.

SNPE uses, for example, six industrial particle sizes that permit the tailoring of burning rates from a few mm/s to 70 mm/s at 7 MPa with burning rate modifiers. They are as follows:

TABLE 9 Some characteristics of the major oxidizers

Oxidizer	"Free" oxygen by weight	Density	Decomposition temperature (°C)	ΔH_{fo} (kcal/kg)	Remarks
Ammonium perchlorate, NH_4ClO_4	34	1.95	> 270	-601	In various particle sizes
Potassium perchlorate, KClO_4	46.2	2.53	> 500	-748	Presence of condensed KCl in the combustion gases
Ammonium nitrate, NH_4NO_3	20	1.72	Very stable	-1098	Numerous allotropic varieties if not stabilized
HMX ($\text{CH}_2\text{N}_2\text{O}_2$) ₄	0	1.91	> 200	+68	Strictly speaking this is not an oxidizer
Nitroguanidine	15	1.76	Very stable	+217	Same as above
$\text{NH}_2-\text{C}(\text{NH})=\text{NO}_2$					

Type	Average diameter (microns)
B	400
b	200
D	100
F	10
M3	3
M1	1

The first two varieties are obtained directly by crystallization, the others by grinding.

2.2.1.2. $KClO_4$

Very dense and oxygen-rich, this oxidizer has the drawback of giving to the propellant limited energetic characteristics. In addition, it also leads to high pressure exponents.

2.2.1.3. NH_4NO_3

This oxidizer, with very low ΔH_{fo} and with little oxygen available, leads to specific impulses that are much lower than those obtained with the perchlorates. Its use is generally limited to gas generator propellants, where low burning temperatures (below 2000K) and slow burning rates (1–2 mm/s) are often sought. In addition, it exhibits a change of allotropic form at $+32^\circ\text{C}$, accompanied by variations of volume causing significant variations in the properties of the propellants, including deterioration. So-called “stabilized” varieties have been obtained through cocrystallization with various salts (such as NiO). This has the drawback of introducing condensable in the propellant [12]. They are, however, more and more used.

2.2.1.4. $(CH_2N_2O_2)_4$: HMX

HMX is not an oxidizer, but it is the only product in the table with a positive enthalpy of formation. As a result, it is used as a supplementary energetic solid in propellants already having a high level of oxygen.

2.2.1.5. Nitroguanidine

Nitroguanidine is not an oxidizer either; but the relatively high value of ΔH_{fo} make it useful as a supplementary charge, like HMX, although at a lesser degree (because of its low density and its deficit in oxygen), particularly as a moderator of the burning rate of ammonium perchlorate propellants.

2.2.2. Fuels

The diagram in Fig. 10 permits classification of fuels based on the energy available for the formation of the fluorides and the oxides. It illustrates:

- The small difference between fluorides and oxides, with an energy higher than the chlorides;
- The following decreasing order of energetic interest of the fuels, $\text{Be} > \text{Li} > \text{B} > \text{Al} > \text{H}$ and C .

However:

- Beryllium is difficult to use, except for very specific applications, because of the toxicity of its combustion products.
- Lithium is not dense enough.
- With boron, B_2O_3 is not obtainable. In reality, sub-oxides are formed due to the thermodynamic conditions in the combustion chamber. Accordingly, this fuel loses its theoretical energetic advantage, except under specific environments very rich in oxygen, in the combustion chamber of ramjets and ramrockets (Chapter 12).

Magnesium is an interesting fuel, although much less dense (1.7) than aluminum (2.7).

Aluminum is virtually the universal fuel for composite propellants. It is available in spherical powders, with small diameters (a few microns to a few tens of microns), and it is well suited for high solid loading. The fine layer of aluminum oxide, which inactivates the grains in humidity, makes it easy to handle.

Carbon and hydrogen, which are always present in a propellant because

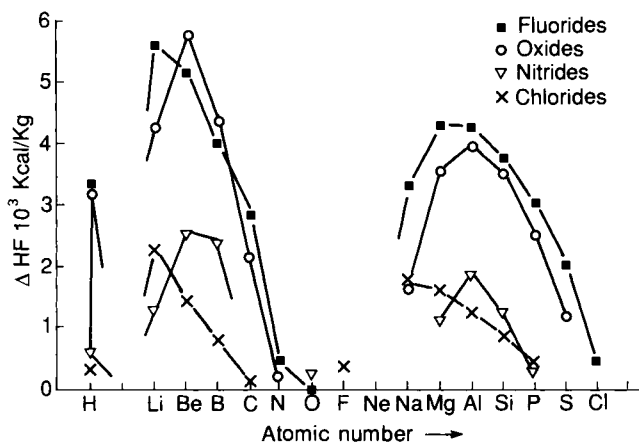


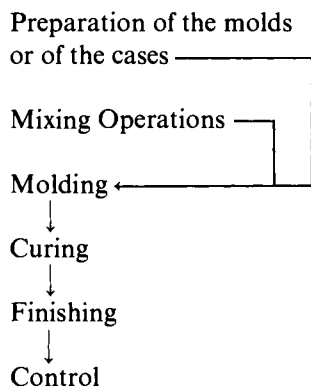
FIG. 10.10. Energies available through formation of exhaust products.

they are essential ingredients of the binder, play a major role in the exothermicity of the combustion, and have a significant advantage over aluminum by producing gaseous combustion products.

Other fuels such as heavy metals have been tried, including Ti, Zr and Pb. None of them is being used, except for zirconium, whose cost remains very high. Its very high density (6.5) and its good combustibility may lend it a certain interest for applications where the amount of space available for the propellant is limited (integral booster for instance).

3. Manufacturing and Quality Control Methods

A complete manufacturing cycle of composite propellants could be represented by the following diagram:



Any of these operations is delicate, and conditions the quality of the propellant grains (microscopic and macroscopic homogeneity, effect on the operational properties). The preparation of the molds and cases is described in Chapter 13.

3.1. MIXING OPERATIONS

The mixing operation consists of the kneading of a solid phase (primarily oxidizer and fuel) and a liquid (the ingredients of the binder). It is designed to produce an homogeneous slurry that can be molded, with a good level of reproducibility of the characteristics of the propellant.

Because of the high investment costs of a mixing facility, all mixing operations that are non-pyrotechnic, and can be done outside of the mixing facility, are done with conventional mixers.

The more important preliminary mixing operations are shown in Fig. 11.

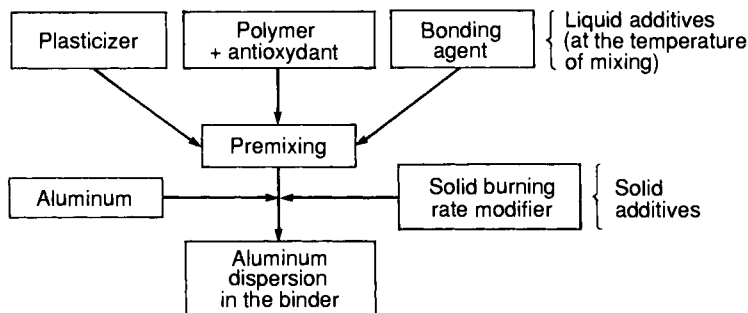


FIG. 10.11. Premixing operations.

3.1.1. Preparation of the binder (Premix)

A typical operation will now be described.

The premixing is done in a container equipped with a mixer. After they have been weighed, the ingredients are put in the container, as follows: the polymer, the plasticizer and the bonding agent. The mixture is heated to 60°C.

The aluminum is poured into the container with the binder, while continuously agitating to ensure a good mixing (this is the case at SNPE; other companies can incorporate aluminum in the propellant mixer).

The kneading is the most important operation in the manufacture of the propellant. It must last long enough to create a homogeneous slurry, suitable for casting. It is also an expensive operation, because of the energy and manpower requirements, and its duration should be as short as possible without affecting the quality.

In the past, the first mixers used for the manufacture of propellants were horizontal mixers. The drum was made of stainless steel to avoid corrosion from the perchlorate. Two rotating Z-shaped blades would knead and cut the slurry. The clearance between the wall of the drum and the edge of the blades was very small — a few millimeters — to minimize the amount of dead space where the blades could not reach, and the intense shearing action was designed to ensure a good level of homogeneity in the slurry.

Some kneading phases require the slurry to be heated; others that it be cooled. This was achieved through a mixer with a double-wall system, where a circulating liquid could be either heated or cooled at will.

Humidity is bad for all propellant compositions. All facilities where there are mixers are air-conditioned, and the mixers themselves are closed with a tight-fitting lid. This lid is equipped with a vacuum device, used to obtain a low residual pressure of about 10 mm of mercury. Volatile components, water, and air trapped in the slurry are easily removed in the course of the kneading phase.

Over the past 15 years the horizontal mixers have been gradually replaced with vertical mixers with two or three blades, and an orbital motion.

The process for the mixing operations on these vertical mixers has remained virtually unchanged from the horizontal mixers; but flexibility and production rates have greatly increased, due to the possibility of exchanging the drums. The time required to load and unload the mixers has been cut down to a minimum.

The vertical position of the blades completely prevents the bearings and seals from having any direct contact with the propellant mixture, thus avoiding contamination of the gearbox: cleaning of the mixer is easier and a higher level of safety is attained.

The sequence of mixing operations is as follows:

The binder is first freed from any gases, after which the oxidizer is introduced. This may be done manually, repeating the operation several times (in the case of a small mixer), or remotely, using a hopper equipped with a vibrating chute or an Archimedes' screw, in a dry environment.

This is a very important phase because the order of introduction of the various oxidizer particle sizes, as well as the timing of the introduction, determine the viscosity of the slurry.

Both the various parameters of the process, as well as the formulation (wetting agents, bonding agents, particle size distribution of the oxidizing solids and the type of aluminum and its particle size), are optimized to obtain a slurry which is as fluid as possible. Better filling of the mixer is possible, and the mixing times are shorter.

In Fig. 12 is an example of the evolution of the torque of the mixer for two

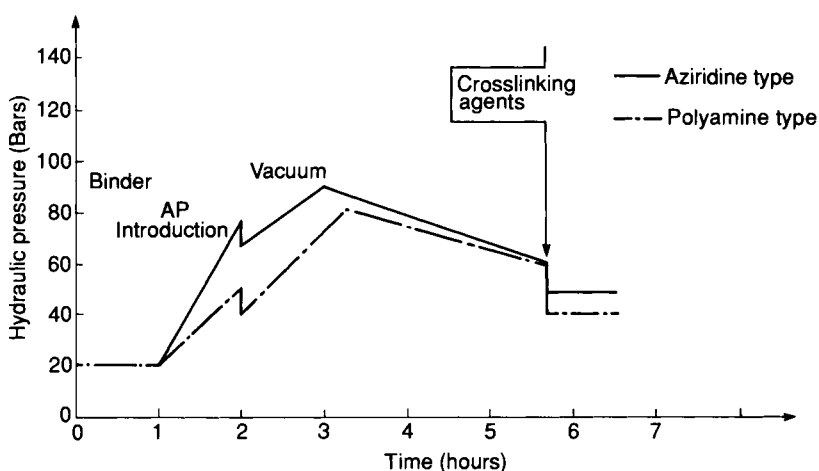


FIG. 10.12. Torque build-up during mixing.

propellant compositions both containing 90% solids, but differing by the bonding agent used.

The introduction of the oxidizer is the most critical phase in terms of safety. The propellant is not a homogeneous slurry yet, and ammonium perchlorate in contact with fuel is sensitive to mechanical stimuli. If this inhomogeneous and porous slurry ignites, the combustion to detonation transition phenomenon may take place.

This phase is followed by a homogenization designed to improve the wetting of the solids by the binder and to decrease the viscosity to the point where casting can be performed under good conditions. Specimens may be taken during this phase to check on the oxidizer content and on the burning rate.

The crosslinking agent and the polymerization catalysts are usually introduced last, a few tens of minutes before the end of the mixing operation.

The propellant slurry is transferred to an isothermic container, when horizontal mixers are used, to be transported to their casting facilities. In the case of a vertical mixer, transport is done by moving the entire drum.

3.1.2. *Continuous mixing processes*

For a long time, research work has been devoted to processes that could lead to continuous mixing as a substitute to the batch mixing process. Since this evolution has an important effect on the whole process of production of the propellant grains it will be described at the end of this book in the chapter devoted to the future of solid rocket propulsion.

3.2. CASTING OF THE GRAINS

3.2.1. *Sequence of operations*

There are three major phases involved in the molding of composite propellant grains:

- First, the filling of the structures and the molding of the central port of the grains, or of the aft face of the grain.
- Second, the polymerization or crosslinking of the propellant. This is the “curing” phase which takes place in an oven, or directly in the casting pit if the grain is very large.
- Third, demolding, machining of the central port and faces when necessary, and finishing operations to give the propellant grain its final aspect.

Typically, the process followed is:

To start, the mold, usually the body of the rocket motor with the inside surface completely coated with the liner, is filled with the propellant slurry, coming directly from the mixer.

This is a delicate operation. There is a wide range of propellants and various types of behaviors can be characterized: some propellants flow well, some propellants stick to the walls, some are very viscous; there is also a great variety of products manufactured, from the small propellant grains for rockets to the grains for space or ballistic missiles. They must, every one of them, be perfectly molded, and devoid of any casting defects.

The most widely used technique is “vacuum casting”; an alternative technique is injection under pressure, called die-casting. Both are described below.

When manufacturing propellant grains that have a central port, conformation is ensured by casting with a mandrel, either as a monoblock or in several parts. The mandrel is placed inside the case before the propellant is cured.

This operation is a simple one when the core can be easily put in place and extracted from one of the end faces of the propellant grain. Furthermore, if the space between the walls of the structure and the mandrel is large enough to allow the propellant to flow well, and for a progressive casting to be done, the mandrel is installed in the case before the casting operation begins. When this is not the case, the molding of the central port is done after the casting has taken place: the mandrel, guided from the outside, is driven progressively into the propellant by applying pressure.

An intermediate solution consists of using a two-part core. The grain is cast with the first, lower part already in place. The top part is placed on the bottom part after the casting has been completed.

3.2.2. Rheologic characteristics and casting processes

The choice of casting process, of the size of the casting devices and the definition of the casting conditions, depends, in addition to the size and the shape of the future grain, on the flowing ability of the non-polymerized propellant slurry.

Data on the behavior of the propellant during vacuum or injection casting is provided by its rheologic behavior law. It is specific to each formulation, and ties the shear stress τ , a function of the load imposed on the material (such as pressure, gravity, and others) to the resulting rate of deformation $\dot{\gamma}$.

This law is determined by using a rheometer, an instrument with a revolving cylinder body placed inside a cylindrical container. A rotation speed Ω is imposed, and the value of the resulting torque \mathcal{M} is recorded.

The law is determined based on the curve \mathcal{M} as a function of Ω , converted into the shear stress τ as a function of the stress rate (τ is expressed in Pascals and $\dot{\gamma}$ in s^{-1}): $\tau = f(\dot{\gamma})$.

Precise plotting is necessary for low levels of shearing ($\dot{\gamma} < 1 \text{ s}^{-1}$), corresponding to the conditions that are typical during gravity casting.

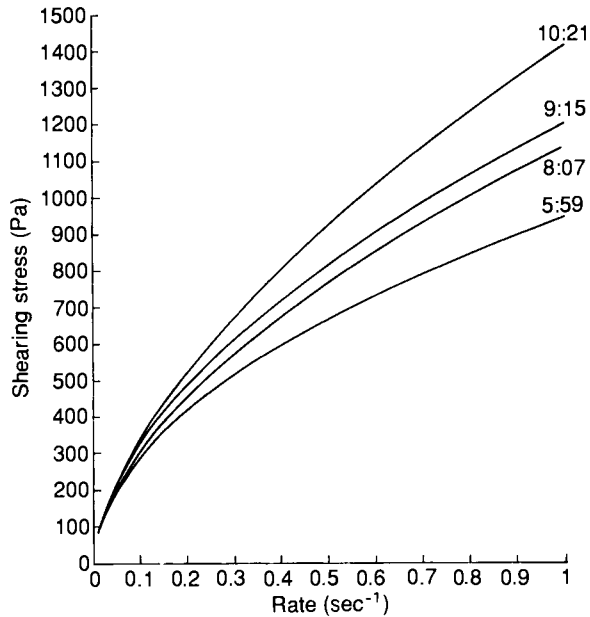


FIG. 10.13. Typical rheograms, as a function of time after introduction of the crosslinking agent (hours-minutes).

The viscosity is determined, for a given shear rate, by the ratio $\tau/\dot{\gamma}$. Typical examples of rheograms are given in Fig. 13.

There are three major types of behavior:

- Compositions exhibiting a Newtonian behavior: their viscosity is constant, therefore independent from the casting conditions.
- Compositions exhibiting a pseudo-plastic behavior: their viscosity diminishes when the shear stress is increased. This particularity occurs regularly, although it is more or less pronounced.

Such a slurry does not spread well, but is well suited for die-casting.

- Compositions exhibiting an expanding behavior: contrary to pseudo-plastic compositions, their viscosity increases with the shear rate. This is fairly rare. Such a propellant would present great difficulties if it had to be injected.

Knowledge of the behavior law provides information that is useful to select the casting process for the propellant and the conditions under which it should take place. It allows the prediction of the flow rate of the slurry in the existing casting facilities and the calculation of the number of grains that can be cast within a period of time compatible with the pot life of the propellant.

3.2.3. Description of the major grain casting processes

3.2.3.1. Vacuum casting process, by gravity

The oldest process is the vacuum casting process, illustrated in Fig. 14.

The mold, which most of the time is a thermally protected case covered inside with a liner, is placed in an enclosure that can be heated, and its pressure lowered between 10 mm and 30 mm of mercury. The purpose is to obtain a complete degassing of the slurry, a necessity for the manufacture of grain without voids.

According to the size of the object manufactured, the enclosure is shaped like a "closet" or a "bell" for small to mid-size grains, or a casting pit for large grains for space launchers or ballistic missiles.

The casting bowl which contains the propellant is placed above the enclosure. It is linked to the top of the enclosure by a duct, called the casting pipe. The end of this pipe opens into the casting enclosure, above the case to be filled. It is equipped with a slit plate.

This slit plate divides the slurry into strips during the casting to ensure efficient degassing of the propellant.

It also organizes the flow of propellant so that it falls directly and is fairly well distributed between the mandrel and the case in grains with a central

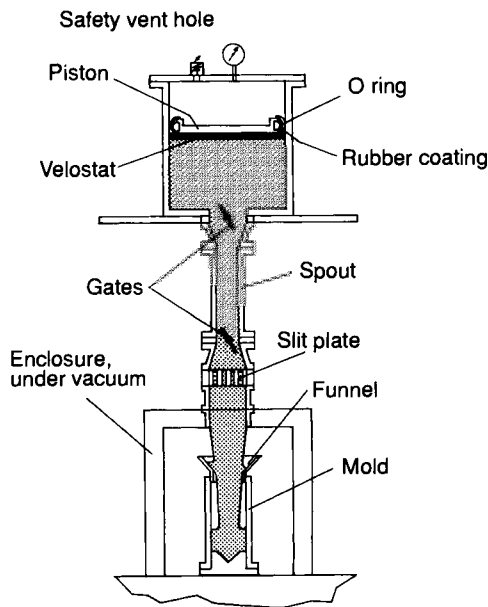


FIG. 10.14. Casting.

port. Because of the difference of pressure between the casting bowl and the enclosure, the propellant flows continuously from the drum to the casting matrix. Coming out of the slit plate, and according to the design of the slit plate, the flow takes the shape of fillets or ribbons of slurry which pile up inside the structure and settle under the effect of their own weight.

The selection of the casting flow rate is the result of a trade-off between:

- The need to have a rapid flow to accommodate time-saving industrial requirements and to avoid a significant increase of the viscosity due to the progress of curing.
- The need for a fairly slow flow to permit sufficient degassing of the slurry after it has gone through the slit plate, and spreading inside the case necessary for a high quality casting.

The selected flow rates are a function of the geometry of the grains, and vary from several kilograms per minute for small grains to flow rates of several hundreds of kilograms per minute for large grains.

The gravity casting process continues to be most widely used today, because it sufficiently satisfies the needs of propellant casting.

It is a simple process, well suited to the use of large quantities of material. In contrast to other casting and molding industries (plastics, loaded polymers and others), large quantities of material are involved for each object.

This process affords all necessary guarantees of safety, considering the sensitivity of the materials used, and ensures good overall quality.

It is well suited for the low production rates most often used in this industry.

3.2.3.3. *Die-casting process*

The characteristics described above also point out the limitations of the process. The design of higher-performance motors, which are highly specialized in terms of their missions and require the lowest possible cost, implies the manufacture of objects with more complex shapes: for example, bi-composition grains, long grains, and grains with small diameter and little space available between the case and the mandrel.

High-performance propellants may also exhibit high viscosity in the casting phase, which is due to the use, for example, of very fine perchlorates or high solid loading ratios.

Finally, the manufacture of certain small objects requires high production rates to allow significant cost reductions.

This led to the study and development of casting processes by injection under pressure: die-casting. This process involves forcing the slurry to move by subjecting it to pressure, and using that pressure to fill the molds rather than simply relying on gravity.

The various methods used to apply pressure have led to the development of several specific processes:

(a) Pressure applied using a gas (Fig. 15)

The propellant is placed in a flexible and deformable pouch. This pouch, located in an air-tight enclosure, is linked to the mold through a suitable linking system. The enclosure is filled with a gas under pressure which presses upon the outside surface of the pouch. The propellant is pushed into the mold.

This process is well suited to the manufacture of small objects with complex shapes, and produced in small series.

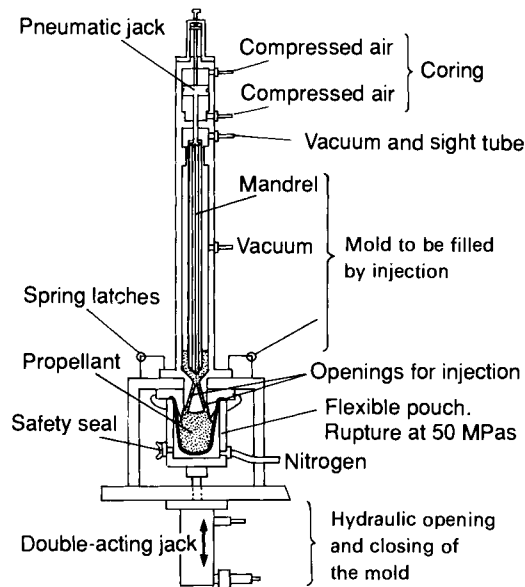


FIG. 10.15. Illustration of injection casting.

(b) Pressure exerted mechanically, using a hydraulic piston

This is the most simple of systems. The propellant is placed in a drum similar to the casting bowls described above. The drum is linked to the bottom of the mold by a pipe. Pressure is exerted on the slurry with a scraping piston placed on top of the propellant.

The propellant, under the pressure of the piston, continuously without any interruption into the mold, and fills it. The level of propellant increases inside the mold. This type of casting is known as spring casting.

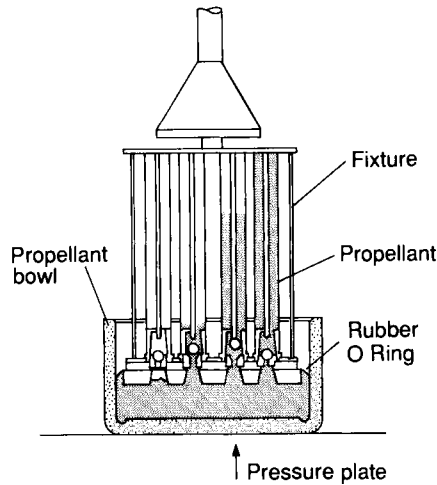


FIG. 10.16. Casting of a propellant in a case under pressure.

One interesting evolution of this classic process has led to the casting process by “stamping” [14]; it is illustrated in Fig. 16.

In order to minimize the waste of slurry inside the pipes linking the drum to the mold, and to allow the casting of a large number of cases in one single operation, the cases are placed directly on the piston, which has been perforated with a specific number of holes, to allow a direct connection between the propellant in the drum and the cases. This setup is mounted on the drum containing the propellant, and is pushed in by applying pressure.

When the pressure is exerted, the propellant goes up and fills the cases. A valve system closes each case when it is filled. The entire setup, piston and cases, is located in an oven. Each propellant-filled case is removed from the piston after cure of the propellant.

This process permits casting of a very large number of case-bonded grains, in one single operation.

(c) Pressure exerted mechanically, using an Archimedes' screw

This process is developed from a special type of mixer: the mixer-extruder (Fig. 17).

The mixing is done in the usual way, in a drum equipped with Z-shaped blades. This mixer, however, has at the bottom an Archimedes' screw used to extrude the product through a threaded-cylinder type of opening at a pressure calculated as a function of the rate of rotation and the rheologic characteristics of the propellant.

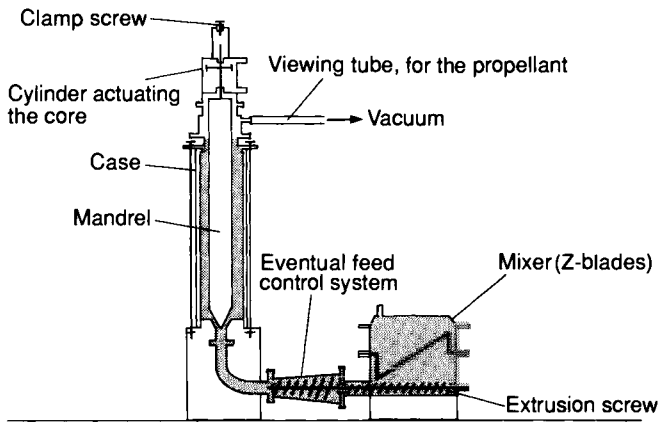


FIG. 10.17. Direct transfer through mixer/extruder.

By linking this opening to the bottom of a case or set of cases, the propellant can be transferred directed from the drum, where it is kneaded under vacuum into the cases without being exposed to atmosphere.

Many grains require central port profiles that cannot be obtained simply by casting. Several techniques are available:

- Machining of the deep axisymmetric slots using an especially designed tool at speeds tailored to the material [15].
- Using segmented mandrels. This technique, although simple in principle, requires in practice the use of complex machinery with safety handling problems that need to be resolved: the mandrel must be kept tight, and there is the issue of safety when removing the pieces of the mandrel. Consequently, this method is used only when central port configurations cannot be obtained through casting with removable monoblock core, or through machining, as with fynocyl grains, for instance. It is also used for maximum loading ratio grains which must be manufactured by integral molding, and for which mechanical finishing operations are not permissible.
- Using mandrels that are destructible after curing of the propellant, or at the time of ignition.

The technological and implementation difficulties involved with multiple-segment mandrels led to research on simpler concepts, and resulted in the creation of mandrels made of a material, either braided or in strips, wrapped in a very specific pattern, compressed and coated with an elastomer or a polyurethane foam. The easiest cases can be handled with a simple foam with sufficient rigidity and capable of disintegrating at ignition. With this process, grain configurations can be obtained that would be completely impossible

using either the machining process or the mechanical removable mandrel. This process places no limitations on configurations or geometry.

This description of casting principles may convey the impression that these technologies are simple. In reality, however, numerous issues have to be checked and eventually resolved to arrive at a qualified and reliable process, such as: air-tightness of the toolings; safety in regard to sensitivity to friction and static electricity of the propellant; compatibility between the inert materials involved and the propellant; and temperature and internal pressure stresses during cure. Without any doubt, most of the knowledge necessary for the manufacture of performing, reliable propellant grains, at an attractive production cost, is applied to this area rather than to the more spectacular area of propellant tailoring.

3.3. TEMPERATURE CURING AND FINISHING

Temperature curing is designed to accelerate the crosslinking reactions, i.e. harden the propellant rapidly. This is done by raising the propellant to a moderate temperature while in the casting pit or in an oven.

Changes in the curing process made to improve the properties of the propellant grains are further described below.

3.3.1. *Curing under pressure*

The 1960s saw the emergence of composite cases, which offer the significant advantage of being lighter than metallic cases but are also more able to deform when subjected to internal pressure.

Benefit can be derived from the latter characteristics to minimize residual stresses/strains occurring in the grain caused by thermal shrinkage when cooling after cure.

The leading concept of this process consists in subjecting the case loaded with the propellant to a pressure during cure such that, when depressurized, the movement of the case will follow, almost perfectly, the predicted contraction of the propellant grain when cooling [16].

By decreasing residual stresses/strains, the mechanical safety coefficient is improved. Curing under pressure is also reflected by an increase of the volumetric loading ratio of the case and higher quality of the propellant.

3.3.2. *Integral molding*

For productivity reasons, or for production of specific grain configurations, as well as for safety reasons (avoiding trimming the grain by machining it with a cutting instrument), the integral casting or molding technology is increasingly being used.

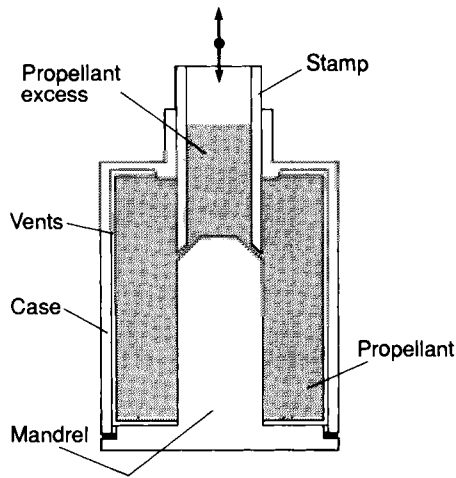


FIG. 10.18. Principle of integral molding.

With this process, which can be coupled with curing under pressure if need be, the propellant grain is obtained directly by casting, as shown in Fig. 18.

The implementation of the integral molding process involves the following considerations:

- An absolute thermal control of the casting-curing cycle — which must be isothermal — only very small temperature changes (positive) are permissible, and after the final tool has been applied to ensure complete confinement, negative temperature changes are forbidden, for risk of creating cavities.
- The viscosity build-up of the slurry and the development of mechanical properties during cure, as well as the thermal characteristics of the grain, determine the curing cycle.

3.4. INFLUENCE OF THE MANUFACTURING PROCESSES OF PROPELLANT GRAINS ON THEIR FUTURE COMBUSTION CHARACTERISTICS AND MECHANICAL AND STRUCTURAL INTEGRITY

3.4.1. *Anisotropy of the combustion characteristics*

Analysis of the pressure and thrust-versus-time curves at firing of the grain demonstrates that the manufacturing processes influence the burning rate of the propellant.

For example, pressure curves recorded during the firing of MIMOSA grains of composite propellant exhibited differences when the propellant was cast with the mandrel already placed in the mold or if the mandrel was introduced after casting.

The pressure-time curve shown in Fig. 19 for the first process shows a characteristic hump occurring approximately halfway through the web burned, while the pressure curve for the second process is flat.

The most important known findings are:

- Halfway through, calculations demonstrate that the burning rate of grains cast with the mandrel in place is always higher by 3–7%.
- The size of the pressure hump is not a function of the burning rate of the propellant.

Other experiments performed on BATES grains confirm these findings. Because experiments where grains of this type manufactured using both processes were extinguished, revealing that the burning surface halfway through the burned web is very similar to the theoretical surface, the pressure hump effect must be attributed to a burning rate variation as a function of web to be burned.

In the United States, AFRPL fired 2500 motors with 7–900 kg of propellants manufactured with 250 formulations for the BATES program. These firings served to reveal the hump effect [17].

Several explanations have been suggested. At the time of casting, binder-rich zones are created, in strata, at contact with the walls of the mandrel and of the case. The binder-rich zones burn slower, which would explain why the burning rate is a function of the web burned [18]; on the other hand, these strata are destroyed when the mandrel is inserted.

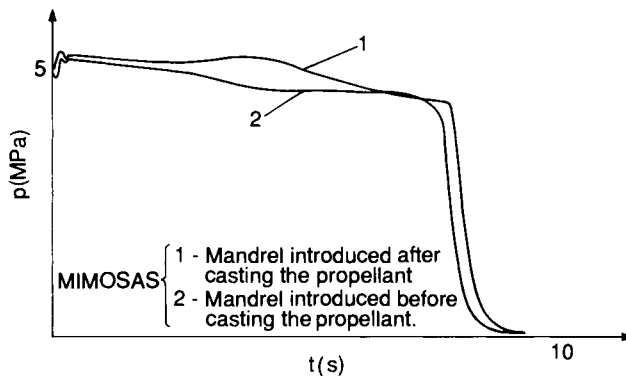


FIG. 10.19. Pressure curves for the same propellant.

3.4.2. *Anisotropy of the mechanical characteristics*

Systematic measurements made on propellant specimens removed from propellant grains tend to demonstrate that these orientation effects, tied to the casting process, may also have an impact on the mechanical characteristics and, consequently, on the effective safety factor of the propellant grains.

The more pronounced the orientation of the successive layers of propellant from the casting operation of the slurry into the case, resulting in significant shearing stresses in the slurry, the greater these effects will be. The viscosity of the propellant, in particular, plays an important role.

- On large case-bonded grains, manufactured with the classic gravity casting process through the base of the aft end of the rocket motor, dissections have shown that the propellant is homogeneous inside the grain but that the structural integrity deteriorates in the “raised collar” usually added to allow casting slightly more slurry than necessary to fill the case of the rocket motor exactly. But this area, considering the local geometrical narrowing, and because it is subjected to the effects of the volume variations of virtually the entire propellant mass during temperature changes, is the most mechanically stressed and strained area at a time when the propellant is already partially crosslinked. In some sense the propellant is “damaged”. Variations of 40% have been recorded between the values of the modulus and the elongation capability of this area and the rest of the propellant grain.
- Die-casting processes involving a high degree of oriented injection coupled with high-level viscosity slurries may lead to variations in the elasticity modulus, ranging from 30% to 40% between the direction of the casting and the perpendicular direction.

This influence resulting from the casting process of the slurry and the geometry of the mold may very well have a considerable impact on the comparisons of characteristics between manufactured grains and grain specimens designed for quality control, cast from the same slurry. Constraints resulting from the manufacturing process require that the specimen designed to control the structural integrity of the grains be an object tailored to industrial production, easily machined, and with the smallest possible size.

Systematic analyses have led to the following conclusions: the mechanical characteristics of the control specimen (parallelepiped obtained through simple casting by gravity) have been found to be representative of the grain in a great number of propellant grains.

On the contrary, in a specific finocyl grain, the mechanical characteristics of the specimen have been shown to be inconsistent with those of the propellant grain. Elastic elongations systematically lower in the propellant grain than in the specimen have been observed. A general analysis of

all test data enabled us to discover that this phenomenon was specific to a particular kind of composite propellant. Further research succeeded in defining a more closely representative although simple specimen, obtained by casting with a star-shaped mandrel.

A number of assumptions or observations were made in the course of analyzing this phenomenon:

- The propellant grain and the specimen must have identical thermal histories. The case of the grain and the core may play a thermal role and influence the final level of the mechanical characteristics.
- The size of the specimen must be sufficiently large to be representative of the propellant grain.
- The liners, and thermal insulations may have some effect (such as migration, for example).
- In the case of significant shearing of the slurry (die-cast or gravity-cast grain), the phenomenon may be intensified.

3.5. QUALITY CONTROL

The mission of the quality control services is to ensure the quality of the product, particularly by controlling the following areas: raw materials, manufacturing operations, finished product.

3.5.1. *Overview*

Quality control operations on finished products can be divided in two major categories:

Destructive tests performed on specimens made with identical propellant: measurement of ballistic and mechanical properties using methods described in Chapters 4 and 6, and comparison with the specifications established for the propellant grain.

Non-destructive tests performed on the propellant grains. The non-destructive quality control tests, although not specific to composite propellants, are described below.

3.5.2. *Non-destructive testing or inspection*

In opposition to destructive tests that may include testing until failure of the specimen, non-destructive tests are designed to ensure the quality and integrity of the material or of their complex assemblies by “inspecting” them without altering them. These tests commonly fall into three categories:

- Inspection of the mass to identify cracks, cavities or heterogeneities.
- Examination of the bonds to identify debondings, cracks or inclusions.
- Control of the geometry to verify the dimensions.

With case-bonded grains, it is very important to inspect the most critical bonding zones which are located, usually at the aft or head ends.

Simple methods, such as visual or dimensional controls, are widely used, either to observe any surface anomalies, or to check the functional dimensions of the finished object.

Generally, these methods do not call for sophisticated principles. But they may very well use very intricate methods, such as endoscopy, surface control devices, television, stereoscopy, laser proximity, and others.

These methods are useless for the control of the interfaces or the mass of the propellant grain. It is therefore necessary to have recourse to advanced technologies that allow us to traverse the material regardless of the nature of the material encountered.

The most widely used of these techniques are based essentially on the analysis or the detection of a wave or a radiation after its absorption, reflection, or emission. The oldest and most prevalent of these techniques call for ultrasound and X-rays. The most recent ones apply newly discovered principles, and make use of powerful automatic computer methods that facilitate the analysis of the information.

The implementation of these techniques usually requires large infrastructures and costly investments. The selection must therefore be very carefully made to ensure that the testing facilities will allow performance of quality control easily, at the best possible price.

The major difficulty encountered comes from the fact that in every case, there are superimposed interfaces, sometimes located behind a zone normally not bonded.

This means that one area can hide another and make the methods suitable for the analysis of the first interface completely useless on the other. The methods used fall into two categories:

- So-called “global” methods, which generally provide qualitative information, over a large area, at one time.
- “Spot” methods, which provide qualitative and quantitative information over a limited area.

It is desirable for one technique to be capable of providing these two types of investigations.

3.5.2.1. Inner control

The oldest and still yet most widely used methods are based on X-rays and ultrasonic waves.

(a) X-ray testing (Fig. 20)

This technique allows us to assess the inner homogeneity of the propellant grain (lack of cracks, bubbles, porosities, foreign matter, for example), the

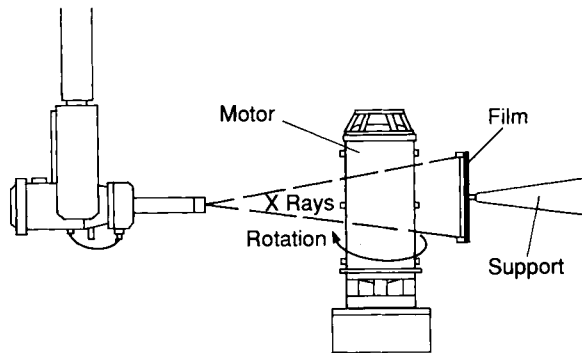


FIG. 10.20. Diagram of an X-ray facility.

quality of the bonds between the various elements of the propellant grain (liner-case or thermal insulation, liner-propellant, propellant-propellant), and also to determine the thickness of the various components. This test is based on the variations in the absorption of X-rays by the elements constituting the grain, which is translated by contrast differences on the various materials used to receive the radiant image. On film, negative film usually, cavities and debonding, which have a low absorption, will show as dark areas; metallic foreign matter, more absorbing, is paler.

X-rays are produced by bombarding fast electrons on a heavy metal target. The resulting energies may range from 50 keV to a few tens of MeV.

An energy of approximately 2 MeV is produced with a Van de Graaf electrostatic generator, while a greater energy will be produced with an electromagnetic linear accelerator.

Analysis of the radiating image, usually captured on photographic film, is a delicate operation, which requires highly qualified personnel regardless of the imaging method used: naked eye or microdensitometer.

This is equally true for the radiologist, who must have knowledge of a collection of parameters which greatly influence the quality, and therefore the analysis, of the final image. These parameters include:

- intensity of the X-ray;
- type of film used;
- distance of the source to the grain;
- positioning of the film in relation to the grain;
- number of angles of exposure;
- exposure time.

The determination of these parameters is often the result of a trade-off: for instance, an increase of the intensity of the X-ray results in a shorter exposure

time, although it increases the graininess of the image on the film. Similarly, increasing the distance to the grain results in a trade-off between a longer exposure time and the depth of field.

The optical density obtained on the film varies significantly according to the area under observation. An average density is necessary to correctly reveal defects, often requiring the use of films with different speeds. For instance, the image of the inhibitor-propellant bonds is done with a slow film, while the central areas will be done with a fast film.

The precision of the measurement of thickness and of the size of the defects is affected by:

- out-of-focus areas, dependent on the focal length of the radiographic camera;
- graininess of the film;
- intensity of the radiation, which affects the contrast.

X-ray radiography, followed by analysis of the image on the film, is a slow and expensive technique for extensive testing; but is a highly precise method for the observation of the inhibitor-propellant bondings and is widely used for large propellant grain.

(b) Ultrasonic testing

This technique is based on the observation of the variations experienced by an ultrasonic wave traversing an object. It is therefore possible to detect the transmission or the reflection of an ultrasonic wave or to analyze the nature of the signal (amplitude, frequency, phase).

This type of control is rarely used for mass exploration because propellant is highly absorbing. It is not very useful in determining the size of a defect. Still, it is frequently used to check the propellant-inhibitor bonding, though limited to the first interface only. It may present some interest for the assessment of the boundaries of bonded areas, and is therefore used as a method to analyze small areas, using portable equipment.

Other techniques, similar to the one just described, may also be used sometimes:

- γ absorption: this is of limited use because of the pyrotechnic threat tied to radioactive sources;
- neutrons: cannot be used for high thicknesses hydrocarbon materials;
- acoustic emission: difficult because of the low emissive power of propellants;
- infrared thermography: this is not suitable for superimposed bondings such as are found in propellants;
- optical holographic interferometry.

New techniques are currently being developed with the help of better-performing and more modern techniques for the recording and analyses of the image.

(c) New investigation methods

The purpose of these new techniques is to:

- remedy the shortcomings of classic radiography by, for instance, aiming for rapidly available information, in real time;
- provide a reception level tailored to the requirements;
- respond to the need for spatial observation;
- answer the necessity of recording the information obtained;
- find a high level of cost-effectiveness.

They include:

Televised radioscopy. This technique, which is increasingly used [19] and is perfectly suited for industrial production, provides the ability for continuous and dynamic observation (Fig. 21). It combines the use of television, video-taping and computers. Total observation in real time of a moving object is

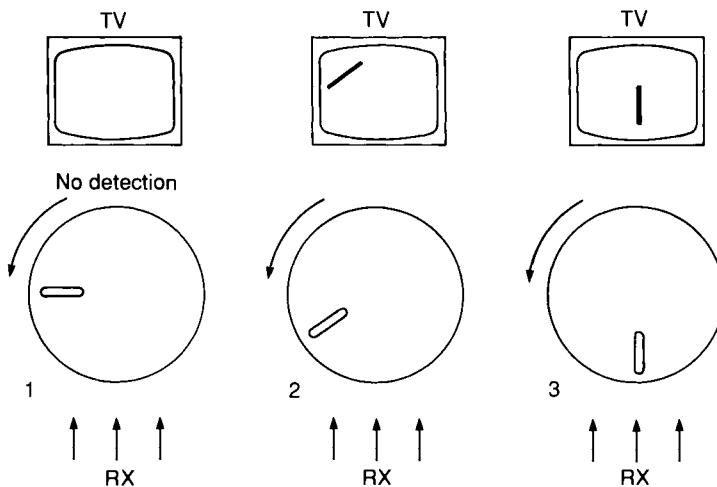


FIG. 10.21. Televised radioscopy: dynamic observation.

possible from a completely automatic observation post. This observation post is divided into three sectors:

- information gathering sector;
- analysis sector;
- memory sector.

Through its new design, this technique offers many advantages and contributes to significant savings in testing operations.

Observation with this new technique of, for example, 64 mm diameter propellant grains, allows us to guarantee the detection of 0.8 by 8 mm cavities, and of foreign objects with an average diameter above 0.5 mm.

Tomodensitometry. In the medical field, this technology is known as “scanning.” It is the result of a logical evolution of tomography (Fig. 22), itself derived from radiography. It permits, using a computer, the reconstruction of images of successive slices of the object, providing a record on film of information that is not accessible with the classic X-ray method, in particular, the observation of the inner configuration of a specimen. Through a reconstruction of a succession of sections it reproduces the three-dimensional aspect of all areas of the object examined. As with televised radioscopy, the completely automatic control is an important advantage, permitting us to acquire, analyze and decide in real time, at a minimum cost (Fig. 23).

This imaging method, used until recently mainly for small objects, is now being applied to stages of ballistic missiles.

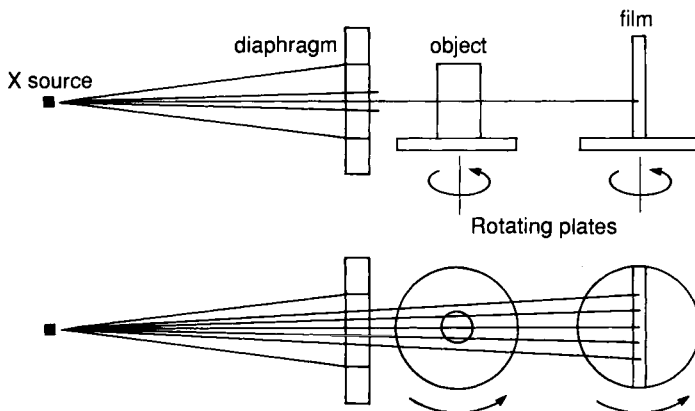


FIG. 10.22. Diagram of the tomography inspection.

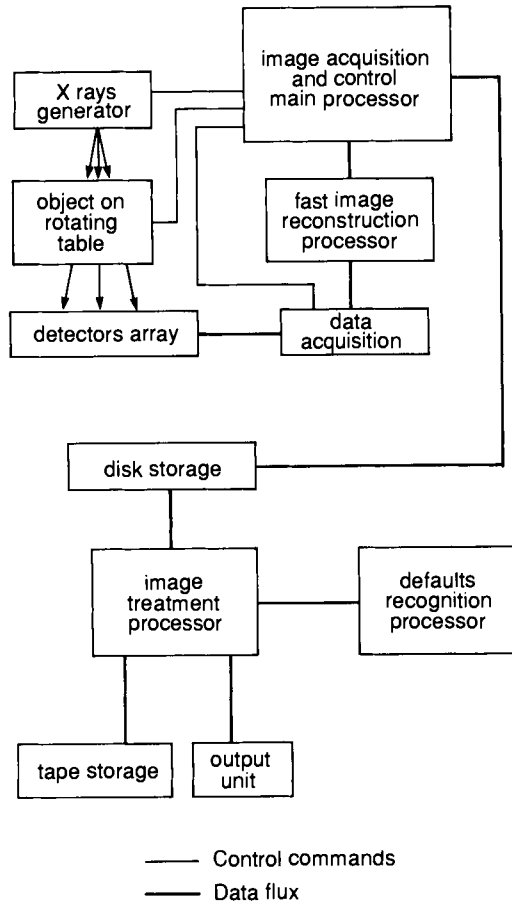
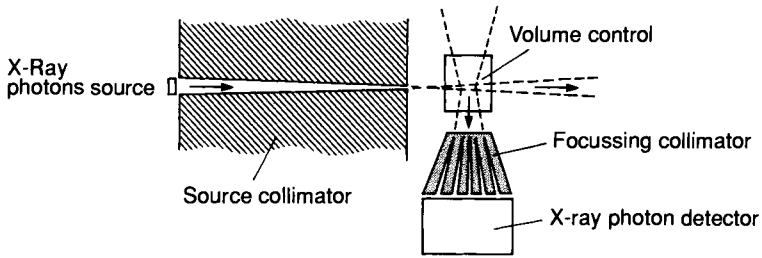


FIG. 10.23. Organization of a tomodensitometry set up.

Compton Scattering. This technique allows the reproduction of images by computers resulting from the observation of the Compton effect, the scattering of an X-ray or gamma-ray upon impact with the object examined. One of the advantages consists of having the source and the detector on the same side of the object (Fig. 24).

When only the periphery of a very thick object is being checked, this technique permits the use of less powerful X-ray generators than would be necessary with the tomodensitometry X-scanning.



Compton scattering technique for the detection and location of density anomalies in the material

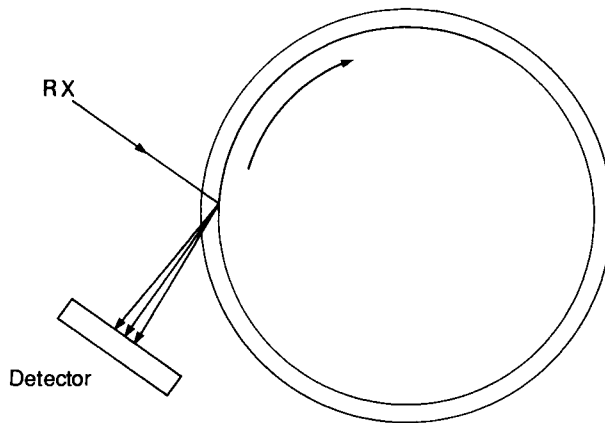


FIG. 10.24. Diagram of the principle of quality control with Compton scattering.

4. Properties of Composite Propellants

4.1. ENERGETIC AND COMBUSTION CHARACTERISTICS (STANDARD DELIVERED PRACTICAL SPECIFIC IMPULSE IS USED)

4.1.1. *Isolites (polyurethane–polyether binder, ammonium perchlorate)*

These non-metallized propellants are used essentially for gas generators, or as “sustainer” compositions for missiles where a low signature (absence of solid particles) is required.

The specific impulse, like the density, is low: some compositions where a portion of perchlorate has been replaced with nitroguanidine to adjust the burning rate at approximately 1–3 mm/s at 7 MPa do not exceed 180–190 s.

4.1.2. *Butalites (polybutadiene binder, ammonium perchlorate)*

The burning rate range of these “reduced smoke propellants” is much wider. They are used for the same purposes, and the tendency is to use them instead of Isolites. The reduced smoke propellants with the highest specific impulse attain I_s ranging from 235 to 239 s, with burning rates at 7 MPa which may exceed 60 mm/s if very fine ammonium perchlorate and a high percentage of ferrocene catalysts are used.

At lower burning rates, on the other hand, the impulses are comparable to those of non-metallized polyurethane propellants, because the ammonium perchlorate has to be replaced, in part, by a cooling charge.

4.1.3. *Aluminized composite polyurethane propellants or Isolanes (polyurethane, ammonium perchlorate, aluminum)*

The standard specific impulse rarely exceeds 240 s, and they are currently replaced by polybutadiene propellants.

4.1.4. *Aluminized composite polybutadiene propellants or Butalanes (polybutadiene, ammonium perchlorate, aluminum)*

The conventional aluminized composite propellants with the highest specific impulse, they are currently manufactured in very large quantities. They contribute an increase of 5 s over the best polyurethanes, with a density capable of reaching 1.86. They are used in the most powerful version of ballistic missiles, as well as in tactical missiles where the range of the burning rate (more than 60 mm/s at 7 MPa) and excellent mechanical properties are very valuable qualities.

4.1.5. *Composites with HMX (Butalanes X)*

These propellants, with some HMX added, offer a gain of 3–4 s in specific impulse over the best Butalanes, including, however, a small loss of density.

4.1.6. *Solid post-boost system propellants: Butamites (polybutadiene binder, nitramine), and nitramine-based propellants*

These propellants, which contain a hydrocarbon binder and a nitramine, are not used in main rocket motors because of their limitations in terms of specific impulse and burning rate. However, their kinetic characteristics, their “cleanliness” and the non-corrosive nature of their gases, and their specific impulse superior to that of AP propellants make them a better choice when severe temperature limitations (2000–2500 K) are placed on the combustion gases in gas generators, or for warhead dispersion systems of ballistic missiles [20]. An illustration is provided in Fig. 25.

The same types of binders are used as in typical propellants: polyesters, polybutadienes, and the nitramines are usually HMX or RDX.

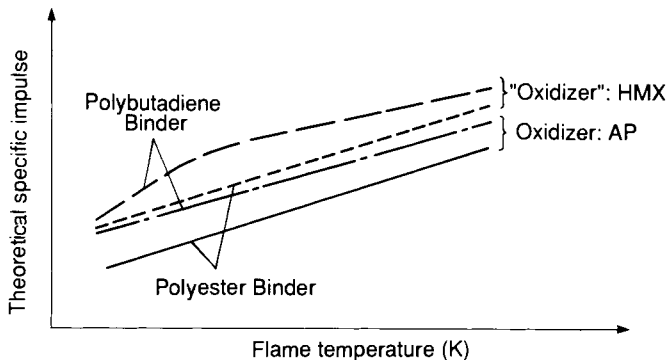


FIG. 10.25. Effect of substitution of AP by HMX for two types of propellants.

Their combustion is rather peculiar: low burning rates, a few millimeters per second; at low pressure, this burning rate increases with the solid loading ratio and decreases with the particle size of the nitramine. The pressure exponents, ranging between 0.5 and 0.7 at low pressure, tend toward 1 above 150 bars, and the burning rate becomes the same as that of pure nitramine [21,22]. This high exponent makes them particularly suitable for the modulation of the flow rate by varying the pressure.

4.1.7. *Gas generator propellants: Butanites and Ammonium nitrate propellants*

Also reserved for use with gas generators, these are the “coldest” of the industrially used propellants ($T_c < 1400$ K). Their burning rates are a few millimeters per second and their specific impulse is low [23,24].

4.2. MECHANICAL CHARACTERISTICS

These are discussed in Chapter 6; consequently, this section describes only certain aspects relating to the chemical composition: capability curves and the kinetic of the development of mechanical properties.

4.2.1. Capability curve

By plotting on a diagram (Fig. 26) the values of the maximum stress S_m versus the maximum strain for various values of the crosslinking or cure ratio — ratio of the reactive functions of the crosslinking agent and the polymer — we see that the corresponding point follows a curve characteristic of the given composition, called the capability curve. For small values of the crosslinking ratio the mechanical capability is very weak, and S_m and e_m decrease simultaneously. For high values of that ratio the elongation capabilities are very small. For values that are overall close to the stoichiometry, the aspect of the curve allows us to determine the best trade-off between S_m and e_m , i.e. determining the mechanical properties of the propellant. Changes resulting from different lots of raw materials — reflected by slight variations in the reactive function concentrations — must be such that, to be acceptable, an identical capability curve is obtained.

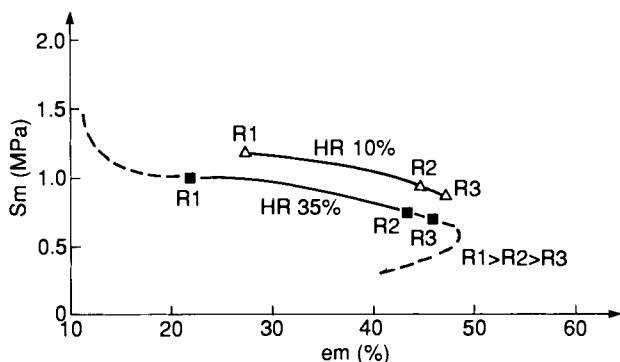


FIG. 10.26. Stress at maximum strain versus maximum strain as a function of the curing ratio (HTPB, AP, Al propellant).

4.2.2. Cure kinetics and development of the mechanical properties

The propellant grains that are being manufactured to be handled without being damaged must have mechanical properties that are virtually stabilized at the end of curing. This explains why the kinetics of the crosslinking must be well determined for each material developed, by measuring the cure state and the mechanical characteristics during the curing operation at various temperatures.

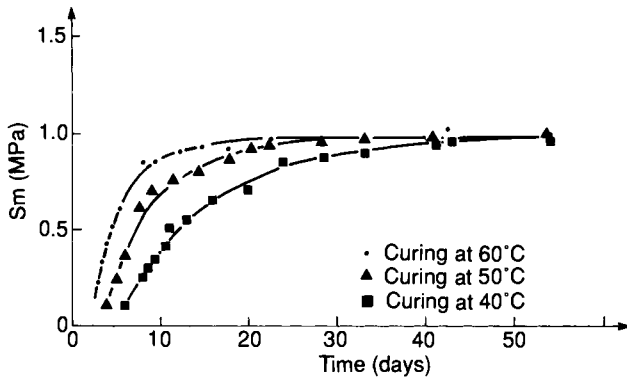


FIG. 10.27. Example of the build-up of maximum stress as a function of the curing temperature.

Figure 27 illustrates the evolution of the maximum stress over time for three cure temperatures. We note that:

- The energy that activates the crosslinking reaction is independent from the temperature, but slightly dependent on the progress of these reactions. The value of energy E which allows the best reproduction of the curve at different temperatures is close to 10 to 15 kcal/mole for propellants formulations based on carboxy or hydroxytelechelic polybutadiene.
- Since generally the cure temperature does not affect the final level of mechanical properties, we may assume that the state of the propellant mechanical properties after complete crosslinking is not dependent, at least within the useful range (40–60°C), on the cure cycle that is being used.
- A simple model can be used to predict the effect of a cure cycle. The development of the mechanical properties — maximum stress, for example — versus time is expressed by formula of the type: $S_m/S_m \text{ stabilized} = f(Q)$ where Q , called “cure quantity,” is related to the cure cycle.
- Having determined the relations $S_m/S_m \text{ stabilized} = f(Q)$ allows us to predict the effect of a given cure cycle on the mechanical properties.

4.3. AGING OF COMPOSITE PROPELLANTS

Experience has shown that it is the mechanical properties that can be the most seriously affected by aging. The thermodynamic and kinetic properties are rarely modified.

There are numerous factors influencing aging, and their incidence varies according to the propellant considered.

4.3.1. Temperature

Temperature accelerates the multiple aging reactions, in various ways, depending on their activation energy.

In practice this means that the determination of the aging characteristics needs to be done at a temperature as close as possible to the temperature that will be really encountered, considering the diversity of the possible reactions, which the temperature does not all accelerate in the same manner.

4.3.2. The environment

Generally, air and humidity are aging factors by initiating oxidation and/or hydrolysis reactions:

- Oxidations of the double bonds of the binder causing an over-crosslinking, followed by a break of the chains through depolymerization.
- Hydrolysis of certain sensitive functions such as the esters bonds, and also the action of the water on the binder-oxidizer bond. Beyond a certain threshold of relative humidity (70–80%), AP absorbs the water, resulting in the destruction of the binder-oxidizer adhesion, eventually surface dissolution, and the acceleration of the oxidizing attack through the formation of perchloric acid.

4.3.3. Mechanical stresses

When the mechanical stresses exceed a certain threshold they may result in a degradation of the material by causing, for example, binder-solid separations.

An accumulation of the degradations (fatigue) may make the propellant useless, as is clearly demonstrated by the previously mentioned case of unstabilized ammonium nitrate propellant (Fig. 28).

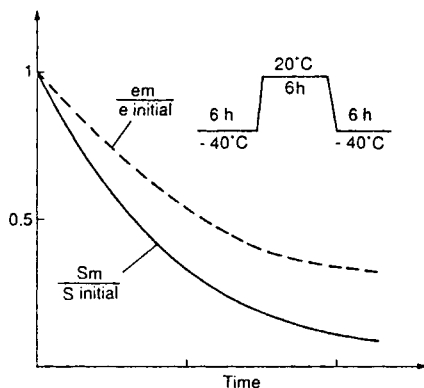


FIG. 10.28. Evolution of the properties of an AN-HTPB propellant during thermal cycles.

4.3.4. *Contact with other organic materials*

The propellant is bonded to a liner or a combustion inhibitor. Some of the elements which are not tied chemically may migrate from the propellant to the rubber; others may migrate in the other direction and significantly modify the composition at the interface with consequences which will naturally not only affect the mechanical properties and the characteristics of the bonding, but also the burning rate, through the migration of catalysts or plasticizers. This issue takes on a great importance for end-burning grains where the burning rate may be greatly disturbed alongside the inhibitor, and cause a modification in the combustion parameters.

4.4 SAFETY CHARACTERISTICS AND PYROTECHNIC BEHAVIOR

The composite propellant types Isolite, Isolane, Butalite, and Butalane generally exhibit high critical detonation diameters, over 1 m, and a low sensitivity. The introduction of oxidizers likely to detonate such as RDX and HMX will of course decrease the critical diameter, but composite propellants may generally be considered not to be very sensitive, thus fulfilling rather well the specifications for low vulnerability or lower risk. The major mode of decomposition from stimuli such as friction, shock, impact, or fire, is combustion. Ammonium perchlorate composite propellants may, however, exhibit a violent reaction (thermal explosion) at slow cook-off, i.e. a few degrees per hour temperature increase.

In terms of the manufacture, an analysis of the history of accidents that have occurred in the composite propellant industry certainly shows that, outside of special cases where the cause is foreign to the product itself (presence of foreign bodies, external stimuli, or equipment malfunction for example), and until the development of high burning rate propellants and HTPB binders, the major causes of accidents were linked to the handling of the wastes, more or less inhomogeneous, of perchlorates and other oxidizers contaminated with grease or organic matters, or to mixtures (dust, for example) of solid oxidizers and fuels. This explains why, in the manufacture of propellants, very rigorous attention must be paid to keeping oxidizers apart from fuels, to the cleanliness of the facilities, and to the handling of wastes or objects contaminated with propellants. Explosions, even detonations, have occurred during the destruction of wastes by burning. Their origin is a transition of combustion to detonation in this sometimes porous and inhomogeneous medium.

Experience, coupled with a systematic characterization of the sensitivity of all products at every stage of the manufacture, has permitted the establishment of concrete measures, reflecting the safety margins of operations carried out during production, that towards the end of the 1960s have generally become the standards for this industry. These measures have had to be

drastically amended, however, with the development in industrial manufacture of two new products: high burning rate propellant with ferrocene additives and HTPB binders which, by making the propellant a very poor conductor, have caused ignitions of electrostatic origin.

4.4.1. High burning rate propellants

High burning rate aluminized composite propellants containing high levels of ferrocene derivatives have been at the origin of many accidents that have occurred in the industry during recent years [25]. This does not mean that they should be rejected because, as we saw, they have unique operational characteristics. However, their greater sensitivity, associated with more violent effects, demands that the production, handling and quality control methods be thoroughly reassessed.

Table 10 lists a certain number of sensitivity characteristics of typical polybutadiene-AP-Al propellants and of propellants with a ferrocene derivative. The sensitivity tests were performed in accordance with the codified standards of SNPE (Chapter 7).

The reactivity of the mixture of ammonium perchlorate with a ferrocene derivative determines the pyrotechnic behavior of the propellant.

Indeed, mixtures of pure products are sensitive to mechanical stimuli, with a sensitivity level identical to that of granular explosives or of a pyrotechnic ignition powder. These characteristics, listed in Table 11, determine the behavior of the finished product, and require that special precautions be

TABLE 10 *Sensitivity characteristics of aluminized polybutadiene composites (Butalanes) with a ferrocene derivative*

Test	Stimuli		Mode of decomposition				
	Thermal		Mechanical		Detonation		
	<i>AI</i> ^a (°C)	Cook-off (°C)	CSF (N)	Shock ^b (m)	<i>CGT</i> ^c	<i>CDD</i> ^d (mm)	Combustion <i>V</i> ^e (mm/s)
<i>With ferrocene derivative</i>							
20–30 mm/s	220	155	50–70	1.75	< 1	60	4–3
30–50 mm/s	196		50–70	1.25	< 1	60	4–5
50 mm/s	190		30–50	0.50	< 1		> 6
<i>Without ferrocene derivative</i>							
7–9 mm/s	320	175	140	2–3	< 1		1
12–15 mm/s	265	175	90	1.75	< 1		1

^a *AI* = Autoignition temperature, heating at 5°C/mm.

^b Shock = 30 kg drop hammer test, no-reaction height.

^c *CGT* = Detonation aptitude index, number of cards (French).

^d *CDD* = Critical detonation diameter.

^e *V* = Burning rate at atmospheric pressure.

TABLE 11 *Sensitivity of mixtures of ammonium perchlorate/ferrocene derivatives compared with explosives*

Test	Pure AP	50/50	72/25	90/10	95/5	HMX	PETN	MIRA*
CSF (Newtons) (friction Julius Peters)	> 360	37	20	22	35	100–200	40	34
CSI (Joules) (impact Julius Peters)	13	5	3	3	2	4–5	3	6
Autoignition (5°C/mm)°C	~400	275	260	260	295	256	184	300

* Pyrotechnic ignition composition.

observed for the production. In addition, the ferrocene derivative facilitates the decomposition of perchlorate. Analyses have shown a decrease of the order of 150°C in the exothermic decomposition peak of the ammonium perchlorate decomposition. Consequently:

- the higher the content of ferrocene derivative,
- the higher the content of perchlorate,
- the smaller the particle size of the AP,
the greater the reactivity will be.

4.4.1.2. *Decomposition modes*

(a) Detonation

The critical diameter of these propellants is much smaller, in some cases as small as 60 mm, setting them clearly apart from those other types of composite propellants, although their response is measured by less than one card at the card gap test.

(b) Combustion

The thermal effects of these formulations present a major threat during manufacturing operations. This is due to the fact that the combustion propagates very rapidly to the surface of the specimen following an accidental ignition.

The regression rate measured during a strand burner test, at atmospheric pressure, is greater than 3 mm/s, and increases with the amount of ferrocene catalyst. A test done on a small star-shaped grain shows that a flame 1 m long appears in a few tenths of a second. This vigorous ignition capability must be taken into account in the determination of the protective zones for the personnel during manufacture, and can require remote operations.

4.4.1.3. Sensitivity to mechanical stimuli

(a) Shock

In a 30 kg drop hammer test, a 4 m fall does not lead to a detonation, and the effects are hardly more violent than the effects obtained with typical compositions. The non-reaction height, however, is much lower than with typical propellants, which show no reaction below a drop of 2 m: the results varied between 0.50 m and 1.75 m.

(b) Friction

These compositions are sensitive to friction, in the conditions created by the Julius Peters testing device (0.4 mm thick blades). Strong reactions were observed, and the higher the content of ferrocene derivative, the more sensitive the compositions are (Fig. 29).

While typical propellants have CSF values greater than 70 N, these propellants exhibit values ranging between 50 and 70 N, lower values can be recorded for formulations whose burning rate at 7 MPa is greater than 50 mm/s.

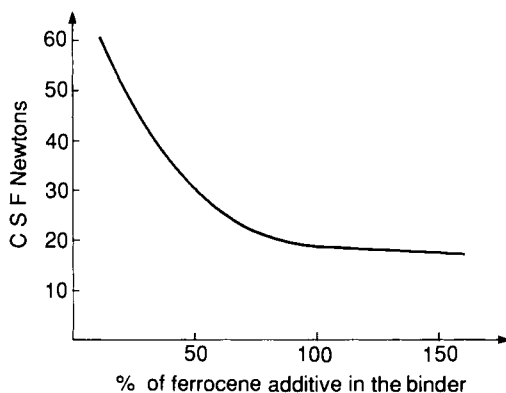


FIG. 10.29. Friction sensitivity.

4.4.1.4. Sensitivity to thermal stimuli

(a) Autoignition temperature

The presence of ferrocene accelerator lowers the autoignition temperature to approximately 200°C, and triggers violent decomposition phenomena in specimens that are not observed with typical propellants, whose reaction temperature is close to 300°C.

(b) Cook-off

The thermal stability of compositions accelerated by a ferrocene derivative is lower than that of typical propellants, and this is more so when the particle size of AP decreases and the amount of ballistic catalyst increases. Cook-off tests performed with a specimen 50 mm in diameter and 50 mm in height have demonstrated a 50°C decrease of critical temperature, which, however, continues to be higher than 125°C.

4.4.1.5. Sensitivity to static electricity

These propellants are sensitive to capacitive discharges only above a certain amount of aluminum (SNPE Test No. 37). Although above that particular amount, the aluminum quality (shape and size of particles) plays a fairly significant role in this type of stimuli, mechanical characteristics and temperature may also be important factors.

4.4.1.6. Production safety measures

While thermal effects are the acknowledged major threat from these compositions when polymerized, it is nonetheless necessary, because of the reactivity of the ferrocene derivative with ammonium perchlorate, to adopt preventive measures for mixing these components.

Ferrocene derivative, for example, may contain volatile ingredients (pure ferrocene), which by condensing on the cold parts of the mixer, may lead to mixtures with AP dust that are particularly sensitive to mechanical stimuli.

In general, these manufacturing operations are done under the highest safety conditions practiced by the industry.

The sensitivity of the various composite propellant families can be illustrated with the diagram of autoignition temperature versus sensitivity to friction shown in Fig. 30.

4.4.2. Detailed presentation of the problems related to sensitivity to static electricity

Table 12, where the resistivities at 20°C of various binders are given, shows that the historical development of these binders was accompanied by an increase of their insulating nature. It is therefore logical that during the manufacturing process that necessarily includes handling, friction, and movement of insulating and conductive materials, we would see an increasing number of occurrences with an electrostatic origin, such as electrostatic discharges that not only are an impressive sight, but also may lead to mechanical rupture of the materials.

The development of these propellants was combined with a development of

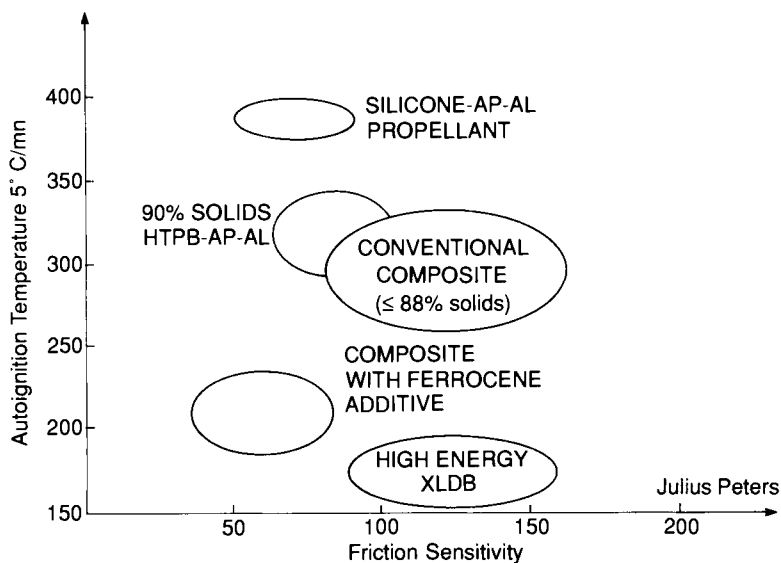


FIG. 10.30. Propellant families sensitivities.

TABLE 12 Volumetric resistivity at 20°C of the major binders of composite propellants, and of several materials

Nature	Resistivity ($\Omega \text{ m}$)
PU binder (polyurethane based on polyoxypropylene glycol)	6×10^8
CTPB binder	7×10^9
HTPB binder	2×10^{12}
PVC inhibitor	10^{12}
Thermal insulation rubber	10^{12}
Thermal insulation rubber, treated for conductivity	10^4

the insulation and case materials. Metallic cases, for example, were replaced by highly insulating composite cases that could only aggravate the problems: the Faraday cage effect of the case disappeared, and the propellant became sensitive to outer electric fields.

Traditional tests to determine sensitivity to electrostatic discharge, typically adapted from tests used for pyrotechnic powders, classified the composite propellants as insensitive but at the same time, accidental ignitions were happening during their manufacture. Little by little the origin of these ignitions was traced back to static electricity. It was SNPE researchers who identified the phenomenon [27,28], created a model reproducing the incidents observed during manufacture, recommended practical measures to minimize these phenomena and, finally, partially clarified the mechanisms involved.

The so-called capacitive discharge test was described in Chapter 7.

For propellants identified as sensitive to capacitive discharges, the analysis of the phenomena observed, such as the occurrence of the cracking phenomenon before the ignition phenomenon, suggests that the reaction mechanism can be broken down into two essential phases:

- | | |
|-----------|---|
| 1st phase | Emergence of a cracking phenomenon, related to a critical potential, |
| 2nd phase | Emergence of an ignition phenomenon, related to a specific critical energy. |

All observations tend to demonstrate that the reaction begins inside the propellant. The existence of a critical potential shows that cracking is caused by one or several electric phenomena.

Among those electric phenomena that have been identified, discharges between aluminum particles may be considered as the most likely one:

- Aluminized compositions alone were found to be sensitive.
- The volumetric resistivity of pure aluminum powder shows that for a given critical potential, the value of resistivity changes from 10^7 to $10^3 \Omega \text{ m}$. This corresponds to a puncture, for a certain number of particles of the aluminum oxide layer that covers the pure aluminum.

A factor analysis of the active ingredients of propellants essentially revealed the influence of:

- ratio, particle size and shape of aluminium particles;
- particle size of ammonium perchlorate;
- resistivity of the binder.

Temperature must also be taken into consideration. Some propellants that are insensitive may become sensitive when the temperature is lowered. When the aluminum ratio is constant, the decrease in diameter of the aluminum particles, i.e. their increase in number, leads to compositions that are more sensitive to capacitive discharges.

A model based on percolation theories was suggested. A “percolation” coefficient P was identified, such that:

$$P = \frac{N_c/N_i}{\sigma_L/V_L}$$

$P > 10^{10} \Omega \text{ m}$ for sensitive propellants;

σ_L = conductivity of the binder;

V_L = unit volume of the binder;

N_c = number of conductive particles (aluminum);

N_i = number of insulating particles (ammonium perchlorate, HMX).

With ammonium perchlorate we note that the influence of the particle size plays a role inverse to that of aluminum.

In addition, the volumetric resistivity measurements of binders have demonstrated that the polyurethane binder with a polyether prepolymer base is the least resistive. Both polybutadiene binders, on the contrary, are much more resistive (HTPB binder resistivity at 20°C: $7 \times 10^9 \Omega \text{ m}$; HTPB binder resistivity: $2 \times 10^{12} \Omega \text{ m}$).

This classification, based on resistivities, also works well for the sensitivity scale of propellants. For instance, polyurethanes are not sensitive at 20°C, and among the polybutadiene HTPBs are the most sensitive.

Bibliography

1. FLORY, P. J., *Principles of Polymer Chemistry*. Cornell University Press, Ithaca, 1953.
2. ABADIE, J. M. *et al.*, Etude des propriétés de polycondensats à base de polybutadiène hydroxytélchélique. *European Polymer Journal*, **23**, 223-228, 1987.
3. ATLANTIC RICHFIELD COMPANY, USA., Procédé de préparation de polymères de diène à terminaison hydroxyle. *Brevet français*, 73.23, 114, 25-6-73.
4. RAYNAL, S. and DORIATH, G., New functional prepolymers for high burning rate solid propellants. AIAA 86-1594, AIAA/SAE/ASME 22nd Propulsion Conference, 1986.
5. LE ROY, M., Agents d'adhésion liant-charge dans les propergols composites. Colloque du Groupe Français des Polymères, Toulouse, 1978.
6. FARRIS, R. J., The influence of vacuole formation on the response and failure of filled elastomers. *Transactions of the Society of Rheology*, **12**, 2, 315-334, 1963.
7. FINCK, B. *et al.*, Agents d'adhésion liant-charge et composition propulsive contenant cet agent d'adhésion. *Brevet français*, 85.13, 871, 19-9-85.
8. OBERTH, A. E. and BRUENNER, R. S., Bonding agents for polyurethane. United States Patent, 4 000 023, 28-12-76.
9. GRAHAM, W. H. *et al.*, Control of cure rate of polyurethane resin based propellants. United States Patent, 4 110 135, 29-8-78.
10. CULLIS, C. F. and LAYER, H. S., The thermal degradation and oxidation of polybutadiene. *European Polymer Journal*, **14**, 571-573, 1978.
11. FARRIS, R. J., Prediction of the viscosity of multimodal suspensions for unimodal viscosity data. *Transactions of the Society of Rheology*, **12**, 2, 280-301, 1968.
12. STRECKER, R. A. H. and LINDE, D., Gas generator propellants for air to air missiles. 53rd Meeting of the AGARD Propulsion and Energetics Panel, 17-1, 17-11, Oslo, 1979.
13. TAUZIA, J. M. *et al.*, Application de la rhéologie au moulage des chargements en propergols composites. ICT Jahrestagung, 37, Karlsruhe, 1987.
14. NIQUET, R. and QUEBRE, E., Procédé de moulage par injection simultanée dans plusieurs moules et appareillage de moulage correspondant. *Brevet français*, 78.02.019, 25-1-78.
15. BROUTIN, C. *et al.*, Procédé de réalisation de blocs de propergol solide et dispositif d'usinage d'un canal interne dans ces blocs. *Brevet français*, 72.06.914, 2-2-72.
16. QUENTIN, D. and PONTVIANNE, G., Procédé de cuisson des blocs de propergols contenus dans une enveloppe. *Brevet français*, 70-44 752, 11-12-70.
17. BECKMAN, C. W. and GEISLER, R. L., Ballistic anomaly trends in subscale solid rocket motors. AIAA 82-1092, AIAA/SAE/ASME 18th Propulsion Conference, 1982.
18. FRIEDLANDER, M. and JORDAN, F. W., Radial variation of burning rate in center perforated grains. AIAA 84-1442, AIAA/SAE/ASME 20th Propulsion Conference, 1984.
19. PATANCHON C. and MESNAGE, R., Application de la radioscopie télévisée au contrôle des moteurs à propergol solide dans la SNPE. ICT Jahrestagung, 137-148, Karlsruhe, 1983.
20. DAVENAS A., Amélioration des propriétés balistiques et des propriétés mécaniques tout temps des propergols sans fumée. AGARD Conference 259 Solid Rocket Motors Technology, 1979.

21. MACCARTY, K. P. *et al.*, Nitramine propellant combustion. AIAA 79-1132, AIAA/SAE/ASME 15th Propulsion Conference, 1979.
22. BECKSTEAD, M. W., Modeling calculations for HMX composite propellants. AIAA 80-1167, AIAA/SAE/ASME 16th Propulsion Conference, 1980.
23. POGUE, G. B. and PACANOWSKY, E. J., Some recent developments in solid propellant gas generator technology. AIAA 79-1327, AIAA/SAE/ASME 15th Propulsion Conference, 1979.
24. BROWN, J. L. and ENDICOTT, D. W., The safe manufacturing of catocene containing propellants. AIAA 87-1705, AIAA/SAE/ASME 23rd Propulsion Conference, 1987.
25. BRUNET, J., Detonation critical diameter of modern solid rocket propellants. ADPA Joint International Symposium on Compatibility, New Orleans, 1988.
26. KENT, R. and RAT, R., Phénomènes d'électricité statique dans la fabrication et la manipulation des propergols solides. *ICT Jahrestagung*, 423-438, Karlsruhe, 1981.
27. KENT, R. and RAT, R., Static electricity phenomena in the manufacturing of solid propellants. 20th Explosives Safety Seminar of the Department of Defense Explosives Safety Board, Norfolk, USA, 1982.

CHAPTER 11

Advanced Energetic Binder Propellants

RENÉ COUTURIER

1. Background

1.1. DEFINITION OF ADVANCED ENERGETIC BINDER PROPELLANTS FAMILY

This family includes all propellants composed of a nitrate ester-based energetic binder in which fillers (oxidizer and, if necessary, metallic fuel) are incorporated.

Due to their composition, these propellants are intermediate between the double-base propellant family (nitrocellulose + nitroglycerine or other liquid nitrate ester) and the composite propellant family (inert binder + charge). Two very different processes can be used to manufacture them.

- A casting solvent process which uses the manufacturing system for traditional double-base propellants. The products manufactured by that process are called composite modified cast double-base propellants (CMCDB) or elastomeric modified cast double-base if they include an isocyanate curable elastomer.
- A slurry cast process similar to the process used to produce composite propellants. These products are referred to as crosslinked double-base propellants (XLDB) or NEPE propellants (nitrate ester–polyether binder including high level of fillers) for specific high energy propellants.

1.2. ADVANTAGES OF ADVANCED ENERGETIC BINDER PROPELLANTS

The necessity to improve performance of conventional propellants for tactical and strategic missiles was at the origin of the development of this propellants family.

Chronologically, the CMCDB propellants were manufactured industrially before the XLDB. Production began in the United States in the 1950s [1,2]. They were a logical continuation of double-base propellants which had significantly evolved since World War Two. As a matter of fact, the transition from a single-base casting powder (nitrocellulose) to a double-base powder (nitrocellulose + nitroglycerine) had allowed a remarkable energetic improvement as well as the possibility of tailoring corresponding propellants to the production of case-bonded grains, due to the improvement of their mechanical properties.

The inclusion of fillers such as nitramines, ammonium perchlorate, and aluminum in double-base casting powder was an additional step toward improvement of the energetic characteristics.

The development of CMCDB propellants, however, ran rapidly into a number of limitations, particularly when applied to strategic missiles, due to the manufacturing process involved. These limitations include:

- impossibility of obtaining solids contents that were as high as those of composite propellants;
- difficulties tied to the production of large case-bonded grains with high fillers contents and increasingly complex geometries.

Because of the potential advantages of these propellants, the formulations were redesigned with the purpose of applying new manufacturing processes. By substituting a nitrocellulosic polymer with synthetic polymers capable of higher plasticizer amounts as well as a high solid content, a manufacturing process related to that for composite propellants could be used. With the advent of XLDB or NEPE propellants a new step had been taken toward the improvement of the performance of strategic and tactical missiles. This family of propellants led to the highest energetic levels that are in fact industrially feasible.

2. Raw Materials

2.1. BACKGROUND

The formulation of a propellant may seem, initially, to be a simple operation, consisting of mixing additives inside a binder. In reality it is a complex operation, requiring that the grain designer takes into account all constraints related to the design of a propellant grain with those of the manufacturing process; for example:

- meeting the performance requirements (ballistic, mechanical, reliability, and safety of handling);

- tailoring of the manufacturing process in order to produce good quality and reproducible propellants, at the lowest cost, and under the best possible safety conditions.

Empirical knowledge inherited from tradition on the one hand, and the emergence of better technical tools on the other hand (computer codes, for example), help determine the best possible solutions to the problems at hand. Nevertheless, before a goal can be successfully achieved it must be assumed that, within a well-established manufacturing process, the raw materials, i.e. the basic ingredients of the propellant, are perfectly known. This implies:

- on the one hand, an in-depth characterization of each of the raw materials;
- on the other hand, the knowledge of their behavior toward each other, i.e. the study of their chemical compatibility. Because propellants are constituted, in large part, of high-energy additives, there naturally exists a problem of reactivity from ingredients likely to be mixed.

Preliminary chemical compatibility analyses are therefore mandatory for any new system. Based on the results obtained, the grain designer may or may not decide to include these additives.

The principle of the chemical compatibility tests typically is based on measurements of the gaseous emissions of vacuum-tested specimens, versus time and temperature. Additional tests may be needed to support the verdict when difficulties are encountered:

- measurement of the enthalpy of decomposition;
- analysis of the decomposition gases;
- use of chemiluminescence for nitrated derivatives testing

2.2. BINDER INGREDIENTS

2.2.1. *Composition of advanced energetic binders*

2.2.1.1. *CMCDB binder*

The major ingredients of CMCDB binders are:

- Polymer: nitrocellulose;
- Energetic plasticizer: nitroglycerine;
- Desensitizing plasticizers: glycerol triacetate (or triacetin);
- Other inert plasticizers: (if necessary): aliphatic or aromatic esters,
- Stabilizers: centralite, 2-nitrodiphenylamine.

With the casting solvent process, binder final composition is acquired in two phases:

First phase: manufacture of a casting powder, with a binder consisting of the nitrocellulose and possibly a portion of the energetic plasticizer.

Second phase: the plasticizer complement is included during the operation where the solvent (nitrate ester + desensitizer) is cast in the mold loaded with the casting powder.

Depending on the plasticizer amount, it may be necessary to crosslink the nitrocellulosic network to obtain a good mechanical behavior of the propellant.

2.2.1.2. *XLDB (or NEPE) binder*

The major ingredients of XLDB (or NEPE) binders are:

- Polymers: nitrocellulose, polyesters, polyethers, polycaprolactones and others;
- Energetic plasticizers: nitroglycerine, butanetriol trinitrate, triethyleneglycol dinitrate, and others;
- Non-energetic plasticizers: if necessary;
- Curing agents: polyisocyanates;
- Chemical stabilizers

With the slurry process the binders are always highly plasticized, and therefore crosslinked.

To be of any advantage, the prepolymers must exhibit specific properties:

- They must be liquid during the premix elaboration (prepolymer and energetic plasticizer).
- They must be capable of handling high plastification ratios without exhibiting any exudation phenomena after crosslinking.
- These prepolymer-plasticizer premixes must be capable of accepting high solids contents (approximately 77–80%) and still be cast into complex shapes. In this regard, the rheology theory of the flow of composite propellant slurries is applicable.
- After crosslinking, they must keep their elastomeric-type properties so as to be more capable of withstanding significant elongations over more or less wide ranges of temperature. This is due to the fact that XLDB propellants are used mainly in case-bonded grains.

2.2.2. *Polymers*

2.2.2.1. *Nitrocelluloses*

Nitrocelluloses, discussed in Chapter 9 on double-base propellants, are primarily characterized by their nitrogen content. The physicochemical and energetic properties of the polymer derive from that characteristic.

Nitrocelluloses used in rocket propulsion have nitrogen contents ranging between 11.5% ($Q_a = 800$ cal/g) and 13% (calorimetric value = 1010 cal/g). In the case of the CMCDDB, however, nitrogen contents close to 12.5% are particularly well suited because the corresponding nitrocellulosic polymers allow one to meet specific requirements such as:

- inclusion of solid charges (such as oxidizers, fuels);
- introduction of high percentages of plasticizers.

However, nitrocelluloses are semi-crystalline polymers that, unlike polyesters or polybutadienes, do not have the chain flexibility that facilitates the incorporation of high contents of charges (70–80%). With CMCDDB, whose basic polymer is nitrocellulose, the solids content compatible with satisfactory mechanical performance is limited to approximately 45%.

2.2.2.2. *Non-energetic prepolymers*

The prepolymers, which must be liquid at the temperature of the manufacturing process, and which are capable, after crosslinking, of both high plasticizer and high solids contents, are recruited essentially from hydroxy terminated polyesters and polyethers. Combined with isocyanates, they will give polyurethane networks.

Some prepolymers that are particularly interesting for XLDB or NEPE propellant are listed in Table 1.

So far, the most widely used prepolymers are the ethylene or diethylene-glycol polyadipates and the polyoxyethyleneglycols (PEG). At ambient temperature, PEG are usually found in a solid state, with a crystalline structure. They are, however, easily melted at temperature compatible with the use of energetic plasticizer (50–60°C). When exposed to high levels of plasticizers the PEG lose their crystalline structure.

The molecular mass of prepolymers ranges from approximately 1500 to 5000. In practice they are adjusted as a function of the propellant specific characteristics (mechanical properties, especially).

2.2.2.3. *Future developments* [3]

The performance improvement of XLDB propellants could conceivably be made by replacing today's inert polymers with energetic products, keeping, if

TABLE 1 Some common inert prepolymers

Prepolymer	Formula	Density ρ (g/cm ³) at 25°C
Polycaprolactone	$\text{HO}-[-(\text{CH}_2)_5-\text{C}(=\text{O})-\text{O}-]_n$	1.15
1,4 Butanediol polyadipate	$\text{HO}-[-(\text{CH}_2)_4-\text{O}-\text{C}(=\text{O})-(\text{CH}_2)_4-\text{C}(=\text{O})-\text{O}-]_n$	1.18
Ethyleneglycol polyadipate	$\text{HO}-[-(\text{CH}_2)_2-\text{O}-\text{C}(=\text{O})-(\text{CH}_2)_4-\text{C}(=\text{O})-\text{O}-]_n$	1.12 (solid) 1.19 (melted)
Diethyleneglycol polyadipate	$\text{HO}-[-(\text{CH}_2)_2-\text{O}-(\text{CH}_2)_2-\text{O}-\text{C}(=\text{O})-(\text{CH}_2)_4-\text{C}(=\text{O})-\text{O}-]_n$	1.19
Polyoxypropyleneglycol (PPG)	$\text{HO}-[-\text{CH}_2-\underset{\text{CH}_3}{\text{CH}}-\text{O}-]_n$	1.03
Polyoxypropyleneglycol (PEG)	$\text{HO}-[-\text{CH}_2-\text{CH}_2-\text{O}-]_n$	1.21 (solid) 1.11 (melted)

possible, the same properties. The synthesis process consists generally of grafting chemical groups with energetic characteristics on the polyester or polyether chains, such as: azide, nitro, nitrate, nitramine, fluoronitrate, etc.

2.2.3. Energetic plasticizers

Energetic plasticizers used in mass production are, for the most part, polyalcohol nitrates (Table 2).

Among these nitrate esters, nitroglycerine is still the most widely used, because of the high values of its calorimetric value (Q_a) and its density. Its drawbacks (vapor pressures, which are rather significant over 50°C, sensitivity to mechanical stimuli, and lower thermal stability over 100°C) are fully appreciated due to the experience acquired, for several tens of years, with double-base propellants.

The development of XLDB or NEPE propellants, with high plasticizers ratios, and whose composition is becoming increasingly different from that of double-base propellants, requires that a choice be made of the nitrate ester best suited to the requirements other than the energetic aspect. These criteria include:

- chemical and thermal stability;
- volatility;
- propensity to migrate;
- manufacturing cost;
- explosive behavior (mechanical stimuli, for example);
- physical and chemical compatibility with the various propellant additives.

Finally, a major effort is being devoted to the synthesis of new energetic plasticizers in order to correct some undesirable characteristics of today's nitrate esters. For example, molecules carrying nitrated groups ($R-NO_2$), azides ($R-N_3$) and fluoronitrated groups are being tested.

2.2.4. Inert plasticizers

The plasticizers incorporated in the advanced energetic propellants are similar to those used in the cast double-base propellants (see Chapter 9). They fulfill, in particular, the same functions: improvement of the manufacturing conditions, and/or of some functional properties of the propellant (ballistic, mechanical, safety).

The most common plasticizers carry ester functions:

TABLE 2 Characteristics of nitrate esters widely used in rocket propulsion*

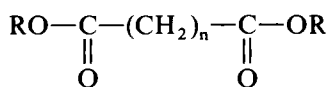
Composite	Abbreviation	Chemical Formula	ρ (g/cm ³)	ΔH_f (cal/g)	Q _a (cal/g)	Melting Point (°C)	Vacuum Stability at 200 h (cm ³ /g) 80°C 100°C
Nitroglycerine	NGL	$\begin{array}{c} \text{CH}_2 - \text{CH} - \text{CH}_2 \\ \quad \quad \\ \text{ONO}_2 \quad \text{ONO}_2 \quad \text{ONO}_2 \end{array}$	1.600 (25°C)	-405	+1750	+13 (stable) +3 (instable)	1.6 23
Triethyleneglycol dinitrate	TEGDN	$\begin{array}{c} \text{CH}_2 - \text{CH}_2 - \text{O} - (\text{CH}_2)_2 - \text{O} - \text{CH}_2 - \text{CH}_2 \\ \quad \quad \quad \\ \text{ONO}_2 \quad \quad \quad \text{ONO}_2 \end{array}$	1.327 (22°C)	-626	+616	-25	0.2 1.6
Butanetriol trinitrate	BTTN	$\begin{array}{c} \text{CH}_2 - \text{CH} - \text{CH}_2 - \text{CH}_2 \\ \quad \quad \quad \\ \text{ONO}_2 \quad \text{ONO}_2 \quad \text{ONO}_2 \quad \text{ONO}_2 \end{array}$	1.520 (20°C)	-283	+1570	-11	1.7 16
Trimethylethane trinitrate	TMETN	$\begin{array}{c} \text{CH}_3 \\ \\ \text{CH}_2 - \text{C} - \text{CH}_2 \\ \quad \quad \\ \text{ONO}_2 \quad \text{CH}_2 \text{ONO}_2 \quad \text{ONO}_2 \end{array}$	1.4568	-364	+1220	+15 +2	0.9 8.7

* The values indicated in this table have been measured at SNPE.

Glycerol triacetate (or triacetin):

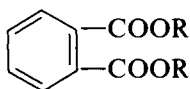


n-alkyl adipates:



(R = CH₃, C₂H₅, ..., C₈H₁₇)

n-alkyl phthalates:



(R = C₂H₅, C₄H₉, ..., C₈H₁₇)

2.2.5. Curing agents

Crosslinking is necessary:

- For propellants using highly plasticized nitrocellulose, in order to strengthen the existing three-dimensional polymeric network whose chains, held by low-energy links (Van der Waals or hydrogen type), are stretched by an excess of plasticizer.
- When using hydroxy-terminated prepolymers, also in a highly plasticized environment; these prepolymers are usually liquid during the mixing (global process).

The curing agents are designed to react with some functions of the polymers or prepolymers so as to create a three-dimensional network that will ensure the cohesion of the cured propellant and, as a result, determine its mechanical properties.

The polyisocyanates are the most used with the energetic binder propellants. Diisocyanate may be enough to ensure the spatial cohesion of nitrocellulose. With diol prepolymers this cohesion can be ensured either with a system of triol/diisocyanate or with a polyisocyanate having a functionality greater than 2. Some of the polyisocyanates widely used in the field of crosslinked propellants are listed in Table 3.

The crosslinking density, which influences the mechanical properties of the final propellant, is controlled by:

- the NCO/OH ratio, which expresses the relationship between the number of available isocyanate functions and the number of alcohol functions;

TABLE 3 *Some common isocyanates*

Type	NCO/kg
<i>Diisocyanates</i>	
Hexamethylene diisocyanate (HMDI)	11.7
Toluene diisocyanate (TDI)	11.4
Isophorone diisocyanate (IPDI)	8.9
<i>Functionality polyisocyanates > 2</i>	
Tri(isocyanato-6 hexyl)-1.3.5 biuret	5.2

- the ratio: (OH of the triol)/(OH of the diol) with diol prepolymers involving a diisocyanate-triol system;
- the nature and the amount of crosslinking catalyst.

For a given composition, in a well-defined environment (temperature, agitation speed), the crosslinking kinetics depends on the nature of the polyisocyanate. It may, however, be regulated by adding catalysts. Very basic amines such as triethanolamine, frequently used for the manufacture of polyurethanes, are prohibited with energetic binders because of their great chemical incompatibility with nitrate esters.

The burning rate modifiers, particularly lead-base, also have a crosslinking catalyst effect, more or less pronounced according to their nature (Example: PbO, PbO₂).

2.3. FILLERS

Performance improvement of energetic binder propellant requires the incorporation of fillers (oxidizers or mixture of oxidizers and fuels).

The maximum of the solids content, compatible with good feasibility and acceptable mechanical properties, is determined by:

- manufacturing process (casting solvent or slurry cast);
- binder composition (nature of the polymer, plasticizing ratio);
- shape and size of the solid particles. The use of several particles sizes — whose average diameter ratios range between 5 and 10 — facilitates high fillers contents;
- use of bonding agents facilitates higher solid level as well as particles greater than 10 microns.

2.3.1. *Oxidizers*

The most common oxidizers used in the advanced energetic propellants are:

- Ammonium perchlorate (NH_4ClO_4)
- Nitramines:
 - RDX ($\text{C}_3\text{H}_6\text{N}_6\text{O}_6$)
 - HMX ($\text{C}_4\text{H}_8\text{N}_8\text{O}_8$)

Their main characteristics are discussed in Chapter 10.

2.3.1.1. Ammonium perchlorate

Incorporated in energetic binders, this oxidizer decreases the self-ignition temperature. Compatibility tests performed on ammonium perchlorate-nitrate ester mixtures reveal a special behavior, which is expressed by a first phase devoid of any noteworthy production of gas, followed by a sudden emission accompanied by a fairly violent decomposition phenomenon.

2.3.1.2. Nitramines

The nitramines are:

- RDX or cyclomethylenetrinitramine,
- HMX or cyclomethylenetetranitramine

RDX crystallizes in an orthorhombic form. HMX, on the other hand, may present four crystalline varieties (α , β , γ and δ). Only the form β , thermodynamically stable and the least sensitive to mechanical stimuli, is used for industrial manufacture. Both varieties α and γ may occur, however, based on the nature of the recrystallization solvent that is used. As for form δ , it is found only beyond 160°C .

As a result it is necessary, during the manufacture of energetic binder propellants, to prevent any possibility of solubilization of HMX (in the cleaning solvent of the tools, for example), to avoid being faced with the risk of later recrystallization in α or γ varieties, which are more sensitive.

Nitramines are powerful explosives, sensitive to shock and to friction. They must therefore be handled with all precautions inherent in high explosives: avoid the creation of dusts and friction areas; use remote handling during the most delicate operations.

RDX and HMX have similar thermodynamic characteristics, but because HMX has a higher density it results in more energetic propellants (if the volumetric specific impulse is considered).

Finally, it must be noted that the manufacturing costs of HMX are much higher than that of RDX.

2.3.1.3. *New oxidizers*

The synthesis research is essentially devoted to the development of dense, high energy molecules [3]. New specifications have been emerging, however:

- reduction of the sensitivity (related to the development of propellant with lower vulnerability);
- possibility of controlling the burning rates.

2.3.2. *Fuels*

Aluminum is widely used in advanced energetic binder propellants as a solid fuel. It is a metal with a high combustion heat, allowing an increase in the burning temperature of propellants. However, for its combustion, a sufficient quantity of available oxygen is necessary. As a result, in the case of high-energy propellants the oxidizer/fuel ratio must be adjusted in order to optimize the specific impulse.

2.4. VARIOUS ADDITIVES

2.4.1. *Chemical stabilizers*

Advanced energetic binder propellants, like all other double-base propellants, present a problem of chemical stability, inherent in the slow decomposition of the nitrate esters.

To delay this self-decomposition phenomenon, additives with a slightly basic nature are incorporated in the propellants, so as to block the nitrogen oxides that are released. The most widely used stabilizers have been described in the chapter on double-base propellants (Chapter 9).

Use of very energetic crosslinked propellants, that sometimes include the combination of products that are not very chemically compatible (nitroglycerine-ammonium perchlorate, for example), requires the development of ever more efficient new stabilizing systems. The criteria for selection are usually based on the following factors:

- the highest possible nitrosation kinetics;
- good solubility of the stabilizer in the propellant;
- good thermal stability of the nitrosated derivatives.

2.4.2. *Ballistic modifiers*

Energetic binder propellants without ammonium perchlorate can be characterized, in a first approximation, by a burning law of the type $r_b = a p^n$

where n , the pressure exponent, is generally high ($n > 0.8$). For these propellants to hold any interest it is necessary to decrease their pressure exponent and to be able to regulate their burning rate.

Burning rate modifiers incorporated in advanced energetic propellants usually come from the classic double-base propellants [3].

2.4.3. Other additives

Specific additives may be included in propellants to take into account the operating characteristics of the grain or its type of application, e.g. instability and/or flash suppressor additives.

3. Manufacturing Processes

3.1. MANUFACTURING PRINCIPLES OF ADVANCED ENERGETIC BINDER PROPELLANTS

The manufacture of these advanced propellants may be done according to two techniques with very different principles:

- A casting solvent process consisting of two major steps:
 - manufacture of a casting powder, made of the nitrocellulosic binder containing all solid additives, and if necessary, a portion of the energetic plasticizer;
 - manufacture of the propellant by injection of a casting solvent into a mold loaded with the casting powders defined for the preceding process; this casting solvent is composed of a nitrate ester and desensitizer mixture. The cohesion of the whole is obtained by curing.
- A slurry cast process is related to the manufacturing process of composite propellants. Its principle is based on the preparation of a slurry, containing all constituent elements of the propellant, which can be poured into the mold either by gravity or by injection. The cohesion of the whole is obtained during curing by the crosslinking of the polymer.

3.2. MANUFACTURING PROCESS OF CMCDB PROPELLANTS

CMCDB propellants are in fact an extension of the cast double-base propellants. Consequently, their manufacturing process is similar to that described in Chapter 8. Therefore, some adjustments are necessary by the presence of fillers, or of necessity of crosslinking.

3.2.1. *Influence of solid fillers (e.g. nitramines, ammonium perchlorate)*

In the manufacturing process of casting powders the charges are introduced during the kneading of the dough. The solvents composition must be optimized to promote the coating of these charges by the nitrocellulosic binder in order to obtain densities that are as high as possible in the finished granules.

In addition, the presence of the fillers is likely to modify the surface of the casting powder (creation of roughness, for example), which has the direct consequence of altering the packing density.

3.2.1.1. *Remarks on the screen loading density (SLD) and the packing density*

To evaluate the packing density, measurements of the screen loading density (defined by the powder weight in a determined volume) are done on the casting powder. These gravimetric densities depend on several parameters:

- density of the granules;
- their geometry: size, length/diameter ratio;
- imperfections of their surface, which affects the flow (importance of the glazing cycle);
- filling method.

According to the theoretical analyses [5] that have been done on casting powders, the screen loading densities are at their maximum when the L/D ratios are close to 1 (Fig. 1). Experimentally, it is preferable to use a L/D ratio

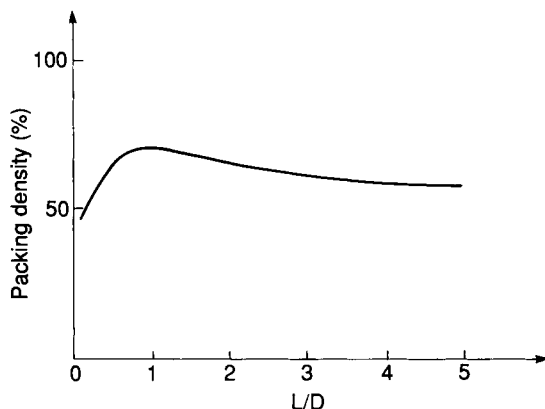


FIG. 11.1. Evolution of the packing density of the molds versus the L/D ratio of casting powders.

close to 1.2 to be in an area of the diagram capable of tolerating some scattering of the dimensions, without necessarily having a significant influence on the packing densities.

The presence of solid charges in the casting powders influences noticeably the values of SLD. Increasing the particle size for a constant filler content or increasing the filler content for a constant particle size leads systematically to a decrease of SLD. The aspect of the surface alone is responsible: more or less granular aspect, which inhibits the sliding of the grains against each other. Figure 2 shows the evolution of SLD of the casting powders loaded with 60 % fillers when the particle size changes from 90 μm to 15 μm . The volumic packing density of the mold follows the same tendency. As for the role played by the fillers contents, it is made quite clear in Table 4.

To increase the packing density one may:

- work with the size of the casting powder (Table 5);
- adapt the industrial process for filling the molds; for example, there are

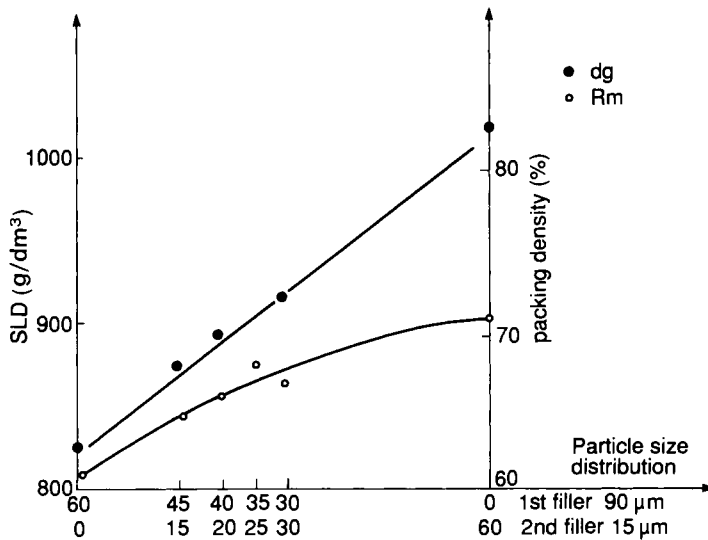


FIG. 11.2. Comparative evolution of screen loading densities (SLD) and of packing densities versus the particle size distribution (casting powder with 60 % solid charges).

TABLE 4 Influence of the fillers content on the screen loading density (SLD) and the packing density of the molds

Fillers content (%)	45	60	45	60
Particle size (μm) of fillers	90	90	15	15
SLD (g/l)	970	825	1035	1010
Volumetric packing density (%)	66.0	60.5	71.0	68.0

TABLE 5 *Influence of the size of casting powders on screen loading density (SLD) and packing density of the molds*

Filler			
Content (%)		60	
Particle size (μm)		90	
<hr/>			
Diameter of casting powders (mm)	0.9	1.5	2.0
SLD (g/l)	810	945	985
Volumetric packing density (%)	60.5	67.0	67.5
<hr/>			

specially designed hoppers which allow both a regular flow rate of the granules, and a good distribution of the granules in the molds.

3.2.2. *Incidence from crosslinking*

The curing agents used to reinforce the highly plasticized nitrocellulosic networks are usually isocyanates which will react with residual alcohol groups of the nitrocellulose (combined if necessary to a hydroxy-terminated prepolymer). The isocyanates, slightly agitated, are introduced in the casting solvent just before the casting operation.

To ensure optimal crosslinking conditions, the humidity content of the various constituents must be as low as possible (a few hundred ppm). Therefore, particular attention must be used when degassing the casting powders and the casting solvent, which is done before the casting.

During the curing phase the casting solvent, which diffuses in the granules, serves also as a vector for the crosslinking agents, which usually have a high steric arrangement. At that time a competition takes place between the diffusion and the crosslinking kinetics, which requires the identification of a curing cycle designed to provide strengthening, as uniform as possible, of the nitrocellulosic network. Should the temperature conditions not be correctly adjusted, a superficial crosslinking of the casting grains may occur, hindering any further diffusion of the casting solvents.

3.3. MANUFACTURING PROCESS OF HIGH-ENERGY PROPELLANTS (XLDB-NEPE)

3.3.1. *Background*

XLDB propellants consist of an energetic binder with a high level of plasticization, in which solid charges are incorporated (oxidizers, fuel, various additives).

The following are the main reasons for the development of this family of propellants:

- possibility of obtaining high total solid contents (up to 75% approximately), allowing an improvement of both the specific impulse and the density;
- manufacture of propellant grains similar to composite propellants, making it possible to benefit from all technologies developed so far.

3.3.2. Manufacturing flow sheet

Although the manufacture of XLDB propellants is related to that of composite propellants, the processes and equipment had to be adapted to take into account the presence of liquid nitrate esters. This is due to the fact that the energetic plasticizers involved (nitroglycerine or others) are mixtures that are sensitive to mechanical stimuli (shock, friction), and that also often have vapor pressures which cannot be ignored beyond 50°C. The different steps of manufacture of a case bonded grain are described in Fig. 3.

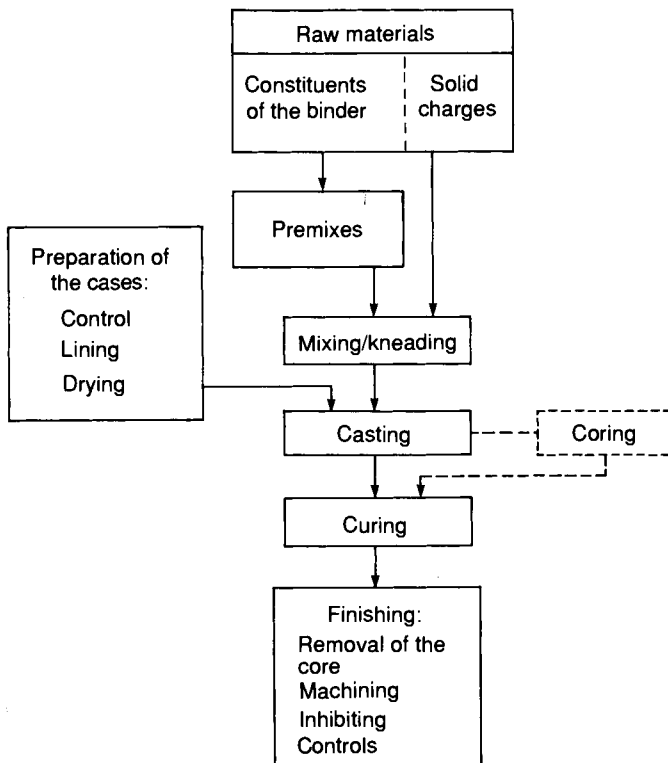


FIG. 11.3. Diagram of the manufacture of high energy propellants.

3.3.3. Cases preparation

3.3.3.1. Background

Two types of cases are currently used with this type of propellant:

- metallic cases made of steel, especially designed to handle significant pressures;
- composite cases which are increasingly used for high-performance applications.

These cases are, of course equipped with thermal protections and coated with a liner, a material for binding with the propellant.

3.3.3.2. Installation of the inert materials

Because the installation process of the various inert materials is described in detail in Chapter 13, this section will provide only a succinct list of the operations sequence necessary to prepare a metallic-type case to receive the propellant slurry. These operations include:

- surface treatment of the cases;
- bonding of the thermal protections;
- coating of the entire surface with a liner.

The process selected for the coating depends both on the nature of the liner and on the shape of the case. Spraying techniques, however, are most widely used.

The quality of these coatings is fundamental for a good adhesion of the liner to the propellant, and of capital importance for the reliability of the propellant grain.

To improve the bonding characteristics (tensile, shear, and peeling strength) between the liner and the propellant, we may have to resort to the use of embedding agents of very specific shapes inside the liner (for example, granules with a cellulosic derivative base), that will function as so many mechanical embedment points for the propellant.

3.3.4. Raw materials preparation

With the exception of energetic binders (nitroglycerine, butanetriol trinitrate, etc.) which require special handling, the other raw materials do not have to be treated or transformed before use. After acceptance according to a determined procedure, the raw materials are stored by homogeneous manufacture batches in the environmental conditions — temperature, humidity — required for their specific nature.

As for the energetic plasticizers, there are several possibilities, according to

the manufacturing processes selected for the propellants and the availability of the mass production of nitrate esters:

- Use of pure nitrate ester, which is possible when a production facility or dynamite extraction facility are located close to the propellant plant. This allows a rapid mixing of the energetic plasticizer with the prepolymer to form a desensitized premixture which can then be stored, i.e., from the time it contains a chemical stabilizer.
- Use of nitrate ester diluted with a volatile solvent (acetone or methylene chloride type) or an inert plasticizer (triacetin type). These solutions are used if the nitrate esters production facilities are located far from the propellant production facilities, or when the manufacturing process requires it.

3.3.5. Manufacture of propellant slurries

The principle of propellant slurry manufacture is based almost exclusively on the preparation of a binder with low viscosity in which the fillers are incorporated. After its homogenization in the suitable mixer, the slurry must maintain a certain level of viscosity to allow its casting by pouring or injection, for as long as the industrial process requires it.

The sequence of incorporation of the propellants ingredients is the result of a trade-off that takes into account, for example:

- evolution of the slurry's viscosity;
- safety problems, related to the use of liquid nitrate esters and/or the use of powerful oxidizers/fuel mixtures such as ammonium perchlorate and aluminum.

Furthermore, it is necessary during this particular phase to maintain very low levels of humidity to facilitate the development of urethane linkages (reaction of isocyanates with alcohols), thereby ensuring good propellant mechanical properties.

For the purpose of illustrating one of the possible manufacture plans, we will use a propellant that contains the following constituents:

Binder

Prepolymer with a tailored molecular weight, polyester or polyether type;
Nitrocellulose (used in low ratios as a crosslinker);
Nitroglycerine;
Stabilizer.

Charges

Nitramine (HMX or RDX);
Ammonium perchlorate.

Curing agents

Polyisocyanate;
Cosslinking catalyst.

The sequence of the operations necessary to obtain a homogeneous slurry can be summarized as follows:

- First, a premix is prepared, containing the prepolymer in which the stabilizer and the nitrocellulose are solubilized.
This operation takes place at atmospheric pressure and at a specific temperature which must take the melting temperature of the prepolymer into consideration.
- Pure nitroglycerine or nitroglycerine in solution is added to this premix. This operation takes place under slight agitation, and at a moderate temperature. Once the energetic plasticizer is completely incorporated, the whole is placed under vacuum, still at a moderate temperature, and is subjected to a degassing, under slight agitation, to ensure both the homogenization and the dwelling of the premix. When the nitroglycerine is introduced as a solution, the degassing operation also permits the removal of the solvent.
- At the end of this operation the curing agent is added. The binder is then ready to receive the solid charges.
- In this particular case the nitramine (RDX or HMX) and the ammonium perchlorate may be introduced in the mixer, either consecutively or in sequenced phases. The tailoring of the incorporation procedure must take into account the various particle sizes that are used in order to avoid problems of unwanted increase of the viscosity of the slurry.

At the industrial level, it is preferable to have a system permitting a continuous introduction of the charges. Such a facility includes one or several hoppers, located above the mixer, containing the various fillers; the charges are fed to the mixer through a vibrating band.

- After the various charges have been incorporated, the mixing of the whole continues at moderate temperature — usually between 40 and 60°C — (under dynamic vacuum pressure below 50 mmHg), with the same goal, i.e. to maintain a humidity level on the slurry that is as low as possible. Approximately 1 hour before the completion of the mixing, the crosslinking agent is introduced into the slurry. From that moment on the polymerization has been started, and the viscosity of the slurry will keep evolving

Vertical mixers are particularly well suited for the manufacture of XLDB slurries because they allow:

- from a quality point of view, a good homogenization of the fillers in the binders;

- from a safety handling point of view, a significant decrease in the risks of diffusion of nitrated oils in the bearings.

3.3.6. *Production of propellant grains (casting, curing, finishing and quality controls)*

Casting, curing and finishing operations leading to the production of the propellant grains are comparable to those described in Chapter 10 on composite propellants. However, some adjustments were necessary to accommodate the presence of explosive charges (nitramines) and, particularly, of energetic plasticizers (nitroglycerine, for example), which are sensitive to mechanical stimuli, have a limited thermal stability, and are likely to migrate. Among the specific adjustments carried out, we may mention:

- use of specific valves preventing shocks and frictions;
- design of fluid-tight equipment, which keeps handling to a minimum — in this regard, integral molding is recommended because it cuts out all finishing operations;
- a greater control of the temperature of the curing facilities, to avoid any change likely to cause a decomposition of the nitrate esters.

Finally, the quality controls include those done on composite propellants, complemented by specific tests, such as chemical stability, and thermal behavior (cook-off tests).

4. Characterization of Advanced Energetic Binder Propellants

4.1. PHYSICAL AND PHYSICOCHEMICAL CHARACTERISTICS

4.1.1. *Density*

Depending on the nature and the fillers content, advanced energetic propellants present a wide range of densities (Table 6).

XLDB, because they accept a higher total solid content than CMCDDB, naturally have higher densities.

The introduction of aluminum ($\rho = 2.7 \text{ g/cm}^3$) in a propellant that already contains an oxidizer (HMX + ammonium perchlorate, for instance) is another determinant for the evolution of the densities.

4.1.2. *Glass transition temperature (T_g)*

The mechanical behavior of propellants may be altered at low temperatures because of structural changes in the binder (glass transition, or of the

TABLE 6 *Densities (ρ) available in advanced energetic propellants*

Propellant type	CMCDB	XLDB		NEPE
Nature of fillers	nitramine	nitramine	nitramine + ammonium perchlorate	nitramine + ammonium perchlorate + aluminum
g/cm^3	< 1.70	< 1.76	< 1.80	< 1.88

second order). The temperatures at which these transitions occur depend primarily, for a specific polymer, on the content level and the nature of the plasticizer (Fig. 4). In fact, in the case of nitrocellulosic binders, they tend toward the second-order transition temperature of the plasticizer when the plasticizing ratio increases [6]. We must remember that the second-order transition temperature of nitroglycerine, when it remains at superfusion, is close to -65°C .

In the case of XLDB binders, which are highly plasticized, the glass transition temperatures typically range between -55°C and -60°C , which

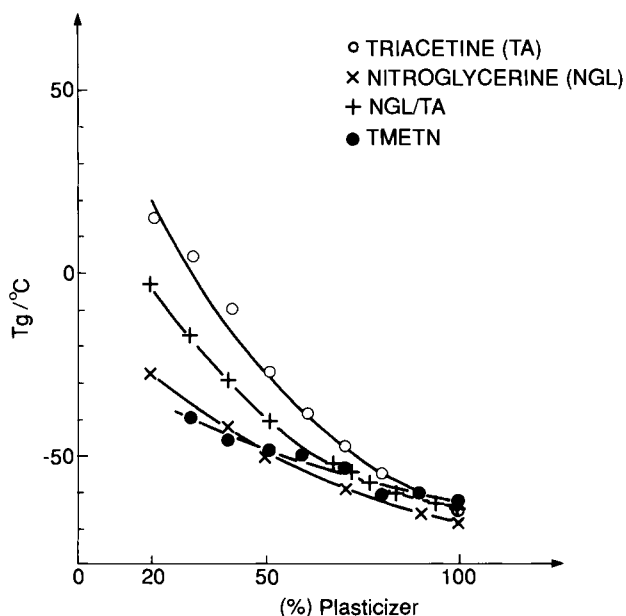


FIG. 11.4. Evolution of the glass transition temperature (T_g) of nitrocellulosic binders versus the amount and the nature of the plasticizer.

explains the good levels of elasticity of this propellant family as far as -40°C to -50°C .

4.1.3. Thermal expansion coefficient (α)

The binders of propellants have thermal expansion coefficients (α) that are greater than those of the charges. Therefore, the higher the fillers content, the more α will have a tendency to decrease.

Additionally, in the case of energetic binder propellants, the plasticizer usually shows the greatest variations of volume versus temperature. Consequently, the more the binder is plasticized, the more α will have a tendency to increase.

Based on these observations, the thermal expansion coefficients of XLDB propellants, measured above the glass transition point, usually range from 1.00×10^{-4} to $1.30 \times 10^{-4} \text{ K}^{-1}$.

4.1.4. Crystallization of energetic plasticizers

In some cycles of low temperature conditioning, XLDB propellants with nitroglycerine base and crosslinked CMCDDB (or EMCDB) with high plasticizing ratio may exhibit an embrittlement phenomenon, detrimental to the operational reliability of the propellant grains. Such embrittlement, which is manifested by a total or partial loss of the elastic properties of the material, is the result of the crystallization of the energetic plasticizer inside the propellant [7,8].

Research done on the crystallization of liquid nitrate esters has provided the following information [7]:

- pure nitrate esters do not crystallize easily;
- crystallization is facilitated through seeding with foreign matter that may be present in the propellant;
- once it has been initiated, the kinetics of crystallization depend on the temperature — with nitroglycerine, for example, the kinetics of crystalline growth has its highest value at around -5°C (Fig. 5).

Energetic plasticizers may be differentiated through their ability to crystallize; nitroglycerine, for example, crystallizes faster than triethyleneglycol dinitrate or butanetriol trinitrate:

- use of specially designed nitrated oils delays or suppresses the crystallization phenomena [7-9].

As far as quality controls are concerned, energetic binder propellants are subject to isothermal conditioning at low temperatures (between 0 and -50°C) or are exposed to daily arctic cycles, for example $-12^{\circ}\text{C} \rightleftharpoons -40^{\circ}\text{C}$,

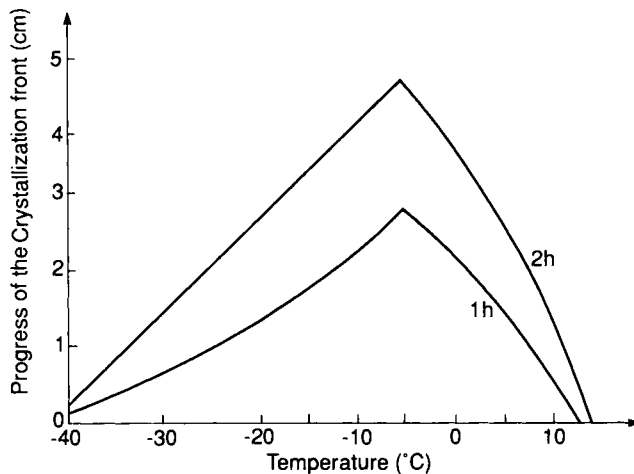


FIG. 11.5. Progress of the crystallization front on nitroglycerin specimens at varying temperatures (readings made one hour and two hours after conditioning).

which are more severe because they facilitate the crystalline germination-growth sequences.

Table 7 gives a description of the behavior at low temperature of two XLDB propellants, one plasticized with nitroglycerine and the other with a mixture of nitrate esters. The propellant containing the nitrate esters resists crystallization, i.e. its mechanical properties are not affected at low temperature, while the propellant containing nitroglycerine becomes embrittled within 10–15 days, depending on the type of conditions selected.

4.2. MECHANICAL PROPERTIES

Depending on the type of grain selected (free-standing or case-bonded), the mechanical characteristics required of the propellant are different:

- Free-standing grains: the propellant is free to deform. The mechanical strains involved mainly concern storage and firing. As far as the material is concerned, sufficient elastic modulus values must be ensured, particularly at high temperatures in the case of tactical missiles.
- Case-bonded grains: the propellant is bound to the case. Its mechanical properties must be tailored to the thermal stress/strains that occur at cooling, right after curing, and for the remainder of the life of the rocket motor. The strain resulting from deformation occurring at firing must also be taken into account.

To be suitable, the propellants must be capable of handling a good level of strain in the entire range of temperatures met during operational conditions

TABLE 7 *Low temperature cycling of XLDB propellants (fillers = 70%) evolution of the strain at maximum stress (ϵ_m)*

Nature of the propellant	XLDB	
	Nitroglycerine	Nitrate ester mixtures
<i>Cycling conditions:</i>		
Isotherm:		
–15°C	Crystallization after 15 days	No crystallization after 6 months
–30°C	Crystallization after 15 days	No crystallization after 6 months
Daily arctic cycle	Crystallization after 10 days	No crystallization after 6 months
–12 \leftrightarrow –40°C		
ϵ_m (%) at –40°C	Crystallized propellant ~ 2%	Non-crystallized propellant ~ 22%

of the grain. In the case of tactical missiles it is particularly important to maintain a good trade-off between the strains at cold temperatures and the values of maximum stress (σ_m), and of the Young's modulus at high temperatures.

These mechanical considerations, related to the design of the grains, determine largely the areas of application of CMCDB/EMCDB propellants and XLDB/NEPE propellants:

- Non-crosslinked CMCDB propellants exhibit a good stress level under high temperatures, but the level of strain at cold temperatures is not suitable for use in case-bonded grains. As a result they are mainly used for the production of free-standing grains.

For these propellants, however, there is a possibility of extending their use to case-bonded grains, in as much as it is possible to increase the plasticizing of the nitrocellulosic binder, involving a strengthening of its network through crosslinking (EMCDB):

- XLDB propellants all exhibit good levels of elongation (including under low temperatures) and satisfactory stress at high temperatures. Consequently, they are well-suited for the production of case-bonded grains.

Mechanical characterizations performed on propellants

A systematic control of mechanical tensile properties is done on all propellants manufactured, first at ambient temperature, and if necessary at low temperature (–40°C, –50°C) and high temperature (approximately +60°C) for propellants intended for tactical applications. For a more detailed characterization, other tests are performed:

- Uniaxial tensile test, at various rates (from 0.5 to 500 mm/min, for example) and various temperatures. Experimental data permit the plotting of master curves necessary during the design of the propellant grain.

- Behaviour at creeping, and at relaxation.
- Simultaneous measurements of the volume variations during a tensile test, recorded with a gas dilatometer. This technique is well suited for the determination of the characteristics of the adhesion between binder and fillers.

4.2.1. Mechanical behavior of CMCDB propellants

Mechanical properties of the different CDB propellants occur during the curing operation, at the time when the casting solvent diffuses into the powder granules, which swell and bond to each other. The more the casting powder is plasticized, the better this diffusion will be. With curing temperatures of the order of 50–65°C, the mechanical properties stabilize within 2–4 days.

4.2.1.1. Influence of the plasticizing ratio

The possibility, on the one hand, of introducing a plasticizer in the casting powder, and on the other hand, of adjusting the casting powder/casting solvent ratio during the filling of the mold, provides the capability of obtaining propellants with a wide range of mechanical properties.

Let us take the case of a casting powder containing 45% of solid charges: up to 30% of nitroglycerine can be introduced, in place of the nitrocellulose. This substitution causes a variation in the plasticizing level (plasticizer/plasticizer + polymer) of the propellant of approximately 50–80%. In terms of the mechanical properties, it is manifested by:

- a decrease of the values of the maximum stress σ_m at all temperatures;
- an increase of the strain values at low temperatures.

Figure 6 illustrates the evolutions of σ_m and ε_m for various plasticizing ratios. At 65–70% the level of maximum stress σ_m at +65°C usually drops to values lower than 0.5 MPa. This may mean that it is no longer acceptable for a propellant grain, and it becomes necessary to crosslink the nitrocellulosic network in order to strengthen the mechanical properties of the propellant.

4.2.1.2. Influence of fillers

The quality of coating by the nitrocellulosic binder is a critical element of the mechanical properties of the finished propellant. As with XLDB or composite propellants, it is necessary to optimize the rheological properties of the binder, and the particle size distribution of the fillers. In addition, the quality of the binder-charge adhesion depends also on the nature of the charge. Figure 7 illustrates the volume variations $\Delta V/V$ recorded with a

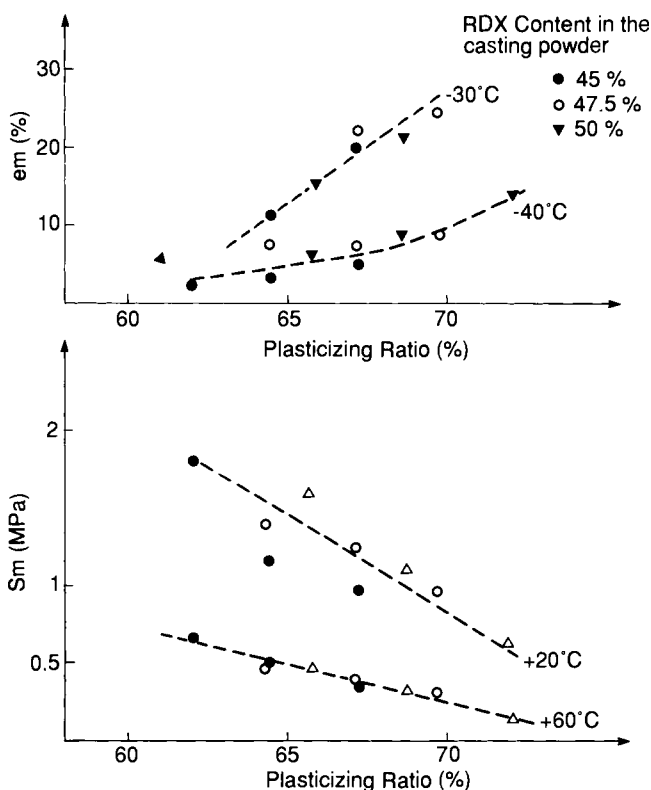


FIG. 11.6. CMCDDB propellants. Evolution of σ_m and ϵ_m in function of the plasticizing ratios.

Farris gas dilatometer for two CMCDDB propellants, one loaded at 30% with ammonium perchlorate, the other at 30% with RDX. It turns out that the ammonium perchlorate compositions exhibit a better binder-charge adhesion than those loaded with nitramines with identical particle sizes; dewetting occurs only at higher strains, and the total volume variation $\Delta V/V$ is clearly smaller.

4.2.1.3. A special case: EMCDDB propellants

With plasticizing ratios greater than 65–70% it is necessary to crosslink the nitrocellulose to strengthen the maximum stress (σ_m) of these advanced CDB propellants at high temperatures. The strain values at low temperature of the resulting propellants are improved, and they may be used in case-bonded grains.

Reinforcement of the polymeric network may be obtained:

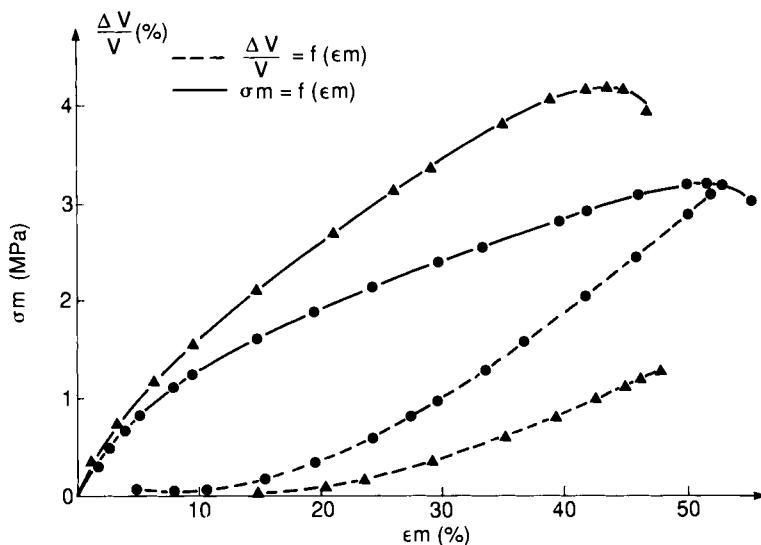


FIG. 11.7. Farris ga. dilatometer behavior of CMCDDB propellants loaded with 30% ammonium perchlorate (▲) or 30% RDX (●).

- either by direct crosslinking of the nitrocellulose;
- or by crosslinking the nitrocellulose with small percentages of hydroxy-terminated prepolymer (preferably polyester) — this prepolymer is introduced in the casting powder or dissolved in the casting solvent before casting.

Small percentages of bi-functional isocyanates are sufficient to obtain an increase in the strain capabilities at high temperatures. Optimization is obtained with NCO/OH ratios lower than 0.1.

The values indicated in Table 8 for the mechanical properties of EMCDB

TABLE 8 *Influence of crosslinking on the mechanical properties of EMCDB propellants containing 30% RDX*

Plasticizing ratio	76%			81%
	No crosslinking of NC*	Direct crosslinking of NC	NC crosslinked with prepolymer	Direct crosslinking of NC
σ_m (MPa) at + 60°C	0.12	0.70	0.60	0.45
ϵ_m (%) at - 40°C	25	20	28-30	40

* NC = Nitrocellulose

propellants with 30% RDX demonstrate the advantage of crosslinking for increasing the σ_m stress capabilities at 60°C and the advantage of the prepolymer for the improvement on strains at -40°C.

4.2.2. Mechanical behavior of XLDB and NEPE propellants

Mechanical properties of these propellants are also obtained after curing, since this phase is designed to activate the crosslinking process of the binder.

The final mechanical properties depend on the composition of the binder, on the fillers incorporated in that binder, and on the manufacturing conditions. Special attention had to be given to the characteristics of the binders of XLDB propellants due to their high contents of plasticizer (up to 70–75%).

4.2.2.1. Characterization of XLDB binders

Studies of the elaboration of XLDB binders have demonstrated the influence of formulation parameters such as: nature of the plasticizer and of the prepolymer, and nature of the isocyanates and of the crosslinking catalysts.

On the basis of crosslinking density measurements, the following tendencies can be observed:

- an increase of the plasticizing level contributes to a decrease in the crosslinking density, which tends to drop significantly when the plasticizer/polymer ratio is close to 3;
- a decrease is also recorded when the molecular weight of the prepolymer increases;
- the incorporation, as crosslinker agents, of polyols with high molecular weights (nitrocellulose and cellulose acetobutyrate, for example) improve the crosslinking density;
- the crosslinking density is optimal when the ratios NCO/OH are slightly greater than the stoichiometry;
- There is a fairly good concordance between the crosslinking densities of the binders and their mechanical properties. It has been possible to establish a linear relationship between these two parameters for simple systems with a polyoxyethyleneglycol or glycol polyadipate base [10].

4.2.2.2. Influence of fillers

As with all composite structures, the mechanical properties are tied to the interaction between the binder and the charge. When there is a transfer of stresses from the binder to the fillers, these function as a physical reinforcement, causing an increase of the modulus, and at the same time a decrease in

TABLE 9 *Mechanical properties evolution of XLDB propellants as a function of the total solid content*

Solid content (%)		65	70	70
Plasticizer content (%) (binder)		71	71	74
σ_m (MPa)	+ 20°C	1.0	0.8	0.7
	+ 60°C	0.8	0.6	0.6
ε_m (%)	+ 20°C	180	130	130
	- 30°C	150	100	110
	- 54°C	23	16	18

the elongations. The loading capability of binders is limited, however, and these limits particularly depend on the nature of the polymer, the plasticizer content and the nature of the fillers. Table 9 indicates some typical, σ_m stress and ε_m strain values for XLDB propellants with a polyester binder with various total solid contents.

As with composite propellants with a polyurethane binder, the optimization of the mechanical properties requires:

- the adaptation of the particle size of the various selected solid fillers;
- the control of the humidity levels, which must remain as low as possible.

Some fillers may have an influence on the elaboration of the polyurethane networks plasticized with nitrate esters. This occurs in particular with ammonium perchlorate, which has a low solubility in the prepolymers rich in ether links such as polyoxyethyleneglycols (PEG). The result in the corresponding propellants is a decrease in the maximum stresses (σ_m) at ambient temperature.

4.2.2.3. *Conditions for propellant curing*

The curing conditions (time, temperature) are determined by the stabilization of the mechanical properties. For case-bonded grains the lowest possible curing temperatures are always sought in order to reduce the thermal stresses due to cooling. Based on the type of propellant, the curing temperatures range from 40 to 60°C and the curing times necessary for the stabilization of the mechanical properties range from approximately 10 to 12 days.

4.3. BURNING RATE OF ADVANCED ENERGETIC BINDER PROPELLANTS

4.3.1. *Burning rate of CMCDB propellants*

CMCDB propellants need to be considered as an extension of the double-case propellant family. Therefore, the adaptation of their characteristics is

done by modifying the characteristics of the binder, using the ballistic modifiers available for these DB propellants.

The introduction of nitramines in these binders compensates more or less for the effects of the “super-rate” caused by the presence of burning rate modifiers. K. Sumi and N. Kubota [11] describe the negative effect of increasing amounts of HMX in a propellant catalyzed with lead salicylate/ethyl-2 lead hexanoate; the plateau effect disappears for amounts higher than about 27%.

In general, less spectacular effects are recorded, which are manifested particularly by a decrease in the level of the burning rate; the plateau effects, although less marked, are nevertheless quite correct for fillers contents up to 40%. There are even ballistic modifiers based on lead or copper salts that remain virtually insensitive to the amount of nitramine [12]: retention of the plateau effect, a very small decrease of burning rate at the plateau (Fig. 8), retention of good temperature coefficient ($< 0.15\%$ per $^{\circ}\text{C}$), and possibility of regulating the burning rate with well-known additives such as carbon blacks.

4.3.1.1. RDX–HMX comparison

Slightly less good burning characteristics have often been observed, experimentally, when HMX replaces RDX: lower burning rate, less marked plateau effect, and a temperature coefficient which is not quite as low.

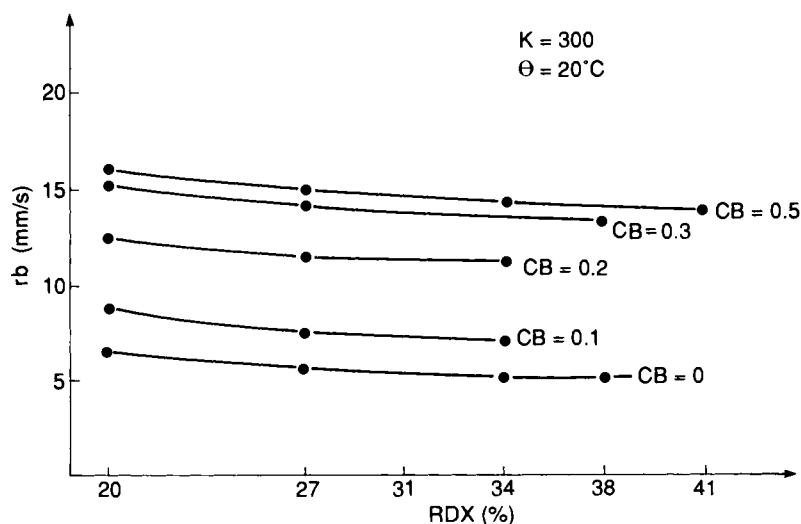


FIG. 11.8. Burning rate of CMCDDB propellants as a function of RDX percentage for different content of carbon black (CB).

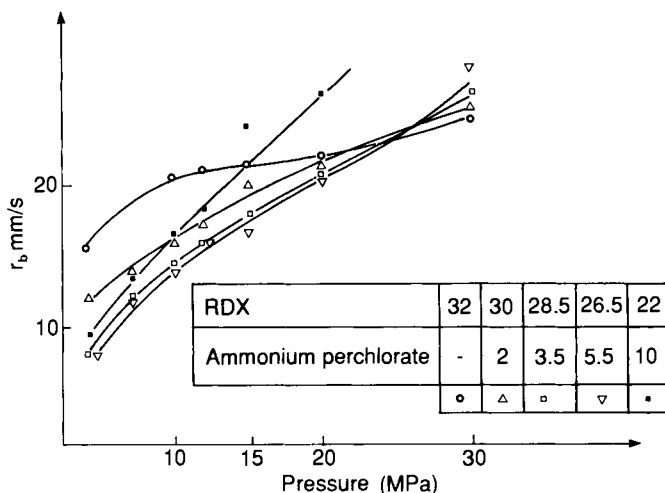


FIG. 11.9. Influence of ammonium perchlorate content on the burning rates of CMCDDB propellants catalyzed with lead aromatic ballistic modifier.

4.3.1.2. Influence of ammonium perchlorate

Introduced in catalyzed CMCDDB or EMCDDB propellants, ammonium perchlorate causes the destruction of the plateau effect, even in very small amounts (Fig. 9).

4.3.2. Burning rate of XLDB and NEPE propellants

4.3.2.1. Nitramine based XLDB propellants

In his synthesis paper, R. A. Fifer points out the difficulties and the few solutions available to affect the burning rate of a propellant with a high content of nitramine [13]. As for the rare catalysts mentioned in the literature, they are not particularly efficient [3,14–16].

Although it is possible to modify the burning behavior of the most widely used binders based on prepolymers of the polyether or polyester type, highly plasticized with nitrate esters, the range of burning rates available remains fairly limited because of the presence of a high amount of nitramine (greater than 50%) [17].

Measures designed to modify the decomposition mechanism of nitramines (RDX or HMX) have not yet succeeded in providing solutions that are applicable industrially.

To sum up, the burning rates of XLDB propellants range from 2 to 15 mm/s at 7 MPa. The pressure exponents are situated between 0.35 and 0.60 and the temperature coefficients are very similar to those of composite propellants (π_k from 0.15 to 0.35 % per °C).

Remark

Research for any new ballistic modifiers implies that a propellant feasibility study be done at the same time. This is due to the fact that some additives, particularly those with a lead base, turn out to be efficient crosslinking catalysts, which may make their use incompatible with mass production.

4.3.2.2. XLDB propellants with nitramine and ammonium perchlorate

Ammonium perchlorate acts as a very efficient ballistic modifier. It is possible to regulate the burning rate over a wide range by varying both the content and the particle size of the oxidizer. Figure 10 gives an idea of the evolution of the burning rate as a function of the evolution of the ammonium perchlorate-octogen proportions in a propellant with a 70% total fillers content.

In addition to the usual role played by the particle size and the amount of ammonium perchlorate, we may also note that:

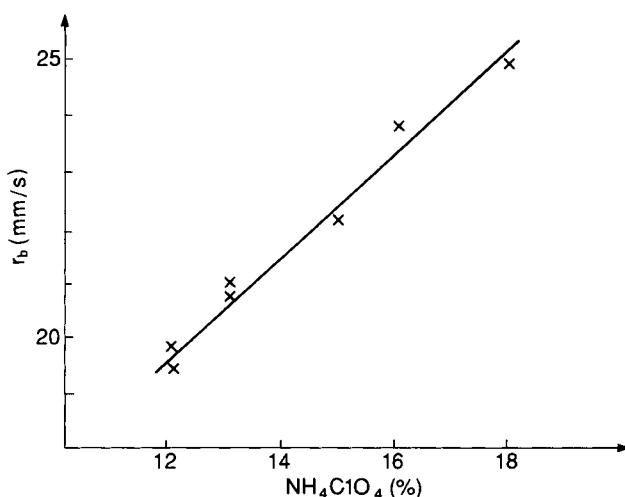


FIG. 11.10. XLDB propellant loaded with 70% fillers (HMX-Ammonium perchlorate). Evolution of the burning rate as a function of ammonium perchlorate content (particle size = 10 μm).

- Polyether binders tend to lead to burning rates that are higher than those obtained with polyester binders.
- Pressure exponents have a tendency to decrease when the ammonium perchlorate content increases. They decrease more rapidly when the particle size of the oxidizer is smaller, reaching minimum values which also depend on the size of the ammonium perchlorate particles. With fine ammonium perchlorate (3 μm), the exponent is around 0.50–0.55, while with somewhat larger perchlorate (10 μm), the exponent may drop to as low as 0.45.

4.4. ENERGETIC CHARACTERISTICS

4.4.1. Recapitulation of theoretical performances

Specific impulse (I_s) and volumetric specific impulse ($I_s \cdot \rho$) theoretically attainable with these propellants are shown in Table 10.

I_s and $I_s \cdot \rho$ evolve differently according to the nature of the solid charges incorporated in the binders:

- If the filler is a nitramine, I_s and $I_s \cdot \rho$ increase in a virtually linear manner when the amount of RDX or HMX increases. Because RDX and HMX have closely related thermodynamic characteristics, the substitution of one by the other has little incidence on the values of I_s . But the difference shows up in the value of the volumetric specific impulse, due to the fact that the density of RDX is lower than that of HMX: respectively 1.818 and 1.903 g/cm^3 .
- A combination of ammonium perchlorate with a nitramine allows a gain in performance provided, however, that the proportions are optimized as a function of the nature of the binders used (Figure 11).

Incorporation of metallic fuel, such as aluminum, combined with an oxidizer (perchlorate ammonium + nitramine) allows to obtain high I_s and

TABLE 10 *Theoretical performance obtainable with advanced energetic binder propellants*

Nature of fillers	Nature of the propellant	I_s (s)	$I_s \cdot \rho$ (s.g.cm ⁻³)
Nitramine	XLDB	250	440
	CMCDB*	245–250	415–425
	EMCDB		
Nitramine + ammonium perchlorate	XLDB	260	465
Nitramine + ammonium perchlorate + aluminum	NEPE	275	515

* The values of I_s and $I_s \cdot \rho$ increase when the propellants are crosslinked, due to the presence of high amounts of nitrate esters in the nitrocellulosic binder.

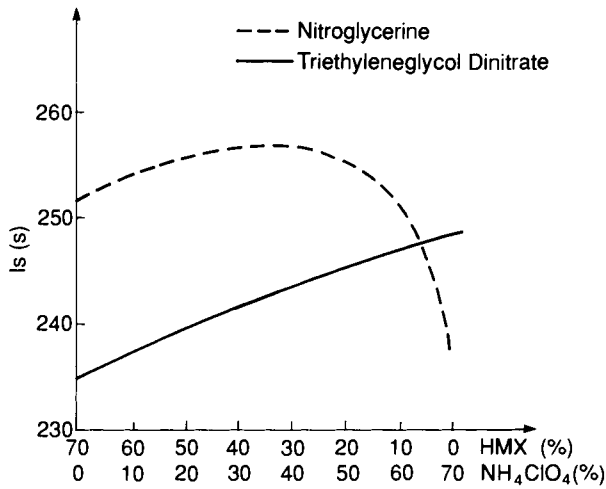


FIG. 11.11. Evolution of I_{sp} as a function of the HMX/Ammonium perchlorate ratios for XLDB propellants with 70% solid fillers whose binder is plasticized either with nitroglycerine, or triethyleneglycol dinitrate.

I_{sp}, ρ values. As in the case with composite propellant, it is necessary, however, to optimize the proportions of the various charges to obtain the maximum performance. The optimum content of aluminum for NEPE propellants ranges between 15 and 20%.

4.4.2. Measured performance

The experimental measurements of specific impulse are done on standardized reference grains during a bench firing test. The propellant grains used have a radial combustion.

The specific impulses measured reveal a shortfall in comparison with the computer predictions, which do not take into account the various losses resulting from the nature of the grain and the firing conditions.

Furthermore, the presence of a metal such as aluminum creates a problem of combustion efficiency (due to the influence of the particle size, of the amount of fuel, the influence of the firing conditions and the size of the grains). Table 11 shows clearly that the shortfalls between theoretical I_{sp} and measured I_{sp} are greater with aluminized propellants.

4.5. FUNCTIONAL CHARACTERISTICS

4.5.1. Signature

Grain signature is assessed on its ability to produce smoke (primary or secondary) or afterburning phenomena (re-ignition of the combustion gases).

TABLE 11 *Theoretical and measured performances of several typical advanced energetic binder propellants*

Propellant	CMCDB	XLDB	NEPE
Nature of fillers	RDX	HMX + ammonium perchlorate	HMX + ammonium perchlorate + aluminum
Theoretical $I_s(s)$ (expansion 70/l)	241	257	270
Measured $I_s(s)$	229	245	249
$\Delta I_s(s)$	12	12	21
Standard motor	Mimosa diam. = 203 mm L = 1000 mm	Bates 12" diam. = 305 mm L = 508 mm	Bates 12" diam. = 305 mm L = 508 mm

Such phenomena, which may affect either the guidance or the detection of the missile, or of the combat platform, are discussed in detail in Chapter 5.

The importance of the signature of advanced energetic binder propellants depends primarily on the nature of the fillers incorporated in the propellant (Table 12).

The ability of these propellants to generate smoke and flashes is examined in the following sections.

4.5.1.1. Primary smoke

Usual energetic binders consisting of atoms C, H, O and N, do not generate primary smoke. This is also true for the oxidizers contained in these binders (RDX, HMX, or ammonium perchlorate). As a result, the release of primary smoke by CMCDB or XLDB propellants is mainly tied to the presence of additives carrying metallic atoms which are incorporated in the propellant to

TABLE 12 *Classification of advanced energetic binder propellants as a function of their ability to generate smoke*

	CMCDB EMCDB		XLDB		NEPE
Fillers	Nitramine	Nitramine	Nitramine + ammonium perchlorate (< 20%)		Nitramine + ammonium perchlorate + aluminum
Classification	Smokeless	Smokeless	Minimum smoke		Smoky

respond to a specific operational requirement. These additives, of which only small amounts are incorporated, include:

- ballistic modifier (lead and copper salts, for example);
- damping particles, sometimes required in some radial burning grains;
- afterburning suppressants including an alkaline ion (most often potassium) which decompose during combustion but may give rise to recombinations in the gaseous phase, which is detrimental to the signature.

4.5.1.2. Secondary smoke

Secondary smoke is characteristic of propellants that contain ammonium perchlorate. The formation of $\text{H}_2\text{O}/\text{HCl}$ aerosols depends, on one hand, on the atmospheric conditions (temperature and relative humidity), and on the other hand, on the amount of NH_4ClO_4 in the propellant.

4.5.1.3. Afterburning

Afterburning phenomena can be suppressed by the introduction of additives with alkaline metals base (sodium and particularly potassium: K_2SO_4 , KNO_3 , K_3AlF_6 and others).

When developing new propellant compositions, however, the choice of an additive must take into account not only its specific afterburning suppressant function, but also such criteria as: influence on the feasibility, ballistic properties, chemical and thermal stability of the propellant, as well as the possible effects on the exhaust plume (primary smoke).

4.5.2. Combustion instabilities

Instabilities, longitudinal as well as transverse, which are typically observed in radial burning grains, are the subject of theoretical research so that computer codes may be developed for predictive analyses (Chapter 4).

This is an interesting approach, in as much as it should allow the reduction of the number of lengthy and expensive tests that need to be performed, particularly in the case of large rocket motors. For modest-size grains destined for tactical purposes, on the other hand, it is possible and even useful to define experimentally the stable combustion zones.

4.5.2.1. Conditions for occurrence of transverse instabilities

In a given propellant, the occurrence of combustion instabilities is tied, on one hand, for the firing conditions, and on the other, to the design of the propellant grains.

(a) Firing conditions

Pressure is a dominant factor. Instabilities usually occur at low pressures, the oscillations increase as the pressure decreases. For a given pressure, the firing temperature may also affect the triggering of instabilities.

(b) Geometry of propellant grains

Starting from free-standing grains with a constant diameter (D), there is a grain length (L) above which combustion instabilities occur. Conversely, starting from grains with a constant length (L), it is possible to determine an initial central port diameter (D) above which the combustion will be stable.

Finally, the combining of these different experimental firing tests allows one to obtain a more accurate definition of the grains size (Fig. 12).

4.5.2.2. Function of damping particles

Damping of the pressure oscillations in the combustion chamber can be obtained through the presence of solid particles in the combustion gases. For each specific vibration, there is a proper particle size.

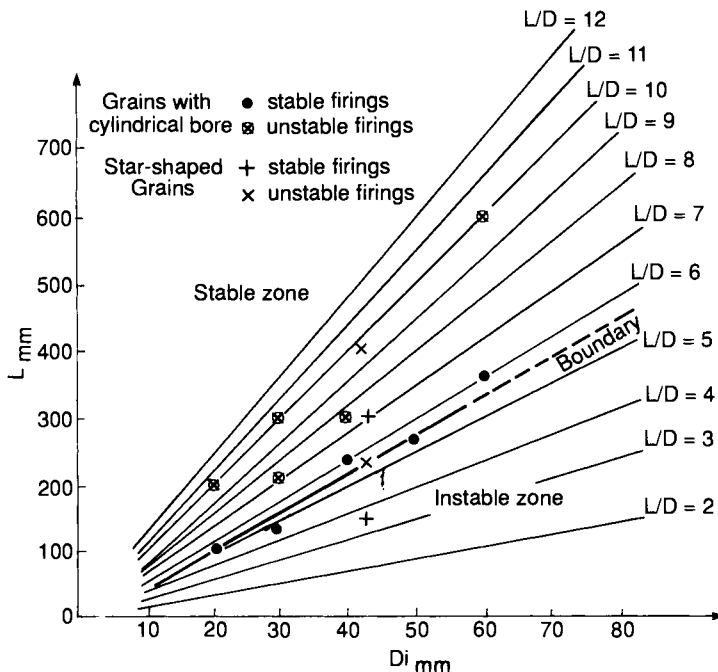


FIG. 11.12. Identification of a stable combustion zone as a function of the dimensional characteristics of the propellant grain. CMCDB propellant with 30% RDX.

When the grain is being designed, there are two ways of proceeding:

- By introducing metallic additives (aluminum or tungsten, for example) which, when they burn, generate oxidation condensed products (AlO_3 , W_2O_3 , etc.). This is the most widely used solution, but it does not afford the possibility of controlling the size of the particles that are generated.
- By introducing refractory additives with melting points that are higher than the combustion temperature of the propellants. This allows a better optimization of the size of the damping particles, provided that the vibration frequencies of the grain are known. The damping particles that can be added to CMCDDB or XLDB propellants belong to the families of oxides (SiO_2 - ZrO_2 - Al_2O_3 for example), carbides (SiC - ZrC - BC), or nitrides.

When it becomes necessary to have recourse to the introduction of an additive to stabilize the combustion of a grain, the consequences on the other properties must be ascertained, such as:

- *Performance*: the metals (aluminum, for instance) contribute to raising the specific impulse; refractory products, on the other hand, are rather detrimental.
- *Burning rate*: these additives may cause perturbations of the burning rate-pressure law, particularly with CMCDDB and XLDB propellants which contain catalysts common in double-base propellants.
- *Signature*: the solid particles released in the exhaust plume are responsible for primary smoke.

4.6. AGING

Aging behavior of propellant grains depends not only on the nature of the propellant, but also on the environmental conditions (temperature, and relative humidity, for example). For the propellant, this aging translates into an evolution of the chemical and/or physicochemical characteristics, which may in turn alter its mechanical and ballistic properties, as well as its safety behavior. Table 13 enumerates the major consequences related to these evolutions.

4.6.1. Chemical stability

The presence of nitrate esters in advanced energetic binder propellants requires, as with all double-base propellants, the incorporation of stabilizers whose function is to trap the nitrogen oxides resulting from the decomposition of the nitrates.

The stabilizers used for CMCDDB and XLDB propellants that contain no ammonium perchlorate are often the same ones used for homogeneous

TABLE 13 *Consequences of aging on the properties of advanced energetic binder propellants*

Type of evolution	Nature of the evolution	Consequences and properties affected
Chemical	Decomposition of nitrate esters	<ul style="list-style-type: none"> ● Chemical stability (consumption of stabilizer) <ul style="list-style-type: none"> ↳ Explosive behavior (risk of ignition) ● Physical integrity (cracks) <ul style="list-style-type: none"> ↳ Operational safety
	Evolution of the polymer network: rupture of chains, creation of links	<ul style="list-style-type: none"> Crosslinking density <ul style="list-style-type: none"> ↳ Mechanical properties
Physicochemical	Mobility of the energetic plasticizer: migration, exudation, volatilization	<ul style="list-style-type: none"> Composition of the material <ul style="list-style-type: none"> ● Mechanical properties ● Ballistic properties ● Explosive properties
	Binder-charge adhesion	Mechanical properties
	Crystallization of the plasticizer (cycling at low temperatures)	<ul style="list-style-type: none"> Mechanical properties <ul style="list-style-type: none"> ↳ Explosive properties

propellants: 2-nitro diphenylamine (2NDPA), and *N*-methyl *p*-nitroaniline (MNA), for example. When they contain ammonium perchlorate, resorcinol (or resorcinol derivatives) combined with 2NDPA is also efficient.

The mechanisms of nitrate esters decomposition, and of the oxides interaction with the stabilizers, are described in depth in Chapter 9.

The chemical stability of advanced energetic binder propellants may be affected by some ingredients of the binder and the nature of the fillers, as well as by the various additives necessary for the functional characteristics of the propellant grain.

4.6.1.1. *Influence of the binders*

- Increase of energetic plasticizer content in the binder is generally manifested by a faster consumption of the stabilizer.
- The polyurethane binders plasticized with energetic nitrate esters usually exhibit a chemical stability that is lower than those of nitrocellulosic binders. Among the parameters that influence this stability are:
 - nature of the polyisocyanates: in general, the aromatic polyisocyanates give a slightly better chemical stability;
 - nature of the prepolymer: prepolymers rich in ether functions lead to less chemical stability.

4.6.1.2. Influence of the fillers

- Nitramines (RDX and HMX) are chemically stable. They do not participate in a significant manner in the degradation of the advanced energetic binder propellants.
- Ammonium perchlorate, on the other hand, plays a particular role by modifying the decomposition mechanisms of the nitrate esters and the interaction mechanisms of the nitrogen oxides with the stabilizers. Under standard aging conditions (50–70°C), this is expressed by a lower consumption of the stabilizer and lower gaseous emissions.

4.6.1.3. Influence of the additives

Incorporation of additives in even small amounts may cause significant modifications in the decomposition kinetics of nitrate esters. This is true in the case of ballistic modifiers.

4.6.2. Cracks caused by aging

The propensity of a grain of a specific size to crack is a function, on one hand, of its chemical and physicochemical behavior, and on the other hand, of its mechanical properties (refer to Chapter 9).

For propellants with similar compositions and mechanical properties, resistance to cracks caused by aging depends mostly on the nature and the proportion of stabilizer(s) included. It has been demonstrated, for example, that centralite is clearly less efficient than 2-nitro diphenylamine (2NDPA). With CMCDDB or XLDB propellants it might be interesting to combine two stabilizers that have very different nitrosation kinetics to improve resistance to cracking.

Included among the other propellant constituents that may affect this type of aging are:

- presence of ballistic modifiers;
- cure agents (nature, content);
- nature of the fillers. The presence of ammonium perchlorate slows down the gases generation, leading as a result to critical sizes much larger than those of double-base propellants or CMCDDB or XLDB propellants loaded with nitramines.

4.6.3. Mechanical aging

The main causes of the evolution of the mechanical properties of the advanced energetic binder propellants are the presence of nitrate esters, the crosslinking systems, mobility of the plasticizers, and environmental factors.

4.6.3.1. *Presence of nitrate esters*

Nitrogen oxides issued from the decomposition of the nitrate esters have the capability of reacting directly with the polymeric chains, or of combining with traces of humidity present in the propellant to produce chemical species (HNO_3 for example) which are particularly aggressive toward the polymers (cutting by acid hydrolysis). The result is a depolymerization causing a decrease of the Young's modulus of the material. However, this mechanical aging can be minimized through the presence of chemical stabilizers performing efficiently inside propellant.

4.6.3.2. *Curing agents*

Circumstances may occur where crosslinking is not entirely completed at the end of the curing phase. During storage the mechanical properties of the propellants may evolve toward a slight hardening, caused by the continuation of the polymerization.

In addition, the eventual formation of secondary products during crosslinking — due to the presence of traces of humidity, for example — may have an influence on the kinetics of self-decomposition of the nitrate esters.

4.6.3.3. *Mobility of the plasticizers*

In the course of aging, the plasticizer may migrate into the materials that are in contact with the propellant (inhibitor, liner, etc.). The localized depletion of plasticizer causes a hardening of the propellant. The development of bonding materials for advanced energetic binder propellants does not completely exclude the risks of diffusion, but does limit them to such low levels that they do not compromise mechanical integrity near the interfaces.

4.6.3.4. *Environment factors*

- *Humidity*: the humidity associated with the decomposition products of nitrate esters accelerates the acid hydrolysis of the nitrocelluloses and polyesters, for example. Humidity most probably also has some effect on the quality of the binder-charge adhesion.
- *Air (oxygen)*: aging in an oxidizing atmosphere (exposed to air, for example) may facilitate a degradation of the mechanical properties. To prevent this process, propellant grains may be stored in inert atmosphere, such as nitrogen.
- *Temperature*: it is quite obvious that the mechanical aging processes in ambient temperature are very slow; however, their kinetics is accelerated whenever the storage temperatures increase.

In practical terms we must remember that non-crosslinked CMCDB propellants have very few problems of mechanical aging. But propellants whose mechanical characteristics are obtained by crosslinking — mainly XLDB propellants — are more sensitive to this type of aging.

4.6.4. Ballistic aging

Advanced energetic binder propellants show no significant modification of their ballistic characteristics over time.

The factors that could have any influence are related to modifications in the composition of the propellant are:

- loss of plasticizer (diffusion to the inhibitors, or volatilization);
- chemical evolution of the burning rate modifiers.

4.7. SAFETY CHARACTERISTICS

4.7.1. Background

Propellants are, above all, materials for which combustion is the major risk. However, the development of new high energetic propellant families has contributed to the identification of techniques and methodologies to study the safety in order to take into account:

- various manufacturing phases;
- various situations in the operational life of the propellant (such as storage, transport, firing).

These methods provide the capability of defining the major risks that must be considered in a given situation: combustion (hazard class 1.3) or detonation (hazard class 1.1). The resulting analyses allow us to deduce information on the nature of the future design of facilities, or on the protective measures needed for personnel and the environment.

4.7.2. Safety behavior during the manufacture of advanced energetic binder propellants

4.7.2.1. CMCDDB propellants

(a) Behavior of the casting powders

The risks involved with casting powders are similar to those from granular products:

- Starting in deflagration in a limited space, they may, under the effect of a sudden increase in the gaseous pressure, lead to a mechanical explosion of the containers, or worse, to a detonation. This is known as the deflagration-detonation transition phenomenon (DDT).

Consequently, it is important to know these mechanisms very well in order to design suitable storage facilities and to determine the conditions of usage that minimize the risks.

Standardized tests allow us to measure the critical explosion heights (CEH) and detonation height (CDH).

Generally, the CEH and CDH decrease when:

- The burning rate of the powder increases. This tendency is clearly demonstrated in the case of casting powders containing mixtures of HMX and ammonium perchlorate. As a matter of fact, when the perchlorate amount increases at the cost of the nitramine, the burning rates increase while the CDH values drop (Fig. 13).
 - The proportion of explosive materials (nitroglycerine + nitramine) increases. In fact the CEH and CDH values are more sensitive to a variation in the amount of nitrate ester than that of nitramine.
 - The size of the casting powder grains decreases.
- The French Card Gap Test also evolves with the size of the granules in a given composition. When the diameter changes from 0.8 to 2.0 mm, the

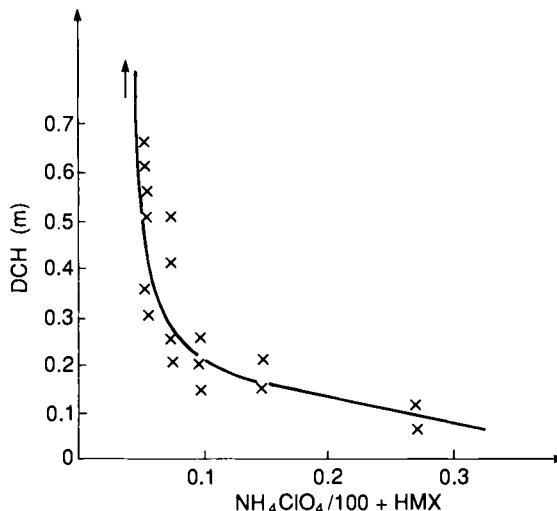


FIG. 11.13. Evolution of the detonation critical height of casting powders as a function of the ammonium perchlorate-HMX ratio.

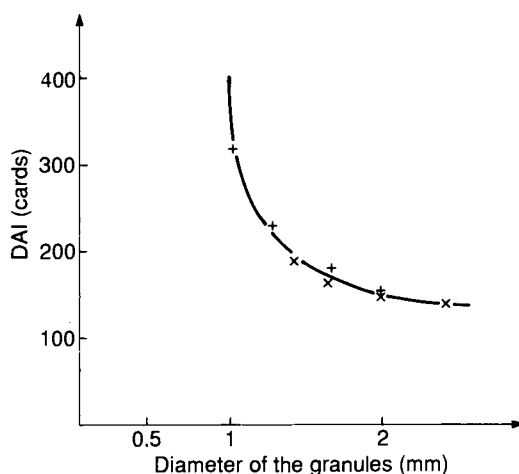


FIG. 11.14. Behavior of french card gap test of casting powders containing 10% nitroglycerin and 15% RDX.

gap drops from 300 to approximately 150 cards (Fig. 14). With granular products the high values of gap may be the result of a deflagration to detonation transition and not the result of a shock to detonation transition, which is the normal case. Indeed, for a weak shock wave, there is no detonation initiation, but only in deflagration; it is this deflagration which later takes on a detonation regime.

- The sensitivity of casting powders loaded with nitramines to mechanical stimuli such as shock or friction does not evolve much with the total solid contents.
- Casting powders may be sensitive to electrostatic discharge if they are not graphitized. To make them perfectly conductive, however, the glazing must be perfect.

A poor distribution of the graphite, often due to a poor surface aspect of the granules, may result in the electric conductivity having virtually no effect.

4.7.2.2. XLDB and NEPE propellants

(a) Premixes behavior

Premixes based on polymers and nitrate esters are sensitive to mechanical stimuli, and in particular to shocks. Their behavior is closely related to that of casting solvents, which is to say that they may manifest two detonation regimes (low and high speed), according to the type of stimulus.

(b) Slurries behavior

The behavior of homogenized slurries at the end of the mixing phase is fairly close to that of finished propellants after curing, as far as mechanical stimuli and propensity to detonate are concerned.

For propellant slurries with solid contents adapted to mass production, it can be observed that:

- these slurries generally exhibit no violent reaction to a 30 kg drop hammer test, below 4 m;
- use of ammonium perchlorate results in an increase in the sensitivity of the slurries to friction — moreover, depending on the nature and the amount of oxidizer, the same behaviour as the most sensitive composite propellants can be found;
- gap of slurries after mixing, measured with the French gap test, is below 240 cards.

4.7.3. Safety behavior of propellant grains

- The gap values, at the French gap test, of advanced energetic binder propellants, are less than 180 cards. These non-confined propellants can be given in the 1.3 hazard classification — the major hazard being combustion — of the French law. Double-base propellants which, we should remember, have been used around the world for over tens of years without any problems, have gap values of around 100 cards. The increase of gap values compared with those of double-base propellants results from the incorporation of explosive fillers, and more precisely nitramines.

As for the conditions of detonation triggering of propellant grains, they have been discussed in detail in Chapter 7. Transition phenomena such as deflagration to detonation or shock to detonation generally imply a prior fragmentation of the propellants. Propellants with good mechanical properties are therefore necessary to allow a minimization of these hazards. In this regard, XLDB propellants, which are designed for use as case-bonded grains, have an excellent mechanical behavior and naturally have a good resistance to fragmentation.

- CMCDB and XLDB propellants, loaded with moderate amounts of nitramines, are not sensitive to friction (behavior identical to that of double-base propellants). The somewhat more greater sensitivity of XLDB propellants comes for the most part from the higher content of nitramines ($> 60\%$). Ammonium perchlorate is a sensitizing element for the propellant in the form of slurry or crosslinked (Fig. 15).
- The shock sensibility behavior (30 kg drop hammer test) of CMCDB or XLDB propellants is not any different from the other current propellant families.

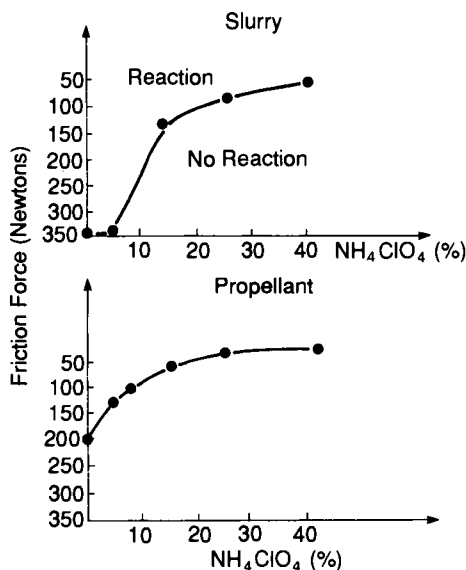


FIG. 11.15. Evolution of the friction sensitivity coefficient of XLDB propellants with 70% fillers (slurry and propellant) as a function of fine ammonium perchlorate content.

- XLDB propellants do not appear to be sensitive to electrostatic discharge test. But some compositions of CMCDDB propellants react to capacitive discharges. However, the normal reaction of the propellant to this type of solicitation is a non-violent combustion (the propellant grain generally does not present any fragmentation).
- In terms of behavior to thermal stimuli (self-ignition or the cook-off test) a distinction needs to be made between compositions with or without ammonium perchlorate. CMCDDB and XLDB propellants without ammonium perchlorate always have critical thermoinitiation temperatures higher than 100°C; these temperatures tend to decrease when the size of the grain increases. On the other hand, propellants containing ammonium perchlorate usually exhibit thermoinitiation temperatures below 100°C, but they are not affected by the size of the grain.

Bibliography

1. STEINGERGER, R. and DRESCHSEL, P. D., Manufacture of cast double-base propellant. *Advanc. Chem. Serv.*, **88**, 1-28. 1969.
2. GORDON, S. and DARWELL, H. M., Composite modified cast double-base propellants — technology and application. Technical report, No. 69/5. IMI Summerfield. Paper presented at the 9th International Aeronautical Congress, Paris, 1969.
3. HELMY, A. M., Investigation of new energetic ingredients for minimum signature propellants. AIAA/SAE/ASME 20th Joint Propulsion Conference, June 1984.

4. COUTURIER, R. and RAT, M., Compatibility of ammonium perchlorate with nitrate ester. ADPA Joint Symposium on compatibility of Plastics and Other materials with explosives, Propellants and Pyrotechnics. Hilton Head, South Carolina, March 1985.
5. TAVERNIER, P., Densité gravimétrique et densité de chargement. *Mémorial des Poudres*, Tome 31, 197-230, 1949.
6. RAT, M., LONGEVIALLE, Y. and COUTURIER, R., Second order transitions in nitrocellulose energetic plasticizers systems. Conference on Nitrocellulose Characterization and Double-Base Propellant Structure. Waltham Abbey, Essex, England, May 1980.
7. BRUN, I., LONGEVIALLE, Y. and RAT, M., Effect of thermal conditions on the crystallization kinetics of different nitrate esters, FhG ICT, Jahrestagung, 1989.
8. HARTMAN, K. O. and SILVER, P. A., High performance non-embrittling double-base propellant. Chemical Propulsion Information Agency Publication No. 340, vol. 1, 1981.
9. ZIMMERMAN, G. A., KIPERSKY, J. P. NAHOULOUSKY, B. D. and NEWAY, S. L. Embrittlement of propellants containing nitrate ester plasticizers, AIAA/SAE/ASME 18th Joint Propulsion Conference, June 1982.
10. CHI, M. S. and HARTMAN, K. O., Relationship of polymer structure to mechanical properties in crosslinked double-base binders. AIAA/SAE/ASME 15th Joint Propulsion Conference, June 1979.
11. SUMI, K. and KUBOTA, N., Reduction of plateau-burning effect of HMX based CMDDB propellants. 11th International Symposium on Space Technology and Science, Tokyo, 1975.
12. DAVENAS, A., Amélioration des propriétés balistiques et des propriétés mécaniques tous temps des propergols sans fumée. AGARD Conference No. 259, Solid Rocket Motors Technology, 1979.
13. FIFER, R. A., Chemistry of nitrate ester and nitramine propellant. *Fundamentals of Solid Propellant Combustion*, Edited by K. K. KUO and M. SUMMERFIELD, *Progress in Astronautics and Aeronautics*, Vol. 90, 1984.
14. STACK, J. S., Double-base propellants with combustion modifiers, US Patent 3.951.704, April 1976.
15. STACK, J. S., Ballistic modifiers, U.S. Patent 3.996.80, December 1976.
16. SARTRIANA, O. R. and BRACUTTI, A. J., Ballistic modifiers. US Patent 4.082.584, April 1978.
17. LENGELLE, G. and DUTERQUE, J., Combustion des propergols à base d'octogène. AGARD/PEP Specialists' Meeting on Smokeless Propellants, Florence, September 1985.

CHAPTER 12

Propellants for Integral Rocket Ramjet Systems

CHRISTIAN PERUT

1. Introduction

Many countries show an increasing interest in better performance for tactical missiles, including range improvements, maneuverability and speed. Solid propellant rocket motor propulsion has proven to be very efficient as long as the range is modest. When using this technology a significant increase in the range and the speed can only be obtained at the cost of a considerable missile weight and volume increase.

In an article published in 1979, R. Marguet, C. Ecary and Ph. Cazin [1] give the example of a 100 km mission at Mach 2 and low altitude with a 200 kg payload. Solid propellant rocket motor propulsion would result in a 9 to 10 m long missile weighing 5000 kg. However, the use of a kerosene ramjet would lead to a missile weighing around 1000 kg and 6 m long.

A ramjet engine (shown in Figure 6 in Chapter 1) consists of several major components. Starting from the front of the missile, they are one or more air inlets followed by the inlet air diffuser, a fuel supply, fuel metering and injection devices, a combustion chamber, and a nozzle. In some configurations the fuel supply is located in the combustor. The air is captured by the air inlet and undergoes compression, resulting in a temperature and pressure increase, and a decrease in speed. The air is heated in the combustion chamber by the burning of a fuel whose introduction also triggers a slight increase in the mass flow rate, of the order of 5–10%. The compressed hot gases are expanded and accelerated in the nozzle.

Although ramjets are capable of functioning at subsonic flight speeds greater than Mach 0.8, albeit with poor performance, they are only advantageous at supersonic speeds ranging between Mach 1.5 and Mach 5, and are in practice used primarily within the Mach 2 to Mach 4 range. Consequently, the operation of a ramjet requires the missile to reach speeds between Mach 1.5 and 2.5 prior to initiation of ramjet engine operation. The initial solution

selected involved the addition of separate, detachable boosters; it was followed by the use of a solid propellant grain located in the ramjet combustion chamber. This last configuration, known as the integral rocket ramjet (Fig. 1), has advantages over the separable rocket booster as it results in a much more compact missile, and the problems of jettisoning the boosters after their use are avoided. The chronology of the various stages of operation of a ramjet with an integral booster is as follows: combustion of the rocket booster, lasting usually between 3 and 6 s; transition over a period of less than 1 s during which the booster nozzle and the inlet port covers are ejected, the fuel is injected into the combustion chamber and ignited and, finally, ramjet operation. The booster may be nozzleless, which avoids the problem of jettisoning the rocket nozzle (Fig. 2).

The ramjet concept was invented in 1911 by a French scientist, R. Lorin. The Frenchman R. Leduc applied it to the propulsion of aircraft, and subsonic flight tests were conducted in 1949. Before and during the Second World War the Germans studied the application possibilities of the ramjet concept to missiles and artillery shells. Between the end of the Second World War and the middle of the 1960s, a large number of countries undertook a major research effort, which took the shape (in France) of many flight tests of experimental missiles called CT41, VEGA, R431 and Stataltex; and of operational developments of ground-to-air or surface-to-air missiles such as the BOMARC (1957) and the TALOS (1959) in the United States; the BLOODHOUND (1959) in Great Britain; and the SA4 (1964) in the USSR. After this period, the research and development effort slackened. Activities began again around the 1970s with, in particular, the following: introduction

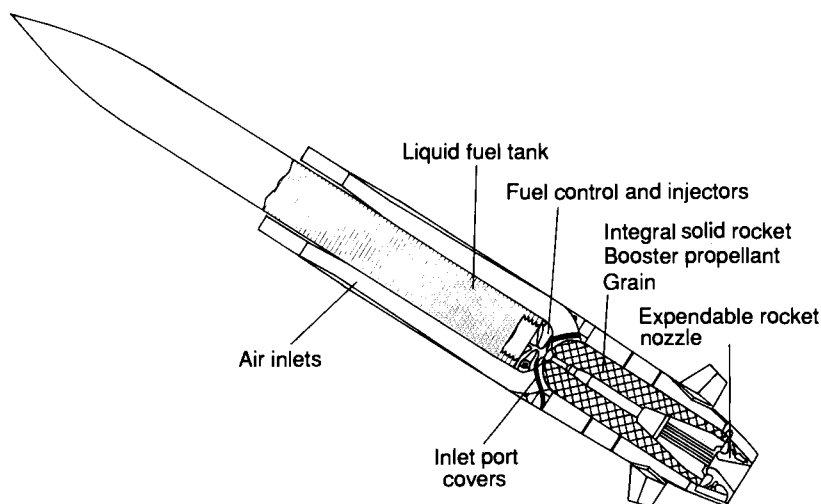


FIG. 12.1. Liquid-fueled integral rocket ramjet.

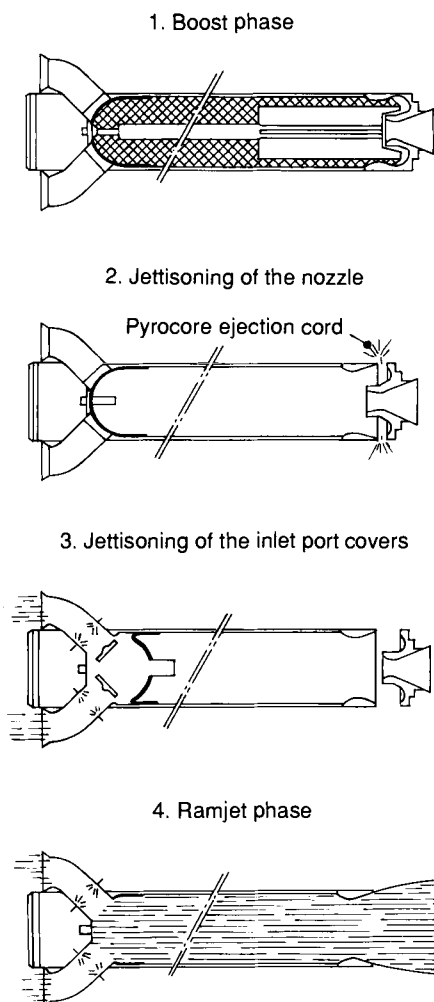


FIG. 12.2. Integral rocket ramjet-operating sequence.

in Great Britain in 1975 of the SEA DART; the in-flight evaluation in the US of the ASALM (advanced strategic air-launched missile) and ALVRJ (advanced low-volume ramjet) experimental missiles; the development of the SLAT (supersonic low-altitude target) [2], which could be operational in 1991 [3]; and in France, the flight test of the ANS missile (supersonic anti-ship) and the operational missile ASMP (medium-range air-to-ground).

The missiles mentioned above are powered with liquid fuel. Another technical solution consists in feeding the combustion chamber with a hot fuel plasma through the decomposition of a fuel-rich solid propellant (the amount

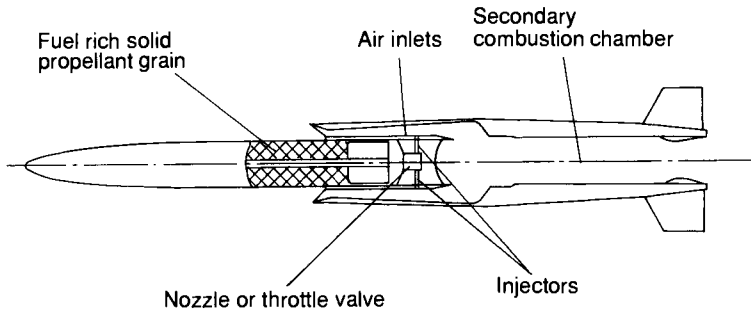


FIG. 12.3. Ducted rocket with choked gas generator.

of oxidizer in the propellant is just sufficient to ensure the required ballistic properties). The fuel-rich grain is placed in a gas generator located upstream from the combustion chamber of the ramjet. Two configurations are used, one with a choked gas generator (Fig. 3) where the combustion pressure of the grain is controlled by one or more nozzles, the other with an unchoked gas generator where the operation of the gas generator is not separated from that of the combustion chamber of the ramjet (Fig. 4). The solid-fueled ramjet engine is referred to as a solid-fueled ducted rocket. In the USSR a ducted rocket-powered antiaircraft missile, the SA-6, became operational in 1967.

The fuel supply for a liquid-fueled ramjet or for a solid-fueled ducted rocket is located upstream of the combustion chamber. On the contrary, in the solid-fuel ramjet concept the fuel is entirely contained in the combustor. The heat feedback from the combustion zone of the fuel decomposition products with air determines the fuel grain regression rate. There are two combustor types [4]. In the non-bypass configuration all of the inlet air passes through the solid fuel grain (Fig. 5). The combustion efficiency is promoted by a mixing device located downstream of the fuel grain [4]. In the bypass arrangement a part of the air is injected downstream of the fuel grain where the combustion of the fuel-rich products is completed (Fig. 6). In the two cases, the flame is

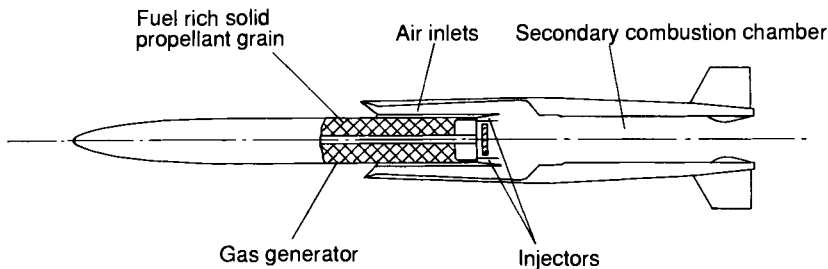


FIG. 12.4. Ducted rocket with unchoked gas generator.

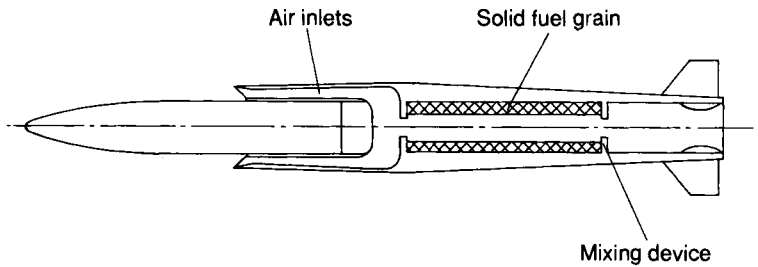


FIG. 12.5. Solid fuel ramjet non-bypass configuration.

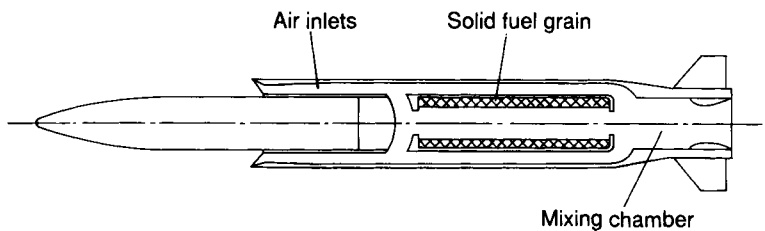


FIG. 12.6. Solid fuel ramjet bypass configuration.

stabilized in the foremost region of the combustion chamber by a recirculation zone created by the inlet step.

Various types of fuel-rich propellant are available. One type is based on pyrolysis of the binder into a fuel-rich plasma. The pyrolysis is caused by the reaction of a small amount of oxidizer with a small portion of the binder. A second type employs a binder and oxidizer in proportions typical of solid rockets, but also contains a large amount of solid-fuel filler. The rocket combustion process generates a hot plasma, containing the solid-fuel filler, and injects it into the secondary combustion chamber where it is mixed with air and recombusted.

This chapter examines the reasons governing the selection of the major fuels likely to be used in the composition of a fuel-rich solid propellant, as well as the main characteristics of typical products belonging to each of the major families, and makes a survey of integral boosters.

2. Fuel-rich Solid Propellants

2.1. SELECTION OF THE MAIN COMBUSTIBLE COMPONENTS

A fuel-rich propellant for ducted rockets consists of:

- A binder, whose function is to ensure the cohesion of the various propellant materials, and to supply combustible fuel fragments through

pyrolysis, an oxidizer is employed to react with the binder to produce a plasma which transports the fuel-rich binder fragments to the secondary combustion chamber.

- Combustion catalysts.
- Additives, generally used in all propellants, to improve their aging, processability, including if necessary one or several fuel fillers to increase energy levels.

An initial selection of the propellant components is feasible on the basis of the combustion heat values which, due to the mode of operation of a ramrocket, allow us to assess their energetic quality. The value of components selected in this manner must later be examined in the light of other selection criteria such as cost, processability, usability in gas generator, combustion efficiency in combustor and, if necessary, the signature.

2.1.1. Selection of a binder

Some of the first criteria to be considered when selecting a binder for a fuel-rich propellant are: the ease of manufacture, and combustion heat values (Table 1).

Polyesters and polycarbonates contain much more oxygen than polybutadiene. Their gravimetric heats of combustion are therefore much lower than those of the polybutadiene binder, and their much greater density is not sufficient to compensate for the difference. The classification of these binders, in a decreasing order of volumetric heating values is as follows:

$$\text{CTPB} = \text{HTPB} > \text{polycarbonate} > \text{polyester}.$$

The plasticizers generally used with propellants are highly oxygenized; their incorporation into a polybutadiene binder results in a drop in the combustion heat.

Another parameter which must be taken into consideration is the amount of fuel-rich solids which can be incorporated into the propellant composition. From a physical properties perspective, this analysis can be based on the experience acquired with propellants loaded with ammonium perchlorate and aluminum. The classification of binders, in a decreasing order of maximum accessible total solids based on processability and mechanical properties, is as follows:

$$\text{plasticized HTPB} > \text{HTPB} > \text{polyester} > \text{polycarbonate}.$$

Polyester and polycarbonate binders, because of their low heating value and their low loading ratio capability, are therefore not very advantageous. The respective importance of each of the criteria discussed above depends on the type of fuel-rich propellant that is considered. In compositions which contain no combustible solid fuel filler the energy level of the material is provided by

TABLE 1 *Properties of binders*

Binder type	Atomic composition % (mass)				Density (g/cm ³)	Heating value		Maximum total solids*
	C	H	O	N		Gravimetric (kJ/g)	Volumetric (kJ/cm ³)	
CTPB	83.9	10.5	4	0.6	1	43.2	40.2	86
HTPB	85.4	11.2	2.4	1		43.4	40	88
Plasticized HTPB	81.6	10.4	7.1	0.9		40.9	38.3	90-91
Plasticized HTPB and ferroceic catalyst	80	9.7	5.3	2.6		39.5	39.5	90-91
Polyester	56.8	8.1	32.7	2.4		25.2	29.3	86
Polycarbonate	57.5	8.3	29.2	5		26.2	30.1	85

* Maximum amount of total solids (A.P. and Al) which can be incorporated into a propellant composition (processability and mechanical properties).

the binder. As we will see later, this type of product contains little oxidizer, and its manufacture does not require the use of a low-viscosity binder. Consequently, the choice will often be a non-plasticized polybutadiene binder.

With compositions containing large percentages of fuel-rich solid particles the energy is primarily contributed by those particles. A plasticizer should, therefore, not be automatically excluded if it allows us to significantly increase the solid loading ratio. Polybutadiene, eventually plasticized, is well adapted to this type of use.

2.1.2. Selection of organic energetic additives

Energy can be added to fuel-rich propellants by replacing a portion of the binder with a solid or liquid hydrocarbonated product. Because polybutadiene-type binders contain little oxygen, the increase in gravimetric heating value likely to be obtained from the substitution of a portion of the binder with such a compound is very limited. But a substantial increase of the volumetric heating value can be obtained by using aromatic or aliphatic cyclical products, which are notably more dense than binders. As for solid products, the focus has been mainly on aromatic products with densities appreciably higher than those of the polybutadiene binders [5,6]. The gravimetric heating value of such products is lower than those of binders, but because of their much greater density, their volumetric heating value is much higher (Table 2). The presence of oxygen or nitrogen in the molecule allows us to significantly increase the density of the product, although not sufficiently to compensate for the loss of gravimetric heating value. The gravimetric heating values obtained with liquid products are greater than those of solid compositions, but the densities are usually lower (Table 3). These two types of products can be used simultaneously in a fuel-rich propellant composition.

TABLE 2 Organic energetic additives (solid products)

Product	Density (g/cm ³)	Formula	m.p. (°C)	b.p. (°C)	Heating value	
					Gravimetric (kJ/g)	Volumetric (kJ/cm ³)
Anthracene	1.28	C ₁₄ H ₁₀	217	340	39.9	51.1
Fluorene	1.20	C ₁₃ H ₁₀	116	294	40.2	48.2
Polystyrene	1.05	(C ₈ H ₈) _n	—	—	39.9	41.9
Poly (alphamethyl styrene)	1.07	(C ₉ H ₁₀) _n	—	—	40.3	43.1
Anthraquinone	1.44	C ₁₄ H ₈ O ₂	286	380	31.4	45.2
Naphthylamine	1.12	C ₁₀ H ₇ NH ₂	50	301	36.9	41.3
Dicyandiamide	1.40	C ₂ N ₄ H ₄	210	d	18.6	26.0

TABLE 3 *Organic energetic additives (liquid products)*

Product	Density (g/cm ³)	Atomic composition % (mass)			Heating value	
		C	H	O	Gravimetric (kJ/g)	Volumetric (kJ/cm ³)
Hydrogenated terphenyl	1.006	90.8	9.2	0	42.6	42.9
Hydrogenated polycyclopentadiene resin	1.053	89.6	10.4	0	44.3	46.6
Poly(styrene-indene)	1.051	91	7.6	1.4	41.0	43.1
Hydrogenated dimer of norbornadiene	1.08	90.2	9.8		43.7	47.2

2.1.3. Selection of inorganic fuel fillers

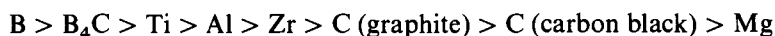
The interest has generally focused on carbon, zirconium, aluminum, magnesium, and boron [6,7]. Boron carbide and titanium are sometimes also mentioned (Table 4).

Although its combustion heat is high, beryllium is excluded, as for all propellants, because of the toxic properties of its oxide as a combustion product.

The order of classification of these products, as a function of their gravimetric heating value, is:



In most cases the performance per unit of volume is the important factor which is sought after. Making a distinction between amorphous carbon black and graphite, the classification is as follows:

TABLE 4 *Inorganic fuel fillers*

Product	Density (g/cm ³)	Heating value	
		Gravimetric (kJ/g)	Volumetric (kJ/cm ³)
Beryllium	1.84	66.5	122.5
Aluminum	2.70	31.1	83.9
Boron (amorphous)	2.22	59.3	131.6
Graphite	2.25	32.8	73.8
Carbon black	1.63	32.8	53.3
Magnesium	1.74	24.7	43.0
Zirconium	6.49	12.0	78.2
Titanium	4.5	19.7	88.8
Boron carbide	2.52	51.5	129.8

Due to their high density, titanium and zirconium now attract more interest.

However, we must point out that for an equal volumetric performance it is preferable to have the highest possible gravimetric energy. This is due to the fact that an increase of the density implies a greater weight for the fuel-rich grain, with the detrimental result of a heavier propulsion system, because of the increase in weight of the gas generator and of the booster, which needs to be more powerful.

A preliminary assessment of the increase in performance that might be obtained by switching from a composition without particles to a particle-laden composition can be made by comparing relative heating values. When taking the gravimetric heating value into consideration, only boron and boron carbide have combustion heats greater than that of a polybutadiene-type binder. But because of their greater density, all of these fillers have volumetric heating value that are greater than those of the binder.

2.1.4. Theoretical energetic performances

The following thermodynamic calculations for various filled and unfilled compositions are provided to demonstrate their relative energy merits. These examples involve one hydrocarbon-fueled composition and compositions with polybutadiene binder with 25 % ammonium perchlorate and 50 % of one of the most common energetic fillers quoted in the field, i.e. aluminum, magnesium, carbon, zirconium or boron. These amounts were selected arbitrarily, and do not take into account either the manufacturing problems specific to each of these additives, or the amount of ingredients that must be selected to ensure the functional properties required from the gas-generating grain.

Before an assessment of the theoretical performances of these fuel-rich propellants can take place, we need to establish standard conditions for the operation of the ramjet. For this chapter we have selected a chamber pressure equal to 0.57 MPa, the enthalpy of formation attributed to air corresponding to a flight at Mach 2 and sea level. In addition, the calculations are done on the basis of different proportions of air and fuel. These proportions are expressed in terms of the value of the equivalence ratio, a term that stands for the quotient of the ratio of the mass flow rate of fuel and air versus the same ratio for a stoichiometric mixture (see Chapter 3).

The evolutions of the specific impulse (I_s) and of the volumetric specific impulse ($I_s\rho$) as a function of the equivalence ratio are illustrated in Figs 7 and 8. The specific impulse is the ratio of the thrust to the product of the acceleration due to gravity and the mass flow rate of the fuel-rich propellant.

For a low equivalence ratio the classification of the combustible solids in a decreasing order of specific impulse is as follows:

$$\text{B} > \text{C} > \text{Al} > \text{Mg} > \text{Zr}$$

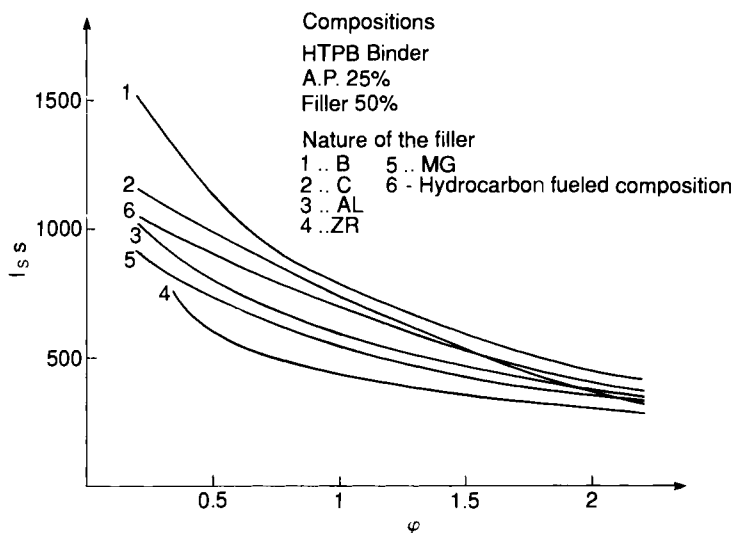


FIG. 12.7. Theoretical performances of fuel-rich propellants ($M = 2$; $Z = 0$; $P = 0.57$ MPa).

This ranking order is identical to that established on the basis of the combustion heat.

Based on the volumetric specific impulse, which is the criterion for the selection when the volume available for the gas generator is limited, the classification is as follows:

$$B > C (\text{graphite}) > Al > Zr > Mg$$

The relative values of a composition without particles are shown on the same diagram, to serve as a reference.

2.2. SELECTION OF A COMPOSITION TYPE

The criteria for selecting the type of composition must take features of future missions other than theoretical energy into consideration.

The combustion in the chamber of the ramjet of the decomposition products from hydrocarbon-fueled compositions and carbon compositions leads exclusively to the production of gaseous products, provided that high levels of combustion efficiency are obtained. Therefore, these compositions produce low levels of exhaust smoke.

The oxides from aluminum, zirconium, magnesium and boron, on the other hand, are solid at ambient temperature. Therefore, these fuel-rich propellants produce high levels of exhaust smoke.

Based on their energy and exhaust smoke levels, fuel-rich propellants can be classified into three categories: metal-loaded compositions with high

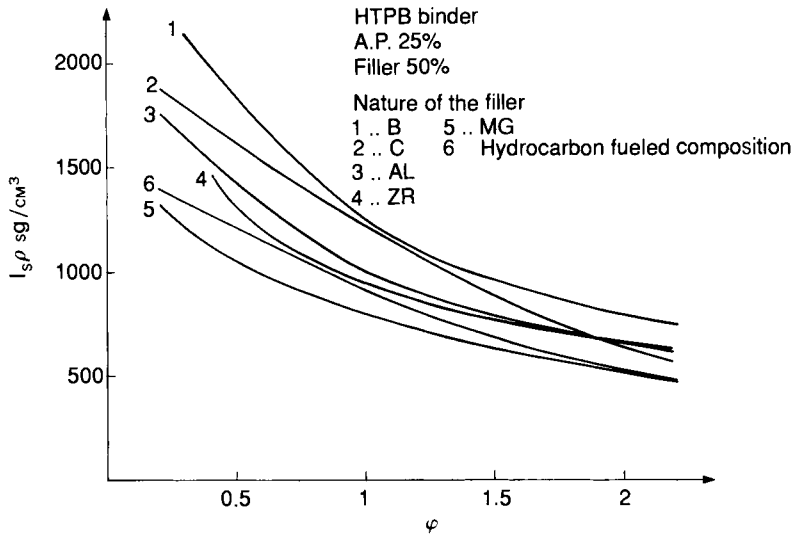


FIG. 12.8. Theoretical performances of fuel-rich propellants ($M = 2$; $Z = 0$;
 $P = 0.57 \text{ MPa}$).

smoke levels, carbon compositions and hydrocarbon-fueled compositions with low smoke level.

The hydrocarbon-fueled compositions generate lower molecular weight hydrocarbon fragments which are burnt later in the secondary combustion chamber. Consequently, these compositions exhibit characteristics of combustion similar to gaseous hydrocarbons.

2.2.1. Compositions with a high content of metal

Four metals offer the desired properties: boron, aluminum, zirconium and magnesium.

The thermodynamic computations demonstrate that boron fuel-rich propellants are potentially highly energetic. However, the expected energy is only likely to be produced if the boron particles ignite and burn in the air within a very short period of time, compatible with the residence time in the combustion chamber, usually less than 5 ms. It is also difficult to burn at low pressures. For these reasons, boron combustion has been the object of very extensive research [8,9].

Boron particles are naturally coated with a layer of boric oxide, which has a very high boiling temperature (2133 K) that interferes with the combustion.

A. Macek's research [8] revealed that boron particle combustion occurs in two successive phases. First, the particle ignites, followed by an extinction phase during which no luminous phenomenon is observed that would

correspond to the end of the evaporation process of the oxide layer, and then to the end of combustion [8,9]. The ignition temperature, defined as the minimal temperature necessary for combustion, is virtually independent of the size of the particle in the case of products with a small particle size. This temperature is 1980 K for a particle measuring 1 μm and 1920 to 1930 K for a particle of 30–40 μm under conditions of a dry atmosphere, and under a pressure of 1 atm and an oxygen molar fraction of 0.2 [9]. With large particles, the burn time varies as the square of the diameter, and it is virtually independent of the pressure, thereby indicating that kinetic behavior is limited to the diffusion phenomena. With fine particles the burn time is proportional to the diameter, and in this case the burning rate is limited by the chemical kinetics and depends on the pressure. There are variations in behavior for diameters of a few tens of microns [9].

The burn time in a gaseous mixture with 20% oxygen and 80% nitrogen at 2240 K is approximately 0.6 ms for particles measuring 1 μm and 1.5 ms for particles measuring 3 μm [9]. Because of the very short residence time in the combustion chamber, these results show that very fine particles must be used. The products usually selected have particle diameters smaller than 3 μm .

Various solutions may be considered to promote the combustion of the boron inside the combustion chamber of a ramjet, such as increase of the temperature, chemical modification of the boron, or optimization of the architecture of the combustion chamber; this last point is discussed in the following section.

The incorporation of a small quantity of metal into the composition may promote the combustion efficiency. The additive is supposed to react rapidly in the zone where the air and the combustible products mix, and cause an increase of the temperature [9].

Some research has demonstrated the advantage of coating the boron particles with lithium fluoride to facilitate their ignition. The mechanism involved is based on the formation of a compound with a boiling temperature that is lower than that of the boron oxide [9].

Fuel-rich propellants with a high content of aluminum cannot be used because of their significant tendency to obstruct the nozzles or the diaphragms of the gas generators.

Thermodynamic computations show that, for an identical solid loading ratio, magnesium compositions have a specific impulse greater than those of zirconium compositions. Due to the fact that zirconium is much more dense than magnesium, this result is inverted when the volumetric specific impulse is considered. Consequently, a comparison between these two types of compositions is only feasible after a final assessment of their applications has been done. In general, magnesium compositions have proven to be more advantageous than zirconium compositions.

Finally, magnesium is introduced in a gaseous state into the combustion chamber because of the very high flame temperature of magnesium composi-

tions, ranging from 1950 to 2400 K, compared to the boiling temperature of magnesium, 1380 K. The combustion of the magnesium in the combustion chamber is therefore very rapid.

2.2.2. Carbon compositions

The burning rate of carbon particles is governed either by the kinetic of the oxygen diffusion, or by the speed of the superficial reaction if one of these two processes is much more rapid than the other; otherwise it is governed by both. The nature of the phenomenon that limits the burning rate depends on the temperature and the particle size.

Major studies reported in the literature demonstrate that it is necessary to use very fine particles, for which the burning rate is probably controlled by the chemical kinetic, and consequently that the nature of the carbon used is a very important parameter in obtaining satisfactory combustion efficiency [11–13].

2.3. THEORETICAL ENERGETIC PERFORMANCES

The performance analyses discussed above were intended to compare the advantage of various fuels, without taking into account any of the other characteristics, in particular the processability characteristics. Figure 9 shows

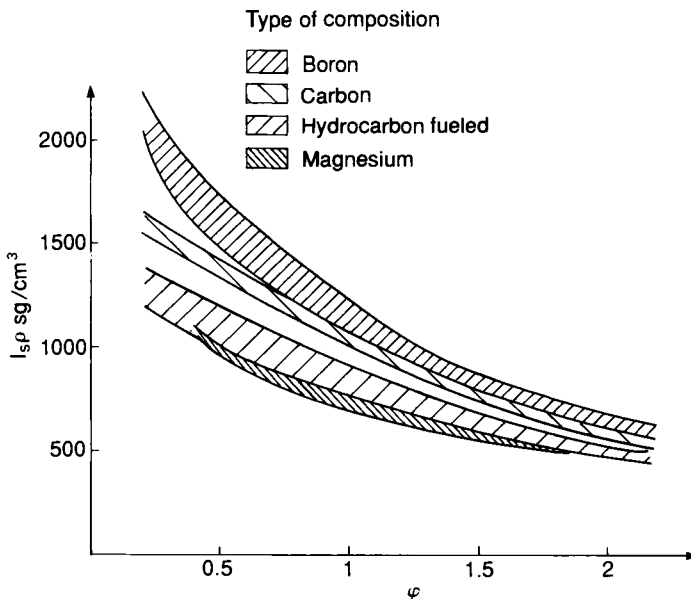


FIG. 12.9. Theoretical performances of fuel-rich propellants ($M = 2$; $Z = 0$; $P = 0.57$ MPa).

the energetic performances of feasible compositions on a graph plotting [volumetric specific impulse] versus [equivalence ratio]. It illustrates the potential advantage of boron compositions which present, for an equivalence ratio of 0.4, a volumetric specific impulse 30–45% greater than the best hydrocarbon-fueled composition included in the figure; and carbon compositions which, together with a low visual signature, have a volumetric specific impulse 12–20% greater than that of the best hydrocarbon-fueled composition. We should add that, within the carbon compositions, we have included carbon black and graphite formulations that are not identical from the point of view of combustion in the chamber of a ramjet. Additionally, hydrocarbon-fueled compositions can be enhanced by the addition of a small amount of metal, carbon or boron.

2.4. MAJOR PROPERTIES OF SEVERAL FUEL-RICH PROPELLANTS

The selection of a fuel-rich propellant is based on various criteria:

- theoretical performances,
- processability,
- mechanical properties,
- safety properties,
- ballistic properties,
- control,
- combustion efficiency,
- signature,
- cost.

Special mention should be made of the capability of modulating the flow rate [14]: it allows us to adjust the combustible flow to the flow of air collected, which varies according to the altitude and the velocity of the missile, in order to remain within a specific range of equivalence ratio. The specification of the ratio of modulation is therefore imposed by the expected flight envelope, speed, and altitude. The more extensive the flight, velocity and altitude envelope, the higher the modulation ratio will have to be. For the trajectory of an air-to-air missile, launched at low altitude, then cruising at high altitude, the range may be increased by over 300% by using a ramrocket with a throttleable gas generator [15].

In the case of the choked gas generator, the modulation of the fuel rate is done by a valve. The modulation ratio can be defined as the ratio of the burning rate at maximum operating pressure for the minimum temperature likely to be encountered by the fuel-rich propellant, versus the burning rate at the minimum operating pressure at the maximum temperature. It is therefore dependent on the pressure exponent (which cannot exceed the value of 0.75 by much for reasons of stability), on the temperature sensitivity coefficient,

and on the operating pressure range, whose highest value is limited by the mechanical strength of the case, and whose lowest value is limited by the stable operation pressure limit of the gas generator, and by the pressure existing in the combustor. The architecture of the valve and the materials it is made of, must be tailored to the particular fuel-rich propellant used, to ensure the valve's resistance to the temperature of the effluents and to prevent obstructions caused by deposits or particles.

The pressure inside an unchoked gas generator is not disassociated from the pressure of the combustor. This means that the grain burns at a pressure directly related to the flight conditions. It is therefore "sufficient" when the fuel-rich propellant has the required ballistic properties to have the fuel flow rate self-adjust to that of the air.

For purposes of illustration, the following sections describe the main properties of a smokeless hydrocarbon-fueled composition, and a boron composition tailored to the operation of a choked gas generator.

2.4.1. Hydrocarbon-fueled composition for a choked gas generator

The major components of hydrocarbon-fueled compositions are a binder, an oxidizer, and sometimes a hydrocarbon filler.

With a given binder, the theoretical performances depend mostly on the nature and the amount of oxidizer. Figure 10 illustrates, in a polybutadiene binder composition, the evolution of the specific impulse and of the volumetric specific impulse versus the amount of ammonium perchlorate. The energetic performances decrease as a function of the oxidizer content; the maximum values correspond to the pure binder.

The combustion of compositions with very low oxidizer content is characterized by the presence after firing of a compact combustion residue in the gas generator. For compositions with an ammonium perchlorate content ratio ranging from 25 to 30 %, the amount of residue in relation to the initial total weight of the grain is usually between 5 and 15 %, depending on the formulation of the fuel-rich propellant. The presence of this residue causes first, a drop in the volumetric specific impulse, mostly due to the decrease of the effective weight of fuel loaded on the gas generator for a given volume. More importantly, the presence of the residue runs the risk of affecting the operational reliability of the gas generator, by obstructing the ejection orifices with fragments breaking away from the main body of the residue.

For these reasons the compositions usually selected today contain an oxidizer amount sufficient to prevent the formation of abundant residue.

The formulation of a hydrocarbon-fueled composition follows various specifications concerning energy level and modulation capabilities. Accord-

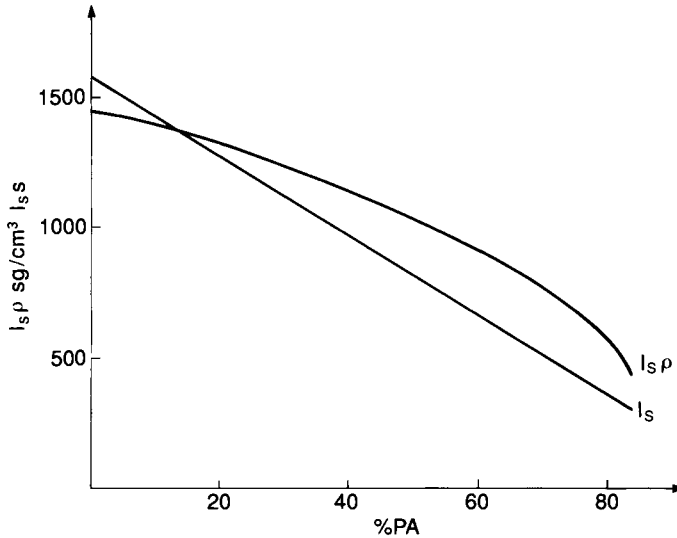
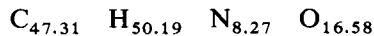


FIG. 12.10. Hydrocarbon fueled compositions influence of the amount of ammonium perchlorate on the theoretical performance ($M = 2$; $Z = 0$; $P = 0.57$ MPa; $\phi = 0.4$).

ing to the type of mission involved and the resulting specifications, the focus is placed on this or that characteristic.

T. D. Myers gives the example of a fuel-rich propellant with extensive modulation capabilities exhibiting a mass flow rate ratio of 1 to 18, for a pressure exponent of 0.55 and a minimum operating pressure of 0.14 MPa [15].

The characteristics described below are those of a hydrocarbon-fueled composition. This composition, which does not contain metal and ammonium perchlorate, is smokeless, but has a low modulation capability. Its basic formula is (1000 g base):



It consists mainly of a polybutadiene binder and an organic oxidizer. Its measured combustion heat is 33 KJ/cm³.

2.4.1.1. Theoretical performance

The temperature inside the gas generator is 1350 K.

The thermodynamic computations for the chamber of the ramjet were made by considering an operational pressure of 0.57 MPa and simulating flight conditions of sea level and Mach number 2.

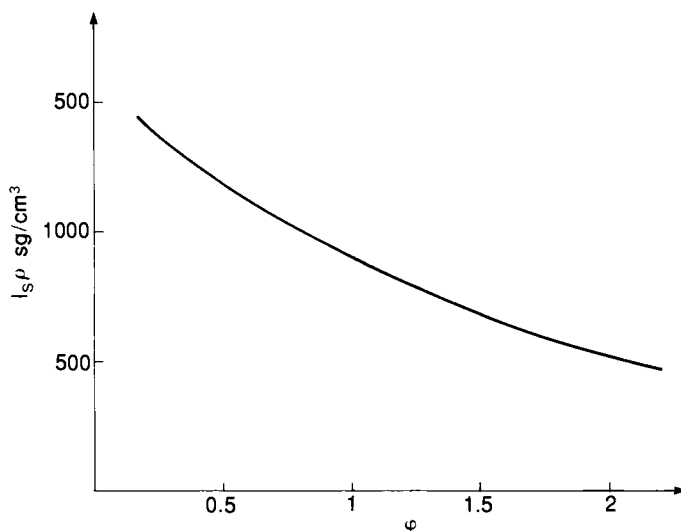


FIG. 12.11. Hydrocarbon fueled composition theoretical performances ($M = 2$; $Z = 0$; $P = 0.57$ MPa).

Figure 11 shows the evolution of the density-specific impulse ($I_s \rho$) versus the equivalence ratio (ϕ).

Figure 12 illustrates the evolution of the temperature as a function of the equivalence ratio. Its maximum value is of the order of 2590 K in an equivalence ratio ranging from 1.1 to 1.35. The stoichiometric fuel-air ratio is 0.143.

2.4.1.2. Processability

Because of its low total solids this composition is very easy to manufacture. The viscosity of the slurry at casting is 2300 poises. Pot-life is excellent: the viscosity is 4400 poises for 12 h after casting.

Consequently, the casting of fuel-rich propellant is very easy, even in the case of grains with very complex shapes. Gravity alone is sufficient to fill the molds, without having recourse to any devices.

2.4.1.3. Mechanical properties

This composition has excellent mechanical properties, also due to its low filler loading ratio. At 20°C, and with a cross head rate of 50 mm/min, maximum stress is 0.8 MPa, the elastic strain 52%, and the strain at maximum stress 120%.

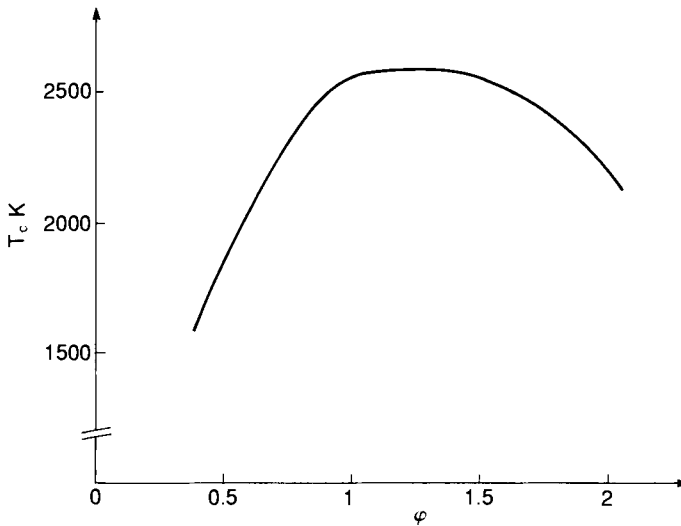


FIG. 12.12. Hydrocarbon fueled composition theoretical combustion temperature in air.

2.4.1.4. Safety properties

Table 5 lists the sensitivity characteristics in accordance with the operational modes described in Chapter 7.

2.4.1.5. Ballistic properties

The burning rate at 5 MPa is 3.8 mm/s. The pressure exponent is 0.45, providing a mass flow rate ratio of 3.8 at 20°C between 0.7 and 15 MPa. The evolution of the pressure curve versus time indicates low-amplitude pressure fluctuations at low pressure.

The modulation ratio between -40°C and 60°C is 3 (Fig. 13).

TABLE 5 Hydrocarbon fueled composition: safety properties

Tests	Results	
Impact sensitivity (30 kg fall-hammer)	Height of non-propagation of violent reaction	≥ 4 m
	Height of non-reaction to impact	2 m
Sensitivity to friction (Julius Peters)	Coefficient of sensitivity to friction	0% at 353 N
Cook-off	Critical temperature	220°C
Card gap test	Number of cards	110

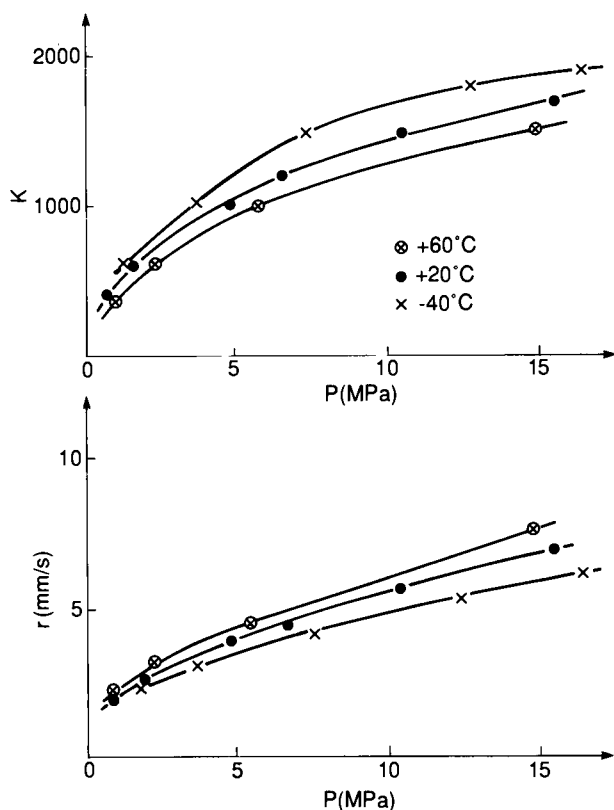


FIG. 12.13. Hydrocarbon fueled composition ballistic properties.

2.4.1.6. Combustion efficiency

The composition has been evaluated in a combustor with 200 mm diameter and four lateral air intakes, simulating a flight speed of Mach 2 and an altitude of 1.5 km.

The gas-generating grain operates at an average pressure of 3.2 MPa and releases 0.250 kg/s for 47 s. The equivalence ratio is 0.38. The combustion efficiency, which is defined as the ratio between the burned gas mass flow rate and the injected gas mass flow rate, is 0.91.

2.4.1.7. Signature

This composition, which does not contain metal and ammonium perchlorate, is smokeless.

2.4.2. Boron composition

Boron composition consists mostly of a binder, ammonium perchlorate, fine boron and sometimes one of several additives designed to facilitate the combustion of the boron.

The boron composition, described here, was selected on the basis of its processability, its mechanical properties, and its operational characteristics in a gas generator. It does not correspond to the higher energetic performances that may be obtained with this type of formulation. It is designed to operate in a choked gas generator.

2.4.2.1. Theoretical performances

The theoretical performance of these compositions depends greatly on the amount of boron. For a 25% content of ammonium perchlorate, the volumetric specific impulse changes, according to our standard calculations ($P = 0.57$ MPa, $M = 2$, $Z = 0$, $\phi = 0.4$), from 1778 to 2028 sg/cm³ (i.e. a 14% increase), when the amount of boron increases from 40 to 50%.

Figures 14 and 15 show respectively the evolution of the volumetric specific impulse and the combustion temperature versus the equivalence ratio for the above composition. The peak temperature is at an equivalence ratio of 1.15.

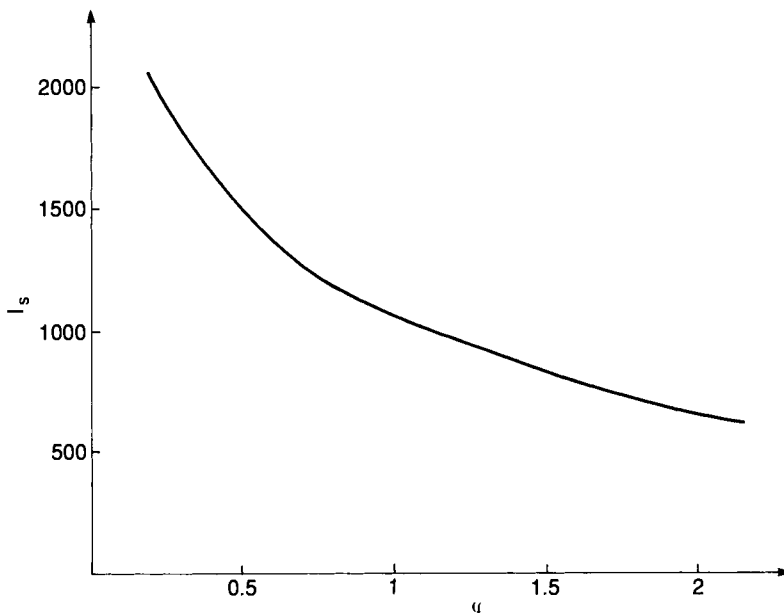


FIG. 12.14. Boron composition theoretical performances ($M = 2$; $Z = 0$; $P = 0.57$ MPa).

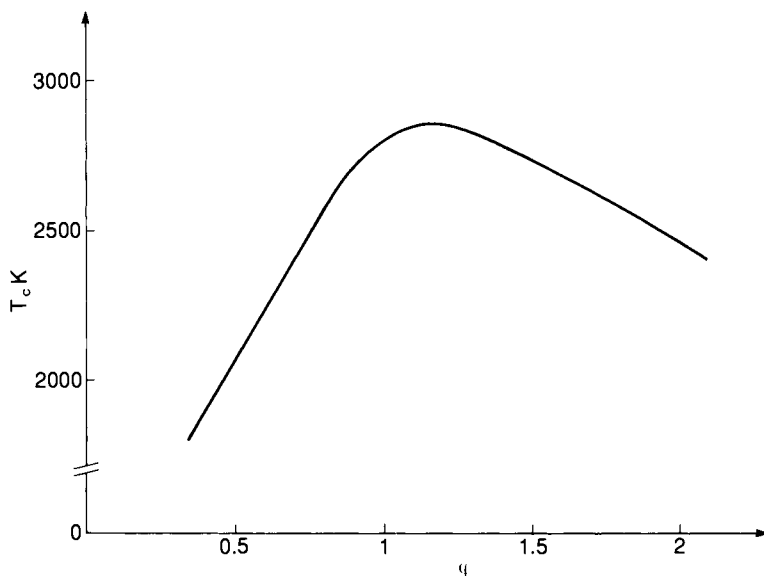


FIG. 12.15. Boron composition theoretical combustion temperature in air.

The temperatures obtained are much higher than with hydrocarbon-fueled compositions.

2.4.2.2. *Processability*

The manufacture of boron compositions with good mechanical properties is made somewhat difficult by the chemical reactions between impurities usually coating boron and the constituents of the binder, requiring a definition of the specification for the raw material, and the creation of a specially designed method for the mixing operation. Once this has been done, the manufacturing qualities and the mechanical properties are highly satisfactory. The viscosity of the slurries at casting is between 10000 and 15000 poises. The manufactured grains are end-burning. They are manufactured using the casting and gravity process.

2.4.2.3. *Mechanical properties*

In terms of the mechanical properties for the binder, the maximum stress is between 1.8 and 2.4 MPa, and the strain at maximum stress is between 37 and 44%.

2.4.2.4. *Safety properties*

These properties are shown in Table 6.

TABLE 6 *Boron composition: safety properties*

Tests	Results	
Impact sensitivity (30 kg fall-hammer)	Height of non-propagation of violent reaction	≥ 4 m
	Height of non-reaction to impact	2.5 m
Sensitivity to friction (Julius Peters)	Coefficient of sensitivity to friction	0% at 253 N
Cook-off	Critical temperature	187°C
Card gap test	Number of cards	≤ 1

2.4.2.5. Ballistic properties

The compositions shown in Fig. 16 burn at a pressure of 5 MPa between 10 and 15 mm/s. They produce no combustion residue, but leave in the gas generator slag with a mass corresponding to less than 1 % of the initial mass of the grain. The compositions discussed here have low-pressure exponents, smaller than 0.1 when the pressure exceeds 3 MPa.

Because the boron compositions are heavily particle-laden they show a high propensity to create obstructions in the nozzle, resulting in pressure evolution curves versus time that are progressive. Two factors have influence

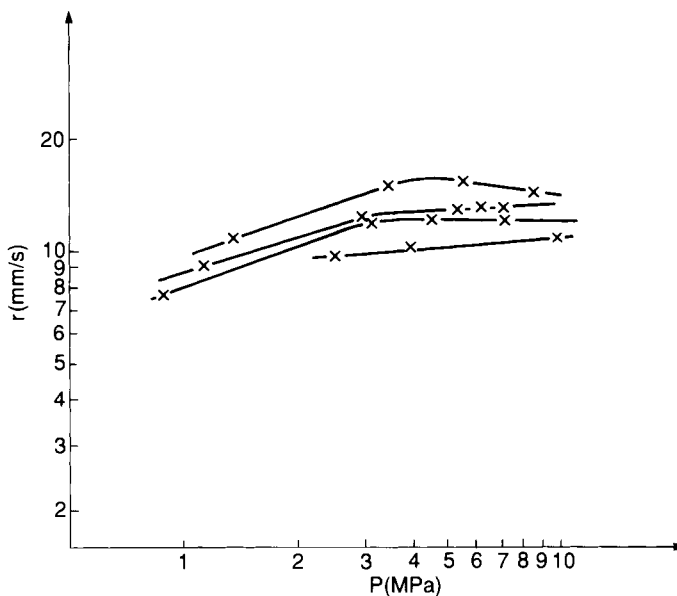


FIG. 12.16. Boron composition ballistic properties (end burning grain—90 or 117 mm diameter).

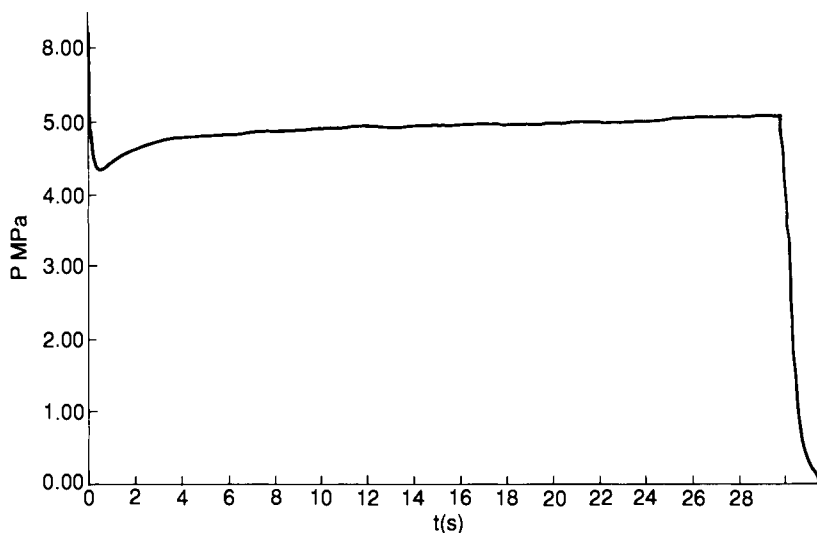


FIG. 12.17. Boron composition static test-end burning grain (177 mm diameter; 300 mm length).

on this phenomenon: one is the internal architecture of the gas generator, and the other is the formulation of the fuel-rich propellant. Figure 17 shows the recording of a firing corresponding to an optimal configuration.

2.4.2.6. Combustion efficiency

For reasons briefly discussed in the preceding section, obtaining high combustion efficiency in a combustor is difficult, and requires a careful organization of the flows inside the combustion chamber.

The research done by K. Schadow [16,17] and S. W. Abbott, L. D. Smoot and K. Schadow [18] demonstrated that because the temperature in the gas generator is generally lower than the 1950 K ignition temperature of boron, good combustion efficiency can be attained only when the gas generated by the composition burn with the air at sufficiently high equivalence ratio levels to produce a temperature high enough to guarantee that the heated boron particles will be able to ignite. They have also demonstrated that combustion efficiency drops when the pressure of the combustor decreases.

C. Vigot, L. Bardelle and L. Nadaud [10] have studied the combustion of a fuel-rich propellant with 35% boron. They demonstrated that the combustion efficiency can be improved by injecting the fuel at the forward end with converging jets, and by introducing only a portion of the air close to the forward end. This arrangement creates an area where the temperature

attained is sufficiently high to guarantee the ignition of the boron, since the ratio of the fuel-air mixture is close to the stoichiometry. The remainder of the air is injected downstream. It is important that the distance separating these two injection planes not exceed a certain specific value. This value depends on many factors such as the geometry of the air intake connections in the combustion chamber, and the distribution of the velocity of the air.

2.4.2.7. *Signature*

Because the boron compositions are heavily particle-laden, they are smoky.

3. Boosters for Integral Rocket Ramjets

Ramjets and ducted rockets are accelerated to or above the minimum required takeover speed by a solid propellant booster [19–22]. Three basic configurations are generally described: externally mounted boosters, whether permanent or droppable, tandem rocket ramjet and integral rocket ramjet. The integral rocket ramjet concept permits the overall missile dimensions to be minimized and so has significant drag, weight and volume advantages when compared to the two other configurations. There are also disadvantages to the integral concept. Specifically, the booster and the combustor share a common chamber. This requires that additional design emphasis be placed on the propellant booster grain, the ramburner thermal protection and the bonding of the grain to the thermal insulator.

The booster operating pressure is between 7 and 14 MPa and the ramjet operates under 1 MPa. The case is fabricated to withstand the high booster pressure and the thermal protection must resist the case mechanical deformation induced during the booster phase. The booster requires a smaller nozzle throat area than the ramjet due to the order of magnitude difference between the ramjet and the booster operating pressures. Two configurations can be used: ejectable nozzle system and nozzleless booster.

The booster is sized to accelerate the missile from ground or air launch speed to a velocity at which ramjet thrust exceeds drag by some margin. The Mach number for ramjet takeover is generally between 1.5 and 2.5.

For a given diameter, this requirement dictates a minimum grain length. Generally, this length exceeds the value required to reach the required ramjet combustion efficiency. This is true even for missiles launched from aircraft. One notable exception is the boron propellant ducted rocket. For a given ramjet configuration, greater booster length results in a shorter fuel tank and therefore a shorter range. According to Myers [19], a 1% increase in propellant grain length could result in a 5–10% loss in vehicle range. Thus a high volumetric specific impulse propellant and a high volumetric ratio grain are important requirements.

It is necessary to restrict drag losses during the booster phase. Consequently, the grain operating time is minimized within the limits dictated by the maximum acceleration allowed by the missile. The grain burn time is generally between 3 and 6 s. Therefore, medium-to-high burning rate propellants are required for boosters.

The thermal protection of the case must withstand heat during the booster and the ramjet phases. During the booster phase the combustion gases are reduced and are produced at temperatures up to 3600 K and pressures up to 14 MPa, but gas velocities and operating times are short. In the ramjet the temperature and the pressure are much lower, but the gases are oxidizer-rich and velocities can reach 300 to 340 m/s with operating times between several tens and several hundred seconds. In order to reduce inert weight and volume, thermal protection thickness is limited.

The different thermal protection concepts are discussed in Chapter 13.

During the transition phase the rocket motor transforms itself to a ramjet combustor (Figure 2). The vehicle drag forces are high and the missile quickly slows down. According to Myers [19] typically slowing down is about 0.1 Mach number per second. Therefore, transition must be done swiftly. Energy is released after booster operation by the combustion of propellant grain slivers, part of liner and decomposition products resulting from booster heating. The fuel injection and its ignition must be timed so that the total energy released does not cause excessive combustor pressure increase which would result in inlet unstart. Shortening the transition phase requires that careful attention be focused on residual booster materials and the careful shaping of booster burning profiles at the end of operation. Consequently, the transition phase dictates new requirements for the booster grain:

- Sliverless grain, although grain slivers always exist to some extent, caused primarily by dimensional tolerance variations during manufacture.
- Minimum liner thickness. One technical answer to direct bonding is described in Chapter 13.

The nozzleless booster represents an alternative concept to the ejectable nozzle system [23,24]. The advantages of this design are indicated in Chapter 2. This configuration places additional requirements by comparison with the nozzled motor design:

- the burning rate must be higher,
- the stress capacity at the high operating temperature must be raised to avoid grain damage under the shear loads caused by the pressure difference between the head-end and the aft-end,
- small pressure exponent — lowering the pressure exponent permits a significant performance increase. According to Procinsky and McHale [23], lowering the pressure exponent from 0.48 to 0.28 induces a 3.0% increase in total impulse.

The booster propellants are generally of the high-energy aluminized composite type as low visual signature is not required (Chapter 10). The formulations are optimized to achieve the mechanical properties suitable for a case-bonded grain. They include a liquid or a solid burn rate catalyst to achieve the required burning rate (between 20 and 35 mm/s at 7 MPa). An alternative propellant composition is one which employs zirconium. The interest in zirconium is due to its high density (6.49). Typical compositions include an HTPB binder, ammonium perchlorate and high loading of zirconium (up to 45%). Typical zirconium propellants possess lower specific impulse, higher density and higher volumetric specific impulse than typical aluminized formulations.

Aluminum and zirconium compositions show some ballistic property differences. The specific impulse efficiency losses for zirconium-loaded compositions are more important than those for aluminum compositions. Also zirconium propellants show greater sensitivity to motor scaling effects [25]. Nevertheless, the substitution of an aluminum composition by zirconium formulation in a given configuration grain would induce a shorter but heavier booster [23]. Another disadvantage of zirconium composition is the relatively high cost of zirconium.

Bibliography

1. MARGUET, R., ECARY, C. and CAZIN, P., Studies and tests of rocket ramjets for missile propulsion, 4th International Symposium on Airbreathing Engines, Orlando, AIAA paper no. 79.7037, 1979.
2. WANSTALL, B., Statofusées pour Longs Parcours à Vitesse Supersonique, *Interavia*, **12**, 1331-1334, 1984.
3. WANSTALL, B., Slat the Mach 3 Target to Test Ship's Defences, *Interavia Aerospace Review*, **44**(3), 242, 1989.
4. MYERS, T. D., Special problems of ramjet with solid fuel, ramjet and ramrocket propulsion systems for missiles. AGARD Lecture Series no. 136, pp. 6.1-6.9, 1984.
5. BESSER, H. L., Solid propellant ramrockets, ramjet and ramrocket propulsion systems for missiles. AGARD Lecture Series no. 136, pp. 7.1-7.30, 1984.
6. COHEN, N. S., Combustion considerations in fuel-rich solid and hybrid propellant systems in airbreathing propulsion. AIAA 6th Aerospace Sciences Meeting, New York, AIAA Paper, no. 68-96, 1968.
7. MCCLENDON, S. E., MILLER, W. H. and HARTY, C. M., Fuel selection criteria for ducted rocket application. AIAA paper, no. 80-1120, 1980.
8. MACEK, A. and MCKENZIE SEMPLE, J., Combustion of boron particles at atmospheric pressure, AIAA 5th Propulsion Joint Specialist Conference US Air Force Academy, Colorado, AIAA paper no. 69-562, 1969.
9. KING, M. K., Ignition and combustion of boron particles and clouds. *Journal of Spacecraft*, **19**(4), 294-306, 1982.
10. VIGOT, C., BARDELLE, L. and NADAUD, L., Improvement of boron combustion in a solid-fuel ramrocket. AIAA/ASME/SAE/ASEE, 22nd Joint Propulsion Conference, Huntsville, AIAA paper no. 86-1590, 1986.
11. SZEKELY JR, G. A. and FAETH, G. M., Combustion properties of carbon slurry drops. *AIAA Journal*, **20**(3), 422-429, 1982.
12. UBHAYAKAR, S. K. and WILLIAMS, F. A. Burning and extinction of a laser-ignited carbon particle in quiescent mixtures of oxygen and nitrogen, *J. Electrochem. Soc. Solid-State Science Technol.*, **123**(5) 747-756, 1976.

13. SMITH, I. W., The intrinsic reactivity of carbons to oxygen, *Fuel*, **57**, 409–414, 1978.
14. THOMAIER, D., Speed control of a missile with throttleable ducted rocket propulsion. 44th Symposium in Air-Launched Weapons, Guidance and Control, AGARD Conference Proceedings 431, pp 24.1–24.15, 1987.
15. MYERS, T. D., *Moteurs à Statoréacteurs/Fusée à Combustibles Solides*. Armada International, no. 3, pp. 122–125, 1984.
16. SCHADOW, K., Boron combustion characteristics in ducted rockets. *Combustion Science and Technology*, **5**, 107–117, 1972.
17. SCHADOW, K., Study of gas-phase reactions in particle-laden, ducted flows, *AIAA Journal*, **11**(7), 1042–1044, 1973.
18. ABBOTT, S. W., SMOOT, L. D. and SCHADOW, K., Direct mixing and combustion efficiency measurements in ducted, particle-laden jets. *AIAA Journal*, **12**(3), 275–282, 1974.
19. MYERS, T. D., Integral boost, heat protection, port covers and transition, ramjet and ramrocket propulsion systems for missiles. AGARD Lecture Series no. 136, pp. 4.1–4.20, 1984.
20. WEBSTER, F. F., Liquid fueled integral rocket ramjet technology. AIAA/SAE 14th Joint Propulsion Conference, Las Vegas, AIAA paper no. 78-1108, 1978.
21. BUTTS, P. G. and MYERS, T. D., Integral booster motor interface requirements. AIAA/SAE 14th Joint Propulsion Conference, Las Vegas, AIAA Paper 78-1060, 1978.
22. MARGUET, R. and CAZIN, PH., Ramjet research in France: realities and perspectives. 7th International Symposium on Air Breathing Engines, Beijing, 1985.
23. PROCINSKY, I. M. and MCHALE, C. A., Nozzleless booster for integral-rocket-ramjet missile systems. *Journal of Spacecraft*, **18**(3), 193–199, 1981.
24. NAHON, S., Nozzleless solid propellant rocket motors: experimental and theoretical investigations. AIAA/SAE/ASME 20th Joint Propulsion Conference, Cincinnati, AIAA Paper no. 84-1312, 1984.
25. COUGHLIN, J. P., Impulse efficiency correlations for aluminum and zirconium propellants, AIAA/SAE/ASME, 17th Joint Propulsion Conference, Colorado Springs, AIAA paper no. 81-1381, 1981.

CHAPTER 13

Thermal Insulations, Liners and Inhibitors

JEAN-MICHEL TAUZIA

1. Inhibiting Materials and Thermal Insulation in Solid Propulsion

The function of a rocket motor is to deliver a thrust according to a predetermined program.

With solid propellant rocket motors, theory allows us to relate the thrust law required by the designer to the evolution versus time of the burning propellant surface [1,2].

The evolution of that surface depends heavily on the presence of organic materials adhering strongly to the propellant. These materials, called combustion inhibitors, limit the initial combustion surface so that the combination of the grain geometry and the combustion law of the propellant results at any instant in the desired thrust.

To completely fulfill their role the inhibitors must present a whole set of characteristics which will be described in detail later in this chapter. The most important is an excellent bonding to the propellant. This property is essential for the reliability of the rocket motor, because any debonding between the inhibitor and the propellant results almost invariably in a failure of the rocket motor due to an uncontrolled pressure rise.

Other inert materials are often present in the combustion chamber, ensuring such functions as the bonding of the propellant with the wall of the motor case (liner), or the thermal insulation of case surfaces exposed to the hot gases (thermal protection).

In the following pages we will use the term "insulating materials" for these various materials (inhibitors, restrictors, liners, thermal protections) illustrated at figure 1.

Very strong interactions take place between the design of the grain, the propellant and the various insulating materials. Consequently, the properties of the latter have a significant influence on performance, service life and cost of rocket motors.

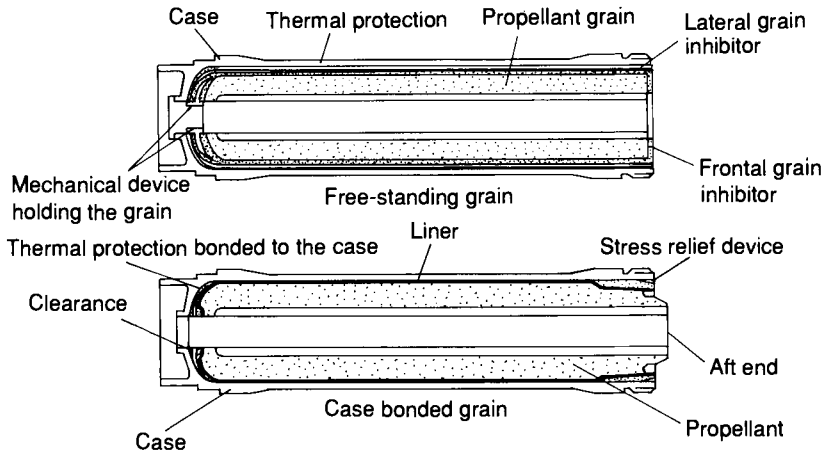


FIG. 13.1. Configuration of a solid propellant rocket motor (without nozzle).

2. Background

2.1. SPECIFICATIONS OF INSULATING MATERIALS

The insulating materials must satisfy many specifications difficult to quantify. They include, but are not limited to:

- Sufficient bonding within the entire range of working temperatures of the motor.
- Low ablation rate, to minimize the inert mass on board. At the same time the resulting “char” must remain porous: the decomposition gases must exhibit a low molecular mass, the pyrolysis of the material must not lead to emission of smoke or flashes.
- Low thermal conductivity.
- High specific heat.
- Low density.
- Mechanical strength compatible at all temperatures with the deformation of the grain during the various manufacturing and storage phases, or with those deformations resulting from various thermal and mechanical stress to which the rocket motor is subjected in the course of its life including, of course, firing.
- Pyrotechnic compatibility with the live constituents of the motor (propellant, ignition powder).
- Sufficient electric conductivity to avoid electric charge build-up.
- Chemical compatibility with the components of the motor: the insulating materials must not upset the chemistry of propellant but maintain the nominal characteristics of the latter.
- Good gas permeability.

- Low humidity absorption.
- Good aging characteristics.

2.2. THEORETICAL DATA REQUIRED FOR THE DESIGN OF INSULATING MATERIALS

The development of insulating materials for rocket motors calls for deep knowledge in multiple fields of studies, such as chemistry, thermodynamics, mechanics, optics and many other branches of physics.

Because of their particular importance for the work of the rocket motor only some aspects, related to the mechanisms of the adhesion, ablation and emission of smokes, are discussed in the following sections.

2.2.1. *Fundamentals of the mechanisms of adhesion*

In spite of the large number of studies dealing with the phenomenon of adhesion during the past 40 years, the basic laws are relatively poorly known and there is no unified theory capable of explaining the entire set of phenomena [3,4].

One of the major difficulties is that adhesion is a multidisciplinary subject requiring the collaboration of experts in the field of chemistry of polymers, the physical chemistry of surfaces, the strength of materials, the mechanics of fracture, and more. In addition, the number of parameters involved in a theoretical modeling exceeds by far the analyses and computation capabilities.

In spite of these somewhat pessimistic premises, bonding theories have emerged. However, we must not forget that their scope is limited and that their capability of prediction does not extend beyond a few typical and particular fields.

2.2.1.1. *Mechanical model*

MacBain was the promoter of a mechanical model where the adhesion is due to a fixing of the bonding agent to the roughness of the substratum. MacBain's research was done more specifically for the bonding of wood, and although his model is in general no longer used, it is regaining interest because of the recent research of Wake.

Broadly speaking, the roughness of the substratum is only a favorable factor inasmuch as the wetting is sufficient. When that is not the case, the portions that have not been wetted form the start of a break themselves. In terms of adhesion between the liner and the propellant, mechanical linking is used when adhesion is difficult, such as with propellants with low chemical reactivity (cast double-base) or those which are highly plasticized (CMDDB).

2.2.1.2. *Electrical model*

In 1948, Deriyagin and Krotova proposed a theory of adhesion based on electrostatic phenomena observed during plucking tests on adhesives. Skinner developed a similar theory in 1953. According to his theory, the system constituted by the bonding agent and the substratum is compared to a capacitor. For example, with an organic bonding agent and a metallic substratum the metal can play the role of the electron donor and the polymer that of the receiver, leading to the formation of a double electric layer.

The difficulties in developing a theory explaining the origin of the electric charges are due to a lack of information about the levels of energy and about the process of conduction in the polymers.

Although experimental work seems to confirm the validity of this model, it is seriously criticized, and many authors agree in their opinion that the electric effects observed are the consequence rather than the cause of a high level of adhesion.

2.2.1.3. *The diffusion model*

The Russian researcher, Voyutskĭ, originated a theory according to which the adhesion results from the diffusion of the molecules of the surfaces in contact, creating a transition layer between the substratum and the bonding agent. The plane interface is replaced by a spatial interphase. The reciprocal solubility of the materials constituting the assembly is a primary condition for obtaining a good bonding. Voyutskĭ suggests, in addition, use of the adhesion as a criterion for the thermodynamic compatibility of the polymers, the best example of perfect compatibility being the self-adhesion of crude rubber to itself, where the interface is quickly impossible to distinguish.

With this model the classic parameters of diffusion influence bonding strength, including time, pressure, temperature, steric configuration of the diffusing products and the crosslinking density of the substratum and, in the case of polymers, they are the structural characteristics such as molecular mass, morphology and crystallinity.

While the diffusion phenomenon is certainly important in the case of self-adhesion, and for the bonding of polymers, it is difficult to imagine its contribution in the case of bonding polymers to glass or metal. Schonborn and Juntzberger, without refuting the existence of diffusion phenomena, feel that they are subordinated to the process of putting in close contact, at the molecular level, the materials to be bonded.

2.2.1.4. *Wetting model*

In 1963, based on thermodynamic considerations and on the research done by Zisman on the critical tension of the wetting of solids, Good, Fowkes and Dann, and Sharp and Schonborn, developed and proposed a new model.

Since the bonding forces have a field of action on the order of the molecular distances, a good bonding is created by an intimate contact between the adhesive and the substratum, such a contact allowing the development of these forces. This is in the occurrence, a criterion of proximity, involving the cleanliness of the surfaces and a perfect wetting.

In this model the bonding energy can be determined, based on the surface energies of the solids to be bonded and considering the wetting to be ideal. Calculated in this manner, the bonding energy corresponds to the energy of formation of the assembly. Experimentally, the debonding energy is often considerably greater.

2.2.1.5. Chemical model

Chemical adhesion involves chemical valence bondings between the adhesives and the substratum. In spite of the obvious interest offered by this type of mechanism, few studies have been done. It is true that demonstrating the chemical reactions at the interface is particularly difficult.

As far as the bonding to propellant is concerned, it is noteworthy that theories of chemical bonding are widely used to create specific molecules known commonly as bonding promoters. These reactive products, exhibiting low molecular mass, are carefully selected and introduced into the inhibitor. They diffuse towards the interface where they react with the polymer of the propellant to create stable chemical bondings, provided the wetting has been done correctly.

2.2.1.6. Model of the interfacial layer with weak cohesion

Bikerman, the author of this model, assumes that the probability of seeing a rupture propagate itself exactly at the interface between the adhesive and the bonded material is extremely low. From this premise it can be deduced that the debonding occurs either in the adhesive or in the bonded material. In fact, according to Bikerman, and more recently also to Sharpe, there is another possibility: that of a debonding propagating itself in an interfacial layer with weak cohesion. These authors distinguish several layers with weak cohesion:

- a first layer consisting of air continues to exist at the interface (imperfect wetting);
- other layers formed when foreign substances with low molecular mass, contained in the adhesive or the bonded material, migrate to the interface;
- yet other layers coming from a reaction between the atmosphere of the ambient medium (humidity for instance) and the bonded material, or the adhesive.

Although Bikerman's analysis is also contested, it allows an explanation of a number of observations made in the field of bonding. In particular it clarifies greatly the role of water vapor absorbed by most of the surfaces.

As for the bonding of propellants on to combustion inhibitors, when combined with the theories of the diffusion and chemical bonding, Bikerman's analysis allows the establishment of a conceptual frame within which the technology used to perform the different bondings in rocket motors can be developed.

2.2.2. *Fundamentals of the thermal protection process through ablation*

If the combustion chamber were to be directly exposed to the propellant combustion gases, the weakening of the structure would lead unavoidably to a rupture by bursting.

Should the inhibitors not play their role, the rapid heating of the propellant would bring on an uncontrollable increase of the burning surface, with consequences similar to those mentioned above.

In practice, the combustion chambers and the propellant grains must be thermally protected against all excessive heating during the operation of the motor. To provide this protection, organic materials coming into contact with hot gases (2000–4000 K) protect the underlying areas through a complex endothermic decomposition mechanism generally known as protection by ablation [5–8].

The temperature of the thermal protection rises by conduction until it reaches its decomposition temperature by pyrolysis. This initiates highly endothermic chemical reactions leading to the creation of gas and leaving a sooty deposit, more or less porous, called "char".

A steady state establishes itself between the combustion gases and the material in the process of pyrolysing. The pyrolysis front regresses. Once this regression is finished, the heat absorption mechanism by thermal decomposition ceases. Only the char, inasmuch as there is any, continues to participate, by conduction and radiation, in the protection of the underlying material.

It is important to note that these materials have a low thermal conductivity which, combined with the short firing times, decreases the heating by conduction of the protected parts.

2.2.2.1. *Examples of experimental test used to evaluate the thermal characteristic of insulating materials*

Several experimental systems are commonly used to compare the materials among themselves or to measure the physical values necessary for modeling the rate of ablation by computer analysis, using specially developed numerical programs.

“*Extension firing*” (using an “exhaust pipe”). The tested materials are placed in a pattern of a hexagonal base cone. They are mounted in pairs in order to limit the dispersions caused by variations of the flow (Fig. 2).

Analysis of these results allows us to plot the ablation curves for a given propellant, linking the ablation rate to the average speed of the flow of the gases. These curves can be plotted for specific chamber temperatures, nature of gases and time of exposure.

Firing of end-burning grains. With the end-burning grain system the ablation can be measured on very low gas flow rates and for long firing times, which is not feasible with exhaust pipe firing. Analysis of the tests results in a curve linking the ablated thickness to the firing time.

The plasma torch. The plasma torch is also used. It allows us to know the behavior of different materials.

Finally, conventional differential thermal analysis (determination of the ablation enthalpy) and thermogravimetric analysis permit the completion of the data used to predict the ablation rate, thanks to numerical programs.

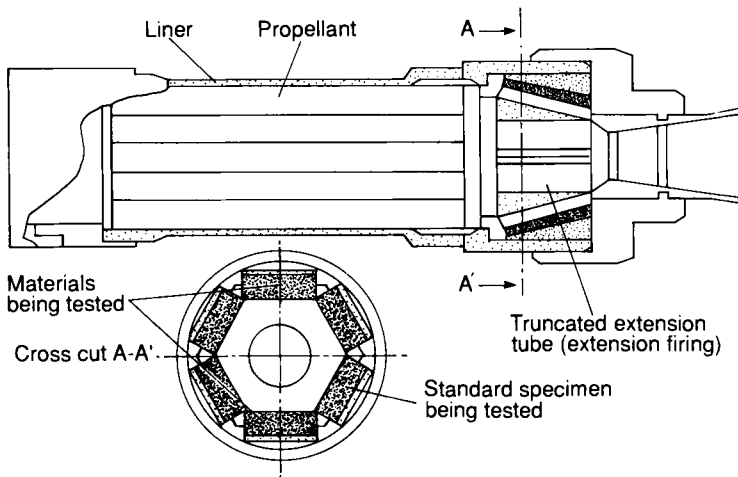


FIG. 13.2. Firing test designed to evaluate the ablation rate of thermal insulations.

2.2.3. *Fundamentals of optical phenomena related to the operation of a rocket motor*

The emission of smoke or flashes by rocket motors is a critical factor for many missile systems [9,10]. The release of smoke reveals the location of the launcher. A smoke trail makes the trajectory of the missile visible at great distances, giving the target the possibility of escape. For wire-guided missiles the plume greatly reduces visibility conditions. The presence of solid particles in the plume may hinder the functioning of the guiding device. The presence of flashes may interfere with tracking systems located on the firing pad.

2.2.3.1. Fundamentals of the smoke phenomena

Smoke may be defined as a condensed liquid or solid phase, in suspension in air. There are, usually, two categories:

- condensation smoke;
- dispersion smoke, formed by the subdivision of very fine particles.

In rocket propulsion the dispersion smoke composed mainly by metallic or refractory particles results from the combustion of the propellant and the pyrolysis of the insulating materials, while condensation smoke comes from low-mass organic molecules existing as vapor in the plume that condenses during the rapid cooling following expansion of the gases in the nozzle.

2.2.3.2. Visibility of an object as a function of the contrast

The visibility threshold of an object is usually expressed in terms of contrast. When an object moves away from the observer, the contrast decreases because of atmospheric absorption. At a fixed distance between the observer and the target, when the luminosity increases, the contrast also increases because the target is more luminous than its background and the opposite occurs when the target is less luminous. Consequently, the plume of a missile is more or less visible whether the missile flies over grassy ground, the sea, or toward the sky.

2.2.3.3. Opacity of the smoke

Visibility of an object through a smoke plume varies according to the manner in which the particles reflect, diffuse or absorb light. The main parameters are morphology, size and density of particles, refraction index and wavelength of incident light.

The opacity of the smoke can be reduced by decreasing the number of particles released, as well as their size, until reaching a diameter much lower than the wavelength of the incident light.

2.2.3.4. Duration of the smoke

Experiments, full-size, have demonstrated that losing sight of a target for 1–2 s is sufficient for the launcher to lose control of the missile. Conversely, a rapid dispersion of the smoke — in less than 1 s — may be compatible with efficient tracking systems.

2.2.3.5. Development of smokeless motors

Insulating materials must be considered as potential sources of smoke which are particularly inconvenient when the propellant has been selected on

the basis of its low signature. There are, however, two categories of inert materials with low or no signature:

- Low or no signature materials due to the fact that no particles are ejected: the “particles” released during their pyrolysis are mainly gaseous, or non-condensable, or very small. This goal can be achieved by using organic materials without refractory fillers.
- The highly refractory materials for which solid particles formed during the pyrolysis are few in number and stay in the combustion chamber.

2.2.3.6. Flashes emitted by the rocket motors

These flashes come from the plume made of heated gases released by the nozzle or from reignition (postcombustion), caused by recombination with the oxygen of reducers contained in the gases. Attenuation of the flashes is usually obtained by introducing appropriate ions in the combustion gases, capable of blocking the recombination reactions that involve free radicals (Chapter 5).

These ions may be contained in the propellant itself, or if the design of the motor allows it, in the inert material subjected to a controlled pyrolysis during the operation of the motor.

2.2.3.7. Experimental methods for the measurement of smoke

Because of the complexity of the phenomena involved, experiments have been conducted during the firing of motors consisting of a cylindrical end burning grain, inhibited laterally and on the front-end surface with the material being tested and for which the grain has been carefully selected, based on its own very low signature, previously measured by firing of non-inhibited grains.

The observations deal primarily with the opacity of the smoke. An experimental device, called an opacimeter, allows us to measure the attenuation in the axis of the jet as well as perpendicular to it, while a film is being taken using a luminous background made of selected color patterns.

2.2.4. Combustion of the propellant along the inhibitor

In the vicinity of the bonding of the propellant and the inhibitor a large number of physicochemical phenomena may occur, which influence the burning rate of the propellant. This alteration is felt particularly for end-burning grains where the existence of a local increase of the burning rate

along the inhibitor may have a strong effect on the pressure and thrust curves [1,2]. This burning rate increase may be the result of:

- heating of the propellant under the inhibitor, due to the circulation of heated gases in the clearance between the chamber and the grain;
- segregation of the fine oxidizer particles in the vicinity of the inhibitor, caused by decanting-type mechanisms — this possibility exists only in the case of grains cast in their inhibitors;
- existence in the liner of compounds which are ballistic modifiers (iron oxide);
- existence of vacuums or microscopic cracks;
- alteration of the local composition of the propellant through the migration of mobile molecules towards and from the inhibitor (plasticizers, crosslinking agents, liquid combustion catalysts and others);
- local variations in the radiation density of the flame in the vicinity of the inhibitor.

For instance, if the plasticizer of a propellant can migrate to the inhibitor, the propellant close to the inhibitor appears, locally, richer in oxidizing species. This results in an increase in the burning rate as well as in the pressure exponent, so that the burning rate enhancement grows with propellant temperature and operating pressure of the motor.

To minimize this phenomenon the grain designer selects materials that are impermeable to the mobile components of the propellants and balances, *a priori*, the chemical potentials on each side of the bonding surface. When equilibrium cannot be obtained, he may, on the other hand, introduce into the inhibitor a plasticizer moderating the burning rate of the propellant.

2.2.5. Method of prediction of the aging of the bonding

As with all other components of the rocket motors, the insulating materials must ensure complete operation for the duration of the service life of the motor. Among these, the “bonding” function is certainly the most sensitive to aging.

The aging of the bonding is caused by the development of chemical reactions, complicated by diffusion phenomena. Each of these reactions exhibits an activation energy which, lacking a more precise theoretical model, can be idealized by an Arrhenius-type law. The aging is evaluated by comparisons of results recorded at ambient temperature at various stages with results recorded at moderate temperatures ranging from 40 to 50°C. The raw materials themselves need to be perfectly stable during the period of time considered.

Accelerated aging experiments on complex materials need to be performed with the greatest circumspection because they usually tend to overestimate.

2.2.6. *Pyrotechnical compatibility—selection of the raw materials*

The raw materials of the insulating materials for combustion chambers must be chemically compatible with the energetic ingredients of the propellants (mineral oxides, nitrated plasticizers, explosives, nitramines and others). Two tests are currently performed for this purpose:

- Differential thermal analysis, where the research worker subjects the energetic ingredient, in powder form and in the presence of the material being tested, to a regular increase of temperature. The verdict is made on the basis of the modification of the decomposition temperature of the live ingredient.
- The “vacuum test”, where the tester puts together, in powder form under heat and vacuum, the live ingredient and the inert materials for testing. The verdict is made on the basis of the volume of gas produced as well as on its rate of production.

2.2.7. *Criteria for the selection of raw materials used in the formulation of insulating materials*

There are many considerations that are principal factors in the development of insulating materials to obtain satisfactory mechanical properties, bonding and other design goals, while other data limit the choice of the designer (for example, pyrotechnical compatibility). In particular, the raw materials must satisfy the following conditions:

- guaranteed availability over a sufficient period of time;
- stability over time;
- reproducibility of the production, process including the control of the impurities coming from the raw materials.

2.3. DETERMINATION OF THE CHARACTERISTICS OF THE BONDING PERFORMANCE OF INSULATING MATERIALS

Once the formulation of an inhibitor has been selected, based on the general rules discussed above, it is necessary to determine its performance.

The mechanical characteristics of inert materials are measured: For a rapid determination of these characteristics the tests are performed at ambient temperature, with tensile loading rates of 50 mm/min, while a complete characterization requires the tests to be performed with several loading rates (from 1 to 1000 mm/min) and several temperatures (-40°C , $+40^{\circ}\text{C}$, $+60^{\circ}\text{C}$).

The bonding characteristics are determined by carrying out tensile, shear-ing and peel tests.

We should note here that the bondings between the insulating material and the propellant behave more or less like their constitutive components, and that, as a result, bonding master curves can be plotted.

The methods selected to design a rocket motor are based on results from tensile and shear tests, since all types of loading involved can be reduced into these two basic stress/strain modes. The peel test, on the other hand, although not used in the determination of the stress and strains of the grain, is widely used for two main reasons:

- peeling is a test of resistance to tearing that simulates very well what occurs at the ends of the grain;
- peeling can be considered as an indication of the quality of the bonding.

2.4. OPTIMIZATION OF INSULATING MATERIALS

The formulation's analysis is done by taking into account the rules of the art and previous experience, and also by performing, during the initial phase, various tests using a wide range of parameters likely to provide the desired performance in order to select the most promising results.

This phase may require a long time. It is also the most difficult one because intuition plays an important role. It leads to selection of a family of formulations that is the first approximation of the composition desired.

Two distinct activities will then take place in close relation to each other; one involving the formulation itself and the other the manufacturing processes. When this work is completed, the formulator is able to define the limits of the composition and the acceptable variations of the raw materials and production processes that can be used to maintain constant properties of the material.

A third phase consists in testing the reproducibility and the aging, after which the industrial documentation is completed.

2.5. MOST COMMONLY EXPERIENCED FAILURES

The type of failure most often observed on a rocket motor involves the bonding between the inhibitor or the liner and the propellant. This may be attributed to the significant variability of the materials used and, to an even greater extent, to the variability of the bondings. The latter problem may be accentuated by anomalies occurring during manufacture:

- insufficient prevention against the environment at the time of preparation of the materials and the actual bonding;
- insufficient knowledge of the raw materials, which may contain impurities such as adhesion poisons;

- insufficient knowledge of the solubility and diffusion properties which cause undesirable chemicals (from a bonding point of view) to migrate and localize at the interfaces (live or inert plasticizers);
- insufficient knowledge of the rates at which the bonding develops resulting in premature stresses and strains in the bonding.

To take precautions against such anomalies it is important to perform, at the commencement of the development of an insulating material, full-size experiments, accelerated aging and overtests, complemented by surveys, so that the real results obtained may be compared to the laboratory tests.

2.6. QUALITY INSPECTION OF BONDINGS

The techniques used to create the bondings today are even more similar to an art that has reached a certain level of maturity than they are to an exact science. Consequently, it is not always sufficient to select the raw materials carefully, and to combine them using a strictly defined process to guarantee that all required specifications are met.

The manufacturer must therefore be able to evaluate by non-destructive means the quality of the work done, in order to discover anomalies such as voids, debonding and porosities. There are numerous non-destructive tests that can be applied to bondings, although only two are widely used for industrial applications. These are described below.

2.6.1. *Quality inspection of bondings by X-ray*

X-rays, using mainly the usually small differences in the density of the various materials, are able to detect debonding only when there is some separation between the materials. However, since X-ray systems generally use powerful generators, sensitive emulsions and highly trained operators, a very high proportion of failures are identified. In addition, it is possible to improve the global resolution power of the method by varying the stress condition of the area examined (moderate cooling of the suspect area, for example).

New technology such as image processing or new analysis tools, such as tomography and Compton scattering, may improve the sensitivity and reliability of this quality inspection technique which, in any case, is not capable of differentiating between a good bonding and a poor one. Finally, video radiography, also slightly less sensitive, allows us to increase significantly the productivity of non-destructive inspection operations.

2.6.2. *Control of bondings by ultrasound*

The propagation of ultrasounds inside materials is disturbed when the beam meets an interface or a heterogeneity. Analysis of the signals received

allows us to perform insurance quality of the bondings. This is a fairly complex task and requires both favorable testing conditions, such as the possibility of using a coupling liquid, and experienced operators.

This method is used mostly with small free-standing grains, in addition to X-rays.

3. Processing Insulating Materials

3.1. INHIBITING PROCESS OF FREE-STANDING GRAINS

The most simple process to inhibit free-standing grains is coating them by casting into a mold.

One method widely used with long pot-life materials consists of mixing all the ingredients in a vertical mixer with a bowl fitted out to allow the injection of the uncured insulator into several molds assembled on a plate distributing the inhibitor.

Another method involves casting the grain inside an inhibiting material (inhibiting tube or restrictor) previously shaped, either through the extrusion process (in the case of a thermoplastic material) or by pressure molding, either with a press or in an autoclave (in the case of a rubber material).

Other basic processes are sometimes used, their selection being often dictated by technical or economical constraints:

- Wrapping ethylcellulose tapes on extruded or cast grain of double-base propellant.
- Soaking of propellant grain in an inhibiting solution. This technique is acceptable only for small objects such as the strands used in the strand-burner test.
- Pushing the propellant grain into a mold containing at the bottom an appropriate quantity of uncured inhibitor.
- Spraying on the propellant grain with a material exhibiting appropriate rheological characteristics.

Except for the first process mentioned, these principles have not been widely developed in the industry.

3.2. PROCESS OF PREPARATION OF THE CASES FOR CASE-BONDED GRAINS

A case-bonded grain includes, in addition to the case, thermal protection, liner and devices designed to accommodate the nozzle.

The application of the liner will be described in detail, while only brief indications will be given concerning the thermal protection.

3.2.1. *Fitting the thermal protection into the case*

For metallic motor cases the thermal protection components, consisting of polymers reinforced with cooling or refractory fillers, are molded in their final form and then bonded inside the case. The adhesives used must give the bonding characteristics required and also be easy and foolproof to apply.

When the cases are obtained through filament winding, the composite is frequently wound around a destructible mandrel coated with the uncured thermal protection. The entire assembly is placed in an oven, both to polymerize the composite and to cure the thermal rubber.

The thermal insulation is often provided with stress relief devices designed to reduce the stresses in the bonding surfaces of case-bonded grains. These features are also known as relief flaps.

3.2.2. *Preparation of the case and the liner*

3.2.2.1. *Inspection of the cleanliness and dryness of the thermal insulation*

It is necessary, to obtain a good bonding, to proceed to the coating on a clean surface.

Wetting tests reveal possible pollution of the surface. In such a case, cleaning (grease removal) operations must be performed again, involving if necessary a mechanical sandblasting before continuing the equipment of the case.

Another important point is the complete absence of humidity. The presence of water may hinder the bonding of the liner to the thermal protection, and later on, also of the propellant to the liner.

3.2.2.2. *Preparation of the liner*

The preparation of the liner can be made in one step (one shot) in a mixer of a type similar to those used for the mixing of the propellant. Such a technique is possible only when the pot-life of the liner is sufficient to allow all sequences of the laying process to be completed. For this purpose, the use of "blocked catalysts" is particularly well-indicated [13,14], or better yet, the use of a blocked curing agent which is thermally activated [15].

The use of liners diluted in a solvent artificially increases the pot-life and facilitates the spraying. Attractive in principle, this process allows only the spraying of thin layers.

The liner may also be prepared in the form of a material with two components which are mixed at the last moment at the site of coating, using precision automatic feeding equipment. The control of the flow rate of the components requires a high and instantaneous precision. Although many

quantity measuring and mixing machines exist on the market, few of them offer the required characteristics and they need to be adapted to meet specific requirements: flow control with the required level of precision, for limited rates of throughput of the order of 50 g/min, while keeping track of the data of operations already performed. The combined use of sufficiently sensitive gages and computer controls allows these requirements to be satisfied [16,17].

3.2.3. Application of the liner to the cases

3.2.3.1. Coating the liner by centrifugation

The principle of the centrifugation process consists of introducing the liner in a liquid state at the bottom of the case and proceeding to polymerization by subjecting the case to a rapid spinning, which plates the liner against the wall of the motor. The operation, thanks to specially designed machines, can be performed for the cylindrical motor case and the front- and aft-ends. Today, this process is being replaced by spraying, which allows reduction of the inert mass involved, and improvement of the propellant mass fraction of the motor.

3.2.3.2. Coating the liner by spraying

The “spraying process” involves spraying the liner in a liquid state in fine droplets onto the inner surface of the case before the crosslinking reaction has taken place. The spraying system, and if necessary the case, must be activated to be moved in relation to each other to ensure that the required thickness of layers of liner is deposited at the right places.

Many systems are used in the industry for the spraying of liquids:

- blowing by compressed air of a liquid jet: pneumatic spraying (Fig. 3);
- sudden expansion of liquid under pressure: airless spraying;
- blowing by centrifugal force with a device such as a disk or a bowl spinning at high speed (Fig. 4).

The blowing of the product can be facilitated with the use of a device generating electrostatic charges: “electrostatic spraying heads”.

The liner spraying systems are derived from commercial equipment. However, it was necessary to redesign them completely to adapt them to using uncured liners exhibiting extremely high viscosities. At the same time they were miniaturized, so that today it is possible to coat cases with an insides diameter of 40 mm.

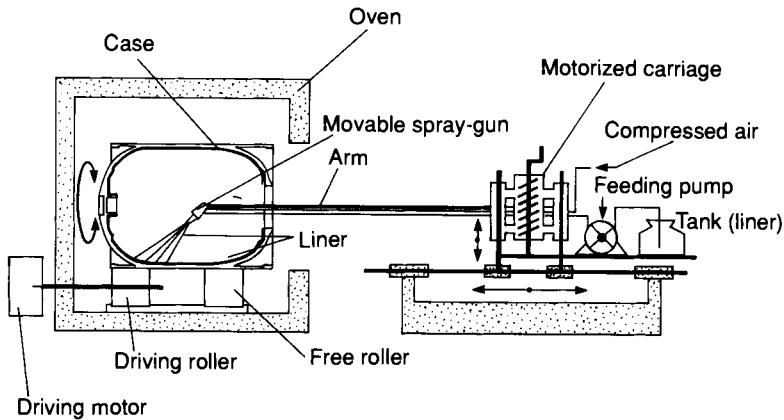


FIG. 13.3. Device used to spray the uncured liner into the case (pneumatic spraying).

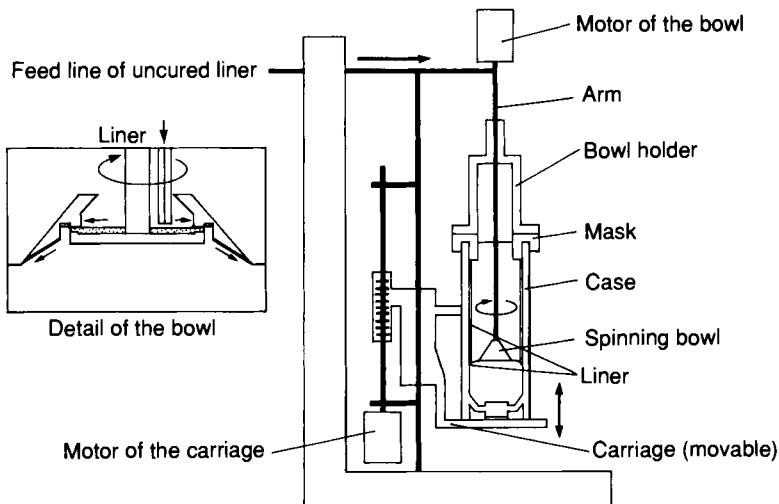


FIG. 13.4. Vertical spraying machine (Mechanical spraying of the liner).

3.2.4. Application of a liner with mechanical embedment

When faced with difficult bondings, as might be the case with highly plasticized propellants, an improvement consists in embedding the liner with particles — typically cylindrical particles — which permit a mechanical embedment between the liner and the propellant [18]. This incrustation can be done by pneumatic spraying of particles on the liner while it is still uncured.

The peel test value of the embedded liner in peel tests is multiplied by a factor of 2 to 3. The incrustations constitute some sort of obstacle to the propagation of tear caused by peeling.

3.2.5. *Recycling of the coated cases with a cured liner out of specifications*

Defects may be present in the materials or the bondings in a case, and they must be detected before proceeding to the casting of the propellant. When the defect cannot be corrected it is desirable to be able to recycle the case. Several techniques are available:

- Prolonged soaking in a solvent, causing a swelling of the materials, which can later be removed by mechanical brushing.
- Removal of the material with a high-pressure water jet. This technique cannot be used with composite materials because it would cause irreversible damage to the case.
- Removal of the material with a heating device locally weakening the mechanical properties of the material to be removed.
- Dissolving the liner to be removed with a solvent selected not to attack the other inert materials present in the case.

4. Examples of Insulating Materials Used In Rocket Propulsion

While the compositions of propellants developed in various countries have a pronounced similarity, due as much to energetic considerations as to the availability of raw materials, the diversity of insulating materials (e.g. polyurethanes, epoxides, silicones, synthetic rubbers and phenolic resins), precludes trying to be exhaustive or even provide detailed descriptions of each type.

For the several examples dealt with in the following sections, reference is made whenever possible to patents and papers listed in the bibliography, particularly when it concerns the chemical aspect of the materials [19].

4.1. INHIBITING MATERIALS FOR FREE-STANDING GRAINS

4.1.1. *Cast inhibitors*

Inhibiting by casting over a propellant grain is interesting in particular for small grains. Nevertheless, some large grains are still produced using this technique.

4.1.1.1. *Cast inhibitors for composite propellants*

This technique is not much used in actual production. The materials used have been prepared based on propellant binders — particularly when it involves polyurethane — correctly adjusted in terms of the crosslinking rate and final mechanical properties.

Polyurethanes, although exhibiting good bonding characteristics — particularly with the peel test — are expensive to produce due to their sensitivity to humidity, and epoxide-based inhibitors are being preferred whenever their mechanical and bonding properties are deemed sufficient for the selected application.

4.1.1.2. *Cast inhibitors for extruded or cast double-base propellants (Table 1)*

Most elastomers which can be crosslinked at low temperature are potential materials for the formulation of cast inhibitors: unsaturated polyesters and silicones curing at ambient temperature, polyurethanes, polysulfides and epoxides can be used. In fact, the selection of one over the other is based on constraints related to the operational mode of the motor and the exact composition of the propellant used.

Table 1 lists the major characteristics of various cast inhibitors belonging to the three most commonly used families, which are briefly described in the following sections.

4.1.1.3. *Unsaturated polyester*

Polyesters are made of unsaturated polymer chains diluted in styrene and capable of crosslinking by free-radical-type reactions with the assistance of appropriate catalysts and accelerators.

The polymer is usually blended with refractory fillers designed to improve the thermal resistance. At the manufacturing level their low initial viscosity makes them ideal for casting, but they can also just as easily be injected with precision automatic feeding equipment.

This family of inhibitors was developed very early, in the 1950s [20], and is still widely used. Its known limitations are related to a high smoke emission, attributable to high amounts of aromatic products contained in the formulation, as well as a propensity — that could be high depending on the type of propellant used — to swell in contact with nitrated plasticizers. The swelling alters the mechanical properties of the material and shortens its service life. Improvements have been obtained by:

- using a primer of the triisocyanate type which, by reducing the rate of migration of nitroglycerine, reduces the swelling;

TABLE 1 Major characteristics of cast inhibitors for extruded or cast double-base propellants

1	2			3	4	5				
	Inhibitors					Behavior at firing				
	mechanical properties					Physicochemistry				
Inhibitors ^a	<i>S_m</i> (MPa)	<i>E</i> (MPa)	<i>σ_r</i> (%)	Test temperature	<i>b</i>	<i>cp^c</i>	Density	Propensity to enhance the burning rate	Ablation rate ^d (%)	Smoke signature ^{d,e} (%)
EPE 01	0.9	540	10	−40°C +20°C +60°C	0.44 1.07 1.67	1.13 1.58 1.76	1.50	yes	15	88
EPE 02	4.5	530	17	−40°C +20°C +60°C	0.55 1.20 1.44	1.17 1.53 1.71	1.50	yes	20	85
SI 111	4.5	1.90	45	−40°C +20°C +60°C	4.1 3.2 4.4	1.54 1.36 1.43	1.32	no	5	88
SI 113	5.5	2.35	37	−40°C +20°C +60°C	1.0 1.0 0.9	1.45 1.33 1.42	1.50	no	5	90
SI 119	2.5	1.92	132	−40°C +20°C +60°C	7.4 5.2 5.3	1.52 1.44 1.51	1.34	no	10	80
SI 117 A	5.3	6.70	15	−40°C +20°C +60°C	4.5 2.9 3.6	1.65 1.27 1.35	1.45	no	2	88
SI 120 A	3.8	3.70	15	−40°C +20°C +60°C	1.0 0.9 0.9	1.42 1.31 1.39	1.43	yes*	2	90
PU 003	7.3	596	30	−40°C +20°C +60°C	0.40 1.30 1.82	1.10 1.68 1.96	1.30	yes	40	90–92

TABLE 1 (continued)

PU 004	8.5	523	35	-40°C +20°C +60°C	0.54 1.25 1.40	1.28 1.76 1.83	1.33	yes	30	90-92
PU 005	7.5	450	50	-40°C +20°C +60°C	0.46 1.30 1.10	1.44 1.73 2.15	1.35	yes	35	90-92
PU 11 C	7.5	517	60	-40°C +20°C +60°C	0.44 1.0 1.58	1.59 1.87 2.29	1.36	no	30	90
PU 51 G	15.0	316	100	-40°C +20°C +60°C	0.44 1.41 1.68	1.17 1.69 1.90	1.54	no	15	85

* Yes, in some cases.

^a EPE = Polyester based inhibitor; SI = silicon-based inhibitor; PU: urethane-based inhibitor.^b Coefficient of thermal expansion (10^{-4}K^{-1}).^c cp = Specific heat coefficient ($\text{J} \times \text{G}^{-1} \times \text{K}^{-1}$).^d Loss of weight of the inhibitor measured after completion of a static firing test.^e Light attenuation through the plume.

- introducing polymer chains with halogen atoms [2] and also reducing and even removing the aromatic diluents which increase the smoke signature.

4.1.1.4. Silicone inhibitors: an excellent inhibiting material once the bonding problems are under control

Silicone inhibitors are produced from polydimethylsiloxane-reactive oils, crosslinking through a condensation mechanism under the influence of the appropriate catalysts. They contain refractory fillers and fibers which lead to the formation, during firing, of a solid char which retains the particles in the combustion chamber of the motor. This factor, combined with the absence of tar formation by condensation, imparts a very low signature to silicone inhibitors.

This family of inhibitors has other specific characteristics such as the absence of any absorption of nitrated plasticizers, giving it a good stability for all of its physical characteristics, such as mechanical properties, shape, etc.

Unfortunately, silicones have a low natural propensity to adhesion on the propellant. The remedy consists usually in using a primer based on a functional silane. The use of such a primer, however, is not economical or desirable in terms of reliability of the bonding.

In France, self-adhesives, particularly high-performing polydimethylsiloxanes, were developed. The process that permits self-adherence is a direct application of the theory of chemical bonding at the interface.

All relevant details on this family of inhibitors are contained in references [10] and [22], which provide a complete review of the chemistry, the performance and the characteristics of production of silicone-based inhibitors.

4.1.1.5. Polyurethane inhibitors; generating only gases during a thermal decomposition (organic inhibitors)

In this class of inhibitors are grouped materials that are made from polymers with a saturated and oxygenized chain without mineral refractory fillers (or with submicron particle sizes). These materials decompose by pyrolysis, preferably in a gaseous form with a minimum formation of soots and tars.

From the binders currently available for elastomers able to crosslink at low temperature, polyethers or hydroxylated polyesters are the best candidates to fulfill the required criteria.

In the case of crosslinking by isocyanates, a first study points to hydroxylated resins with polyoxyethylenic and polyoxypropylenic chains, with a carbon versus oxygen ratio of 2 and 3, respectively. In practice, however, the best compromise between a low signature and thermal resistance is obtained

with polymers made by opening C4 or C5 rings including oxygen [23] and further progress is still being made.

The possibilities for choice of refractory fillers are more limited, inasmuch as there is not a great number of highly oxygenized thermostable organic products. Oxamide appears to be the best one; but in the case where the thermal resistance would prove to be insufficient, a dense mineral filler, with appropriate particle size and capable of providing oxygen, can be added.

Another means consists of incorporating into the formulations a low quantity of fibrous mineral or organic filler. The ablation ratios are improved by 20–25 % and the signature properties are not altered [24]. The viscosity of the mixtures continues to be compatible with injection casting.

Injection with precision automatic feeding equipment at high or low pressure makes it possible to reduce the cost of inhibiting, particularly for high rates of production. However, this manufacturing process requires a formulation of inhibiting composition based on two components preferably exhibiting similar viscosities and equivalent masses.

4.1.1.6. Future cast inhibitors

It seems that some applications, such as rocket motors for antitank missiles, will continue to use free-standing grains inhibited by cast inhibitors for a long time. The future ideal inhibitor should combine the simplicity of the polyester, the stability of the silicone and the low signature and excellent bonding of the polyurethane. A compromise of this sort is not easy to come by, although the epoxide systems cured at low temperature, handicapped for a very long time by the low pyrotechnic compatibility of the amine curing agent, may hold the key to future progress. Methods have been recently found that are both easy and may be industrially feasible, allowing the use of curing agents in the presence of double-base propellants, which offers prospects of development attractive in terms of cost and performance.

4.1.2. Restrictors for free-standing grains

Restrictors are made from elastomeric material presenting sufficient thermal resistance (polyvinyl chloride, thermoplastic rubber or synthetic rubber) molded in advance with the external shape of the grain into which the propellant in its slurry form is cast before curing. This process results in a particularly economic manufacture. It requires the use of elastomers selected for their adhesive properties with the propellant (such as EPDM rubber or butyl in the case of composite propellant with polyurethane binder) or their low signature, for cast double-base propellants. A reader interested in this particular area will find numerous details on the composition of restrictors for composite propellants in reference [25] or double-base propellants in [26] and [27].

4.2. LINERS FOR CASE-BONDED GRAINS

Free-standing grains do not permit the construction of motors with large diameters. The development of case-bonded technology provided an answer to this need.

This is not the place for an historical review of the development of this process. Interested readers may refer to articles listed in the bibliography [28–30]. But the emergence of this motor design led to the development of a new elastomer material, called binding material or liner, designed to ensure the mechanical bond between the case and the propellant or between the thermal protection and the propellant. In the beginning, the adhesion between the liner and propellant was obtained by keeping the same binder for both materials. Without a doubt this was done to have the best thermodynamic compatibility possible, as well as sufficient wetting of the interface. Later, research demonstrated that the optimum binding was often obtained with a chemical composition of the liner that was different from that of the propellant binder.

The following factors play an important role in the creation of the binding:

- curing level of the liner at the moment when the propellant is cast: presence or not of reactive chemical functions;
- presence in the liner of chemical species capable of diffusing and of chemically binding with the propellant binder: presence of adhesion promoters;
- crosslinking density of the liner: allowing sterically the thermodynamically possible diffusion.

4.2.1. *Detailed formulation of a liner for a propellant with a CTPB binder (Table 2)*

The base polymer will be a polybutadiene in order to ensure good thermodynamic compatibility. For reasons of reactivity and low viscosity, a hydroxytelechelic (HTPB)-type polybutadiene was selected; and to be able to tailor the mechanical properties, a hydroxylated chain extensor with low mass was added to the prepolymer.

A mineral filler (carbon black, titanium oxide) also regulates the mechanical characteristics, increases mechanical resistance and controls the rheology of the material before polymerization. The stoichiometric ratio allows adjustment of the level of the mechanical properties with great precision.

In order to ensure a high level of adhesion between the liner and the propellant, the liner will include an adhesion promoter capable of creating linkage through covalent bonds at the interfaces.

Finally, a catalytic system will not only allow control of the rate of crosslinking but also, in some cases, will control the nature of the chemical reactions at the interfaces.

TABLE 2 *Composition and characteristics of a liner designed for an aluminized composite propellant using a CTPB binder*

<i>Physical properties of the liner</i>	
Density at 20°C	1.14
Electrical resistivity	$10^{12} \Omega\text{m}$
Linear thermal expansion coefficient	$120 \cdot 10^{-6}/^{\circ}\text{C}$
Specific heat	0.4 Cal/g
<i>Composition of the liner</i>	
HTPB	66.0%
Chain extender	8.0
Antioxidizer	0.3
Bonding promoter	3.6
Filler	13.0
Crosslinking agent	8.6
Catalyst	0.5
Pot-life—20 min at 20°C	
<i>Mechanical properties of the liner^a</i>	
Temperature	+ 20°C
S_m (MPa)	2.2
(%)	250
E (MPa)	0.8
e_m (%)	800
e_r (%)	800
<i>Bonding properties</i>	
C = shear strength (MPa)	0.65
T = tensile strength (MPa)	0.65
P = peeling strength (daN/cm)	2.5

^a Tensile loading rate 20 mm/min.^b Test rate 10 mm/min.

Test temperature 20°C.

Of course, the propellant will be cast on a liner that is not completely cured, to facilitate the adhesion, and that is free of poisons such as absorbed water, tensio-active agents, etc.

The selection of the set-point is made by using a methodology that allows us to localize rationally the optimum of a function of several variables (experimental design factorial studies).

Table 2 provides the composition and the major characteristics of a liner for composite propellant (CTPB binder).

4.2.2. *Other examples of liner development in response to specific situations*

For the most part, the general ideas proposed in relation to the development of a liner for CTPB liner propellant are also true for the other types of

binders. However, particular situations arise where special requirements are needed.

For instance, a propellant may, because of its composition, be sensitive to electrostatic discharges. In this case appropriate precautions must be taken to eliminate the risks during the manufacture or handling of the grains. Such precautions include, for example, devices to eliminate the charges and equipotentiality of all elements. A specific means of protection consists, for instance, of building a Faraday cage around the grain, thereby eliminating all outside influences. A family of conductive lines has been developed for this purpose. Their extreme viscosity in the uncured state required the development of highly original spraying systems.

4.2.3. *Liners designed for tactical case-bonded grains manufactured at high rates of production*

The development of case-bonded propellant grains in tactical missiles was a consequence of requirements for high propulsion performances.

A review of possible concepts has been published by E. Gonzales and F. Marks [31], which demonstrates the usefulness of taking into account, in particular, the inert components of the motor.

Similarly, R. T. Davis and J. D. Byrd pointed out the economic advantages expected from the use of a liner with a blocked isocyanate as a crosslinking agent [15].

These types of liners have been developed in France during recent years. They have a pseudo-plastic behavior which eliminates all risks of dripping during manufacture, and crosslink through the use of a blocked isocyanate linked to an appropriate catalytic system.

The selection of the blocked isocyanate was made in such a way that it not only contributes to a very long pot-life at ambient temperature, but also provides (during the deblocking through thermal activation at 60°C — in particular during the curing of the propellant) the isocyanate functions allowing an improvement of the cohesion at the interface between liner and propellant. In addition, the blocking agent acts as a plasticizer for the propellant, improving the binding behavior at low temperature.

In terms of mass production, the very long pot-life results in a great flexibility of use, significantly reducing manufacturing cost.

4.2.4. *Liners designed for grains using propellant with high levels of nitrated plasticizers (XLDB)*

In terms of their compositions these propellants resemble the conventional composite propellants already discussed in this chapter, with several additional particularities (undesirable in terms of bonding) linked essentially to the presence of a significant quantity of nitrated plasticizer.

The liners are similar in their composition, as well as in the quality control methods, to those we just examined. However, in order to improve peel behavior a form of mechanical linking, known as mechanical embedment [18], was used in the past. Recently, with the purpose of simplifying the process, improving the reliability of the bonds between the liner and the propellant and reducing the costs, a family of liners with direct bonding has been developed.

4.3. THERMAL PROTECTION DESIGNED FOR THE INSULATION OF COMBUSTION CHAMBERS

Excellent descriptions of these materials are available in the bibliography [32,33] or in commercial brochures [34]. Protection through the ablation mechanism was described earlier. We will therefore limit ourselves here to pointing out that the elastomers used to manufacture flexible thermal protection are most often made of rubber (NBR, NR, EPDM and Hypalon) with cooling fillers (oxalate, carbonate and hydrate) and refractory charges such as carbon, silica or asbestos fibers. In contrast, the majority of the rigid thermal protections are made of phenolic resins (or derivatives) reinforced with refractory fibers such as asbestos, silica, carbon, alumina or even nylon. The selection is always guided by the particular characteristics required for good operation of the motor.

However, the thermal protection for integral boosters located in the propulsion chamber of a missile powered by a ramjet calls for special attention in this section.

The reader may find in this book, as well as in the bibliography, pertinent information about the functioning of these ramjets [35].

The point that needs to be emphasized here has to be with the fact that the material ensuring the bonding of the propellant to the case during the boost phase of the missile must also later work as the thermal protection of the combustion chamber of the ramjet. Consequently, this thermal protection must have the usual performance characteristics of a liner. In particular, it must be sufficiently elastic to withstand, without breaking, the deformation induced by the operation at high pressure of the booster grain. This virtually forbids the use of phenolic compounds reinforced with silica. Of course, the elastomer selected must withstand the oxidizing atmosphere of the ramjet combustion chamber without burning.

Because of these two requirements, the number of choices is drastically limited. Only polysiloxanes (or derivative materials) are capable of satisfying all of these specifications. Table 3 gives the composition and main characteristics of such a thermal protection.

However, the siloxanic materials due to their very low critical wetting tension (the second lowest after PFTE) have a very poor natural adhesion with the propellant. This resulted, in the United States in particular, in the

TABLE 3 Major characteristics of a thermal protection for integral booster for a ramjet missile

<i>Physical characteristics, at 20°C</i>					
Density at 20°C				1.45	
Electrical resistivity				$10^6 \Omega\text{m}$	
Linear Thermal expansion coefficient				$4.7 \times 10^{-4} \text{K}^{-1}$	
Thermal conductivity				$0.40 \text{ W/}^\circ\text{C m}$	
Specific heat				$1.13 \text{ J/}^\circ\text{C}$	
<i>Composition</i>					
Bicomponent silicone elastomer					
RTV type				46%	
Granular refractory charge				23%	
Fibrous refractory charge				18%	
Catalyst				7.0%	
<i>Mechanical characteristics^a</i>					
Temperature	S_m (MPa)	(%)	E (MPa)	e_m (%)	e_r (%)
-40°C	5.6	4.6	122.0	55	55
+20°C	4.7	3.8	138.0	51	51
+60°C	4.5	4.6	96.0	52	52
<i>Bonding characteristics^b</i>					
			Shear strength (MPa)	Tensile strength (MPa)	Peeling strength (daN/cm)
HTPB Composite propellant with liquid burning rate modifier			6.5	7.5	1.5
Aluminized HTPB composite propellant			5.0	7.0	2.0

^a Tensile loading rate 50 mm/min.^b Test rate 10 mm/min.

Test temperature 20°C.

development of complex solutions to ensure the bonding of the booster grain to the chamber [36].

In France, the research was oriented in two directions:

- improvement and simplification of the bonding techniques of the integral booster in the combustion chamber of the ramjet;
- improvement of the thermal performance of the material in terms of a decrease in thermal conductivity and a rise of mechanical strengthening of the residual char, to make it capable of withstanding flow instabilities in the combustion chamber of the ramjet.

To improve the bonding of the propellant to the thermal insulation much attention has been paid to the chemistry of the propellant binder.

HTPB, which is used to manufacture the propellant of the booster, crosslinks through a reaction of the isocyanate functions on mobile hydrogens. Advantage has been taken of this reaction in the selection of polydimethylsiloxane as a binder for the thermal protection, and to introduce in the latter adhesion promoters, such as functional silane or blocked isocyanates. These chemicals improve the bonding by creating strong chemical links at the interfaces with the propellants. The result is that the propellant may be directly bonded onto the thermal protection. Among other things, this solves the problem of combustion of residues at the transition between the boost phase and the operation of the ramjet chamber.

Simultaneously, an improvement of the mechanical strength of the pyrolyzed portion is attempted by using polymers leading to a higher amount of ceramic-like residues than with polydimethylsiloxanes, and by increasing the efficiency of the endothermic reactions during the exposure of the thermal protection to a high heat flux. Significant progress has been made in the following areas:

- use of fibrous refractory reinforcements to improve the thermomechanical resistance of the char;
- use of polymers similar in type to those used as precursor for the production of silicon carbide fibers;
- use of polysilarylene-polysiloxane as a replacement for polydimethylsiloxane as a binder for the thermal protection material, leading to a significantly higher amount of refractory residues [37].

5. Conclusion

This chapter, devoted to insulating materials for propellant motors, shows that the preparation of a case or the inhibition of a grain are very complex tasks, because they must reach a fine compromise between a large number of often contradictory requirements.

The reader will have noted that making the appropriate materials available to the designer of the motor is a crucial factor, for the following characteristics:

- access to complex design, permitting adjustment of the internal ballistics;
- decrease of the inert mass in the motor;
- reliability and safety of operation;
- wide range of firing temperatures;
- industrial costs.

In the end, it turns out that for the reasons previously mentioned, the development of insulation materials is one of the most difficult and time-consuming of the tasks involved in the development of solid rocket motors.

Here more than in any other area, it may be true that the predominantly experimental nature of the techniques used must rest on the best-known theories and a very rigorous experimental research, while leaving a large place to the intuition and the experience of the designers.

Bibliography

1. BARRÈRE, M., and JAUMOTTE, A., *La propulsion par fusée*. Paris: Dunod, 1957.
2. *Propellants manufacture, hazards and testing*. Advances in chemistry series no. 88. Washington: American Chemical Society, 1969.
3. SCHULTZ, R., *Actes du colloque "Adhesion"*. Université de Bordeaux I. Université du Haut-Rhin, France, 1979.
4. KAEBLE, M., *Physical Chemistry of Adhesion*. North American Rockwell Corporation — Science center, Thousand Oaks, California; Van Nostrand, 1967.
5. SUTTON, G. W., The initial development of ablation heat protection: a historical perspective. *Journal of Spacecraft and Rockets*, **19**(1), 3-11.
6. SCHMITT, D. L., Ablative polymers in space technology. *Journal of the Macromolecular Chemical Society*, **13**(C3), 326, 1969.
7. LACAZE, H., La protection thermique par ablation. *Doc. Air Espace*, nos. 105, 106 and 107, July-Sept.-Nov. 1967.
8. YOUREN, J. W., Ablation mechanism for elastomeric rocket motor case insulation. *Composites*, no. 2, pp. 180-184, 1971.
9. EVANS, C. I., Minimum smoke solid propellants rocket motors. AIAA paper no. 72-1192, New Orleans, 1972.
10. GONTHIER, B., and TAUZIA, J. M., Minimum smoke rocket motor with silicones inhibitors. AIAA paper no. 84-1418, Cincinnati, 1984.
11. PROBSTER, M., and SCHUCKER, R. M., Ballistics anomalies in solid rocket motors due to migration effects. *Acta Astronautica*, **13**(10), 599-605, 1986.
12. GONTHIER, B., MAUCOURT, J., and TAUZIA, J. M., Burning rate enhancement phenomena in end-burning solid propellant grains. AIAA paper no. 85-1435, Monterey, California, 1985.
13. GRAHAM, H., and SHEPARD, G., Composition et procédé pour régler la vitesse de durcissement des résines polyuréthannes. Thiokol corporation USA. *Brevet français* no. 2.386-570, 1977.
14. BATS, J. P., LALANDE, R., and TAUZIA, J. M., Systèmes catalytiques retardés pour élastomères polyuréthannes. Application à la préparation d'inhibiteurs de combustion de blocs de propergols. *European Polymer Journal*, **20**(10), 997-1001, 1984.
15. DAVIS, R. T., and BIRD, J. D., Reduction in cost of rocket motors manufactured by use of liners with controlled cure. *JANNAF propulsion meeting*, Vol. V, pp. 435-465, Monterey, California, 1980.
16. TAUZIA, J. M., Elaboration d'adhésifs bicomposants sur le site d'utilisation. Fiabilité et qualité des assemblages. *Actes du congrès Adhécom*. Université de Bordeaux, France, 1986.
17. DESSUGE, P. H., Automatisation d'une installation de dosage bicomposants. *Mémoire du Conservatoire National des Arts et Métiers*. Centre de Bordeaux, France, 1987.
18. SCHAFFLING, O., Process for preparing a rocket motor. OLIN corporation, US patent no. 4-131.051, December 1978.
19. KIRK-OTHMER, H., *Encyclopedia of Chemical Technology*. New York: John Wiley and Sons, 1967.
20. DELACARTE, J., and QUENU, P., Inhibiteurs à base de polyesters insaturés. SNPE. *Brevet français*, no. 1.194.649, 1959.
21. CAIRE-MAURISIER, M., and TRANCHANT, J., Inhibiteurs halogénés pour propergols homogènes. SNPE. *Brevet français* no. 223.7117, 1975.
22. LEFORT, M., and BRISSON, P., Les silicones: synthèse, propriétés et applications. *Actualité chimique*, no. 8, 7-11, 1983.
23. CARTER, R. E., and WRIGHT, J., Procédé de préparation de polyuréthannes destinés à revêtir une charge de propergol pour en inhiber la combustion périphérique et polymère et charges revêtus ainsi obtenus. *Brevet français* no. 2.444.689, 1979.

24. TAUZIA, J. M., GONTHIER, B., and GRIGNON, J., Nouveaux inhibiteurs de combustion à base d'élastomères polyuréthannes oxygénés comportant des fibres. SNPE. *Brevet français* no. 2.538.578, 1982.
25. MAUCOURT, J., and COMBETTE, C., Inhibiteur préformé pour propergol composite à liant polyuréthane. SNPE. *Brevet français* no. 8.610.820, 1986.
26. TAUZIA, J. M., and ZILIOLI, F., Revêtement inhibiteur pour propergol solide à combustion frontale comportant des charges organiques. SNPE. *Brevet français* no. 2.495.133, 1980.
27. Case bonding composite for double-base propellants, US patent no. 3.960.088, 1976.
28. KLAGER, K., Polyurethanes, the most versatile binders for solid rocket propellants, AIAA paper no. 84-1239, Cincinnati, 1984.
29. SUTTON, E. S., From polysulfides to CTPB binders. A major transition in solid propellant binder chemistry. AIAA paper no. 84-1236, Cincinnati, 1984.
30. BYRD, J. D., Consideration on the binding of large rocket motors. AIAA paper no. 76-638, 1976.
31. GONZALES, F., and MARKS, F., Concept analysis for a low cost four-inch advanced tactical rocket. AIAA/SAE, 13th Propulsion Conference, AIAA paper no. 77-868, Orlando, Florida, 1977.
32. DAY, J. M., and HORTZ, W. A., Nitrile butadiene rubber in ablative applications. *Applied Polymers Symposium* no. 25, pp. 261-274, 1974.
33. TAUZIA, J. M., and MAUCOURT, J., Protection thermique pour propulseur à poudre exempté d'amiant. SNPE. *Brevet français* no. 2.458.687, 1979.
34. *Doc Fiberite*. Fiberite corporation Europe; ICI, PO Box 6, Bessemen Road, Welwyn Garden City. Hertfordshire, UK.
35. CAZIN, P. H., Les statoréacteurs à combustion liquide. Onera-Agard lecture, series no. 186, 1984.
36. BUTLS, P. G., and MYERS, T. D., Integral booster motor interface requirements, AIAA paper no. 78.160, Las Vegas, 1978.
37. DVORNIC, P. R., and LENTZ, R. W., Exactly alternating silylene siloxane polymers. *Polymers*, **24**, 763-768, 1983.

CHAPTER 14

Future of Solid Rocket Propulsion

ALAIN DAVENAS

1. Increase of Solid Propellant Energy

The progress made in the energetic characteristics of solid propellants during the 1950s and the 1960s was followed by a period of disillusionment.

As with all new technology, the initial progress had been very rapid. It resulted from an excellent synergy between the needs related to applications and the emergence on the market of chemicals supplied by the chemical industry, well suited for the formulation of binders for solid propellants: PVC, polyurethane, followed by more specific products such as various kinds of liquid functional polybutadienes. This led to the creation of today's typical composite propellant, associating a polybutadiene binder with excellent mechanical characteristics in a very wide range of temperatures to a high content of oxidizers and fuels: ammonium perchlorate and aluminum respectively. This is a particularly stable system, and involves a reasonably easy production process in facilities where, aside from a few specific production phases, the only hazard of concern is that of fire. Consequently, this type of composition has progressively spread to a great number of applications, such as missiles, rockets, and gas generators. For these applications the immediate availability, long service life and good performance represent major advantages, at least where the dimensions of the motor are not too limited by space constraints, such as in the case of strategic missiles on submarines, portable ground-air systems, or integral boosters on ramjets.

The research work done during the 1960s encountered great difficulties in the synthesis and production of new molecules designed to increase the energy of these propellants.

A great number of oxidizers more powerful and denser than ammonium perchlorate were synthesized, tested and abandoned because of a high chemical reactivity or a lack of stability (NO_2ClO_4 , for example) made them incompatible with the existing binders, or because of high sensitivity to shock or friction for industrial production (hydrazine mono or diperchlorate, for example).

Techniques were subsequently developed to improve the compatibility of energetic solid oxidizers included in the propellant: surface modifications and, in particular, encapsulation of the particles by organic polymers insoluble in the binder and compatible with the rest of the composition. These techniques resulted in a decrease of the energy gain expected from the formulation, and a significant cost increase for the preparation of the propellant, but they may conceivably be used again in the future.

Many failures were also experienced with metallic fuels. Metallic hydrides either exhibited densities that were too low to be interesting when the hydrides were stable (LiH , LiAlH_4), or they were not stable unless complexed with an organic molecule, thereby losing a good deal of their advantage (AlH_3 , BeH_2). Extensive research has been done during the 1960s, in the United States as well as in France and probably in the USSR, on composite propellants containing beryllium. The reason for this is that the addition of this metal significantly increases the specific impulse, without creating any problems of compatibility with the hydrocarbon binders or ammonium perchlorate. These developments were virtually abandoned because of the very high toxicity of beryllium and particularly of its oxide resulting from combustion, although there are controversies concerning the real toxicity of oxide formed at the very high temperature of combustion in the motor. This approach appears closed for the moment, although the possibility of starting the research again comes up periodically, particularly for space applications. There is one metal, however, that could have a definite future in some applications, and in particular for tactical missiles of smaller sizes, such as ramjet boosters. This is zirconium, with its very high density (6.49), resulting in propellant with a volumetric specific impulse clearly above that of the conventional polybutadiene-AP-Al propellant.

The thermochemistry and energetics of these various compositions are particularly well described in the work from Boisson [1] which, although not recent, continues to be recommended as a reference.

In the end, there seem to be two approaches open for the future: one is the use of nitrated or nitro derivatives; the other, in the distant future, may be the use of molecules containing fluorine not highly chemically bound in radicals of the NF_2 type.

Among today's most widely used energetic compounds, special attention has been given to HMX which, in spite of its highly explosive nature, exhibits high density, energy and stability. Two applications are: (1) the development of specific polybutadiene-AP-Al formulations with some percentages of HMX (12-20%); (2) XLDB type of formulation whose energetic binder, more highly oxygenated, provides a higher specific impulse due to a possible high content of HMX. These two types of compositions are being applied either in apogee motors for space launchers (American PAM D₂, for example), or in advanced ballistic missiles for space launchers: Trident 1 C4, Trident 2 D5, the third stage of the MX, and Midgetman in the United States.

Research continues in many countries on energetic solids or binders, or on nitrated plasticizers that are more energetic or stable than binders with a very high content of nitroglycerine. Molecules such as hexanitrohexa aza adamantane or wurtzitane are the object of intensive research.

The avenue of the difluoraminated-type binders and oxidizers, which was pursued because of the potential of very high specific impulse and density, continues to be a highly difficult area of research direction. It seems to be particularly oriented toward gem-difluoraminate molecules which preferably include the geminal $C(NF_2)_2$ rather than the vicinal $CHNF_2$, which is unstable. This chemistry, which uses the difluoramine NF_2H as a starting material, is a difficult chemistry and it is very expensive.

However, an outside candidate has emerged that leads us to believe that in the very near future we will be able to increase the energetic levels of today's propellants. It has been discovered in the United States that aliphatic molecules containing the azide entity, N_3 , are stable and not very sensitive to shock or friction. One particular polymer is presently under development, the glycidyl azide polymer (GAP) [2].

Table 1 summarizes the main chemical features that are involved in the research on new energetic compounds with high heat of formation and high heat of combustion.

In the end there seems to be a definite trend again toward the research of higher energies, which will be discussed in the next section. This has occurred after a period during which research budgets for the improvement of thermodynamic characteristics were drastically cut because of the disappointments encountered in the chemistry of high energy materials. These disappointments result in a great diversification of the more conventional compositions in terms of their applications, which we will also discuss later.

TABLE 1 *High energy groups*

Group	ΔH_f (kcal/mole)	Use
$-C-O-NO_2$	-19.4	plasticizers
$-C-NO_2$	-15.8	solids polymers plasticizers
$-N-NO_2$	17.8	solids plasticizers
$-C-N_3$	80	plasticizers polymers
$-C-NF_2$	-7.8	solids plasticizers polymers

2. Propulsion of Strategic Missiles

The search for optimal propellant performance — specific impulse I_s and volumetric specific impulse $I_s \rho$ — will continue to be the most important research mission, coupled with other expected technological progress which will improve the propellant mass fraction (composite cases with very high specific resistance, nozzle materials, and thermal protection) and with the miniaturization of the nuclear warheads. These energetic gains will provide the flexibility of design and usage corresponding to the various constraints of the missions. It will involve, for example:

- For a missile of a given size (missiles on board submarines), increasing the range or the number of warheads, countermeasures (decoys), or the number of potential targets.
- A miniaturization of strategic missiles (the Midgetman concept in the United States, project SX in France) to facilitate their transport and their utilization, while at the same time decreasing their cost, allowing a corresponding increase in the number of missiles.
- The evolution of past performances and those possible in the future is illustrated in Table 2, which shows the improvement in performance of propellants (in terms of the volumetric impulse I_s) over the years, based on the American missiles until 1984, and then extrapolating from today's state of the art (propellants existing but not yet manufactured industrially). The source for this table is a paper written by D. Quentin [3], to which we will refer to a number of times in the following sections.

TABLE 2 *Past and predicted evolution of solid propellants for strategic missiles*

Formulation	Theoretical I_s standard conditions	ρ g/cm ³	$I_s \rho$	Estimated date of completion of industrial development
Butalane 68/20	265	1.815	481	1968
Nitralane Trident C4	271	1.84	498	1973
Nitralane Trident C5	273	1.87	510	1978
F1	276	1.89	522	1985
F2	280	1.91	535	1995
F3	296	1.91	565	2010

Note: The performances assigned to the future formulations (F1, F2 and F3) are the results of calculations, and consequently involve a certain amount of uncertainty concerning the possibility of attaining them in practice.

The dates correspond to the demonstration of the industrial feasibility of the propellants rather than their introduction in a missile program.

F1 and F2 compositions are based on nitrated or azide ingredients.

F3 composition contains difluoramined derivatives.

Based on these elements, we see that, taking only thermodynamics into account, there is a considerable potential for improvement.

However, we should point out that these propellants, in comparison with the conventional composite propellants, present the same drawbacks as those experienced with high-energy XLDB propellants: (1) small critical diameter; (2) manufacturing involving delicate phases because of the use of large amounts of explosive ingredients. Solving the latter requires high investments, and thorough knowledge and control of the deflagration-detonation transition phenomenon. The approach taken in the United States with the ballistic missiles of the Trident and MX family shows, however, that these various aspects can be handled, resulting in reliable, high-performance systems.

Before they can be produced, these future propellants will also need to have sufficient mechanical properties allowing them to be case-bonded, and aging properties that are compatible with the typical service life of the ballistic missiles motors, i.e. at least 10 years.

The architecture of the grains, based on the levels attained today (loading ratio greater than 95%), should not evolve noticeably if the architecture of the motor remains the same (we will discuss the concept of integrated stages further).

Another general possible evolution is related to the hardening of the main stages of the missiles against space-based lasers that could be used in the SDI concept. This hardening could involve rotation of the missile and much lower burn times of the stages, phases during which it is the most sensitive. So high-rate, high-energy propellants would be considered.

Special propulsion systems need to be contemplated for the post-boost control systems which require special solid propellants. The best propellant energy management in these systems implies the availability of solid propellant with modifiable flow rates or the availability of extinguishable and re-ignitable (start-stop) systems.

The future trends seem to be as follows: for ground-based missiles with a large number of warheads to deliver we are experiencing a return to liquid propellants systems. This is due to the fact that they allow a greater amount of flexibility in adjusting the thrust, and easy control of the extinction and re-ignition of the motor, with very high specific impulses.

In the case of systems on board submarines, the liquid propellants are less acceptable (risks of leaks from the tanks, corrosion, limited space available, and low density of the propellants). Two types of systems are possible for present and next future systems. The classical post boost system used on missiles of the Poseidon and Trident family, which uses propellant gases produced by a generator modulated by a valve. At the technical level this implies the availability of the propellant with low burning rates (the operational times must last several minutes) and the highest possible specific impulse, while not exceeding gas temperatures acceptable for the valves and

the pipes of the system. In the United States the materials used are generally Colomium alloys, which limit the temperatures to approximately 1900 K. In France extensive work is being done with carbon-carbon composite materials allowing temperatures up to 2400–2500 K, and consequently, higher specific impulses. Butamites or nitramites, with “cold” nitrated binder and high HMX content, are propellants well suited for this type of need. Another characteristic of these types of systems is the need for very clean combustion gases, to avoid clogging of valves and pipes. Mineral compounds are generally not used in the composition of the propellant; as for inhibitors and the thermal protection of the chamber, gasifiable formulations, also used in low-signature tactical missiles, are preferable.

With the throttleable or controllable system, with separate solid propellants, the main motor functions only when a gas generator — with low combustion rate — generates flows inside the combustion chamber. When the gas injection is interrupted the main grain extinguishes. The corresponding propellant compositions are often fairly reducing for the generator, and oxygenated for the main grain. High specific impulses, associated with an operation that includes more than ten thrust pulses separated by motor extinction phases of varying duration, have been demonstrated in France.

A concept studied by Aerojet [4] is similar to this system. It features two solid propellant generators: one for oxidizing gases and the other for the reducing gases. Their flow rates are independently adjustable; they both flow into one single combustion chamber.

We should also mention that in the area of general architecture for multi-stage ballistic missiles, an interest is developing in an integrated stage concept, whereby the front end of the lower stage forms the exit cone for the nozzle of the next higher stage. This concept would lead to a 20% increase in range. A “forced deflection” nozzle, using a special boron-based propellant, has been demonstrated in the United States in a chamber simulating high-altitude conditions [5]. A related system, though less ambitious in terms of the innovations involved, has been recently demonstrated [6].

Finally, we should also note, in relation to the development of solid propellant boosters for space launchers, the trend of manufacturing facilities toward the processing of very large quantities of composite propellants in one manufacturing operation, still using the batch process. The unit operation has grown from 2–3 tons to approximately 15 tons. Today, modern automation technology results indicate significant drops in manufacturing costs.

For the longer-term continuous processes, presenting revolutionary possibilities are being developed and will be addressed in the section on space boosters.

3. Propellants for Tactical Missiles

Each mission has its own specifications and requirements, as illustrated in Table 3. Although this presentation is largely arbitrary — for instance no

TABLE 3 *Characteristics of solid propellants for tactical missiles as a function of their missions*

Types of Missiles	$I_s \rho$	Signature	Temperature coefficient	Duration of combustion
Artillery rockets	×		×	×
<i>Anti-tank</i>				
Rockets		×	×	very short
SR	×	×	×	
M and LR	×	×	×	
<i>Ground-air</i>				
VSR	×		×	long
MR	×	×	×	
LR	×	×	×	
<i>Air-ground</i>				
Rockets	×	×	×	long*
Missiles	×	×	×	
<i>Air-air</i>				
SR	×	×	×	long*
MR	×	×	×	
Sea-sea	×	×	×	long*

Note: ×, not an important criterion; × ×, of average importance; × × ×, highly important.
 SR = short range; MR = medium range; LR = long range; VSR = very short range.

missile manufacturer believes that the cost of the propellant is marginally important — it still allows us to identify the trends. Naturally, the service life and storage and operational safety are also included in the main specifications.

Before getting to the solutions (propellants, grain geometry) for these problems, it would be interesting to take a closer look at the evolution of some specifications.

3.1. EVOLUTION OF THE NEED

3.1.1. *Signature and penetration*

The lowering of the electromagnetic, infrared, and optical signatures of missiles is intended above all to delay the use of countermeasures. In fact, a low signature is one of the means of ensuring the superiority of the attack over defense, so that future missiles will retain their capability of penetration.

Extensive efforts are devoted to reducing the visible, infrared, and electromagnetic signatures. A reduction of the electromagnetic signature — characterized by the radar cross-section — is obtained mostly by changing the architecture or the materials: limiting “bright spots”, using coatings that absorb or diffuse radar waves and special shapes, which could lead to missiles

with elliptical or triangular sections. This in turn would result in completely new problems in terms of the propellant grain.

We will not discuss decoy systems, although we will comment briefly on the maneuvering capability the manufacturers would like to provide their missiles in order to outwit the defense systems. In terms of propulsion, such a capability would imply several indispensable attributes, including: (1) the modulation of the thrust which may lead, even for a missile, to three or even four successive thrust levels which, of course, becomes extremely problematic for a single grain; (2) the capability of the grain to withstand acceleration factors.

3.1.2. *Environment*

The number and severity of constraints under which future missiles will be used are continually increasing, particularly in terms of the extreme temperatures of operation and storage. In the course of the last 30 years these have progressed from propellants usable in a -30°C to $+50^{\circ}\text{C}$ temperature range to propellants with a working range from -54°C to $+70^{\circ}\text{C}$, and able to resist to peaks reaching temperatures close to 100°C . This corresponds, in particular, to the extension of the flight domains (altitude and speed) of aircraft, for air-launched missiles.

These constraints present the grain designers with two critical problems. Not only is it necessary to maintain the mechanical and physical integrity of the grain within the operational ranges, and its reliability after severe thermal cycles — consequently requiring excellent mechanical properties at all temperatures — but it is also necessary to maintain the performance (thrust, pressure versus time) in the same range (reduction of temperature coefficient).

The problems linked to the temperature ranges involve several other parameters, including:

- the intrinsic mechanical properties of the propellant;
- the geometry of the grain;
- the grain-case interaction, related to deformation under pressure from the case and to its thermal expansion characteristics.

This last point is an important one. Indeed, the evolution toward increasingly thinner metallic cases, made feasible by flow-turning processes and the use of filament-wound cases (Kevlar and carbon fibers), modifies considerably the behavior of the motors in terms of deformations under pressure (to which are added the difficulties of calculation and local anisotropies). It also modifies the need to take into account the whole composite propellant-case to calculate the stresses and strains which determine the safety coefficient and the service life of the motor.

Naturally, the improvement of the mechanical characteristics of the propellant give the grain designer a greater amount of flexibility in his search

for a solution. In addition, the generalization of the three-dimensional analyses validated through experiments, and the use of more sophisticated rheological models, improve the reliability of the predictions and the estimation of the service life.

3.1.3. *Maneuverability; thrust modulation*

We mentioned, when discussing the signature, the necessity for maneuverability on part or all of the trajectory to defend against anti-missile weapons. Without a doubt the next generation of air-sea or sea-sea missiles will feature a supersonic final path to foil the enemy defenses. Conversely, anti-missile missiles design will have to be able to react almost instantly, to maneuver with agility once the target has been detected.

3.1.4. *Increase range*

For air-ground, air-sea, and sea-sea missiles the possibilities of detection or identification of remote targets and the desire to escape from enemy defenses (such as launching aircraft or battleship) requires significant increases in missiles range, which, as we will discuss later, demonstrates the value of the air-breathing type of solutions.

3.1.5. *Vulnerability*

Low vulnerability specifications of the type described in Chapter 8 will certainly be imposed for all missiles. In the United States the objective, a very ambitious one, is to use missiles meeting "insensitive munition" requirements by 1998.

3.2. EVOLUTION OF THE TACTICAL PROPULSION

3.2.1. *Propellants*

Propellants are generally classified into three families:

- double-base (extruded or cast);
- composite with inert binder;
- composite modified double-base with energetic binders, CMDB or XLDB type.

The first two families — also the oldest — will continue to develop in two major directions: increase of burning rate ranges, and development of low-cost processes for industrial production.

The third family will be affected by the application of high-energy, low-signature propellants and their development within the framework of low vulnerability specifications.

The expected improvement, over the years, of the performance of the low-signature propellants for tactical missiles ($I_s \rho$) is illustrated in Table 4.

One of the major difficulties encountered with the newer types of smokeless high-energy propellants is the present limitations in rates of combustion available. This is certainly one of the main subjects for research in the near future.

3.2.2. Grains for thrust modulations

There are already many grains that have two thrust rates and thrust ratios capable of reaching factors of 7 to 8. These rates, however, are currently predetermined, while the missile designers wish to be able to trigger an "overrate" on request, as a function of the proximity of the target. Designs with complex geometries — with an increase of the burning surface at the desired moment — are being developed and are expected to be operational within the next few years, particularly for applications on the new sea-sea, air-surface, or air-air missiles [7,8].

3.2.3. Increase range: air-breathing systems

With air-ground and sea-sea missiles, and sometimes also ground-air, the ranges are limited by the weight of the missile, and also by the burn time available for the sustainer grains (more than 150 s is now available).

A simple solution, in principle, consists in using the air-breathing propulsion. There are several alternative development paths: turbojet, ramjet and ramrocket, and in the longer term, air turboramjet and turboramjet.

The adaptation of aircraft turbojets by simplification of the compressor, and of the lubrication and injection systems, and the use of low-cost materials

TABLE 4 *Past and potential development low-signature solid propellants for tactical missiles*

Formulation	Theoretical I_s standard conditions	Density ρ g/cm ³	$I_s \rho$	Estimated date of industrial development
EDB—CDB	229	1.66	380	1970
CMDB	241	1.67	403	1982
XLDB	256	1.76	450	1985
F1	259	1.77	458	1988
F2	261	1.81	472	1993
F3	262	1.83	479	2000

Note: All of these formulations correspond to basic compositions of the CHON type — mixtures of ingredients containing only these atoms — possibly with the addition of low amounts of ballistics modifiers.

for application where the operational time is limited to several hours, makes this propulsion system competitive with the rocket motors. Currently they are limited, however, to subsonic and slightly supersonic flights.

The technology of the ramjets and ramrockets is ready for numerous applications to missiles. The systems now developed actually reach ranges of several hundred kilometers [9], and ranges of several thousand kilometers are a possibility being investigated. The development of this type of propulsion is going to take several directions. The integral boosters (in the combustion chamber of the ramjet) without ejectable nozzles (for launching from aircraft in particular) will become widely used on combat platforms, implying such related problems as: design of nozzleless grains, prediction of the performance, and precise thrust vector control. The bonding and thermal protection materials of the combustion chamber will have to be capable of two functions: booster function and very long-lasting ramjet function, for which the temperatures and composition of the gaseous mixtures are very different.

Because of volume and space limitations, the desired increase in range requires the use of high-energy propellants or high volumetric impulse propellant types for the booster phase, and dense liquid fuels or boron or carbon solid fuel-rich propellants for the sustainer phase.

The search for simplicity in manufacture, if not in design, has led to the creation of the experimental model known as the “rustique ramjet” where a single chamber contains both the booster and the sustainer grains. This type of ramrocket has been flight-tested several times in France [10].

The turboramjet is a newer design intended to operate as a turbojet at subsonic speeds and as a ramjet at supersonic or hypersonic speeds. It includes, briefly described: an air intake, a compressor, a turbine, a generator of reducing gases, a combustion chamber, and a nozzle.

The air entering into the motor is compressed by the low-pressure compressor, which is driven by a high-pressure turbine powered by the reducing gases from the generator. The system is capable of accelerating up to its cruising speed, without any additional boosters.

The major advantages of this design are: (1) better thrust and specific impulse, as well as a more stable burning rate than in a ramjet alone; (2) a turbine less complex than the conventional turbines; and (3) a better thrust/weight ratio than with the ramjets.

Among possible applications there are stand-off supersonic missiles, cruise missiles, air-ground missiles, and drones.

3.2.4. Low vulnerability propellants

This topic, particularly sensitive for missiles on board ships or on aircraft, requires research into propellants with a low vulnerability to stimuli from projectiles, fire, static electricity, and in addition possessing a pyrotechnical

behavior preventing the combustion-to-detonation transition. It is likely that, during the coming years, this theme of “low-vulnerability” propellants will become very important. The most important question, still undecided to this day, will be whether a trade-off with energy performances will be tolerated. It is certain that it will be extremely difficult to significantly lower the vulnerability while maintaining the high levels of performance obtained today, although this is the goal of a large number of important research programs [11,12].

Many of the ingredients being studied for an energy increase in today’s propellants could also serve to decrease the vulnerability, for an equal level of energy.

3.2.5. Processes; decrease in costs

Decreasing costs is a permanent goal. It is sought both at the level of the design of the grain, by performing value analysis in cooperation with the missile manufacturer to satisfy the operational requirements, and at the level of the manufacture:

- reduction of manufacturing cycles;
- automation of industrial production;
- integrated processing systems;
- selection of materials;
- highly economical, non-destructive quality control tests.

The large industrial production processes already being tested, involve:

- the use of continuous screw extruders: extruded double-base and composite propellants with thermoplastic binders but also now with thermosetting binders;
- the implementation of high production rates, short cycles, and inhibiting techniques;
- high rate of injection systems for composite propellants, and reduction of the cure cycles.

For composite propellants, revolutionary progress (costs decreased by more than half) will be obtained only through extensive modifications of the active parts of the manufacturing process, such as continuous mixing. So far, the difficulties facing this development do not involve basic issues such as mechanical components, but rather the amount of precision required in the continuous feeding of raw materials, and the high level of sensitivity of the propellants to minute variations in the amounts of crosslinking agent, or catalyst. Therefore, progress should come from improvements in the precision of the feeding control equipment, and from the modification of the compositions to render them less sensitive in this area.

4. Propulsion of Shells

An area related to that of tactical missiles, where we will see the use of propellants and semi-propellants increase during the coming years, is the area of projectiles launched from a gun. Increasing the range of ballistic artillery projectiles, and increasing their velocity on the flat trajectory are constant goals.

Beyond the range increase through reduction of the base drag discussed in Chapter 10, research efforts are focusing on air-breathing propelled shells. The major problem consists in placing and having a ramrocket function inside a projectile launched from a gun, and often spin-stabilized. For these, the range of a 155 mm projectile could be increased to 50 km. In the case of a projectile stabilized by tail fins, ranges of 70 km are being predicted. Tubular projectiles, with a kinetic effect resulting from an air-breathing propulsion, are also being studied for anti-tank applications.

At any rate, all solid fuels to be used will have to produce combustible gases capable of burning efficiently in combustion chambers very limited in their lengths. The nature of these solid fuels and the design of these grains will have to overcome problems associated with a gun environment: very high pressures, high initial axial and radial accelerations, and rapid drop of pressure — for instance, when exiting the gun — while ensuring a consistent performance.

5. Space Launchers and Space Motors

This area is one where solid propellants are not doing as well as liquid propellants. All of the following factors have led to a wide use of liquid-fuel rocket engines on heavy launchers: (1) higher levels of specific impulse, and the possibility of easily modulating the thrust; (2) the ability to feed the propellant tanks at the last minute, unlike military missiles, thereby allowing the use of propellants not suitable for long-term storage; (3) less strict volume/weight limitations. Solid propellant rocket motors (Diamant A or B in France, from 1964 to 1972, and the first Japanese launchers, Scout in the USA) were used at the beginning of the space era, either because they were directly derived from the military technology of ballistic missiles, or because the payload was fairly small.

Solid propellant grains continued to be used in two types of motors related to the development of space applications: additional boosters for take-off, allowing an increase in the payload of a liquid propellant launcher (Ariane 3 and 4, for example), and the perigee and apogee motors designed to place satellites on geostationary transfer orbits from parking orbits.

Many motors of this type have been developed in Europe (motors for the MAGE family) or in the United States (STAR family), some of them attaining large dimensions, such as the Inertial Upper Stage SRM-2.

With the American space shuttle emerged an architecture already tested on the Titan III launcher, whereby the whole is designed in such a way that the central liquid propellant motor is not capable of ensuring take-off of the system by itself. At that point, 80 % of the thrust is provided by the boosters of the space shuttle. This type of launcher architecture, which utilizes solid propellant grains that are gigantic in comparison with what is used on the larger stages of military ballistics missiles, could become widely developed because the same type of architecture is being considered for the future European Ariane 5 launcher and for the future Japanese heavy launcher (HII).

The mass of propellants involved in these motors (several hundreds of tons) prevented in the past the production of monolithic grains. These grains are consequently case-bonded, and made of segments manufactured separately and later assembled. The propellants used, for reasons of safety and cost are generally polybutadiene-AP-Al propellants.

The progressive use of space for military purposes may confirm this trend toward solid propellant motors: the Department of Defense of the United States defines the main objectives that must be reached by the technologies to be used in the future military space systems as follows:

- immediate availability,
- low vulnerability,
- affordable cost,
- simplified logistics,
- reliability.

These are the very characteristics that have guaranteed the success of the solid propellant motors used on the strategic missiles, leading in the past to a success rate over 90 % for American military satellites launched by solid propellant launchers. To this, we may add that, for the very high mass flow rates considered, solid propellants give efficient and easy solutions and that the costs of development and production of solid boosters are lower than with liquids. MacDonald [14] has done a very detailed study of the various possibilities of development of these solid propellant space systems, using either existing motor assemblies, in particular the boosters of the shuttle, or improved-technology motors, focusing in particular on their competitiveness with the liquid fuel engines. More recently the AIAA Solid Rocket Technical Committee has emphasized [15] the potentials of solid rocket motors in the frame of US studies on a future ALS (advanced launch system). The stringent requirements for improvement of cost and reliability related to these applications, and perhaps environmental considerations, may lead to dramatic evolutions of this technology [16].

The present technology used on space boosters is a 20-30-year-old technology based on previous experience in tactical or strategic missile systems. In its most advanced form the propellant used is a composite

propellant: polybutadiene (HTPB), AP, Al with 86–88 % solids. This is a low-cost binder with a very good processability; it has a very attractive curing system which gives to the propellant a long pot-life and short cure times and a low viscosity enabling easy casting and high quality. The reliability of the cured propellant grains is good: good mechanical properties are achieved, good liners giving good bonding are available. There is an important experience with tactical and ballistic systems using this type of propellant. It will be used in the Ariane 5 boosters, HII boosters, Titan IV boosters and ASRM for the shuttle.

The processing facilities use batch mixing for the propellant and the nondestructive testing inspection is done with radiographic static controls with a progressive evolution toward automatic dynamic inspection using computer-aided radioscopy or tomodensitometry for exploration of the whole grain.

In their most advanced form these facilities represented by Bacchus West Hercules facility or the facility that is being built in Kourou (French Guyana) for the Ariane 5 boosters have the following characteristics:

- Specialization in the case of the Kourou facility; it is designed to manufacture only the main (100-ton) segments of the booster. This facility is close to the launch pad, enabling minimum handling.
- High level of automatization and computer on-line data acquisition and control.
- Batch processing, using for cost the highest capacity available mixer (1800 gallons, 13 tons of propellant per mix).

For the future continuous mixing is being considered.

Like any transformation industry the solid propellants industry has considered very early [17] the use of continuous processes that would be — compared to the batch processes — more economically efficient and safer, since a smaller quantity of propellant is worked on at a given time. The competition between increased size of the batch mixers and the continuous mixers has been favorable to the batch mixers in the past 30 years, even if Aerojet had operated a continuous mixing facility in the sixties [18].

The situation is changing since Aerojet will use a continuous process [19] for the new improved boosters for the shuttle (ASRM).

The main technical problems involved in continuous mixing have been described in Chapter 10. They are mostly related to precise continuous metering of the raw ingredients and to continuous in-line chemical control of the propellant. A Polybutadiene-AP-Al propellant will still be used.

Other more exotic processes are being researched, but are far less advanced so that their future is unpredictable. Some of them could use thermoplastic elastomers as binder for the propellant; no curing would be needed. A process called MEGABAR uses as oxidizers ammonium nitrate-based eutectic

oxidizers which are liquids during the mixing operation, which thus becomes easy and very rapid.

Besides the evolutions that originate because of the work on process improvement some research is devoted to clean or non-polluting propellants [16,20,21].

The AP propellants generate a very high level of hydrochloric gas and aluminum oxide, typically more than 20% of HCl and about 35% of Al_2O_3 can be found in the exhaust gases of our HTPB, AP, Al reference propellant.

The simple solution to the problem is to use an HCl scavenger like KNO_3 or NaNO_3 . HCl will be replaced by KCl or NaCl in the exhausts. The penalty on specific impulse — a loss of 15–20 s — will be severe. The use of NH_4NO_3 instead of AP would also lead to a severe performance loss. This could be compensated by using an energetic binder — and since in that application we do not want a too-sensitive one — quite a lot of work is devoted to GAP-TMETN binder.

5.1. MONOLITHIC GRAINS FOR SPACE BOOSTERS

The monolithic (non-segmented) boosters could have greater simplicity and reliability, and may have some advantages for cost. The main problems encountered would be [22]:

- the size of the molding tools and mandrels (they could be segmented, etc.);
- the casting of the propellant;
- the handling of these gigantic assemblies (we could imagine that all the operations would be done with the case in the same position until the final assembly, etc.);
- safety problems involved with such big masses of propellant;
- the size of the nondestructive inspection systems;
- the overall cost of demonstrating the validity of the concept.

Other avenues of technological evolution seem to have been opened by the Strategic Defense Initiative (SDI) of President Reagan toward either counter-measures by the “hardening” of strategic missiles and re-entry vehicles, which should lead to a requirement of very high energy and very high burning rate propellants (taking into account the increase in mass), or development of propulsion systems of anti-satellite or anti-re-entry-vehicle missiles, with conventional explosive warheads. The specifications for these systems are not completely developed, although they will certainly lead to:

- Attempts to reduce costs to a minimum, based on the large numbers of launches that may be involved for ground-based interceptors designed to intercept in the high atmosphere or exoatmosphere, or for launching of a large number of satellites at the last minute [23–25].

- Very high volumetric performance and special resistance to thermal cycles for interceptors based on satellites.

6. Conclusions

In the final analysis it appears that, as in many cases, the technological progress of propulsion systems using solid propellants is due at least as much to the expression of new requirements and the emergence of diversified applications, as to the results of basic research disconnected from any requirement specifications.

We have seen that a potential for improvement of the characteristics of solid propellants does exist, and that the development of these characteristics — especially for diversified space applications and the replacement of tactical missiles with newer, more versatile ones — should constitute an important field of study.

The applications of propulsion systems using solid or liquid propellants could also become more intertwined than in the past. We have seen, for instance, the return to bipropellant systems for the upper stages of ballistic missiles, while at the same time large solid propellant boosters were making a breakthrough on space launchers. And while liquid propellants seem to be useless for tactical missiles (with the exception of drone missiles and the possibility of using liquid propellants in a gel form), there will be strong competition for the middle- and long-range tactical missiles between the liquid fuel ramjet, the solid propellant ramrocket, the turbojet and the turboramjet.

Beyond applications to very high-performance military missiles, the emphasis will be placed on costs, particularly for mass industrial productions and very large missiles (artillery rockets and space launchers). This emphasis will not only be on production costs but also on development costs, implying significant changes in the methods of development: systematization of the approach by value analysis done at the pre-design phase; computer-aided automatic methods for the design phase; overtests performed within the framework of the development program, etc.

Finally, three new directions of effort have recently emerged that may have significant consequences on the renewal of the family of solid propellants: low vulnerability research, the various projects related to the American Strategic Defense Initiative and the technology evolution of the new space boosters.

Bibliography

1. TAVERNIER, P., BOISSON, J., and CRAMPEL, B., *Propergols hautement énergétiques*. AGAR-Dographi 141, AGARD, Paris, 1970.
2. FLANAGAN, J. E., and FRANEKL, M. B., An energetic binder comprises a hydroxy terminated aliphatic polymer having pendant alkyl azide groups and method for processing, US Patent 4 268450, 1981.

3. QUENTIN, D., Les propergols solides de l'an 2000, *Air et Cosmos*, **1000**, 243, 1984.
4. Solid staged combustion demonstrated. *Aviation Week and Space Technology*, p. 99, 12 April 1982.
5. MACPARTLAND, G. G., *et al.*, Integrated stage system study results. AIAA 22nd Propulsion Conference, 86-1581, 1986.
6. CALABRO, M., *et al.*, Reverse forward dome for a missile first stage. AIAA 23rd Propulsion Conference, 87-1989, 1987.
7. DOIN, B., Chargement pyrotechnique à combustion frontale comportant un canal longitudinal inhibé qui comporte des éléments de mise à feu. *Brevet français*, **78**, 21455, 1978.
8. JONES, R. A., and MABRY, W., Barrier systems for dual pulse rocket motors. US Patent 4085584, 1978.
9. LANGEREUX, P., La France met en service le missile air-sol nucléaire ASMP. *Air et Cosmos*, **1087**, 35, 1986.
10. LANGEREUX, P., Premier essai au banc du missile à statoréacteur rustique, *Air et Cosmos*, **935**, 27, 1983.
11. ROCHIO, J. J., Low vulnerability solid propellant, AIAA 22nd Propulsion Conference, 86-1589, 1986.
12. DERR, R. L., and BOGGS, T. L., Hazards/performance trade offs for smokeless solid propellant rocket motors. AGARD Conference Proceedings, 391, 1, 1985.
13. GUNNERS, N. E., and HELLGREN, R., Gun projectile arranged with a base drag reducing system, US Patent 4 213393, 1980.
14. MACDONALD, A. J., Solid rockets, an affordable solution to future space propulsion needs, AIAA 20th Propulsion Conference, 84-1188, 1984.
15. Low Cost Access of Space: "a solids approach". The Solid Rocket Technical Committee of AIAA, July 1988.
16. DAVENAS, A., Propergols solides et applications spatiales. *L'Aeronautique et l'Astronautique*, 1989.
17. *Propellants Manufacture, Hazards and Testing*. Advances in Chemistry series, ACS, Washington, 1964.
18. KEATING, J. W., SAGE, F., and KLAGER, K., Review of the continuous mixing process for solid propellants, ICT Jahrestagung, Karlsruhe, 1984.
19. NASA selects Lockheed/Aerojet to build shuttle's advanced solid rocket motor. *Aviation Week*, 1-5.89. p. 32.
20. SASSO, S., Solid rocket motors for future space launch vehicles. 25th Propulsion Conference, AIAA 89-2417, 1989.
21. KUBOTA, N., *Neusho Kenkyu*, 88-1, Japanese Combustion Institute, 1988.
22. BROWN, E. D., Processing issues for monolithic large scale booster rocket motors. ADPA Joint International Symposium on Compatibility, 1988.
23. CHASE, C. A., Solid booster propulsion for the late 1990s. AIAA 22nd Propulsion Conference, 86-1637, 1986.
24. DOLL, D. W., *et al.*, Low cost propellants for large booster applications, AIAA 22nd Propulsion Conference, 86-1706, 1986.
25. GAUNT, D. C., Understanding costs of solid rocket motors. AIAA 22nd Propulsion Conference 86-1638, 1986.

Index

- Ablation 105, 195, 554, 558, 559, 572, 575
- Acceleration 42, 48, 49, 59, 139, 351, 550, 592
- Acoustic balance 177, 186
- Acoustic modes 65, 173–175
- Adhesion 554–558, 574, 576
- Afterburning 199, 341, 400, 402, 511, 513, 561
- Aging 364, 365, 370, 408, 409, 432, 465, 517–519, 554, 561, 562
- Airbreathing motors 26, 106–109, 594, 595
- Aluminum 5, 11, 42–46, 96, 126, 139, 357, 403, 438, 462, 488, 497, 498, 533, 551
- Ammonium nitrate 416, 429, 437, 463, 466, 599
- Ammonium perchlorate 42–46, 96, 125, 127, 197, 316, 341, 348, 357, 416, 428, 435, 460, 461, 462, 487, 490, 496, 498, 504, 509, 510, 517, 520, 534
- Anisotropy 451–454
- Antioxidant 432
- Azide 483, 587, 588

- Ballistic modifier 123, 128, 372, 376, 396, 408, 427–428, 488, 513
- Base bleed 349
- Beryllium 438, 586
- Binder 42, 46, 126, 130, 237, 415, 416, 417, 418, 430, 433, 440, 471, 479, 480, 505, 516, 530, 571, 576, 585
- Blast tube 8
- Bond 265–269, 454
- Bonding 185, 215, 294, 417, 455, 494, 549, 554, 556, 562, 563, 564, 565, 567, 580
- Bonding agent 430, 486, 555
- Boron 357, 438, 533, 534, 537, 545, 549, 590
- Burning area 55–57, 75, 100
- Burning rate 10, 12, 13, 58, 61, 63, 82, 100, 111–117, 307, 334, 335, 351, 356, 375, 394, 395, 468, 488, 489, 506, 508
- Burning rate accelerator 427
- Burning rate enhancement 83, 136, 561, 562
- Burning rate law 14, 59, 112, 128
- Burning rate models 124, 129, 132
- Burning rate moderator 428

- Carbon-carbon 8
- Card gap test 309, 312, 322, 412, 520, 521
- Case 2–5, 50, 343, 344, 454, 472, 494, 549, 567, 568, 570, 592
- Case bonded grain 5, 37, 79, 218, 280, 338, 343, 415, 417, 448, 453, 455, 478, 493, 500, 503, 549, 566, 567, 576
- Casting 37, 383, 388, 416, 442–450, 453, 497, 502, 566
- Casting powder 42, 371, 377, 383, 385, 387, 478, 490, 491, 492, 502, 520, 521
- Casting solvent 383, 386, 387, 480, 502
- Catalyst 431, 442, 486, 571
- Centrifugation 568
- Char 554, 558, 574
- Chemical stability 371, 404–408, 497, 515
- Clean propellant 600
- Combustion instability 64, 80, 81, 172, 373, 401–404, 513–515
- Combustion mechanism 121, 124, 131
- Combustion efficiency 26, 530, 537, 544, 548
- Compatibility 376, 416, 434, 483, 554, 556, 562, 563, 586
- Condensed phase 24, 85, 142
- Conductive combustion 305, 307
- Coning 41, 83
- Continuous mixing 442, 596, 599
- Convective combustion 305, 306, 308
- Cook-off 218, 306, 317, 318, 347, 348, 411, 467, 471, 497
- Cost 4, 42, 81, 343–345, 351, 361, 551, 553, 596, 598, 600, 601
- Creep 243, 246
- Crosslinking 416, 418, 423, 425, 464, 466, 480, 492, 496, 504, 505, 568, 574, 576
- Crystallization 487, 499–500
- Curing 4, 5, 220, 383, 388, 416, 431, 450, 464, 485, 496, 497, 506, 518, 522, 576, 599

- Damage 261, 288, 294, 453
- Damping 179, 188, 376, 403, 514
- Deflagration 305, 520
- Deflagration to detonation transition 309–311, 323, 520, 522, 589
- Density 8, 10, 21, 332, 385, 386, 387, 391, 436, 490, 493, 497, 510, 531, 532, 533, 554, 572, 580, 594
- Design to cost 362
- Detonation 304, 306, 308, 314, 316, 346, 347, 411, 467, 469, 521
- Detonation critical diameter 49, 308, 325, 347, 348, 412, 469
- Discharge coefficient 10, 11, 20, 89
- Dynamic loads 297–300

- End burning grains 40, 41, 83, 97, 383, 390, 548, 559
- Equivalence ratio 534, 539, 545, 548
- Erosive burning 52, 61–63, 75, 157–164, 404
- Expansion ratio 7, 23, 55, 75, 89
- Extrusion 42, 379, 383, 384

- Failure criteria 71, 77, 257–261
- Ferrocenic derivative 128, 427, 461, 468–471
- Finocyl 40, 137, 156, 175, 453
- Flash suppressor 210, 376, 400, 408, 513
- Flow 15, 24, 31, 59, 86, 140, 153–157, 194
- Flow rate 10, 11, 89, 335, 356, 534, 539, 544
- Fluoramino compounds 587, 588
- FMECA 76
- Free standing grain 5, 37, 40, 222, 343, 500, 566, 575
- Friction sensitivity 314, 315, 411, 470, 521, 522, 543
- Fuel rich propellants 106, 527, 529, 532, 535, 538–545, 548

- GAP 587
- Gas generator 2, 106, 158, 350, 351–354, 460, 463, 528, 539, 545, 548, 590
- Glass transition temperature 336, 421, 497, 498

- Hazard division 320–324, 345, 522
- Heat capacity 391
- Heat of combustion 530, 532
- Heat of explosion 386, 391, 398, 403, 407
- Heat transfer 15, 159, 160, 168, 354
- HMX 42–46, 125, 344, 437, 462, 487, 507, 586, 590
- Hump effect 59, 136, 137, 451, 452

- Igniter 354, 355, 356
- Ignition 3, 4, 9, 42, 51, 63, 67, 75, 80, 167–172, 304, 314, 316, 317, 338, 351, 354, 356, 372, 379, 410, 469, 473, 537
- Ignition delay 169
- Ignition compositions 356–359
- Impact sensitivity 313, 411, 543
- Incompressible 67, 68, 250, 282–286
- Infrared 201, 203, 208, 399
- Inhibitor 380, 381, 553, 566, 570, 571, 590
- Insensitive munitions 4, 345–347
- Integral booster 81, 526, 549, 579
- Integral molding 450, 486, 497
- Isocyanate 423, 485, 492, 496, 571, 574, 576

- Klemmung (burning area to throat area ratio) 11, 13, 14, 75, 93, 185, 323
- Kneading 377, 378, 384

- L* instabilities 173, 177
- Labor regulations 320, 322
- Liner 6, 38, 417, 454, 494, 550, 553, 567, 576, 578
- Longitudinal instabilities 173, 181, 401
- Loss 24, 25, 97, 180

- Mandrel 3, 4, 38, 443, 446, 449, 452, 567
- Mass flow rate 1, 17, 19, 27, 48, 63, 75, 130
- Mass flow rate response 175, 176
- Mechanical behavior 66, 67, 227, 235, 239, 251, 274, 298, 336, 393, 502, 505, 522
- Mechanical capability 66, 71, 77, 217, 268, 339, 341, 463, 464
- Mechanical imbedment 569
- Mechanical loads 35, 68, 70, 77, 218, 338, 416
- Migration 427, 454, 466, 518, 562
- Mixer 384, 441, 496, 599
- Mixing 383, 384, 416, 439–442, 496, 568, 600
- Molding 450
- Monolithic boosters 600

- Nitramine 125, 483, 487, 490, 496, 498, 510, 517, 520, 562
- Nitrocellulose 42, 329, 370, 373, 377, 383, 384, 477, 481, 504
- Nitroglycerine 42, 329, 370, 374, 377, 383, 384, 386, 477, 483, 496, 499, 500, 587
- Nitroguanidine 374, 429, 437, 461
- Nondestructive inspection 364, 454–461, 565, 599, 600

- Nozzle 6-9, 15, 16, 17, 18, 27, 50, 51, 59, 75, 89, 92-94, 107, 180, 194, 344, 525, 526, 547, 549, 590
- Nozzleless motors 81-82, 549, 550, 595
- Operating pressure 7, 12, 22, 75, 102, 402
- Optical transmission 95, 201, 206, 399, 559-561
- Overtest 78
- Oxamide 429, 575
- Paste 378
- Peeling 270, 563, 570
- Plasticizer 371, 375, 422, 425, 427, 479, 480, 481, 483, 495, 498, 499, 562, 571, 578
- Plateau 372, 395, 396, 397, 507-508
- Plume 48, 97, 193, 199, 204, 560
- Poisson ratio 227, 229, 230, 283
- Polybutadiene 45, 96, 417, 423, 427, 432, 461-462, 471, 474, 530, 534, 540, 576, 585, 598, 599
- Polyester 421, 432, 462, 474, 481, 504, 510, 530, 571, 574
- Polyether 421, 460, 481, 510, 574
- Post boost control system 462, 589
- Pot life 416, 431, 542, 566, 567, 599
- Preliminary design 3, 20, 21, 36, 52, 72-75
- Pressure coupling 175, 178, 181
- Pressure effect 249, 252-261
- Pressure exponent 58, 112, 128, 396, 427, 463, 489, 510, 547, 550
- Pressurization 70, 220, 223, 224
- Primary smoke 196, 211, 341, 512
- Pyrolysis 41, 118, 554, 558, 561, 574
- Pyrotechnic behavior 304, 467, 595
- Radar attenuation 200, 206, 210
- Ramjet 26-31, 106-109, 335, 351, 525, 526, 528, 535, 549, 579, 595, 601
- Ramrocket 26-31, 335, 351, 539, 595, 601
- RDX 42-46, 125, 487, 504, 507
- Relaxation 67, 243, 244
- Reliability 35, 37, 49, 75-78, 218, 362, 574, 592, 598, 600
- Resonance rod 187
- Reynolds number 161
- Rolling 379, 383
- Safety 49, 303, 345, 358, 410-412, 442, 449, 467, 495, 519-523, 543
- Safety coefficient, safety factor 65, 70, 71, 72, 74-77, 216, 288-297, 519
- Safety margin 65, 77, 217
- Screw extrusion 343, 377, 382, 390, 596
- Secondary smoke 197, 212, 341, 512
- Segmented grain 79, 80, 598
- Service life 35, 40, 360, 363, 405, 406, 553, 571, 589, 592
- Shear 233, 443, 454
- Shell 349, 597
- Shock sensitivity 386, 470, 521, 522
- Signature 193, 194, 333, 341, 342, 399, 460, 511, 515, 530, 544, 549, 561, 572, 591
- Space motors 79, 80, 597-600
- Specific impulse 19, 21, 25, 27, 81, 85, 96-106, 332-333, 398, 426, 434, 460, 493, 510-512, 534, 538, 542, 545, 549, 586, 588, 589, 594, 595, 597
- Spraying 566, 568
- Stabilizer 317, 371, 375, 376, 405, 408, 488, 516
- Stamping 343, 381, 448
- Standard motor 11, 99, 116
- Standard specific impulse 10, 54, 105, 106, 108
- Static electricity 319, 411, 471-473, 523, 578
- Steady state combustion 10, 93, 135
- Steady state flow 91, 92
- Strain 67, 70, 128, 217, 225-229, 237, 270, 276, 291, 417, 501, 502, 503, 592
- Strand burner 113, 307
- Stress 67, 70, 138, 217, 225-229, 237, 270, 276, 293, 417, 466, 501, 502, 503, 592
- Structural analysis 36, 52, 53, 65, 74, 215
- Structural integrity 52, 82, 216
- Swelling 377, 380, 419, 571
- T burner 181, 182
- Tear 262
- Temperature coefficient 14, 59, 112, 335, 372, 375, 395, 507, 539
- Tensile test 71, 233-236, 240-242, 501
- Terminology 47-48
- Theoretical specific impulse 24, 96
- Thermal conductivity 391, 554, 580
- Thermal cycles 42, 48, 49, 295, 338-340, 501, 592, 601
- Thermal expansion coefficient 340, 391, 417, 499, 580
- Thermal explosion 307, 317
- Thermal insulation 5, 6, 50, 454, 553, 554, 567, 590
- Thermal protection 3, 44, 494, 549, 550, 558, 579
- Thermal shrinkage 280
- Thermoinitiation 317, 410, 470, 523
- Thrust 1, 15, 17, 19, 30, 48, 52, 53, 79, 80, 416, 598
- Thrust coefficient 18, 31, 89
- Thrust law 13
- Thrust measurement 97, 98

- Thrust modulation 592, 593, 594, 597
Thrust vector control 8
Time-temperature equivalence 246-249
TNT equivalency 308, 309
Total impulse 20, 48, 55, 75, 96, 550
Toxicity 586
Transverse instabilities 174, 185, 401, 513
Turbojet 594, 601
Turboramjet 595, 601
- Unsteady combustion 140, 141, 164, 175
- Value analysis 361, 362
- Velocity coupling 175, 178, 183
Viscoelasticity 235, 251, 336, 417, 418
Viscosity 374, 380, 422, 431, 433, 442, 444, 451, 453, 495, 542, 568, 575, 578, 599
Volume change 241, 388, 503
Volumetric loading fraction 41, 55, 81, 549, 589
Vulnerability 49, 345, 488, 593, 595, 598, 601
- XDT 311
- Zirconium 336, 403, 533-535, 537, 551, 586